APPLICATION OF SOLID-PHASE MICROEXTRACTION FOR THE DETERMINATION OF PESTICIDES IN VEGETABLE SAMPLES BY GAS CHROMATOGRAPHY WITH AN ELECTRON CAPTURE DETECTOR

Chai Mee Kin[1], Tan Guan Huat[2] and Asha Kumari[3]

[1]*Dept. of Science and Mathematics, College of Engineering,Universiti Tenaga Nasional,*
Km 7, Jalan Kajang-Puchong,43009 Kajang, Selangor.
Fax:03-89263506
[2,3]*Dept. of Chemistry, Faculty of Science,*
Universiti Malaya, Lembah Pantai,
50603 Kuala Lumpur.

Abstract

A solid-phase microextraction (SPME) method has been developed for the determination of 9 pesticides in 2 vegetables - cucumber and tomato - samples, based on direct immersion mode and subsequent desorption into the injection port of a gas chromatograph with an electron capture detector (GC-ECD). The main factors affecting the SPME process such as extraction time and temperature, desorption time and temperature, the effect of salt addition and fiber depth into the liner were studied and optimized. The analytical procedure proposed consisted of a 30-minute ultrasonic extraction of the target compounds from 1.0 g vegetable samples with 5 mL of distilled water. Then, the samples were filtered and topped up with distilled water to 10 mL. The analytes in this aqueous extract were extracted for 15 minutes with a 100 μm thickness polydimethylsiloxane SPME fiber. Relative standard deviations for triplicate analyses of samples were less than 10%. The recoveries of the pesticides studied in cucumber and tomato ranged from 52% to 82% and the RSD were below 10%. Therefore, the proposed method is applicable in the analysis of pesticides in vegetable matrices. SPME has been shown to be a simple extraction technique, which has a number of advantages such as solvent free extraction, simplicity and compatibility with the chromatographic analytical system.

Introduction

One of the major fields in analytical chemistry is the development of faster and easier methodologies for characterization and quantification of trace compounds in complex matrices. A special attention is given to substances that can compromise food safety, such as pesticide.

Pesticides are widely used for agricultural and non-agricultural purpose throughout the world. Although various methods, using highly efficient instruments such as gas chromatography (GC), high performance liquid chromatography (HPLC), Liquid chromatography (LC) and their combination with mass spectrometry (MS), have been developed for pesticide analysis, most analytical instruments cannot handle the sample matrices directly. In general, the analytical method involves processes such as sampling, sample preparation, separation, detection and data analysis and more than 80% of the analysis time is spent of sampling and sample preparation steps that include homogenization of samples, extraction of the analytes with an organic solvent, and clean up of the final organic extract. Therefore, it is not an exaggeration to say that the choice of an appropriate sample preparation method greatly influences the reliable and accurate analysis of food.

In contrast to conventional techniques, Solid Phase MicroExtraction (SPME) is a solvent-free extraction that minimizes sample preparation allowing the extraction and concentration steps to be focused into a single step. This technique, whose initial concepts were developed by Pawliszyn and co-workers in 1990 [1], is based on absorption of analytes onto a polymeric-coated fused-silica fiber, usually housed in a modified syringe. The total analytes retained in the fibers are thermally desorbed in the injector port and deposited at the head of the GC

column. Due to its advantages over classic extraction methods, SPME has received increasing attention since its commercial introduction in the nearly 1990s [2]. SPME has been applied to the determination of several organic compounds especially in gas and liquid samples, but also in a few solid samples, in combination with both GC and HPLC determination. Two modes of application of SPME have been extensively reported [1]: Direct Immersion (DI-SPME) and Headspace (HS-SPME) extraction. In DI-SPME, the fiber is directly immersed in the liquid sample or in the sample suspension and the analytes are transported from the sample matrix to the fiber coating. In headspace extraction mode, the analytes are extracted in a three-phase system: sample (liquid or solid), headspace, and fiber coating.

SPME has been successfully applied to the determination of pesticide residue analysis in water, soil, food and biological samples as reported in recent reviews published by Beltran et al. [3] and Kataoka et al. [1]. Water samples are by far the most widely analyzed by this technique [4-6].

The number of applications of SPME to complex matrices such as biological fluids is still limited; the headspace mode is the most attractive approach in this field [7-12]. Analysis of other samples such as soil [13-16] or food commodities [1, 17-18] is generally based on a solvent extraction of the analytes before application of SPME.

The low number of references about pesticide determination in food samples by SPME derives from the complexity of these matrices, which makes an extraction of the sample prior to determination by direct immersion SPME necessary in most of cases. This problem can be overcome if headspace SPME is applied, as described in several papers dealing with pesticide residue determination in fruits [19-21] or in a large number of papers related to determination of volatile compounds in food commodities [22-25].

Determination of non-volatile pesticides has received increasing attention in the recent years in order to solve some of the problems related with the application of DI-SPME in complex matrices. Several papers deal with direct immersion of the SPME fiber into a slurry of fruit with water [19,26]. Complex matrix problems can be solved by prior extraction of pesticide and the subsequent application of DI-SPME over the separated aqueous extract. Once the aqueous extract is obtained, the presence of interfering substances can reduce the efficiency of SPME. This problem can be overcome by simply diluting the extract in order to simplify the matrix complexity [27-28]. Still another problem, closely related with pesticide residue determination in fruits by SPME, is the difficulty of quantification; in most cases it is necessary to use calibration curves prepared using blank matrix, standard addition calibration, and internal standards [20].

The aim of this work is to investigate the feasibility of developing a single-step clean up enrichment procedure for pesticides extracted from vegetables based on SPME prior to gas chromatography with electron capture detection (GC-ECD). Nine pesticides: Carbaryl, Diazinon, Chlorothalonil, Malathion, Chlorpyrifos, Quinalphos, Profenofos, Alpha-Endosulfan, Beta-Endosulfan were selected as the model compounds because residues of these compounds are very often detected in vegetable samples. Table 1 showed the properties of nine selected pesticides. In this study, SPME-GC-ECD conditions have been optimized for the target compounds. The developed procedure was then successfully applied to the analysis of vegetable samples such as cucumber and tomato.

Table 1: Name, Molecular Formula, Molecular Weight, Chemical Class of the selected Pesticides.

Name	Molecular Formula	Molecular Weight	Chemical Class
Carbaryl	$C_{12}H_{11}NO_2$	201.22	Carbamate
Diazinon	$C_{12}H_21N_2O_3PS$	304.35	OP
Chlorothalonil	$C_8Cl_4N_2$	265.92	OC
Malathion	$C_{10}H_{19}O_6PS_2$	330.36	OP
Chlorpyrifos	$C_9H_{11}C_{l3}NO_3PS$	350.62	OP
Quinalphos	$C_{12}H_{15}O_3N_2PS$	298.18	OP
Profenofos	$C_{11}H_{15}Br_{Cl}O_3PS$	373.60	OP
α-Endosulfan	$C_9H_6Cl_6O_3S$	406.96	OC
β-Endosulfan	$C_9H_6Cl_6O_3S$	406.96	OC

Experimental

Chemicals and Reagent

All solvents used were HPLC grade. Methanol was purchased from Fischer Scientific, Loughborough, U.K. Deionized water and methanol were filtered through a 0.45 μm membrane filter purchased from Millipore. The

use of high purity reagents and solvents help to minimize interference problems, pesticide standards (carbaryl, diazinon, chlorothalonil, malathion, chlorpyrifos, quinalphos, profenofos, α-endosulfan, β-endosulfan) were > 95% pure and purchased from AccuStandard Inc. New Haven CT, USA. Stock solutions of each pesticide at different concentration level, 50-2000 mg/kg were prepared in methanol and stored at 4 ^{o}C. Preparation of different concentration level of stock solution is due to their sensitivity to the ECD detector. Working standard solutions of pesticides mixture were prepared by volume dilution in distilled water. In order to avoid the influence on the results from the possible degradation of pesticides, the working solution was freshly prepared everyday. 1-chloro-4-fluorobenzene (2mg/kg) was used as internal standard to compensate for sample and was added to the vial prior to GC analysis.

Gas Chromatography – Electron Capture Detector (GC-ECD)
A Shimadzu GC 17A version 2.21 gas chromatograph with an electron capture detector ECD was used. A SGE BPX5, 30m x 0.32 mm id capillary column with a 0.25 μm film was used in combination with the following oven temperature program: initial temperature 120 ^{o}C, then 7 ^{o}C/min ramp to final temperature at 250 ^{o}C, held for 4.5 min. The total run time was 23.07 min. The injector temperature was at 240 ^{o}C and the detector temperature was at 300 ^{o}C. Nitrogen gas (99.999%) was used as the carrier gas with a gas flow at 24.4 cm/sec linear velocity and the pressure at 94 kPa and the split mode ratio of 1:36.

SPME Procedure
The SPME fiber holder for manual extraction and the fibers of polydimethylsiloxane (PDMS, 100 μm film thickness) were purchased from Supelco (Bellefonte, PA, USA). SPME fibers were conditioned by heating at 250 ^{o}C for 0.5 hour in the gas chromatography (GC) injection port according to the manufacturer recommendations in order to remove contaminants and to stabilize the polymeric phase.

Preliminary experiments were carried out to optimize the main parameters affecting the SPME of the pesticides investigated from aqueous solution (i.e. extraction time and temperature, desorption time and temperature, the effect of salt addition, stirring speed of the solution and fiber depth into the liner). In these studies, distilled water samples spiked with the appropriate amount of the standard solution was used.

After optimization, a typical experiment consisted of the direct immersion of the conditioned fiber into the spiked water sample, 10mL in a 15 ml clear glass vial and capped with a PTFE-faced silicone septum (Supelco). The SPME holder needle was inserted though the septum and the fiber was directly immersed in the sample solution for 15 minutes under magnetic stirring at room temperature (25 ^{o}C) in order to improve mass transfer from the aqueous sample into the fiber coating. After extraction, the fiber was withdrawn into the holder needle, removed from the vial and immediately introduced into the GC injector port for 7 min at 240 ^{o}C for thermal desorption in a split mode injector.

Calibration curves were constructed by SPME of the target compounds from aqueous samples spiked at 7 concentration levels and the constant volume of internal standard under above experimental condition. Three extractions were made for each concentration level of mixture solution. The calibration graph was plotted by the ratio of the peak area of the analyte against the peak area of the internal standard from the spiked samples versus the concentration of the analyte. These calibration lines were used for quantification in subsequent experiments.

Vegetable Samples
In order to evaluate the pesticide recoveries, 2 types of vegetables, cucumber and tomato were obtained from pesticide free farms under study. 1.0 g of vegetable samples was finely chopped and placed in a 15ml clear glass vial and capped with a PTFE-faced silicone septum. 5 mL of distilled water was added and spiked with three concentration levels of stock solution. The mixture was shaken for 30 minutes in an ultrasonic bath. Then, the samples were filtered, added with internal standard and topped up with distilled water to 10 mL. Pesticides were then extracted by direct dipping of the PDMS fiber in the solution. Recoveries of pesticides were determined by comparison of the ratio of the peak area of the analyte against the peak area of the internal standard from the spiked samples with that of the standard calibration solutions.

Result and discussions

Method Optimization

Preliminary experiments were performed by direct injection of pesticides for GC-ECD conditions optimization; the temperature program developed was capable of a good separation of the investigated analytes. In order to developed the SPME described method for pesticides selected extraction in vegetables, several parameters such as extraction time and temperature, desorption time and temperature, the effect of salt addition, stirring speed of the solution and fiber depth into the liner were studied.

On the basis of the results previously published for the target compounds, a 100 μm PDMS fiber was chosen as this material has been reported to have satisfactory extraction efficiency for a variety of compounds, including pesticides selected in this study. The 100 μm PDMS fiber (a non-polar phase) is recommended in the literature because it is a rugged liquid coating able to withstand high injector temperature up to 300 ^{o}C. Fibers coated with thicker films required a longer time to achieve extraction equilibrium, but might provide higher sensitivity due to the greater mass of the analytes that can be extracted.

Effects of Extraction Temperature and Time

In order to study the effect of temperature on the extraction process, vials were immersed in a water bath heated by the magnetic stirring unit. A thermometer was used to monitor the water temperature. The temperature effect was evaluated by varying the temperature from 25 to 70 ^{o}C. An increase in extraction temperature causes an increase in the extraction rate and a simultaneous decrease in the distribution constant between the analytes and the fiber [27]. The analysis of the 9 pesticide compounds was performed at room temperature for the subsequent experiments.

The sorption time profile for the selected fiber was obtained by plotting the detector response (peak area) versus the extraction time for each pesticide in order to obtain the partition equilibrium curve (figure 1). Blank aqueous samples (10mL) spiked at 0.1 mL standard solution were analyzed at experimental conditions described in the SPME procedure. Sorption time profiles indicated that a sampling time higher than 30 minutes is necessary to reach the equilibrium. According to the literature [1,12,29-31], the sorption time can be shortened by working in non-equilibrium condition because the amount of analyte adsorbed from the sample onto the fiber is proportional to the initial concentration in the sample matrix, if the agitation and the sampling time are held constants amongst samples. Thus, considering a compromise between the extraction time and the chromatographic analysis time, an extraction time of 15 minutes was selected for further experiments. This time still allowed a good, reproducible extraction response for all pesticides while minimizing analysis time.
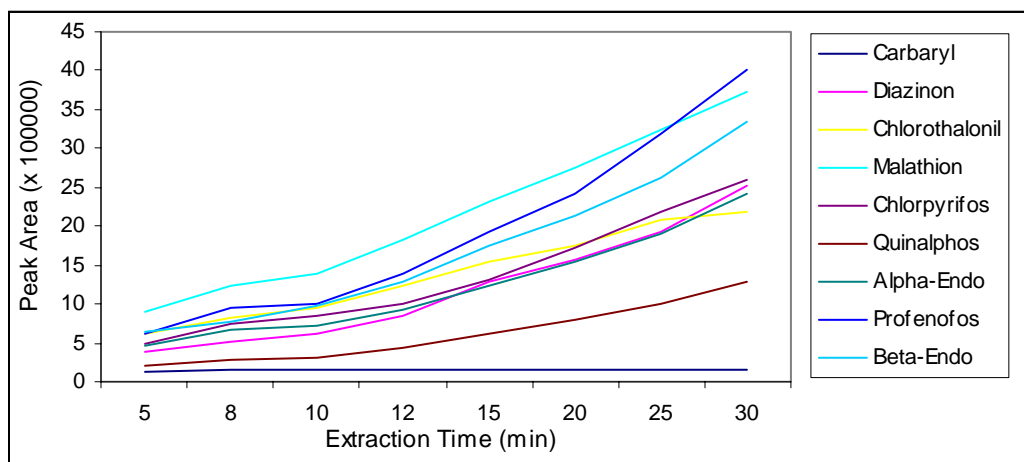

Figure 1: Peak area versus extraction time for 9 investigated pesticide

Effects of Desorption Temperature and Time

The temperature of GC injector and desorption time were tested in order to guarantee the complete desorption of pesticides to avoid carryover. For the PDMS fiber, temperatures ranging between 200 and 280 ^{o}C were tested (selected according to the recommended temperature range indicated by the manufacturer). High desorption temperature can enhance the process but they can also degrade analytes. Desorption at 200 and 230 ^{o}C was not

capable of desorbing completely the analytes; they were completely removed from the coating at 240 – 280 °C and not much significant differences were observed within this range of temperature. Hence a temperature of 240 °C was selected since high temperatures can shorten the coating lifetime and can result in the bleeding of the polymer, causing problems in the separation and quantification [29].
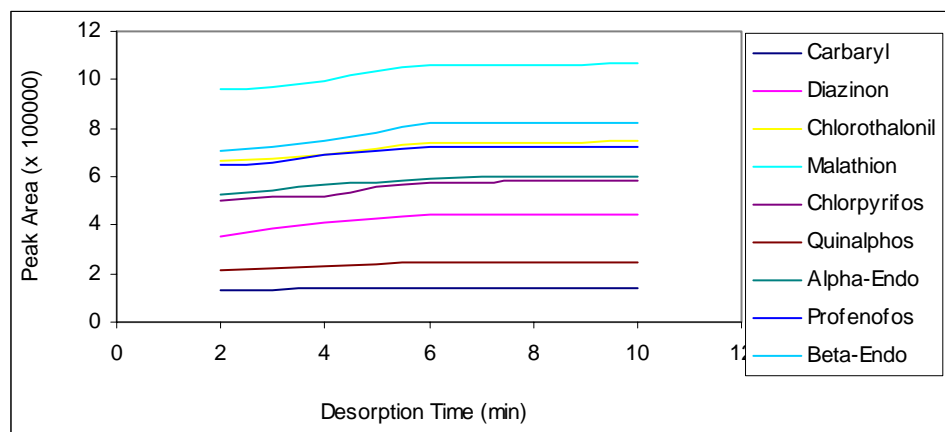

Figure 2: Peak area versus desorption time for 9 investigated pesticide.

Desorption profiles of the pesticides were obtained by plotting the detection response versus different desorption times, 1 – 10 minutes. Desorption profiles showed that a 6 minute-period was sufficient to desorb pesticides in the GC injector port (Figure 2); therefore a 7 minute-period was chosen to guarantee a reproducible desorption.

Effects of Salt Addition
The addition of salts into the samples can modify the extraction efficiency, because the partition coefficients are partially determined by matrix-analyte-fiber interactions [29]. Pesticides that are more soluble in water have a lower affinity for the fiber coating. The amount of these analytes extracted by the fiber can be increased if the solubility of the analytes in water is decreased by adding sodium chloride to alter the ionic strength [27]. The effect of increasing the ionic strength of the sample was determined with samples containing no salt, 5, 10, 15, 20 and 25% (w/v) of sodium chloride. Result showed that the amount of compounds extracted decreased when the salt concentration increased. The best results were obtained when no salt was added; this could possibly be due to the formation of a thin layer of salt around the fiber, which decreases the extraction efficiency [29].

Effects of Stirring Speed
The use of a magnetic stirrer allows the control of the stirring speed as well as the mode of stirring, and hence a cyclic change in stirring direction. The results showed the responses increased if the stirring speed is increased which agrees with the fact that SPME is a technique based on equilibrium and that good diffusion through the phases is essential to reach equilibrium faster. Although the equilibrium time progressively decreases with increasing agitation rate, faster agitation tends to be uncontrollable and the rotational speed might cause a change in the equilibrium time and poor measurement precision. A constant gentle stirring speed was selected in this study to increase the rate of extraction.

Effects of Fiber Depth into the Liner
The effect of the fiber depth into the liner was also checked, and the results showed that peak areas increased when the depth of the fiber into the injector glass-liner was higher, which is closer to the column entrance and the center of the hot injector zone.

Method performance
After optimization of all the variables considered, the recommended procedure was established as follows: extraction of 10 mL of water sample containing no salt under magnetic stirring for 15 min at room temperature using a PDMS, 100 μm fiber coating and subsequent desorption at 240 °C over 7 min. The optimum procedure developed was applied to the extraction of nine pesticides in spiked water samples. With the selected conditions for the SPME procedure, quality parameters of the SPME-GC-ECD method such as linearity, limits of detection and quantitation, and recovery were calculated.

5

The linearity of the method was tested using a series of aqueous solution (distilled water) in the difference concentration range (7 levels, three replicates for each level). After plotting the ratio of analyte peak area relative to that of the peak area of internal standard versus the analyte concentration to generate the calibration curves, a statistical regression model was applied to obtain the corresponding values for slope and intercept for each compound. The SPME procedure showed a linear behavior in the ranges tested with r^2 values > 0.9900. Linear ranges and determination coefficients (r^2) obtained for each pesticide are given in Table 2. The loss of linearity observed at higher concentrations can be justified due to overloading of the SPME fiber capacity.

The detection limit (LOD) was calculated by comparing the signal-to-noise ratio (S/N) of the lowest detectable concentration to a S/N=3. A S/N of 10 was applied for the calculation of the quantification limit (LOQ). The results obtained are shown in Table 2.

Table 2: Coefficients (r^2), linear range, limits of detection (LOD) and limits of quantification (LOQ) of the investigated pesticides using the optimized SPME extraction method.

Name	R^2	Linear Range (mg/kg)	LOD (mg/kg)	LOQ (mg/kg)
Carbaryl	0.9976	0.2 – 200	0.01	0.05
Diazinon	0.9968	0.05 – 50	0.005	0.02
Chlorothalonil	0.9988	0.02 – 20	0.001	0.005
Malathion	0.9965	0.05 – 50	0.005	0.02
Chlorpyrifos	0.9986	0.005 – 5	0.0005	0.001
Quinalphos	0.9985	0.05 – 50	0.005	0.02
Profenofos	0.9941	0.01 – 10	0.001	0.005
α-Endosulfan	0.9952	0.005 – 5	0.0005	0.001
β-Endosulfan	0.9972	0.005 – 5	0.0005	0.001

Vegetable Samples
The developed method has been applied to the vegetable samples, cucumber and tomato, treated as described in the Experimental section. From Figure 3, it is clear to show that all the target analytes were detectable in the sample and appeared completely separated from interfering peaks. The extraction efficiencies were calculated by comparing the chromatogram (Figures 3) obtained from the extracts of the spiked samples by SPME with those obtained by direct GC injection of non-extracted (Figure 4). It is shown that SPME is effective in the extraction of all the pesticides investigated without absorbing any other unwanted compounds from the samples.
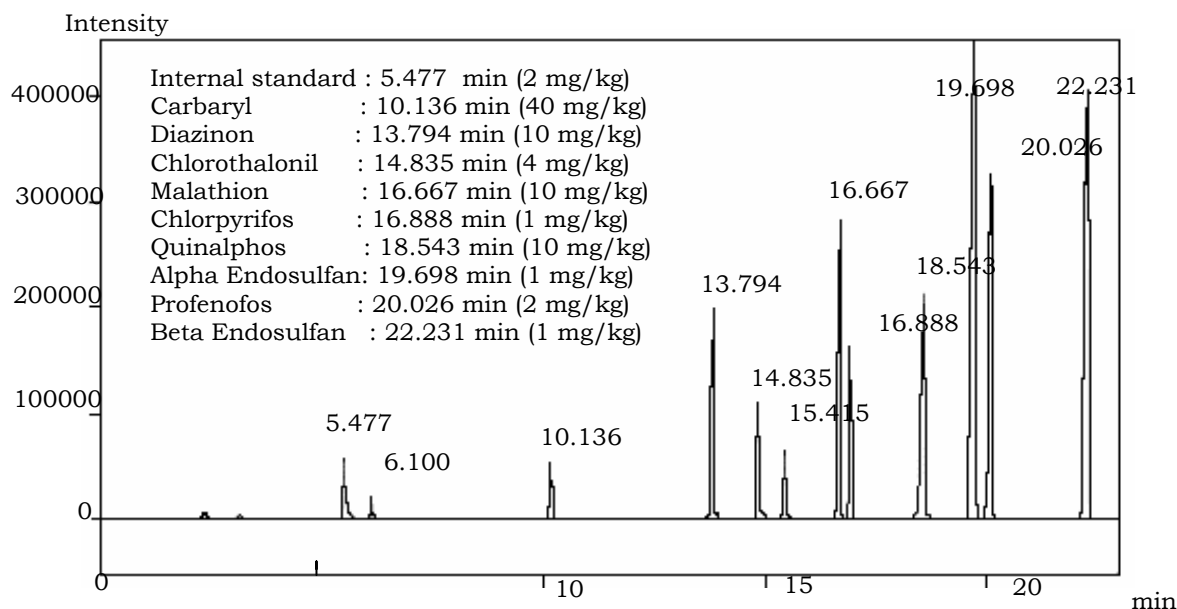

Figure 3 : Chromatogram on recovery of spiked cucumber and extracted by SPME.

Recovery tests were performed in order to study the accuracy. These tests were based on the addition of known amounts of standard solution of pesticides to the vegetable samples. The study was carried out in triplicate at

three concentration levels. The peak areas obtained when these samples were analyzed by the same procedure were compared with the standard calibration curves. Mean recoveries and RSD obtained in the analysis of fortified cucumber and tomato samples are listed in Table 3. For fortified cucumber samples, the recoveries were between 53 – 75 % and for the tomato, the recoveries were between 53 – 82 % with is quite similar to that of the fortified cucumber. The precision determined using the same conditions was good, with the vast majority yielding relative standard deviations (RSDs) below 10 %.
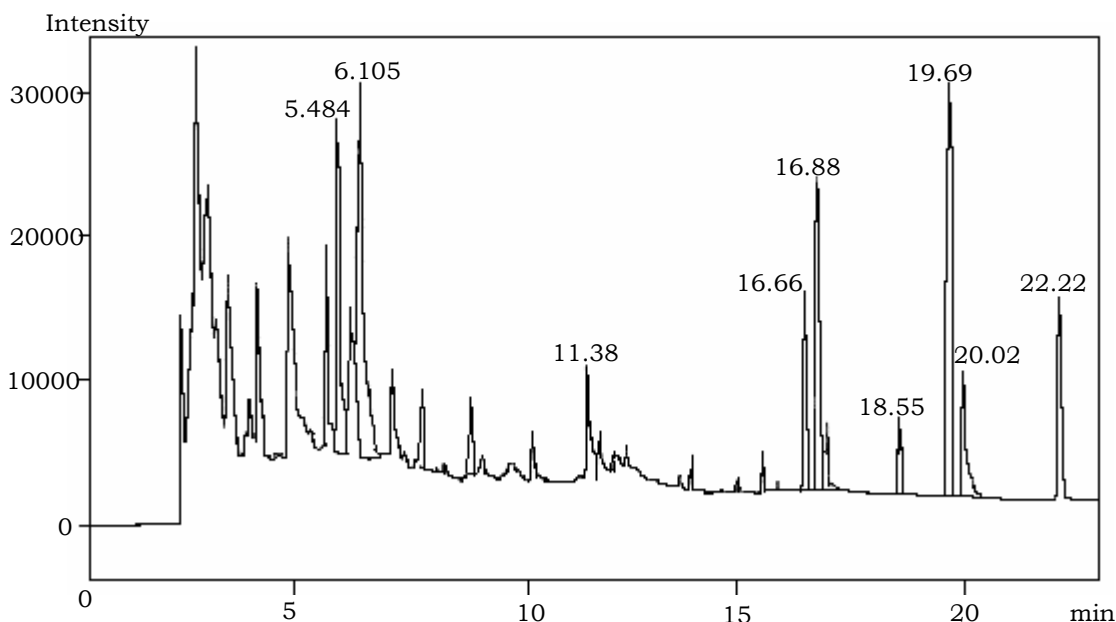

Figure 4: Chromatogram on recovery of spiked cucumber and direct injection

Table 3: Average recoveries and relative standard deviations (RSDs) from three representative
commodities fortified vegetable samples using the optimized SPME extraction method.

Name	Cucumber (n=3)		Tomato (n=3)	
	Recovery (%)	RSD (%)	Recovery (%)	RSD (%)
Carbaryl	74.10	8.22	82.17	1.26
Diazinon	53.96	1.43	54.13	1.57
Chlorothalonil	58.26	1.27	56.44	1.00
Malathion	75.03	2.11	71.79	0.47
Chlorpyrifos	55.36	8.93	56.90	9.30
Quinalphos	54.76	2.53	52.57	0.99
Profenofos	56.47	3.94	58.41	5.99
α-Endosulfan	60.09	6.05	53.08	3.83
β-Endosulfan	65.27	4.39	58.40	6.92

Conclusions

A fast, simple, solvent free screening method based on a 30 min ultrasonic extraction of a 1.0 g vegetable samples with distilled water and subsequent SPME of the analytes from the aqueous solution and detected by gas chromatography with an electron capture detector has been developed for the determination of nine pesticides. The main experimental parameters affecting the SPME step were optimized. This method offers very low detection limits for all nine pesticides. The recoveries of the pesticides studied in cucumber and tomato ranged from 53% to 82% and the RSD were below 10%. Therefore, the proposed method is applicable in the analysis of pesticides in vegetable matrices. SPME has been shown to be a simple extraction technique, which has a number of advantages such as solvent free extraction, simplicity and compatibility with the chromatographic analytical system.

References
1. Beltran J, Peruga A, Pitarch E, Lopez, FJ and Hernandex F (2003), " Application of solid-phase microextraction for the determination of pyrethroid residues in vegetable samples by GC-MS", Anal. Bional. Chem. 376, 502-511.
2. Betran J, Lopez F.J, Hernandez F (2000), "Solid-phase microextraction in pesticide residue analysis.", J. of Chromatography A, 885, 389-404.
3. Goncalves C, Alpendurade MF (2004), "Solid-phase micro-extraction-gas chromatography – (tandem) mass spectrometry as a tool for pesticide residue analysis in water samples at high sensitivity and selectivity with confirmation capabilities." J. of Chromatography A, 1026, 239-250.
4. Blanco MC, Rodriguez BR, Grande BC, Gandara JS (2002), "Optimization of solid-phase extraction and solid-phase microextraction for the determination of α- and β- endosulfan in water by gas chromatography-electron capture detection." J. of Chromatography A, 976, 293-299.
5. Tomkins BA, Barnard AR (2002), "Determination of organochlorine pesticides in ground water using solid-phase microextraction followed by dual-column gas chromatography with electron-capture detection." J. of Chromatography A, 964, 21-33.
6. Hernandez F, Pitarch E, Beltran J, Lopez FJ (2000), "Headspace solid-phase microextraction in combination with gas chromatography and tandem mass spectrometry for the determination of organochlorine and organophosphorus pesticides in whole human blood.", J.of Chromatography B, 769, 65-77.
7. Lopez FJ, Pitarch E, Egea S, Beltran J, Hernandez F (2001), "Gas chromatographic determination of organochlorine and organophosphorus pesticides in human fluids using solid phase microextraction.", Anal. Chimica Acta, 433, 217-226.
8. Snow NH (2000), "Solid-phase microextraction of drugs from biological matrices.", J. of Chromatography A, 885, 445-455.
9. Kumazawa T, Suzuki O (2000), "Separation methods for amino group-possessing pesticides in biological samples." J. of Chromatography B, 747, 241-254.
10. Theodoris G, Koster EHM, Jong GJ (2000), "Solid-phase microextraction for the analysis of biological samples." J. of Chromatography B, 745, 49-82.
11. Navalon A, Prieto A, Araujo L, Vilchez JL (2002), "Determination of oxadiazon residues by headspace solid-phase microextraction and gas chromatography-mass spectrometry." J. of Chromatography A, 946, 239-245.
12. Hernandez F, Beltran J, Lopez FJ, Gaspar JV (2000), "Use of solid-phase microextraction for the quantitative determination of herbicides in soil and water samples." Anal. Chem. 72, 2313-2322.
13. Zambonin CG, Palmisano F (2000), "Determination of triazines in soil leachates by solid-phase microextraction coupled to gas chromatography-mass spectrometry." J. of Chromatography A, 874, 247-255
14. Baciocchi R, Attina M, Lombardi G, boni MK (2001), "Fast determination of phenols in contaminated soils." J. of Chromatography A, 911, 135-141.
15. Bouaid A, Ramos L, Gonzalez MJ, Fernandez P, Camara C (2001), "Solid-phase microextraction method for the determination of atrazine and four organophosphorus pesticides in soil samples by gas chromatography." J. of Chromatography A, 939, 13-21.
16. Eisert R, Jackson S, Krotzky A (2001), "Application of on-site solid-phase microextraction in aquatic dissipation studies of profoxydim in rice." J. of Chromatography A, 909, 29-36.
17. Fidalgo N, Centineo G, Blanco E (2003), "Solid-phase microcextraction as a clean-up and preconcentration procedure for organochlorine pesticides determination in fish tissue by gas chromatography with electron capture detection." J. of Chromatography A, 1017, 35-44.
18. Simplicio AL, Boas LV (1999), " Validation of a solid-phase microextraction method for the determination of organophosphorus pesticides in fruits and fruit juice." J. of Chromatography A, 833, 35-42.
19. Lamprodon DA, Albanis TA (2002), "Headspace solid-phase microextraction applied to the analysis of organophosphorus insecticides in strawberry and cherry juices." J. of Agricultural and Food Chemistry, 50, 3359-3365.
20. Matich AJ, Rowan DD, Banks NH (1996), "Solid-phase microextraction for quantitative headspace sampling of apple volatiles." Anal. Chem. 68, 4114-4118.

21. Holt Ru (2001), "Mechanisms Effecting analysis of volatile flavour components by solid-phase microextraction and gas chromatography." J. of Chromatography A, 937, 107-114.
22. Mestres M, Busto O, Guasch J (1998), "Headspace solid-phase microextraction analysis of volatile sulphides and disulphides in wine aroma." J. of Chromatography A, 808, 211-218.
23. Song J, Gardner BD, Holland JF, Beaudry RM (1997), "Rapid analysis of volatile flavour compounds in apple fruit using SPME and GC/Time-of-Flight Mass Spectrometry." J. of Agricultural and Food Chemistry, 45, 1801-1807.
24. Song J, Fan L, Beaudry RM (1998), "Application of solid-phase microextraction and Gas Chromatography/Time-of-Flight Mass Spectrometry for rapid analysis of Flavour volatiles in tomato and strawberry fruits." J. of Agricultural and Food Chemistry, 46, 3721-3726.
25. Beltan J, Peruga A, Pitarch E, Lopez FJ (2003), " Application of solid-phase microextraction for the determination of pyrethroid residues in vegetable samples by GC-MS." Anal. Bioanal. Chem. 376, 502-511.
26. Fernandez M, Padron C, Marconi L, Ghini S, Colombo R, Sabatini AG, Girotti S (2001), "Determination of organophosphorus pesticides in honeybees after solid-phase microextraction.", J. of Chromatography A, 922, 257-265.
27. Sen NP, Seaman SW, Page BD (1997), "Rapid semi-quantitative estimation of N-nitrosodibutylamine and N-nitrosodibenzylamine in smoked hams by solid-phase microextraction followed by gas chromatography thermal energy analysis." J. of Chromatography A, 788, 131-140.
28. Otero RR, Ruiz CY, Grande BC, Gandara JS (2002), "Solid-phase microextraction-gas chromatographic-mass spectrometric method for the determination of the fungicides cyprodinil and fludioxonil in white wines." J. of Chromatography A, 942, 41-52.
29. Zambonin CG, Cilenti A, Palmisano F (2002), " Solid-phase microextraction and gas chromatography-mass spectrometry for the rapid screening of triazole residues in wine and strawberries." J. of Chromatography A, 967, 255-260.
30. Michelle LR, Jennifer SB (2001), " Analysis of fine ant pesticides in water by solid-phase microextraction and gas chromatography/mass spectrometry of high-performance liquid chromatography/mass spectrometry." Analytical Chimica Acta, 436, 11-20.

9

ANALISIS TOLUENA RESIDU DALAM PEMBUNGKUS MAKANAN DENGAN KAEDAH PENGEKSTRAKAN RUANG KEPALA KROMATOGRAFI GAS

Lim Ying Chin[1] dan Mohd Marsin Sanagi[2]

[1]*INTEC, Universiti Teknologi MARA Section 17 Campus, 40200 Shah Alam, Selangor.*
[2]*Department of Chemistry, Faculty of Science, Universiti Teknologi Malaysia, 81310 Skudai, Johor.*
e-mail: [1]*limyi613@salam.uitm.edu.my;* [2]*marsin@kimia.fs.utm.my*

Abstrak

Bahan polimer banyak digunakan sebagai bahan pembungkusan makanan. Toluena residu yang tertinggal di dalam bahan pembungkusan boleh meresap masuk ke dalam makanan yang dibungkus dan seterusnya menjejaskan kualiti makanan. Dalam kajian ini, penganalisisan ruang kepala yang manual telah berjaya direkabentuk dan dibangunkan. Penentuan kepekatan toluena residu dilakukan dengan kaedah penambahan piawai dan kaedah pengekstrakan ruang kepala berbilang ,MHE) menggunakan kromatografi gas-pengesan pengionan nyala ,GC-FID. Pengenalpastian toluena dilakukan dengan perbandingan masa penahanan toluena piawai dan GC-MS. Kajian mendapati suhu pemanasan yang paling sesuai ialah 180 ^{o}C dengan masa optimum ialah 10 minit. Kajian juga menunjukkan sampel berbilang warna mempunyai kepekatan toluena residu yang lebih tinggi berbanding sampel satu warna. Sampel yang dianalisis dengan kaedah penambahan piawai didapati mempunyai kepekatan toluena residu yang lebih tinggi berbanding dengan kaedah MHE. Walau bagaimanapun, perbandingan dengan kepekatan toluena residu yang diperoleh daripada makmal De'Paris, Perancis mendapati bahawa sampel berkepekatan rendah yang dianalisis dengan kaedah MHE mempunyai peratus ketepatan yang tinggi. Sementara itu, sampel berkepekatan tinggi pula mempunyai peratus ketepatan yang rendah disebabkan oleh ralat bersistem. Perbandingan kaedah penentuan toluena mendapati kaedah MHE adalah lebih presis berbanding dengan kaedah penambahan piawai.

Abstract

Polymeric materials are used in many food contact applications as packaging material. The presence of residual toluene in this food packaging material can migrate into food and thus affect the quality of food. In this study, a manual headspace analysis was successfully designed and developed. The determination of residual toluene was carried out with standard addition method and multiple headspace extraction ,MHE) method using gas chromatography-flame ionization detector ,GC-FID). Identification of toluene was performed by comparison of its retention time with standard toluene and GC-MS. It was found that the suitable heating temperature was 180 ^{o}C with an optimum heating time of 10 minutes. The study also found that the concentration of residual toluene in multicolored sample was higher compared to monocolored sample whereas residual toluene in sample analyzed using standard addition method was higher compared to MHE method. However, comparison with the results obtained from De'Paris laboratory, France found that MHE method gave higher accuracy for sample with low analyte concentration. On the other hand, lower accuracy was obtained for sample with high concentration of residual toluene due to systematic errors. Comparison between determination methods showed that MHE method is more precise compared to standard addition method.

Pengenalan

Pembungkusan merupakan suatu proses yang tersusun untuk menyediakan barangan bagi tujuan pengangkutan, pengedaran, penyimpanan, pemasaran dan penggunaan akhir [1]. Kini, bahan pembungkusan bertindak sebagai alat komunikasi untuk membolehkan pengguna mengenalpasti produk atau jenama yang baru, mengetahui kandungan nutrient yang hadir dan dalam sesetengah kes, bahan pembungkus memberi maklumat tentang cara penyediaan makanan tersebut [2]. Pembungkus fleksibel seperti lamina mengandungi beberapa lapisan filem dan pelarut toluena biasanya digunakan dalam percetakan grafik pada filem ini [3-5].

Perhatian perlu diberikan kepada bahan pembungkus apabila terdapat kemungkinan berlakunya keracunan makanan yang disebabkan oleh resapan bahan pencemar ke dalam makanan semasa penyimpanan makanan. Peresapan bahan ini mempunyai kesan dari segi kualiti dan ketoksikan makanan [6]. Ia mungkin mempunyai bau

dan boleh memberi kesan kepada rasa makanan. Keadaan sebaliknya seperti penyerapan rasa makanan oleh pembungkus juga boleh mengurangkan intensiti rasa makanan dan aroma makanan [7]. Bahan pencemar dalam pembungkus makanan bukan sahaja menjejaskan kualiti makanan malahan ia mungkin membawa kesan negatif ke atas kesihatan pengguna sekiranya kepekatan bahan pencemar melebihi had kepekatan yang dibenarkan.

Kajian ini melibatkan perekabentukan dan pengubahsuaian penganalisisan ruang kepala yang manual. Dalam kajian ini, suhu dan masa pemanasan dioptimumkan dan seterusnya kuantiti toluena residu akan ditentukan menggunakan kaedah penambahan piawai dan kaedah pengekstrakan ruang kepala berbilang ,MHE) menggunakan kromatografi gas-pengesan pengionan nyala ,GC-FID). Perbandingan kepekatan toluena turut dilakukan di antara sampel satu warna dan berbilang warna dalam 6 jenis pembungkus makanan.

Eksperimen

Reagen

Larutan piawai toluena ,99 %) daripada keluaran J. T. Baker, Phillipsburg, USA. Heksana ,95 %) gred GC diperoleh daripada Fisher Scientific, New Jersey, USA. Hidrokarbon piawai, nonana ,C_9H_{20}) adalah gred analar daripada jenama BDH, England. Gas helium pula dibekalkan oleh Syarikat MOX, Pasir Gudang, Johor.

Alat radas

Vial jenis ruang kepala dengan bukaan luas bersaiz 10 mL ,22.5 mm × 46 mm) dan 2 mL ,12 mm × 32 mm) daripada Supelco, Bellefonte, PA, USA. Penutup pembebasan tekanan jenis aluminium yang mempunyai septum dengan pelapis jenis silikon / PTFE yang bersaiz 20 mm dan penutup yang mempunyai septum teflon ,11 mm) juga daripada Supelco, Bellefonte, PA, USA. Penyuntik jenis kedap udara dengan saiz 100 µL keluaran Hamilton, Reno, Nevada, USA. Penyuntik kedap udara yang bersaiz 1 mL pula daripada SGE, Australia. *Crimper* tangan yang dapat dilaraskan bukaan saiznya jenis 20 mm dan *decapper* tangan jenis 20 mm yang digunakan untuk membuka penutup vial ruang kepala pula adalah keluaran Kimble Glass Inc, Vineland, NJ, USA.

Instrumentasi

Analisis toluena residu dijalankan dengan menggunakan kromatografi gas Hewlett Packard model 6890 GC dengan pengesan pengionan nyala ,FID). Turus pemisahan yang digunakan ialah turus rerambut Ultra 1 ,dimetilpolisiloksana) keluaran Hewlett Packard, USA. Turus yang berukuran 30 m ini berdiameter 0.25 mm dengan ketebalan filem 0.17 µm. Dalam kajian ini, helium digunakan sebagai gas pembawa pada kadar alir 2 mL/min. Suhu liang suntikan pada 150°C dan suhu pengesan ialah 250°C. Suhu GC isoterma digunakan pada 150 ^{o}C dan masa analisis yang diperlukan adalah 5 minit. Gas ruang kepala ,1 mL) disuntik dengan menggunakan mod suntikan berpecah 1:10.

Pensampelan

Enam jenis pembungkus yang digunakan dalam kajian ini iaitu sampel TE, CCB, MCP, PM, TC dan PDC disumbangkan oleh Kilang BBM Sdn. Bhd., Tampoi, Johor. Sampel diletakkan bersama untuk membentuk blok yang padat. Blok sampel yang padat ini dibungkus ketat dengan kerajang aluminium yang mempunyai ketebalan 30 - 40 µm. Nisbah di antara luas spesimen ,dalam cm^2) terhadap isipadu vial ,dalam mL) ditetapkan pada 5. Sebanyak 15-20 kepingan sampel dikeluarkan daripada "blok" sampel tanpa memisahkannya. Setelah mengeluarkan sekurang-kurangnya satu lapisan kepingan sampel daripada bahagian atas blok sampel, kepingan sampel yang seterusnya diambil dan spesimen dipotong menggunakan templat. Spesimen itu digulung dan dimasukkan ke dalam vial dengan segera. Selepas itu, vial ditutup dengan cepat menggunakan *crimper* tangan.

Prosedur

Dalam kajian ini, dua kaedah digunakan dalam penentuan kuantitatif toluena residu iaitu kaedah penambahn piawai dan kaedah MHE. Kedua-dua kaedah ini merupakan kaedah piawai seperti yang tercatat dalam EN 261 WI 190 [8]. Dalam pengoptimuman parameter dalam pengekstrakan ruang kepala,

suhu penyuntik kedap udara ditetapkan pada 100 ^{o}C dan suhu pemanasan vial yang mengandungi sampel ditetapkan pada 180 ^{o}C. Sampel dipotong, dimasukkan ke dalam vial dan ditutup dengan segera. Botol sampel bersama dengan sampel dipanaskan pada 180 ^{o}C selama 2, 5, 10, 15 dan 20 minit ± 10 saat. Dalam pengoptimuman suhu pemanasan, botol sampel bersama dengan sampel dipanaskan pada 100,120, 140, 160 dan 180 ^{o}C berdasarkan masa pengoptimuman yang diperoleh. Gas ruang kepala disuntik dan dianalisis dengan GC-FID.

Kaedah penambahan piawai

Dalam kaedah penambahan piawai, sebanyak 5 vial disediakan. Spesimen yang disediakan ,10 cm × 5 cm) digulung dan dimasukkan ke dalam vial 10 mL. Vial ditutup dengan segera. Jisim vial bersama sampel ditimbang. Seterusnya, larutan piawai dengan isipadu yang meningkat ,0-4 µL) disuntik ke dalam vial yang telah tertutup melalui septum.Setiap vial ditimbang untuk mendapatkan jisim larutan piawai yang telah ditambah. Semua vial dipanaskan pada suhu 180 ^{o}C selama 10 minit secara berterusan. Analit dalam fasa gas itu ,1 mL) kemudian disuntik ke dalam GC-FID menggunakan penyuntik yang telah dipanaskan pada suhu 100 ^{o}C.

Kaedah pengekstrakan ruang kepala berbilang (MHE)

Kaedah MHE yang digunakan adalah secara piawai dalaman. Kaedah ini melibatkan 2 bahagian iaitu penentuan faktor gerak balas dan seterusnya penentuan toluena residu dalam sampel [8]. Dalam penentuan faktor gerak balas*,* vial 10 mL yang tertutup ditimbang. Sebanyak 1 µL larutan piawai toluena disuntik ke dalam vial yang tertutup dan kemudian vial ditimbang sekali lagi untuk mendapatkan jisim 1 µL larutan toluena. Kemudian, 1 µL larutan nonana ,piawai dalaman) disuntik ke dalam vial menggunakan penyuntik yang berbeza. Sekali lagi, vial ditimbang untuk mendapatkan jisim nonana. Vial dipanaskan pada suhu 180 ^{o}C selama 10 minit. Analit dalam fasa gas disuntik ke dalam GC-FID dengan menggunakan penyuntik kedap udara 1 mL yang telah dipanaskan pada 100 ^{o}C terlebih dahulu. Dalam penentuan toluena residu dalam sample, vial yang mengandungi spesimen ujian ditimbang. Kemudian, 1 µL larutan nonana disuntik ke dalam vial menerusi septum menggunakan penyuntik dan vial ditimbang semula untuk mendapatkan jisim larutan nonana yang disuntik. Vial dipanaskan pada suhu 180°C selama 10 minit. Analit, 1 mL) dalam fasa gas disuntik ke dalam GC-FID dengan menggunakan penyuntik kedap udara 1 mL yang telah dipanaskan pada 100 ^{o}C terlebih dahulu. Vial yang masih panas kemudian melalui proses pembebasan tekanan. Dalam proses ini, satu jarum yang telah disambung ke sumber gas helium dimasukkan ke vial melalui septum vial dan satu lagi jarum terus dicucuk ke dalam vial. Gas helium dialirkan pada kadar alir 15 mL/minit selama 1 minit ± 10 saat. Selepas itu, kedua-dua jarum dikeluarkan daripada vial dan vial dimasukkan semula ke dalam ketuhar. Untuk pengekstrakan kali kedua dan seterusnya, langkah pemanasan vial, analisis GC dan proses pembebasan tekanan diulang untuk vial yang sama sebanyak 4 kali.

Keputusan dan perbincangan

Pengoptimuman masa pengekstrakan

Keseimbangan yang berdasarkan partisi toluena dalam fasa pepejal dan fasa gas dalam vial tertutup amat diperlukan dalam teknik analisis ruang kepala [9]. Daripada Rajah 1 yang ditunjukkan, didapati luas puncak toluena tidak memberikan perbezaan yang ketara pada masa pemanasan 2 minit dan 5 minit. Ini disebabkan kedua-dua tempoh masa ini terlalu singkat untuk toluena mencapai keseimbangan antara fasa gas dan fasa pepejal dalam vial tertutup.
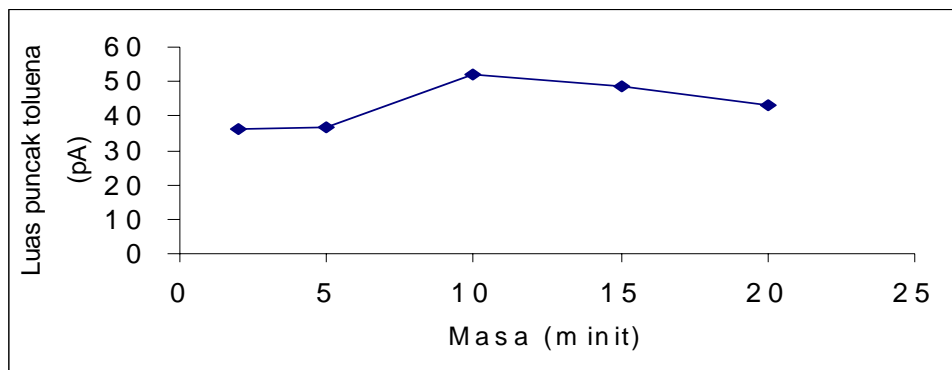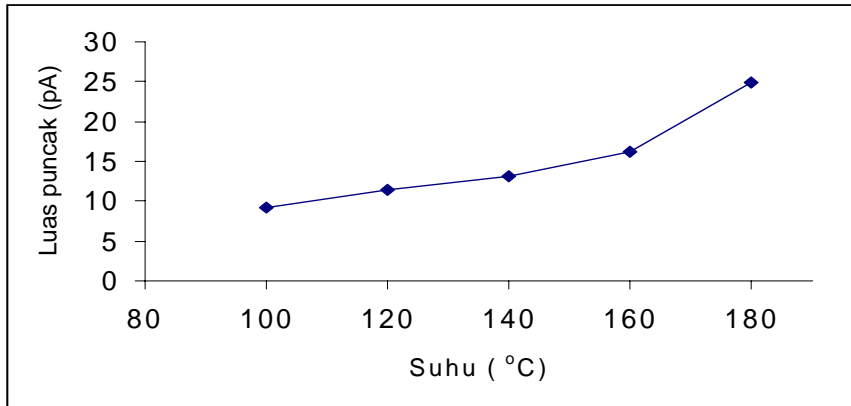

Rajah 1: Luas puncak melawan masa pemanasan (minit) bagi toluena

Sebaliknya, masa pemanasan selama 10 minit merupakan masa pengestrakan yang paling optimum. Ini menunjukkan keseimbangan toluena antara fasa gas dan fasa pepejal telah tercapai. Daripada Rajah 1 juga, didapati masa pemanasan yang lebih lama iaitu selama 15 minit dan 20 minit memberikan luas puncak toluena yang semakin menurun. Dalam erti kata yang lain, masa pemanasan yang lama akan mengganggu keseimbangan

fasa toluena dalam vial. Dengan ini, masa pemanasan selama 10 minit dipilih sebagai masa pemanasan yang paling optimum.

Pengoptimuman suhu pengestrakan
Daripada Rajah 2, ia jelas menunjukkan luas puncak bagi toluena adalah berkadar langsung dengan suhu pemanasan iaitu semakin tinggi suhu pemanasan yang digunakan, semakin tinggi luas puncak toluena yang diperoleh. Ini menunjukkan suhu 180°C merupakan suhu yang paling sesuai.


Rajah 2: Luas puncak melawan suhu pemanasan bagi toluena

Suhu pengekstrakan melebihi 180 ^{o}C tidak digunakan disebabkan kekangan penganalisian ruang kepala. Septum pada tudung aluminium mungkin akan lebur pada suhu yang terlalu tinggi. Selain itu, pemegangan vial yang telah dipanaskan pada suhu yang tinggi, contohnya 200 ^{o}C adalah sukar walaupun sarung tangan digunakan. Dengan ini, suhu 180 ^{o}C dipilih sebagai suhu pengesktrakan yang paling sesuai dan digunakan dalam analisis ruang kepala dalam kajian seterusnya.

Pengenalpastian sebatian toluene secara masa penahanan dan GC-MS
Dalam kajian ini, masa penahanan toluena adalah 2.653 minit dan ia hampir sama dengan masa penahanan toluena piawai, (Rajah 3).
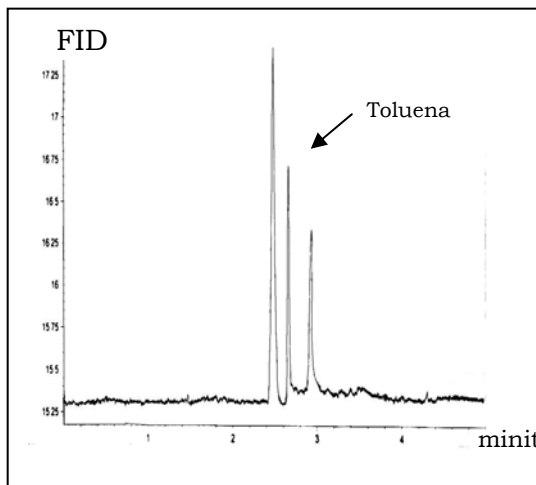
Rajah 3: Pemisahan GC bagi sebatian toluena dalam sampel
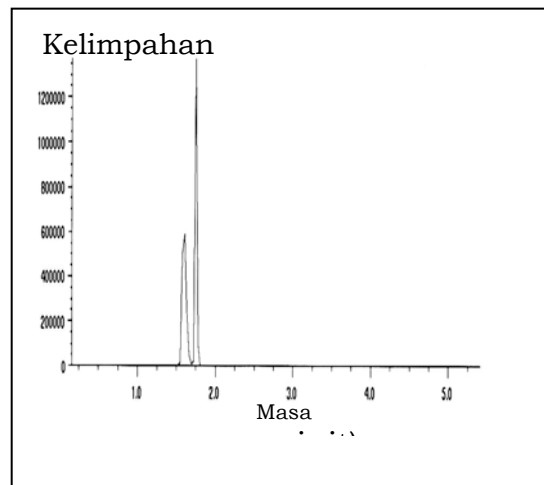
Rajah 4: Kromatogafi ion

Analisis GC-MS telah dilakukan untuk mengenalpasti puncak toluena dan puncak sampingan yang terhasil apabila penyuntik dipanaskan. Kromatografi ion jumlah seperti yang ditunjukkan dalam Rajah 4 menunjukkan kehadiran 2 puncak dengan tertib pengelusian yang sama. Puncak 2 dapat dikenalpasti sebagai puncak toluena.

Perbandingan spektrum jisim toluena dengan spektum jisim toluena daripada pangkalan data Wiley memberika kebarangkalian yang melebihi 90 %.

Perbandingan kepekatan toluena residu antara kaedah penambahan piawai dan kaedah MHE
Perbandingan kepekatan toleuan residu antara kaedah penambahan piawai dan kaedah MHE hanya dapat dilakukan ke atas 3 jenis sampel sahaja iaitu sampel TC, PM dan MCM. Perbandingan ke atas sampel CCB, TE dan PDC tidak dapat dilakukan disebabkan kehabisan sampel dari kelompok sampel yang sama untuk dianalisis dengan kaedah MHE. Jadual 1 jelas menunjukkan kepekatan toluena residu yang ditentukan melalui kaedah penambahan piawai adalah lebih tinggi berbanding dengan kaedah MHE. Ini mungkin disebabkan anggaran kuantiti toluena residu dalam sampel perlu dibuat sebelum analisis sampel sebenar dilakukan menggunakan kaedah penambahan piawai. Dengan erti kata lain, anggaran toluena residu mempengaruhi keputusan analisis.

Jadual 1: Perbandingan kepekatan toluena residu antara kaedah penambahan piawai dan kaedah MHE

Sampel	Kepekatan toluena ,mg/m^2)			
	Kaedah penambahan piawai		Kaedah MHE	
	satu warna	berbilang warna	Satu warna	berbilang warna
TC	15.55 ± 2.16	18.33 ± 1.14	5.09 ± 0.27	7.21 ± 0.18
PM	10.78 ± 1.57	16.82 ± 1.02	2.81 ± 0.17	4.53 ± 0.13
MCM	8.32 ± 1.12	12.09 ± 1.09	4.19 ± 0.15	5.89 ± 0.15

Ujian awal mendapati anggaran kepekatan toluena residu adalah sekitar 8 mg/m^2. Oleh itu, kepekatan toluena residu yang ditentukan melalui kaedah penambahan piawai adalah lebih tinggi nilainya. Sebaliknya, anggaran sebegini tidak perlu dilakukan dalam kaedah MHE. Analisis toluena residu dilakukan secara terus secara pengekstrakan berterusan dalam kaedah MHE.

Perbandingan kepekatan toluena residu antara makmal
Dalam kajian ini, perbandingan kepekatan toluena residu telah dilakukan di antara makmal disebabkan kesukaran untuk mendapatkan bahan rujukan piawai bagi sampel bahan pembungkusan. Perbandingan keputusan analisis antara makmal dilakukan bertujuan untuk mengatasi ketakpastian kaedah dan seterusnya meningkatkan kebolehpercayaan hasil analisis. Bagi sampel TC, PM dan MCM, perbandingan kepekatan toluena residu telah dilakukan di antara makmal UTM dan makmal Dannone, Paris seperti yang ditunjukkan dalam Jadual 2 [10].

Jadual 2: Perbandingan kepekatan toluena residu antara makmal

Sampel	Makmal UTM		Makmal Dannone, Paris	Peratus ketepatan ,%)	
	Kaedah MHE	Kaedah penambahan piawai		Kaedah MHE	Kaedah penambahan piawai
TC 1	7.2114	18.3280	6.2	116.31	295.61
TC 2	5.0876	15.5480	6.2	82.06	250.77
PM 1	4.5293	16.8200	10.7	42.33	157.20
PM 2	2.8100	10.7766	10.7	26.26	100.72
MCM 1	5.8890	12.0946	11.1	53.05	108.96
MCM 2	4.1859	8.3186	11.1	37.71	74.94

Daripada Jadual 2 yang ditunjukkan, dapat diperhatikan bahawa kepekatan toluena residu dalam sampel TC yang dianalisis dengan kaedah MHE mempunyai peratus ketepatan yang baik iaitu sekitar 82.06% hingga 116.31% berbanding dengan kaedah penambahan piawai. Sebaliknya, untuk sampel PM dan sampel MCM pula, kaedah penambahan piawai didapati mempunyai peratus ketepatan yang lebih baik iaitu di sekitar 74.94% hingga 157.20% berbanding dengan kaedah MHE. Corak peratus ketepatan yang dapat diperhatikan ialah sampel dengan kepekatan toluena residu yang tinggi iaitu melebihi 10 mg/m^2 apabila dianalisis dengan kaedah penambahan piawai memberikan peratus ketepatan yang tinggi berbanding dengan kaedah MHE. Keadaan sebaliknya diperhatikan untuk sampel dengan kepekatan toluena residu yang rendah iaitu kurang daripada 10 mg/m$^{2.}$ disebabkan nilai anggaran kepekatan toluena residu dalam sampel yang dianalisis dengan kaedah penambahan piawai ditetapkan pada nilai kepekatan yang agak tinggi iaitu 8 mg/m^2.

Perbandingan kaedah penentuan toluena residu

Perbandingan kaedah dilakukan bertujuan untuk menguji sama ada kaedah MHE dan kaedah penambahan piawai berbeza dari segi kejituan iaitu sama ada perbezaan dua sisihan piawai bererti.

Jadual 3 : F_{kiraan} bagi sampel TC, PM dan MCM

Kaedah Sampel	Penambahan piawai MHE
TC 1	41.1555
TC 2	62.0135
PM 1	58.4552
PM 2	84.0046
MCM 1	50.3499
MCM 2	59.6905

*Daripada jadual F, $F_{2,2} = 39.00$

Daripada Jadual 3, dapat diperhatikan bahawa F_{kiraan} bagi semua sampel adalah lebih besar daripada F_{jadual}. Ini menunjukkan terdapat perbezaan bererti antara sisihan piawai kaedah MHE dan kaedah penambahan piawai pada aras 5 %. Oleh kerana varians kaedah penambahan piawai lebih besar daripada varians kaedah MHE pada 5 % aras kebarangkalian, maka dapat disimpulkan bahawa kaedah MHE adalah lebih presis dalam penentuan toluena residu dalam sampel.

Kesimpulan

Dalam kajian ini, kaedah pengekstrakan ruang kepala menggunakan analisis GC-FID dapat diaplikasikan dalam analisis toluena residu. Toluena terelusi dalam masa kurang daripada 3 minit. Didapati masa pemanasan yang paling optimum adalah 10 minit sementara suhu pemanasan yang paling sesuai pula ialah 180 ^{o}C. Kajian yang dilakukan menunjukkan bahagian berbilang warna dalam sampel pembungkus yang dianalisis dengan kaedah penambahan piawai mahupun kaedah MHE memberikan kepekatan toluena yang lebih tinggi berbanding dengan bahagian satu warna. Bagi sampel dengan kepekatan toluena residu yang rendah ,kurang daripada 10 mg/m^2), analisis toluena residu menggunakan kaedah MHE mempunyai peratus ketepatan yang baik iaitu sekitar 82.1% hingga 116.3%. Sebaliknya, untuk sampel sampel dengan kepekatan toluena residu yang tinggi ,melebihi 10 mg/m^2), peratus ketepatan yang rendah diperoleh iaitu di antara 26.3% hingga 53.1%. Ujian F yang digunakan dalam perbandingan kaedah penentuan toluena residu menunjukkan kaedah MHE adalah lebih presis dalam penentuan toluena residu dalam sampel.

Rujukan
1. Paine, F. A. 1990. The packaging user's handbook. London: Blackie and Son Ltd. 4-7.
2. Marsihi, R. 1993. Testing packaging material : why and how. Weeks Publishing Company.
3. Oswin, C. R. 1975. Plastic films and packaging. London: Applied Science Publishers Ltd.: 20-21.
4. Aurela, B, Ohra-aho, T and Soderhjelm, L. 2001. Migration of alkilbenzenes from packaging into food and tenax. *Packag. Technol. Sci*. 14: 71-77.
5. Wenzl, T and Lankmayr, E. P. 2000. Reduction of adsorption phenomena of volatile aldehydes and aromatic compounds for static headspace analysis of cellulose based packaging materials. *J. Chromatogr. A*. 897: 269-277.
6. Hotchkiss, J. H. 1988. Food and packaging interactions. Washington, D. C.: American Chemical Society:. 1-9.
7. Vermeiren, L., Devlieghere, F., Beest, M. V., Kruijf, N. and Debevere, J. 1999. Developments in the active packaging of foods. *Trends in Food Sci & Technol*. 10: 77-86.
8. European Committee for Standardization. 1998. Flexible packaging material determination of residual solvents by static headspace gas chromatography - Part 2: industrial methods. EN 261 WI 190:.1-16.
9. Grob, R. L. 1995. Modern practice of gas chromatography. 3rd Ed. New York: JohnWiley and Son Inc. 815-816.
10. Janiah Ibrahim 2002. Komunikasi persendirian, Kilang BBM Sdn. Bhd. Tampoi, Johor.

DETERMINATION OF POLYCYCLIC AROMATIC HYDROCARBONS IN PALM OIL MILL EFFLUENT BY SOXHLET EXTRACTION AND GAS CHROMATOGRAPHY-FLAME IONIZATION DETECTION

Nor Fairolzukry Ahmad Rasdy, M. Marsin Sanagi,* Wan Aini Wan Ibrahim, Ahmedy Abu Naim

Department of Chemistry, Faculty of Science, Universiti Teknologi Malaysia
81310 UTM Skudai, Johor, Malaysia
*E-mail: marsin@kimia.fs.utm.my

Abstract

A method has been developed for the determination of polycyclic aromatic hydrocarbons (PAHs) from palm oil mill effluent based on gas chromatography-flame ionization detection. Extraction of spiked PAHs (napthalene, fluorene phenanthrene, fluoranthene and pyrene) in palm oil waste was carried out by Soxhlet extraction using hexane-dichloromethane (60:40 v/v) as the solvent. Excellent separations were achieved using temperature programmed GC on Ultra-1 fused-silica capillary column (30 m × 250 μm ID), carrier gas helium at a flow rate of 1 mL/min.

Introduction

Polycyclic aromatic hydrocarbons (PAHs) are a class of diverse organic compounds containing two or more fused aromatic rings of the carbon and hydrocarbon atoms. They are ubiquitous pollutants formed from the combustion of fossil fuels and are always found as a mixture of individual compounds. PAHs as one of the typical persistent organic compounds (POPs) featured in regional and global cycling. PAHs are emitted mainly into the atmosphere and have been detected at long distances from their source. Because of their low vapor pressures, compounds with five or more aromatic rings exist mainly adsorbed to airborne particulate matter, such as fly ash and soot [1].

The analysis of these PAHs is of great interest because of their toxicity and persistence in the environment. PAHs are adsorbed strongly to the organic fraction of sediments and soils [2]. Therefore, it can be concluded that sediments and soils are usually considered as the main sinks for PAHs in the environment. Polycyclic aromatic hydrocarbons (PAHs) are reported to have mutagenic and/or carcinogenic effects. The ability of PAHs to induce cancer has been documented by epidemiological studies of worker in coal tar, creosote, coal gas, coke, and cutting oil industries [1]. Some analogues of these compounds, such as polycyclic aromatic sulfur heterocycles (PASHs), are also potentially mutagenic and carcinogenic. But, although they have a high bioaccumulation and have been found in some water and sediment samples, they have not been studied as extensively as PAHs.
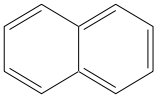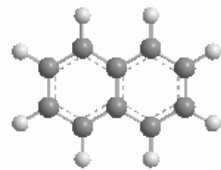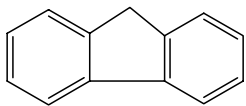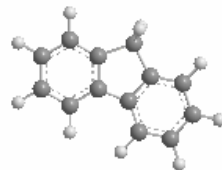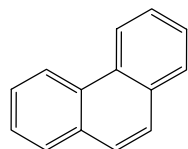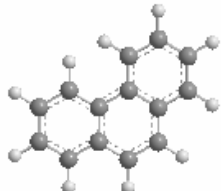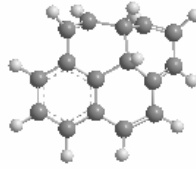
PAHs are routinely analyzed by one-dimensional capillary gas chromatography (GC). Normally, high-resolution mass spectrometry can detect the PAHs in sample [3]. This study will discuss more about analysis of PAHs using one-dimensional gas chromatography-flame ionization detection (GC-FID). This is significant for screening PAHs present in environmental sample before further analysis.

Experimental

Reagents

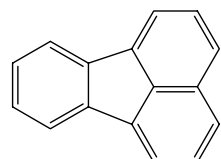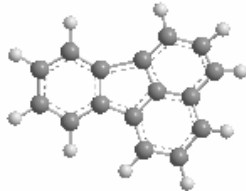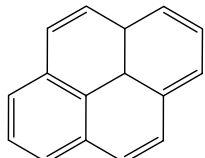Methanol was obtained from HyperSolv, BDH Laboratory, (England). Acetonitrile, dichloromethane, hexane (all in HPLC grade) were supplied by Fisher Chemicals (USA). The polycyclic aromatic hydrocarbons (napthalene, fluorene, phenanthrene, fluoranthene and pyrene) were obtained from Fluka Chemika, Sigma-Aldrich Chemic, Steinheim, (Switzerland). The molecular weight and molecular structures of the PAHs are shown in Table 1. Double-distilled deionized water of at least 18 MΩ was purified by Nano ultra pure water system (Barnstead, USA).

Table 1: Properties of four polycyclic aromatic hydrocarbons (PAHs)

Compound	Formula Structure	Molecular Weight	3D Molecular Structure
Napthalene	$C_{10}H_8$	128	
Fluorene	$C_{13}H_{10}$	166	
Phenanthrene	$C_{14}H_{10}$	178	
Fluoranthene	$C_{16}H_{10}$	202	
Pyrene	$C_{16}H_{10}$	202	

Chromatographic conditions

The GC-FID system consist of a Hewlett Packard Model 6890GC gas chromatography (GC) equipped with a flame ionization detector (FID) and a data processor (USA). The gas chromatographic column used was Ultra-1 932530, a non-polar, fused-silica capillary column (30 m length × 250 μm inner diameter × 0.20 μm film thickness) (USA). Helium gas was used as the carrier gas at a flow rate of 1 mL/min at a pressure of 75 kpa. The injector temperature was set at 250°C and the detector temperature at 310°C. The temperature program used was; 2 minute s hold time at 250°C, a ramp to 130°C at 30°C/min followed by 3 minutes hold time, a ramp to 240°C at 7°C/min and a final ramp to 285°C at 12°C with an 8 minutes hold time.

Procedure

The mixture of standard solution was prepared from the 1000 ppm stock solution. The mixed standard solution was prepared to produce the calibration graph of each PAHs to determine the limit of detection. The prepared mixture solution (80, 60, 40, 20, 10 ppm) was injected in triplicate onto the column.

About 10 g of dried palm oil mill effluent sample, thoroughly mixed with anhydrous sodium sulphate (10 g) was Soxhlet extracted with dichloromethane (200 mL) for 6 hours. The solvent was concentrated to 5 mL in a rotary evaporator under reduced pressure. 0.5 M potassium hydroxide (100 mL) in methanol was added and the mixture was refluxed for 4 hours in a water bath at 80ºC. After cooling, deionized water (20 mL) was added and extraction was performed with hexane (3×50 mL). The combined organic extracts were dried over anhydrous sodium sulphate (0.5 g). The decanted extract was evaporated at 40ºC in a rotary evaporator under reduced pressure to near dryness, dissolved in isooctane (1 mL) for silica clean-up.

The glass column (1.2 cm I.D.) was slurry packed with silica gel (10 g) in dichloromethane and a top layer of anhydrous sodium sulphate (0.5 g). The column was rinsed with hexane (40 mL) before use. The extract was transferred on to the column and sequentially eluted with hexane (25 mL) and hexane-dichloromethane, 60:40 (30 mL) to give fractions enriched in alkanes and PAHs, respectively. The second eluate was evaporated under reduced pressure to near dryness and replaced with acetonitrile (1 mL) before injection can be made. After cleaning up the sample, 1 μL was injected into GC-FID column. The temperature program used was exactly same with the temperature used for standard solution described above. For detection, peaks interfere were compared to the standard and from peak area, recovery value was calculated for spiked sample.

Results and Discussion

PAHs peak was identified in the mixture standard solution based on their retention time. All of the PAHs were eluted within 25 minutes. Based on the chromatograms obtained (Figure 1), it was noted that the elution orders for the five PAHs on Ultra-1 column were strongly in order of increasing molecular weight. Napthalene (8.182 min) with the lowest molecular weight was first eluted across the column followed by fluorene (14.591 min), phenanthrene (17.917 min), fluoranthene (22.279 min) and pyrene (23.004 min). Even fluoranthene and pyrene with the same molecular weight value can be separated accordingly. The chromatograms were very clear with no interfering peaks appearing in the areas of interest.

In order to examine the sensitivity of gas chromatography system, the limits of detection for PAHs are investigated. Theoretical limits of detection (LOD) were determined taking the usual definition, which that gives a peak with a height three times the background noise level. The calibration graph obtained was used to determine the limit of detection (LOD). A linear calibration graph was produced for each standard PAHs with the correlation coefficient ranging between 0.9914-0.9989. The value of the correlation coefficient obtained for each calibration graph shows that the correlation between relative peak area and concentration is good. The calibration graph of naphthalene, fluorene, phenanthrene, fluoranthene and pyrene are shown in Figure 2. Table 2, given the regression equation, correlation coefficient and LOD for each PAHs.
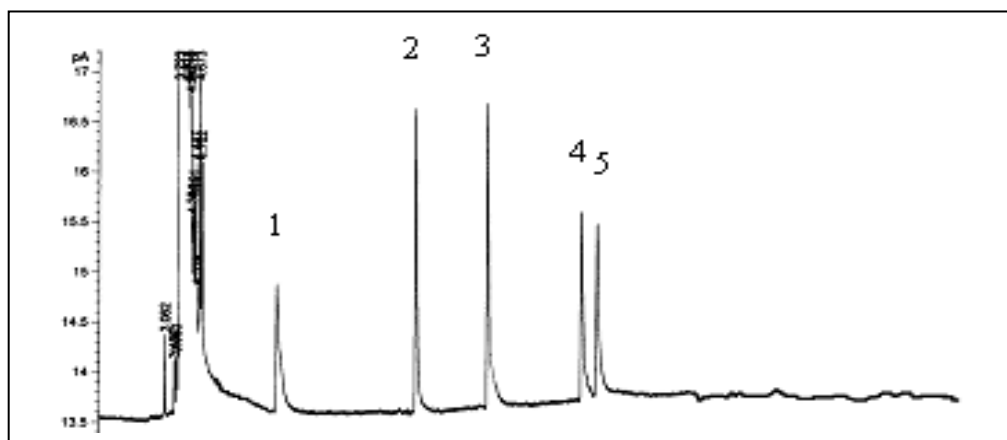

Figure 1: Chromatogram of PAHs study (100 ppm). Peaks identification: (1) naphthalene, (2) fluorene, (3) phenanthrene, (4) fluoranthene (5) pyrene

Table 2: Limit of detection, regression equations and correlation coefficient of PAHs studied using GC-FID

PAHs	Regression Equation	Correlation Coefficient, r^2	LOD in ppm (From calculation)	RSD (%) (n = 3)
Naphthalene	y = 0.6486x + 6.3900	0.9989	3 (2.83)	9.0
Fluorene	y = 1.1729x + 3.8878	0.9930	8 (7.22)	5.2
Phenanthrene	y = 0.9770x + 0.5149	0.9914	8 (7.28)	13.1
Fluoranthene	y = 0.6152x + 0.7479	0.9910	5 (4.30)	5.3
Pyrene	y = 0.6904x + 3.4882	0.9927	5 (4.33)	4.9

The silica gel column clean-up provided all PAHs in second fraction together with alkylbenzenes, but these monoaromatic hydrocarbons did not interfere with GC analysis. Hence the use of silica gel for clean-up extracts appeared more suitable for PAHs determination. Saponification also improved the determination of PAHs. Associations between minor PAHs and lipid palm oil waste fraction are reduced when the raw extract is submitted to a basic treatment, and liquid-liquid partitioning allows fatty acid removal and therefore, extract clean-up is made easier. After doing the clean-up using the same procedure, the sample (1 μL) was injected into the GC-FID injection port. According to their retention times, PAHs should be identifiable in the palm oil waste if they are present above the detection limits. However, in this work, none of them were identified, probably because they are non-existent or present in a concentration lower than the detectable limit (chromatogram not shown). The effectiveness of the method was assessed with the analysis of a palm oil waste spiked with PAHs. The chromatogram obtained (Figure 3) showed that all the peaks of analyte studied were well resolved but there were some peaks corresponding to other organic products present in sample observed but did not interfere with the PAHs peaks studied.

The concentration of spike sample was obtained from peak area value from calibration graph equation. The recovery percentage was then calculated by dividing with the standard spike value, which is 100 ppm. Table 3 gives the peak area value and concentration for each PAHs obtained. Recoveries of PAHs from palm oil waste sample ranged from 36.14 % to 67.57 % for Soxhlet extraction with silica gel clean-up (Figure 4). The chromatogram of spiked standard PAHs in palm oil waste is shown in Figure 4.

Table 3: Peak area, concentration and percentage recovery of PAHs studied using GC-FID

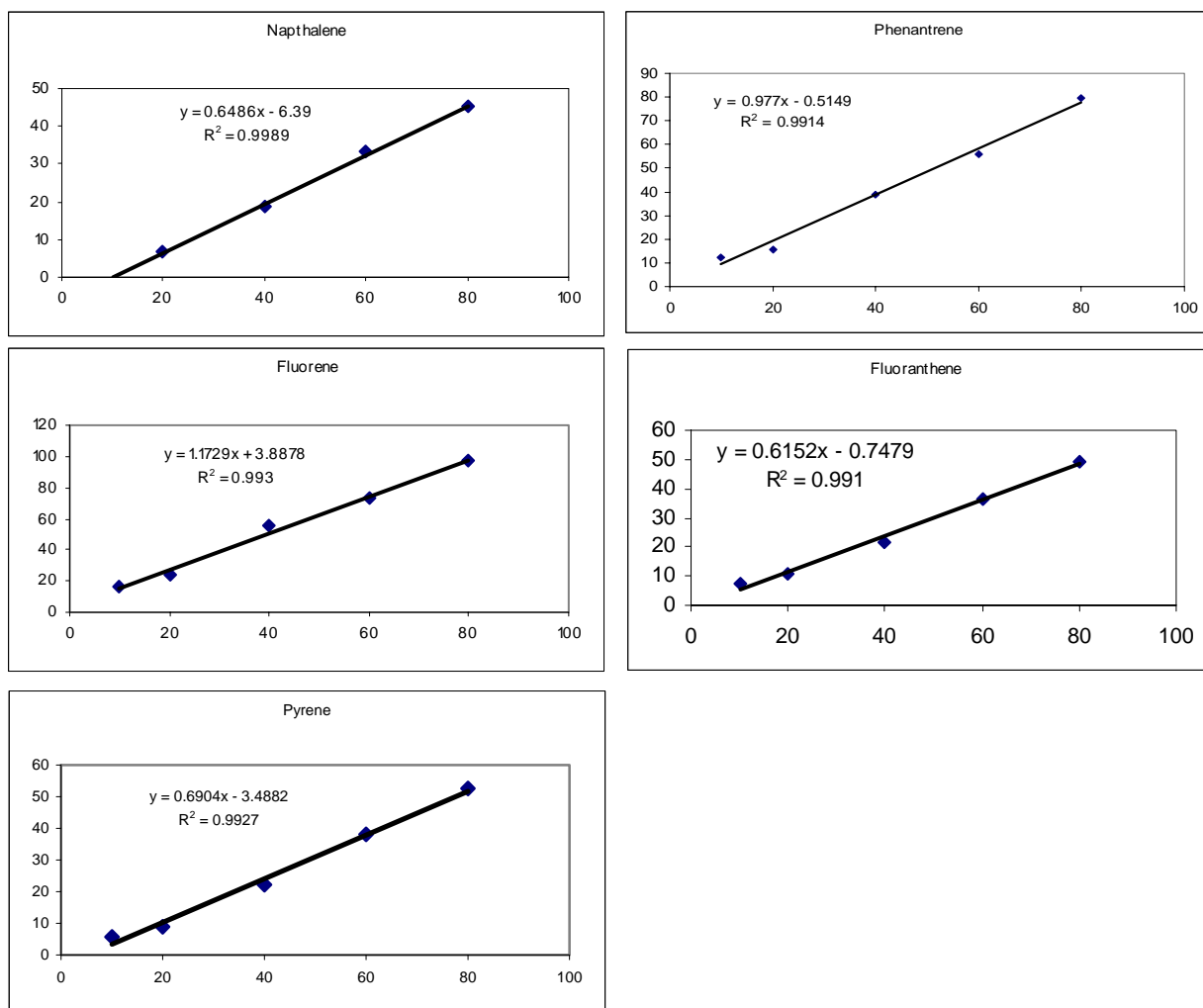| PAHs	Peak Area	Concentration (ppm)	% Recovery (RSD)
Naphthalene	17.050	36.14	36.14 (8.36)
Fluorene	53.583	42.37	42.37 (5.22)
Phenanthrene	37.216	38.62	38.62 (11.47)
Fluoranthene	31.734	52.80	52.80 (6.35)
Pyrene	43.162	67.57	67.57 (3.13)

Figure 2: Calibration graph of the five PAHs studied: naphthalene, fluorene, phenanthrene, fluoranthene and pyrene
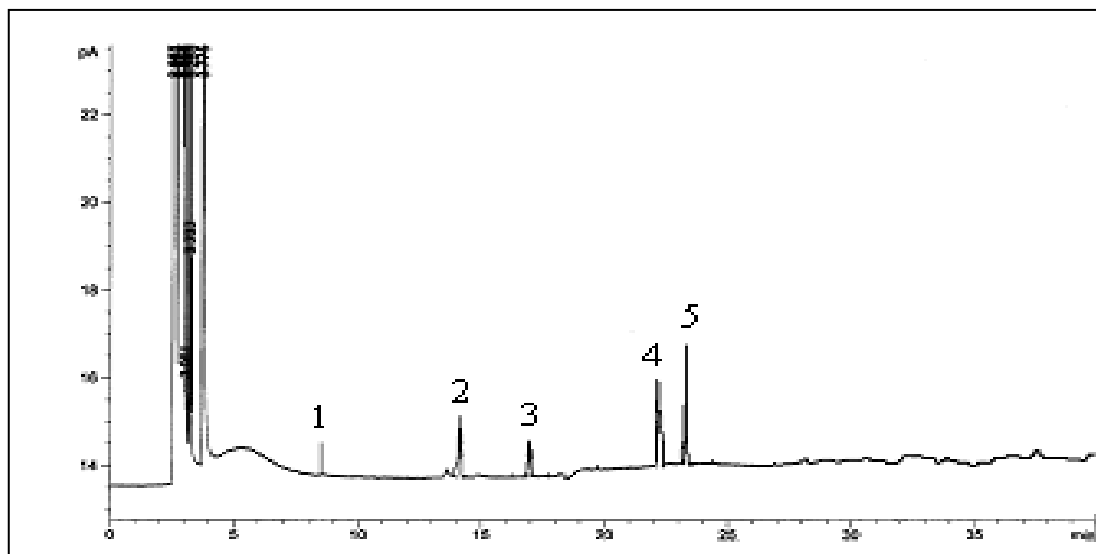

Figure 3. Chromatogram of standard PAHs (100 ppm) spiked in palm oil mill effluent using GC-FID after Soxhlet extraction. (1) naphthalene, (2) fluorene, (3) phenanthrene, (4) fluoranthene (5) pyrene
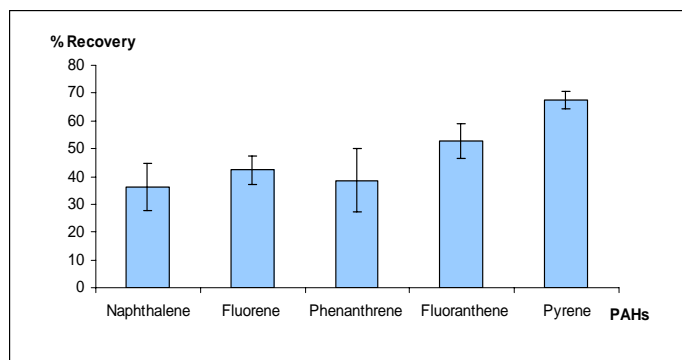
Figure 4. Percentage of extracted PAHs (100 ppm) in palm oil mill effluent after
Soxhlet extraction and GC-FID analysis

Conclusions

The separations of polycyclic aromatic hydrocarbons by GC-FID with temperature programming have been examined. It was observed that a good separation and linearity was achieved during the operating temperature. The LOD is still considered acceptable since EPA method indicated 50 to 1000 ppm is moderately toxic, which means method limits of detection are below the risk-based values. Therefore, Soxhlet extraction with GC-FID detection can be chosen as a preliminary and as an alternative analysis technique for PAHs detection.

Acknowledgements

References

1. Zakrzewski, S. F. 1991. Principles of Environmental Toxicology. ACS Professional Reference Book. American Chemical Society, Washington D.C.
2. Flotron, V, Houssou, J, Bosio, A, Delteil, Bermond, A, Camel, V. 2003. Rapid Determination of polycyclic aromatic hydrocarbons in sewage sludges using microwave-assisted solvent extraction comparison with other extraction methods. *J. Chromatogr. A*, 999. 175-184.
3. Korytar, P., Leonards P. E. G. 2002. High-resolution separation of polychlorinated biphenyls by comprehensive two-dimensional gas chromatography. *J. Chromatogr. A*, 958. 203-218.
4. Chen, C.S., Rao, P.S.C. and Lee, L. S. 1996. Evaluation of Extraction and Detection Methods for Determining Polynuclear Aromatic Hydrocarbons From Coal Tar Contaminanted Soils. Pergamon. 32. 1123-1132.
5. Codina, G., Vaquero, M. T., Commellas, L, Broto-Puig, F. 1994. Comparison of various extraction and clean-up methods for the determination of polycyclic aromatic hydrocarbons in sewage sludge-amended soils. *J. Chromatogr. A*, 673, 21-29.
6. Dadan Hermawan, M. Bachi Amran and Buchari ,2002. Study of Polycyclic Aromatic Hydrocarbon, PAH Content in Sediment by HPLC Method. Proceeding InSECT 2002. 206-212.
7. Berset, J. D. and Holzer, R. 1995. Organic micropollutants in Swiss agriculture: Distribution of Polycyclic Aromatic Hydrocarbons ,PAHs and Polychlorinated Biphenyls (PCBs) in Soil, Liquid Manure, Sewage Sluge, and Compost Samples; A Comparative Study. *J. Environ. Anal. Chem.* 59. 145-155.
8. Miege, C., Dugay, J. and Hennion, M. C. 2003. Optimization, validation and comparison of various extraction techniques for the determination of PAH in sewage sludges by liquid chromatography coupled to diode-array and fluorescence detection. *J. Chromatogr. A*. 995. 87-97.

SUBCRITICAL WATER EXTRACTION OF ESSENTIAL OIL FROM CORIANDER (*Coriandrum sativum L.*) SEEDS

Norashikin Saim*, Rozita Osman, Wan Azriza Hirmi Md Yasin, Rossuriati Dol Hamid

Fakulti Sains Gunaan, Universiti Teknologi MARA,40450 Shah Alam, Selangor

Abstract

Subcritical water extraction (SWE) is a technique based on the use of water as an extractant, at temperatures between 100 and 374 ºC and at a pressure high enough to maintain the liquid state. As the temperature of liquid water is raised under pressure, the polarity decreases and it can be used as an extraction solvent for a wide range of compounds. The application of SWE in the extraction of essential oil from coriander (*Coriandrum sativum L.*) seeds was studied. Ground coriander seeds (3-4 g) were subjected to SWE with water for an extraction time of 15 min under several extraction conditions (pressures of 870 and 1000 psi and temperatures of 65, 100 and 150 ºC). The SWE method was compared with hydrodistillation performed by treating 10 g of ground coriander seeds with 100 mL of water for 3 hours. Compounds were removed from the aqueous extract with hexane and determined by gas chromatography mass spectrometry (GC-MSD). It was found that the efficiency (g oil/g of coriander) of SWE was higher than that provided by hydrodistillation with reduced extraction time. The major compounds found were linalool, isoborneol, citronellyl butyrate and geraniol. SWE method has the possibility of manipulating the composition of the oil by varying the temperature and adjusting the pressure.

Introduction

Before the essential oils of plants can be analyzed, they have to be extracted and concentrated, and a number of different methods can be used for that purpose such as hydrodistillation, steam distillation and solvent extraction. Air dried leaves are usually subjected to hydrodistillation or steam distillation for about 3-8 hours and the essential oils are dried over anhydrous sodium sulfate. In solvent extraction (cold or hot), extraction of the air-dried plant material is carried out using an appropriate solvent depending on the nature of the essential oils. Several drawbacks such as low yield, losses of volatile compounds, long extraction times, degradation of unsaturated compounds and toxic solvent residue in the extract may be encountered with the current extraction methods [1]. These shortcomings have led to the emergence of new techniques in the extraction of essential oils such as supercritical CO_2 extraction (SFE) [1,2] and solvent free microwave extraction [3].

In recent years extraction with superheated water or subcritical water extraction (SWE) has been used widely for the extraction of polar and non polar analytes from environmental samples. SWE has also been applied in the extraction of essential oil from plants [4,5]. In this work subcritical water extraction of coriander seeds was compared to hydrodistillation in terms of extraction yields and essential oil composition. The influence of extraction conditions (temperature and pressure) on the composition of essential oil was analyzed.

Experimental

Sample preparation
Coriander seeds were purchased from local stores. The seeds were crushed before analysis.

Subcritical water extraction (SWE)
SWE was performed using an accelerated solvent extraction system, ASE 200, equipped with a solvent controller unit from Dionex Corporation. Extractions were performed using water with a static extraction time of 15 min at different extraction temperatures and pressures (SWE 1: 870 psi, 65 ˚C, SWE 2: 870 psi, 100 ˚C, SWE 3: 870 psi, 150 ˚C, SWE 4: 1000 psi, 65 ˚C, SWE 5: 1000 psi, 100 ˚C, SWE 6: 1000 psi, 150 ˚C)   All extractions were performed in 22 mL extraction cells, containing 3 g of sample. The extraction procedure was as follows: (i) sample is loaded into cell; (ii) cell is filled with solvent up to a specific pressure and temperature (iii) a static extraction is performed for 15 min (v) the cell is rinsed (with 60% cell volume using extraction solvent);

and (vi) solvent is purged from the cell with N_2 gas. Following SWE, liquid-liquid extraction step was performed using hexane and HCl was added to facilitate the breaking of emulsion. The obtained oil was separated and the yield was determined in terms of dry basis yield. The oil was stored in a freezer at -4 °C until analyzed by GC–MSD.

Hydrodistillation
Ten grams of crushed coriander seeds were subjected to hydrodistillation using 100 mL of distilled water for 3 h after the mixture had reached boiling point (100 °C). Liquid-liquid extraction step was performed using hexane. The obtained oil was separated, and the yield was determined. It was stored in a freezer at -4 °C until analyzed by GC–MSD.

Gas chromatography-mass spectrometry (GC-MS) analyses
GC-MS analysis was performed on an Agilent gas chromatography model 6890N coupled to a mass selective detector 5973 *inert*. Compounds were separated on a cross-linked fused silica capillary column HP5-MS (30m x 250µm x 0.25µm). The head pressure of the carrier gas helium (high purity) was 50 kPa. The temperature programmed was set at an initial 60 °C, followed by an increase by 10 °C min^{-1} to 200 °C and held for 15 minutes. The MS detector was operated in the full scan mode with 70 eV electrons ionization, by scanning a mass range of *m/z* 35-450 in 0.45 s. The system was computer-controlled using Agilent GC-MSD ChemStation. Compounds were identified by matching their mass spectra with the flavour spectral library with a resemblance percentage above 90 %.

Results and Discussion

Extraction yield and time
The yields (in terms of g of essential oil/1 g of coriander seeds) of SWE under these conditions (0.6 -0.8%) were found to be higher than that obtained by hydrodistillation (0.06-0.1%). Lower yields (~ 0.4%) of SWE were obtained at high temperature (150 °C) under both pressure conditions. The decreased in yield at higher temperature was also reported by other researchers [4,6]. It was observed that there were no significant difference in the amounts of extracted oil obtained under different pressures but same temperatures. The reduced extraction time (3 hours for hydrodistillation against 15 min for SWE) is clearly advantageous for the SWE method.

Composition of essential oil
For SWE extraction of coriander seeds, experiments were performed at different combination of extraction pressure and temperature. Identification of compounds extracted using these techniques were performed by GC-MS. Figure 1 shows the total ion current (TIC) chromatogram of coriander seed extract obtained using the two methods. Major compounds identified were linalool, isoborneol, citronellyl butyrate and geraniol. Comparison in the composition of coriander extracts obtained using various extraction techniques is shown in Table 1.
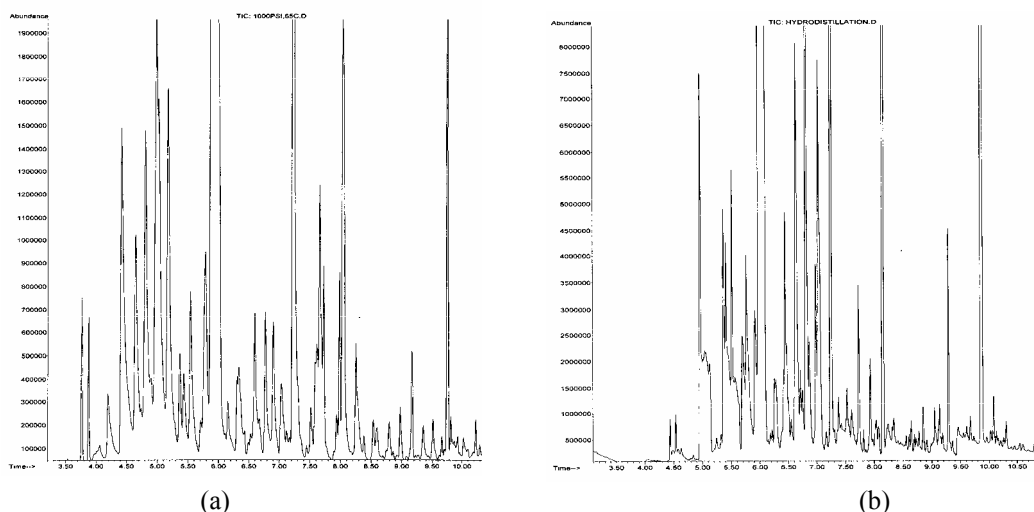

| (a) | (b) |

Figure 1: Total ion current (TIC) chromatograms of compounds of coriander seeds extracted by SWE (a) and HD (b).

Table 1: Compounds (%)* extracted from coriander by HD and SWE under different conditions.

Compound	HD	SWE 1 (870 psi, 65 ˚C)	SWE 2 (870 psi, 100 ˚C)	SWE 3 (870 psi, 150 ˚C)	SWE 4 (1000 psi, 65 ˚C)	SWE 5 (1000 psi, 100 ˚C)	SWE 6 (1000 psi, 150 ˚C)
Linalool	66.5	87.8	87.7	68.7	88.6	85.4	79.5
Isoborneol	6.8	6.1	3.8	0.8	6.1	2.9	4.3
Citronellyl butyrate	13.4	2.2	1.2	3.7	1.6	1.4	1.3
Geraniol	13.3	4.0	7.3	26.8	3.6	10.4	14.9

*Percent of component based on area normalization.

In general, the relative amounts of the major compounds obtained using HD and SWE under different conditions are comparable. Linalool is the most abundant composition of coriander isolated either by SWE under all conditions (68.7-88.6%) and HD (66.5%). However, the relative amount of citronellyl butyrate obtained using SWE is slightly lower than those obtained using hydrodistillation. For SWE, a change in extraction temperature resulted in a slight change of composition of the extracted oil. The percentage of geraniol increases with temperature while the percentage of linalool and isoborneol decreases at high temperature. Therefore using SWE, specific composition of essential oils can be obtained by optimizing the extraction temperature. Extraction pressure however did not seem to give significant effect on the oil composition as shown by the similarity of the oil composition for the extracts obtained under different pressures but same temperature ie. SWE 1 vs SWE 4 and SWE 2 vs SWE 5. It is noteworthy that the coriander extracts obtained using SWE produced a pleasant odor similar to the starting plant material.

Conclusions
The use of SWE has shown to be a good alternative for the extraction of essential oils. Essential oil of coriander obtained using SWE (at temperature 65-150 ˚C and pressure 870-1000 psi) was comparable to that obtained from hydrodistillation. SWE enables rapid extraction and has the advantage of being selective because it is possible to manipulate the extract composition under a given working conditions.

Acknowledgement

References
1.   Khajeh, M., Yamimi, Y., Bahramifar, N., Sefidkon, F., Pirmoradei, M.R. (2005) "Comparison of essential oils compositions of *Ferula assa-foetida* obtained by supercritical carbon dioxide extraction and hydrodistillation methods" *Food Chemistry*. 91. 639-644.
2.   Diaz-Maroto, M.C., Pérez-Coello, M.S., Cabezudu, M.D., (2002) "Supercritical carbon dioxide extraction of volatiles from spices. Comparison with simultaneous distillation-extraction" *J. Chromatogr. A*. 947. 23-29.
3.   Lucchesi, M.E., Chemat, F., Smadja, J., (2004) "Solvent-free microwave extraction of essential oil from aromatic herbs: comparison with conventional hydro-distilation" *J. Chromatogr. A*. 1043. 323-327.
4.   Ozel, M.Z., Gogus, F., Lewis, A.C. (2003) "Subcritical water extraction of essential oils from *Thymbra spicata*" *Food Chemistry*. 82. 381-386.
5.   Ozel, M.Z., Gogus, F., Kaymaz, H. (2004) "Superheated water extraction, steam distillation and Soxhlet extraction of essential oils of *Origanum onites*" *Anal Bioanal Chem*. 379. 1127-1133.
6.   Soto Ayala, R., Luque de Castro, M.D. (2001) "Continuous subcritical water extraction as a useful tool for isolation of edible essential oils" *Food Chemistry*. 75. 109-113.

FORENSIC ANALYSIS OF EXPLOSIVE RESIDUES FROM HAND SWABS

Umi K. Ahmad*, Sumathy Rajendran and Syahidah Abu Hassan

Department of Chemistry, Faculty of Science,Universiti Teknologi Malaysia, 81310 UTM Skudai, Johor,

Abstract

In the forensic examination of physical evidence for organic explosives, cotton swabs are often used to collect residue from surfaces, such as skin and post-blast debris. A preliminary study has been conducted to develop extraction method of a common energetic compound, pentaerythritol tetranitrate (PETN) from hand swabs followed by direct analysis of the resulting extract solution using high-performance liquid chromatography (HPLC) with ultraviolet (UV) detector. Analysis was performed on an octadecylsilane-based (C_{18}) column using acetonitrile-water mixture (55:45) as mobile phase. The mobile phase was pumped at 1.0 mL/min and separation affected using an isocratic mode with the detection wavelength of 230 nm. The explosive residue was extracted from cotton swabs using acetone in an ultrasonic cold bath. The developed method was later applied to the real hand swabs samples, which were taken from three army personnel who handled PETN during a munition disposal operation at Asahan Camp Military Firing range. The acetone extract obtained using sonication method was found to be effective in recovering PETN from cotton swabs with relatively high recovery (89.5%) and good sensitivity with detection limit as low as 2 ng. The content of PETN in the real hand swab samples were found to be in the range of 4.7-130 mg.

Abstrak

Dalam pemeriksaan forensik bagi bukti fizikal seperti letupan organik, sapuan kapas lazimnya digunakan untuk mengumpul residu daripada permukaan, contohnya kulit dan saki baki letupan. Satu kajian awal telah dilakukan untuk membangunkan kaedah pengekstrakan sebatian bertenaga pentaeritritol tetranitrat (PETN) daripada sapuan tangan diikuti dengan analisis ekstrak menggunakan kaedah cecair berprestasi tinggi (HPLC) dengan pengesanan ultralembayung (UV). Analisis menggunakan turus silika oktadesil (C_{18}) dengan campuran acetonitril-air (55:45) sebagai fasa bergerak. Fasa bergerak dialirkan pada 1.0 mL/min dan pemisahan berlaku pada mod isokratik dan pengesanan pada 230 nm. Residu letupan diekstrak daripada sapuan kapas menggunakan aseton dalam rendaman ultrasonik. Kaedah tersebut digunakan untuk analisis sampel sebenar sapuan tangan yang diambil daripada tiga anggota tentera yang telah memegang PETN semasa Operasi Pelupusan bahan letupan di Lapang Sasar Kem Asahan. Ekstrak aseton yang diperolehi menggunakan kaedah ultrasonik didapati berkesan dalam mengekstrak PETN daripada sapuan kapas dengan peratus pengembalian yang tinggi (88.2%) dan kepekaan yang baik dengan had pengesanan serendah 2 ng. Kandungan PETN dalam sampel sebenar didapati dalam linkungan 4.7-130 mg.

Introduction

Researches on explosives residues are often based on two aspects, which is either an environmental study [1-4] or forensic investigation. From an environmental aspect, there has been an increased concern that routine military training and testing exercises involving munitions could potentially cause a buildup of explosive residues in soil that can result in contamination of underlying groundwater. Studies have showed that candidate energetic sources for this contamination include releases from breached casings of unexploded (UXO) or partially exploded ordinance, poor disposal practices, open burn and open detonation operations, and the accumulation of high-order detonation residues in impact area (mostly at military training camp) [1,2]. Research conducted in this area could improve the current state of knowledge concerning the nature and extent of contamination [3] and the fate of residues of explosives to the environments [4].

However from the forensic point of view, information obtained from forensic laboratories during investigation of an explosion can yield valuable data for future investigations [5-7]. Data from one event can often be applied to other cases, thus improving the probability of locating and identifying crucial evidence. In the forensic examination of physical evidence for organic explosives, cotton swabs are often used to collect residue from

surfaces, such as skin and post-blast debris. According to the literature reviews, most of the analysis relies on organic solvents to wet and extract cotton swab [8]. Organic solvents such as acetone, ethanol or methanol are used because explosive compounds dissolve readily in them. Swab analysis of explosives could also been used as quality assurance testing as reported in a recent study [9].

This report describes a preliminary study of hand swabs analysis for the forensic analysis of pentaerythritol tetranitrate (PETN) residues. PETN is the major component of detonation cord often used during demolition activities Hand swabs were taken during sampling activities at Asahan Camp Military Firing Range, Malacca. The main purpose of this study was to develop an extraction method for explosive residues using HPLC with UV detector, which can be used to analysis hand swabs in real samples.

Experimental

Materials

Reagents
Double distilled deionized water (DDDW) was used throughout the analysis. Organic solvents such as acetone and acetonitrile used were of analytical grade (Merck) and HPLC grade (Merck) respectively. The mobile phase solvents for HPLC; DDDW and acetonitrile (MeCN) were filtered through a 0.45-μm-filter membrane prior to use.

Standard solutions
A stock solutions of 1000 ppm was prepared by dissolving 0.0100 g PETN with acetone in a 10 mL volumetric flask and then diluted to volume with MeCN. The stock solution was kept in a 10 mL vial, which was covered with aluminum foil and stored in the refrigerator. Working solutions (20-100 ppm) were prepared by dilution of suitable amount of the stock solution.

Cotton Swabs for Sampling
A packet of cotton balls meant for facial use was purchased at a local provision store. The average cotton ball was a sphere with approximately 3-cm diameter and weighing 500 mg. The cotton balls were cleaned by soaking in distilled water and followed by acetone for 30 minutes. Most of the solvent was squeezed out from the cotton prior to drying the cotton balls at room temperature for 12 hr. The cleaned and dry swabs were then stored in a zip lock plastic bag at room temperature.

Hand Swab Samples
Real hand swab samples were obtained from three army personnel who molded PETN during a munition disposal practice at Asahan Camp Military Firing Range, Malacca. At the sampling site, cotton balls were wetted with about 1 mL of acetone prior to use. The damp cotton ball was handled with gloved hand, swabbed against the surface of the volunteer's hand to collect residues, and then stored in a labeled zip lock bag. The zip lock bag was sealed properly to protect the swab from contamination. Hand swabs from all three army personnel were placed in a cool icebox before being transported back to the laboratory and were kept cold in refrigerator prior to analysis.

Spiked Samples for Recovery Study
Spiked samples were prepared in the laboratory for analyte recovery study. A cotton ball damped with acetone was placed in a 10 mL vial. The sample was spiked with 500 μL of PETN (1000 ppm). Duplicate spiked samples were prepared. Blank cotton swabs prepared were treated in a similar manner except that the blank samples were not spiked with the target analyte.

Instrumentation

Apparatus
All glasswares, spatula, forceps and sample bottles used for the analysis were previously soaked in 10% nitric acid overnight and rinsed carefully for at least three times with deionized water and thoroughly dried prior to use.

HPLC Instrument
Standard solutions and sample extracts were analyzed by using HPLC (Agilent 1100 series). The instrument was equipped with a quaternary pump, degasser, variable wavelength detector (VWD) and a computerized data acquisition and instrument control system (HPLC Chemstation Software G2170AA). Manual injector was used to inject samples onto the column. The HPLC column used was an Agilent Zorbax Eclipse XDB-C18 (4.6 x 150 mm, 5 µm).

Procedure

Extraction of PETN from Cotton Swabs
To extract explosive residues from a swab, acetone was added into the vial up to the 5-10 mL graduation to cover the cotton ball with solvent. The filled vial was placed in a sonic bath for approximately 10 minutes. Bath temperature was maintained at less than 10 ºC with cooling water. The acetone extract was removed from the vial and the extract was filtered through a gravity filter paper (Whatman, 90 mm). The cotton was pressed tightly to the bottom of the vial using forceps to remove the last few drops and the supernatant was collected in a vial. The sample solution was evaporated to near dryness under nitrogen gas flow, and acetonitrile was added to bring the volume to 10 mL [8]. Samples that were very cloudy or showed a large amount of particulate were made up to a known dilution factor. Spiked samples and blank samples were treated in a similar manner.

HPLC Analysis

HPLC analysis was performed using MeCN-Water mixture (55:45, v/v) under isocratic mode. The mobile phase was pumped in at a flow rate of 1.0 mL/min and the analyte was detected using a variable wavelength UV-Vis detector set at 230 nm. An aliquot (20 µL) of sample solution was introduced into the system via a Rheodyne six port injection valve fitted with a 20 µL sample loop.

Calibration Graph

A series of standard solutions ranging from 20 ppm up to 100 ppm were used to obtain a calibration graph for the determination of PETN. The concentrations of analyte in the samples were obtained by interpolation of the peak areas of the analyte from the calibration graph.

Limit of Detection

A standard solution of PETN with lower concentration was prepared by serial dilution of a 100 ppm stock solution. The limit of detection was assessed for the peak area of the lowest concentration of PETN that yielded a signal to noise ratio of 2:1.

Results and Discussion

Qualitative Analysis
Analysis of PETN was affected using HPLC in the isocratic mode employing MeCN-water mixture with analyte detection at 230 nm (Figure 1). The PETN peak was found to elute close to the solvent (acetone) peak. Peak due to the diluent (MeCN) was not apparent due to the nature of MeCN, which is transparent in the UV region at wavelengths above 200 nm.
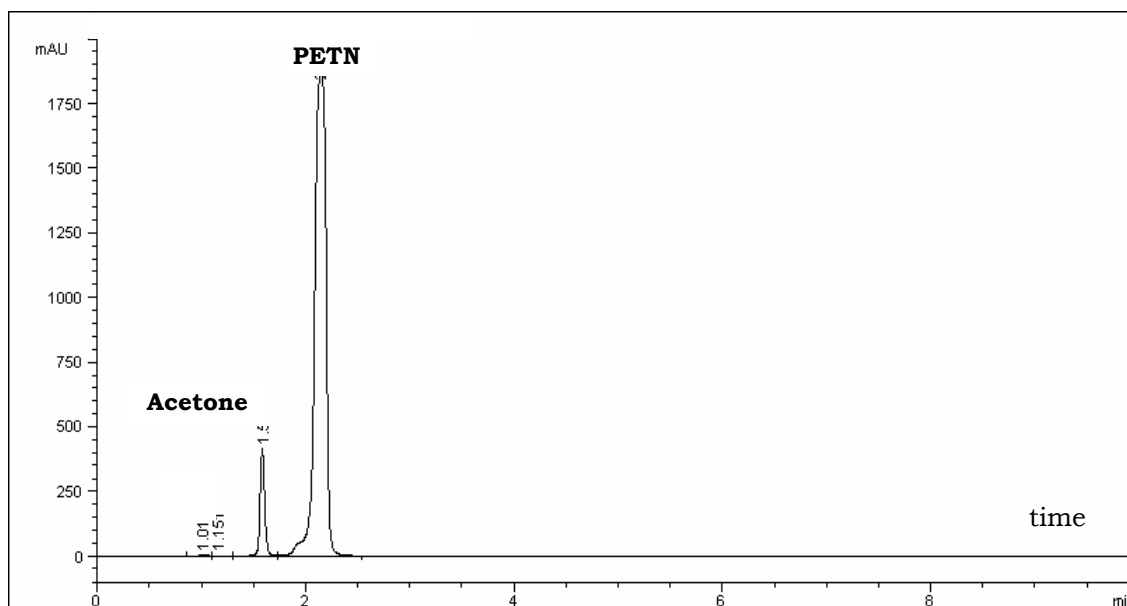
Figure 1. HPLC chromatogram of PETN standard solution (1000 ppm). HPLC conditions; mobile phase: 55% ACN : 45% Water, flow rate: 1.00 mL/min, detection wavelength: 230 nm.

Calibration Graph and Limit of Detection
Various concentration of PETN was injected to obtain chromatograms, which were used to plot a calibration graph of PETN. The concentrations of PETN standard chosen for this analysis were in the range of 20 to 100 ppm (Figure 2).
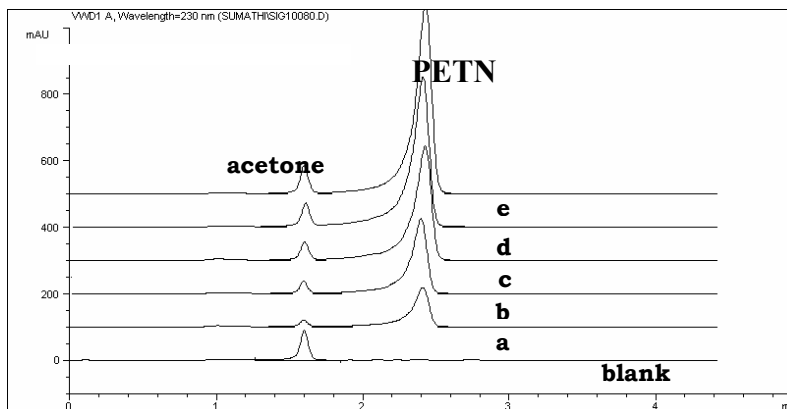
Figure 2. HPLC chromatograms of serial dilution of PETN standard with concentrations of (a) 20, (b) 40, (c) 60, (d) 80, (e) 100 ppm. HPLC conditions as in Figure 1.

The calibration graph plotted gave a regression line of y = 52.122x + 88.209 where y and x are peak area (mAU) and PETN concentration (ppm) respectively (Figure 3). Good correlation coefficient was obtained, with R^2=0.9995. Peak area was linear with the amount injected PETN over the range up to 100 ppm (2   g). The limit of detection (LOD) of an analyte can be described as the minimum concentration which gives an instrument signal significant different from the blank and background signal [10]. In this study, the limit of detection was assessed to be 2 ng.

28
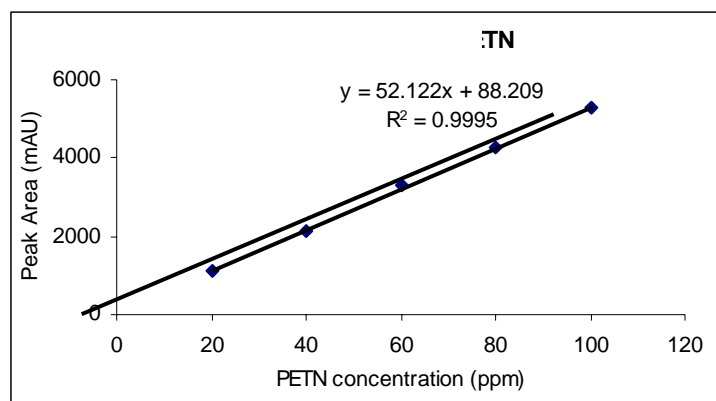
Figure 3. Calibration graph of PETN

Recovery Study

In order to evaluate efficiency of extraction using the cool bath ultrasonication technique [8], recoveries of the analyte from spiked samples were determined. Peak areas of both blank and spiked sample were measured and were used to calculate the percent recovery. Figure 4 shows the chromatogram of a sample spiked with 500   g analyte, which was used in the recovery study. The blank chromatogram at 230 nm is nearly flat with the exception of the solvent peak. The percent recovery of the extraction method used was found to be 89.5 % , indicating that a large fraction of the explosives was extracted from the cotton ball, and only a small amount of explosive residues could have remained bounded in the cotton swab. The recovery of PETN was comparable to that reported by Thomson *et al.* [8] who reported recoveries of over 80% for a mixture of explosives analysed.
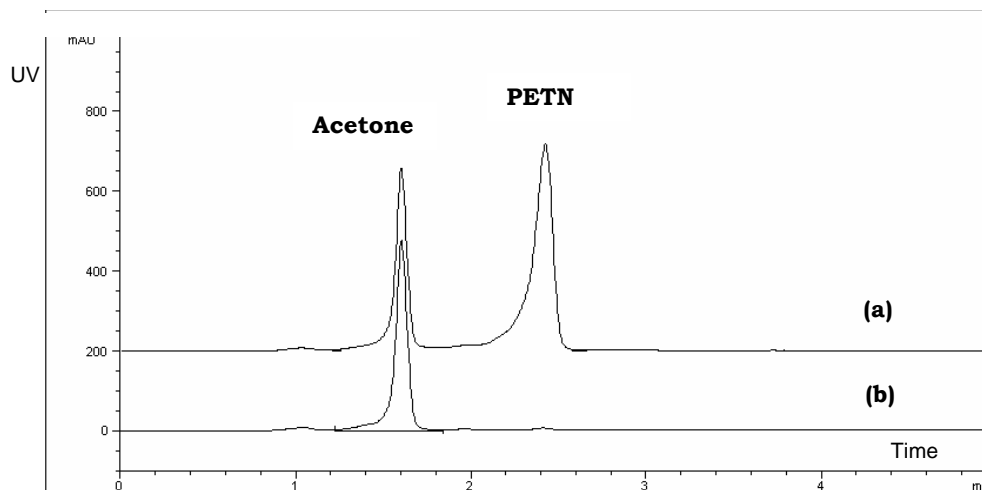
Figure 4. HPLC chromatogram of (a) Spiked cotton swab (500 μL of 1000 ppm PETN) and (b) Blank cotton swab. HPLC conditions as in Figure 1.

Real Samples Analysis

From the analysis, it was found that all three hand swabs samples taken during sampling contained PETN. Due to the high concentration of PETN, the hand swabs samples were diluted 10 to 100 times to yield responses with peak area with the range of the calibration graph. Extracts of sample HS1 (bare hand) was diluted 10 times (Figure 5) meanwhile extracts of sample HS2 and HS3 (gloved hands) were diluted 100 times. Table 1 shows the details of hand swabs analysis of the real samples.
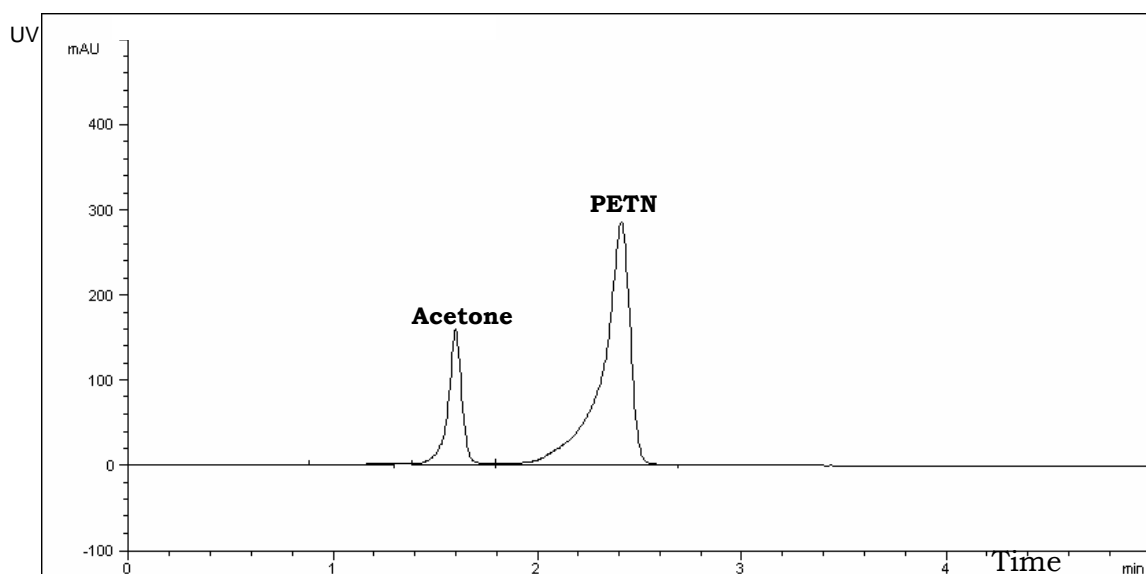
Figure 5: HPLC chromatogram of a real hand swab sample. Sample extract HS1 with 10 times dilution. HPLC conditions as in Figure 1.

Table 1: Amount of analyte in real hand swab samples

Sample Code	Dilution Factor, **DF**	Peak Area, **y** (mAU)	Amount of PETN in extracts, (**x × DF**), (mg)
HS1	10	2573.74	4.7
HS2	100	6805.14	129
HS3	100	6874.79	130

*Equation of calibration graph was used: $y = 52.122x + 88.209$

Conclusions

The extraction of hand swabs using cool bath sonication method developed in this study shows a relatively high recovery (88.2%) and reasonably good sensitivity with detection limit of 2 ng. The method was easily conducted and applicable to the analysis of the real hand swab samples using HPLC-UV at 230 nm. Significant amounts of PETN (4.7-130 mg) were extracted from the real samples analysis.

References

1. Hewitt, A.D., Jenkins T.F., Ranney T.A., Stark J.A.,. Walsh M.E, Taylor S., Walsh M.R., Lambert D.J., Perron N.M., Collins N.H., and Karn R. (2003). "Estimates for Explosives Residue From the Detonation of Army Munitions". US Army Corps of Engineers: Cold Regions Research and Engineering Laboratory.
2. Monteil-Rivera, F., Beaulieu, C., Deschamps, S., Paquet, L. and Hawari, J. (2004). "Determination of Explosives in Environmental Water Samples by Solid Phase Microextraction-Liquid Chromatography". *J. Chromatogr. A*. **1048(2).** 213-221.
3. Oxley, J.C., Smith, J.L., Resende, E., Pearce, E., and Chamberlain, T. (2003) "Trends in Explosive Contamination" *J. Forensic Sci*. **48**. 1-9.
4. Pennington J.C.; Brannon J.M. (2002). "Environmental fate of explosives" Thermochimica Acta, **384(1)**, 163-172.

5.   Samuels, J. E., Boyd, D. G. and Rau, R. M. (2000). *A Guide for Explosion and Bombing Scene Investigation*. Washington: National Institute of Justice.
6.   Furton, K. G., Almirall, J. R., J. Wang and Wu L. (2000). Application of Solid-phase Microextraction to the Recovery of Explosives and Ignitable Liquid Residues from Forensic Specimens. *J. Chromatogr. A*. **885**: 419-432.
7.   Yinon, J. and Zitrin, S. (1993). *Modern Methods and Applications in Analysis of Explosives*. West Sussex, England: John Wiley & Sons.
8.   Thompson, R.Q., Fetterrolf, D.D., Miller, M. L., Mothershead, R.F. (1998). "Aqueous Recovery from Cotton Swabs of Organic Explosives Residue Followed by Solid Phase Extraction". *J. Forensic Sci.* **97-10.** 795-804.
9.   Crowson, A., Hiley, R.W., and Todd, C.C. (2001). "Quality Assurance Testing of an Explosive Trace Analysis Laboratory". *J Forensic Sci.* **46(1)**. 53-56.
10. Miller, J.C. and Miller, J.N. (1984). "Statistics for Analytical Chemistry". England: Ellis Horwood Limited. 96-100.

A HOME-MADE SPME FIBER COATING FOR ARSON ANALYSIS

Umi K. Ahmad*, Abdul Rahim Yacob and Geetha Selvaraju

Department of Chemistry, Faculty of Science, Universiti Teknologi Malaysia, 81310 UTM Skudai, Johor, Malaysia.

Abstract

A number of adsorbents are available commercially as coatings for SPME fibers but some analytical methodologies might demand specific properties for the extraction of selected compounds, special coatings that have particular volume and a selectivity towards particular analytes. This paper presents a simple, fast, effective and environmental friendly methodology for the determination of accelerants in arson samples using headspace solid-phase microextraction coupled to gas chromatography. A new fiber prepared by sol-gel method, containing 1:1 molar ratio of octyltriethoxysilane (C_8-TEOS): methyltrimethoxysilane (MTMOS) was employed in this technique. The efficiency of the new fiber coating prepared by sol–gel technology for the determination of accelerants was compared to that of commercial PDMS/DVB fibers. Polydimethylsiloxane divinylbenzene (PDMS/DVB) is the most common fiber coating for the extraction of hydrocarbon compounds. Compared with commercial PDMS/DVB fiber, the new homemade fiber exhibited higher extraction capability and good selectivity for accelerants. The homemade fiber was also applied for the simulated arson samples. The home-made SPME adsorbent was shown to be a good alternative to commercially available fiber for the determination of accelerants in arson cases.

Abstrak

Pelbagai jenis gentian penjerap bagi teknik SPME wujud di pasaran. Namun demikian, ciri-ciri khas bagi pengekstrakan sebatian yang terpilih, salutan khas dengan isipadu tertentu dan keterpilihan terhadap analit tertentu diperlukan dalam beberapa kaedah analisis. Kertas kerja ini membentangkan suatu kaedah yang mudah, pantas, efektif dan mesra alam sekitar untuk menentukan bahan penggalak kebakaran dalam sampel kebakaran yang disengajakan dengan menggunakan teknik pengekstrakan fasa pepejal mikro yang dihubungkan dengan kromatografi gas. Gentian baru yang digunakan dalam teknik ini disediakan melalui kaedah "sol-gel", di mana ia terdiri daripada C_8-TEOS dan MTMOS dalam nisbah 1:1. Keberkesanan gentian penjerap baru yang disediakan melalui teknologi "sol-gel" untuk penentuan bahan penggalak kebakaran dibandingkan dengan gentian penjerap yang diperolehi secara komersil (PDMS/DVB). Gentian PDMS/DVB adalah gentian yang biasa digunakan dalam pengekstrakan sebatian hidrokarbon. Berbanding dengan gentian PDMS/DVB, gentian buatan sendiri yang baru menunjukkan kapasiti pengekstrakan yang lebih tinggi dan keterpilihan yang baik bagi bahan penggalak kebakaran. Gentian buatan sendiri ini juga diaplikasikan pada sampel simulasi kebakaran yang disengajakan. Gentian buatan sendiri untuk teknik SPME menunjukkan suatu alternatif yang baik kepada gentian komersial bagi penentuan bahan penggalak kebakaran dalam kes kebakaran yang disengajakan

Introduction

Arsons are particularly difficult crimes to prove due to the usual lack of physical evidence associating a suspect to the crime. The accelerants most commonly used by offenders because of their volatility, availability and flammability are petrol, kerosene and diesel. The more volatile components of an accelerant evaporate at a faster rate than the heavier components so that overall chemical profile of the accelerant will change during the fire and before sampling [1, 2].

It is difficult to conclusively determine if a sample of an accelerant was the same as that to initiate or propagate a fire, because of the universal composition of the common accelerants. The chemical components of the common accelerants are aliphatic and aromatic hydrocarbons and oxygenated hydrocarbons such as alcohols. The oxygenated hydrocarbons are to a degree water soluble and therefore washed away during the extinguishing of the blaze, so that little trace remains [3-6].

The amount of accelerant remaining at the fire scene available for sampling is governed by the initial loading of the accelerant, volatility of the accelerant, severity of the fire, water solubility of the accelerant, porosity of the substrate material, dryness of the area after the fire and the elapsed time between the fire and sampling [3-6].

An important aspect of an investigation of a suspected arson case involves the chemical analysis of the debris remaining after the fire. Currently, accelerant extraction and analytical techniques have been refined to improve sample turnover and to reduce the number of inconclusive findings. For this purpose, solid-phase micro extraction (SPME) have been introduced. The major advantage of SPME is that it uses no solvents and can be used for either direct sampling or sample clean-up. It is fairly economical and is a relatively simple and sensitive technique. The qualities that enable an SPME adsorbent to be successfully used for accelerant extraction and analysis are its selectivity towards accelerant components which separates and concentrates the accelerant from the headspace to yield a sample that is suitable for introduction to GC-FID [7].

Recently, many novel coatings have been developed using different techniques and technology for use in SPME. Compared with commercially available SPME adsorbents, the new materials exhibited higher thermal stability (350 $^{\circ}$C), solvent stability (organic and inorganic) and extraction capability [8-19]. However, up to now, none of the novel fibers have been evaluated for the determination of accelerants in arson analysis. This paper presents a recent development in the forensic aspects of fire investigation. As a preliminary study, a home-made SPME adsorbent comprising of sol-gel derived C_8-coating was developed and evaluated for the determination of accelerants in arson samples, with the aim of improving the quality of ignitable liquid residue analysis.

Experimental

Chemicals and Materials

Samples of diesel and unleaded gasoline were purchased from a petrol station in Skudai, Johor while kerosene was obtained from a grocery shop at Taman Universiti, Skudai, Johor. Samples of carpet were purchased from a carpet retail shop in Taman Ungku Tun Aminah, Skudai, Johor.

Apparatus

A glass apparatus (400 cm^3) for sample preparation step of headspace SPME was specially designed [20]. A Supelco SPME holder, commercially available PDMS/DVB fibers (Bellefonte, Pennsylvania, U.S.A.), and home-made sol-gel derived C_8-coated fibers containing (1:1, C_8-TEOS:MTMOS) [21] were employed for the extraction of accelerants.

Instrumentation

Gas chromatography was conducted using a Hewlett-Packard 6890 GC (Wilmington, Delaware, U.S.A.). The HP 6890 gas chromatograph was equipped with FID and a HP ChemStation for data processing. An Ultra-1 capillary column (Agilent) of dimensions 25 m x 0.20 mm x 0.11 μm film thickness was used. Helium was used as the carrier gas at a flow rate of 1.2 mL/min. The injection port temperature was set at 250 °C and FID temperature at 310 °C. SPME injections were performed using a split mode injection (1:5).

Preparation of Spiked Fire Debris sample

A sample of carpet (15 cm x 10 cm) placed on a sheet of aluminium foil was ignited with a fire starter and left to burn until about 1/3 remained on the aluminium foil. Fire was extinguished and the partially burnt carpet was exposed to the surrounding air for 30 minutes to cool down. 100 μL of accelerant (petrol, kerosene and diesel) were individually spiked on to the burnt carpet fire debris sample. The spiked sample was placed in the glass apparatus prior to headspace SPME .

Procedures for Headspace SPME

The spiked fire debris sample was placed in the sample preparation apparatus that was immersed in a hot water bath and heated for 15 min at 100 $^{\circ}$C. The C_8-coated fiber was exposed in the headspace and the fiber extracts were analyzed using GC-FID. The oven temperature was initially set at 40 $^{\circ}$C, programmed at a rate of 10 $^{\circ}$C/min until a final temperature of 270 $^{\circ}$C. The headspace SPME procedure was repeated using PDMS/DVB fiber for comparison.

Results And Discussion

Selectivity of C$_8$-coated fiber for accelerants

In order to examine selectivity of the home-made SPME fiber towards petroleum based accelerants, burnt carpet samples were individually spiked with known amount of gasoline, kerosene and diesel. The samples were subjected to headspace SPME using sol-gel derived C$_8$-coated fiber and the GC profiles were compared with that from direct injection. As seen in Figure 1 (b), all the hydrocarbon components in gasoline spiked burnt carpet sample were recovered by using C$_8$-coated fiber and the chromatogram was comparable with the profile of gasoline from direct injection (Figure 1 (a). The hydrocarbon components in kerosene (Figure 2) and diesel (Figure 3) spiked burnt carpet sample were also effectively extracted using the home-made fiber and similar comparisons were obtained with direct injection of the respective accelerants. This indicated that the home-made SPME fiber favored the extraction of hydrocarbons, thus providing a good selectivity towards accelerants. The GC profiles of gasoline, kerosene and diesel spiked samples obtained in this study were in good agreement with those obtained by Borusiewicz [1] using Tenax as adsorbent and Yong [20] using commercially available fibers.

Extraction capability of the C$_8$-coated fiber

The extraction capability of the sol-gel derived C$_8$-coated fiber was determined by comparing it with the commercially available PDMS/DVB fiber. PDMS/DVB fiber was selected for comparison because previous work done in this lab [20] proved that the fiber has the highest sensitivity towards hydrocarbon compounds and most suitable for accelerants identification. Both C$_8$-coated fiber and PDMS/DVB fiber is capable of extracting early, middle and late eluting hydrocarbon compounds sufficiently. However, the C$_8$-coated fiber showed a slightly higher extraction capability by contrast with conventional PDMS/DVB fiber for all the accelerants as shown in Figure 4. This result was comparable to that reported by Gbatu *et al.* [8]. A higher extraction capability could be due to the existence of higher surface area for the C$_8$-coated fibers [8]. Up to now, all the headspace SPME extractions were carried out with the optimized conditions of the commercially available PDMS/DVB fiber [20]. A study is now underway to optimize the extraction and desorption time of the C$_8$-coated fiber. The optimized conditions of the C$_8$-coated fiber might result in faster extraction time as reported by Gbatu *et al.* [8].

(a)

(b)

(c)
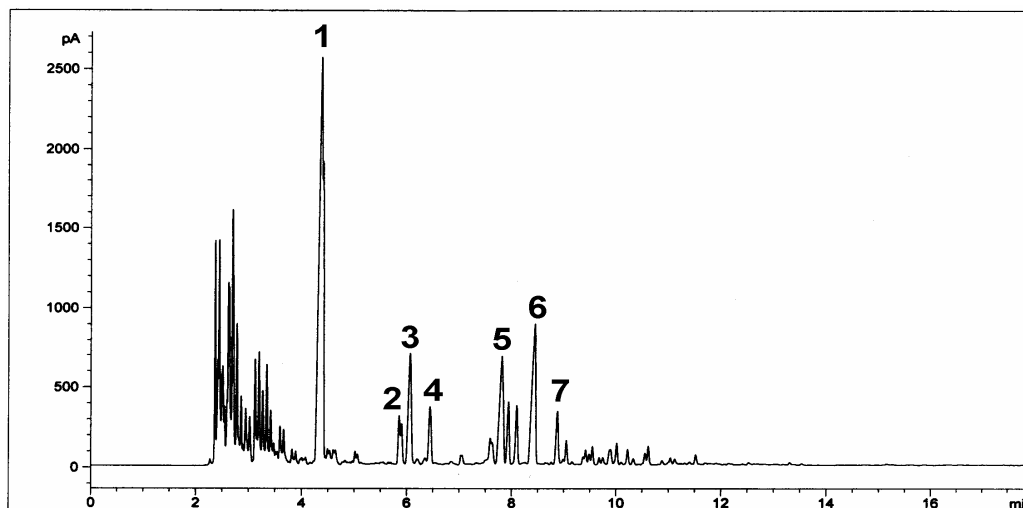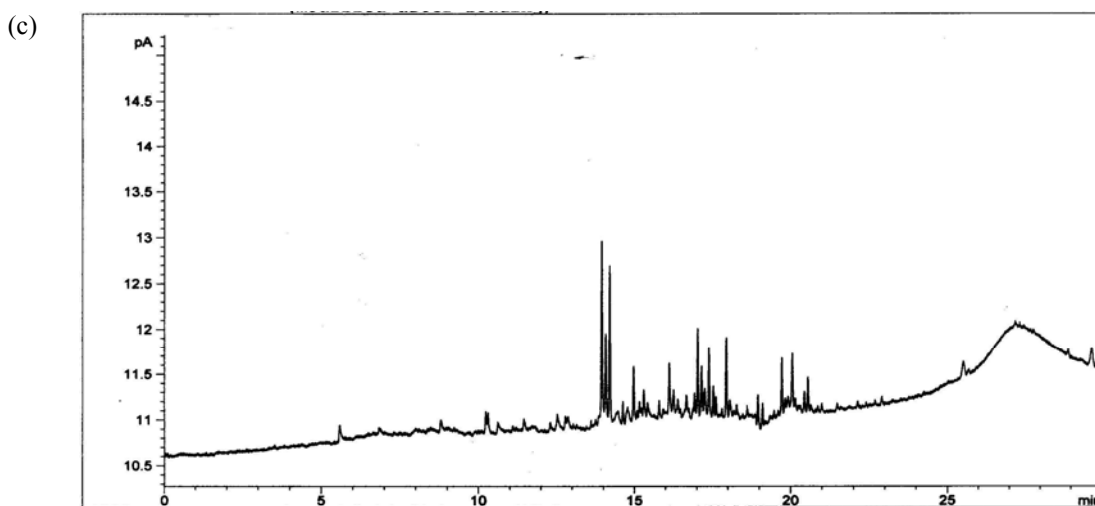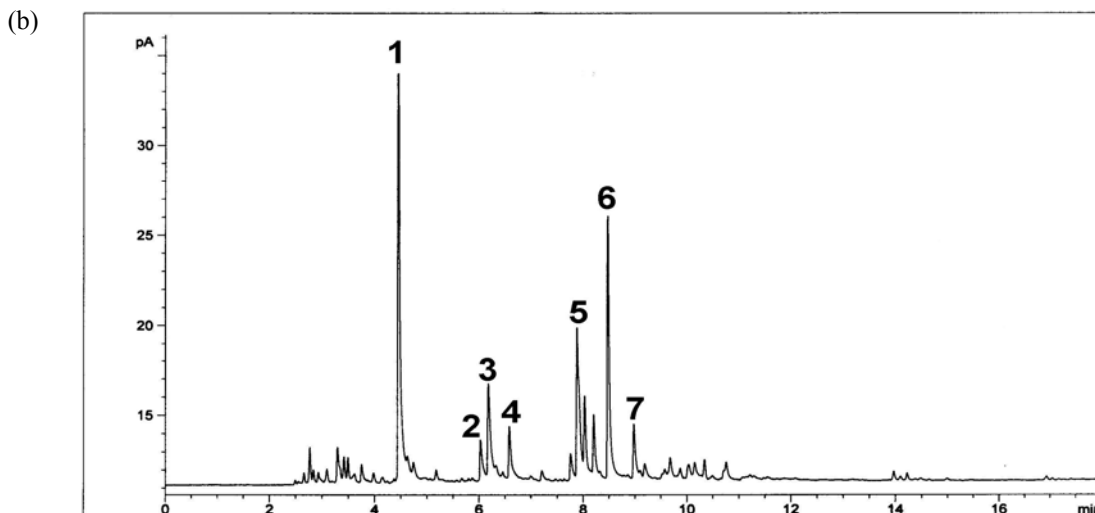
Figure 1**:** GC profiles of (a) direct injection of gasoline, (b) gasoline spiked burnt carpet sample and (d) the blank burnt carpet sample using C_8-coated fibers. Peak identities: (1) methylbenzene, (2) ethylbenzene, (3) 1, 3-dimethylbenzene, (4) 1, 2- dimethylbenzene, (5) 1-ethyl-2-methylbenzene, (6) 1, 2, 4-trimethylbenzene, (7) 1, 2, 3- trimethylbenzene.

(a)
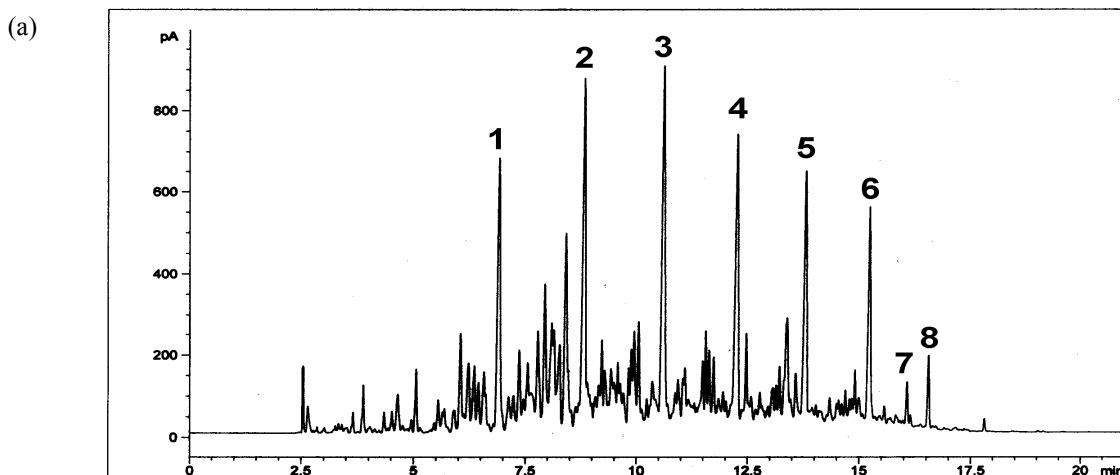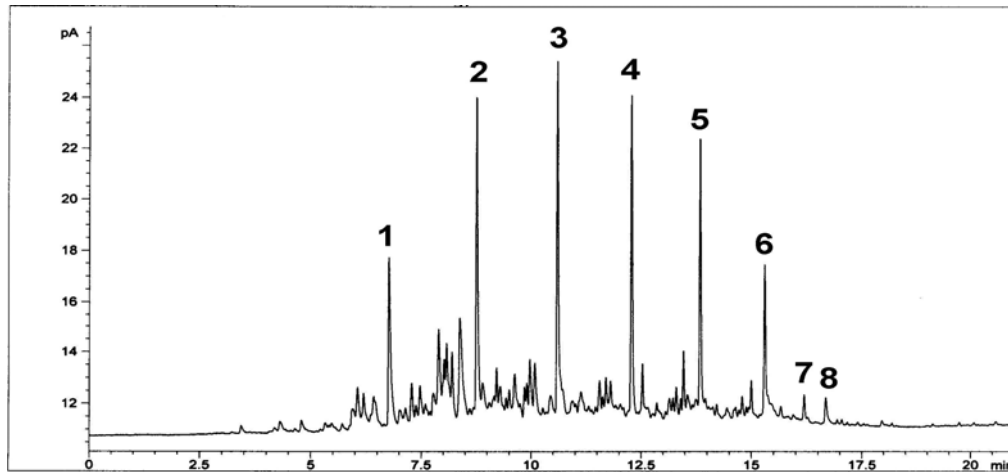
(b)

Figure 2: GC profiles of (a) direct injection of kerosene and (b) kerosene spiked burnt carpet sample using C_8-coated fibers.Peak identities: (1) C_9, (2) C_{10}, (3) C_{11}, (4) C_{12}, (5) C_{13}, (6) C_{14}, (7) 2, 6-dimethylnapthalene, (8) C_{15}
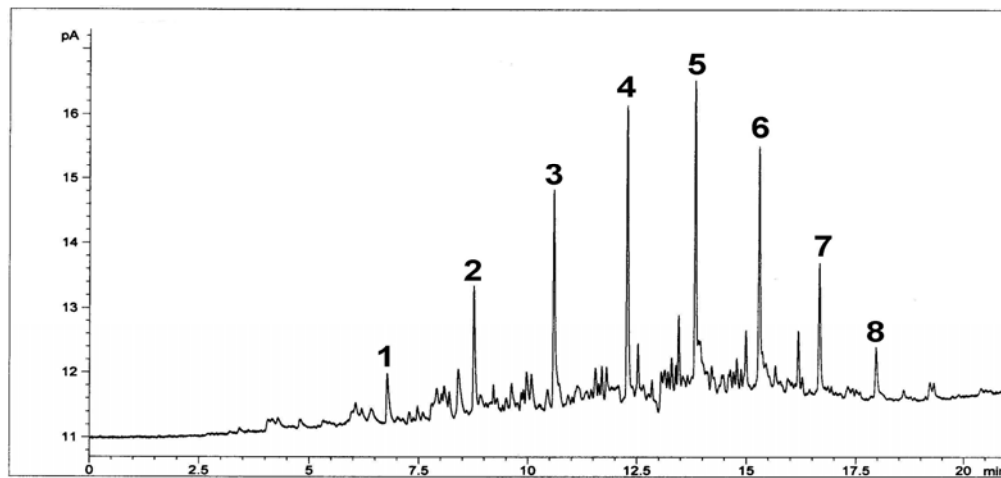
Figure 3: GC profiles of direct injection of diesel spiked burnt carpet sample using C_8-coated fibers.
Peak identities: (1) C_9, (2) C_{10}, (3) C_{11}, (4) C_{12}, (5) C_{13}, (6) C_{14}, C_{15}, (7) C_{16}

(a)

Label identities: (1) methylbenzene, (2) ethylbenzene, (3) 1, 3-dimethylbenzene,(4) 1, 2-dimethylbenzene, (5) 1-ethyl-2-methylbenzene, (6) 1, 2, 4-trimethylbenzene, (7) 1, 2, 3-trimethylbenzene.

(b)

Label identities: (1) C_9, (2) C_{10}, (3) C_{11}, (4) C_{12}, (5) C_{13}, (6) C_{14}, (7) 2, 6-dimethylnapthalene, (8) C_{15}

(c)

Label identities: (1) C_9, (2) C_{10}, (3) C_{11}, (4) C_{12}, (5) C_{13}, (6) C_{14}, C_{15}, (7) C_{16}
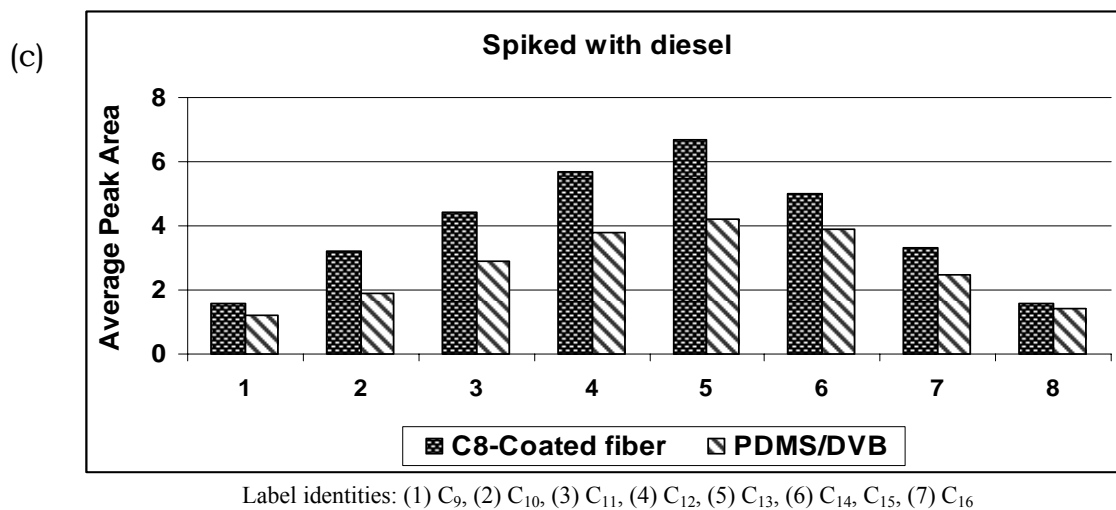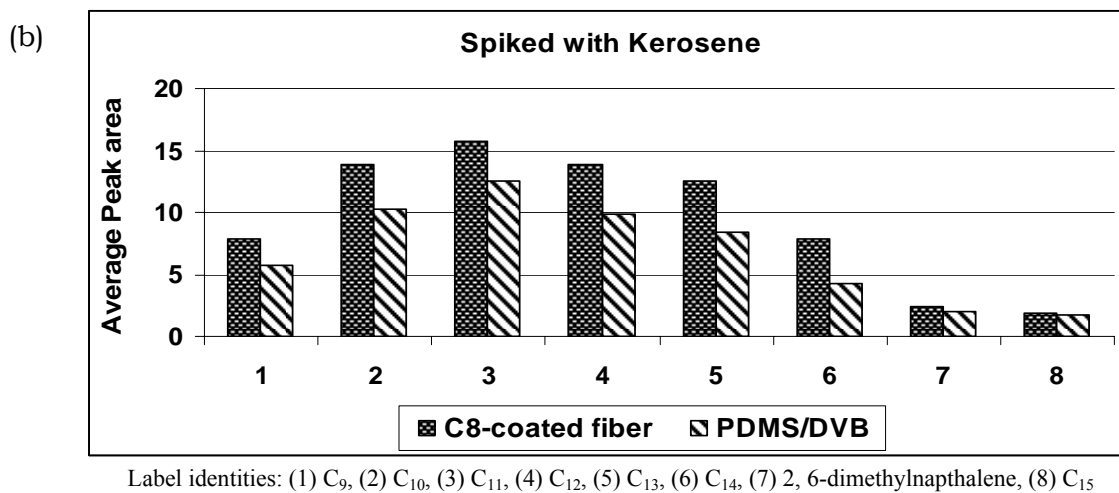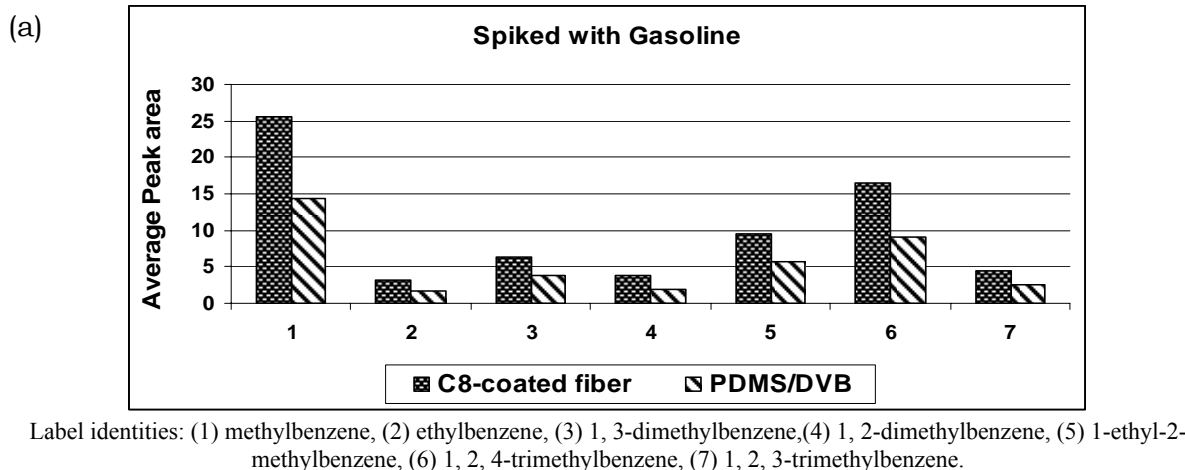
Figure 4: Comparison of sol-gel derived C_8-coated fiber and commercially available PDMS/DVB fiber in extracting hydrocarbon compounds from (a) gasoline, (b) kerosene and (c) diesel spiked burnt carpet

Conclusions

The sol-gel derived C_8-coated fiber was successfully evaluated for the determination of accelerants in arson samples. The home-made fiber was capable of extracting hydrocarbon compounds from simulated arson samples

and showed a good selectivity towards accelerants. The C_8-coated fiber exhibited a slightly higher extraction capability by contrast with conventional PDMS/DVB fiber. The experiments performed proved that the developed fiber could be successfully applied for arson analysis.

References

1. R. Borusiewicz, G. Zadora and J. Z. Palus (2004). "Application of headspace analysis with passive adsorption for forensic purposes in the automated thermal desorption GC-MS system." *Chromatographia supplement.* 60. S113-S142.
2. T. Ma, S. M. Olenick, M. S. Klassen and R. J. Roby (2004). "Burning rate of liquid fuel on carpet (porous media)." *Fire Tech. 40.* 227-246.
3. J. S. Almirall and K. G. Furton (2004). "Characterization of background and pyrolysis products that may interfere with the forensic analysis of fire debris." *J. Anal. Appl. Pyrolysis.* 71. 51-67.
4. J. S. Almirall, K. G. Furton and J. C. Bruna (1996). "A novel method for the analysis of gasoline from fire debris using headspace solid-phase microextraction." *J. Forensic. Sci.* 71. 12-22.
5. K. Cavanagh, E. D. Pasquier and C. Lennard (2002). " Background interference from car carpets-the evidential value of petrol residues in cases of suspected vehicle arson." *Forensic. Sci. Int.* 125. 22-36.
6. P. M. L. Sandercock and E. D. Pasquier (2003). "Chemical fingerprinting of unevaporated automotive gasoline samples." *Forensic. Sci. Int* 134. 1-10.
7. J. Dolan (2003). " Recent advances in the applications of forensic science to fire debris analysis." *Anal. Bioanal. Chem.* 376. 1168-1171.
8. T. P. Gbatu, K. L. Sutton and J.A Caruso (1999). "Development of New SPME Fibers By Sol-gel Technology for SPME-HPLC Determination of Organometals."
   Anal Chim Acta. 402. 67-79
9. A. kabir, C. Hamlet, K. S. Yoo, J. R. Newkome and A. Malik (2004) "Capillary Microextraction on Sol-gel Dendrimer Coatings," *J. Chromatogr. A.* 1034. 1-11.
10. C. Basheer, S. Jagadesan, S. valiyaveetil and H. K. Lee (2005). "Sol-gel coated oligomers as novel stationary phases for solid-phase microextraction." *J.Chromatogr. A.* Article in Press.
11. Y. Hu, Y. Yang, J. Huang and G. Li (2005). "Preparation and application of poly(dimethylsiloxane)/B-cyclodextrin solid-phase microextraction membrane." *Anal. Chim. Acta.* Article in Press.
12. L.Yun (2003). "High Extraction Efficiency Soild-phase Microextraction Fibers Coated with Open Crown ether Stationary phase using Sol-gel Technique." *Anal Chim Acta.* 486. 63-72.
13. J. Yu, L. Dong, C. Wu, L. Wu and J. Xing (2002). " Hydroxyfullerene as a Novel Coating for Solid-phase Microextraction Fiber with Sol-gel technology." *J. Chromatogr. A.* 978. 37-48.
14. V. G. Zuin, A. L. Lopes, J. H. Yariwake and F. Augusto (2004). "Application of a Novel Sol-gel Polydimethylsiloxane-Poly(vinyl alcohol) SPME Fiber for Gas Chromatographic Determination of Pesticide Residues in Herbal Infusions." *J. Chromatogr. A.* 1056. 21-26.
15. J. Yu, C. Wu and J. Xing (2004). "Development of New SPME Fibers By Sol-gel Technology for The Determination of Organophosphorus Pesticide Multiresidues in Food." *J. Chromatogr. A.* 1036. 101-111.
16. C. Basheer, S. Jagadesan, S. valiyaveetil and H. K. Lee (2005). "Sol-gel coated oligomers as novel stationary phases for solid-phase microextraction." *J. Chromatogr. A.*Article in Press.
17. D. Wang, J. Xing, J. Peng and C. Wu (2003). " Novel benzo-15-crown-5 Sol-gel Coating for Solid-phase Microextraction." *J. Chromatogr. A.* 1005. 1-12.
18. J. Wu and J. Pawliszyn (2004). "Solid-phase microextraction based on polypyrrole films with different counter ions." *Anal. Chim. Acta.* **520**.257-264.
19. R. Aranda, P. Kruus and R. C. Burk (2000) "Assessment of polycrystalline graphites as sorbents for solid phase microextraction of non-ionic surfactants." *J. Chromatogr. A.* **888**. 35-41.
20. T. Y. Yong (2004) "Development of Headspace SPME-GC Technique for the Forensic Analysis of Ignitable Liquid Residues in Fire Debris." Universiti Teknologi Malaysia: Master of Science Thesis.
21. U. K. Ahmad, A. R. Yacob and G. Selvaraju (2005) "A New SPME Adsorbent for the Forensic Analysis of Accelerant Residues." Ibnu Sina Institute, Universiti Teknologi Malaysia: Proceeding of the Annual Fundamental Science Seminar.

HARNESSING ELECTRO DRIVEN SEPARATION TECHNIQUE FOR THE SEPARATION OF SELECTED AGROCHEMICALS

Wan Aini Wan Ibrahim[1], S. M. Monjurul Alam[2] and Azli Sulaiman[1]

[1]*Separation Science Research Group (SSRG)Chemistry Department, Faculty of Science,
University Teknologi Malaysia, 81310 Skudai, Johor*
[2]*Chemistry Department, Rajshahi University, Rajshahi-6205, Bangladesh*

Abstract

Electro driven separation techniques offer a different approach to the analysis of complex mixtures than do traditional pressure-driven chromatographic system; it may rely on electrophoresis, the transport of charged species through a medium by an applied field or may rely on electro driven mobile phase to provide a true chromatographic separation. In the current work the potential of an electro driven separation technique viz. micellar electrokinetic chromatography (MEKC), is harnessed for the separation of selected agrochemicals (organophosphorus pesticides, OPPs) widely used in the agriculture sector in Malaysia. The current study compares the use of MEKC in normal mode (NM) and reverse mode (RM) for the separation of the selected OPPS. This study also highlights the difference in separations produced by performing separations in normal mode-MEKC (NM-MEKC) and reverse mode-MEKC (RM-MEKC) for the selected OPPs. In RM-MEKC, separation is conducted at acidic pH (pH 2.5 in the current work) where the electroosmotic flow (EOF) is weak whereas in NM-MEKC, the separation is carried out under basic pH (9.3 in this work) where the EOF is strong. A reverse migration order of the OPPs was observed under RM-MEKC. Separation under NM-MEKC was found to be superior to those of RM-MEKC. A comparison is also made between separations performed under sweeping-NM-MEKC and sweeping-RM-MEKC. In sweeping, the OPPs are prepared in the same background solution (BGS) minus the micelles and is adjusted to the same conductivity as the BGS. The study showed that NM-MEKC is more sensitive than RM-MEKC but sweeping-RM-MEKC is superior to sweeping-NM-MEKC. However, sweeping-RM-MEKC only separates two of the OPPs in a single run whereas sweeping-NM-MEKC separates four OPPs in a single run. The better choice of separation mode would be sweeping-NM-MEKC for more OPPs separation in a single run.

Abstrak

Teknik pemisahan pacuan elektro menawarkan satu pendekatan berlainan analisis suatu campuran kompleks berbanding dengan sistem kromatografi pacuan tekanan; ia boleh bergantung kepada elektroforesis, pengangkutan spesis bercas melalui media oleh medan yang dikenakan atau bergantung kepada fasa bergerak pacuan elektro untuk memberikan pemisahan kromatografi sejati. Dalam kajian ini keupayaan teknik pemisahan pacuan elektro iaitu kromatografi elektrokinetik misel (MEKC) digunakan untuk pemisahan bahan kimia agro terpilih (pestisid organofosforus) yang banyak digunakan dalam sektor pertanian di Malaysia. Kajan ini membandingkan penggunaan MEKC dalam mod normal (NM) dan mod terbalik (RM) untuk pemisahan OPPs terpilih ini. Kajian ini juga menonjolkan perbezaan pemisahan yang dihasilkan dalam mod NM-MEKC dan mod RM-MEKC. Dalam mod NM-MEKC, pemisahan dijalankan di dalam keadaan berbes (pH 9.3 dalam kajian ini) di mana daya electroosmosis (EOF) adalah kuat sementara dalam mod RM-MEKC, pemisahan dijalankan dalam keadaan berasid (pH 2.5) di mana EOF adalah lemah. Tertib migrasi yang dicerap dalam RM-MEKC adalah berlawanan dengan tertib migrasi dalam NM-MEKC.   Perbandingan juga dibuat antara pemisahan secara sapuan-NM-MEKC dan sapuan-RM-MEKC. Dalam mod sapuan, OPPs disediakan dalam larutan latarbelakang (BGS) tanpa misel dan kekonduksian diubahsuai supaya sama dengan kekonduksian BGS. Kajian ini menunjukkan bahawa NM-MEKC lebih sensitif berbanding RM-MEKC tetapi sapuan-RM-MEKC lebih baik berbanding sapuan-NM-MEKC. Walau bagaimanapun, sapuan-RM-MEKC hanya mampu memisahkan dua OPPs dalam satu larian berbanding dengn sapuan-NM-MEKC yang dapat memisahkan empat OPPs dalam satu larian. Pemilihan mod pemisahan yang lebih baik adalah sapuan-NM-MEKC untuk pemisahan lebih banyak OPPs dalam satu larian.

Introduction

Capillary electrophoresis (CE) has become a powerful separation technique and has been applied to the analysis of a wide range of molecules. Electrokinetic chromatography (EKC) is a mode of CE and was first introduced

by Terabe and co-workers [1, 2] in 1984. Since the first introduction of EKC, it has become widely popular as a powerful separation technique for both neutral and ionic compounds [3-5]. In EKC, the use of charged pseudostationary phases (PSP) like sodium dodecyl sulphate (SDS) is by far the most famous experimental form of EKC and called micellar electrokinetic chromatography (MEKC). Species having the same charge as the micelles do not interact with the micelle, while those having opposite charge strongly interact with the micelles. The separations of charged species depend on the species difference in electrophoretic mobility. The formation of micelles provides a unique chromatographic process for the separation of neutral molecules where partitioning between the micellar PSP and the electroosmotically pumped aqueous phase take place. The use of untreated silica capillaries and separation in basic buffers with positive potential were considered as the standard features in most of the MEKC works [6-8]. In these particular conditions, the bulk electroosmotic flow (EOF) is dominant and that ultimately drives the anionic sodium dodecyl sulphate (SDS) micelles toward the cathode end. However, in few works, especially those described in the newer online concentration techniques [9-12] have studied the effect of buffers pH in relation with the overall separation performances.

In the current work the potential of an electro driven separation technique, micellar electrokinetic chromatography (MEKC), is harnessed for the separation of selected agrochemicals (organophosphorus pesticides, OPPs) widely used in the agriculture sector in Malaysia. Electro driven separation techniques offer a different approach to the analysis of complex mixtures than do traditional pressure-driven chromatographic system; it may rely on electrophoresis, the transport of charged species through a medium by an applied field or may rely on electro driven mobile phase to provide a true chromatographic separation. The current study compares the use of MEKC in normal mode (NM) and reverse mode (RM) for the separation of the selected OPPS. This study also highlights the difference in separations produced by performing separations in normal mode-MEKC (NM-MEKC) and reverse mode-MEKC (RM-MEKC) for the selected OPPs. In RM-MEKC, separation is conducted at acidic pH (pH 2.5 in the current work) where the anionic micelles (sodium dodecyl sulphate, SDS) move faster than the electro-osmotic flow (EOF), which is weak; thus positive potential is applied at detector end in order to detect the analytes. In NM-MEKC, the separation is carried out under basic pH (pH 9.3 in this work) where the EOF is strong.

In CE, the injected sample volumes are typically limited to 1% of the total capillary volumes in order to maintain efficiency. Therefore to increase detection sensitivity, various concentration techniques can be used. In this study, sweeping is used and a comparison of sweeping in NM-MEKC and RM-MEKC is also made. Sweeping is one of the on-line concentration techniques in MEKC and is based on the accumulation of analyte molecules by an additive in the background solution (BGS), which they have a considerable affinity for [10, 13].

Experimental

Reagents All pesticides were analytical standards purchased from Dr. Ehrenstorfers GmbH laboratory (Augsburg, Germany). SDS was purchased from Fisher Scientific (Loughborough, UK), methanol from BDH (Poole, England), acetonitrile and disodium tetraborate 10-hydrate ($B_4Na_2O_7$ $10H_2O$) from MERCK (Germany), hydrochloric acid (37.5%) from Sigma (St. Louis, MO, USA), sodium hydroxide pellets and disodium hydrogen phosphate 12-hydrate (Na_2HPO_4 $12H_2O$) from Riedel-de Haen (Seelze, Germany).

Instrument

Capillary electrophoresis was performed on a CE – L1 instrument (CE Resources Pte. Ltd. Singapore) fitted with a UV-Visible detector (SPD – 10A VP) from Shimadzu (Kyoto, Japan). Electropherograms and data were recorded by *Chromatography Station* software (*CSW*) for Windows at 202 nm. Uncoated fused-silica capillaries (total and effective lengths are 82 and 42 cm, respectively) from SGE (Victoria, Australia) of 50 μm ID were used.

Procedures

Standard solutions of about 1 mg mL^{-1} of each pesticide were prepared in methanol. Working standard solutions were prepared by diluting the corresponding stock solutions in buffer, surfactant and modifiers, and the ionic strengths of sample matrix and running buffers were maintained at same level. Dilutions in sweeping procedures, corresponding pH of sample and buffer matrices were mentioned in respective places. All the stock buffers and surfactants were prepared in distilled deionized (DD, 18 MΩ) water. Concentrations of buffers, SDS, methanol and acetonitrile are reported based on the final volume in the running buffer. All running buffers were filtered through 0.45 μm nylon filter disc from Whatman (Clifton, New Jersey, USA). Separation voltage of 25 kV

(either + or − mode) was employed depending on the requirements. Sample injections were performed electrokinetically at 15 kV in all separations where basic running buffer were involved, while samples were injected hydrodynamically at 2.8 kPa for various times where separations were performed in RM-MEKC. All experiments were conducted at an ambient temperature of 25°C. At the beginning of each day, the capillary was rinsed for at least 10 min with 0.1 M NaOH solution followed by DD water for 10 min and conditioned with running buffer for 10 min. In between runs, the capillary was also conditioned by running buffer for 5 min. At the end of the day, the capillary was rinsed with DD water for 30 minutes followed by passing air.

Results and Discussions

Separation in NM- MEKC

The five OPPs chosen for the study are hydrophobic compounds (Figure 1) and were baseline separated in normal mode MEKC (NM-MEKC) within 20 minutes run. A representative electropherogram is shown in Figure 2. The elution order is consistent with their water solubility (Table 1). Methidathion elutes first and the elution continues in the order of decreasing water solubility or in the order of increasing hydrophobicities (taking the upper value in the range). The limit of detection for separation in NM MEKC is in the range 1.6-6.4 ppm and migration time relative standard deviation (RSD) is less than 1%.
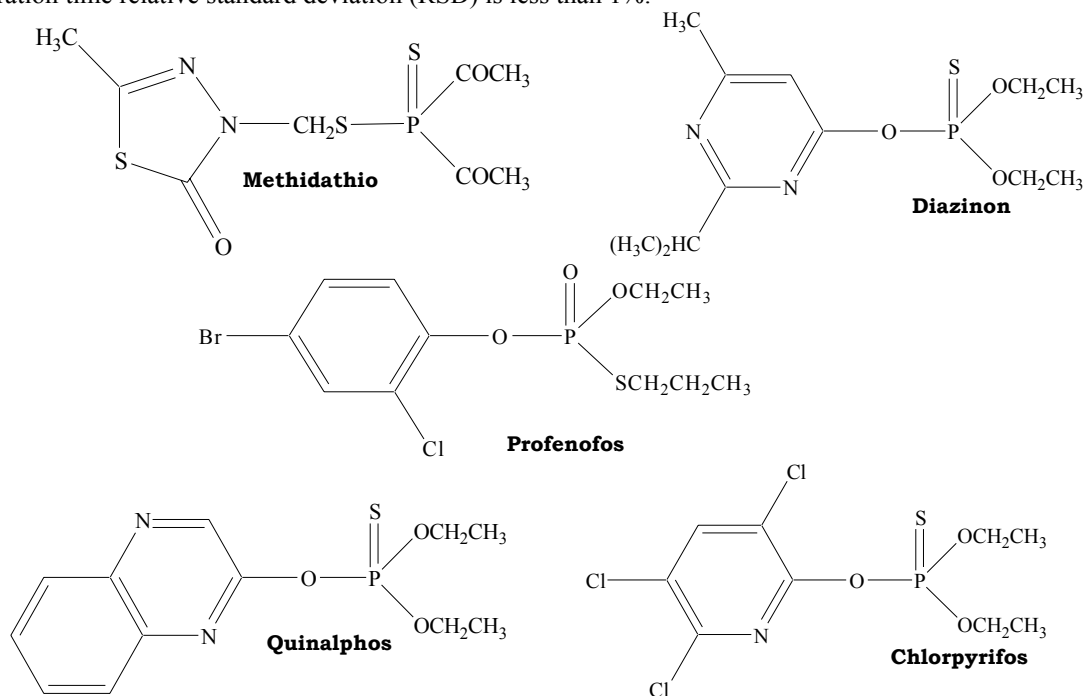
Figure 1:. Names and structures of OPPs used in the current work

Table 1: Selected properties of investigated OPPs [14-15].

Name (mp/bp, °C)	Mol. weight	S_w (g/L, 20°C)	Log K_{ow}
Methidathion (mp 39-40)	302.31	0.25	1.58-2.42
Diazinon (bp 83-84)	304.35	5.35×10^{-2}	3.02-3.86
Quinalphos(bp 142)	298.3	2.4×10^{-2}	3.04-4.44
Profenofos (bp 110)	373.64	2.0×10^{-2}	4.68-4.8
Chlorpyrifos (bp decom. 160)	350.59	0.73×10^{-3}	4.68-5.3

S_w = Solubility in water; Log K_{ow} = log value of octanol, water partition coefficient
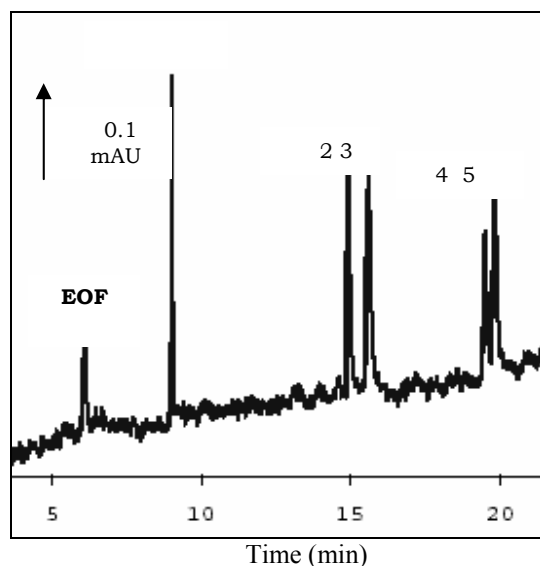
Figure 2: OPPs separation in NM-MEKC. Conditions: separation buffer contained 10 mM 1:1 Na_2HPO_4-$Na_2B_4O_7$ (pH 9.3), 10 mM SDS and 10 % 1:1 methanol-acetonitrile; applied potential 25 kV; sample prepared in 10 mM 1:1 Na_2HPO_4-$Na_2B_4O_7$ (pH 9.3), 10 mM SDS and 10 % 1:1 methanol-acetonitrile; sample injection: 10 s at 15 kV. Peaks: EOF electroosmotic flow marker (methanol); 1, methidathion (20 ppm); 2, diazinon (20 ppm); 3, quinalphos (5 ppm); 4, chlorpyrifos (5 ppm); 5, profenofos (5 ppm).

Separation in RM-MEKC

RM-MEKC was investigated for the possibility of better sensitive detection. In acidic condition the use of borate in running buffer is limited and the 20 mM phosphate buffer is found optimal in the range of 5-80 mM. The presence of organic modifier (especially methanol) in buffer and sample matrix is also found crucial but only 5-10% methanol is necessary. The concentration of SDS remained at 10 mM as before. Sample injections were performed hydrodynamically at 2.8 kPa for 10 s, as electrokinetic sample injection (here by negative potentials) causes peak disappearances. Diazinon, profenofos and chlorpyrifos co-eluted and the possible optimisation schemes could not resolve these three peaks. Runs by single compound have shown that the sensitivity of diazinon is very weak and the resolution of profenofos and quinalphos peak is poorer than the chlorpyrifos and quinalphos peaks. Therefore, only metidathion, quinalphos and chlorpyrifos were separated in acidic phosphate buffer at pH 2.5. A typical electropherogram of the separation is shown in Figure 3. The concentration of quinalphos and chlorpyrifos are the same as in Figure 2 except for methidathion where the concentration is half. In RM-MEKC, the migration order is reverse the migration order in NM-MEKC. Chlorpyrifos eluted first followed by quinalphos and finally methidathion. The three OPPs were separated in less than 18 minutes with baseline resolution. The limit of detection (LOD) in RM-MEKC is in the range of 0.63-6.7 ppm and a RSD migration time of 0.69-1.4%.

Sweeping-NM- MEKC

Sweeping is a technique for on-column sample concentration of non-polar molecules based on the analytes ability to partition into the pseudo-stationary phase (PSP) in MEKC. The effectiveness of sweeping is closely related to the analyte/s affinity for the micellar phase. The greater the affinity of the analyte toward the micelle or the higher the retention factor of the analyte, the greater the concentrating effect. Sweeping requires low EOFs and thus is often constrained to separations performed in acidic conditions. Sweeping is defined as the picking and accumulation of analytes by the PSP that fills the sample zone that bears no micelles in it during application of voltage [10]. Samples are prepared in buffer of equivalent ionic strength to the running buffer but without any micelles, and a longer plug is injected in sweeping. Utility of sweeping in various micellar systems has been tried and recently reviewed [16]. Figure 4 shows the sweeping of five selected OPPs used in this study. It is to be noted that the concentration range in sweeping is five times lower and sample injection time is five times higher than the NM-MEKC run (Figure 2 and Figure 4).

Time/min
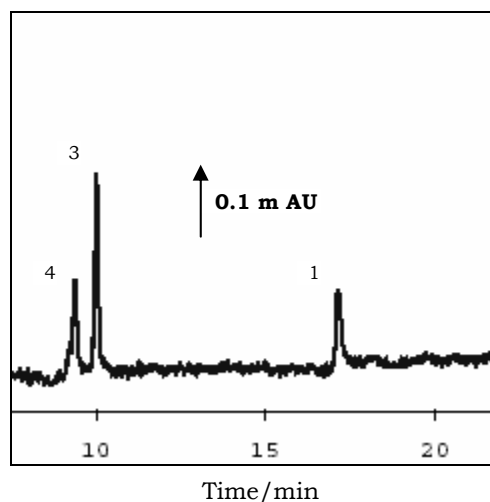
Figure 3: OPPs separation in RM-MEKC. Conditions: separation buffer contained 20 mM Na_2HPO_4 (pH 2.5), 10 mM SDS and 5 % methanol. Sample prepared in 20 mM Na_2HPO_4 (pH 9.3), 10 mM SDS and 5 % methanol; sample injection: 10 s at 2.8 kPa; Peaks: 1, methidathion (10 ppm); 3, quinalphos (5 ppm); 4, chlorpyrifos (5 ppm).

The presence of 10% organic solvents in sample matrices has actually increased the solubility of pesticides, especially for profenofos and chlorpyrifos. The question of non-suitability of sweeping phenomenon for methidathion can be explained by the theories that were proposed initially that characteristically sweeping depends on the retention factor, therefore is effective to strongly retained analytes [10, 17]. The LOD in sweeping-NM-MEKC is in the range 0.15-3.0 ppm with a migration time RSD less than 0.5%.
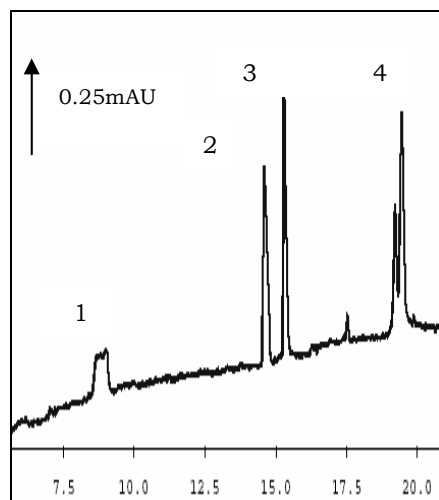
Figure 4: OPPs separation by sweeping-NM-MEKC. Conditions: separation buffer contained 10 mM 1:1 Na_2HPO_4-$Na_2B_4O_7$ (pH 9.3), 10 mM SDS and 10 % 1:1 methanol-acetonitrile; applied potential 25 kV; sample prepared in 10 mM 1:1 Na_2HPO_4-$Na_2B_4O_7$ (pH 9.3) and 10 % 1:1 methanol-acetonitrile. Sample injection: 50 s at 15 kV; Peaks: 1, methidathion (4 ppm); 2, diazinon (4 ppm); 3, quinalphos (1 ppm); 4, chlorpyriphos (1 ppm); 5, profenofos (1 ppm).

Sweeping-RM-MEKC
Sweeping can offer better results where EOF is weak when neutral hydrophobic analytes were used [10]. Therefore, sweeping in RM-MEKC was tried as an effort to further increase the sensitivity. However, in sweeping-RM-MEKC, mixture of only quinalphos and chlorpyrifos was used, as the methidathion peak cannot be uniquely focused. As the profenofos and chlorpyrifos co-eluted, therefore, another mixture of quinalphos and profenofos was also swept to compare the peak sensitivity of quinalphos with respect to both of chlorpyrifos and profenofos. Here, significantly longer sample plug (ca. 10 cm that corresponds to 400s injection at 2.8 kPa) can

be injected. Figure 5A & 5B shows the respective electropherogram. Both peaks were eluted within 10 minutes. The LODs for the quinalphos-chlorpyrifos and quinalphos-profenofos pair is in the range of 0.27-0.86 ppm and 0.19-0.29 ppm respectively.

Table 2 summarises the LODs of the various MEKC modes used in the study. As can be seen from the table, sweeping-RM-MEKC gives the lowest LOD but the separation is only limited to two of the selected OPPS in a single run. Sweeping in NM-MEKC separates all the five OPPs but the separation of methidathion in this mode is not suitable as the peak is broad and short. A better way of online concentration for methidathion would be stacking [18, 19]. Sweeping-NM-MEKC also produces low migration time RSD (less than 0.5%). Table 2 summarises the LODs for the various modes of MEKC used in the study.

Table 2: Limit of detection of various MEKC modes

| Mode	*LOD, ppm*
NM-MEKC	1.6-10.4
Sweeping-NM-MEKC	0.15-3
RM-MEKC	0.63-6.7
Sweeping-RM-MEKC	0.19-0.86
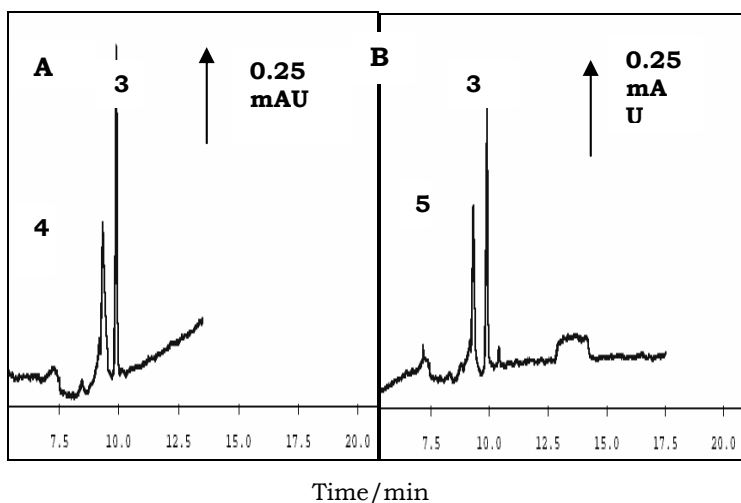
Figure 5: OPPs separation in sweeping-RM-MEKC. Conditions: separation buffer contained 20 mM Na_2HPO_4 (pH 2.5), 10 mM SDS and 5 % methanol; sample prepared in 20 mM Na_2HPO_4 (pH 9.3) and 5 % methanol; sample injection: 400 s at 2.8 kPa; Peaks: 3, quinalphos (0.25 ppm); 4, chlorpyrifos (3 ppm). (B) Conditions: As in (A); sample prepared in 20 mM Na_2HPO_4 (pH 9.3) and 5 % methanol; sample injection: 400 s at 2.8 kPa. Peaks: 3, quinalphos (0.25 ppm); 5, profenofos (1 ppm)

Conclusions

The study carried out showed that NM-MEKC is more sensitive than RM-MEKC for the selected OPPs. In both normal MEKC and RM-MEKC, sensitivity enhancements were found to be at least one order higher but sweeping-RM-MEKC is superior to sweeping-NM-MEKC. However, separation in acidic buffer is limited, as the short optimisation scheme could not resolve the co-elution of few OPPs. Instead of anionic SDS surfactant, the use of cationic surfactant and the use of coated capillaries where EOF is absent could be worth trying in further investigation of sweeping for this particular set of hydrophobic OPPs. Even though sweeping-RM-MEKC gave lowest LOD but it only separates 2 OPPs in a single run. The better mode of separation for the selected OPPS would be sweeping-NM-MEKC as it separates 4 OPPs in a single run with LOD in the sub-ppm level. Off-line extraction such as liquid-liquid extraction (LLE) or solid phase extraction (SPE) in combination with sweeping-NM-MEKC would achieve ppb levels needed for pesticide analysis.

References

1. Terabe, S., Otsuka, K., Ichikawa K., Tsuchiya, A. and Ando T., (1984) "Electrokinetic Separations with Micellar Solutions and Open-Tubular Capillaries" *Anal. Chem*. 56. 113.
2. Terabe, S., Otsuka, K. and Ando T., (1985) "Electrokinetic Chromatography with Micellar Solution and Open-Tubular Capillary" *Anal. Chem*. 57. 834.
3. Wan Ibrahim, Wan Aini, Monjurul Alam, S. M., Sulaiman, A. B., (2005) "Comparative Study of Two Common Surfactants in Micellar Electrokinetic Chromatography for the Separation of Organophosphorus Pesticides", *ACGC Chemical Research Communications*. 18. 43.
4. Wan Ibrahim, Wan Aini, Monjurul Alam, S. M., Sulaiman, A. B., (2005), "Organic modifier and Effect of Sample Matrix in the Separation of Organophosphorus Pesticides", *Mal. J. Chem*. 7(1). 26.
5. Zakaria, P., Macka, M. and Haddad, P. (2003) "Mixed-mode electrokinetic chromatography of aromatic bases with two pseudo-stationary phases and pH control" *J. Chromatogr. A,* 997. 207.
6. Farran, A., Ruiz, A., Serra, C., Aguilar, M., (1996)   "Comparative study of high-performance liquid chromatography and micellar electrokinetic capillary chromatography applied to the analysis of different mixtures of pesticides" *J. Chromatogr. A*. 737, 109.
7. Penmetsa, K. V., Leidy, R. B, Shea, D., (1996) "Herbicide Analysis by Micellar Electrokinetic Chromatography" *J. Chromatogr. A*. 745. 201.
8. Hinsmann, P., Arce, A., Rios, A., Valcarcel, M. (2000) "Determination of pesticides in waters by automatic on-line solid-phase extraction–capillary electrophoresis" *J. Chromatogr. A*. 866. 137.
9. Molina, M., Wiedmer, S. K., Jussila, M., Silva, M., Riekkola, M.L. (2001) "Use of a partial filling technique and reverse migrating micelles in the study of *N*-methylcarbamate pesticides by micellar electrokinetic chromatography–electrospray ionization mass spectrometry" *J. Chromatogr. A*. 927. 191.
10. Quirino, J. P., Terabe, S. (1998) "Exceeding 5000-fold Concentration of Dilute Analytes in Micellar Electrokinetic Chromatography" *Science.* 282.465.
11. Quirino, J. P., Terabe, S. (1998) "On-line Concentration of Neutral Analytes for Micellar Electrokinetic Chromatography. 3. Stacking with Reverse Migrating Micelles" *Anal. Chem*. 70. 149.
12. Quirino, J. P., Otsuka, K., Terabe, S. (1998) "On-line concentration of neutral analytes for micellar electrokinetic chromatography. VI. Stacking using reverse migrating micelles and a water plug" *J. Chromatogr. B*. 714. 29.
13. Quirino, J. P., Kim, J.B., Terabe, S., (2002) 'Sweeping: Concentration Mechanism and Applications to High-Sensitivity Analysis in Capillary Electrophoresis" *J. Chromatogr. A*. 965. 357.
14. Montgomery, J. H. (1997) "Agrochemicals Desk Reference", Boca Raton: Florida, USA, CRC Press, Lewis Publisher.
15. Verschueren, K. (1996) Handbook of Environmental Data on Organic Chemicals", USA: Von Nostrand, Reinhold.
16. Kim, J.B., Terabe, S., (2003) "On-line sample preconcentration techniques in micellar electrokinetic chromatography". *J. Pharm. Biomed. Anal.* 30. 1625.
17. van Zomeren, P. V., Hilhorst, M. J., Coenegracht, P. M. J., de Jong, G. J. (2000) "Resolution optimisation in micellar electrokinetic chromatography using empirical models" *J. Chromatogr. A*. 867. 247.
18. Beckers, J. L and Bocek, P. (2000) "Sample Stacking in Capillary Zone Electrophoresis: Principles, Advantages and Limitation" *Electrophoresis*. 21. 2747.
19. Wan Ibrahim, Wan Aini, Monjurul Alam, S. M., Sulaiman, A. B., (2004) "Stacking as an Online Concentration of Neutral Organophosphorus Pesticides using Micellar Electrokinetic Chromatography" *Buletin Kimia*, 20. 23.

APPLICATION OF SOLID PHASE MICROEXTRACTION (SPME) IN PROFILING HYDROCARBONS IN OIL SPILL CASES

Zuraidah Abdullah Munir*, Nor'ashikin Saim, Nurul Huda Mamat Ghani

Department of Chemistry, Faculty of Applied Sciences, Universiti Teknologi MARA
40450 UiTM Shah Alam, Selangor, Malaysia.

Abstract.
In environmental forensic, it is extremely important to have a fast and reliable method in identifying sources of spilled oil and petroleum products. In this study, solid phase microextraction (SPME) method coupled to gas chromatography-mass spectrometry was developed for the analysis of hydrocarbons in diesel and petroleum contaminated soil samples. Optimization of SPME parameters such as extraction time, extraction temperature and desorption time, was performed using 100-μm polydimethylsiloxane (PDMS) fiber. These parameters were studied at three levels by means of a central composite experimental design and the optimum experimental conditions were determined using response surface method. The developed SPME method was applied to determine the profiles of hydrocarbons in several oil contaminated soil sample. The SPME method was also used to study the effects of weathering on the profiles of hydrocarbons in unleaded gasoline, diesel and kerosene contaminated soil samples. After several days, significant losses of the lighter hydrocarbons were observed compared to the heavier ones. From these data, SPME method can be used to differentiate possible candidate sources in oil spill cases.

Introduction

Gasoline, diesel and kerosene are all created from crude oil by a variety of refining and distillation processes. Each product is produced by the combination of multiple individual hydrocarbon compounds all of which have slightly different vaporization and boiling temperatures. Gasoline is the combination of many lower boiling range compounds while the middle boiling range compounds are used in differing proportions to create kerosene and diesel. The profile of hydrocarbons in oil may hence be used to characterize the oil. This enables the identification of the candidate source of oil spill cases. In forensic chemistry, ability to identify the sources of an oil spill is very important and hydrocarbon fingerprinting method is now realized as one of the fastest and reliable method for identifying the origin of oil spill cases.

In this study, a solid phase microextraction (SPME) method coupled to gas chromatography with mass spectrometry detector (GC-MSD) was developed for analyzing the profile of several types of oils. The simplicity of operation, sensitivity, selectivity, portability, and the solvent-free nature of the SPME method makes it a powerful tool for sample introduction method for gas chromatographic analyses of organic chemicals [1]. It is based on the enrichment of analytes on a polymer or adsorbent-coated fused-silica fiber either directly to the sample or its headspace. The extraction efficiency of SPME technique is dependent on several experimental parameters such as the extraction time, extraction temperature and desorption time [2,3]. These operating parameters were optimized using an experimental design approach that consisted of three stages; identifying the factors which may affect the result of an experiment, designing the experiment so that the effects of uncontrolled factors are minimized, and using statistical analysis to separate and evaluate the effects of the various factors involved. The optimized SPME method was used to analyze the effect of weathering on three types of oils: unleaded gasoline, diesel and kerosene.

EXPERIMENTAL

Preparation of spiked sample
Three types of oil (unleaded gasoline, diesel and kerosene) were used in this study. About 1 L of each type of oil was poured into three separate plots of soil. After 2 weeks, the contaminated soil for each plot was mixed thoroughly, sieved and stored in an amber bottle at -4 ˚C until analysed for optimizing the experimental conditions.

For the weathering study, three plots of soil measuring 2' x 1.5' each were chosen for three types of oil (unleaded gasoline, diesel and kerosene). Each plot was divided into 20 small sections. About 1 L of oil sample was poured into each dedicated plot. For each analysis, 100 g of two small sections of soil were thoroughly mixed and a 5 g sample was placed in a headspace vial (10 mL volume) and capped for SPME analysis. Soil was analysed 1 day, 2 days, 1 week, 2 weeks and 1 month after oil spillage.

Solid phase microextraction (SPME)
A 100-μm polydimethylsiloxane (PDMS) fiber (Supelco, Bellafonte, Pennsylvania, USA) was conditioned in a hot GC injection port at 250 °C for 30-60 min prior to sample extraction. In the optimization study, the SPME needle was inserted through the septum of the vial and the fiber was released and exposed to the headspace of the sample at a specified temperature (maintained using a water bath) for a specified extraction time. The fiber was then withdrawn, SPME needle was removed from the headspace and immediately injected into the gas chromatography (GC) with a desorption time of 35 sec. For the weathering study, the sample was extracted at 90 °C for 45 min. The compounds were then transferred into the GC with desorption time of 35 sec.

Experimental design
Statistical software package Design-Expert 6.0.6, an expert system for the design and analysis of experiments was purchased from Stat-Ease Inc., Minneapolis. Preliminary work on the optimization of SPME for the extraction of hydrocarbons in soil using three experimental variables (extraction temperature, extraction time and desorption time) showed that the desorption time was not significant within the range 20 to 50 seconds and from the response surface analysis, optimum extraction was achieved at desorption time of 35 sec. Optimization using central composite design was then focused on two experimental variables, namely extraction temperature and extraction time. The response variables selected were the GC area count for several common compounds of unleaded gasoline, diesel and kerosene. The response variables selected were the gas chromatograph area count for tridecane, hexadecane, and octadecane. The design matrix of the central composite design is shown in Table 1. The order of these experiments was randomized to remove any systematic error.

GC-MS analysis
GC-MS were performed on Agilent Technologies 6890 Network GC System with Agilent Technologies 5973 inert Mass Selective Detector. The flow rates of gases were set to manufacturer's specifications. The column used was a HP-5MS fused silica capillary column, 30.0 m x 250 μm I.D and 0.25 μm capillary thickness. Injections were made in the splitless mode. The temperature programmed was set at an initial 60 °C for 2 min, followed by an increase of 10 °C min^{-1} to 200 °C and held for 15 min. Both the injector temperature and the detector temperature were set at 250 °C. Compounds were identified by matching their mass spectra with the NIST spectral library with a resemblance percentage above 90%.

Table 1: Central composite design of the optimization experiment

Run Order	Extraction Time (min)	Extraction Temperature ($°C$)
1	50.0	60.0
2	80.0	60.0
3	50.0	90.0
4	80.0	90.0
5	65.0	75.0
6	65.0	75.0
7	43.8	75.0
8	86.2	75.0
9	65.0	53.8
10	65.0	96.2
11	65.0	46.0
12	65.0	40.0

Results And Discussion

Optimization of SPME conditions

The results from the central composite design were fitted to a quadratic model. Analysis of variance (ANOVA) was performed on the design in order to determine which variables (A:extraction time and B:extraction temperature), if any, had a significant effect on the recovery of each compound. From the statistical analysis of the experimental design, it was found that extraction temperature was the important factor influencing the amount of hexadecane and octadecane extracted from soil. The influence of temperature on the extracted amount of hexadecane and octadecane was further studied using spiked sample with SPME extraction time of 45 min and desorption time of 35 sec. It was found that in both cases, the amount extracted increases as the extraction temperature increases, but at temperature more than 90 °C the amount of hexadecane and octadecane extracted decreases. Based on these analyses, the optimum operating conditions for SPME were: extraction time 45 min, extraction temperature 90 °C and desorption time 35 sec.

Profile of hydrocarbons in spiked sample

The optimized SPME method was applied in the extraction of unleaded gasoline, diesel and kerosene from spiked soil samples.

Gasoline is a complex mixture of hydrocarbons compounds predominantly in the range of $C_3 - C_{12}$. It is the light distillate product of petroleum containing more lower molecular weight hydrocarbons but higher fraction of both light hydrocarbons and aromatics. It contains about 41% alkanes with undecane, dodecane, tridecane and tetradecane as major compounds. In the profile of hydrocarbons in gasoline [Figure 1(a)], the hydrocarbons were eluted in the range between 5.50 min to 12.00 min.

Kerosene is a light end middle distillate of petroleum. It is composed of hydrocarbons mostly in the range of $C_9 - C_{16}$. It contains 50.5% aliphatic hydrocarbons and 30.9% naphthenes, the rest being aromatics hydrocarbons. Major compounds in kerosene are dodecane, tridecane, tetradecane and pentadecane. The hydrocarbons of kerosene were eluted in the range of 7.00 min to 13.50 min [Figure 1(b)].

iesel is a higher boiling point fraction composed of essentially C_{10} to C_{25} aliphatic hydrocarbons. It has a wide range of polyaromatic hydrocarbons such as naphthalenes and phenanthrenes. Diesel contains 55% paraffins, 24% aromatics, 12% naphthenes, and 5% olefins. It is similar in chemical composition to kerosene with the exception of additives. As shown in Figure 1, the hydrocarbon profile of diesel [Figure 1(b)] is quite similar to that of kerosene [Figure 1(c)], with additional compounds eluted up to 18.00 min.
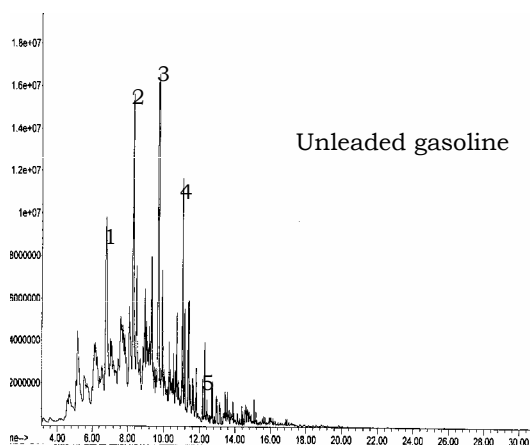
(a)
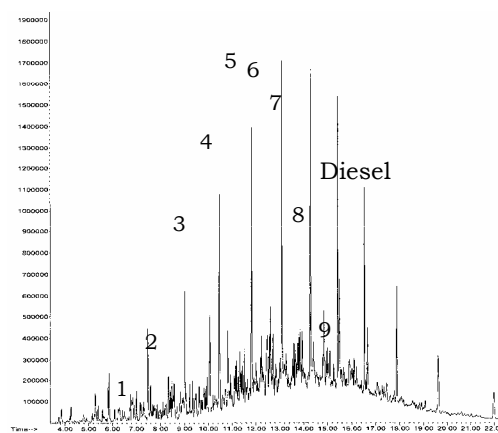
(b)
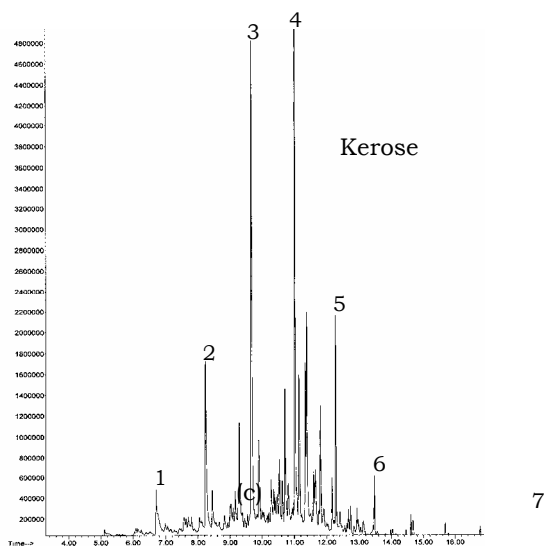
Figure 1. GC-MS total ion chromatogram of
(a) unleaded gasoline (b) diesel and (c) kerosene recovered from spiked soil sample.
Identification of compounds:
1: undecane   2: dodecane   3: tridecane
4: tetradecane 5: pentadecane 6: hexadecane 7: heptadecane 8: octadecane   9: nonadecane

Effects of weathering on oil hydrocarbon fingerprinting
When oil or petroleum products are accidentally released to the environment, they are immediately subjected to a wide variety of weathering process that can affect their chemical properties [4]. In the short term after a spill (hours to days), evaporation is the single most important and dominant weathering process, in particular for the light petroleum products. The lower boiling points components tend to volatilize more rapidly than the components of higher boiling points. The hydrocarbon profile of the spiked soil was obtained using SPME method using the optimized conditions. Figure 2 shows the profile of unleaded gasoline in soil after differing levels of weathering. It was found that after 1 week, the more volatile compounds, dodecane and tetradecane were reduced by 46% and 44% respectively while naphthalene 1, 6, 7-trimethyl was reduced by less than 1%. After 2 weeks, dodecane and tetradecane were reduced by 98% while naphthalene 1, 6, 7-trimethyl was reduced by 96% and after one month the more volatile compounds (dodecane and tetradecane) were undetected while the amount of naphthalene 1, 6, 7-trimethyl was further reduced by 96%.

(a)

(b)

(c)
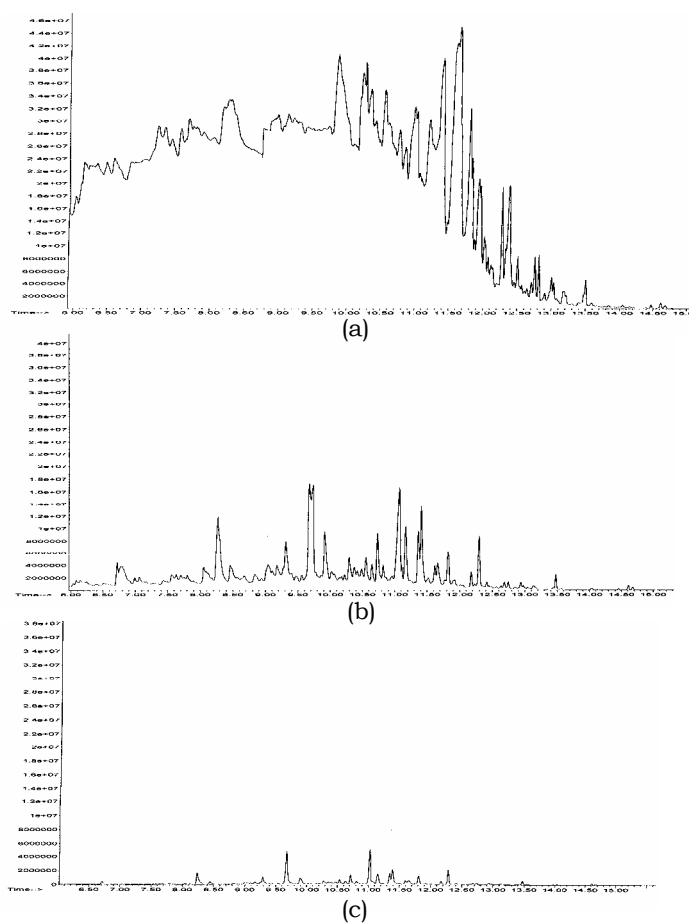
Figure 2. Hydrocarbon fingerprint of unleaded gasoline in soil sampled (a) 2 days,
(b) 1 week and (c) 2 weeks after spillage.

Figure 3 shows the profile of diesel in soil after differing levels of weathering. These chromatograms clearly showed a decreased in peak intensity due to volatilization.   It was found that after 2 weeks, the most volatile compound (dodecane) was not detected while tridecane, pentadecane and heptadecane were reduced by 93%, 92% and 88% respectively. However, after one month most compounds were reduced by 99%.
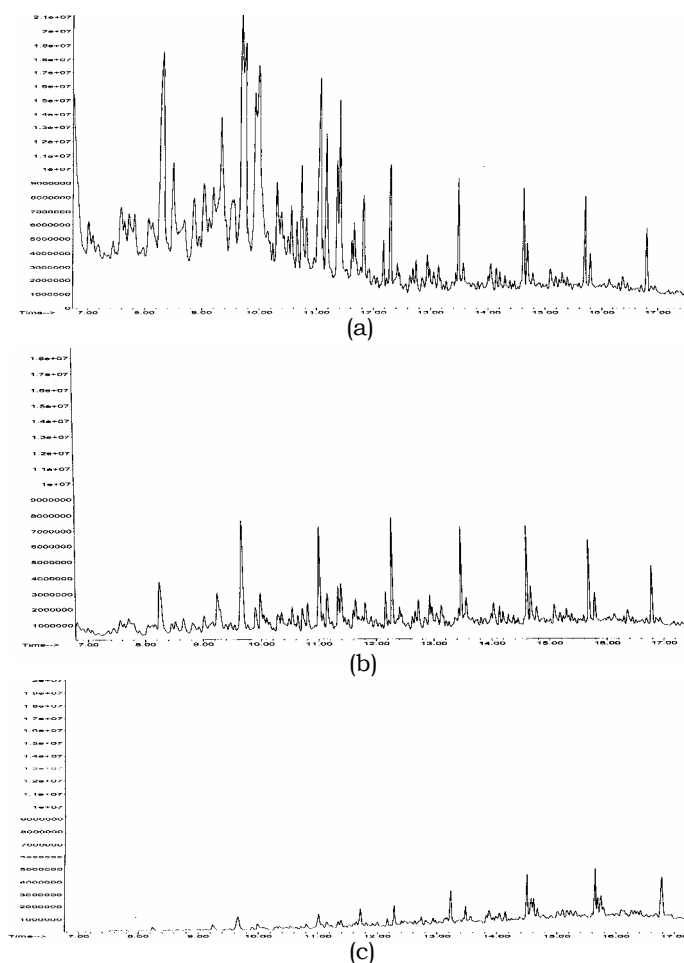
Figure 3. Hydrocarbon fingerprint of diesel in soil sampled (a) 2 days, (b) 1 week and (c) 2 weeks after spillage.

Figure 4 shows the profile of kerosene in soil after differing levels of weathering. After 2 weeks, most of the compounds in kerosene had almost disappeared. Tetradecane and pentadecane had disappeared by 96% while heptadecane had 86% evaporated. After 1 month these compounds were almost insignificant in the soil sample analysed.

CONCLUSIONS

The use of SPME-GC-MSD provides a reliable method for hydrocarbon fingerprinting of oil from soil. SPME technique, which enables the simultaneous extraction and pre-concentration steps, has been the method of choice for the analysis of these compounds in soil because it is fast, solvent-less extraction method, inexpensive and can handle the matrix sample directly. Therefore, it reduces analysis time (allowing processing a higher number of samples) and avoids loss of analytes. Study of weathered oils of spiked soil samples using SPME was able to show the change in the profiles of their chemical properties.
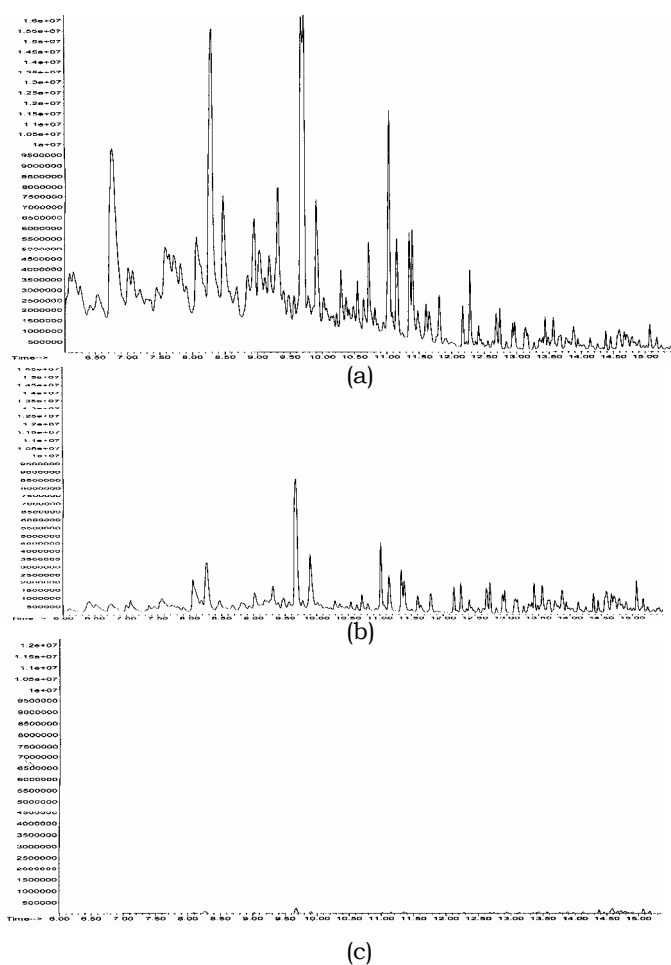
Figure 4. Hydrocarbon fingerprint of kerosene in soil sampled (a) 2 days, (b) 1 week
and (c) 2 weeks after spillage.

References
1. Hook, G.L., Kimm, G.L., Hall, T., and Smith, P.A. (2002) "Solid-phase microextraction (SPME) for rapid
    field sampling and analysis by gas chromatography-mass spectrometry (GC-MS). Trends in analytical
    chemistry, 21,8, 534-543.
2. Pawliszyn, J. (1997) Solid Phase Microextraction, Theory and Practice. New York, Wiley-VCH Inc., 97.
3. Supelco. (2001) "Control Your "T"s for Better Quantitation with Solid Phase Microextraction (SPME)".
    The Reporter, vol 19.7
4. Wang, Z., Fingas, M.F. (2003) " Development of oil hydrocarbon fingerprinting and identification
    techniques", Marine Pollution Bulletin. 47. 423-452.

HEAVY METAL CONCENTRATIONS IN THE RAZOR CLAMS (*SOLEN* SPP) FROM MUARA TEBAS, SARAWAK

Devagi Kanakaraju*, Connie anak Jios., and Shabdin Mohd Long

Faculty of Resource Sciences and Technology,
University of Malaysia Sarawak,
94300 Kota Samarahan, Sarawak

Abstract

The razor clams (*Solen* spp) or locally known as 'ambal' in Sarawak collected from Muara Tebas were studied for their heavy metals contents in tissues and shells. Sediment samples were also tested for their metal contents. Concentrations of Pb, Fe, Zn, Cu, Cd and Mn were determined by using Flame Atomic Absorption Spectrophotometer (FAAS). Tissues of razor clams showed highest concentrations of Fe and Zn, while shells accumulated highest concentrations of Pb and Mn. The lowest metal concentrations found were Cu and Cd. In general, the levels of metals in 'ambal' were within the permissible limit recommended by international standard, the Food and Agricultural Organization (FAO). However, the study revealed that the sediments at Muara Tebas fall under the category of slightly polluted (for Pb) when compared to the guidelines suggested by United States Environment Protection Agency (USEPA).

Abstrak

Razor clam **(***Solen* spp) atau lebih dikenali sebagai ambal di Sarawak telah dipungut dari Muara Tebas untuk kajian kandungan logam berat dalam bahagian tisu dan cengkerangnya. Sampel sedimen juga telah dikaji kandungan logam beratnya. Kepekatan logam Pb, Fe, Zn, Cu, Cd dan Mn telah ditentukan dengan menggunakan Spektroskopi Serapan Atom Nyala (FAAS). Bahagian tisu ambal mengandungi kepekatan Fe dan Zn yang tertinggi manakala cengkerang pula menunjukkan kepekatan Pb dan Mn yang paling tinggi. Kepekatan logam yang paling rendah ialah Cu dan Cd. Secara keseluruhannya, tahap kepekatan logam dalam ambal berada dalam had yang disyorkan oleh piawai *Food and Agricultural Organization* (FAO). Walau bagaimanpun, kajian ini menunjukkan bahawa sedimen di Muara Tebas berada dalam kategori sedikit tercemar (untuk Pb) apabila perbandingan dibuat dengan piawai yang disyorkan oleh *United States Environment Protection Agency* (USEPA).

Introduction

Various species of edible bivalve mollusks such as clams, oyster and cockles are found on the mangrove mudflats and intertidal sandy beaches in Peninsula Malaysia as well as Sarawak. Razor clam (*Solen* spp) or locally known as "ambal" is found abundantly in the intertidal sandy beaches in Kuching and Samarahan Division of Sarawak. There are three different species of Ambal in the genus *Solen* that commonly found in Sarawak [1]. The three species are Solen corneus, Solen species and Solen vagina and they are locally known as "Ambal Biasa', 'Ambal Jernang', and 'Ambal Riong' respectively.

Heavy metals pollution has been a hot issue in environmental studies for many years. Even though, metals occurs naturally in the environment but due to the anthropogenic inputs which originate from various human activities the concentrations have been rising. Heavy metals tend to accumulate in the food chain and eventually will be consumed by organisms. Bivalve mollusks are well-known to accumulate heavy metals and have been widely used as bioindicator for monitoring heavy metal pollution in aquatic environment [2-4]. There is very little documented information available about the metal contents in 'ambal' despite the popularity as a source of seafood item in Sarawak. Owing to limited studies on 'ambal', various aspects on 'ambal' are still unexplored such as the feeding behavior, biology and population dynamics. A study was conducted on the stock assessment and some biology perspective of 'ambal' [5]. Some work was also done on the bacterial density and quality of water in 'ambal' from Asajaya Laut and Kampung Buntal, Sarawak [6].

Thus, this study was undertaken to determine the amounts of heavy metals (Pb, Fe, Zn, Cu, Cd and Mn) in tissues and shells of razor clam and sediments at Muara Tebas. The suitability of 'ambal' as a seafood item was evaluated by comparing with an international standard (FAO).

Experimental

Sample Collection
This study was carried out along the beach at Muara Tebas during low tide in the month of September and November 2004, the harvesting periods of 'ambal' (Figure 1). The sampling stations was divided into 3 positions namely low tide station (S1), middle tide station (S2 and S3) and high tide station (S4, S5).
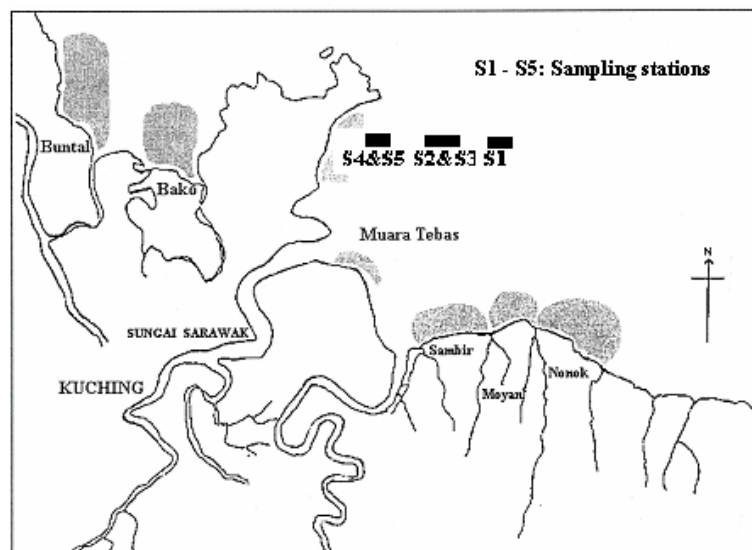
Figure 1 : Map showing the sampling stations at Muara Tebas

The razor clams were collected using long, elongated, slender stick of four feet in length a mixture of limestone powder, ashes and salt. Razor clam samples ranging between 3.0 and 10.0 cm in length were collected. About 10-15 individuals were collected at each station to prepare a pooled sample. Immediately after collection, the samples were washed with seawater to remove sediment before being kept in the labeled glass jar. The samples were kept in a cool box. Sediment samples were collected from each sampling stations around the area inhabited by the razor clam using the PVC tubes. Three to four random surface sediment samples were collected from each station were divided into two sub-ranges, 0 - 5 cm and 5 - 10 cm.

Chemical analysis
Razor clam samples were thawed and carefully washed with tap water and deionized water to remove any extraneous material. Tissues and shell samples were freeze-dried. Subsequent to the drying process, the samples were ground to fine powder using pestle and mortar and stored in polyethylene bottles. The composite homogenates were divided into three sub-samples for replicate analyses.

Acid wet digestion method modified from [2] was employed to the razor clam samples. One gram of tissue sample was weighed and digested with 6 ml of concentrated nitric acid (63 %) and 1 ml of 30 % hydrogen peroxide using hot plate digester. While for the shell samples, one gram of shell samples was digested with the mixture of 2 ml of concentrated nitric acid (63 %), 5 ml of concentrated hydrochloric acid (37 %) and 1 ml of 30 % hydrogen peroxide. The samples were dissolved for one hour and then digested for another one hour. The digested samples were filtered and diluted to 50 ml with deionized water.
Oven-dried sediment samples were ground to the size of 50 mesh. One gram of sediment samples was digested for three hours with freshly prepared mixture 1:3 of 20 ml of nitric acid and hydrochloric acid using hot plate digester. The levels of heavy metals in the filtrate were determined with Flame Atomic Absorption Spectrophotometer (Perkin – Elmer Model 3110). The quantitative measurement was made using calibration curves obtained with five standard solutions of each elements analyzed in this study. Fresh working standard solutions were prepared using AAS stock solution (1000 ppm). Acid blank for every batch was analyzed to evaluate any contamination. All results reported in this study are expressed in dry weight.

Statistical Analysis

One-way analysis of Variance (ANOVA) is used to study differences in metal concentrations at different sampling period and at two different depths for sediments. Correlation coefficient (r) was used to test the relations between the concentrations of metals in sediments with tissues and shells of razor clam.

Results and Discussions

Metals concentrations in sediments

The pH of the surrounding sediments of Muara Tebas was found to be alkaline (8.13 – 8.36) (Table 1). Temperature and dissolved oxygen (DO) was in the range of 28.5 – 33.7 ^{o}C and 5.2 -7.4 mg/L. Metals contents in sediments at two different depths (0 – 5 cm and 5 – 10 cm) Muara Tebas are shown in Table 2.

Table 1. Mean pH, temperature and DO of sediments at Muara Tebas

Station	pH	Temperature (^{o}C)	DO (mg/L)
Low tide	8.13	28.5	7.4
Mid tide	8.36	30.3	5.2
High tide	8.30	33.7	6.6

Table 2. Metal contents (µg/g dry wt) in sediments from Muara Tebas

	Pb		Cu		Fe		Zn		Cd	
	0-5	5-10	0-5	5-10	0-5	5-10	0-5	5-10	0-5	5-10
S1*	36.67 ± 0.03	35.83 ± 0.03	5.17 ± 0.01	4.67 ± 0.01	529.17 ± 0.05	477.67 ± 0.05	32.50 ± 0.01	34.33 ± 0.01	3.33 ± 0.01	3.33 ± 0.01
S2	35.50 ± 0.04	36.50 ± 0.06	4.33 ± 0.01	4.67 ± 0.01	520.33 ± 0.02	499.00 ± 0.04	32.50 ± 0.01	33.33 ± 0.01	2.83 ± 0.01	1.83 ± 0.01
S3	51.83 ± 0.04	53.17 ± 0.06	5.17 ± 0.01	5.67 ± 0.01	557.00 ± 0.04	523.67 ± 0.01	37.67 ± 0.01	32.83 ± 0.01	1.67 ± 0.01	1.67 ± 0.01
S4	41.83 ± 0.06	44.50 ± 0.08	5.17 ± 0.01	5.67 ± 0.01	546.33 ± 0.03	484.00 ± 0.03	32.67 ± 0.01	35.33 ± 0.01	2.67 ± 0.29	2.67 ± 0.01
S5	38.17 ± 0.05	45.17 ± 0.08	5.17 ± 0.01	4.67 ± 0.01	497.83 ± 0.02	463.67 ± 0.03	29.33 ± 0.01	29.17 ± 0.01	1.67 ± 0.01	1.83 ± 0.01
S1**	49.17 ± 0.07	47.83 ± 0.03	5.17 ± 0.01	4.33 ± 0.01	534.17 ± 0.04	514.83 ± 0.05	30.83 ± 0.02	30.67 ± 0.01	1.50 ± 0.01	2.00 ± 0.01
S2	53.83 ± 0.07	54.17 ± 0.06	4.83 ± 0.01	5.83 ± 0.01	571.50 ± 0.02	571.50 ± 0.05	31.50 ± 0.01	35.17 ± 0.01	1.83 ± 0.01	2.50 ± 0.01
S3	51.83 ± 0.04	53.17 ± 0.06	5.17 ± 0.01	5.67 ± 0.01	546.33 ± 0.04	523.67 ± 0.01	37.67 ± 0.01	32.83 ± 0.01	1.67 ± 0.01	1.67 ± 0.01
S4	54.50 ± 0.03	56.33 ± 0.05	5.67 ± 0.01	5.67 ± 0.01	566.50 ± 0.03	573.33 ± 0.06	34.83 ± 0.01	33.50 ± 0.01	1.83 ± 0.01	2.33 ± 0.01
S5	52.50 ± 0.04	53.67 ± 0.04	4.33 ± 0.01	4.33 ± 0.01	539.33 ± 0.05	527.83 ± 0.05	33.67 ± 0.01	30.33 ± 0.01	1.33 ± 0.01	0.83 ± 0.01

S1* : Data obtained during first sampling
 S1**: Data obtained during second sampling

The amounts of Fe, Pb, Zn, Cu and Cd was found in the range from 463.67 µg/g – 573.33 µg/g, 35.50 µg/g – 56.33 µg/g, 29.17 µg/g – 37.67 µg/g, 4.33 µg/g – 5.83 µg/g and 0.83 µg/g – 3.33 µg/g respectively. Fe occurs in the highest level whereas Cd was found in the least amount. Fe is naturally abundant in the earth's crust. There

was no much difference observed for the metals concentrations at two different depths. The amounts were quite close for both depths. Even, statistical analysis also showed that there was no significant difference between the depths ($p < 0.05$). The sediments were assessed by doing comparison with United States Environment Protection Agency (USEPA) guidelines [7].

The sediments at Muara Tebas fall under the category slightly polluted with Pb (40-60 µg/g). This could be due to the anthropogenic sources which contribute to Pb contamination. The major source of Pb in the environment is related to the burning of fossil fuels and via atmosphere [8]. Hence, Pb contamination in Muara Tebas may be resulted from burning of fossil fuels from boats used for fishing and also leisure activities at Kuching Bay.

Table 3. USEPA guidelines classification for sediments (µg/g)

Elements	Unpolluted	Slightly polluted	Heavily polluted
Pb	<40	40-60	>60
Cu	<25	25-50	>50
Zn	<90	90-200	>200
Cd	-	-	-

Metal concentrations in razor clam

Table 4 represent the metal concentrations and standard deviation of six elements analyzed in 'ambal' collected from Muara Tebas. The metals contents in tissues and shells of 'ambal' at Muara Tebas revealed major variations. It was further proved by statistical analysis ($p < 0.05$) which showed that there were significant differences of Pb, Fe, Zn, Cu, Cd and Mn in tissues and shells. The most abundant elements in tissues of razor clam were Fe and Zn which ranged from 276.17 µg/g – 1161.00 µg/g and 72.17 – 97.00 µg/g respectively. The shells indicated the highest levels of Pb (52.00 µg/g–58.17 µg/g) followed by Mn (30.83 µg/g – 67.00 µg/g), Cu (12.67 µg/g – 23.83 µg/g) and Cd (7.33 µg/g – 9.00 µg/g).

The wide variations of metals in two different parts of 'ambal' could be expressed by the complex relationship between environmental concentrations and bioaccumulation [9]. There are various factors which influence the metals accumulation in bivalves. Among the factors known include metal bioavailability, season of sampling, size, hydrodynamics of the environment and reproductive cycle [3].

Cd was also found in a very trace amount in tissues and shells likewise in sediments. There was moderate significant negative correlation for Cd in shells with sediments at Muara Tebas (r = - 0.51., P = 0.00). This may be attributed to the low bioavailability of Cd in sediments and water environment. Metals concentrations obtained in this study were compared with the international standards for metals in mollusks/shellfish compiled by Food and Agricultural Organization (FAO) of the United Nations [9] (Table 4). All metals were within the regulated limits except for Pb contents in shells. FAO permissible limit for Pb was 5 – 30 µg/g and the results obtained ranged 52.00 µg/g – 58.17 µg/g. The Pb concentration possibly originated from the surrounding sediments as Pb was found in slightly polluted range. However, poor correlation (r = 0.17) was attained between Pb concentrations in shells and sediments at Muara Tebas. The results need to be further verified with other techniques as contamination could have occurred during the sample preparation and analysis.

Ambal' collected from Muara Tebas can be classified as safe for human consumption even though the level of Pb in the shells exceeded the permissible limit as 'ambal' are famous for their tissues. The shells are thrown away during the cooking process and only the tissues are consumed.

Table 4. Metal concentrations in tissues and shells (in µg/g dry weight) at Muara Tebas

	Pb		Cu		Fe		Zn		Cd		Mn	
	Tissue	Shell	Tissue	Shell	Tissue	Shell	Tissue	Shell	Tissue	Shell	Tissue	Shell
S1*	15.00 0.02	56.83 ± 0.04	2.67 ± 0.01	19.50 ± 0.01	289.33 ± 0.02	165.17 ± 0.02	77.83 ± 0.01	11.67 0.01	1.17 ± 0.01	7.33 ± 0.01	16.17 ± 0.01	47.17 ± 0.01
S2	15.33 ± 0.08	52.17 ± 0.01	2.17 ± 0.01	22.17 ± 0.01	298.00 ± 0.01	171.83 ± 0.02	85.50 ± 0.01	7.83 ± 0.01	1.17 ± 0.01	7.33 ± 0.01	19.17 ± 0.01	64.83 ± 0.01
S3	16.17 ± 0.07	56.00 ± 0.02	2.17 ± 0.01	22.00 ± 0.01	276.17 ± 0.01	105.83 ± 0.01	86.17 ± 0.01	7.33 ± 0.01	1.17 ± 0.01	7.33 ± 0.01	15.17 ± 0.01	38.67 ± 0.01
S4	15.33 ± 0.03	58.17 ± 0.01	2.33 ± 0.01	21.17 ± 0.01	312.50 ± 0.03	97.67 ± 0.02	82.17 ± 0.01	6.17 ± 0.01	0.67 ± 0.01	7.83 ± 0.01	18.67 ± 0.01	37.67 ± 0.01
S5	15.50 ± 0.07	55.33 ± 0.06	10.67 ± 0.01	20.67 ± 0.01	377.83 ± 0.04	157.67 ± 0.01	75.67 ± 0.01	4.33 ± 0.01	1.83 ± 0.01	8.67 ± 0.01	16.17 ± 0.01	67.00 ± 0.01
S1**	9.67 ± 0.02	52.17 ± 0.02	4.33 ± 0.01	12.83 ± 0.01	782.50 ± 0.06	95.17 ± 0.01	78.83 ± 0.01	6.33 ± 0.01	2.17 ± 0.01	8.33 ± 0.01	24.17 ± 0.01	30.83 ± 0.01
S2	9.50 ± 0.03	56.33 ± 0.03	4.67 ± 0.01	12.67 ± 0.01	940.33 ± 0.08	143.00 ± 0.02	83.17 ± 0.01	7.83 ± 0.01	1.17 ± 0.01	7.83 ± 0.01	24.67 ± 0.01	35.67 ± 0.01
S3	14.83 ± 0.04	54.83 ± 0.02	4.33 ± 0.01	16.83 ± 0.01	1161.00 ± 0.03	134.17 ± 0.03	72.17 ± 0.01	17.67 ± 0.01	2.00 ± 0.01	8.17 ± 0.01	41.83 ± 0.01	31.33 ± 0.01
S4	9.50 ± 0.04	55.17 ± 0.05	3.83 ± 0.01	23.83 ± 0.01	459.17 ± 0.01	82.67 ± 0.01	97.00 ± 0.04	19.17 ± 0.01	2.83 ± 0.01	8.67 ± 0.01	15.33 ± 0.01	40.33 ± 0.01
S5	13.83 ± 0.03	52.00 ± 0.01	4.17 ± 0.01	19.33 ± 0.01	323.83 ± 0.06	125.83 ± 0.01	89.67 ± 0.01	20.17 ± 0.01	2.17 ± 0.01	9.00 ± 0.01	11.33 ± 0.01	43.33 ± 0.01
FAO limits	5-30 µg/g		50-150 µg/g		-		200-500 µg/g		10 µg/g		-	

S1* : Data obtained during first sampling   S1**: Data obtained during second sampling

Conclusions

Accumulation of the selected metals Pb, Fe, Zn, Cu, Cd and Mn in the tissues and shells of razor clam was evaluated. Tissues showed highest accumulation of essential elements like Fe and Zn while shells accumulated highest concentrations of Pb and Mn. The level of Pb in shells exceeded the limit designated by FAO.

Acknowledgment

References

1. Pang, S.C., 1992. Razor clams (*Solen* sp) Fishery in Sarawak. Jabatan Perikanan Kementerian Pertanian Malaysia, Kuching Sarawak, 1 - 6.
2. Lau, S., Mohamed, M., Tan Chi Yen, A. and Su'ut, S., 1998. Accumulation of Heavy Metals in Freshwater Mollusks. The Science of the Total Environmental 214, 113 - 121.
3. Otchere, F.A., 2003. Heavy metals concentrations and burden in the bivalves (*Anadara (Senilia) senilis, Crassostrea tulipa and Perna perna*) from Lagoons in Ghana:Model to describe mechanism of accumulation/excretion. African Journal of Biotechnology 2(9), 280 - 287.
4. Liang, L.N., He, B., Jiang, G.B., Chen, D.Y. and Yao, Z.W., 2004. Evaluation of Mollusks as Biomonitors to investigate Heavy Metal Contaminations along the Chinese Bohai Sea. Science of the Total Environmental 324, 105 - 113.
5. Pang, S. C., 1993. A Study of Some Aspects of the Biology and Stock Assessment of Razor clam (*Solen brevis*) in Sarawak, Malaysia. Fishery Research Institute Report, Kuching, Sarawak.

6. Apun, K., Ridan, T. M. M. and Bujang, B., 2001. Microbiological quality of Razor clam (ambal) and Water of their Growing Area. Proceedings of the Regional Conference on Natural Resources and Environmental Management, 18-20 October 2001, Kuching, Sarawak.

7. Cheggour, M., Chafik, A., Langston, W.J., Burt, G.R., Benbrahim, S. and Texier, H., 2001.Metals in Sediments and the Edible Cockle *Cerastoderma edule* from two Moroccon Atlantic lagoons: Moulay Bou Selham and Sidi Moussa. Environmental Pollution 115, 149-160.

8. Avelar, W. E. P., Mantelatto, F. L. M., Tomazelli, A. C., Silva, D. M. L., Shuhama, T. and Lopes, J. L. C., 2000. The Marine Mussel *Perna Perna* (Molluscsa, Bivalvia, Mytilidae) as an Indicator of   Contamination of Heavy Metals in the Ubatuba Bay, Sao Paulo, Brazil. Water, Air and Soil Pollution 118, 65-72.

9. Wagner, A. and Boman, J., 2004. Biomonitoring of Trace Elements in Vietnamese Freshwater Mussels. Spectrochimica Acta Part B: Atomic Spectroscopy 59, 1125-1132.

HUBUNGAN PERMINTAAN KLORIN DENGAN KUALITI AIR MENTAH

Lim Fang Yee & Md. Pauzi Abdullah

*Pusat Pengajian Sains Kimia & Teknologi Makanan, Fakulti Sains & Teknologi,
Universiti Kebangsaan Malaysia, 43600 Bangi, Selangor.*

Kata Kunci: Permintaan klorin, ammonia, jumlah karbon organik, lembangan Sungai Semenyih

Abstrak.

 Klorin sebagai agen disinfeksi dalam air minuman telah digunakan secara meluas sejak ia berjaya dipraktikkan dalam bekalan air minuman di Jersey City pada 1908. Kebanyakan loji rawatan air di Malaysia menggunakan klorin sebagai agen disinfeksi untuk membunuh patogen dan bahan pencemar yang membahayakan para pengguna. Oleh kerana klorin merupakan agen disinfeksi yang kuat, ia boleh bertindak balas dengan komponen-komponen kimia seperti mangan, ferum, hidrogen sulfida, ammonia, dan fenol dalam air. Tindak balas ini berlaku dengan pantas, dan klorin tidak akan bertindak sebagai agen disinfeksi sehingga semua sebatian organik dan inorganik yang hadir dalam air telah bertindak balas dengan klorin. Komponen-komponen kimia yang boleh bertindak balas dengan klorin akan menyebabkan permintaan klorin dalam air. Permintaan klorin dalam air perlu dipenuhi sebelum klorin bebas terhasil. Klorin bebas ini seterusnya akan mengurai kepada asid hipoklorus dan ion hipoklorit yang penting dalam proses disinfeksi untuk membunuh patogen dan bahan pencemar dalam air. Kebanyakan loji rawatan air mengekalkan klorin bebas sebanyak 0.2 mg/l dalam sistem pengagihan sebelum sampai kepada pengguna. Kajian ini melibatkan penentuan parameter-parameter yang dipercayai boleh bertindak balas dengan klorin di sembilan stesen pensampelan di sepanjang Sungai Semenyih dan empat stesen di loji rawatan air. Parameter-parameter yang ditentukan terdiri daripada ammonia, sianida, sulfida, fenol, fosforus, nitrit, mangan, ferum, dan karbon organik jumlah. Secara keseluruhannya, kajian ini mendapati ammonia dan karbon organik jumlah merupakan sebatian yang paling banyak bertindak balas dengan klorin untuk menghasilkan trihalometana dan kloramina. Selain itu, kepekatan sebatian-sebatian sianida, sulfida, fenol, fosforus, nitrit, mangan, dan ferum juga menurun selepas proses pengklorinan. Hasil kajian ini boleh digunakan menilai tahap permintaan klorin di Sungai Semenyih.

Pengenalan

Disinfeksi merupakan proses yang paling penting dalam proses rawatan air mentah kerana proses ini berupaya membasmi penyakit yang disebabkan oleh mikroorganik patogen [1]. Sebarang bentuk proses disinfeksi adalah perlu untuk menyingkirkan mikroorganisma yang boleh membahayakan. Klorin digunakan secara meluas sebagai disinfektan kerana ianya murah dan berkesan. Hampir semua loji rawatan air di Malaysia menggunakan klorin dalam proses disinfeksinya [2-5]. Di sebalik keberkesanan proses pengklorinan bagi membunuh patogen dalam air, pengklorinan didapati dapat menjanakan hasil sampingan seperti trihalometana (THM) yang merupakan sebatian halo-organik yang terbukti bersifat karsinogenik dan mutagenik [6,7]. Klorin yang digunakan sebagai agen disinfeksi dalam proses rawatan air telah menyebabkan isipadu air terawat mengandungi sebatian berklorin yang tinggi [8].

Klorin merupakan agen pengoksidaan yang kuat. Gas klorin sangat larut dalam air dan dapat membentuk asid hipoklorus (HOCl) dan ion hipoklorit (OCl$^-$) dengan cepat [9]. Klorin bebas ialah jumlah HOCl dan OCl$^-$ yang hadir. HOCl adalah agen disinfeksi yang lebih cekap daripada OCl$^-$. Keberkesanan pembasmian kuman HOCl adalah 40 kali lebih cekap daripada OCl$^-$. Klorin adalah kurang berkesan sebagai disinfektan pada pH di bawah 6 dan pH yang melebihi 8 [10]. Klorin boleh mengoksidakan banyak komponen yang hadir dalam air. Apabila klorin dilarutkan dalam air, sebatian organik dan agen penurun yang lain akan bertindak balas dengan klorin bebas ini dan menyebabkan permintaan klorin dalam air. Klorin yang selebihnya akan memusnah dan merosakkan protein dan asid nukleik mikroorganisma dalam air [11,12]. Kepekatan sebatian organik dan pepejal terampai yang tinggi dalam air mentah sering menyebabkan permintaan klorin yang tinggi dan mengurangkan keberkesanan klorin sebagai disinfektan [13,14]. Akibatnya, klorin yang lebih perlu didoskan untuk membunuh patogen dalam air.

Disinfeksi air minum dengan menggunakan klorin akan menghasilkan bahan sampingan yang boleh memudaratkan kesihatan orang awam [15,16]. Kebimbangan yang dinyatakan akhir-akhir ini tentang adanya kepekatan surihan sebatian organoklorin dalam air adalah penyebab barah apabila diuji pada dos yang tinggi terhadap haiwan. Kewujudan trihalometana dalam air minum di Malaysia boleh membimbangkan masyarakat kerana ianya berhubungkait dengan kesihatan manusia [17]. Penemuan saintifik ini telah menyebabkan isu THM menjadi satu perkara yang dibimbangkan dan perlu diberi penekanan dan perhatian pada peringkat kebangsaan dan juga antarabangsa [18]. Selain itu, agen penurun yang hadir dalam air boleh bertindak balas secara reaktif dengan klorin. Permintaan klorin ini mesti dipenuhi sebelum klorin dapat bertindak sebagai disinfektan. Adalah perlu supaya kajian dan penyelidikan dibuat dengan memberikan kawalan proses yang berhati-hati dan penggunaan dos klorin yang sesuai dalam proses disinfeksi. Penggunaan dos klorin yang optimum supaya tidak terlalu kurang dan tidak menentu luar daripada yang diperlukan adalah penting. Kajian ini bertujuan untuk mengenalpasti komponen-komponen yang boleh bertindak balas dengan klorin serta punca-puncanya, supaya pengurusan dan tindakan dapat diambil untuk menyingkirkan pelopor yang boleh menyebabkan permintaan klorin.

Experimen

Kawasan Kajian
Loji pembersihan air Sungai Semenyih terletak di Presint 19, Putrajaya. Loji ini mendapatkan sumber air mentahnya dari Sungai Semenyih. Air mentah dipamkan melalui saluran paip sepanjang 8 km dari Jenderam Hilir ke loji pembersihan air untuk proses perawatan.

Pensampelan air dilakukan di empat stesen di dalam loji pembersihan air. Keempat-empat stesen ini adalah mengikut susunan proses rawatan air, iaitu air mentah, air mendap, air tapisan, dan air bersih. Pendosan klorin dilakukan selepas air dituraskan dengan pasir deras untuk menyingkirkan jisim pepejal dalam air, iaitu klorin ditambahkan ke dalam air tapisan. Selepas proses pengklorinan, air disalurkan ke tangki air bersih dan seterusnya dipam ke kolam imbang. Dari kolam imbang, air bersih disalurkan secara graviti ke kolam agihan sebelum disalurkan kepada pengguna.

Jadual 1 Lokasi Stesen Pensampelan di Sungai Semenyih

Stesen	Latitud	Longitud	Lokasi
SS1	N 03° 04.572'	E 101° 53.034'	Empangan
SS2	N 03° 00.520'	E 101° 52.125'	Sungai Semenyih
SS3	N 02° 56.866'	E 101° 50.891'	Sungai Saringgit
SS4	N 02° 56.615'	E 101° 50.808'	Sungai Semenyih
SS5	N 02° 54.308'	E 101° 48.690'	Sungai Rinching
SS6	N 02° 54.213'	E 101° 48.533'	Sungai Semenyih
SS7	N 02° 53.160'	E 101° 48.373'	Sungai Beranang
SS8	N 02° 53.021'	E 101° 47.560'	Sungai Semenyih
SS9	N 02° 53.021'	E 101° 49.163'	Stesen Pam Air Mentah

Sumber air mentah iaitu Sungai Semenyih mengalir melalui tiga mukim, iaitu Hulu Semenyih, Semenyih, dan Beranang. Dalam kajian untuk menentukan punca-punca yang menyebabkan permintaan klorin, sebanyak sembilan stesen telah dipilih bagi mewakili kawasan kajian. Terdapat beberapa aktiviti yang dijalankan di lembangan Sungai Semenyih yang berpotensi mencemarkan Sungai Semenyih, iaitu perindustrian, pembinaan, pertanian, dan penternakan. Kawasan kajian mempunyai topografi yang seimbang dengan adanya kawasan landai, beralun, dan tanah tinggi. Lebih kurang 65 % lembangan Sungai Semenyih adalah bergunung-ganang dan kawasan hilir sungai adalah berpaya. Semua stesen pensampelan yang tersebut di atas ditunjukkan dalam rajah 1. Pemilihan sembilan stesen pensampelan ini adalah berasaskan kepada beberapa kriteria dan kesesuaian pensampelan dilakukan. Selain itu, kehomogenan air, bentuk muka bumi, sumber pencemaran, serta pertemuan anak-anak sungai dengan Sungai Semenyih merupakan faktor yang dipertimbangkan dalam pemilihan stesen-stesen seperti yang ditunjukkan dalam Jadual 1.
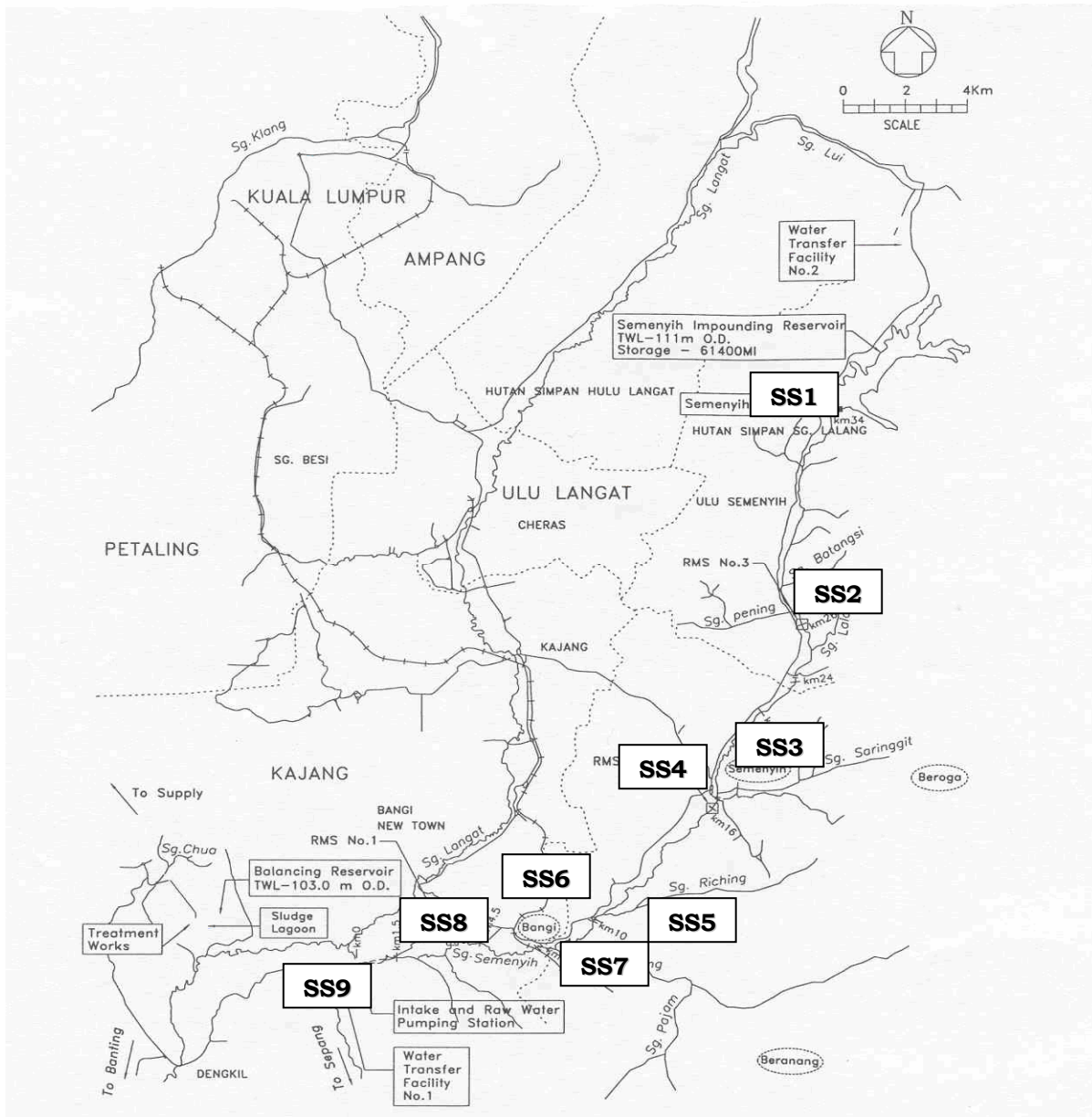
Rajah 1   Peta kawasan kajian dan stesen-stesen pensampelan di lembangan Sungai Semenyih

Bahan dan Kaedah

Dalam kajian ini, sebanyak 14 kali pensampelan telah dijalankan antara bulan Disember 2004 hingga bulan Julai 2005. Sampel diambil dengan menggunakan kaedah "grab sampling", iaitu dengan menggunakan bekas untuk menimba air di permukaan sungai atau lebih kurang 1 m dari permukaan sungai. Empat botol sampel yang berisipadu 1 liter digunakan, iaitu dua botol kaca dan dua botol plastik. Semasa pensampelan air, beberapa parameter kualiti air diukur secara *in situ*. Pengukuran parameter *in situ* dilakukan dengan menggunakan YSI 556 Multiprobe System (MPS) dan Ultrameter keluaran syarikat Myron L. Company. Parameter-parameter yang diukur secara *in situ* ialah suhu, konduktiviti, kemasinan, jumlah pepejal terlarut, oksigen terlarut, pH, klorofil A, dan keupayaan pengoksidaan dan penurunan.

Parameter-parameter kimia seperti ammonia, sianida, sulfida, fenol, fosforus, nitrit, karbon organik jumlah, ferum, dan mangan dianalisis di makmal kimia Universiti Kebangsaan Malaysia. Semua sampel dianalisis secepat mungkin setelah pensampelan dilakukan. Dalam kes dimana sampel air tidak dapat dianalisis dengan

serta merta, sampel air diawet dengan menggunakan asid sulfurik atau asid nitrik kepada pH 2 dan disimpan pada suhu 4 °C. Kesemua parameter ini dianalisis mengikut kaedah piawai yang telah ditetapkan [19].

Keputusan dan Perbincangan

Permintaan klorin terhasil daripada pelbagai tindak balas dimana klorin digunakan untuk mengoksidakan komponen-komponen yang hadir dalam air. Data yang terhad selama lapan bulan ini menunjukkan permintaan klorin di loji rawatan air Sungai Semenyih adalah disebabkan oleh ammonia, sianida, sulfida, fenol, fosforus, nitrit, mangan, ferum, dan karbon organik jumlah.

Ammonia

Dalam proses pengklorinan, tindak balas di antara ammonia dan klorin tidak dapat dielakkan. Tindak balas klorin dengan ammonia akan menghasilkan satu siri sebatian kloro-ammonia yang dipanggil kloramina. Rajah 2(a) di bawah menunjukkan pengurangan kepekatan ammonia di sepanjang proses rawatan air. Paras ammonia didapati berkurang sebanyak 88 % daripada air tapisan (L3) kepada air bersih (L4) selepas klorin didoskan. Rajah 2(b) menunjukkan tahap pencemaran ammonia di sepanjang Sungai Semenyih sebelum air dipamkan ke loji rawatan air. Punca pencemaran ammonia berlaku di stesen 5 (SS5) dan stesen 7 (SS7). Kedua-dua SS5 dan SS7 terletak berhampiran dengan Pusat Bandar Rinching dan Bandar Tasik Kesuma. Pencemaran ammonia boleh berpunca daripada kumbahan domestik dan sistem rawatan kumbahan yang belum siap. Permintaan klorin adalah berkadar dengan banyaknya ammonia yang hadir dalam air mentah. Tindak balas klorin dengan ammonia bergantung kepada suhu, pH, kepekatan ammonia, dos klorin, dan masa sentuhan [20].

2(a) 2(b)
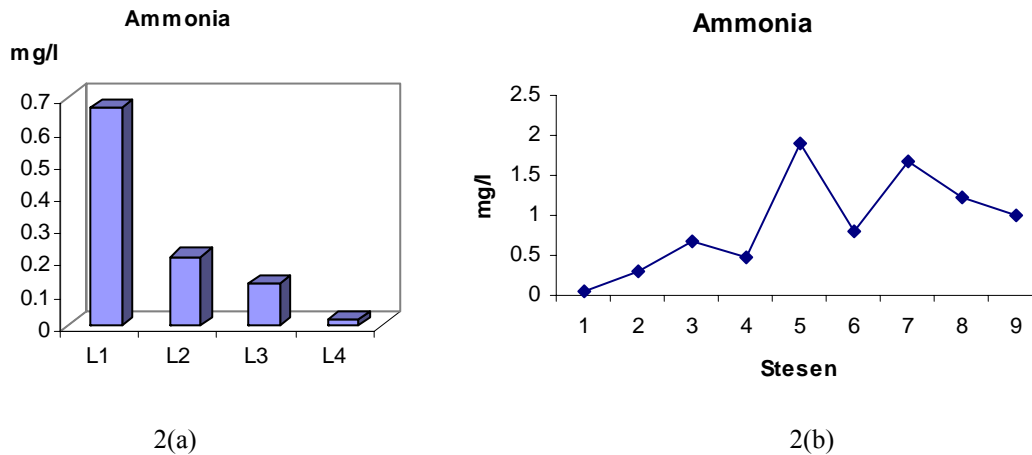
Rajah 2: (a) Tahap pengurangan ammonia di loji rawatan air (b) Punca pencemaran
ammonia di 9 stesen pensampelan di Sungai Semenyih

Sianida

Dalam loji rawatan air Sungai Semenyih, sianida hadir dalam kepekatan yang rendah. Rajah 3(a) menunjukkan kepekatan sianida adalah kurang daripada 0.5 ppb dalam air bersih. Kajian yang dijalankan mendapati kepekatan sianida berkurang sebanyak 73.68 % selepas klorin didoskan. Punca pencemaran sianida berlaku di SS3, SS5, dan SS7 seperti yang ditunjukkan dalam rajah 3(b). Pencemaran sianida ini adalah disebabkan oleh pembuangan industri dan aktiviti pelupusan sampah yang terletak berhampiran dengan sungai. Sianida dihasilkan terutamanya oleh industri yang berasaskan elektropenyaduran dan racun insektisid [10].

3(a)   3(b)
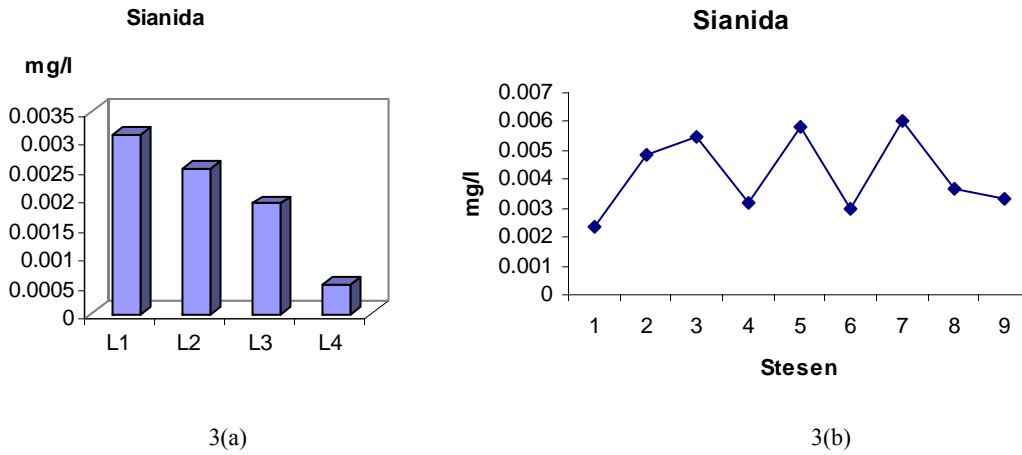
Rajah 3: (a) Tahap pengurangan sianida di loji rawatan air (b) Punca pencemaran sianida
di9 stesen pensampelan di Sungai Semenyih

Sulfida

Ion sulfida biasanya dilepaskan daripada sisa industri yang berasaskan kimia, kertas, tektil, dan aktiviti menyamak kulit binatang. SS5 dan SS7 mencatatkan bacaan sulfida yang tertinggi seperti yang ditunjukkan dalam rajah 4(b). Rajah 4(a) menunjukkan pengurangan kepekatan sulfida sepanjang proses rawatan air. Ion sulfida mengalami pengurangan sebanyak 61.46 % daripada air tapisan (L3) kepada air bersih (L4). Tindak balas sulfida dengan klorin berlaku dengan pantas dan menghasilkan sulfat dan hidrogen klorida.

4(a)   4(b)
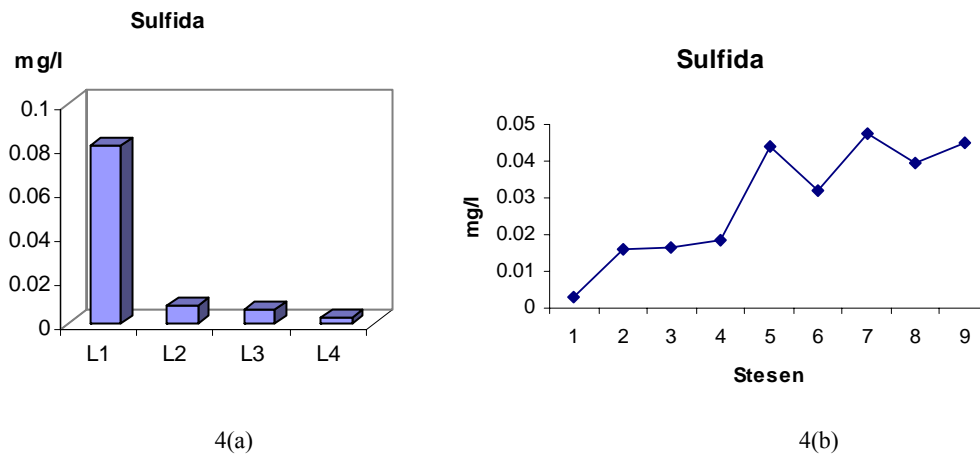
Rajah 4: (a)   Tahap pengurangan sulfida di loji rawatan air (b)   Punca pencemaran sulfida
di 9 stesen pensampelan di Sungai Semenyih

Fenol

Alley [10] mendapati klorin dapat bertindak balas dengan fenol dengan mudah, dan sekiranya klorin hadir, kepekatan fenol dapat dikurangkan kepada tahap yang paling rendah. Rajah 5(a) menunjukkan pengurangan fenol dalam loji rawatan air sebelum dan selepas proses pengklorinan. Fenol didapati berkurang sebanyak 42 % selepas klorin ditambahkan. Rajah 5 (b) menunjukkan pencemaran fenol yang berlaku di SS5 dan SS7 yang mencatatkan bacaan sebanyak 0.26 mg/l dan 0.28 mg/l masing-masing. Pencemaran fenol di kedua-dua stesen ini adalah berpunca daripada aktiviti perindustrian yang menyalurkan sisanya ke dalam Sungai Semenyih.

Fenol

mg/l

5(a)

Fenol

5(b)
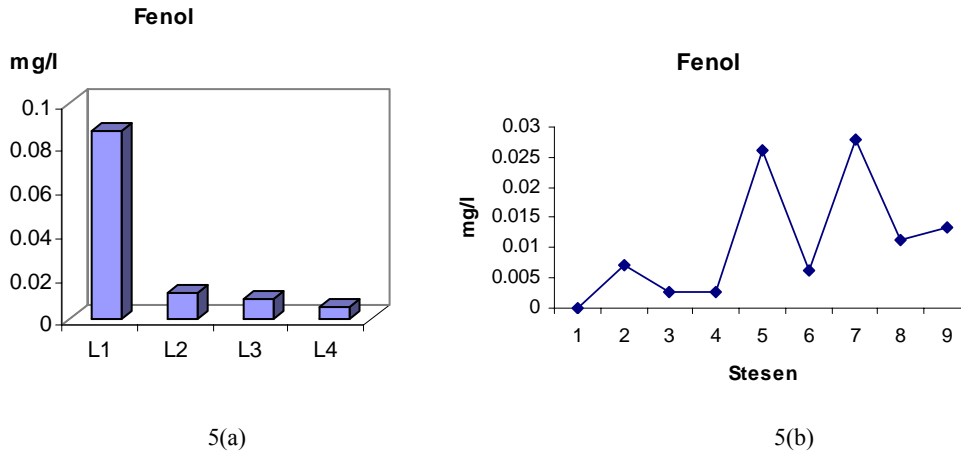
Rajah 5: (a) Tahap pengurangan fenol di loji rawatan air (b) Punca pencemaran fenol
di 9 stesen pensampelan di Sungai Semenyih

Fosforus

Fosforus yang hadir secara semulajadi biasanya wujud dalam bentuk fosfat. Kehadiran fosfat juga boleh disebabkan oleh detergen sintetik dan bahan pencuci. Rajah 6(a) menunjukkan tahap pengurangan fosforus sepanjang proses rawatan air. Fosforus berkurang sebanyak 78.69 % selepas klorin ditambahkan. Rajah 6(b) menunjukkan trend pencemaran fosforus di sembilan stesen di lembangan Sungai Semenyih. Punca pencemaran fosforus berlaku pada SS1, SS2, dan SS5. Selain detergen, kehadiran fosforus juga boleh dikaitkan dengan penggunaan baja dalam aktiviti pertanian.

Fosforus

mg/l

6(a)

Fosforus

6(b)
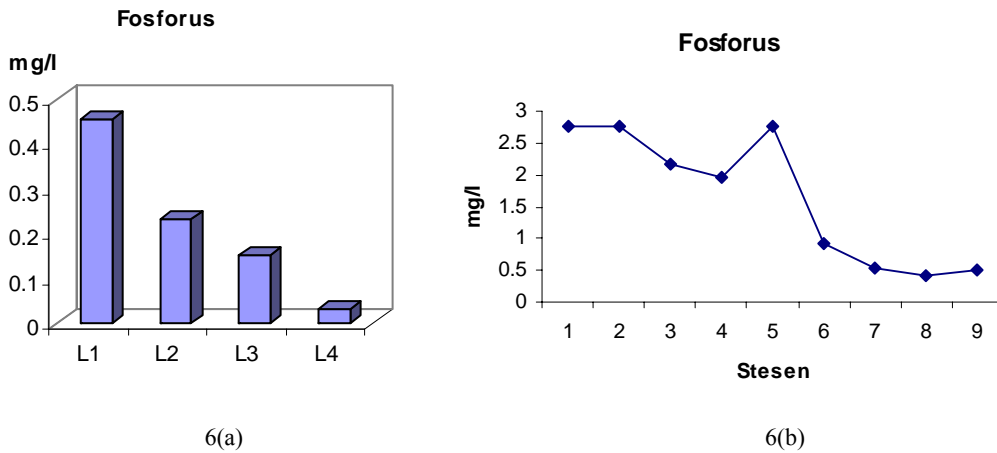
Rajah 6: (a)   Tahap pengurangan fosforus di loji rawatan air (b)   Punca pencemaran fosforus di 9 stesen
pensampelan di Sungai Semenyih

Nitrit

Nitrit merupakan sebahagian daripada bentuk nitrogen yang hadir dalam kitaran nitrogen. Nitrit terbentuk sebagai proses perantaraan dalam proses nitrifikasi [19]. White [1] mendapati nitrit boleh menghasilkan permintaan klorin yang tinggi apabila bertindak balas dengan klorin. Rajah 7(a) menunjukkan pengurangan nitrit selepas klorin ditambahkan pada L4. Secara amnya, nitrit yang hadir tidak memberikan permintaan klorin yang tinggi di loji rawatan air Sungai Semenyih. Pengurangan nitrit selepas proses pengklorinan ialah sebanyak 42.86 %. Kajian ini mendapati pencemaran nitrit adalah rendah di lembangan Sungai Semenyih kecuali SS5. Rajah 7(b) menunjukkan trend pencemaran nitrit di sembilan stesen di lembangan Sungai Semenyih. Kehadiran nitrit di SS5 boleh dikaitkan dengan sisa buangan industri dan aktiviti penternakan yang berhampiran.

Nitrit

7(a)
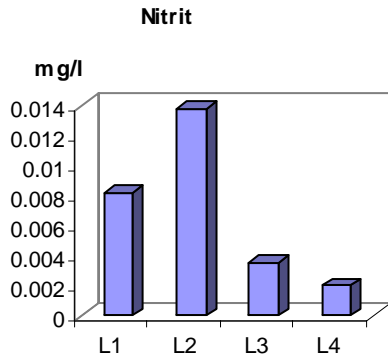
Nitrit

7(b)

Rajah 7: (a) Tahap pengurangan nitrit di loji rawatan air (b)   Punca pencemaran
nitrit di 9 stesen pensampelan di Sungai Semenyih

Mangan

Mangan merupakan logam berat yang boleh disingkirkan melalui proses pengoksidaan dengan klorin. Ini menunjukkan tindak balas boleh berlaku antara mangan dan klorin dan mangan boleh menyebabkan permintaan klorin dalam air. Pengurangan mangan dalam air bersih ialah 49.37 % selepas klorin didoskan seperti yang ditunjukkan dalam rajah 8(a).

Mangan

8(a)

Mangan

8(b)

Rajah 8: (a) Tahap pengurangan mangan di loji rawatan air, (b) Punca pencemaran
mangan di 9 stesen pensampelan di Sungai Semenyih

Pencemaran mangan di lembangan Sungai Semenyih adalah paling tinggi di SS7 seperti yang ditunjukkan dalam rajah 8(b). Pencemaran di SS7 adalah disebabkan oleh tapak pelupusan sisa pepejal yang berhampiran dengan Sungai Beranang. Selain itu, mangan juga hadir secara semulajadi dalam kepekatan yang rendah.

Ferum
Ferum biasanya wujud sebagai ferus bikarbonat yang larut separa dalam air. Klorin akan bertindak balas dengan ferum untuk menghasilkan ion ferik. Rajah 9(a) menunjukkan pengurangan ferum sepanjang proses rawatan air. Kebanyakan ferum boleh disingkirkan setelah air dimendapkan. Walaubagaimanapun, kepekatan ferum telah berkurang sebanyak 46 % selepas proses pengklorinan. Tindak balas ferum dengan klorin boleh berlaku dalam julat pH yang luas (pH 4-10). Kehadiran ferum dalam loji rawatan air adalah berpunca daripada SS5 dan SS7 seperti yang ditunjukkan dalam rajah 9(b). Sumber pencemaran ferum di kedua-dua SS5 dan SS7 berpunca daripada larut lesap dari tapak pelupusan sampah, kakisan daripada jambatan yang berhampiran dengan sungai, dan sisa buangan industri.

9(a)
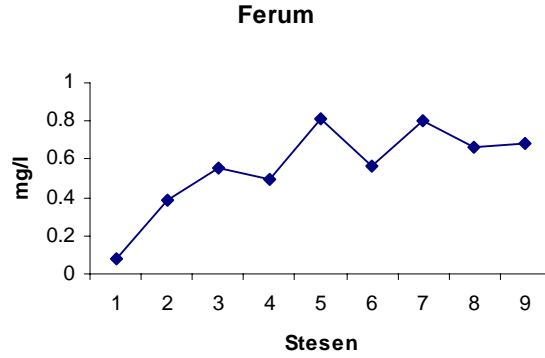
9(b)

Rajah 9: (a) Tahap pengurangan ferum di loji rawatan air, (b)   Punca pencemaran ferum
di 9 stesen pensampelan di Sungai Semenyih

Karbon Organik Jumlah

Karbon yang ditentukan dalam kajian ini ialah karbon organik terlarut (DOC). DOC meliputi semua bentuk karbon seperti karbon organik, karbonat tak organik, karbon dioksida, dan spesis yang lain seperti HCN yang larut dalam air. Rajah 10(a) menunjukkan kepekatan DOC dalam loji rawatan air, dimana DOC mengalami pengurangan sebanyak 33.91 % selepas proses pengklorinan. DOC merupakan pelopor yang boleh bertindak balas dengan klorin untuk menghasilkan THM, asid haloasetik, dan haloasetonitril yang boleh membawa kesan kepada kesihatan manusia. Oleh itu, punca pencemaran DOC perlu dikenalpasti. Rajah 10(b) menunjukkan SS5 dan SS7 merupakan dua stesen yang paling tercemar dengan karbon organik. Secara amnya, kepekatan DOC adalah paling tinggi berbanding dengan parameter-parameter yang lain yang boleh menyebabkan permintaan klorin. Jadi pengawalan pencemaran DOC dari buangan domestik, industri, dan pertanian adalah penting dalam menangani masalah permintaan klorin.

10(a)

10(b)

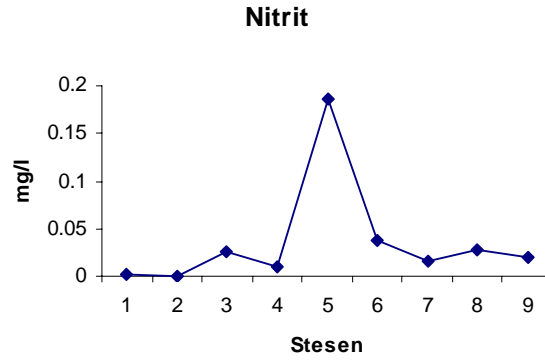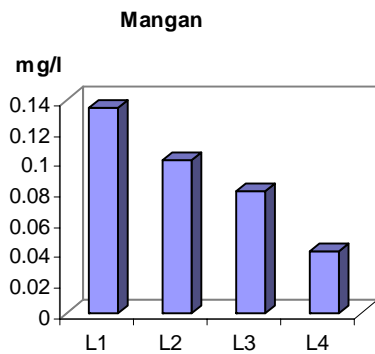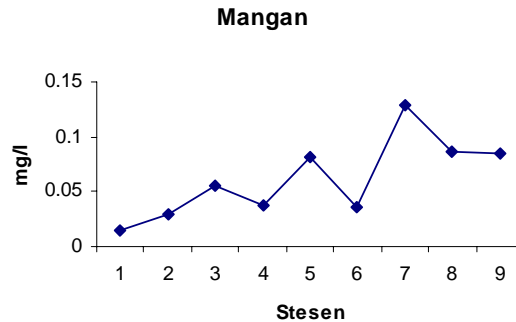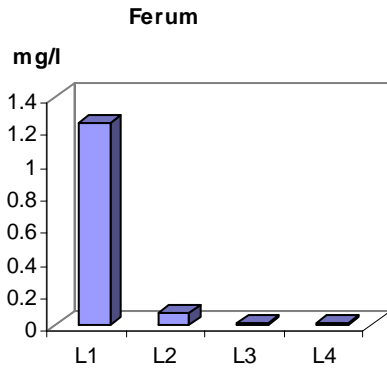Rajah 10: (a)   Tahap pengurangan DOC di loji rawatan air, (b) Punca pencemaran
DOC di 9 stesen pensampelan di Sungai Semenyih

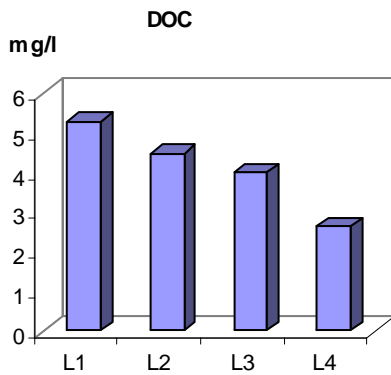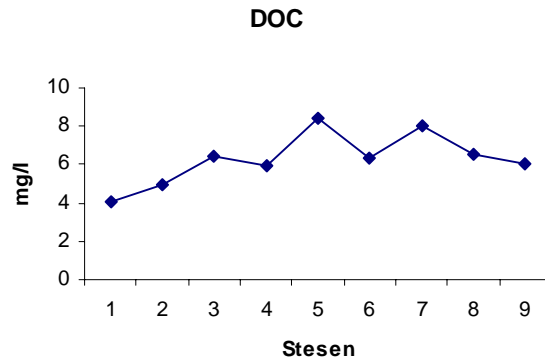Jadual 2   Kepekatan komponen-komponen yang menyebabkan permintaan klorin dalam air tapisan

Komponen	Min (mg/l)	Julat (mg/l)
Ammonia	0.1255	0-0.36
Sianida	0.0019	0.001-0.003
Sulfida	0.0056	0.001-0.008
Fenol	0.0095	0.004-0.006
Forforus	0.1525	0.11-0.25
Nitrit	0.0035	0.001-0.005
Mangan	0.0797	0.018-0.116
Ferum	0.0141	0-0.020
DOC	4.0070	2.454-5.125

Faktor dan punca yang menyebabkan permintaan klorin di loji rawatan air Sungai Semenyih, yang merupakan salah satu sumber bekalan air utama di daerah Hulu Langat. Data yang terkumpul selama lapan bulan ini mendapati komponen-komponen yang menyebabkan permintaan klorin ialah ammonia, sianida, sulfida, fenol, fosforus, nitrit, mangan, ferum, dan karbon organik terlarut. Jadual 2 menunjukkan kepekatan komponen-komponen ini dalam air tapisan (sebelum pengklorinan). Keputusan kajian menunjukkan karbon dan ammonia boleh menyebabkan permintaan klorin yang tinggi berbanding dengan komponen-komponen yang lain.

Kesimpulan

Secara puratanya, kandungan karbon dan ammonia berkurang sebanyak 1.36 mg/l dan 0.111 mg/l masing-masing selepas klorin ditambahkan. Selain itu, kepekatan parameter-parameter yang lain seperti sianida, sulfida, fenol, nitrit, fosforus, mangan, dan ferum juga berkurang selepas proses pengklorinan. Parameter-parameter ini tidak mempengaruhi permintaan klorin dengan banyak berbanding dengan DOC dan ammonia kerana hadir dalam kepekatan yang rendah. Kajian ini turut mendapati terdapat dua stesen di lembangan Sungai Semenyih yang menjadi punca yang menyebabkan permintaan klorin, iaitu SS5 dan SS7. Punca pencemaran yang dikenalpasti di SS5 dan SS7 ialah aktiviti perindustrian, kumbahan domestik, pertanian, penternakan, dan larut lesap dari tapak pelupsan sisa pepejal. Langkah-langkah yang bersesuaian perlu diambil untuk melaksanakan pendekatan pengurusan yang bersistematik supaya pencemaran sungai dapat diminimumkan, dan seterusnya permintaan klorin dapat dikurangkan untuk menjimatkan kos rawatan air.

Penghargaan

Rujukan

1. White, G.C. (1992). *Handbook of Chlorination and Alternative Disinfections*. Ed. ke-3. New York: Van Nostrand Reinhold Publisher, Inc.
2. Sukiman, S. & Pauzi, A. (1993). Chemical Quality of Malaysian Drinking Water Sources. *Drinking Water Quality: Microbiological and Public Health Aspects*, UKM: 63-69.
3. Johari, M. A. (1994). Perkembangan Teknologi Dalam Sistem Bekalan Air. Paper Presented at SKAM-7, Kuala Lumpur. 27-29 Sept.
4. Wan, K. J., Ki, D. K., Jong, I. D. & Yong. C. (2005). Multi-route Trihalomethane Exposure in Households Using Municipal Tap Water Treated with Chlorine or Ozone-Chlorine. *Sci. of the Tot. Environ*. 339: 143-152.
5. Sukiman, S. & Pauzi, A. (1993). Chemical Quality of Malaysian Drinking Water Sources. *Drinking Water Quality: Microbiological and Public Health Aspects*. UKM: 63-69.
6. Rook, J. J. (1974). Formation of Haloforms During Chlorination of Natural Water. *Water Treat. Exam.* 23: 234-243.
7. Bellar, T. A., Lichtenberg J. J. & Kroner, R. C. (1974). The Occurrence of Organohalogens on Chlorinated Drinking Waters. *J. AWWA*. 66: 703-706.
8. Tachkikawa, M., Aburada, T., Tezuka, M. & Sawamura, R. (2005). Occurrence and Production of Chloramines in The Chlorination of Creatinine in Aqueous Solution. *Water Res.* 39: 371-379.
9. Macolo, G., Lopez, A., James, H. & Fielding, M. (2001). By-Products Formation During Degradation of Isoproturan In Aqueous Solution. II: Chlorination. *Water Res.* 35(7): 1705-1713.
10. Alley, E. R. (2000). *Water Quality Control Handbook*. New York: McGraw-Hill Inc.

11.   Chanratchakool, P. (1995). White Patch Disease of Black Tiger Shrimp (*Penaeus Monodon*). *AAHRI Newsletter.* 4(1): 3.

12.   Aacher, A., Fischer, E., Turnheim, R., Manor, Y. (1997). Ecologically Friendly Wastewater Disinfection Techniques. *Water Res..* 31(6): 1398-1404.

13.   Hopkins, J.S., Hamilton, R.D. II, Sandifier, P.A., Browdy, C.L., Stokes, A.P. (1993). Effects of Water Exchange Rate On Production, Water Quality, Effluent Characteristics and Nitrogen Budgets of Intensive Shrimp Ponds. *J. World Aquacult. Soc.* 24(3): 304-320.

14.   Dierberg, F. F., Kiattisimkul, W. (1996). Issue, Impacts, and Implications of Shrimp Aquaculture in Thailand. *Environ. Man*. 20(5): 649-666.

15.   Rook, J. J. (1976). Haloforms in Drinking Water. *J. AWWA.* 68: 168-172.

16.   Cotruvo, J. A. & Wu, C. (1981). Controlling Organics. Why Now?. *J. AWWA*. 70: 590-594.

17.   Morrow, C. M. & Minear, R. A. (1987). Use of Regression Models to Link Raw Water Characteristics to Trihalomethanes Concentrations in Drinking Water. *J. Wat. Res*. 21: 41-48.

18.   El-Dib, M. & Ali, R. (1995). THMs Formation During Chlorination of Raw Nile River Water. Egypt. *J. Wat. Res.* 29: 375-378.

19.   APHA. (1998). *Standard Method For the Examination of Water and Wastewater.* Ed. ke-20. Washington: American Public Health Association.

20.   Faust, S. D. & Aly, O. M. (1998). *Chemistry of Water Treatment*. Ed ke-2. New York: Lewis Publishers.

POLYCYCLIC AROMATIC HYDROCARBONS IN URBAN SOILS OF KEMAMAN

Norhayati Mohd Tahir*[1], Lee Boon Jeen[1], Hasra Masrifah Abd. Rahim[1],
Marinah Ariffin[1], Suhaimi Suratman[1] and Mhd Radzi Abas[2]

[1]*Department of Chemical Sciences, Faculty of Science and Technology,Universiti Malaysia Terengganu,
Mengabang Telipot, 21030 Kuala Terengganu, Terengganu*
[2]*Department of Chemistry, Faculty of Science, Universiti Malaya (UM), 50603 Kuala Lumpur*

Abstract

A study has been carried out to determine the concentration and distribution of polycyclic aromatic hydrocarbons (PAHs) in urban soils of Kemaman, Terengganu. Surface soil samples (< 500 μm) were ultrasonicated using dichloromethane as solvent and the extracts fractionated on silica-alumina column. Detection and quantification of 16 priority PAHs compounds were carried out using GC-FID. With the exception of two stations, results generally indicated that the sum of 16 priority PAHs concentration (total PAHs) in soils ranged from to 6.3 to 176 μg/kg (dry weight); the two stations which exhibited significantly higher levels of total PAHs was at the main road junction located at the heart of the commercial centre of the town (535 μg/kg) and at an industrial estate, adjacent to a sawmill (547 μg/kg). Statistical analysis suggests that there is a significant difference in total PAHs concentration ($p<0.05$) with sampling sites. Most common PAHs compound observed in almost all the soil samples was BgP indicating the importance of vehicular emission as a source of PAHs in these soils. In addition, contribution of biomass burning to the presence of PAHs in these soils was also observed as indicated by a positive correlation between Benzo[a]pyrene with total PAHs.

Abstrak

Satu kajian bagi menentukan kepekatan dan agihan hidrokarbon polisiklik aromatic (PAH) dalam tanah di Bandar Kemanan, Terengganu telah dijalankan. Sampel tanah permukaan (< 500 μm) diekstrak menggunakan kaedah pengekstrakan ultrasonik dengan DCM sebagai pelarut dan hasil ekstrak dipisahkan menggunakan turus silika-alumina. Pengenalpastian dan pengkuantitian 16 sebatian PAH keutamaan dilakukan menggunakan GC-FID. Keputusan secara amnya menunjukkan bahawa jumlah PAH dalam tanah adalah dalam lingkungan 6.3 μg/kg ke 176 μg/kg (berat kering) kecuali pada dua stesen dimana kepekatan adalah jauh lebih tinggi; satu stesen terletak di simpang jalan utama di kawasan pusat Bandar (535 μg/kg) dan satu lagi terletak di kawasan estet perindustrian, berhampiran kilang kayu   (547 μg/kg). Analisis statistik menunjukkkan bahawa terdapat perbezaan ketara dalam kepekatan PAH jumlah diantara stesen persampelan. Hampir semua sampel tanah mengandungi BgP dimana kehadirannya sering dikaitkan dengan sumber kenderaan bermotor manakala sumbangan daripada sumber pembakaran biojisim terhadap kandungan PAH dalam tanah juga dikenalpasti berdasarkan korelasi positif antara BaP dan total PAH.

Introduction

Polycyclic aromatic hydrocarbons (PAHs) are ubiquitous in the global environment and soil remains as one of the most important sinks for these compounds. Due to their mutagenic and carcinogenic potentials as well as their persistence, the presence of PAHs in the environment is of great global concern. PAHs are formed from the incomplete combustion of fossil and biomass fuels. Main sources of these compounds in soil include wildfires and biomass burning for agricultural land clearing, municipal incinerators, vehicular emission, residential heating and through the atmospheric deposition as a result of long-range atmospheric transport [1-6]. In this context, knowledge on the PAHs level and its dispersion on regional and national scale are essential. At present in Malaysia, even though studies to determine the concentration, composition and possible sources of PAHs in soils are being reported in the literature [7,8], this type of studies is still limited, particularly in the east coast states of Peninsular Malaysia. In view of this, a study has been initiated to address this gap in knowledge. This paper presents the results of a study to determine the concentrations, composition and possible sources of PAHs in soils of Chukai, the capital of the district of Kemaman, Terengganu, Malaysia.

Experimental

Study area and sampling

Chukai with a population of 45,873 density, lies on the southeast end of the Terengganu state (Fig.1a) and is sandwiched between the booming oil town of Kerteh, Terengganu and the fast growing industrial area of Gebeng, Pahang. It acts as the center for business activities and public agencies for the fastest growing district in the state of Terengganu, largely due to the booming petroleum and related industries in Paka-Kerteh belt. Owing to its strategic location, Chukai also acts as a residential town to those who work in Paka-Kerteh belt as well as Gebeng and Kuantan, the capital of Pahang.

Soil sampling was carried out around the urban area of Chukai (Table 1 and Fig. 1b). These sites were chosen based on traffic density, residential and industrial activities and were generally diffuse source oriented. Where possible soil samples were collected ca. one metre from the roadside. Twenty sampling sites were ascertained and classified to three zones. Zone A was located in the centre part of this town, where most of the economic activities were found with major road network, Zone B emphasized on residential areas whereas Zone C is located in the industrial zone of the town. Sampling involved the collection of 20 surfacial soil samples (0-10 cm) using metal spades, wrapped in pre-cleaned aluminum foil and transported to the laboratory in an icebox to minimize sample degradation. Once in the laboratory, soil samples were homogenized and sieved through a 500 μm sieve.
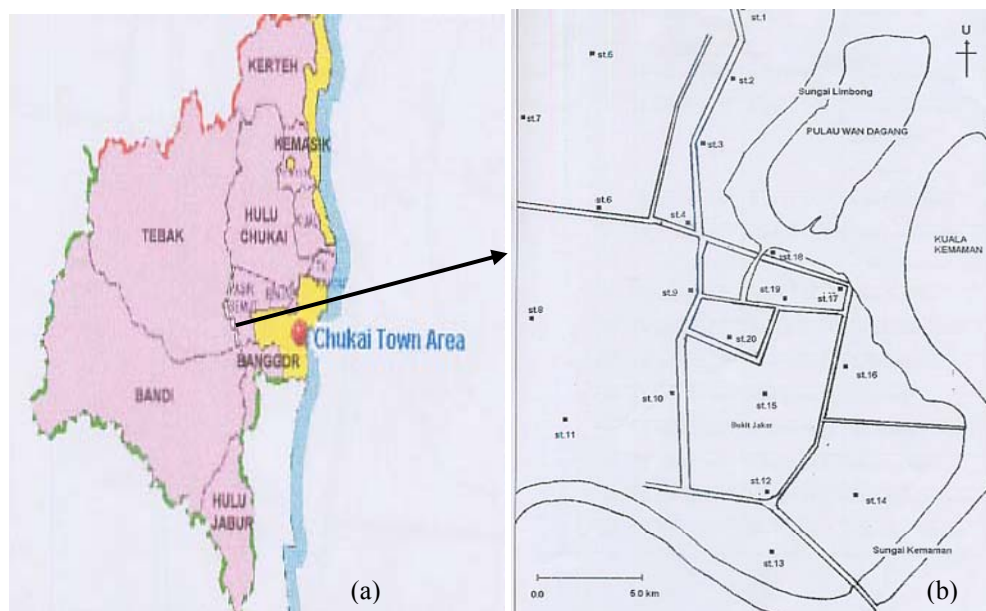
Figure 1. Chukai Town Map (a) and Sampling site map (b)

Table 1 : Longitude and latitude of the sampling site

Zone	Site No	Longitude	Latitude	Sampling Sites
Zone A	1	E 103°25'29.5''	N 04°15'07.4''	Jln Bakau Tinggi
	2	E 103°25'29.5''	N 04°14'50.8''	Sek. Men. Sultan Ismail Kemaman
	3	E 103°25'19.0''	N 04°14'21.4''	Jln Penghiburan
	4	E 103°25'02.5''	N 04°14'21.4''	Center Road Junction of Jln Da Omar
	9	E 103°25'17.3''	N 04°13'56.4''	Jln Da Omar
	10	E 103°25'11.2''	N 04°13'27.0''	Jln Kubang Lurus
	15	E 103°25'25.8''	N 04°13'39.1''	Bukit Jakar
	16	E 103°25'43.5''	N 04°13'49.6''	Jln Jakar
	17	E 103°25'10.1''	N 04°14'09.1''	Bus station
	18	E 103°25'38.8''	N 04°13'54.2''	Jln Sulaimani
	19	E 103°25'33.5''	N 04°13'48.7''	Jln Abd. Rahman
	20	E 103°25'25.8''	N 04°13'39.1''	Jln Mak Donyang
Zone B	5	E 103°24'31.7''	N 04°14'44.8''	Kg Gong Limau
	6	E 103°25'02.5''	N 04°14'10.2''	Jln Air Putih
	7	E 103°23'24.4''	N 04°14'16.0''	Kompleks Quarters Pend. Kemaman
	8	E 103°23'06.0''	N 04°13'31.7''	Kg Mentok
	11	E 103°24'49.6''	N 04°13'32.6''	Jln Pengkalan Lama
Zone C	12	E 103°25'20.8''	N 04°13'10.8''	Jln Jakar (Fire Station)
	13	E 103°25'31.3''	N 04°12'59.6''	Jakar II Industrial Estate (electronic)
	14	E 103°25'48.2''	N 04°13'22.6''	Jakar I Industrial Estate (sawmills)

Analytical procedure

PAHs were extracted from soils (< 500 μm fraction) with dichloromethane (DCM) as solvent using ultrasonic method. The extracts were then fractionated on partially deactivated (5%) silica-alumina columns. PAHs compounds were eluted using a combination of 20ml of 10% DCM in hexane followed by 20ml of 50% DCM in hexane [9].

Identification and quantification of the 16 priority PAHs compounds were carried out using gas chromatography fitted with flame ionization detector (GC-FID) based on the retention times compared to that of external PAHs standards. These compounds were naphthalene (NAP), acenaphtylene (ACY), acenaphtene (ACE), fluorene (FLU), phenanthrene (PHEN), anthracene (ANT), fluoranthene (FTH), pyrene (PYR), benzo(a)anthracene (BaA), chrysene (CHR), benzo(b)fluoranthene (BbF), benzo(k)fluoranthene (BkF), benzo(a)pyrene (BaP), dibenz(a,h)anthracene (DA), benzo(g,h,i)perylene (BgP) and indeno(1,2,3,cd)pyrene (IP). Sums of these 16 compounds were collectively known as total identified PAHs (TIP).

The GC-FID with fused silica column (30 m x 0.25 mm i.d.; 0.25 μm filmed thickness); was set with injection temperature of 290°C using a splitless mode; column temperature was programmed at hold at 50°C for 1 min, first temperature ramp of 50 - 140°C at 5°C min^{-1} followed by the second temperature ramp of 140 - 290°C at 3°C min^{-1} and then maintained at 290°C for 13 min resulting in a total run time of 82 min; helium was used as the carrier gas with a flow rate at 1.2 mL. min^{-1}; detector temperature was set at 300°C.

Total organic carbon (TOC) in soils was analysed using Walkley and Black's rapid titration method [10].

Results and Discussion

Soil Organic Carbon (SOC)

Numerous studies have shown that PAHs are strongly retained by the soil matrix [11, 12]. The partitioning concept of soil sorption of organic contaminants implies that the sorption of hydrophobic organic molecules is determined by the organic carbon content of the substrate [13-14]. The organic matter content is considered to be a very important variable related to PAHs pollution of soils [15]. In this study, the soils exhibited rather low

organic carbon content with values ranging from 0.09% to 0.53% with a mean of 0.27% (Table 2 and Fig. 2). A regression analysis (Fig. 3) showed a negative and weak relationship between the concentrations of the TIP and the amounts of soil organic carbon (SOC, %). Because of the very low SOC in soils, it is probable that this parameter does not play an important role in influencing the concentration of TIP in these soils.
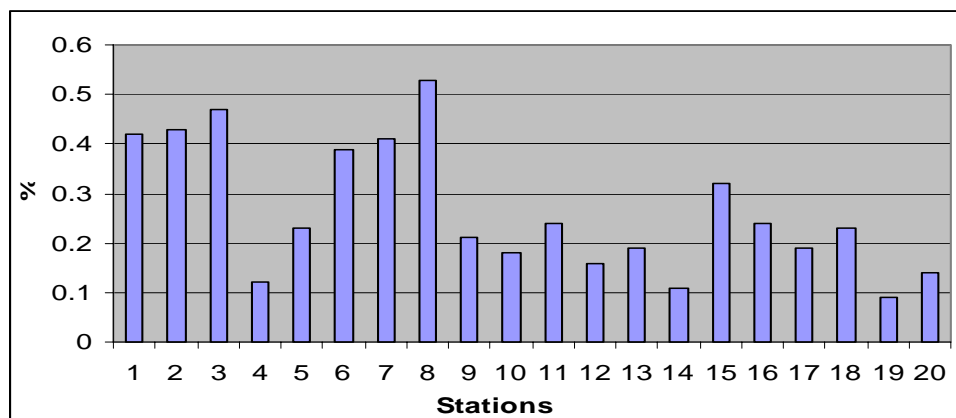
Figure 2: Distribution of SOC in soil samples

$$y = -473.25x + 255.11$$
$$R^2 = 0.1734$$
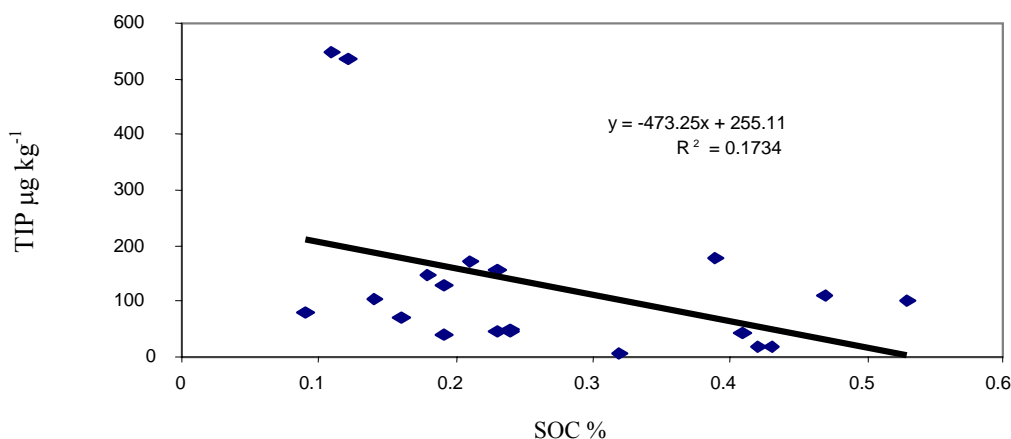
Figure 3: Correlation between TIP and SOC

Total identified Polycyclic Aromatic Hydrocarbon (TIP)
The distribution of TIP obtained in this study is shown in Figure 4. With the exception of two stations (Stations 4 and 14) which exhibited significantly higher TIP than the other remaining stations, the range of TIP values found in this study was between 6.27 µg/kg to 176.3 µg/kg (Table 2); the mean concentration of TIP values obtained for the 20 sites was 129.7 µg/kg whilst the median was 101.4 µg/kg. Statistical analysis showed significant differences (p<0.05) of TIP values between the stations monitored. These values are generally in great excess of the reported natural concentration of PAHs in soil (1-10 µg/kg) [16] but within similar range to those reported in soils of Kuala Lumpur [7, 17] and Kuala Terengganu [8]. Comparison between the three sampling zones showed that TIP values in Zone A ranged from 6.27µg/kg to 534.6µg/kg with mean value of 127.2 µg/kg and a median of 106.1µg/kg, Zone B ranged 43.66µg/kg to 176.3µg/kg with mean value of 82.08µg/kg and a median of 44.62µg/kg and Zone C ranging from 71.13µg/kg to 547.3µg/kg with mean value of 219.0 µg/kg and a median of 71.13µg/kg. The stations which recorded exceptionally high TIP values were located in Zone A and Zone C, respectively and it is conceded that their values does exhibit an influence on the mean values calculated for the respective zone, particularly in the case of Zone C where there were only three stations monitored; Station 4 was located at the busiest road junction in Chukai (Zone A) whereas Station 14 is located in the vicinity of a sawmill in Zone C. In addition, as expected, it was also observed that most of the sampling sites located by major roadside generally exhibited relatively higher TIP values (e.g. Stations 3, 4, 8, 9, 10) than sites located in the residential areas (Stations 5, 7, 11, 16).
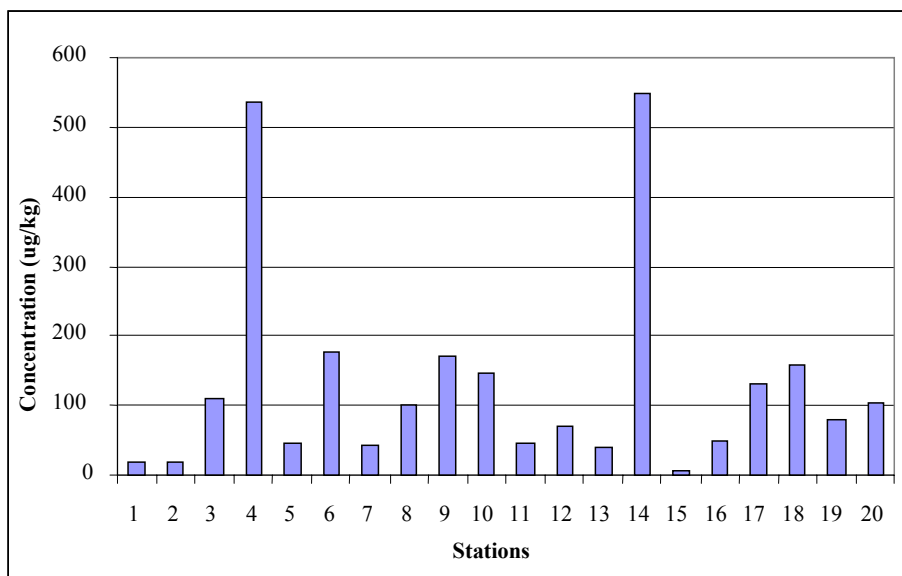
Figure 4: Distribution of TIP in soil samples

The distribution of the 16 PAHs compounds monitored at each sampling site were found to differ with stations, with station 4 showing the presence of all compounds except the very low molecular weight PAHs (with two benzene rings), viz. NAP, ACY and ACE. In fact, NAP was absent from all stations whilst ACY and ACE were found in only few stations at rather low concentrations (< 3 µg/kg). This observation is not surprising as these compounds are generally more volatile compared to the other higher ring number PAHs [18, 19]. Almost all stations exhibited the presence of BgP, the heavy molecular weight PAHs commonly associated with vehicular emissions resulting from internal engine combustion of gasoline [20]; BgP concentration found in this study ranged from 22.08µg/kg to 126.44µg/kg with station 4 exhibiting highest BgP concentration relative to other stations. Other high molecular weight PAHs that were present in almost all stations monitored includes DA and IP. BaP, a high molecular weight PAHs generally taken as a signature of an incomplete burning of biomass or organic matter was also present but only at selected stations with station 14 exhibiting extremely high concentration of this compound (423.5 µg/kg) accounting > 70% of the PAHs recorded for this site. These observations are consistent with the fact that Station 4 is located at the busiest road junction in Chukai whilst Station 14 is located in the vicinity of a sawmill with obvious signs of wood burning activities.

Table 2 : TIP and selected parameters

Site No	TOC %	TIP (µg/g)
1	0.42	19.53
2	0.43	19.32
3	0.47	109.2
4	0.12	534.6
5	0.23	44.47
6	0.39	176.3
7	0.41	43.66
8	0.53	101.4
9	0.21	170.4
10	0.18	146.8
11	0.24	44.62
12	0.16	71.13
13	0.19	38.66
14	0.11	547.3
15	0.32	6.27
16	0.24	49.92
17	0.19	130.1
18	0.23	157.1
19	0.09	80.48
20	0.14	102.9

Phenanthrene to antracene ratio (PHEN/ANT) has often been used to investigate possible sources of PAHs compounds in the environment where a low ratio (PHEN/ANT < 10) is generally considered as indicative of a predominance of pyrolytic sources (i.e. combustion sources) over petrogenic sources (i.e. oil spill) [21-24]. In this study, the PHEN/ANT ratios in soil samples of Chukai ranged from 1.2 to 7.5 suggesting that the PAHs compounds found in these soils were derived from pyrolytic sources.

Differentiating between the two major pyrolytic source, viz. internal engine or biomass combustion require the use of other molecular markers; as indicated above, presence of BaP in the environment is generally indicative of incomplete combustion sources, in particular combustion of organic whilst the association of BgP with vehicular emission has long been established [20]. A linear correlation analysis between TIP and BaP and between TIP and BgP for the 20 stations monitored gave an r-value of 0.68 and 0.58, respectively (Figs.5 and 6) which suggest that both sources contribute to the presence of PAHs in these soils. Station 14 is interesting in that BaP contributes over 70% of the TIP observed at the station, thus to eliminate possible bias, a second linear correlation analysis was calculated between TIP and BaP and between TIP and BgP by excluding this station giving an r value of 0.44 and 0.86. Similarly, since Station 4 is suspected to have a high contribution from vehicular emission, another correlation analysis was carried out by removing the contributions of the two extreme stations; the r value obtained was 0.41 and 0.63 for correlation between TIP and BaP and between TIP and BgP, respectively. The results of the latter two correlation analyses clearly show a stronger correlation exist between BgP and TIP suggesting that vehicular emissions is the more dominant contributor to the PAHs in the soils around Chukai. The contribution from the vehicular emission is expected as samplings were conducted in an urban area with a number of stations located close to major trunk road. The presence of a relatively weaker but positive correlation between BaP and TIP suggests that biomass burning also contributes to the presence of PAHs in these soils. Apart from Station 14, it is most likely that these PAHs were contributed from activities of open burning of rubbish and garden refuse by local residents [17] which are still prevalent in the east coast states particularly in Terengganu and Kelantan.
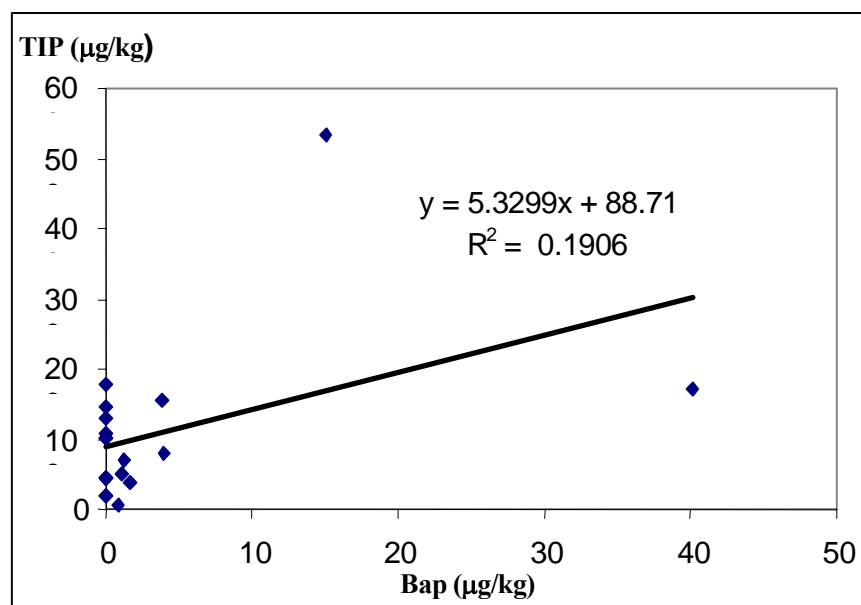
Figure 5: Correlation between TIP and BaP (20 stations)
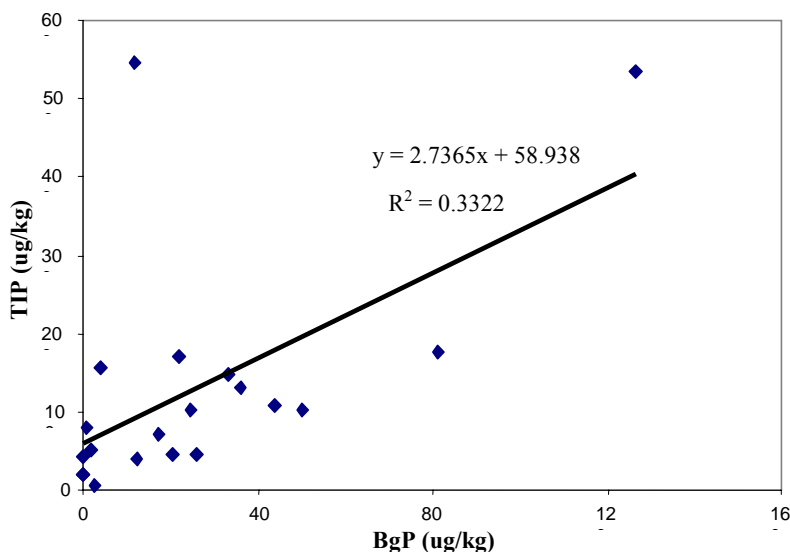
Figure 6: Correlation between TIP and BgP (20 stations)

Conclusion

Total concentration of PAHs found in urban soils of Chukai, Kemaman ranged from 6.27 μg/kg to 547.3 μg/kg with two stations exhibiting exceptionally high TIP values. Almost all stations showed the presence of BgP, a signature PAHs compounds known to be associated with vehicular emissions resulting from gasoline combustion in engines. A strong correlation between BgP and TIP and low PHEN/ANT ratio (< 10) provide further evidence for the importance of vehicular emission sources of PAHs in these soils. In addition, contribution of biomass burning to the presence of PAHs in these soils, through open burning of rubbish and
garden refuse by local residents, was also observed as indicated by a positive albeit a weaker correlation between BaP with TIP relative to the correlation between BgP and TIP.

Acknowledgement

References

1. Van Brumelen, T.C., Verweij, S.A. Wedzinga, S.A and Van Gestel, C.A.M. (1996). Enrichment of polycyclic aromatic hydrocarbons in forest soils near a blast furnace plant. Chemosphere, 32:293-314.
2. Kim, Eun-Jung, Oh Jeong-Eun, Chang, Yoon-Seok (2003). Effects of forest fire on the level and distribution of PCDD/Fs and PAHs in soil. The Sci. Total Env., 311:177-189.
3. Lunde, G. and Bjorseth, A. (1977). Polycyclic aromatic hydrocarbons in long –range transported aerosol. Nature, 268: 518-519
4. Aanot, E., Steinnes, E. and Schmid, R. (1996). Polycyclic aromatic hydrocarbons in Norwegian forest soils: impact of long range atmospheric transport. Environ. Poll., 92:275-280.
5. Bakker, M.I., Casado, B., Koerselman, J.W., Tolls, J and Kollofel, C. (2001) Polycyclic aromatic hydrocarbon in soil and plant samples from the vicinity of an oil refinery. Sci. Total Env., 263: 91-100
6. Simoneit, Bernd R.T. (2002). Biomass burning - a review of organic tracers for smoke from incomplete combustion. Appl. Geochem., 17:129-162.
7. Nasr, Yousef M. J. Omar, M. Radzi Abas, Kamal Aziz Ketuly and Norhayati Mohd Tahir (2002). Concentrations of PAHs in atmospheric particles (PM-10) and roadside soil particles collected in Kuala Lumpur, Malays. Atmos. Environ., 36:247-254.
8. Norhayati Mohd Tahir, Abd. Ghani Abd. Manas, Hasra Masrifah Abd Rahim, Suhaimi Suratman and Mhd Radzi Abas (2005). Distributions of polycyclic aromatic hydrocarbons in soils of Kuala Terengganu: a preliminary study. Malays. J. Anal. Sci., In press.
9. UNEP. 1992. Reference method for marine pollution studies no.20 (IOC, IAEA). United Nation Environmental Programme.

10.   Lim HK (1975). Working manual for soil analysis. Ministry of Agriculture Malaysia, Kuala Lumpur.
11.   Chung N. and Alexander, M. (1998) Differences in sequestration and bioavailability of organic compounds aged in dissimilar soils. Environ Sci Technol, 32:855–860.
12.   Chung N. and Alexander M. (2002) Effect of soil properties on bioavailability and extractability of phenanthrene and atrazine sequestered in soil. Chemosphere, 48:109–115.
13.   Chiou,.T. Peters L.J. and Freed, V.H. (1979) A physical concept of soil–water equilibria for nonionic organic compounds. Sci., 206:831–832.
14.   Chiou, C.T. McGroddy, S.E. and Kile, D.E. (1998) Partition characteristics of polycyclic aromatic hydrocarbons on soils and sediments. Environ. Sci. Technol., 32:264–269.
15.   Boehm, P.D. Burns, W.A., Page, D.S. Bence, A.E. Mankiewicz, P.J. and Brown, J.S. (2002) Total organic carbon, an important tool in a holistic approach to hydrocarbon source fingerprinting. Environ Forensics, 3:243–250.
16.   Edward, N. T .J. (1987). Polycyclic aromatic hydrocarbons (PAHs) in the terrestrial environment – review. J. Environ. Qual., 12:427-441.
17.   Nasr, Y.M.J.O.(2001). Characterization of solvent-extractable hydrocarbons from particulates and street dust of Kuala Lumpur. MSc. Thesis. University of Malaya, Malaysia.
18.   Hathairatana, G. (1999). A study on air pollution by airborne polycyclic aromatic hydrocarbons (PAHs) in Banngkok urban atmosphere. AIT Dissertation No. EV-99-1.
19.   Kim-Oanth, N. T., Botz Reutergardh, L. and Dung, N. Tr. (1999). Emissions of polycyclic aromatic hydrocarbons and particulate matter from domestic combustion of selected fuels. Environ. Sci. Technol., 33:2703-2709.
20.   Zheng, M., Fang, M., Wang, F. and To, K.L. (2000). Characterisation of the solvent extractable organic compounds in PM2.5 aerosols in Hong Kong. Atmos. Environ., 34:2691-2702.
21.   Yunker, M.B. Macdonald, R.W. Gpyette, D. Paton, D.W. Fowler B.R. and Sullivan D. (1999), Natural and anthropogenic inputs of hydrocarbons to the Strait of Georgia. Sci Total Environ., 225:181–209
22.   Sanders, M. Sivertsen S. and Scott, G. (2002) Origin and distribution of polycyclic aromatic hydrocarbons in surfacial sediments from the Savannah River. Arch Environ. Contam Toxicol., 43:438–448.
23.   Colombo, J.C. Pelletier, E. Brochu,C. and Khalil, M. (1989) Determination of hydrocarbon sources using n-alkanes and polyaromatic hydrocarbon distribution indexes. Case study: Rio de La Plata Estuary, Argentina. Environ Sci Technol, 23:888–894.
24.   Baumard, P., Budzinski, H. and Garrigues, P. (1998). Polycyclic aromatic hydrocarbons in sediments and mussels of the Western Mediterranean Sea. Env. Toxicol. Chem., 17(5):765-776.

DEGRADATION STUDIES ON PARAQUAT AND MALATHION USING TiO$_2$/ZnO BASED PHOTOCATALYST

Rusmidah Ali and Siti Habsah Hassan

Chemistry Department, Faculty of Science, Universiti Teknologi Malaysia,
81310 Skudai, Johor Bahru, Malaysia.

Abstract

Paraquat, a herbicide and malathion, an insecticide are pesticides that are always polluting our water system. Thus a lot of efforts has been conducted to treat the polluted water. The latest technology proposed is using photocatalyst. In this study, ZnO and TiO$_2$ were used as photocatalysts to degrade the pesticide in the presence of UV light (λ=354 nm). The photodegradation rate was measured using UV-Visible spectrophotometer and TOC analyzer. Malathion showed the absorption peak at λ=210 nm while for paraquat at λ=258 nm. The best coupled photocatalyst for degrading malathion solution is ZnO/TiO$_2$ with % weight ratio 1:0.05 and the best coupled photocatalyst in degrading paraquat solution is TiO$_2$/ZnO with % weight ratio 1:0.03. The result shows that Fe^{2+} ion present in the reaction mixture was better than Fe^{3+} ion present as a dopant (which is added during the catalyst preparation). The optimum photocatalyst calcinations temperature for degrading paraquat and malathion were 550°C for TiO$_2$ and 500°C for ZnO. The physical properties of the best catalyst were characterized using SEM, XRD, UV-Vis-NIR spectrophotometer and elipsometer. By increasing the calcinations temperature up to 600°C, XRD data showed the transformation of TiO$_2$ anatase to rutile phase while for ZnO, the increment of the intensity of ZnO catalyst was observed, indicating that, the quality of ZnO wurtzite crystal was improved. The thicknesses for ZnO, ZnO/TiO$_2$ 1:0.05 and ZnO/TiO$_2$ doping with Fe^{3+} thin film were 130.57 nm, 150.68 nm and 153.84 nm respectively. The band gap energy values measured using UV-Vis NIR were in the range of 2.95 – 3.09 eV.

Abstrak

Parakuat, sejenis racun rumpai dan malation sejenis racun serangga merupakan pesitisid yang mencemar sistem akuatik. Banyak usaha telah dijalankan masa kini untuk merawat air yang tercemar. Antara kaedah yang terbaru adalah teknik pemangkin foto. Dalam kajian ini, mangkinfoto TiO$_2$ dan ZnO telah digunakan untuk mendegradasikan larutan racun perosak dengan kehadiran sinaran ultralembayung (λ=354 nm). Kadar fotodegradasi diukur dengan menggunakan Spektrofotometer Ultralembayung-Nampak dan analisis TOC. Malation menunjukkan serapan pada λ=210 nm manakala parakuat pada λ=258 nm. Pasangan mangkin yang terbaik mendegradasi larutan malation adalah TiO$_2$/ZnO dengan nisbah % berat 1:0.05 manakala mangkin yang terbaik untuk mendegradasi larutan parakuat adalah pasangan mangkin TiO$_2$/ZnO dengan nisbah % berat 1:0.03. Kehadiran dopan yang ditambahkan dalam penyediaan mangkin, merencatkan tindak balas fotodegradasi manakala penambahan ion logam dalam larutan tindak balas meningkatkan peratus fotodegradasi. Mangkin TiO$_2$ yang dikalsin pada suhu 550°C dan mangkin ZnO yang dikalsinkan pada suhu 500°C memberikan peratus degradasi yang paling tinggi. Pencirian sifat fizik mangkin dikaji dengan menggunakan SEM, XRD, UV-Vis-NIR spektrofotometer dan elipsometer. Data XRD menunjukkan bahawa apabila suhu pengkalsinan dinaikkan ke 600°C, fasa anatas TiO$_2$ telah bertukar kepada fasa rutil. Sebaliknya untuk ZnO, peratus intensiti puncak ZnO didapati bertambah dengan pertambahan suhu pengkalsinan. Ini menunjukkan bahawa kualiti kristal wurzit ZnO bertambah baik. Ketebalan saput tipis bagi ZnO, ZnO/TiO$_2$ 00.05 dan ZnO/TiO$_2$ didop dengan Fe^{3+} ialah masing-masing 130.57 nm, 150.68 nm 153.84 nm. Nilai E$_{bg}$ saput tipis ZnO adalah dalam lingkungan 2.95 – 3.09 eV.

Introduction

Paraquat and malathion can be introduced into aquatic environments especially in the river through intentional application (controlling of aquatic weeds, algae, fish or unwanted invertebrates), aerial drift, runoff from agricultural applications or runoff from accidental release. Rivers are directly linked to estuaries, coasts and open seas where the pollutants can be transported by the flow, and contact with the atmosphere through volatilization [1].

Several methods were used in treating wastewater such as coagulation, photodegradation, ozonation, biological treatment, filteration, etc. The advantages of using photodegradation are, there are no sludge produced and foul

odors are greatly reduced, safety application of the reactions being performed at atmospheric pressure and near ambient temperature and requires only dissolved oxygen in water [2].

The molecular orbital of semiconductors has a band structure that consult highest occupied valence band and lowest unoccupied valence band separated by band gap energy, E_{bg}. When the semiconductor is illuminated with ultra violet light with photon energy greater or equal to the band gap energy of the semiconductor, valence band electrons are excited to the conduction band leaving a hole behind (Equation 1). TiO_2 anatase band gap energy is 3.2 eV while ZnO band gap energy is 3.17 eV. Superoxide anion radicals ($•O_2^-$) and hydroxyl radicals ($•OH$) are being generated (Equation 2 and 3) in the aqueous medium and these spescies are responsible to accelerate the oxidation of pollutants [3, 4]. The efficiency of the photocatalysts activity can be enhanced by coupling the ZnO and TiO_2 (ZnO /TiO_2) semiconductor [5].

$$Semiconductor \; + \; h\nu \; \rightarrow \qquad e^- \; + \quad h^+ \tag{1}$$
$$O_2 \; + \; e^- \; \rightarrow \; •O_2^- \tag{2}$$
$$H_2O + \; h^+ \; \rightarrow \; •OH + H^+ \tag{3}$$
$$OH^- \; + \; h^+ \rightarrow \; •OH \tag{4}$$
$$•OH + H^+ \rightarrow \; •OH_2 \tag{5}$$
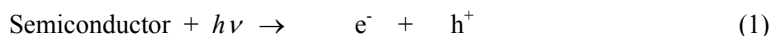
This research studies the degradation reaction of paraquat and malathion using single and couple semiconductor. The best ratio of TiO_2/ZnO coupled photocatalyst for both pesticides will then doped with Fe^{3+} ions. The photocatalyst was characterized further using X-Ray Diffraction (XRD) and Scanning Electron Microscopy (SEM) technique. The photodegradation was conducted in the presence of UV-light and monitored by UV-Visible spectroscopy and the mineralization was monitored using TOC analyzer. Degradation process is the process of breaking the organic molecules into smaller organic molecules, while mineralization process is a process that converts organic molecules into minerals such as NO_3^-, PO_4^{3-}, CO_3^{2-}, depending on the elements present in the molecule.

Experimental

Reagents and Chemicals

The commercial paraquat dichloride "Gramoxone PP910" with active ingredients 25 % w/w was purchased from CCMB Agrochemical Sdn. Bhd. Shah Alam. The standard paraquat (1,1'-dimethyl-4,4'-bipyridylium dichloride) was purchased from Reference Material for Residue Analysis, Germany, malathion (active ingredients about 57 % w/w), ferric nitrate nonahydrate ($Fe(NO_3)_3.9H_2O$) and ferrous sulfate heptahydrate ($FeSO_4.7H_2O$) were obtained from GCE (Goodrich Chemical and Emory). TiO_2 powder (99 % anatase, sigma), titanium tetraisopropoxide (TTIP), ethanol (absolute ≥ 99 %) and polyethylene glycol 2000 (PEG 2000), were obtained from Fluka Chemika while diethanolamine (DEA) from Riedel de Haen AG. Zinc acetate ($Zn(OAc)_2$) is obtained from Analar (BDH), and sodium hydroxide (NaOH) from Ashland Chemical and 2-propanol from J.T Baker.

Apparatus

Photocatalytic tests were performed in a batch photoreactor of 1000 mL made of pyrex glass cylinder. The calcination of the photocatalyst was carried out in the furnace Nabertherm L3/S17 model. Ultra violet lamp (Yamato, λ=354 nm, 6 W, 100 V) was used as the UV light sources with the support of a Teletron step down transformer (Model TSD 100 W). The instruments for monitoring and characterizing of samples are Perkin Elmer UV-Visible spectrophotometer, Shimadzu (TOC 500) Total Organic Carbon Analyzer, Siemens D5000 X-Ray diffractometer   (XRD) equipped with Cu-K_α (λ=1.54 Å) radiation, Scanning Electron Microscopy (SEM Phillips XL 40), Ellipsometer Geatner and Shimadzu UV-3101PC UV-Vis-NIR Spectrophotometer.

Preparation of TiO_2 sol-gel

Polyethylene glycol (PEG 2000) (6 g) was dissolved in ethanol (600 mL) in a 1 L volumetric flask. The solution was stirred continuously until PEG was completely dissolved before 31.8 g diethanolamine (DEA) was added to the solution followed by 85.2 g of titanium(IV) isopropoxide (TTIP). The solution was left for a few minutes before 5.4 mL deionized water was added. The solution was stirred continuously for 3 hours at ambient temperature until it forms homogeneous solution. The conical flask was kept close during the sol-gel preparation to prevent the evaporation of ethanol as the process was exothermic [6].

Preparation of ZnO sol-gel
Zinc acetate (0.5 g) was dissolved in 2-propanol (100 mL) in a volumetric flask at 50-60°C and stirred continuously. At the same time, sodium hydroxide (NaOH) (10 mg) was dissolved in 2-propanol (100 mL) and stirred at the same temperature. These two solutions were mix together and continuously stirred in ice bath (at 0°C), then the solution was kept in water bath at room temperature for an hour [7].

Thin Film Preparation
The thin film was coated on glass support using the dip-withdraw method by repeating the dip-withdraw process for five times. The support used in this study is a microscope slide glass (76 x 26 x 2 mm). The coated slides were calcined in the furnace where the temperature was elevated at 1°C min^{-1} up to 550°C for TiO$_2$ photocatalyst and 2°C min^{-1} up to 500°C for ZnO and kept at this temperature for an hour [8].

Photocatalytic measurement
Photocatalytic study of TiO$_2$ and ZnO thin film was examined in degrading 200 mL pesticide solutions (1 x 10^{-4} M paraquat and 2 x 10^{-4} M malathion) under various experimental conditions. This photocatalytic reaction was carried out in a glass reactor and irradiated with UV lamp for 4 hours in the presence of photocatalyst. An aliquot (4 mL) was taken at specific time intervals. For the degradation process the samples were analyzed using UV-Vis spectrophotometer (Equation 6) and the Total Organic Carbon analyzer was used to analyze the mineralization of the pesticides (Equation 7).

$$\% \text{ Degradation} = (A_o/A_t) \times 100, \qquad\qquad (6)$$
where,
A_o= initial absorption
A_t= absorption at t time.

$$\% \text{ Mineralization} = (TOC_o/TOCt) \times 100 \qquad\qquad (7)$$
Where,
TOC_o= total organic carbon value before irradiation
TOC_t= total organic carbon value after irradiation

Photodegradation using TiO$_2$, ZnO and a mixture of TiO$_2$/ZnO thin film
Seventeen microscope slide glasses containing TiO$_2$, ZnO and a mixture of TiO$_2$/ZnO (ratio 1:$\leq$ 0.08) thin film as shown in Table 1 were used in paraquat and malathion degradation.

Photodegradation using the best photocatalyst doped with Fe^{3+}
The two best photocatalysts each for paraquat and malathion was doped with Fe^{3+} (ratio 1:0.005). 0.05062 g and 0.0035 g Fe(NO$_3$)$_3$.9H$_2$O containing Fe^{3+} was weighed and added into 75 mL of the best TiO$_2$/ZnO and ZnO/TiO$_2$ sol-gel respectively and stirred. A clean microscope slide was dipped into the sol-gel and withdrew gently with a constant speed. The process was repeated for five times.

Table 1: Mixture ratios of TiO$_2$: ZnO ($\leq$ 5%) and ZnO: TiO$_2$ ($\leq$ 8%)

% Weight ratio TiO$_2$:ZnO (g)	TiO$_2$ sol-gel (mL)	ZnO sol- gel (mL)	Total sol-gel volume (mL)
1:0.05	30	43.75	73.75
1:0.03	40	35	75
1:0.01	60	17.5	77.5
0.08:1	80	0.22	80.22
0.05:1	80	0.14	80.14
0.03:1	80	0.07	80.07
0.01:1	80	0.03	80.03

Photodegradation using the best photocatalyst with Fe^{2+} ion dissolved into the working solution
20 mL of 55.84 ppm Fe^{2+} (9.998 x 10^{-5} M) ion solution was pipetted into 500 mL volumetric flask containing 200 mL pesticides and diluted with deionized water to make the working solution. The 200 mL working solution was place in a pyrex reaction cell and was treated as stated earlier in the photocatalytic measurement.

Effect of photocatalyst calcination temperature on the photodegradation process
The two best photocatalyst for each paraquat and malathion were calcined at different temperatures as shown in Table 2. The photocatalytic measurement was carried out as stated earlier.

Table 2: Calcination temperatures of the best photocatalyst

Number of slide	Calcination temperature (°C)	
	ZT03 (paraquat)	ZT05 (malathion)
2	600	600
2	200	200

ZT03: The best photocatalyst for paraquat, TiO_2 : 3% ZnO
ZT05: The best photocatalyst for malathion, ZnO : 5% TiO_2

Effect of support on photodegradation process
Prepared photocatalyst powder was weighed with the same amount of thin film coated onto the glass slide. Photocatalytic measurement was carried out as stated before using thin film and the prepared powder of the best photocatalyst.

Results and Discussions

Calibration of total organic carbon
A linear calibration curve was matched with UV absorption value in the same range in order to determine the suitable working solution concentration for further degradation process. The suitable concentration of formulated paraquat is 1×10^{-4} M (29.52 ppm) with UV absorption value, 1.363 and for formulated malathion, the suitable concentration is 2×10^{-4} M (59.89 ppm) with UV absorption value, 2.135.

Effect of TiO_2 thin film and commercial TiO_2 on paraquat and malathion photodegradation
Degradation and mineralization of paraquat with commercial TiO_2 was higher than TiO_2 thin film as shown in Figure 1 and Figure 2. 77.67% paraquat was mineralized by using commercial TiO_2 while only 42.21% was mineralized using prepared thin film. Commercial TiO_2 performed better as photocatalyst in which 58.57% malathion was degraded compared to 50.09% using TiO_2 thin film after 4 hours reaction. Mineralization process using commercial TiO_2 was better compared to TiO_2 thin film through out the reaction time due to the fact that commercial TiO_2 had a pure anatase crystal structure with high active surface area [9]. While the thin film catalysts prepared from the sol-gel method does not have a perfect lattice as the commercial catalyst thus giving a detrimental affect on their photocatalytic activity [10]. Even though the photocatalytic activity of commercial TiO_2 is better than the prepared thin film, the entire research was focused on the thin film photocatalyst to study the synergy effect of ZnO and TiO_2 semiconductor in degrading and mineralizing paraquat and malathion solution.
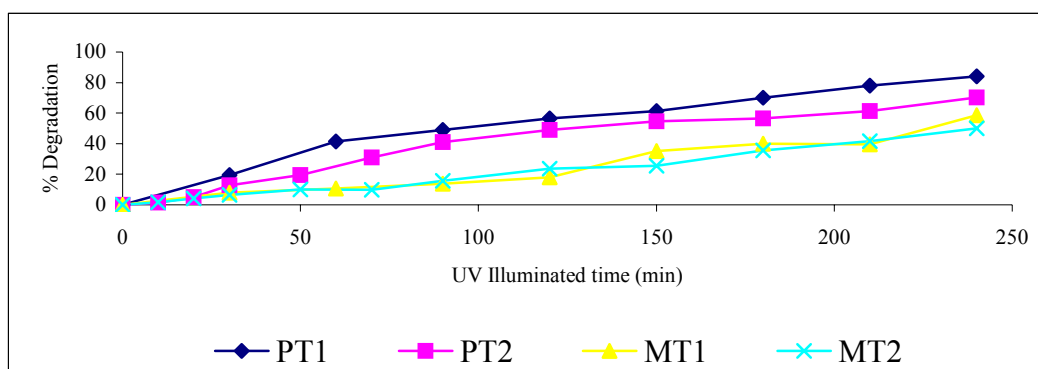
Figure 1: Percent degradation of paraquat (P) and malathion (M) at different illumination time. (PT1: commercial TiO_2 in paraquat, MT1: commercial TiO_2 in malathion, PT_2: TiO_2 thin film in paraquat and MT2: TiO_2 thin film in malathion).
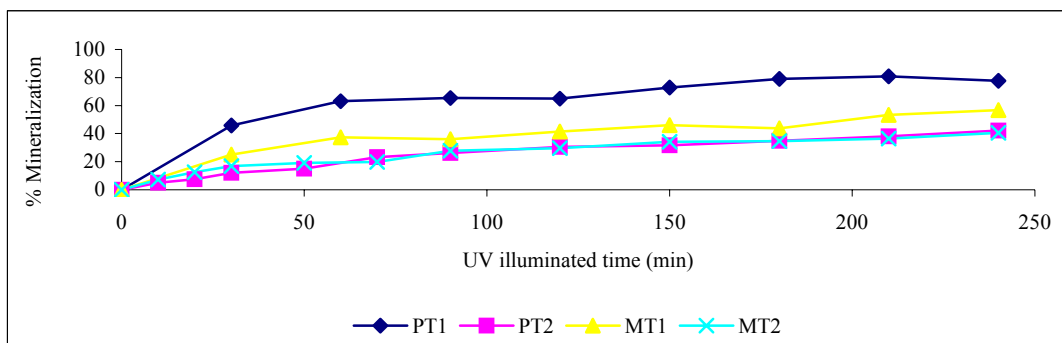
Figure 2: Percent mineralization of paraquat (P) and malathion (M) at different illumination time. (PT1: commercial TiO_2 in paraquat, MT1: commercial TiO_2 in malathion, PT_2: TiO_2 thin film in paraquat and MT2: TiO_2 thin film in malathion).

Effect of single TiO_2, ZnO and coupled TiO_2/ZnO semiconductor on paraquat and malathion photodegradation
The degradation and mineralization of paraquat were higher in the presence of TiO_2 photocatalyst than ZnO as shown in Figure 3. Modifying the surface properties of TiO_2 with $\leq 5\%$ ZnO, significantly enhances the rate of photocatalytic degradation of this cationic pollutant. TiO_2/ZnO (TZ0.3; 1:0.03) couple semiconductor, containing 97% TiO_2 and 3% ZnO was chosen as the best photocatalyst in degrading paraquat solution (% degradation :80.12%, % mineralization: 52.32%). In contrast, the photodegradation of malathion was higher in the presence of ZnO as shown in Figure 4. The best photocatalyst in degrading malathion solution is zinc oxide couple with 0.05 titanium dioxide (95% ZnO and 5% TiO_2). The optimum degradation of malathion is 84.92% while the total mineralization is 58.66% after 4 hours reaction.
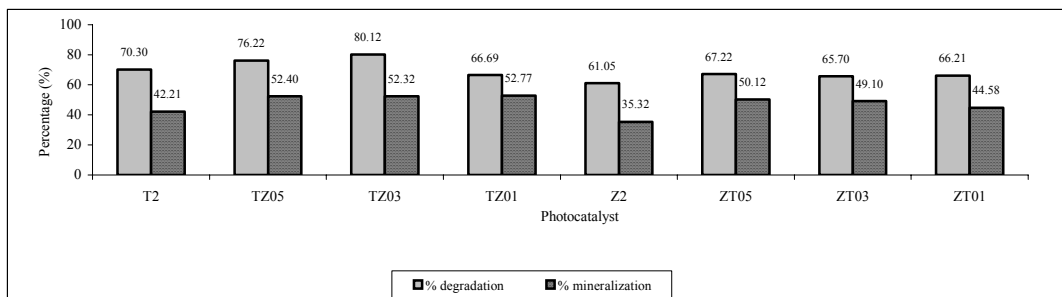
Figure 3: Percent of degradation and mineralization of paraquat with single and couple semiconductor photocatalyst TiO_2 and ZnO after 4 hours UV radiation.
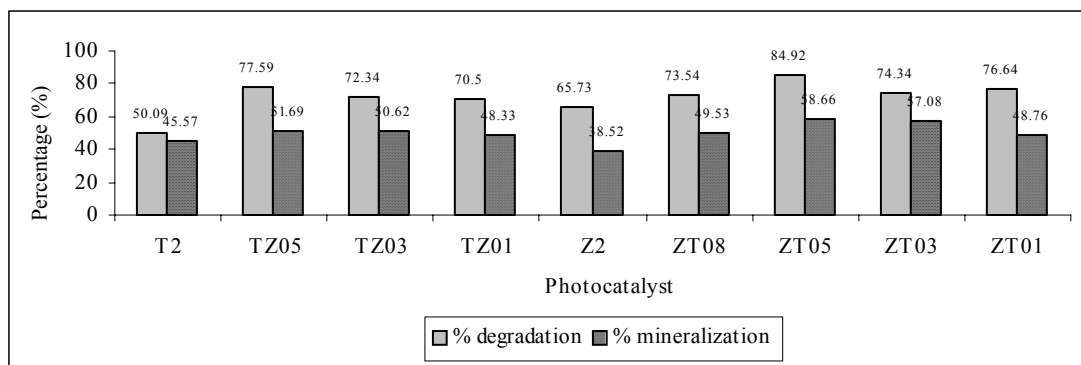
Figure 4: Percent of degradation and mineralization of malathion with single and couple semiconductor photocatalyst TiO_2 and ZnO under UV light within 4 hours reaction.

81

Effect of Fe^{3+} as dopant (co-catalyst) and the addition of Fe^{2+} ions into the working solution.
Theoretically, the presence of metal ions can delay the recombination process of generated electrons and holes as shown in Equation 8 and 9. Therefore the photodegeadation results are expected to be higher. 92.71% total degradation and 77.07% total mineralization of paraquat while 94.74% degradation and 81.17% mineralization of malathion were observed when Fe^{2+} ion was added into the pesticide solution after 4 hours illumination as shown in Figure 5 and Figure 6.

$$M^{n+} + e \rightarrow M^{(n-1)+} \tag{8}$$
$$M^{(n-1)+} + h^+ \rightarrow M^{n+} \tag{9}$$

In contrast, the use of Fe^{3+} as dopant gave detrimental effect. When the metal is deposited on the photocatalyst, it was scattered in the bulk of the catalyst therefore increasing the recombination process of e^-h^+ pairs.
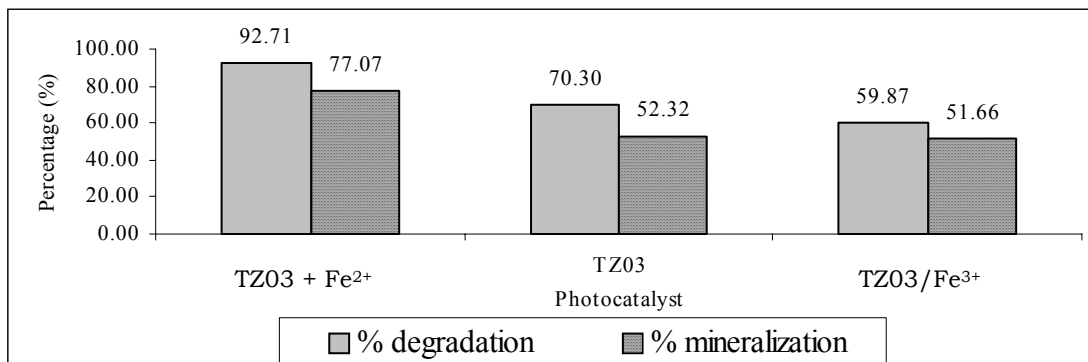
Figure 5: Percent of degradation and mineralization of paraquat with the best of photocatalyst doping with Fe^{3+} (TZ03/Fe^{3+}) and the addition of Fe^{2+} into paraquat solution (TZ03 + Fe^{2+}).
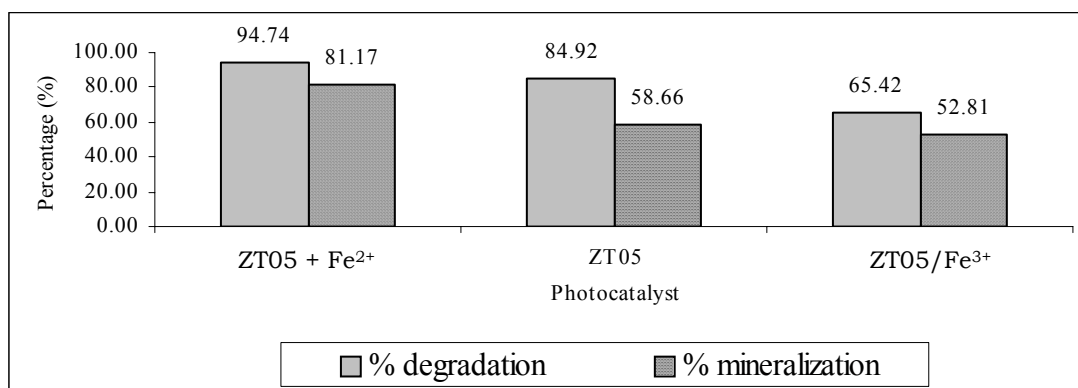
Figure 6: Percent degradation and mineralization of malathion with the best of photocatalyst doped with Fe^{3+} (ZT05/Fe^{3+}) and the addition of Fe^{2+} into the malathion solution (ZT05 + Fe^{2+}).

Effect of calcinations temperature.
The optimum degradation was observed with catalyst calcined at 550°C. 80.12% paraquat was degraded at this temperature compared to 600°C (48.01%) and 200°C (21.36%) as shown in Figure 7. A similar pattern was observed for mineralization. Catalyst prepared at 550°C gave the highest percent of mineralization followed by 600°C and 200°C. The amorphous titania is known to have very low photocatalytic activity compared to that of the anatase or rutile phase due to an increased of electron – hole pairs recombination rate [11]. At 550°C the anatase phase is fully formed while at a temperature of 600°C, the rutile phase starts to appear. Anatase phase has a high photocatalytic activity because it contain more surface hydroxyl group that can react with holes to generate hydroxyl radicals. The recombination process was thus delayed by the presence of hydroxyl radical.
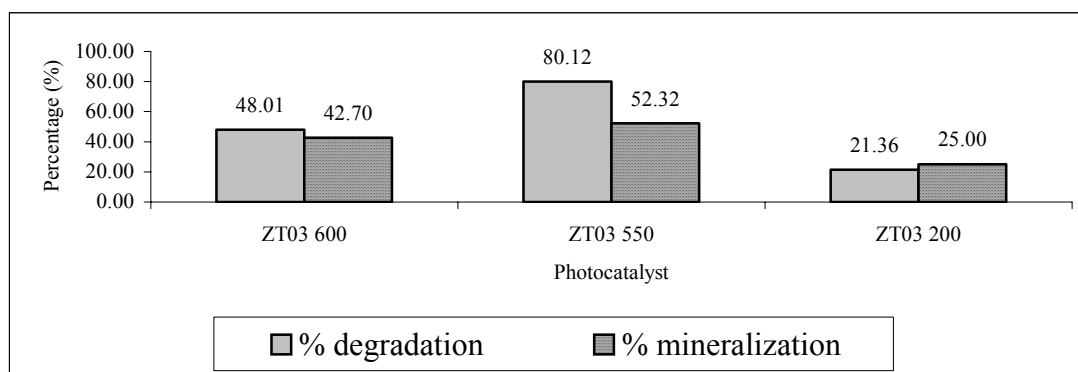
Figure 7: Percent degradation and mineralization of paraquat with the best of photocatalyst with various calcinations temperature (TZ03 600: 600°C, TZ03 550: 550°C, TZ03 200: 200°C)

From Figure 8, the optimum degradation (80.12%) and mineralization (52.32%) were observed using catalyst calcined at 500°C. At this temperature, the ZnO wurtzite crystal has fully formed [12]. At 600°C, the percentage of the degradation and mineralization of the pesticide decreases. Agglomeration of the photocatalyst will occur which attributed to the low surface area. This condition will lower the photocatalytic activity of the photocatalyst. While at 200°C,   crystallization of crystalline ZnO is incomplete.
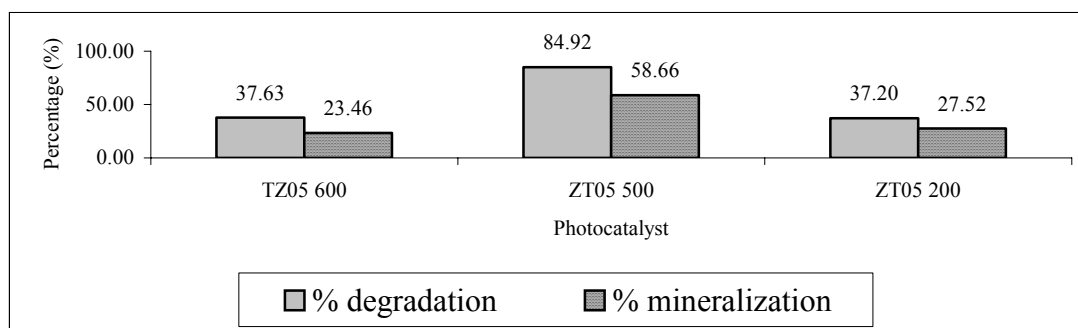
Figure 8: Percent of degradation and mineralization of malathion with the best of photocatalyst with various calcinations temperature (ZT05 600: 600°C, ZT05 500: 500°C, ZT05 200: 200°C)

Supported photocatalyst
The catalyst coated on support were observed to perform better than the powder (unsupported) as shown in Figure 9 and Figure 10. The greater substrate degradation and mineralization is due to the availability of surface adsorption site in the prepared thin film. Catalyst activity of the unsupported photocatalyst was lower because the catalyst particles were trapped inside the agglomeration particle where radiation cannot penetrate. This will avoid the maximum generation of electron and hole pairs.
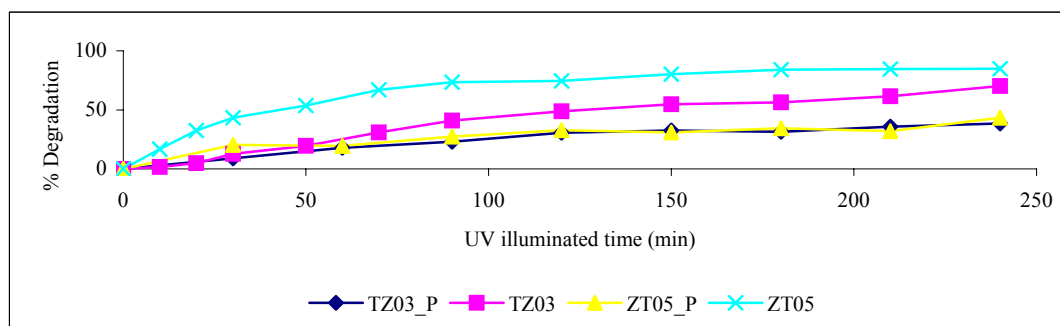
Figure 9: Percent degradation of pesticide with the best photocatalyst thin film (TZ03) and powder form (TZ03_P) for paraquat and the best photocatalyst thin film (ZT05) and powder form (ZT05_P) for malathion.
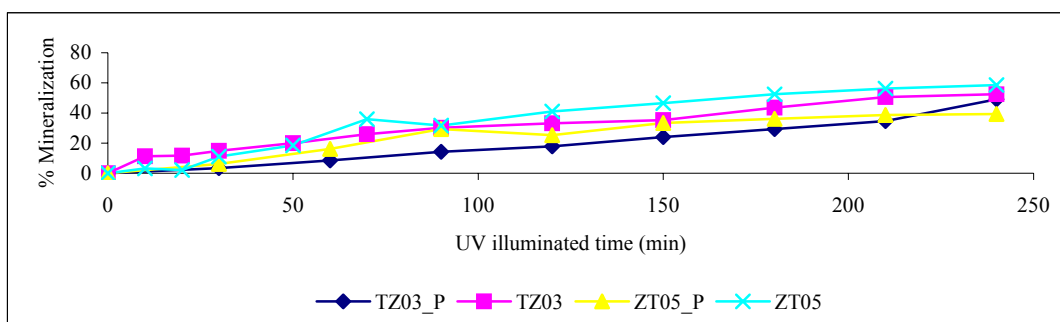
Figure 10: Percent mineralization of pesticide with the best photocatalyst thin film (TZ03) and powder form (TZ03_P) for paraquat and the best photocatalyst thin film (ZT05) and powder form (ZT05_P) for malathion.

SEM analysis

As shown in Figure 11, TiO_2 thin films were mainly composed of small uniform spherical particles monodispersed on the surface of the glass slide with a calcination temperature of 550°C. The surface of the films exhibited a certain degree of roughness and the thin film become rougher when coupled with zinc oxide.

(a)   (b)
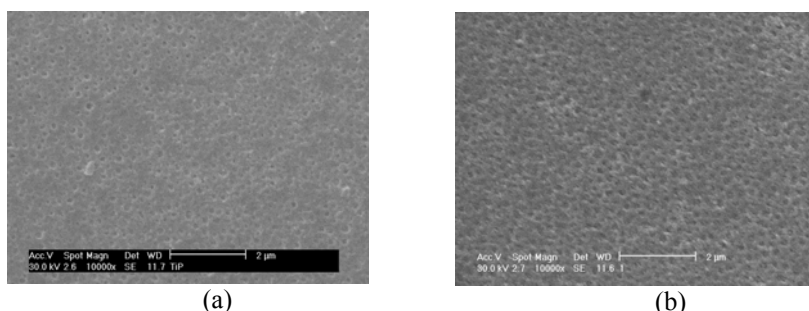
Figure 11**:** SEM micrographs of a) TiO_2 thin film b) TiO_2/ZnO 0.03 couple semiconductor thin film calcined at 550°C (magnification factor: 10000x)

The SEM micrographs for ZnO photocatalyst calcined at the same temperature of 500°C is shown in Figure 12 which indicates the irregular shape of particle formed. The second thin film, which was couple with 5%, TiO_2 shows smooth surface with a fine microstructure without cracks and voids. The grains of the film become larger and denser if coupled with TiO_2.

(a)   (b)
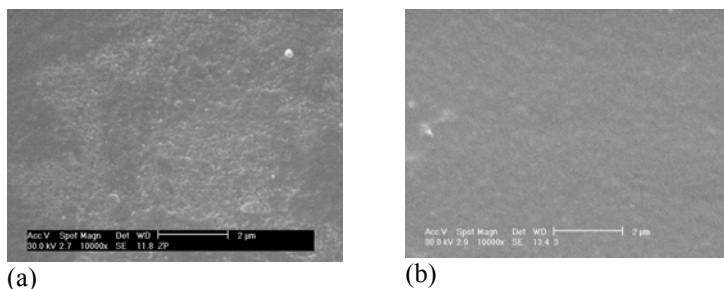
Figure 12: SEM micrographs of a) ZnO thin film b) ZnO/TiO_2 0.05 couple semiconductor thin film calcined at 500°C (magnification factor: 10000x).

XRD analysis

Diffractogram of catalyst calcined at 200°C indicated that the catalyst was an amorphous phase as shown in Figure 13. By increasing the temperature up to 450°C, transformation of phase occurred whereby amorphous phase was transformed to anatase phase. At 600°C, the rutile phase started to appear, therefore forming a mixture of anatase and rutile catalyst. The presence of rutile phase will decrease the performance of catalyst due to the lack of hydroxyl ion surface species. Thus will increased the $(e^- - h^+)$ pairs recombination process.

Intensity %
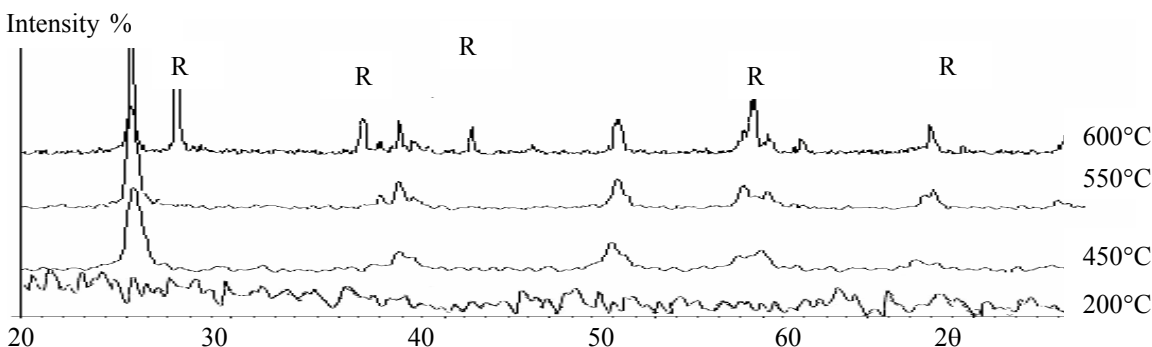
Figure 13: Diffractograms of TiO_2/ZnO 0.03 prepared using sol-gel method and calcined at 200°C, 450°C, 550°C and 600°C (R=rutile).
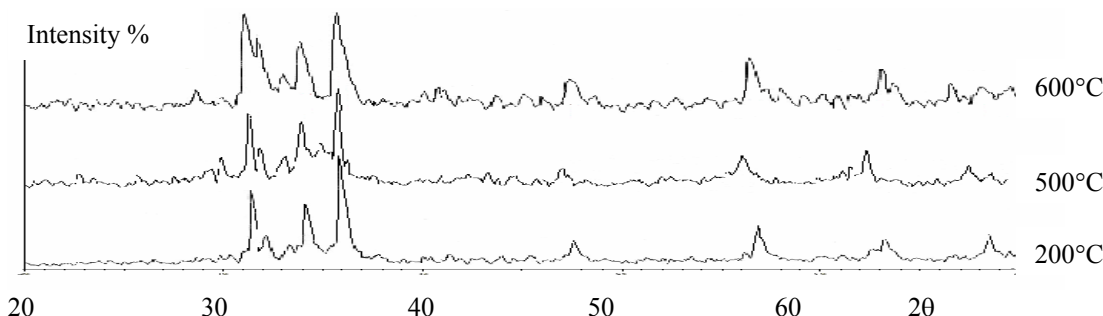
Intensity %

Figure 14: Diffractograms of ZnO/TiO_2 0.05 prepared using sol-gel method and calcined at 200°C, 500°C and 600°C.

By increasing the calcinations temperature of ZnO photocatalyst to 500°C, the increment of intensity become stronger, which indicated that the quality of ZnO catalyst in thin film has improved as shown in Figure 14. At 200°C, the formation of the metastable ZnO phase occurred. This was supported by Yang *et. al.* [13] who reported that low temperature portion of the $ZnO-TiO_2$ phase diagram is difficult to study due to the sluggishness of the reactions and the similarities of the XRD patterns.

Ellipsometer (Thickness measurement)
The values of polarizer (P), analyzer (A), thickness and refractive index of the thin film photocatalyst are shown in Table 3. The thickness of the thin film increases as it was coupled with different semiconductor and doped with Fe^{3+} ions. As the second semiconductor and metal ion were added, the viscosity of the sol-gel increased.

Table 3: The angle value of polarizer (P), analyzer (A) and the value of thickness and refractive index of the thin film photocatalyst.

Parameter	Angle value for thin film (°)		
	ZnO	**ZnO/TiO$_2$ 0.05**	**ZnO/TiO$_2$ 0.05/Fe^{3+}**
A$_1$	22.9	18.8	24.3
P$_1$	130.4	128.0	127.3
A$_2$	149.2	158.5	154.7
P$_2$	199.8	214.4	218.2
Thickness (nm)	**130.57**	**150.68**	**153.84**
Refractive Index	**2.4946**	**2.1984**	**2.2042**

UV-Vis-NIR analysis (Band gap Energy measurement)
The band gap energy, E_{bg} values for all thin films were determined by plotting $[\alpha hc/\lambda]^{1/2}$ versus the equivalent energy at wavelength λ (h = Planck constant, c = light velocity). The α (absorption coefficient) was derived from the measured transmittance (T) and reflectance (R) factors with a wavelength ranging from 300-500 nm. The α can be obtained by using the following relationship:

$$T = (1-R^2) \exp(-\alpha d) \tag{10}$$

Where d is the thickness of the thin film. The resulting diagram is called Tauc's plot (Figure 15) and the respective band gap energy was obtained by extrapolation of the Tauc plot dataset to $[\alpha hc/\lambda]^{1/2} = 0$. Coupled TiO_2 have the lowest bandgap energy (2.95 eV) than single ZnO photocatalyst (3.04 eV). Band gap energy for doped catalyst was higher (3.09 eV) than coupled TiO_2. These data were in a good agreement with the results obtained in the photodegradation reaction data. The higher value of E_{bg} will reduce the formation of $(e^- h^+)$ pair, therefore reducing the performance of the photocatalyst.
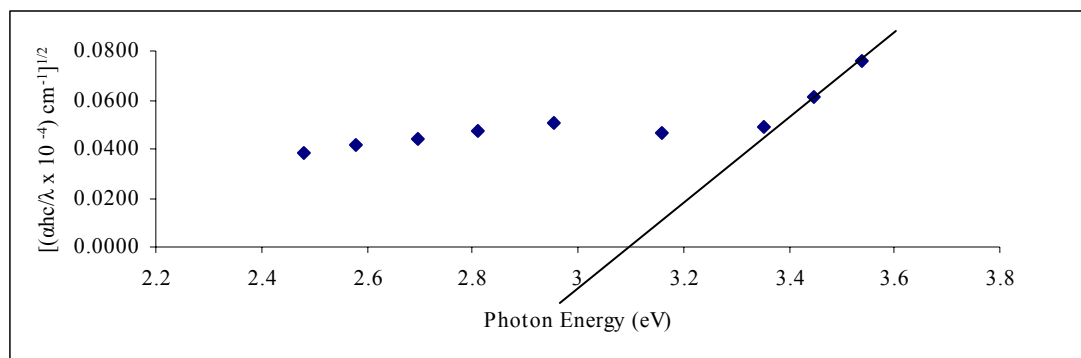
Figure 15: Tauc's plot for indirect band gap of ZnO (E_{bg}: 3.04 eV)

Conclusion

Zinc oxide is an efficient catalyst in degrading malathion solution while titanium dioxide is found to be more efficient in degrading paraquat solution. The best coupled photocatalyst degrading malathion solution is $ZnO:TiO_2$ with a ratio of 1:0.05. In contrast the best coupled photocatalyst in degrading paraquat solution is $TiO_2:ZnO$ in a ratio of 1:0.03. Dissolved Fe^{2+} ions have showed the highest photocatalytic activity in degrading paraquat and malathion solution. Coupled photocatalyst doped with Fe^{3+} ion exhibited lower photodegradation compared to undoped coupled photocatalyst. The best calcination temperature for TiO_2 based photocatalyst is 550°C while for ZnO based photocatalyst is 500°C. This result was supported by XRD diffractograms and SEM micrographs. Supported catalyst plays an important role giving the high dispersion rate and enhanced the photodegradation process of paraquat and malathion rather than the unsupported one. The thickness of ZnO, ZnO/TiO_2 0.05 and ZnO/TiO_2 0.05 doped with Fe^{3+} thin film are 130.57 nm, 150.68 nm and 153.84 nm. The band gap energy values measured using UV-Vis NIR are in the range of 2.95 – 3.09 eV.

References

1. Petit, V., Cabridenc, R., Swannell, R.P.J. and Sokhi R.S. (1995) " Review strategies for modelling the environmental fate of pesticides discharged into riverine systems." *Environ. International*. **21** (2). 167-176
2. Robertson, P.K.J. (1996) "Semiconductor photocatalysis: an environmentally acceptable alternative production technique and effluent treatment process" *J. Cleaner Prod.* **4** (3-4). 203-212.
3. Mills, A. and Le Hunte, S. (1997). "An overview of semiconductor photocatalysis" *J. of Photochem. and Photobiol. A: Chemistry*, **108**. 1-35.
4. Vidal, A., Dinya, Z., Mogyorodi Jr., F. and Mogyorodi, F. (1999). "Photocatalytic of thiocarbamate herbicide active ingredients in water." *Applied Catalyst B: Environ.*. **21**. 259–267.
5. Yang, J. and Swisher, J.H. (1996). "The phase stabilization of $Zn_2Ti_3O_8$." *Material Characterization*. **37**. 153-159.
6. Adilah Bt Hj Abdul Aziz. (1999). *Sintisis dan pencirian mangkin TiO₂ serta kajian fotodegradasi racun makhluk perosak*, Tesis Sarjana, Universiti Teknologi Malaysia.
7. Dindar, B. and Icli, S. (2001). "Unusual photoreactivity of Zinc Oxide irradiated by concentrated sunlight." J. of Photochem. And Photobiol..140. 263-268.
8. Ganesh Subramanium. (2002). "*The optimization of photocatalytic degradation of paraquat using Titanium(IV) oxide Thin film*. Master Thesis, Universiti Teknologi Malaysia.
9. Florencio, M.H., Pires, E., Castro, A.L., Nunes, M.R., Borges, C. and Costa, F.M. (2004). "Photodegradation of Diquat and Paraquat in aqueous solutions by titanium dioxide: evolution of degradation reactions and characterization of intermediates." *Chemosphere*. **55**. 345-355.

10. Araña, J., González, D.O., Doña, R.J.M., Herrera M.J.A., Cabo, C.G., Pérez P.J., Hidalgo, M.C. and Navio-Santos, J.A. (2003). "Role of Fe^{3+}/Fe^{2+} as TiO_2 dopant ions in photocatalytic degradation of carboxylic acids." *J. of Molecular Catalysis A: Chemical*. **197.** 157-171.

11. Su, C., Hong, B.-Y. and Tseng, C.-M. (2004). "Sol-gel preparation and photocatalysis of titanium dioxide." *Catalysis Today*. **96**. 119-126

12. Li, H., Wang, J., Liu, H., Yang, C., Xu, H., Li, X. and Cui, H. (2004). "Sol-gel preparation of transparent zinc oxide films with highly preferential crystal orientation.

13. Yang, J. and Swisher, J.H. (1996). "The phase stabilization of $Zn_2Ti_3O_8$." *Material Characterization*. **37**. 153-159.

KANDUNGAN TOLUENA DAN XILENA DALAM DEBU JALAN DI SEKITAR KUALA LUMPUR

Mohd Rozali Othman dan Nor Faizawati Zulkifli

Pusat Pengajian Sains Kimia dan Teknologi Makanan, Fakulti Sains dan Teknologi
Universiti Kabangsaan Malaysia, 43600 UKM Bangi, Selangor Darul Ehsan, Malaysia.
e-mail: rozali@pkrisc.cc.ukm.my

Abstrak

Kajian telah dilakukan untuk menentukan kehadiran toluena dan xilena dalam debu jalan yang bersaiz <38 μm dan 38 – 63 μm di sekitar Kuala Lumpur. Kedua-dua bahan ini dipercayai digunakan dalam minyak petrol sebagai bahan tambah untuk meningkatkan nombor oktana petrol berkenaan. Setelah dilakukan pengekstrakan untuk mengeluarkan kedua-dua parameter kajian dari fasa pepejal (debu) kepada fasa cecair, analisis seterusnya dijalankan menggunakan kromatografi gas yang dilengkapi dengan pengesan pengionan nyala. Hasil kajian mendapati debu yang dikutip di kawasan pusat bandar memberikan kepekatan toluena dan xilena yang lebih tinggi berbanding dengan yang dikutip di kawasan pinggir bandar. Ujian ANOVA yang dilakukan menunjukkan bahawa terdapat perbezaan yang bererti antara lokasi persampelan yang berbeza dari segi struktur kawasan dan bilangan kenderaan yang melaluinya dan juga antara saiz debu yang berbeza. Ini menunjukkan bahawa kedua-dua bahan pencemaran ini adalah lebih bersifat setempat dan lebih bergantung kepada puncanya.

Abstract

The objective of this study is to determine the content of toluene and xylene in street dust (<38 μm and 38 – 63 μm in diameters) collected at various sites in the vicinity of Kuala Lumpur. Both pollutants were believed had been used as an additive in petrol to increase an octane number. After extraction by either soxhlet or agitating method, gas chromatography with flame ionization detector was used to quantify the amount of both parameters in street dust samples. Result obtained showed that the samples collected in urban areas recorded a higher concentration of toluene and xylene. ANOVA test showed that there are a significant differences between locations due to traffic flows and between two different sizes of dust particles.

Pendahuluan

Kemerosotan kualiti alam sekitar merupakan salah satu masalah yang semakin meruncing dari semasa ke semasa. Dunia semakin maju dan pesat membangun dalam pelbagai sektor, di mana ini secara tidak langsung akan memberikan impak yang begitu besar terhadap alam sekitar malah juga mengganggu kesihatan manusia sejagat. Pencemaran udara adalah salah satu masalah kualiti alam sekitar yang semakin parah pada masa kini. Terdapat banyak punca yang menyebabkan berlakunya pencemaran udara. Antaranya pembakaran secara terbuka, pembebasan asap daripada kilang–kilang, penggunaan kenderaan dan sebagainya. Dalam bahan pencemaran udara terkandung pelbagai jenis bahan pencemar yang berbahaya terhadap kesihatan manusia sama ada bahan-bahan organik atau bukan organik.

Debu terutamanya debu jalan raya terhasil daripada pelbagai punca. Debu jalan raya juga dikenalpasti sebagai unsur bahan pencemaran yang memberikan kesan buruk kepada manusia, haiwan dan tumbuhan. Debu boleh dikelaskan mengikut sumber dan kesannya kepada kesihatan manusia dan alam sekitar. Debu dikenali sebagai pepejal aerosol dan kebanyakannya tidak toksik [1], tetapi debu juga boleh dikatogerikan sebagai toksik jika bersaiz kurang dari 10μm [2, 3].

Debu adalah merupakan zarah–zarah kecil pepejal yang terkandung dalam udara di persekitaran. Zarah–zarah kecil ini wujud bersama–sama dengan gas, wap dan asap [4]. Debu juga boleh terhasil daripada pelbagai proses yang lain contohnya seperti daripada asap dari ekzos kenderaan, emisi dari industri dan pembakaran hutan, di mana zarah-zarah kecil ini akan bergabung dengan unsur-unsur lain di atmosfera dan membentuk zarahan yang

lebih besar dan kemudian akan termendap dan membentuk debu. Debu merupakan zarah yang cuba memendap dalam masa yang agak singkat [5]. Kehadiran debu dalam udara juga adalah hasil daripada proses penyepaian mekanikal dalam proses pemecahan, peleburan atau penggerudian yang kemudiannya terampai ke udara hasil daripada percampuran dengan gas [6]. Walaupun debu jalan raya mengandungi kepekatan bahan pencemar yang tinggi, namun ia hanya mewakili penumpukan pencemar semasa [7].

Dengan adanya sifat debu yang boleh terampai, mempunyai saiz yang sangat kecil dan berkemampuan untuk termendap, maka debu boleh digunakan sebagai matriks yang sesuai untuk analisis tahap pencemaran udara di sesuatu kawasan. Di samping itu debu boleh terampai dalam atmosfera atau dalam gas-gas lain serta tidak boleh meresap tetapi boleh mengenap dengan pengaruh graviti [8]. Salah satu contoh analisis terhadap debu yang telah dijalankan dalam banyak kajian terdahulu ialah analisis kandungan logam berat [3, 9, 10]. Di samping itu debu juga sesuai untuk analisis bahan pencemar organik seperti toluena dan xilena kerana dipercayai terkandungan dalam minyak petrol kenderaan.

Toluena dan xilena merupakan suatu bahan yang merbahaya kepada hidupan di mana pendedahan yang maksimum kepada sebatian ini boleh memudaratkan kesihatan manusia [11]. Kedua-dua bahan ini dapat memberi kesan jangka panjang dan jangka pendek kepada manusia bergantung kepada tahap atau paras pendedahannya. Antara kesan jangka pendek ialah simptom seperti pening kepala, alergi dan muntah [12]. Manaka kesan jangka masa panjang ialah menyebabkan barah, kerosakan jantung, hati dan buah pinggang [13].

Bahan–bahan ini dipercayai ditambah ke dalam minyak petrol untuk meningkatkan nombor oktananya. Bahan ini merupakan antara bahan yang ditambah ke dalam petrol tanpa plumbum untuk menggantikan plumbum yang bersifat anti-ketuk, di mana bahan-bahan ini akan terbebas ke udara sama ada bersama asap sekiranya pembakaran tidak sempurna ke atas petrol berlaku atau akan meruap bersama-sama petrol sekirangnya proses peruapan berlaku [14]. Bahan pencemar ini dilaporkan terkandung dalam minyak petrol kenderaan dalam kuanttiti yang kecil, tetapi yang menjadi masalahnya kepada persekitaran ialah penggunaannya adalah tidak terhad iaitu tiada piawai yang ditetapkan untuk kedua-dua bahan berkenaan [14, 15, 16]. Menurut kajian yang telah dilakukan amaun toluena dan xilena yang ditambahkan ke dalam minyak petrol adalah sedikit iaitu dalam jumlah antara 0.1 – 0.6% sahaja, terutamanya apabila penggunaan petrol tanpa plumbum semakin meningkat [16].

Sehubungan dengan itu kajian ini dilakukan untuk melihat kandungan toluena dan xilena yang terdapat di permukaan debu serta mengaitkannya dengan kesesakan lalulintas sesuatu lokasi persampelan. Kawasan persampelan yang terlibat ialah kawasan bandar dan kawasan pinggir bandar Kuala Lumpur di mana kedua-dua kawasan ini mempunyai kadar kesesakan lalulintas atau bilangan kenderaan yang berbeza.

Eksperimental

Lokasi Kajian

Lokasi kajian atau kawasan persampelan terbahagi kepada dua kawasan iaitu kawasan bandar dan kawasan pinggir bandar. Pemilihan kawasan persampelan adalah berdasarkan kepada pemerhatian tahap kesibukan lalulintas kawasan berkenaan. Kedudukan stesen-stesen persampelan adalah seperti yang diringkaskan dalam Jadual 1. Persampelan telah dilakukan sebanyak tiga kali di setiap lokasi.

Jadual 1. Kedudukan kawasan persampelan.

Kategori	Singkatan	Stesen
Kawasan bandar	PD	Puduraya
	DM	Dataran Merdeka
	BSK	Perhentian bas Klang
Kawasan pinggir bandar	DK	Danau Kota
	BU	Bukit Unggul

Bahan kimia dan alat radas

Bahan-bahan kimia utama yang digunakan dalam kajian ini adalah seperti petroleum eter (60-80°C takat didihnya) sebagai pelarut, toluena dan xilena (kesemuanya bergred Analar, BDH Chemical Limited). Manakala alat-alat radas yang digunakan ialah seperti alat-alat kaca yang berkaitan, pengayak (bersaiz 38 dan 63 μm), pengekstrak soxhlet yang dilengkapi dengan didal (thimble) selulosa, penggoncang mekanikal (Grant

instrument), Penyejat berputar (Bünchi Rotavapor) dan Kromatografi Gas (Hewlett-Packard Company) yang dilengkapi dengan pengesan pengionan nyala sebagai pengesan untuk analisis toluena dan xilena.

Persampelan dan Pengolahan Sampel
Pengambilan debu dilakukan dengan cermat iaitu menggunakan berus dan penyodok khas yang bebas xilena. Di mana permukaan jalan disapu secara perlahan-lahan untuk memastikan hanya debu di permukaan sahaja yang diambil. Kepanjangan jalanraya lebih kurang 100 m diperlukan untuk memastikan sampel yang cukup diperolehi. Sampel diambil di kawasan pusat bandar dan kawasan pinggir bandar. Sampel debu yang dikutip ini dimasukkan ke dalam beg plastik untuk dibawa ke makmal. Berat debu kira-kira dua kilogram diambil bagi setiap stesen. Di makmal sampel debu seterusnya dipindahkan ke atas piring kertas untuk proses pengeringan di udara sekurang-kurangnya selama 72 jam untuk memudahkan proses pengayakan. Saiz debu yang dikehendaki adalah berukuran <38 μm dan 38-63 μm. Saiz butiran debu ini diayak menggunakan pengayak bersaiz tertentu yang telah ditetapkan.

Kedua-dua kaedah pengekstarakan secara soxhlet dan penggoncangan (menggunakan penggoncang mekanikal) digunakan dalam kajian ini, dimana kedua-dua kaedah ini adalah merupakan kaedah klasik yang digunakan untuk mengekstrak bahan organik dari sampel pepejal [17]. Dalam kedua-dua kaedah pengekstrakan ini petroleum eter dengan takat didih dalam julat antara 60-80ºC dan debu seberat lebih kurang 1.0 gram (yang telah ditimbang dengan tepat) digunakan. Proses pengekstrakan ini dilakukan selama dua jam untuk kedua-dua kaedah pengekstrakan.

Alikuot sampel yang terhasil daripada proses pengekstrakan di atas seterusnya dikeringkan sehingga ke isipadu kira-kira 5 ml menggunakan alat pengeringan penyejat berputar sebelum dipindahkan ke dalam botol sampel yang bebas daripada toluena dan xilena [18]. Pemekatan alikuot sampel ke isipadu kira-kira 1.0 ml seterusnya dilakukan menggunakan aliran gas nitrogen sebelum disuntik ke dalam turus kromatografi. Sampel seterusnya dianalisis secara kualitatif dan kuantitatif menggunakan kromatografi gas.

Analisis Kromatografi Gas dan Kuantifikasi
Larutan ekstraksi dianalisis menggunakan kromatografi gas (model GC-HP5890 series II, Hewlett-Packard Company, USA). Keadaan pengoperasian alat kromatografi gas adalah seperti yang diringkaskan dalam Jadual 2.

Jadual 2. Pengoperasian kromatografi gas

Parameter	Peralatan/Keadaan/nilai
Pengesan	Pengesan Pengionan Nyala (FID)
Turus	Silika
Suhu pengesan	200°C
Suhu penyuntik	150°C
Gas pembawa	Nitrogen
Masa pemisahan	40 minit

Nota: Masa pemisahan yang panjang digunakan untuk memisahkan bahan lain yang hadir bersama

Pengesanan kehadiran toluena dan xilena ditentukan berdasarkan kepada masa penahanan bagi larutan piawainya dan juga kaedah penambahan piawai. Satu siri kepekatan larutan piawai toluena dan xilena yang sesuai digunakan untuk menyediakan lengkuk kalibrasi. Selain daripada untuk menentukan kehadiran toluena dan xilena, kaedah penambahan piawai juga digunakan untuk menentukan kepekatan toluena dan xilena dalam larutan sampel.

Hasil dan Perbincangan
Contoh kromatogram yang diperolehi dari analisis kromatografi gas untuk salah satu larutan sampel debu yang telah diekstrak adalah seperti yang ditunjukkan dalam Rajah 1. Manakala Jadual 3 dan 4 pula meringkaskan kepekatan toluena dan xilena dalam debu jalan yang telah diperolehi dalam kajian ini.

Dalam kajian ini dua kaedah pengekstrakan telah digunakan untuk mengekstrak sampel debu. Kaedah pengekstrakan tersebut ialah pengekstrakan soxhlet dan penggoncangan. Kedua-dua kaedah ini adalah merupakan kaedah klasik yang digunakan untuk mengekstrak bahan organik dari sampel pepejal [17]. Hasil

analisis menunjukkan kepekatan paling tinggi bagi bahan cemar organik toluena dan xilena dikesan pada sampel debu yang diekstrak menggunakan kaedah pengekstrakan soxhlet. Ini adalah kerana kesan daripada penggunaan isipadu pelarut yang digunakan dan juga kesan dari pemanasan. Jika pelarut yang digunakan adalah banyak maka lebih banyak bahan organik yang dapat dijerap keluar daripada permukaan butiran debu begitu juga dengan pemanasan. Aspek kelarutan dan pemanasan juga mungkin memainkan peranan dalam menentukan peratus kecekapan pengektrakan. Hasil kajian juga mendapati peratus perbandingan antara kedua-dua kaedah ini adalah lebih tinggi bagi toluena berbanding xilena (Jadual 3). Keadaan ini menunjukkan bahawa toluena lebih mudah terekstrak berbanding xilena walaupun kaedah pengekstrakan yang mudah seperti penggoncangan digunakan. Analisis secara kuantitatif dilakukan untuk menghitung kepekatan kedua-dua bahan pencemar organik toluena dan xilena dalam sampel debu menggunakan kalibrasi yang telah disediakan. Jadual 4 menunjukkan purata kepekatan toluena dan xilena dalam sampel debu yang telah digunakan.

Jadual 3.   Kepekatan purata bahan cemar dalam sampel menggunakan kaedah pengekstrakan soxhlet dan pengoncangan untuk saiz debu jalan <63 µm

Kaedah pengekstrakan	Kepekatan (μgg^{-1})	
	Toluena	Xilena
Soxhlet	203	847
Penggoncangan	163	183
%(Penggoncangan/soxhlet)	80.3%	21.6%

Jadual 4. Purata kepekatan toluena dan xilena dalam sampel debu

Saiz debu	Stesen persampelan	Kepekatan (μgg^{-1})	
		Toluena	Xilena
<38 µm	PD	163	100
	DM	114	td
	BSK	203	172
	DK	407	572
	BU	td	td
38-63 µm	PD	132	183
	DM	572	td
	BSK	491	938
	DK	953	td
	BU	td	td

Nota:td=tidak dapat dikesan

91
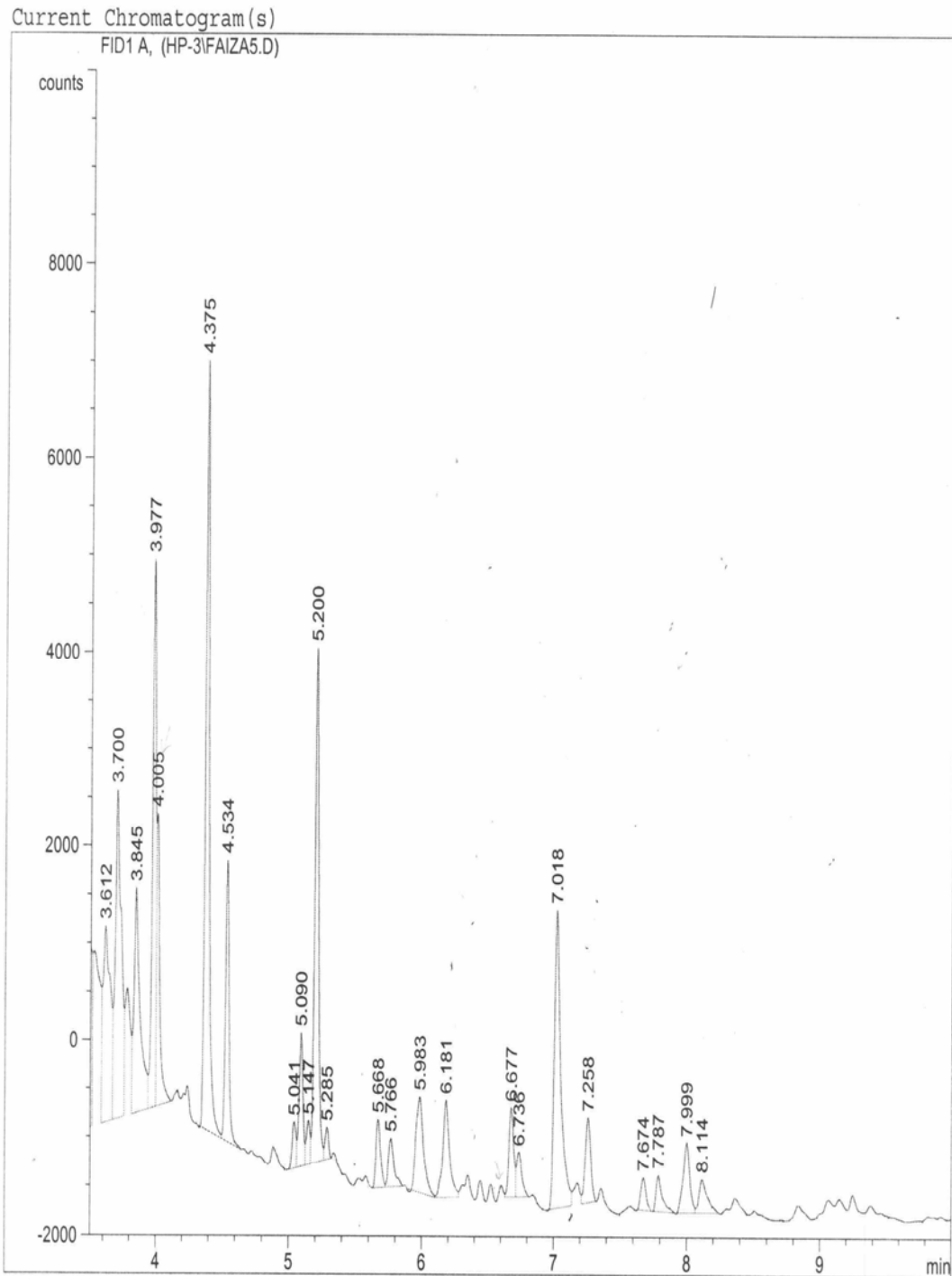
Rajah 1. Contoh kromatogram bagi sampel yang diekstrak dengan kaedah pengekstrakan soxhlet

Toluena dan xilena adalah merupakan bahan organik yang sangat berbahaya. Bahan pencemar organik ini adalah sangat bersifat sangat toksik dan memberikan kesan kepada kesihatan manusia walaupun bahan-bahan ini hanya wujud dalam kuantiti yang sedikit. Antara gejala yang wujud jika tahap dedahan tinggi kepada seseorang individu ialah sesak nafas, sakit kepala dan keletihan. Hasil daripada analisis yang telah dijalankan didapati kehadiran bahan organik berkenaan dalam kajian di dalam sampel debu jalan adalah kecil, namun ianya tidak boleh dipandang ringan kerana kedua-duanya merupakan antara bahan yang boleh menyebabkan pembentukan asbut fotokimia di udara dan ini hanya dikesan pada permukaan debu sahaja. Kandungan bahan pencemar organik berkenaan yang diperolehi dalam kajian ini adalah bergantung kepada latar belakang kawasan persampelan. Kehadiran bahan organik kajian tertinggi dapat dikesan dalam sampel dari kawasan bandar yang sibuk dengan kenderaan. Ini membuktikan bahawa bahan organik ini adalah terkandung dalam minyak petrol kenderaan.

Penggunaan kenderaan di kawasan pusat bandar adalah lebih banyak jika dibandingkan di kawasan pinggir bandar. Maka tahap kepekatan pencemaran yang disebabkan oleh toluena dan xilena yang diperolehi adalah lebih tinggi di kawasan pusat bandar. Pelepasan bahan pencemar ini ke atmosfera adalah mungkin secara tumpahan minyak petrol, kebocoran enjin kenderaan atau melalui peruapan petrol. Bahan pencemar ini mempunyai sifat meruap, maka bahan-bahan ini akan meruap di atmosfera dan bergabung dengan zarah-zarah debu yang terampai di udara dan kemudiannya akan termendap secara graviti [8].

Hasil daripada kajian mendapati terdapat perbezaan kepekatan bahan organik yang dikesan bagi kawasan persampelan yang berlainan. Kandungan toluena dan xilena yang paling tinggi dapat dikesan adalah sampel kawasan pusat bandar iaitu stesen Puduraya. Kepekatan toluena dan xilena bagi stesen yang lain boleh dilihat pada Jadual 4. Bagi sampel debu dari kawasan pinggir bandar iaitu stesen Bukit Unggul tiada kehadiran toluena dan xilena dapat dikesan. Ini menunjukkan kebergantungan antara kadar penggunaan kenderaan dengan amaun bahan organik yang dikesan. Namun pegecualian dapat dilihat di stesen Danau Kota (Jadual 4). Keadaan ini berkemungkinan berlaku kerana debu di kawasan berkenaan adalah debu yang telah lama, kerana kawasan berkenaan tidak dibersihkan sekerap di kawasan pusat bandar, oleh itu penumpukan toluena dan xilena berlaku. Ujian ANOVA sehala tanpa replikasi pada paras keyakinan 95% menunjukkan bahawa kawasan persampelan di pusat bandar dan kawasan pinggir bandar memberi perbezaan yang bererti.

Dalam kajian ini, sampel debu yang diperoleh dari kawasan persampelan yang telah dipilih terbahagi kepada dua iaitu dengan saiz butiran bersaiz <38 µm dan 38-63 µm. Tujuan menggunakan saiz butiran debu yang berlainan ialah untuk mengetahui kebergantungan kepekatan bahan pencemar organik yang dapat diekstrak dengan saiz butiran debu.

Hasil daripada analisis yang dijalankan bagi saiz butiran debu mempengaruhi kepekatan toluena dan xilena yang terdapat di permukaan debu berkenaan (Jadual 4). Di mana didapati saiz debu yang lebih besar iaitu antara 38-63 µm memberikan kepekatan toluena dan xilena yang lebih tinggi (kecuali ada lokasi terentu memberikan nilai yang sebaliknya) (Jadual 4). Ini mungkin disebabkan oleh peratus fraksi yang bersaiz <38 µm adalah kecil dan berbeza antara lokasi. Contohnya kawasan yang berpasir mempunyai saiz butiran debu bersaiz kecil yang lebih rendah dan begitu juga sebaliknya. Ujian ANOVA satu hala tanpa replikasi pada paras keyakinan 95% menunjukkan bahawa secara amnya terdapat perbezaan yang bererti antara saiz butiran debu, iaitu debu yang bersaiz 38-63 µm memberikan kepekatan toluena dan xilena yang lebih tinggi berbanding debu bersaiz <38 µm bagi hampir kesemua lokasi kajian.

Hasil kajian juga mendapati bahawa tidak terdapat trend yang tetap antara kandungan toluena dan xilena (Rajah 3). Namun berdasarkan kepada Rajah 3, dapat dilihat dengan lebih jelas bahawa sekiranya kaedah pengekstrakan soxhlet digunakan kandungan xilena adalah lebih tinggi berbanding dengan toluena. Keadaan ini menunjukkan bahawa terdapat kemungkinan penggunaan xilena yang lebih tinggi berbanding toluena dalam petrol dan juga mungkin kerana xilena lebih sukar meruap di udara, menjadikannya lebih mudah termendap pada zarah-zarah debu.

Kesimpulan

Secara keseluruhannya, hasil daripada kajian yang telah dijalankan mendapati bahan pencemar oganik seperti toluena dan xilena terdapat dalam sampel debu jalan raya yang dianalisis. Hasil daripada analisis terhadap sampel debu dilakukan didapati kepekatan bahan pencemar organik toluena dan xilena yang paling tinggi dapat

dikesan adalah di kawasan pusat bandar. Perbezaan kedua-dua kawasan persampelan ini adalah dari segi kesibukan kenderaan, maka ini membuktikan bahawa kehadiran bahan pencemar organik ini adalah berpunca daripada minyak petrol kenderaan. Penggunaan dua kaedah pengekstrakan yang berbeza menunjukkan bahawa toluena lebih mudah diekstrak berbanding dengan xilena. Saiz butiran juga mempengaruhi kandungan toluena dan xilena dalam debu jalan. Secara amnya kandungan xilena juga adalah lebih tinggi berbanding dengan toluena dalam debu jalan yang digunakan yang mungkin disebabkan oleh pengunaannya yang lebih meluas.

Rujukan
1. Katyal, T., Satake, M., Kumar, R. 1989. Environment Pollution, New Dehli: Anmol Publications, 10-57.
2. Rozali, M. O., Lim Sun Hoo, 2000. Kajian Beberapa Parameter Fizis dan Kandungan Kimia Debu Jalan Raya di Sekitar Kuala Lumpur, Kajang, Bandar Baru Bangi, Bangi Lama, Nilai dan Seremban. *Malays. J. Anal. Sci*. 6 (1). 162-172.
3. Rozali, M.O., Mohamed Nazir Ramlan, 2000. Analisis Kandungan Logam Berat dalam Dampel Debu Jalan Raya di Sekitar Kuala Lumpur, Kajang, Bandar Baru Bangi, Bangi Lama, Nilai dan Seremban. *Malays. J. Anal. Sci.* 6(1). 112-119.
4. Laharne, S., Charleswort, D., Chowdhry, B., 1992. A Survey of Metal Lives in Street Dust in Inner London Neighbourhood. *Environ. Inter.* 18. 236-270.
5. Sani, S., 1975. Iklim Bandar dan Pencemaran Udara. Kuala Lumpur: Dewan Bahasa Dan Pustaka. Hlm 81-83.
6. Davies, B.E., Elwood, P.C., Gallacher, J.E., Ginnerer, R.C., 1985. The Relationship between Heavy Metals in Garden Soils and House Dust in an Old Lead Mining Area of North Wales, Great Britain. *Environ. Pollut.* 9 (Series B). 255-266.
7. Harrison, R.M., Mora, S. J., Rapsomakins, S., Johnston, W.R., 1992. Introductory Chemistry for Environmental Sciences. New York: Cambridge University Press.
8. Zaini, H., 1997. Pengenalan Pencemaran Udara. Kuala Lumpur: Dewan Bahasa Dan Pustaka.
9. Rozali, M. O., Mohd Kamal Md. Zin, 1997. Kandungan Logam Berat Dalam Debu Jalan Di Sekitar Bandar Kota Kinabalu, Sabah. *Malays. J. Anal. Sci*. 3(1). 101-112.
10. Massadeh, A.M., 2003. Distributions of Copper and Zinc in Different Fractions of Particle Sizes in Road Dust Samples in Irbid City, Jordan using Atomic Absorption Spectrometry. *Res. J. Chem. Environ.* 7(4). 49–54.
11. Dictionary Organic Compaunds, 1983. Ed. Ke-5. New York: Chapman & Hall.
12. Butler, J.D., 1979. Air Pollution Chemistry. London: Academic Press.
13. Kupchella, C.E., Hyland, M.C., 1993. Environment Science: Living within the System of Nature. Ed. Ke-3.
14. Simons, C., 1995. The Lies of Unleaded Petrol - Part 2. Highly Toxic Chemicals are Replacing the Lead in Our Fuel, yet Government Authorities Continue to Underestimate the Serious Risks to Public Health. *NEXUS Magazine.*. 2(26). http://www.nexusmagazine.com/articles/ulp2.html
15. Crabtree, J.M, Roziah Hj. Mohamed, Zani bin Assim, 1997. Aromatics (Benzene, Toluene and Xylene) and Oxygenate (Methly tert-Butyl Ether) Contents in Unleaded Gasoline. *Abstracts 2nd International Conference on Environmental Chemistry and Geochemistry In The Tropic (Geotrop)"*, hlm. 31. Kuala Lumpur: Malaysia.
16. Kokosa, J.M., Andrzej, P., 2002. Headspace Microdrop Analysis- An Alternative Test Method for Gasoline Diluent and Benzene, Toluene, Ethlybenzene and Xylenes in used Engine Oils. *J. Chromatogr.* 983. 205-214.
17. Dean, J.R., Guohua Xiong, 2000. Extraction of Organic Pollutants from Environmental Matries: Selection of Extraction Technique. *Trends in Anal. Chem.* 19(9). 553-558.
18. Buch, A., Sternberg, R., Meunier, D., Rodier, C., Laurent, C. (2003) "Solvent Extraction of Organic Molecules of Exobiological Interest for *in-situ* Analysis of the Martin Soil" *J. Chromatogr.* A(999). 165-174.

KANDUNGAN LOGAM BERAT DI DALAM BEBERAPA SIRI TANAH OKSISOL DI SEKITAR TASIK CHINI, PAHANG

Sahibin Abd. Rahim, Muhd. Barzani Gasim, Mohd. Nizam Mohd Said, Wan Mohd Razi Idris,
Azman Hashim, Sharilnizam Yusof dan Masniyana Jamil

Program Sains Sekitaran, Pusat Pengajian Sains Sekitaran dan Sumber Alam
Fakulti Sains dan Teknologi, UKM 43600 Bangi Selangor, Malaysia
e-mail: haiyan@pkrisc.cc.ukm.my

Abstract

This study was carried out to determine heavy metal content and physico-chemical properties of soil's influencing heavy metal accumulation in some series surrounding the Chini Lakes. A total of 15 topsoil sample were collected randomly from 6 stations. The physical properties that were analyzed include particle size distribution and soil organic matter. Meanwhile, the chemical characteristics determined were pH, electrical conductivity and cation exchange capacity. It was found that heavy metal content of Cd, Cr, Cu, Co, Pb, Zn and Mn were low whereas Fe content was high. The textures of soil studied were clay, loamy sand, sandy loam, clay loam and silty clay loam. The mean of organic matter ranged from 2.68 to 11.46%. The soil pH showed that the soil studied was acidic with values ranged between 3.36 to 3.72. The range of electrical conductivity mean was between 2150 μScm^{-1} to 2403 μScm^{-1}. Cation exchange capacity mean ranged from 2.85 hingga 8.59 $cmol_c/kg$. Correlation analysis showed that there were positive and negative significant correlations between soils parameters heavy metal concentration. Analysis of variance (ANOVA) showed that there were significant differences in organic matter percentage, pH, cation exchange capacity and heavy metals except cadmium between sampling station.

Abstrak

Kajian ini dijalankan untuk menentukan kandungan logam berat dan ciri fiziko-kimia tanah yang mempengaruhi pengayaan logam berat dalam beberapa siri tanah di sekitar Tasik Chini, Pahang. Sebanyak 15 sampel tanah daripada 6 stesen telah diambil berdasarkan jenis tanah. Ciri fizik yang ditentukan termasuklah taburan saiz partikel dan kandungan bahan organik tanah. Manakala ciri kimia yang ditentukan pula adalah pH, kekonduksian elektrik dan kapasiti pertukaran kation. Didapati bahawa kandungan logam berat Cd, Cr, Cu, Co, Pb, Zn dan Mn adalah rendah manakala kandungan Fe adalah tinggi. Tanah kawasan kajian terdiri daripada tekstur lempung, pasir berlom, lom berpasir, lom lempung dan lom lempung berkelodak. Kandungan bahan organik berjulat di antara 2.68 hingga 11.46%. Nilai pH menunjukkan tanah di kawasan kajian adalah berasid iaitu pada julat antara 3.36 hingga 3.72. Manakala julat kekonduksian elektrik pula berada di antara 2150 μScm^{-1} hingga 2403 μScm^{-1}. Purata kapasiti pertukaran kation berjulat di antara 2.85 hingga 8.59 $cmol_c/kg$ tanah. Analisis korelasi menunjukkan terdapat perhubungan yang signifikan positif dan negatif di antara parameter tanah dengan kandungan logam berat. Analisis varians (ANOVA) pula menunjukkan terdapat perbezaan yang signifikan di antara stesen bagi kandungan bahan organik, kapasiti pertukaran kation serta logam berat kecuali logam kadmium.

Pendahuluan

Luluhawa dan pedogenesis merupakan dua proses utama yang menyumbang dalam pembentukan tanah. Luluhawa fizik adalah proses di mana batuan dipecahkan dan dihancurkan oleh agen iklim seperti haba, air yang mengalir, graviti dan angin melalui proses pengembangan dan penguncupan yang berterusan. Luluhawa kimia pula melibatkan proses seperti pengoksidaan, penurunan, hidrasi, hidrolisis dan pengkarbonan sementara luluhawa biologi pula melibatkan peranan benda-benda hidup seperti sesetengah hidupan seni, akar tumbuhan primitif seperti liken dan lumut [8].

Saling tindakan iklim, topografi dan juga masa ke atas bahan induk mengakibatkan pembentukan pelbagai jenis tanah di Malaysia. Sebagai contoh, tanah yang terbentuk daripada batuan granit berbeza dengan tanah yang terbentuk daripada batuan basalt. Perbezaan tersebut bukan sahaja dari segi mineraloginya, malahan juga morfologinya [10]. Tanah di kawasan kajian didasari oleh batuan metasedimen daripada batupasir, batu lodak dan batu lumpur yang telah mengalami canggaan hebat. Komposisi batuan adalah berbagai dengan sebahagiannya mempunyai kandungan ferum yang tinggi. Ini menunjukkan tanaih di sini adalah tanah oksisol.

Perbezaan komposisi batuan induk menyebabkan terbentuk beberapa siri tanah di sekitar Tasik Chini. Antara siri tanah yang ditemui di sini adalah siri Melaka, Bungor dan Rasau. Siri Melaka dikenali dengan warna merah gelap berkomposisi laterit yang tinggi. Horizon pada profil tidak begitu jelas. Siri Bungor berwarna kekuningan, manakala siri Rasau berkomposisi pasir dengan dicirikan oleh warna cerah. Kajian ini cuba melihat kepada ciri fiziko-kimia tanah yang terdapat di kawasan sekitar Tasik Chini.

Bahan Dan Kaedah

Lokasi dan stesen kajian

Kawasan kajian iaitu Tasik Chini adalah terletak di mukim Penyur, Pahang. Kedudukan lokasi kajian adalah merangkumi garis lintang 3°24' hingga 3º28' utara dan garis bujur di antara 102°55' hingga 102°60' timur. Tasik Chini terletak kira-kira 100 km dari Kuantan terbahagi kepada 12 cabang saliran yang dikenali sebagai laut.

Stesen 1 merupakan tanah siri Melaka yang terdiri daripada tanah laterit yang mengandungi logam ferum yang tinggi. Kawasan persampelan meliputi tanah hutan dan tanah pertaniah kelapa sawit tua.

Stesen 2 pula terdiri daripada tanah siri Rasau berwarna cerah putih meliputi kawasan pertanian kelapa sawit yang baru ditanam dan hutan sekunder. Tanah di stesen ini mempunyai struktur yang halus dan peroi.

Stesen 3 terletak di Kampung Gumum yang terdiri daripada kawasan terbuka dan tanah hutan yang kecerunannya lebih kurang 4º. Tanah di stesen ini dikategorikan sebagai tanah siri Bungor.

Stesen 4 terletak di Bukit Jerangking yang mempunyai kecerunan lebih kurang 20 hingga 25° dengan litupan sebanyak 60 hingga 70%. Tanah di stesen 4 juga dikategorikan sebagai tanah siri Bungor.

Stesen 5 pula adalah lokasi Kampung Chenahan yang terdiri daripada kanopi sebanyak 30% tetapi tiada litupan pada lantai hutan serta mempunyai kecerunan lebih kurang 5º. Tanah di stesen 5 ini pula dikategorikan sebagai Siri Melaka.

Stesen 6 merupakan kawasan hutan yang mempunyai litupan kanopi lebih kurang 90% dan litupan sebanyak 70% pada lantai hutan. Stesen ini terletak di Pulau Babi. Tanah di sini adalah siri Melaka. Selain itu di stesen keenam ini terdapat banyak daun dan sampah-sarap pada lantai hutan yang menyumbang kepada pembentukan humus.

Kaedah Kajian

Kaedah yang digunakan dalam kajian ini dikelaskan kepada 4 peringkat yang terdiri daripada cerapan di lapangan, persampelan tanah, analisis makmal dan analisis data.

Persampelan Tanah

Persampelan tanah dijalankan dengan mengambil secara rawak kira-kira 1kg berat tanah permukaan atas (0-20cm) dengan menggunakan *dutch auger*. Sampel tanah tersebut dimasukkan ke dalam beg plastik dan dilabelkan mengikut lokasi masing-masing untuk analisis makmal.

Penyediaan Sampel

Analisis makmal merangkumi proses penyediaan sampel di mana semua sampel tanah dibiarkan kering udara pada suhu bilik. Semasa proses pengeringan yang dijalankan, gumpalan sampel tanah dipecahkan kepada bahagian yang lebih kecil untuk mempercepatkan proses pengeringan. Sampel tanah kering udara kemudian ditumbuk dengan menggunakan penumbuk lesung kayu. Pecahan-pecahan tanah diayak dengan menggunakan ayak bersaiz 2mm. Hasil ayakan tanah yang mempunyai saiz yang kurang daripada 2mm dibahagikan di mana satu bahagian tanah digunakan untuk analisis parameter fiziko-kimia manakala bahagian yang lain disimpan untuk kajian ulangan. Sebanyak 3 replikasi digunakan untuk setiap penentuan.

Analisis Makmal

Penentuan saiz partikel dilakukan mengikut kaedah pipet berserta ayakan kering [1]. Kandungan bahan organik ditentukan secara pembakaran [3]. Pengukuran pH tanah dilakukan di dalam nisbah 1:2.5 bagi tanah:air suling [6] menggunakan meter pH berelektrod kaca Model WTW INOLAB Level 1. Kekonduksian elektrik ditentukan

daripada ekstrak $CaSO_4.2H_2O$ tepu [5] menggunakan alat meter kekonduksian Model H 18819 Hanna. Kation asid boleh tukar ganti Al^{3+} dan H^+ diekstrak dengan larutan 1M KCl dan kemudian ditentukan secara titratan. Kepekatan kation boleh tukar K^+, Na^+, Ca^{2+} dan Mg^{2+} daripada ekstrak 1M Ammonium Asetat [7] ditentukan menggunakan alat Spektrometer Serapan Atom Nyalaan (FAAS). Kandungan logam berat di dalam tanah diekstrak dengan menggunakan kaedah Archer and Hodgson (1987) [2], kemudian kepekatannya di dalam larutan ekstrak ditentukan dengan Spektrometer Serapan Atom Nyalaan (FAAS).
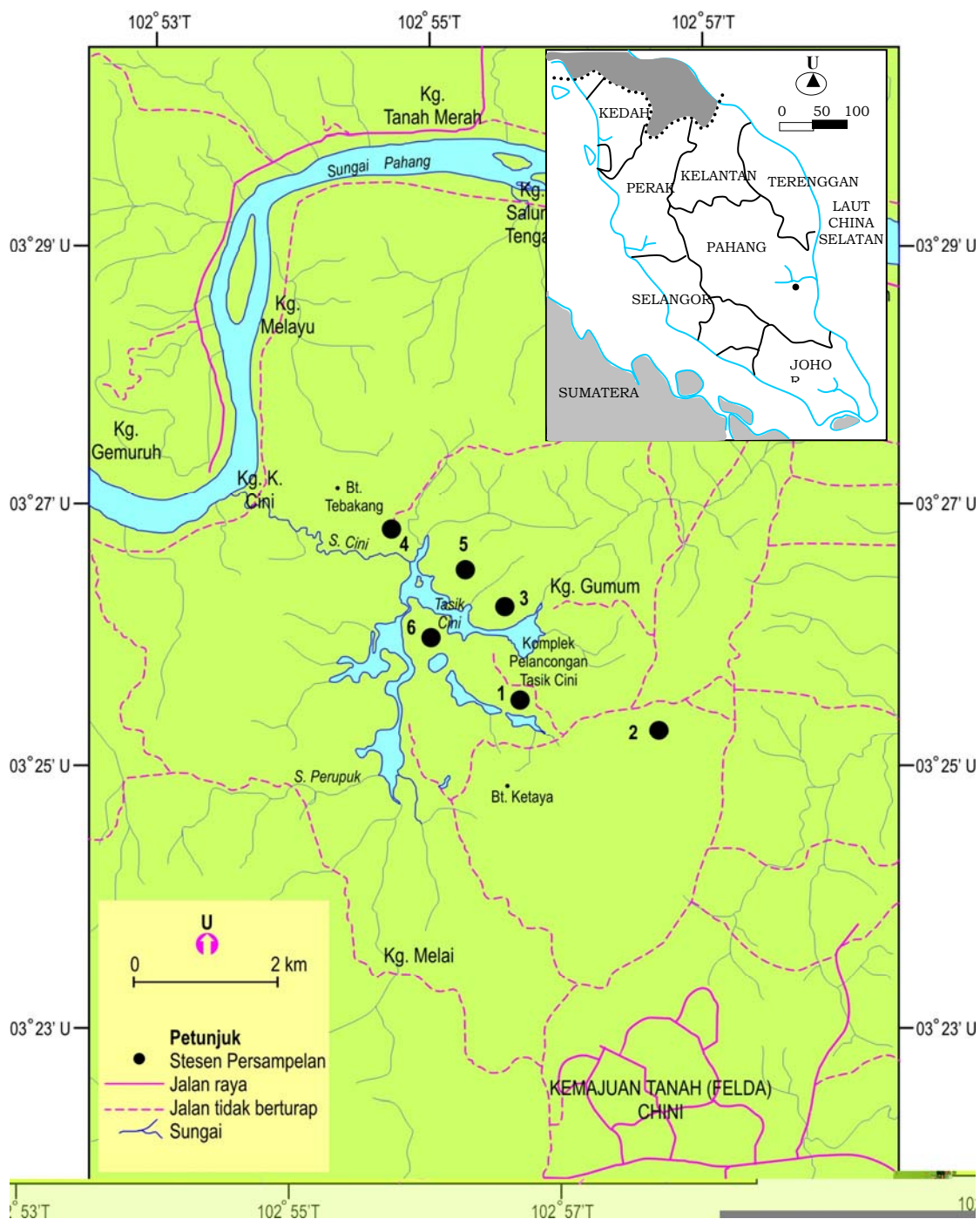
Rajah 1. Peta menunjukkan kawasan kajian dan persampelan

Hasil Dan Perbincangan

Kandungan Logam Berat Dalam Tanah

Purata dan sisihan piawai bagi setiap logam yang dikaji di kesemua stesen cerapan ditunjukkan pada Rajah 1 dan 2. Julat purata kepekatan bagi logam kadmium (Cd) di dalam tanah adalah di antara 1.03 hingga 2.03 mg/kg. Kepekatan tertinggi dicatatkan pada stesen 5 dan yang terendah dicatatkan pada stesen 6 dengan nilai masing-masing ialah 2.03 ± 0.93 mg/kg dan 1.03 ± 0.77 mg/kg. Analisis varians menunjukkan tidak ada perbezaan signifikan di antara purata kandungan Cd di dalam tanah di stesen yang dikaji. Ini menunjukkan kandungan Cd dalam siri tanah yang berbeza adalah lebih kurang sama sahaja.

Purata kepekatan logam kobalt (Co) pula adalah di antara 7.44 hingga 19.85 mg/kg. Kandungan logam berat Co yang paling tinggi dicatatkan oleh stesen 6 iaitu 19.85 ± 1.71 mg/kg dan yang paling rendah adalah stesen 2 iaitu 7.44 ± 0.81 mg/kg. Analisis varians menunjukkan terdapat perbezaan signifikan di antara purata kandungan Co di antara stesen 2 dengan stesen-stesen yang lain. Stesen 2 adalah tanah siri Rasau yang didominasi oleh pasir.
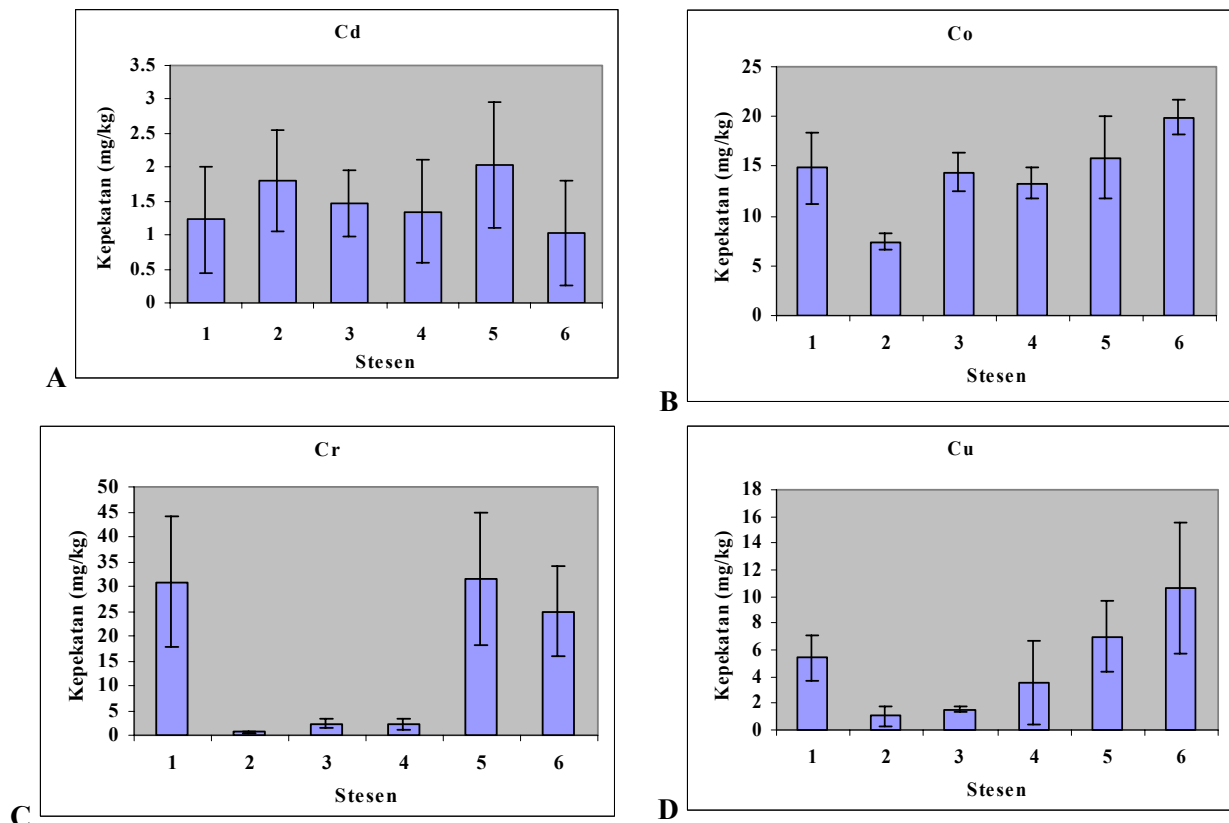
Rajah 2. Kandungan logam berat (Cd, Co, Cr, Cu) dalam sampel tanah di kawasan kajian

Bagi kandungan unsur kromium (Cr) di dalam tanah pula purata kepekatannya berada pada julat 0.57 hingga 31.63 mg/kg yang mana stesen 5 mencatatkan nilai kepekatan tertinggi iaitu 31.63 ± 13.34 mg/kg. Manakala stesen 2 mencatatkan nilai kepekatan Cr yang terendah iaitu 0.57 ± 0.32 mg/kg. Analisis varians menunjukkan terdapat perbezaan signifikan di antara purata kandungan Cr di dalam tanah di stesen 1, 5, 6 dengan stesen 2, 3 dan 4. Tanah stesen 1, 5 dan 6 merupakan tanah siri Melaka.

Purata kepekatan logam kuprum (Cu) pula terletak pada julat di antara 1.04 hingga 10.65 mg/kg iaitu kepekatan logam ini dicatatkan paling tinggi pada stesen 6 iaitu 10.65 ± 4.87 mg/kg dan paling rendah pada stesen 2 iaitu 1.04 ± 0.70 mg/kg. Analisis varians menunjukkan terdapat perbezaan signifikan di antara purata kandungan C di dalam tanah di stesen 2, 3 dengan stesen 1, 5 dan 6. Tanah stesen 1, 5 dan 6 merupakan tanah siri Melaka.

Secara keseluruhannya, logam ferum (Fe) mencatatkan nilai purata kepekatan yang paling tinggi di kawasan kajian dengan nilainya berada pada julat 1156.80 hingga 2898.40 mg/kg. Stesen 1 mencatatkan nilai purata tertinggi iaitu 2898.40 ± 98.10 mg/kg manaakala stesen 2 mencatatkan nilai purata kepekatan logam Fe yang paling rendah iaitu 1156.80 ± 511.60 mg/kg. Analisis varians menunjukkan terdapat perbezaan signifikan di antara purata kandungan Fe di dalam tanah di antara stesen 2, 3 dan 4 dengan stesen 1, 5 dan 6. Tanah stesen 1, 5 dan 6 merupakan tanah siri Melaka
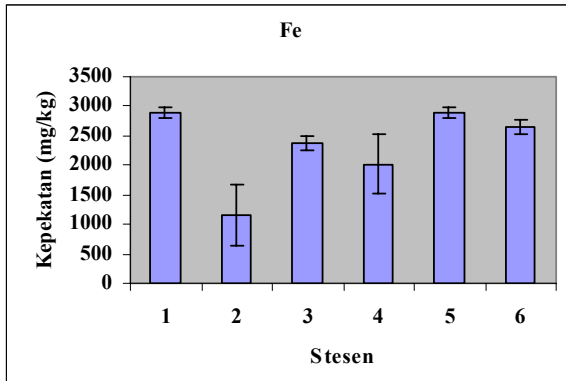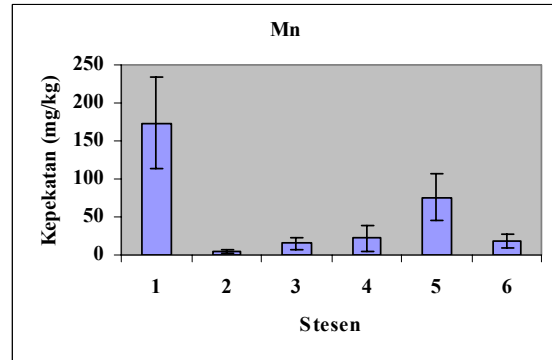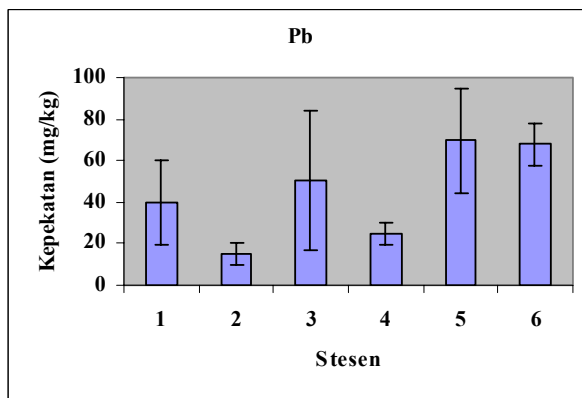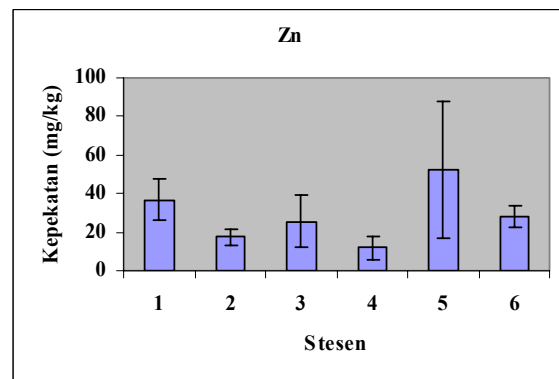
Rajah 3. Kandungan logam berat (Fe, Mn, Pb, Zn) dalam sampel tanah di kawasan kajian

Purata kepekatan unsur mangan (Mn) berada pada julat di antara 4.58 hingga 173.60 mg/kg. Stesen 1 mencatatkan kepekatan logam Mn yang paling tinggi iaitu sebanyak 173.60 ± 59.68 mg/kg dan stesen 2 pula mencatatkan kepekatan yang paling rendah iaitu 4.58 ± 1.82 mg/kg. Analisis varians menunjukkan perbezaan signifikan di antara purata kandungan Mn di dalam tanah di stesen 2, 3, 4 dan 6 dengan stesen 1 dan 5.

Purata kepekatan logam plumbum (Pb) pula berada pada julat di antara 15.30 hingga 69.59 mg/kg di mana kepekatan Pb yang paling tinggi dicatatkan pada stesen 5 iaitu 69.59 ± 25.35 mg/kg, sementara stesen 2 mencatatkan kepekatan logam Pb yang terendah iaitu 15.30 ± 5.19 mg/kg. Analisis varians menunjukkan perbezaan signifikan di antara purata kandungan Pb di dalam tanah di stesen 2 dan 4 dengan stesen 5 dan 6.

Bagi logam zink (Zn) pula, purata kepekatannya berada pada julat 12.10 hingga 52.20 mg/kg. Secara puratanya, stesen 5 mencatatkan kepekatan logam Zn yang paling tinggi berbanding stesen persampelan yang lain iaitu 52.20 ± 35.55 mg/kg, sementara stesen 4 mencatatkan kepekatan yang paling rendah iaitu 12.10 ± 6.06 mg/kg. Terdapat perbezaan signifikan di antara purata kandungan Zn di dalam tanah di stesen 1 dan 6 dengan stesen 2 dan 4.

Berdasarkan analisis varians yang dijalankan, didapati terdapat perbezaan yang signifikan di antara keenam-enam stesen persampelan bagi setiap unsur logam berat kecuali Cd. Secara umumnya kandungan logam berat dalam tanah siri Melaka adalah lebih tinggi daripada kandungan logam berat di dalam siri Bungor dan Rasau. Kandungan logam berat dalam siri Rasau adalah paling rendah.

Kebiasaannya, kuprum di dalam tanah adalah berbentuk ion Cu^{2+} yang akan dijerap oleh tanah lempung atau bersebati dengan bahan organik. Penahanan kuprum di dalam tanah bertambah dengan peningkatan bahan organik [12]. Keterdapatan kuprum juga akan berkurangan dengan peningkatan pH.

Zink pada tanah berasid kebiasaannya mudah diserap oleh tumbuhan, manakala dalam keadaan tanah beralkali, ia tidak mudah diserap [12]. Secara umum, dalam keadaan tanah berasid Fe^{2+} dan Mn^{2+} hadir dalam larutan tanah untuk keperluan tumbuhan. Dalam tanah yang terlalu berasid, kehadiran ferum dan mangan adalah pada kepekatan yang toksik.

Sementara itu, kerendahan nilai pH juga bertindak mempengaruhi penjerapan logam berat iaitu melalui jerapan proton-proton asid lemah atau jerapan spesifik hasil hidrolisis atau pembentukan mendakan permukaan dari hidroksid atau silikat [4].

Ciri Fiziko-kimia Tanah
Ciri fizik tanah
Nilai purata dan sisihan piawai parameter fizik tanah seperti peratusan pasir, kelodak, lempung, kandungan bahan organik dan tekstur tanah ditunjukkan dalam Jadual 1.

Peratusan lempung, kelodak dan pasir serta tekstur tanah
Purata peratusan lempung yang diperoleh daripada kajian ini adalah berjulat di antara 7.55% hingga 70.96%. Purata peratusan lempung yang tertinggi dicatatkan ialah pada stesen 1 iaitu sebanyak 70.96 ± 19.35%, manakala stesen 2 pula mencatatkan purata peratusan kandungan lempung yang terendah iaitu sebanyak 7.55 ± 1.64%. Bagi purata peratusan kelodak di keenam-enam stesen pula adalah berjulat di antara 8.59% hingga 47.94% di mana stesen 5 menunjukkan nilai peratusan tertinggi iaitu 47.94 ± 10.47%, manakala nilai purata peratusan yang paling rendah dicatatkan oleh stesen 1 iaitu sebanyak 8.59 ± 10.02%. Purata bagi peratusan kandungan pasir pula adalah berjulat di antara 7.87% hingga 80.43%. Nilai tertinggi bagi purata peratusan kandungan pasir ini dicatatkan oleh stesen 2 iaitu sebanyak 80.43 ± 3.57% dan nilai terendahnya pula dicatatkan oleh stesen 6 iaitu sebanyak 7.87 ± 1.99%.

Hasil yang diperoleh daripada data yang telah dianalisis menunjukkan bahawa stesen 1 dan stesen 6 terdiri daripada tekstur lempung, stesen 2 terdiri daripada tekstur pasir berlom sementara stesen 3 bertekstur lom berpasir. Manakala didapati stesen 4 dan 5 masing–masing mempunyai tekstur lom lempung dan lom lempung berkelodak.

Jadual 1. Purata dan sisihan piawai bagi kandungan bahan organik, peratus pasir, kelodak, lempung dan tekstur tanah

Stesen	% Bahan organik	% Pasir	% Kelodak	% Lempung
1 (Melaka)	11.46 ± 2.23	20.30 ± 9.79	8.59 ± 10.02	70.96 ± 19.35
2 (Rasau)	2.68 ± 1.08	80.43 ± 3.57	12.02 ± 1.97	7.55 ± 1.64
3 (Bungor)	3.41 ± 0.14	54.80 ± 6.28	27.21 ± 7.06	17.93 ± 0.73
4 (Bungor)	3.70 ± 0.31	35.39 ± 9.80	45.10 ± 8.33	19.52 ± 1.51
5 (Melaka)	9.50 ± 2.10	12.98 ± 1.94	47.94 ± 10.47	39.08 ± 10.43
6 (Melaka)	9.81 ± 3.10	7.87 ± 1.99	33.32 ± 1.66	58.81 ± 3.06

Ciri kimia tanah
Nilai purata berserta sisihan piawai bagi setiap parameter kimia tanah di setiap stesen persampelan yang telah dianalisis ditunjukkan di dalam pada lampiran A, B dan C. Hasil yang didapati menunjukkan bahawa tanah di kawasan kajian adalah bersifat asid memandangkan nilai pH yang diperoleh bagi semua stesen persampelan adalah rendah.

pH tanah
Purata pH serta sisihan piawai bagi setiap stesen persampelan ditunjukkan di dalam Rajah 4. Nilai purata pH yang diperoleh adalah berada pada julat 3.36 hingga 3.72. Secara puratanya, tanah di stesen 1 mencatatkan

bacaan bagi nilai pH yang tertinggi berbanding stesen cerapan yang lain iaitu 3.72 dengan sisihan piawainya 0.45. Tanah di stesen 4 pula mencatatkan nilai pH paling rendah iaitu 3.36 ± 0.18.

Secara keseluruhannya, didapati bahawa kesemua tanah yang dikaji bagi setiap stesen persampelan adalah bersifat asid kerana purata pH yang rendah. Terdapat perbezaan yang signifikan bagi nilai pH di antara stesen 1 dan stesen 4. Keasidan tanah berpunca daripada humus atau bahan organik, tanah lempung alumino-silikat, hidrus oksida ferum dan aluminium, aluminium tukarganti, garam larut dan karbon dioksida [12].

Jadual 2. Purata dan sisihan piawai bagi pH, kekonduksian elektrik (EC) (μScm^{-1}) dan KPK (cmolc/kg).

Stesen	pH	Kekonduksian elektrik	Kapasiti Pertukaran Kation
1 (Melaka)	3.72 ± 0.45	2403 ± 122.8	3.85 ± 0.81
2 (Rasau)	3.57 ± 0.25	2282.5 ± 9.6	2.85 ± 1.48
3 (Bungor)	3.56 ± 0.05	2287.5 ± 63.4	6.21 ± 1.67
4 (Bungor)	3.36 ± 0.18	2150 ± 59.4	7.91 ± 0.26
5 (Melaka)	3.60 ± 0.14	2262.5 ± 5.0	7.67 ± 0.28
6 (Melaka)	3.44 ± 0.08	2267.5 ± 65	8.59 ± 1.11

Nilai purata pH yang didapati rendah bagi semua stesen kerana kebanyakannya terdiri daripada kawasan hutan dengan litupan 100%. Oleh itu, kawasan ini mengandungi banyak bahan organik dan humus hasil pereputan daun yang menyumbang keasidan tanah. Ini adalah kerana pereputan bahan organik terutamanya humus akan mengeluarkan asid organik dan asid mineral. Bahan organik tanah atau humus mengandungi kumpulan reaktif karboksil, fenolik dan amino yang mana ia boleh mengikat ion H^+. Kumpulan yang tepu H^+ tersebut bersifat seperti asid lemah dan H^+ yang terikat secara kovalen akan terurai bergantung kepada penguraian asid yang terbentuk [12].

Keasidan tanah juga berlaku disebabkan oleh titisan air hujan yang lebat yang mengakibatkan kebanyakan garam yang terkandung di dalam tanah mengalami larut lesap. Kehilangan bes Na^+, K^+, Ca^{2+} dan Mg^{2+} ini digantikan oleh ion H^+ dan Al^{3+}. Kehadiran H^+ dan Al^{3+} di tapak pertukaran kation inilah yang bertanggungjawab terhadap keasidan tanah [8].

Di samping itu, kawasan kajian yang juga terdiri daripada kawasan pertanian mengaplikasikan penggunaan baja sebagai sumber nutrien kepada tanaman. Kandungan nitrogen dan sulfur di dalam baja akan mengalami tindakbalas mikrobiologi. Nitrogen dioksidakan kepada ammonium, manakala sulfur dioksidakan kepada sulfur trioksida. Gas-gas ini masing-masing larut di dalam air untuk membentuk asid nitrik dan asid sulfat. yang kemudiannya terjerap ke dalam tanah [8].

Kekonduksian elektrik tanah
Purata kekonduksian elektrik tanah yang diperoleh daripada setiap stesen adalah berada pada julat 2150.0 μScm^{-1} hingga 2403.0 μScm^{-1}. Berdasarkan Rajah 4.5, didapati stesen 1 mencatatkan nilai kekonduksian elektrik yang tertinggi iaitu 2403.0 $\pm$ 122.8 μScm^{-1}. Manakala stesen yang mencatatkan nilai kekonduksian yang paling rendah ialah stesen 4 iaitu 2150.0 $\pm$ 59.4 μScm^{-1}.

Analisis ANOVA yang dijalankan menunjukkan terdapat perbezaan yang bererti pada aras keertian 5% bagi stesen 1 dengan kelima-lima stesen yang lain iaitu stesen 2, stesen 3, stesen 4, stesen 5 dan stesen 6. Manakala stesen 2 dan 3 menunjukkan perbezaan yang signifikan dengan stesen 4.

Secara keseluruhannya, nilai kekonduksian elektrik yang dicatatkan oleh semua stesen cerapan adalah rendah. Ini menunjukkan kepekatan garam dalam tanah adalah rendah. Jadi, ia tidak menyekat pengambilan air oleh tumbuhan dan tumbuhan juga tidak menunjukkan simptom-simptom kekeringan. Oleh itu, tanah di kawasan kajian adalah sesuai untuk aktiviti pertanian berdasarkan indisis bagi kekonduksian elektrik tanah yang digunakan oleh MAFF (1988) [13] yang mana nilai kekonduksian yang diperoleh berada di bawah indeks 3 iaitu tidak merosakkan tumbuhan.

Kapasiti pertukaran kation (KPK)
Purata kapasiti pertukaran kation (KPK) bagi keenam-enam stesen ditunjukkan dalam Rajah 4.12 adalah berjulat di antara 2.85 hingga 8.59 $cmol_c/kg$. Stesen 6 mencatatkan nilai KPK tertinggi berbanding stesen yang lain iaitu 8.59 ± 1.11 $cmol_c/kg$, manakala stesen 2 pula mencatatkan nilai KPK yang paling rendah iaitu 2.85 ±1.48 $cmol_c/kg$. Daripada ujian ANOVA dapat dinyatakan bahawa stesen 1 dan stesen 2 berbeza secara signifikan dengan keempat-empat stesen yang lain. Selain itu, stesen 3 menunjukkan perbezaan yang signifikan dengan stesen 1, stesen 2, stesen 4 dan stesen 6. Stesen 4 dan 6 pula mempunyai perbezaan yang signifikan dengan stesen 1, stesen 2 dan stesen 3, sementara stesen 5 berbeza secara bererti dengan stesen 1 dan stesen 2.

Kapasiti pertukaran kation adalah paling tinggi di stesen 6 mungkin kerana tanahnya yang bertekstur lempung. Ini kerana lempung merupakan konstituen tanah yang paling halus serta mempunyai luas permukaan spesifik yang besar. Lebih-lebih lagi, lempung tanah terdiri daripada cas elektronegatif yang aktif secara kimia serta berupaya menarik kation yang bercas positif.

Penentuan KPK ini adalah merupakan penggantian semua atau sebahagian daripada kation tukarganti pada kompleks pertukaran. Tanah lempung atau tanah organik mempunyai KPK yang tinggi berbanding tanah pasir atau tanah yang tidak begitu organik memandangkan keupayaannya yang kecil serta mudah hilang menerusi larut lesap. Koloid lempung yang bermuatan negatif membolehkan kation tertarik oleh partikel lempung dan diikat secara elektrostatik [11].

Kation bes tukarganti Ca^{2+}, Mg^{2+}, Na^+ dan K^+ boleh terlekat pada koloid tanah oleh cas elektrik dan boleh tertukarganti sesama sendiri atau dengan H^+. Nilai purata KPK bagi stesen 6 adalah paling tinggi kerana kepekatan kation Al^{3+} tukarganti yang tinggi serta menyumbang kepada peningkatan KPK tanah.

Korelasi antara parameter tanah dengan logam berat
Jadual 2 menunjukkan terdapat perhubungan signifikan secara positif pada aras keertian 5% antara pH dengan logam kromium (Cr) dan korelasi signifikan positif yang bererti dengan logam mangan (Mn). Kandungan bahan organik tanah juga mempunyai perhubungan signifikan yang kuat dengan logam Cr, Fe dan Mn, sementara terdapat perhubungan signifikan yang lemah dengan logam Co dan Cu.

Selain itu, peratusan kandungan pasir juga mempunyai perhubungan dengan logam yang dikaji walaupun perhubungan yang negatif. Peratusan pasir menunjukkan terdapatnya korelasi signifikan negatif yang kuat pada aras keertian 5% dengan logam Cr, Co, Cu and Fe. Sementara itu, ia juga mempunyai korelasi signifikan negatif yang lemah dengan logam Pb dan Zn.

Jadual 3. Nilai korelasi di antara parameter tanah dengan kandungan logam berat (mg/kg)

	Cr	Co	Cu	Cd	Pb	Fe	Mn	Zn
pH	0.397*	0.186	0.016	-0.194	0.347	0.298	0.614*	0.441
% BOT	0.674*	0.404*	0.392*	-0.178	0.304	0.698*	0.697*	0.543
% Pasir	-0.650*	-0.618*	-0.698*	0.105	-0.450*	-0.798*	-0.371	-0.393*
% Kelodak	-0.058	0.267	0.261	0.056	0.486*	0.046	-0.327	0.219
%Lempung	0.620*	0.386*	0.461*	-0.128	0.098	0.686*	0.540*	0.215
KE	0.308	-0.025	0.069	-0.039	0.012	0.278	0.596*	0.220
KPK	-0.091	0.416*	0.422*	0.017	0.221	0.150	-0.461*	-0.094

Aras keertian = 5% (*), KE, kekonduksian elektrik; KPK, kapasiti pertukaran kation.

Bagi peratusan kandungan kelodak dalam tanah pula menunjukkan korelasi signifikan positif dengan logam Pb tetapi dalam perhubungan yang lemah. Sementara bagi peratusan kandungan lempung pula menunjukkan korelasi signifikan positif yang kuat pada aras keertian 5% dengan logam Cr, Fe dan Mn. Perhubungannya dengan logam Co dan Cu pula, menunjukkan korelasi signifikan positif yang lemah.

Nilai kekonduksian elektrik pula hanya menunjukkan korelasi signifikan yang agak kuat dengan logam Mn. Kapasiti pertukaran kation (KPK) pula menunjukkan perhubungan signifikan yang lemah dengan logam Co dan Cu, manakala ia menunjukkan korelasi signifikan negatif yang lemah dengan logam Mn.

Ini menunjukkan bahawa kandungan bahan organik, pasir, kelodak, lempung, pH, kekonduksian elektrik dan kapasiti [pertukaran kation mempunyai pengaruh ke atas pengayaan dan pengurangan jumlah logam berat di dalm tanah.

Korelasi di antara logam berat dengan logam berat dalam tanah
Berdasarkan Jadual 4, didapati Co mempunyai perhubungan signifikan yang positif dengan semua logam kecuali Mn dan Cd. Logam Co menunjukkan korelasi signifikan positif yang kuat dengan Cu ($p<0.05$, r = 0.5339), Cr ($p<0.05$, r = 0.6026), Fe ($p< 0.05$, r = 0.6316), Pb ($p< 0.05$, r = 0.6187), sementara ia mempunyai korelasi signifikan positif yang kurang kuat dengan Zn ($p<0.05$, r = 0.4135).

Jadual 4. Korelasi di antara logam berat dengan logam berat dalam tanah(μg/g).

	Co	Cu	Cr	Fe	Mn	Pb	Zn	Cd
Co	1.000							
Cu	0.5339*	1.000						
Cr	0.6026*	0.6182*	1.000					
Fe	0.6316*	0.5244*	0.7014*	1.000				
Mn	0.2675	0.1699	0.6858*	0.6031*	1.000			
Pb	0.6187*	0.5058*	0.5977*	0.4877*	0.2120	1.000		
Zn	0.4135*	0.2880	0.7365*	0.5650*	0.5413*	0.7339*	1.000	
Cd	-0.3695	-0.0306	-0.1316	-0.1370	-0.2254	-0.0002	0.1903	1.000

Aras keertian = 0.05 (*)

Logam Cu pula menunjukkan korelasi signifikan positif yang agak kuat dengan logam Cr ($p<0.05$, r = 0.6182), Fe ($p<0.05$, r = 0.5244) dan Pb ($p<0.05$, r = 0.5058). Selain itu, didapati logam Cr menunjukkan perhubungan signifikan positif yang kuat dengan logam Fe, Mn, Pb dan Zn yang mana nilai r masing-masing ialah 0.7014, 0.6858, 0.5977 dan 0.7365 pada aras keertian 5%.

Logam Fe juga mempunyai perhubungan signifikan positif yang kuat dengan logam Mn dan Zn yang mana nilai r masing-masing ialah 0.6031 dan 0.5650. Manakala perhubungannya dengan logam Pb ($p<0.05$, r =0.4877) adalah signifikan positif yang lemah pada aras keertian 5%. Logam Mn pula mempunyai korelasi signifikan positif yang kuat dengan logam Zn ($p<0.05$, r = 0.5413). Sementara itu logam Pb menunjukkan korelasi signifikan positif yang kuat dengan Zn ($p<0.05$, r =0.7339). Manakala logam Cd pula tidak menunjukkan korelasi dengan mana-mana logam sama ada secara positif atau negatif pada aras keertian 5%.

Kesimpulan
Secara keseluruhannya, tanah di sekitar Tasik Chini boleh dikategorikan sebagai berasid berdasarkan nilai pH yang rendah bagi kesemua stesen persampelan. Ini kerana kawasan yang dikaji kebanyakannya terdiri daripada kawasan hutan dan pertanian yang mengandungi banyak bahan organik dan humus yang menyumbang kepada keasidan tanah. Dari segi tekstur pula, tanah di kawasan kajian boleh dikelaskan kepada beberapa kategori iaitu lempung, pasir berlom, lom berpasir, lom lempung dan lom lempung berkelodak.

Selain itu, nilai kekonduksian elektrik yang diperoleh bagi setiap stesen persampelan adalah rendah iaitu di bawah indeks 3 yang tidak merosakkan tumbuhan (MAFF 1998). Oleh kerana kepekatannya yang rendah, maka ia tidak akan menyekat pengambilan air oleh tumbuhan dan tahap kesuburannya adalah tinggi.
Kepekatan logam ferum adalah paling tinggi di dalam tanah yang dikaji berbanding logam berat yang lain memandangkan ia merupakan salah satu juzuk major di litosfera. Selain ferum, kepekatan logam mangan yang diperoleh juga adalah tinggi. Kepekatan kedua-dua jenis logam ini tinggi kerana tanah di kawasan kajian adalah bersifat asidik. Logam-logam berat ini berkemungkinan mempunyai potensi yang besar untuk mencemar tasik sekiranya langkah kawalan yang berkesan tidak dilaksanakan.

Penghargaan

Rujukan

1. Abdulla, H. H. (1966). *A study of the development of podzol profiles in Dovey forest*. Tesis Ph.D Aberystwyth: University of Wales.
2. Archer, F. C., Hodgson, I. H. (1987). Total and extracatable trace element content of soils in England and Wales. *Journal of Soil Science 38, 421-432*.
3. Avery, B. W., Bascomb, C.L. (1982). Soil Survey Laboratory Methods. *Soil Survey Technical Monograph No. 6. Harpend*en.
4. Khairiah Jusoh (1987). *Kajian Pencemaran Logam Berat Di Dalam Sistem Sungai Dengan Rujukan Khas Kepada Kawasan Perbandaran Kuala Lumpur*. Tesis Sarjana Sains. Bangi: Universiti Kebangsaan Malaysia.
5. Massey, D.M., Windsor, G.W. (1967). *Replication Glasshouse Crops Response Inst*., hlm. 72.
6. Metson, A.J. (1956). *Method of Chemical Analysis for Soil Survey samples*. N.Z.D.S.I.R. Soil Bureau Bulletin no. 12
7. McLean, E.O. (1965). *In Methods of Soil Analysis Pt 2, ed. C.A. Black, 978-997*
8. Othman Yaacob (1982). *Sains Tanah*. Kuala Lumpur : Dewan Bahasa dan Pustaka.
9. Rowell, D.L. (1994). *Soil science: methods and applications*. London: Longman Rowell, Group UK Limited.
10. Shamshuddin, J. (1981). *Asas Sains Tanah*. Kuala Lumpur: Dewan Bahasa dan Pustaka.
11. Tan, K.H. (1994). *Environmental Soil Science*. Marcel Dekker, Inc., New York.
12. Havlin, J. L., Tisdale, S. L., Nelson, W. L., Beaton, J.D. (1999). *Soil Fertility and Fertilizers. An Introduction to Nutrient Management*. Prentice Hall, NY.
13. MAFF (1988). Agricultural Land Classification of England and Wales. *Revised guidelines and criteria for grading the quality of agricultural land.*

COMPARATIVE STUDY ON CLEANUP PROCEDURES FOR THE DETERMINATION OF ORGANOPHOSPHORUS PESTICIDES IN VEGETABLES

Alvin Chai Lian Kuet[1] and Lau Seng[2]

[1]*Agriculture Research Centre, Semongok, Kuching, Sarawak*
[2]*Universiti Malaysia Sarawak, 94300 Kota Samarahan, Sarawak*

Abstract

A study was carried out to compare the cleanup procedures for the determination of organophosphorus pesticides in vegetables. Eleven organophosphorus pesticides were extracted with acetone and methylene chloride. Extracts were cleanup by solid-phase extraction (SPE) mixed-mode column using quaternary amine and aminopropyl (SAX/NH$_2$) or octadecyl (C$_{18}$) sorbents. The pesticides were determined by gas chromatography with flame photometric detector. The recovery results obtained from the SPE SAX/NH$_2$ and C$_{18}$ cleanups in carrot, cucumber and green mustard samples were in the range of 71.0 % to 115 %. Lower recoveries were obtained for polar pesticides, methamidophos and dimethoate. These results were compared to the method currently used in the laboratory which does not include any cleanup**.**

Abstrak

Satu kajian telah dijalankan untuk membandingkan kaedah-kaedah pembersihan untuk menentukan racun perosak organopfosforus di dalam sayur-sayuran. Sebelas racun perosak organofosforus diekstrak dengan aseton dan dwiklorometana. Ekstrak dibersihkan dengan pengekstrakan fasa pepejal (SPE) menggunakan amina quaterina dan aminopropil (SAX/NH$_2$) atau turus oktadesil, C$_{18.}$ Racun perosak ditentukan dengan kromatografi gas yang dilengkapkan dengan pengesan fotometrik nyala. Pengembalian racun perosak dalam tiga jenis sayur-sayuran iaitu lobak merah, timun dan sawi hijau adalah di antara 71.0 % dan 115 %. Pengembalian yang rendah diperolehi untuk racun perosak yang berkutub iaitu methamidophos dan dimethoate. Keputusan ini dibandingkan dengan kaedah tanpa pembersihan yang digunakan di makmal pada masa ini.

Introduction

Organophosphorus (OP) pesticides have replaced the organochlorine pesticides due to concern regarding the persistence and polluting effect of these compounds to the environment. However, due to its low persistency, a greater number of applications to a crop may be necessary during the course of the growing season. Numerous methods have been developed for the analysis of OP pesticides in fruits and vegetables. Some of these methods advocate the use of solid-phase extraction (SPE) cartridges. A method using acetonitrile for extraction of pesticide residues in fruits and vegetables was reported [1]. The pesticides were detected on gas chromatograph (GC) equipped with flame photometric detector (FPD). A simple and efficient cleanup method for GC determination of twenty-three OP pesticides in crops was reported [2]. The sample was extracted with acetone and benzene. Cleanup was performed on silica catridges. It was reported that water-soluble pesticides such as dichlorvos and dimethoate gave poor recoveries in all crops. A method for the determination of twenty-eight OP pesticides in fatty and non-fatty foods was reported [3]. Extraction was carried out using acetone and mixture of acetone-water. Carbon-celite was used as cleanup. A multi-residue method for determination of forty-three OP insecticides in plant and animal tissues was reported [4]. The OP insecticides were extracted with methanol-dichloromethane (1 : 9) and cleaned up using gel permeation chromatograph and silica gel mini columns. Determination of OP pesticides in fruits and vegetables using octadecyl, carbon and aminopropyl cartridges was reported [5]. The pesticides were determined by GC equipped with mass selective detector. Gravity-fed C$_{18}$ SPE as cleanup for detection of pesticides in spinach, oranges, tomatoes and peaches was also reported [6]. The method was used to analyze forty-eight OP pesticides. A method using SPE cleanup of chlorpyrifos, methidathion and methyl parathion in oranges was reported [7]. Samples were extracted with anhydrous sodium acetate with ethyl acetate. The ethyl acetate extract was concentrated and cleaned up by passing through tandem

SAX and PSA SPE columns. In this study, the cleanup procedures for the determination of OP pesticides in vegetables using the SPE mixed-mode column; quaternary amine and aminopropyl (SAX/NH$_2$) and octadecyl (C$_{18}$) sorbents were employed.

Experimental

Eleven OP pesticides; namely methamidophos, dimethoate, diazinon, tolcofos-methyl, fenitrothion, chlorpyrifos, phenthoate, prothiofos, triazofos, cyanofenfos and azinphos-ethyl were selected for this study.   These pesticides were fortified in carrot, cucumber, and green mustard at 0.5 and 0.1 ppm levels. Three replicate fortifications for each matrix type were prepared. Extraction was carried out based on procedures described by Steinwandter [8]. 10 g of sample was homogenised in a blender containing 100 mL acetone, 75 mL dichloromethane and 15 g sodium chloride for three minutes. The organic phase was transferred to a beaker and 3 g of sodium sulphate was added to remove the remaining water. For SPE SAX/NH$_2$ cleanup, the tube was conditioned with 10 mL of acetone : petroleum ether (1 : 2). 2 mL of extract was transferred to the SPE tube, followed by eluting with 10 mL of conditioning solvent at the flow rate of 1 mL/min. For SPE C$_{18}$, the tube was conditioned with 10 mL hexane : petroleum ether (1 : 1 v/v). 2 mL of extract was transferred to the tube, followed by eluting with 10 mL conditioning solvent. The eluates collected were analysed by GC-FPD on a HP 5, 15 m x 0.53 mm x 1.5 μm column. A Hewlett-Packard GC 5890 Series II equipped with FPD was used for the determination of the OP pesticides. GC conditions were: injector temperature, 260 °C; detector temperature 250 °C; carrier flow (nitrogen) 4 mL/min; oven temperature, 120 °C (1.0 min), rate 30 °C/min to 150 °C, rate 5 °C/min to 270 °C (10 min); air flow : 80 mL/min; hydrogen flow : 67 mL/min.

Results and Discussion

Recoveries of the OP pesticides at 0.5 ppm and 0.1 ppm levels from carrot samples with SAX/NH$_2$, C$_{18}$ cleanup and without cleanup are shown in Table 1. At 0.5 ppm fortification level, the recoveries obtained for eleven OP pesticides using the method without cleanup were within the acceptable range of 70 -120 % [9]. The recoveries for these pesticides ranged from 76 % to 108.3 % with CV of 5.0 - 11.0 %. Comparable results were obtained for the SPE SAX/NH$_2$ cleanup for nine OP pesticides.   Their recoveries were in the range of 92.0 % to 115.0 % with CV of 4.0 - 7.2 %. A low recovery of 30.3% was obtained for dimethoate, while methamidophos was totally absorbed in the SPE during the cleanup. Both dimethoate and methamidophos were more polar as compared to the other OP pesticides. The solubility of methamidophos and dimethoate in water are 200,000 mg/L and 25,000 mg/L respectively as compared to 0.05 mg/L for prothiofos [10]. The low recoveries of these polar pesticides were because of their strong retention by polar anion exchange sorbents, SAX/NH$_2$. For the C$_{18}$ cleanup, the recoveries obtained were within the acceptable range except for methamidophos. Their recoveries were in the range of 80.0 % to 107.7 % with CV of 1.5% to 5.9 %. The recovery obtained for methamidophos was 6.7 %.

Table 1. Recovery of OP pesticides from carrot samples using different cleanup methods

Pesticide	0.5 ppm			0.1ppm		
	SAX/NH$_2$	C$_{18}$	No cleanup	SAX/NH$_2$	C$_{18}$	No cleanup
	% Rec.[a] ± CV	% Rec.[a] ± CV	% Rec.[a] ± CV	% Rec.[a] ± CV	% Rec.[a] ± CV	% Rec.[a] ± CV
Methamidophos	0	6.7 ± 2.5	76.0 ± 5.0	0	40.7 ± 5.9	108.3 ± 10.5
Dimethoate	30.3 ± 17	107.7 ± 2.3	108.3 ± 6.0	71.0 ± 6.6	99.7 ± 8.7	118.0 ± 3.5
Diazinon	92.0 ± 6.1	92.7 ± 3.2	89.3 ± 9.3	95.7 ± 3.5	93.7 ± 3.1	97.3 ± 4.2
Tolcofos-methyl	113.3 ± 5.8	92.0 ± 1.7	98.7 ± 10.7	94.7 ± 4.0	93.3 ± 6.7	97.0 ± 2.7
Fenitrothion	108.7 ± 5.7	91.7 ± 1.5	102.0 ± 6.1	92.3 ± 4.7	97.0 ± 4.6	110.1 ± 1.2
Chlorpyrifos	112.3 ± 5.8	84.7 ± 5.9	99.3 ± 11	92.7 ± 1.2	97.0 ± 2.0	96.0 ± 2.0
Phenthoate	109.7 ± 5.7	92.3 ± 2.1	97.0 ± 8.9	99.3 ± 2.5	91.0 ± 2.7	94.0 ± 1.7
Prothiofos	115.0 ± 7.2	80.0 ± 1.0	103.7 ± 10	93.0 ± 4.4	85.3 ± 2.5	94.0 ± 1.0
Triazofos	105.3 ± 4.0	102.0 ± 2.0	95.7 ± 8.1	98.0 ± 6.1	92.7 ± 5.7	124.0 ± 1.0
Cyanofenfos	112.7 ± 4.0	88.0 ± 1.7	99.7 ± 7.2	90.3 ± 5.5	96.0 ± 4.4	99.7 ± 0.6
Azinphos-ethyl	102.3 ± 6.8	102.3 ± 5.0	97.3 ± 9.2	97.0 ± 4.4	92.0 ± 6.6	112.0 ± 1.0
AV	107.9	91.7	98.1	92.4	93.8	104.2
SD	7.2	7.2	4.1	8.0	4.0	10.9

AV = average mean   CV = coefficient of variation   SD = standard deviation   (a) n = 3

At 0.1 ppm fortification level, all the OP pesticides except methamidofos showed good recoveries of 71 % to 99.3 % using the SAX/NH$_2$ cleanup with CV of 1.2 % to 6.6 %. None of the methamidofos was recovered in this cleanup. The higher recovery obtained for dimethoate as compared to 0.5 ppm level showed that the amount of

semi polar pesticide being retained by the SAX/NH$_2$ varied depending on the concentration of the pesticides. Better recoveries were obtained for method without cleanup. The recoveries for the OP pesticides without cleanup ranged from 94.0 % to 124.0 % with CV of 0.6 % to 10.5 %. For C$_{18}$ cleanup, the recoveries obtained for 10 OP pesticides were from 85.3 % to 99.7 % with CV of 2.0 % to 8.7 %. Methamidophos had lower recovery of 40.7 %.

Recoveries of the OP pesticides at 0.5 ppm and 0.1 ppm levels from cucumber samples with SAX/NH$_2$, C$_{18}$ cleanup and without cleanup are shown in Table 2. At 0.5 ppm fortification level, the recoveries for 9 OP pesticides using the SAX/NH$_2$ cleanup were within the acceptable range of 80.3 % to 95.3 % with CV of 2.5 % to 7.1 %. Low recovery of 51.7 % was obtained for dimethoate. Methamidophos was totally absorbed during the cleanup. Good recoveries were obtained for method without cleanup. Their recoveries ranged from 69.3 % to 111.0 % with CV of 1.2 % to 6.2 %. For the C$_{18}$ cleanup, the recoveries were from 76.3 % to 104.0 % with CV of 1.5 % to 7.9 %. Low recovery of 8 % was obtained for methamidophos.

Table 2. Recovery of OP pesticides from cucumber samples using different cleanup methods

Pesticide	0.5 ppm			0.1ppm		
	SAX/NH$_2$	C$_{18}$	No cleanup	SAX/NH$_2$	C$_{18}$	No cleanup
	% Rec.[a] ± CV	% Rec.[a] ± CV	% Rec.[a] ± CV	% Rec.[a] ± CV	% Rec.[a] ± CV	% Rec.[a] ± CV
Methamidophos	0	8.0 ± 4.4	69.3 ± 1.5	0	30.7 ± 1.5	92.0 ± 2.7
Dimethoate	51.7 ± 6.0	104.0 ± 6.2	111.0 ± 6.2	43.3 ± 8.5	111.0 ± 9.5	100.3 ± 10.7
Diazinon	86.7 ± 4.6	82.7 ± 3.2	96.3 ± 4.0	80.7 ± 1.5	86.7 ± 7.1	98.7 ± 1.5
Tolcofos-methyl	87.0 ± 5.3	76.3 ± 1.5	94.3 ± 3.1	71.0 ± 1.0	94.3 ± 8.1	94.0 ± 2.7
Fenitrothion	89.0 ± 6.1	79.7 ± 2.1	98.3 ± 1.5	77.3 ± 3.5	95.7 ± 8.7	101.0 ± 2.7
Chlorpyrifos	82.0 ± 7.0	87.0 ± 7.2	91.7 ± 4.2	92.3 ± 3.1	88.7 ± 7.0	94.3 ± 1.5
Phenthoate	95.3 ± 5.9	92.3 ± 7.0	97.3 ± 1.2	85.3 ± 3.8	103.0 ± 6.0	87.0 ± 7.9
Prothiofos	80.3 ± 7.1	92.3 ± 3.2	92.3 ± 4.0	95.3 ± 2.5	82.7 ± 1.2	93.7 ± 7.1
Triazofos	94.0 ± 3.5	98.3 ± 7.9	97.0 ± 2.0	79.7 ± 1.5	104.3 ± 1.2	99.3 ± 7.1
Cyanofenfos	91.3 ± 6.1	86.7 ± 7.4	89.3 ± 1.5	80.3 ± 4.0	95.7 ± 7.5	91.0 ± 1.7
Azinphos-ethyl	91.3 ± 2.5	96.3 ± 6.7	101.0 ± 4.0	88.3 ± 6.4	89.0 ± 7.9	111.7 ± 2.1
AV	88.5	88.0	95.3	79.3	93.3	98.6
SD	5.1	7.5	3.7	14.6	7.3	11.0

AV = average mean   CV = coefficient of variation   SD = standard deviation   (a) n = 3

At 0.1 ppm fortification level, the recoveries obtained for the nine OP pesticides using SAX/NH$_2$ cleanup ranged from 71 % to 95.3 % with CV of 1.0 % to 6.4 %. A low recovery of 43.3 % was obtained for dimethoate, while methamidophos was totally absorbed in the sorbent. Good recoveries were obtained for method without cleanup. Their recoveries ranged from 87.0 % to 111.7 %, with CV of 1.5 % to 10.7 %. For C$_{18}$ cleanup, the recoveries obtained for 10 OP pesticides ranged from 86.7 % to 111 % with CV of 1.2 % to 9.5 %. Low recovery of 30.7 % was obtained for methamidophos.

The recovery results obtained from green mustard samples with SAX/NH$_2$, C$_{18}$ cleanup and without cleanup are shown in Table 3. At 0.5 ppm fortification level, the recoveries obtained for 10 OP pesticides using SAX/NH$_2$ cleanup were within the acceptable range. They were in the range of 82.0 % to 102.0 % with CV of 2.7 % to 9.9 %. The only pesticide with low recovery was methamidophos. As compared to carrot and cucumber, higher recoveries were obtained for dimethoate. For semi polar pesticides such as dimethoate, the amount of absorption into the SAX/NH$_2$ also varies depending on the samples types. Therefore, there is a wide variation of recoveries obtained among the three types of vegetables tested. Good recoveries were obtained from the method without cleanup. Their recoveries were in the range of 74.3 % to 118.3 % with CV of 0.6 % to 6.1 %. For C$_{18}$ cleanup, the recoveries obtained were in the range of 71.0 % to 97.3 % with CV of 2.0 % to 8.3 %. Lower recovery of 38.0 % was obtained for methamidophos.

At 0.1 ppm fortification level, the recoveries obtained for nine OP pesticides using SAX/NH$_2$ cleanup ranged from 77.0 % to 88.0 % with CV of 0.7 % to 5.7 %. As encountered in the cucumber and carrot samples, the recovery for dimethoate was low; 34.5 %, while, methamidophos was totally absorbed by the SPE sorbent. Good recoveries were obtained for method without cleanup. Their recoveries ranged from 86.3 % to 114.7 % with CV of 2.5 % to 10.4 %. For the C$_{18}$ cleanup, the recoveries obtained were in the range of 83.7 % to 106.3 % with CV of 1.7% to 8.7 %. The recovery obtained for methamidophos was 37.0 %.

107

The chromatograms for SPE cleanups and without cleanup are shown in Figure 1. All the   chromatograms showed no interference peaks which co-eluted with the 11 OP pesticides. The FPD in phosphorus mode is selective and specific responding only to phosphorus compounds. It was noted that a large peak at 21 min has substantially reduced after the SAX/NH$_2$ and C$_{18}$ cleanups.

Table 3 Recovery of OP pesticides from green mustard samples using different cleanup methods

Pesticide	0.5 ppm			0.1ppm		
	SAX/NH$_2$	C$_{18}$	No cleanup	SAX/NH$_2$	C$_{18}$	No cleanup
	% Rec.[a] ± CV	% Rec.[a] ± CV	% Rec.[a] ± CV	% Rec.[a] ± CV	% Rec.[a] ± CV	% Rec.[a] ± CV
Methamidophos	15.3 ± 4.5	38.0 ± 27.8	74.3 ± 1.5	0	37.0 ± 10.2	93.3 ± 10.4
Dimethoate	102.0 ± 9.9	97.3 ± 8.3	118.3 ± 6.1	34.5 ± 9.2	96.7 ± 8.7	99.0 ± 7.6
Diazinon	88.3 ± 6.5	84.0 ± 2.0	92.3 ± 1.5	84.0 ± 5.7	94.7 ± 3.8	91.3 ± 2.5
Tolcofos-methyl	92.0 ± 4.6	80.0 ± 2.0	89.7 ± 1.5	80.5 ± 0.7	104.3 ± 2.3	89.0 ± 4.0
Fenitrothion	91.3 ± 4.7	80.0 ± 7.6	93.3 ± 5.9	77.0 ± 5.7	96.3 ± 3.8	100.3 ± 6.8
Chlorpyrifos	94.0 ± 5.2	71.0 ± 7.9	96.7 ± 2.1	77.5 ± 2.1	83.7 ± 3.1	90.3 ± 3.2
Phenthoate	89.7 ± 4.5	85.7 ± 7.6	93.3 ± 3.2	88.0 ± 1.4	99.3 ± 6.0	86.3 ± 4.9
Prothiofos	90.7 ± 7.4	71.0 ± 3.6	97.3 ± 0.6	78.0 ± 2.8	84.0 ± 5.0	91.3 ± 6.7
Triazofos	86.0 ± 2.7	77.5 ± 7.9	89.7 ± 4.0	80.5 ± 7.8	105.7 ± 4.0	96.3 ± 6.7
Cyanofenfos	88.0 ± 5.3	80.7 ± 5.5	91.3 ± 3.2	84.5 ± 2.1	88.0 ± 1.7	88.3 ± 4.0
Azinphos-ethyl	82.0 ± 4.6	83.0 ± 3.6	92.3 ± 6.1	87.5 ± 3.5	106.3 ± 6.7	114.7 ± 8.1
AV	90.4	81.0	95.5	77.2	95.8	94.7
SD	5.3	7.6	8.4	15.5	8.9	8.4

AV = average mean   CV = coefficient of variation   SD = standard deviation   (a) n = 3
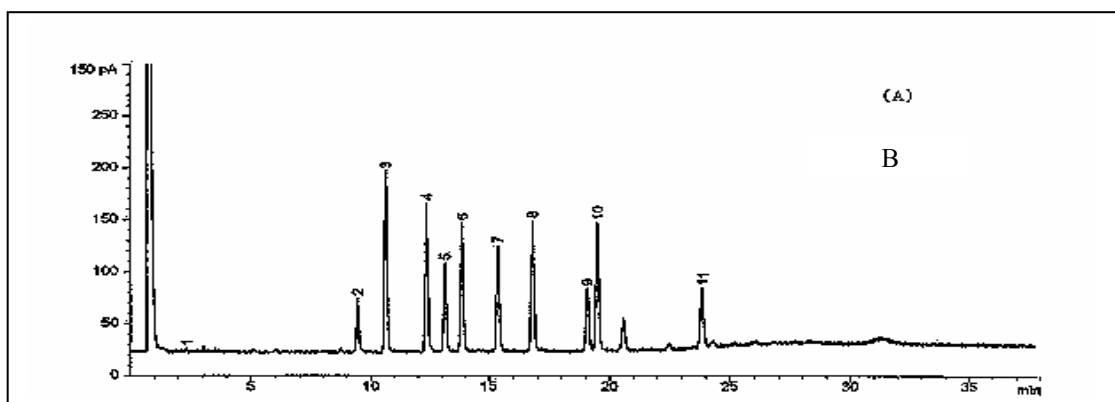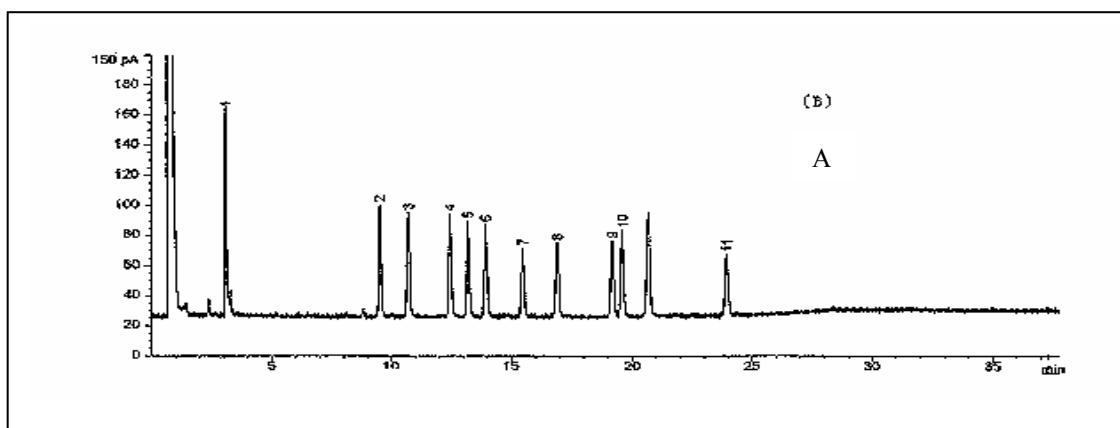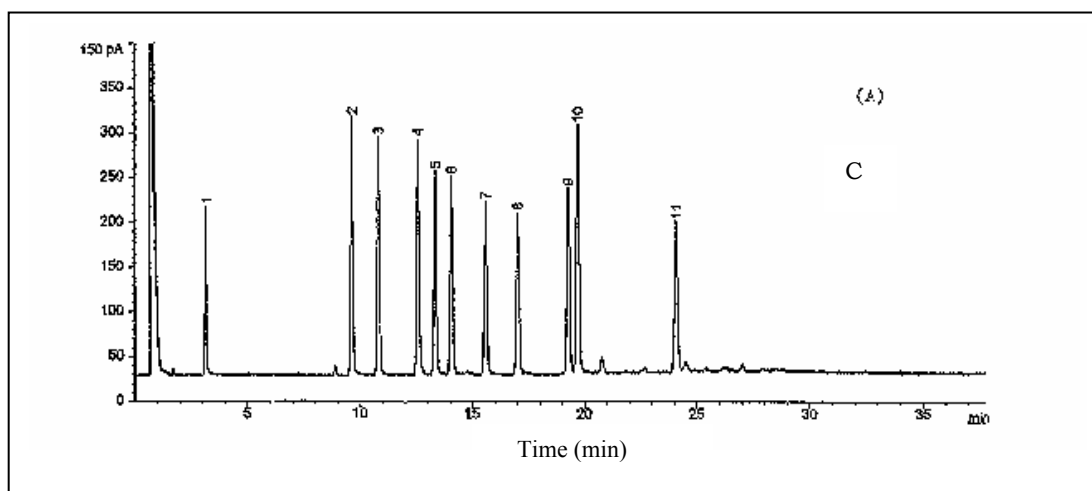
Figure 1. Typical GC chromatogram of vegetable sample without cleanup (A), after SAX/NH$_2$ cleanup (B) and C$_{18}$ cleanup (C). Peaks : 1, methamidophos; 2, dimethoate; 3, diazinon; 4, tolcofos-methyl; 5, fenitrothion; 6, chlorpyrifos; 7, phenthoate; 8, prothiofos; 9, triazofos; 10, cyanofenfos; 11, azinphos-ethyl

Conclusion

The studies on the SPE cleanup methods showed that SAX/NH$_2$ and C$_{18}$ have the potentials to be used as cleanup method for OP pesticides in the laboratory. The advantage of the SPE method over the current method without cleanup is that the former removed a substantial amount of coloured compounds and matrix interferences from the samples. This can reduce the cost of GC maintenance especially for the GC inlet and column. Except for more polar pesticides such as methamidofos and dimethoate, comparable results were obtained for the other OP pesticides using SPE cleanup methods. No interfering peaks were encountered in the chromatograms. In spite of the limited range of this study, it can be predicted that the SPE cleanup can be successfully extrapolated to other pesticides and vegetables. The benefits of the SPE method compared to the other cleanup methods were the reduction of organic solvents use, possibility of concentration the samples, less sorbent is used, no cross-contamination and shorter analysis time.

References

1. Lee, S.M., Papathakis, M.L., Feng, H.M., Hunter, G.F. & Carr. J.E. (1991) Multipesticide residue method for fruits and vegetables. *Fresenius J. Anal. Chem.*, **339**, 376 – 383.
2. Sasaki, K., Takashhi, S. & Saito, Y. (1987) Simplified cleanup method and gas chromatographic determination of organophosphorus pesticides in crops. *J. Assoc. Off. Anal. Chem.*, **70**, 460 – 464.
3. Leoni, V., Caricchia, A.M. & Chiavarini, S. (1992). Multiresidue method for quantitation of organophosphorus pesticides in vegetable and animal foods. *J. AOAC Int.* **75**, 511 - 518.
4. Holstege, D.M., Scharberg, D.L., Richardson, E.R. & Moller, G. (1991). Multiresidue screen for organophosphorus insecticides using gel permeation chromatography-silica gel cleanup. *J. Assoc.Off. Anal. Chem.* **72,** 394 – 399.
5. Fillion, J., Saure, F. & Selwyn, J. (2000) Multiresidue methods for the determination of residues of 251 pesticides in fruits and vegetables by gas chromatography with florescence detection. *J.AOAC Int.*, **83**, 698 – 713.
6. Cook, J., Beckett, M.P., Reliford, B., Hammock, W. & Engel, M. (1999) Multiresidue analysis of pesticides in fresh fruits and vegetables using procedures developed by the Florida Department of Agriculture and Consumer Services *J. AOAC Int.*, **82**, 1419 - 1435.
7. Yamazaki, Y. & Ninomiya, T. (1999) Determination of benomyl, diphenyl, o-phenylphenol, thiabendazole, chlopyrifos, methidation and methyl parathion in oranges by solid-phase extraction, liquid chromatography and gas chromatography. *J. AOAC Int*, **82**, 1474 – 1478.
8. Steinwandter, H. (1985) Universal 5-min on-line method for extracting and isolating pesticide residues and industrial chemicals. *Fresenius Z. Anal. Chem.*, **322,** 752 – 754.

9.   Parker, G.A. (1991). Validation of methods used in the Florida Department of Agriculture and Consumer Services Chemical Residue Laboratory. *J. Assoc. Off. Anal.Chem*. **74,** 868 - 871.

10. Worthing, C.R., & Hance, R.J. (1991). *The Pesticide Manual*, 9th Ed. Surrey : Unwin Brothers Limited.

REMOVAL OF DYE BY IMMOBILISED PHOTOCATALYST LOADED ACTIVATED CARBON

Zulkarnain Zainal*, Chang Sook Keng and Abdul Halim Abdullah

Department of Chemistry, Faculty of Science, Universiti Putra Malaysia, 43400 UPM Serdang, Selangor Darul Ehsan, Malaysia

Key words: Photodegradation; Adsorption; Methylene Blue; Titanium Dioxide; Activated Carbon

Abstract

The ability of activated carbon to adsorb and titanium dioxide to photodegrade organic impurities from water bodies is well accepted. Combination of the two is expected to enhance the removal efficiency due to the synergistic effect. This has enabled activated carbon to adsorb more and at the same time the lifespan of activated carbon is prolonged as the workload of removing organic pollutants is shared between activated carbon and titanium dioxide. Immobilisation is selected to avoid unnecessary filtering of adsorbent and photocatalyst. In this study, mixture of activated carbon and titanium dioxide was immobilised on glass slides. Photodegradation and adsorption studies of *Methylene Blue* solution were conducted in the absence and presence of UV light. The removal efficiency of immobilised TiO_2/AC was found to be two times better than the removal by immobilised AC or immobilised TiO_2 alone. In 4 hours and with the concentration of 10 ppm, TiO_2 loaded activated carbon prepared from 1.5 g/15.0 mL suspension produced 99.50% dye removal.

Abstrak

Kebolehan karbon teraktif untuk menjerap and titanium dioksida untuk memfotodegrasi bendasing organik dalam sumber air adalah amat diterima. Penggabungan dua teknik ini dipercayai dapat meningkatkan kecekapan penyingkiran disebabkan kesan sinergik. Ini membolehkan karbon teraktif untuk menjerap lebih banyak dan pada masa yang sama tempoh penggunaan karbon teraktif dapat dipanjangkan memandangkan beban kerja penyingkiran pencemar-pencemar organik dikongsi antara karbon teraktif dan titanium dioksida. Sekatan gerak dipilih untuk mengelakkan daripada penapisan bahan penjerap dan fotopemangkin. Dalam kajian ini, campuran karbon teraktif dan titanium dioksida disekat gerak pada kepingan kaca. Kajian fotodegradasi dan penjerapan *Methylene Blue* dilakukan dalam kehadiran dan ketidakhadiran cahaya ultralembahyung (UV). Kecekapan penyingkiran oleh TiO_2/AC tersekat gerak adalah dua kali lebih baik berbanding penyingkiran dengan AC tersekat gerak atau TiO_2 tersekat gerak. Dalam masa 4 jam dan dengan kepekatan 10 ppm, karbon teraktif termuat titanium dioksida yang disediakan dari 1.5 g/15.0 mL ampaian menghasilkan 99.50% penyingkiran pewarna.

Introduction

The idea of conserving the environment does not come in one or two days time. It has become a necessity to enlighten each an everyone of us of the problem faced by the Mother Nature. Pollution in water bodies is escalating and the fear of living in dirty environment has encouraged researchers to come out with or design techniques to overcome the problem. Developing techniques ranging from distillation, ion exchange, filtration, ultrafiltration, reverse osmosis, ultraviolet (UV) radiation to carbon adsorption has become a necessity.

Combined adsorption-photodegradation process is another alternative in the development of wastewater treatment method and is expected to give better results in removing organic pollutants [1-3]. Adsorption can be done by using a variety of materials such as sawdust, coconut shell, rice husk, banana pith, chitosan, chitin, orange peel, activated carbon and so on. On the other hand, photodegradation is applied by using semiconducting compound such as TiO_2, SnO_2, SiO_2, ZrO_2 and many more. It is proven that titanium dioxide photocatalyst, anchored or embedded onto co-adsorbent with large surface area such as activated carbon produced promising results due to the high capacity of activated carbon to adsorb most of the pollutants and the synergistic effect between these two materials [4-8].

In order to ensure the water treatment system works effectively, immobilisation of titanium dioxide loaded activated carbon onto glass slides is introduced in this study. The purposes of immobilising the photocatalyst-

adsorbent are to avoid the filtration step, reduce losses of the materials and increase the efficiency of the whole system [9-12].

Experimental

Preparation of Immobilised Titanium Dioxide Loaded Activated Carbon (TiO₂/AC)

Particle size of titanium dioxide and activated carbon powders were characterized using particle size analyzer Malvern Mastersizer S.

The suspension for TiO_2/AC coating was prepared by mixing 0.30 g titanium dioxide powder (BET surface area = 50 m²/g, pH 4 suspension, Aeroxide Degussa P25) with 1.20 g AC (iodine number = 1150-1200, carbon total content = 70%-80%, bulk density = 0.40-0.44, ash = maximum 5%) before adding 15.0 mL of distilled water. The mixture was stirred for 1 hour to ensure homogeneity.

The binder was prepared by adding 5.0 g polyvinylalcohol into 80.0 mL formaldehyde at 70 °C under continuous stirring. Transparent, sticky polymer glue was formed and was kept in a sealed bottle to prevent it from rapid hardening.

Later, pieces of glass slides with dimension of 2.54 cm x 7.62 cm were applied with a thin layer of the binder. Then, TiO_2/AC suspension was brushed onto the layer of binder and let to dry. The samples were stored in the dark to prevent preactivation.

Preparation of Methylene Blue

Methylene Blue stock solution with the concentration of 200 ppm was prepared by dissolving 0.2 g Methylene Blue powder in 1000 mL distilled water. Dye solutions used in the removal process were prepared from the stock solution.

Photocatalytic Degradation with Ultraviolet Lamp

The photodegradation experiments were run by illuminating the dye solution (200 mL) containing immobilised TiO_2/AC using an ultraviolet (UV) lamp. Air was continuously pumped into the solution to ensure a constant supply of oxygen. The experimental set-up was covered to avoid unnecessary exposure to light and the temperature was maintained at 28 ºC using a water bath. UV-Visible analysis was performed on the sample solutions using Perkin Elmer UV/VIS Lambda 20 Spectrophotometer.

Results and Discussion

Particle Size of Titanium Dioxide (TiO₂) and Activated Carbon (AC)

TiO_2/AC prepared from TiO_2 and AC powders were studied using Malvern Mastersizer S. Size and characteristics of the particles may affect the stability, chemical reactivity, opacity, flowability and material strength of many materials. This analyzer applied dispersion mechanism whereby particles were accelerated within a compressed air stream and this resulted collision between the particles and wall. Therefore, parameters like feed rate and dispersion air pressure of the particle size analyzer were set at 20% and 3 bar respectively in analyzing both powders. Figure 1 illustrates the size distribution of titanium dioxide and activated carbon. From the figure, it was found that activated carbon has a wide range of sizes whereas titanium dioxide is more uniform whereby it has about the same cumulative percentages in the range of 10 μm to 100 μm. The particle size of titanium dioxide is smaller than activated carbon as it shows higher cumulative percentage at smaller particle size. On the other hand, the cumulative percentage of activated carbon soars higher than titanium dioxide after 350 μm. This shows the compatibility between these two materials when they are mixed together. TiO_2 with smaller particle size will go in between or into the pores of activated carbon that have bigger particle size. This enables TiO_2 and activated carbon to perform effectively in the adsorption-photodegradation process.
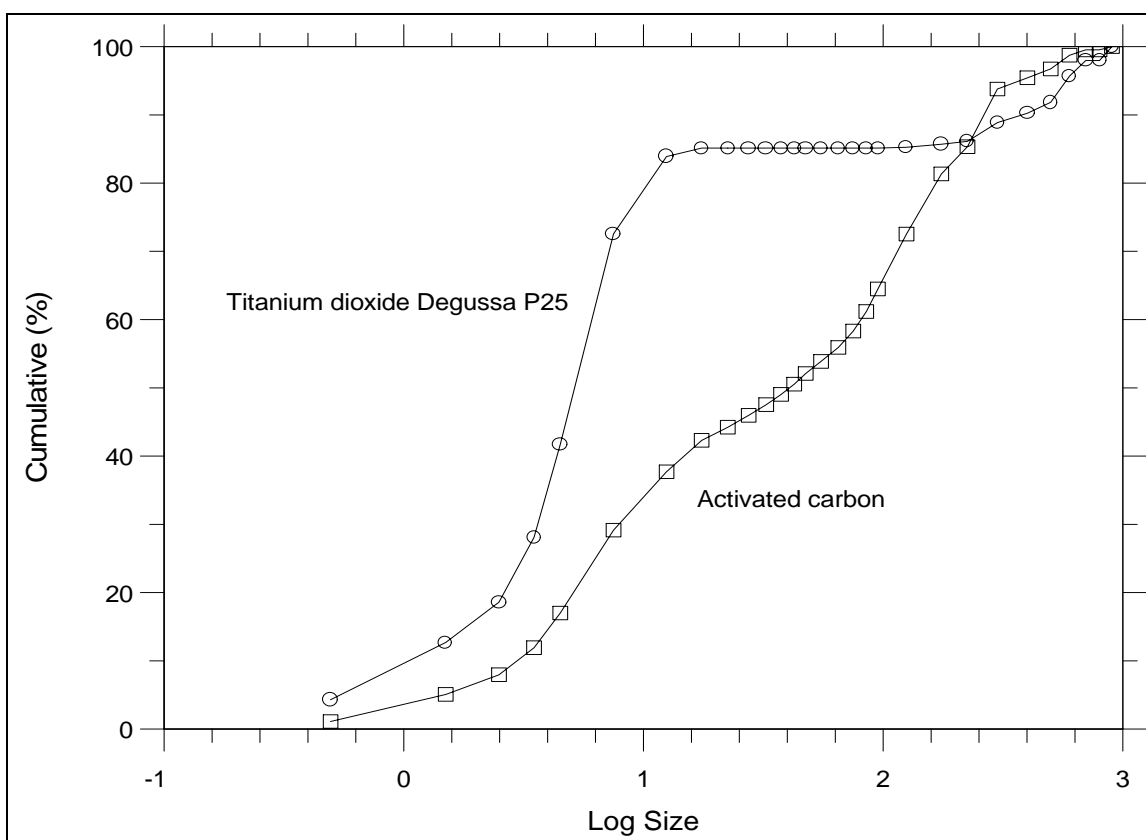
Figure 1: Graph of particle size of titanium dioxide and activated carbon powders.

Comparison between Titanium Dioxide, Activated Carbon and Titanium Dioxide/ Activated Carbon
The removal of Methylene Blue by using the three different samples is depicted in Figure 2. From the graph, it shows that a mixture of TiO_2/AC gives a better efficiency by achieving 99.50% of the dye removed after 4 hours. With the usage of immobilised activated carbon samples, 74.33% of the dye was removed and the percentage of removal goes down to 46.60% by using immobilised TiO_2 samples. These results proved that the combination of titanium dioxide and activated carbon is the best option in removing Methylene Blue. The amount removed by TiO_2/AC is 6.70×10^{-6} mol followed by AC (4.65×10^{-6} mol) and TiO_2 (2.76×10^{-6} mol). Photodecomposition of adsorbed Methylene Blue enhances the adsorption rate of this dye by keeping the adsorptive capacity of activated carbon unsaturated [8]. Dye molecules adsorption by activated carbon followed by a transfer of the molecules to TiO_2 where photocatalysis occurred has created a mutual combination for the enhancement of the dye removal system. This has enabled the adsorption capacity of activated carbon to be maintained and to perform effectively for a longer period of time.

Effect of Suspension Loading in the Preparation of Immobilised TiO_2/AC
Figure 3 shows the effect of suspension loading of TiO_2/AC on the removal of Methylene Blue. Increasing suspension loading of TiO_2/AC resulted the removal system to reach saturation faster as the surface area provided is greater for more adsorption to occur. The removal effect of TiO_2/AC was studied by using kinetics models namely first-order and pseudo-second-order while intraparticle diffusion model was applied to obtain the diffusion rate of the dye molecules into TiO_2/AC. The removal effect of TiO_2/AC by using first-order model is depicted in Figure 4 whereas pseudo-second-order model can be seen in Figure 5. A plot of q_t against the square root of t for the intraparticle diffusion model of Methylene Blue onto TiO_2/AC can be found in Figure 6. The results in Table 1 shows the correlation coefficient, r^2 and first-order apparent rate constant, k compared with correlation coefficient, r^2, sorption capacity, q_2, sorption rate constant of pseudo-second-order rate constant, k_2 and initial sorption rate, h and correlation coefficient, r^2 and intraparticle diffusion rate constant, k_i at various suspension loading of TiO_2/AC, m. From this table, the results can be better represented by pseudo-second-order based on the correlation coefficients (> 0.990). As the amount of TiO_2/AC increases, sorption capacity, q_2 decreases. This trend is in agreement with Ho and McKay [13] where by these researchers studied the sorption

of Basic Red 22 and Acid Red 114 by biosorbent waste product pith. Correlation coefficients for the intraparticle diffusion parameter are the lowest and this suggests that the diffusion controlled mechanism is not predominant. Figure 7 illustrates the variation of apparent rate constant, k_1 and amount of removal against the suspension loading of TiO$_2$/AC. 1.5 g/15.0 mL gives the highest apparent rate constant and greatest amount of removal with the value of 4.91×10^{-2} min^{-1} and 6.70×10^{-6} mol respectively. The results revealed that Methylene Blue removal efficiency increases up to the optimum amount (1.5 g/15.0 mL), beyond which the amount of removal decreases. It is due to the difficulty of light penetration into the immobilised samples for photocatalysis to occur.
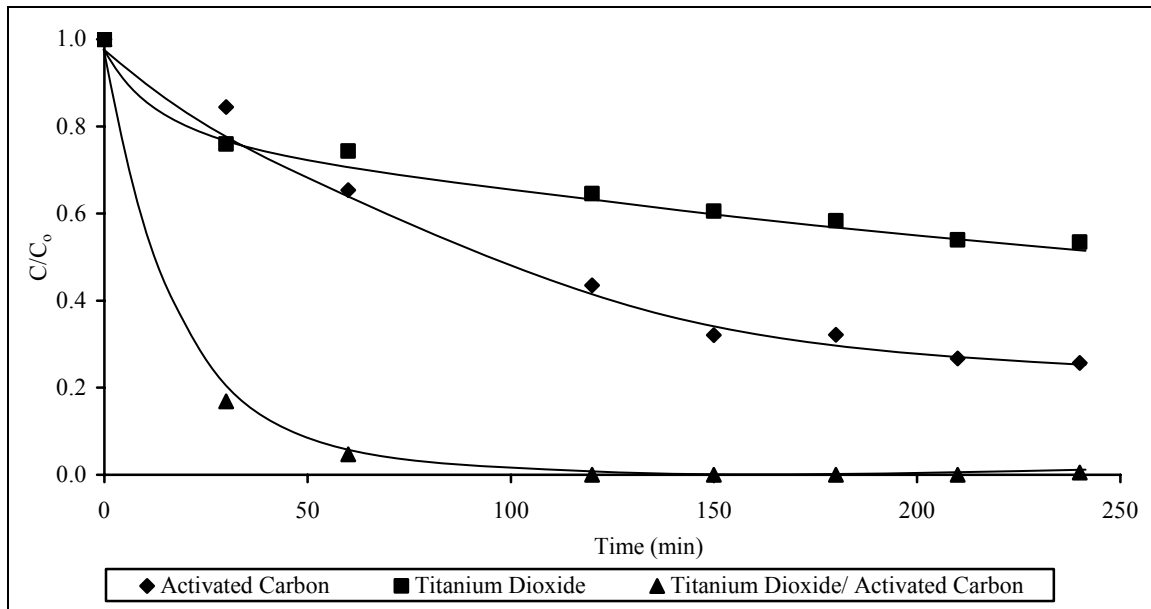
Figure 2: The removal of Methylene Blue by activated carbon, titanium dioxide and TiO$_2$/AC conducted on 5 pieces of glass slides in 200 mL of 10 ppm Methylene Blue solution at 28 ºC.
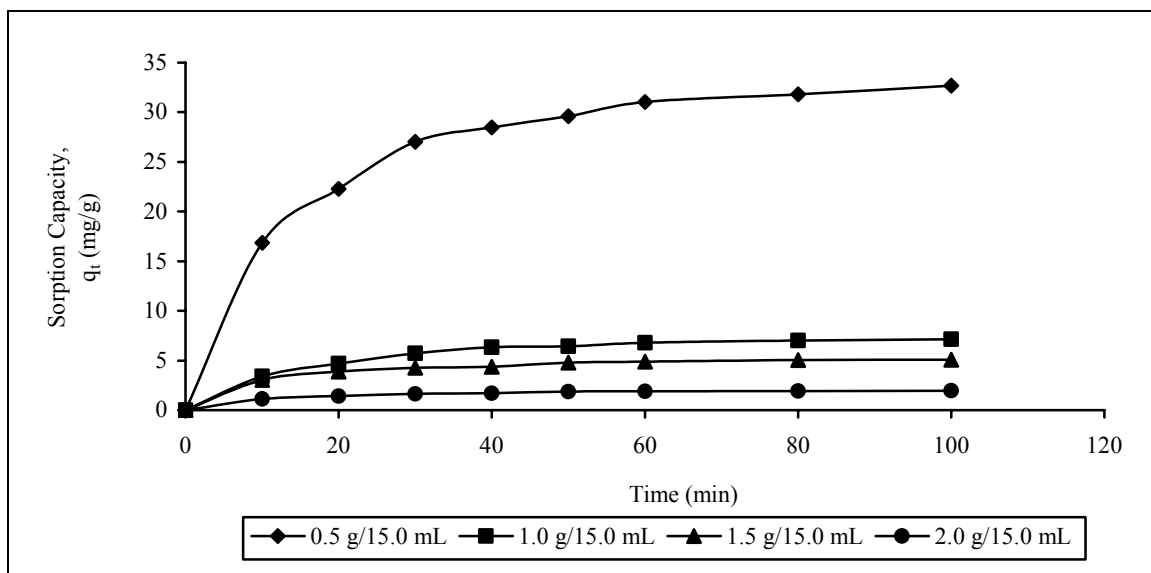
Figure 3: The removal of Methylene Blue by immobilised TiO$_2$/AC at different suspension loading in the preparation of immobilised TiO$_2$/AC conducted on 5 pieces of glass slides in 200 mL of 10 ppm Methylene Blue solution at 28 ºC under UV illumination (1 ultraviolet lamp).
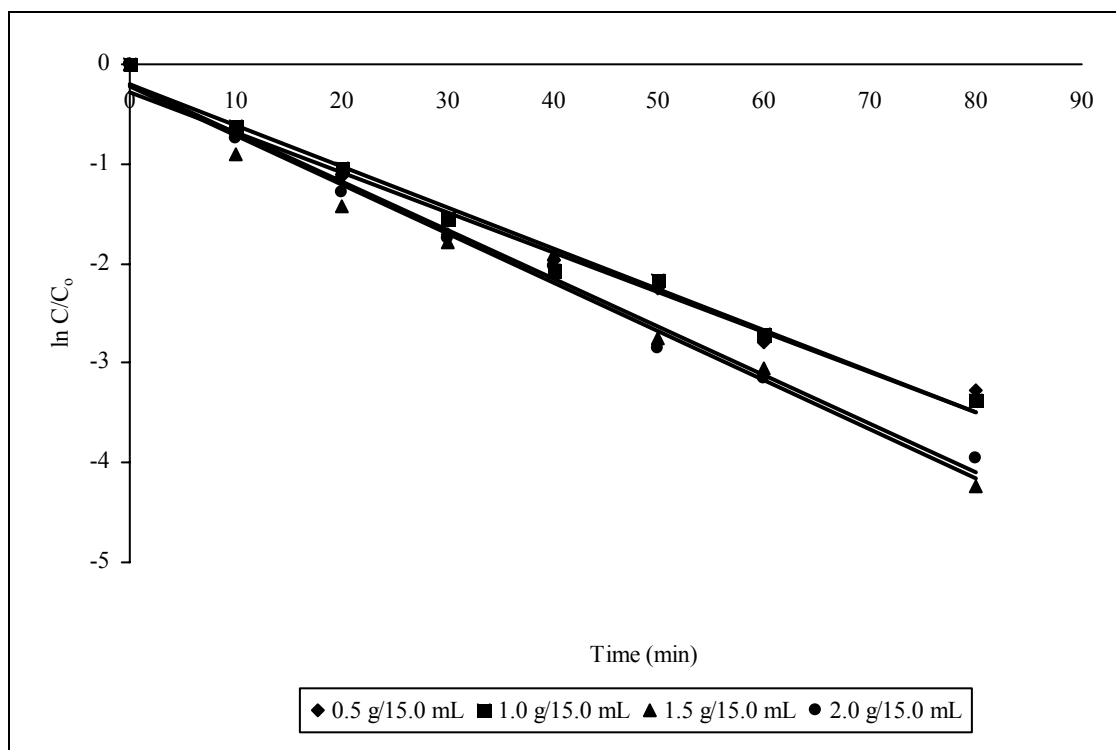
Figure 4: Graph of first-order kinetics of Methylene Blue removal for the effect of suspension loading in the preparation of immobilised TiO_2/AC conducted on 5 pieces of glass slides in 200 ml of 10 ppm Methylene Blue solution at 28 ºC under UV illumination (1 ultraviolet lamp).
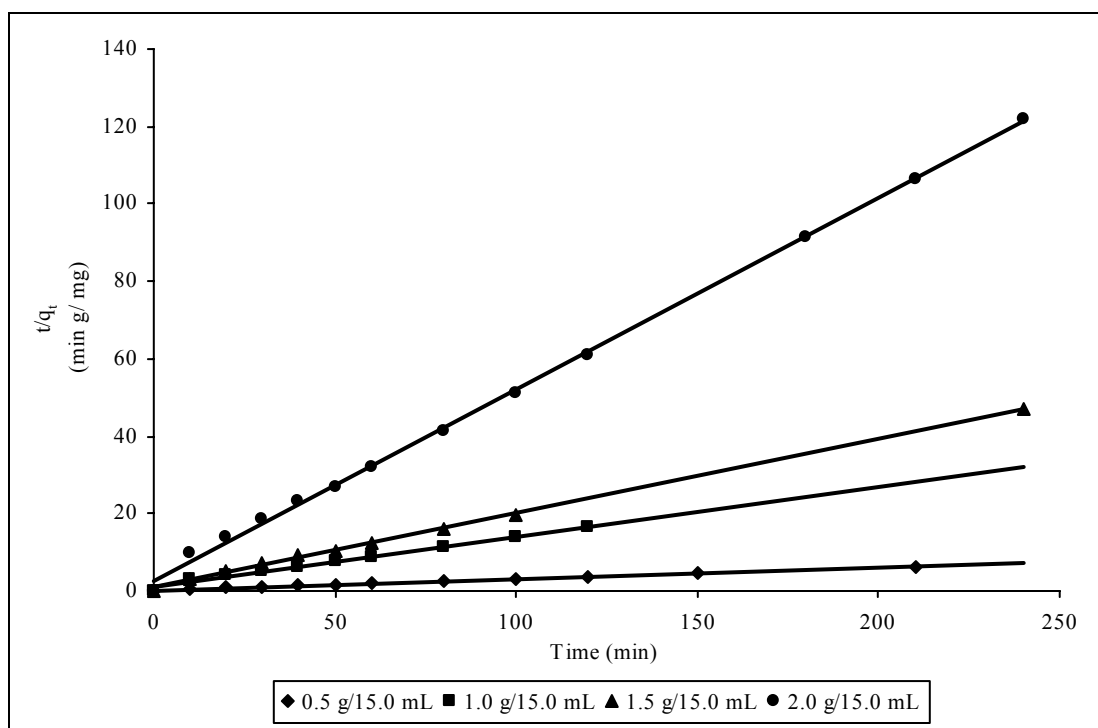
Figure 5: Graph of pseudo-second-order kinetics of Methylene Blue removal for the effect of suspension loading in the preparation of immobilised TiO_2/AC conducted on 5 pieces of glass slides in 200 ml of 10 ppm Methylene Blue solution at 28 ºC under UV illumination (1 ultraviolet lamp).
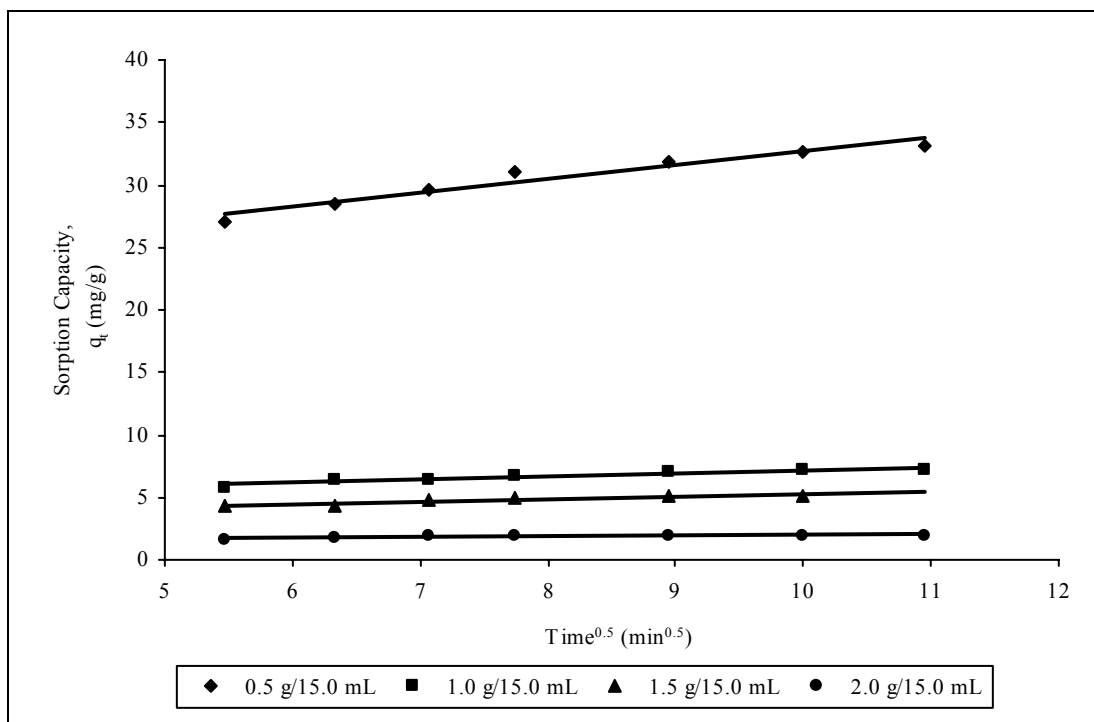
Figure 6: Graph of intraparticle diffussion of Methylene Blue for the effect of suspension loading in the preparation of immobilised TiO_2/AC conducted on 5 pieces of glass slides in 200 ml of 10 ppm Methylene Blue solution at 28 ºC under UV illumination (1 ultraviolet lamp).
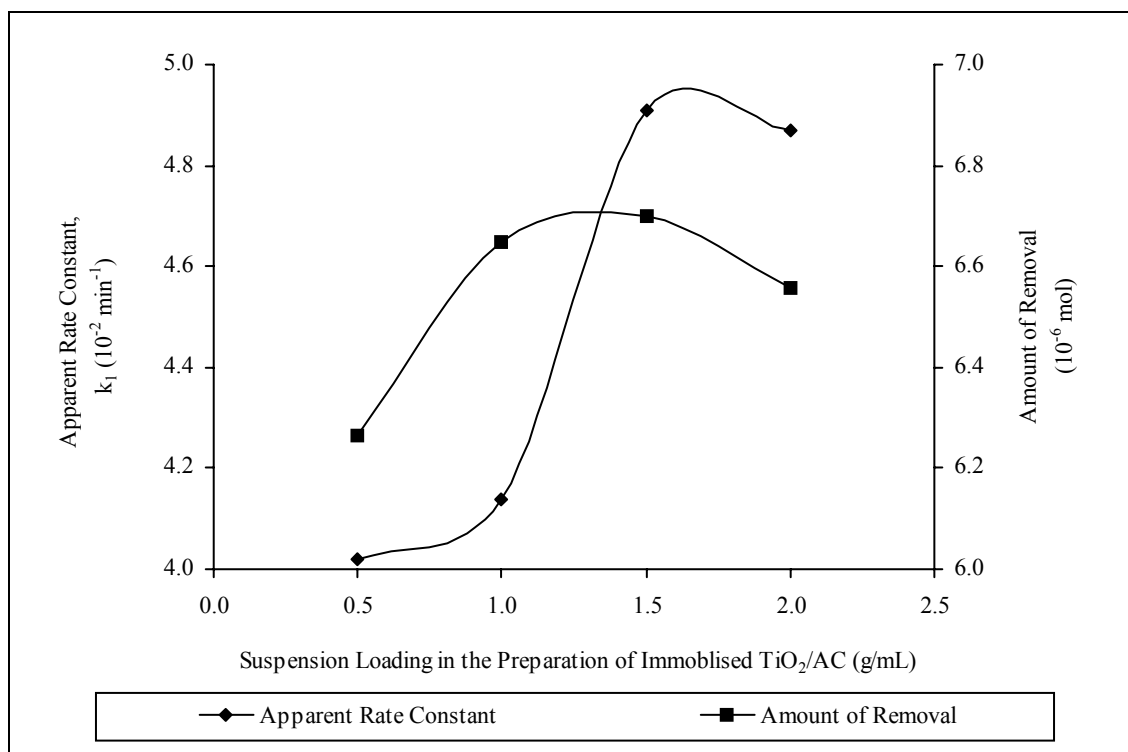
Figure 7: Graph of apparent rate constant and amount of removal versus suspension loading in the preparation of immobilised TiO_2/AC in the removal of Methylene Blue.

Table 1: Parameters for the effect of suspension loading in the preparation
of immobilised TiO_2/AC in the removal of Methylene Blue.

m (g /15.0 mL)	First-order Kinetics		Pseudo-second-order Kinetics				Intraparticle Diffusion	
	r_1^2	k_1 (x10^{-2} min^{-1})	r_2^2	q_2 (mg/g)	k_2 (x10^{-2} g/mg per min)	h (mg/g per min)	r_i^2	k_i (mg/g per min$^{0.5}$)
0.5	0.9767	4.02	0.9979	34.2466	0.43	5.01	0.9429	1.1008
1.0	0.9856	4.14	0.9917	7.7220	1.49	0.89	0.8947	0.2577
1.5	0.9797	4.91	0.9987	5.2219	4.00	1.09	0.8762	0.1962
2.0	0.9873	4.87	0.9990	2.0247	9.06	0.37	0.8076	0.0582

Conclusion

Combination of activated carbon and titanium dioxide has proven to be efficient in removing dye molecules compared with neat TiO_2 and neat AC. Moreover, shorter time frame is required in achieving saturation when TiO_2/AC is applied to the dye removal system. TiO_2/AC is able to remove 95.50% of Methylene Blue whereas activated carbon gives 74.33% efficiency and the dye removal by TiO_2 only shows 46.60%. The dye removal system is initialized by the adsorption of Methylene Blue on activated carbon followed by a mass transfer to titanium dioxide to photodegrade the dye molecules. The removal rate of Methylene Blue was affected by the suspension loading used and the removal of this dye followed pseudo-second-order chemical reaction kinetics model in which best correlation coefficients were shown.

References

1.	S., Qourzal, A., Assabbane, Y., Ait-Ichou (2004). Synthesis of TiO_2 via Hydrolysis of Titanium Tetraisopropoxide and its Photocatalytic Activity on a Suspended Mixture with Activated Carbon in the Degradation of 2-naphthol. J. Photochem. Photobio. A: Chem. 163:317-321.

2.	N., Takeda, N., Iwata, T., Torimoto, H., Yoneyama (1998). Influence of Carbon Black as an Adsorbent Used in TiO_2 Photocatalyst Films on Photodegradation Behaviors of Propyzamide. J. Catal. 177:240-246.

3.	R., Yuan, R., Guan, J., Zheng (2005). Photocatalytic Degradation of Methylene Blue by a Combination of TiO_2 and Activated Carbon Fibers. J. Colloid Interface Sci. 282:87-91.

4.	E., Carpio, P., Zúñiga, S., Ponce, J., Solis, J., Rodriguez, W., Estrada (2005). Photocatalytic Degradation of Phenol Using TiO_2 Nanocrystals Supported on Activated Carbon. J. Mol. Catal. A: Chem. 228:293-298.

5.	B., Tryba, A.W., Morawski, M., Inagaki (2003). Application of TiO_2-mounted Activated Carbon to the Removal of Phenol from Water. Appl. Catal. B: Environ. 41:427-433.

6.	J.-M., Herrmann, J., Matos, J., Disdier, C., Guillard, J., Laine, S., Malato, J., Blanco (1999). Solar Photocatalytic Degradation of 4-chlorophenol Using the Synergistic Effect Between Titania and Activated Carbon in Aqueous Suspension. Catal. Today 54:255-265.

7.	J., Matos, J., Laine, J.-M., Herrmann (1998). Synergy Effect in the Photocatalytic Degradation of Phenol on a Suspended Mixture of Titania and Activated Carbon. Appl. Catal. B: Environ. 18:281-291.

8.	P., Fu, Y., Luan, X., Dai, X. (2004). Preparation of Activated Carbon Fibers Supported TiO_2 Photocatalyst and Evaluation of its Photocatalytic Reactivity. J. Mol. Catal. A: Chem. 221:81-88.

9.	S., Gelover, P., Mondragón, A., Jiménez (2004). Titanium Dioxide Sol-gel Deposited Over Glass and its Application as a Photocatalyst for Water Decontamination. J. Photochem. Photobio. A: Chem. 165:241-246.

10.	K., Ventaka Subba Rao, A., Rachel, M., Subrahmanyam, P., Boule (2003). Immobilization of TiO_2 on Pumice Stone for the Photocatalytic Degradation of Dyes and Dye Industry Pollutants. Appl. Catal. B: Environ. 46:77-85.

11.	V.K.S., Rao, M., Subrahmanyam, P., Boule (2004). Immobilized TiO_2 Photocatalyst During Long-term Use: Decrease of its Activity. Appl. Catal. B: Environ. 49:239-249.

12.	N., Serpone, E., Borgarello, R., Harris, P., Cahill, M., Borgarello, E., Pelizzetti (1986). Photocatalysis Over TiO_2 Supported on a Glass Substrate. Sol. Energy Mater. 14:121-127.

13.	Y.S., Ho, G., McKay (1999). A Kinetic Study of Dye Sorption by Biosorbent Waste Product Pith. Resour. Conserv. Recycl. 25:171-193.

PYROLYSIS AND LIQUEFACTION OF ACETONE AND MIXED ACETONE/TETRALIN SWELLED MUKAH BALINGIAN MALAYSIAN SUB-BITUMINOUS COAL – THE EFFECT ON COAL CONVERSION AND OIL YIELD

Mohd Fauzi Abdullah*, Mohd Azlan Mohd Ishak and Khudzir Ismail

Fuel Combustion Research Laboratory,Faculty of Applied Sciences,University Technology MARA, Arau Campus, 02600, Arau, Perlis

Abstract

The effect of swelling on Mukah Balingian (MB) Malaysian sub-bituminous coal macrostructure was observed by pyrolysing the swelled coal via thermogravimetry under nitrogen at ambient pressure. The DTG curves of the pyrolysed swelled coal samples show the presence of evolution peaks at temperature ranging from 235 – 295 °C that are due to releasing of light molecular weight hydrocarbons. These peaks, however, were not present in the untreated coal, indicating some changes in the coal macrostructure has occurred in the swelled coal samples. The global pyrolysis kinetics for coal that follows the first-order decomposition reaction was used to evaluate the activation energy of the pyrolysed untreated and swelled coal samples. The results thus far have shown that the activation energy for the acetone and mixed acetone/tetralin-swelled coal samples exhibit lower values than untreated coal, indicating less energy is required during the pyrolysis process due to the weakening of the coal-coal macromolecular interaction network. Moreover, liquefaction on the swelled coal samples that was carried out at temperatures ranging from 360 to 450 °C at 4 MPa of nitrogen pressure showed the enhancement of the coal conversion and oil yield at temperature of 420 °C, with retrogressive reaction started to dominate at higher temperature as indicated by decreased and increased in oil yield and high molecular weight pre-asphaltene, respectively. These observations suggest that the solvent swelling pre-treatment using acetone and mixed acetone/tetralin can improve the coal conversion and oil yields at less severe liquefaction condition.

Introduction

Coal liquefaction is usually carried out at temperatures higher than 400 °C and at relatively high pressure. Many attempts have been made to develop methods of dissolving coal at less severe conditions in order to increase coal liquefaction efficiency [1-4] and to reduce capital and operation costs [5]. It is known that, by lowering reaction severity, coal conversion reaction rates and liquid product yields will also be reduced, unless the intrinsic coal reactivity can be sufficiently enhanced [4]. Joseph [1] reported that pre-swelled US bituminous and lower rank coals (i.e. sub-bituminous and lignite) with tetrabutylammonium hydroxide, tetrahydrofuran and methanol prior to liquefaction at 400 °C and at 7.6 MPa enhanced coal conversion and product quality. He found that the enhancement depends on the coal rank and the type of swelling agent being used and suggested that the beneficial effect of swelling might be due to the expansion of the coal macromolecular structure, making it more accessible to the hydrogen donor solvent during liquefaction. In another work, Simsek [2] studied the effect of pre-swelling with various organic solvents and acid-demineralised (pre-treatment) Turkish coals on the supercritical toluene extract yield at 350 °C and at 7 MPa. They found that the highest improved liquid yields for each coal was obtained by the combined effects of pre-treatment and pre-swelling of coals. Although the combination effects proved to increase liquid yields, no simple trend between reactivity improvements with properties of the coals was observed.

In our study [6], we carried out the solvent swelling pre-treatment using hydrogen and non-hydrogen-bonding solvents on low-rank Malaysian coal. The pyrolysis of the untreated and swelled coal using thermogravimetric analyzer (TGA) under nitrogen atmosphere thus far has shown that the activation energy barrier in the swelled coals was lower with an increase in the volatile yield in comparison to the untreated sample. Moreover, the results of the treated samples also show the increase of coal reactivity as revealed by DTG results. Thus, these

preliminary results might provide useful information for coal extraction and liquefaction processes. Hence, this study investigates the effect of acetone and mixed acetone/tetralin-swelled, respectively on the pyrolysis behaviours using TGA and the conversion and product yields from the liquefaction using 1-liter high-pressure high-temperature batch-wise reactor system with tetralin as the hydrogen-donor solvent.

Materials And Methods

Coal Preparation
The sample used in this study is Mukah Balingian (MB) originating from Sarawak, Malaysia. The procedure for coal preparation has been reported earlier [7]. Table 1 represents the ultimate, proximate and petrography analyses of the untreated MB coal sample.

Solvent Swelling Procedure
The volumetric method described by Onal and Akol [8] was adopted in the measurement of swelling ratio without density correction. Acetone (analytical grade solvent from Fisher Chemicals) is used as swelling solvent. For the mixed solvent, which consists of acetone and tetralin, the volume mixed ratio was 80:20. The swelling ratio of the coal samples was measured at room temperature (30 °C) and at ambient pressure. After the swelling procedure, the swelled coal was filtered, dried in vacuum-oven at 80 °C for overnight and finally stored in bottle prior to liquefaction experiments. The determination of activation energy and volatile yield of the coal samples have been reported earlier [6]. The results of swelling ratio, activation energy and pyrolysis volatile yields of the coal samples are given in Table 2.

Coal Liquefaction Experiments
All liquefaction experiments were carried out in a 1-liter magnetically stirred (at 500 rpm) high-pressure high-temperature batch-wise reactor (Parr, 4571 model) fitted with stainless steel tubing condenser cooled with ice to ensure maximum capture of the volatile materials. The procedure of coal liquefaction has been reported earlier [7]. Briefly, 20 g of untreated or acetone-swelled coal and 200 g of tetralin were mixed in the reactor and the liquefaction was carried out at temperature ranging from 360 – 450 °C and at 4 MPa nitrogen pressure. However, for mixed acetone/tetralin coal sample, the reaction temperature used was at 420 °C. After reaching at the particular temperature, the reaction was held for 30 minutes before the system was cooled to ambient temperature. Coal conversion and the product yields of all the samples were finally evaluated [7] and are shown in Table 3.

Sample Analyses
The procedure of ultimate and proximate analyses has been reported earlier [7]. The ultimate analyses were carried out using Elemental Analyser Leco 932 model. The proximate analyses were done using Thermogravimetric analyzer DTA/DSC TA model SDTQ600 under nitrogen gas atmosphere with heating condition follows the ASTM D2974 [9].

Table 1: Characteristics of MB coal sample.

Ultimate analysis	(wt% daf)	Proximate analysis	(wt% db)
Carbon	63.9	Volatile matter	44.7
Hydrogen	5.1	Fixed Carbon	51.1
Nitrogen	1.9	Ash content	4.2
Sulphur	0.5		
Oxygen*	28.6		
	Calorific Value = 24.60 MJ/kg		

*Calculated by difference.

Table 2: Results of swelling ratio (Q), activation energy (Ei, kJ/mol) and pyrolysis volatile yield (VY) of MB coal.

Sample	Q	Ei	VY(%)
Untreated	1.0	312.2	37.6
Tet-sw	1.0	246.3	41.4
Ace-sw	1.3	230.5	40.4
Ace+Tet-sw	1.4	131.6	49.8

Tet-sw Tetralin-swelled
Ace-sw – Acetone-swelled
Ace+Tet-sw – Acetone/Tetralin-swelled

Results And Discussion

Effect of Swelling On Coal by Pure and Mixed Solvents During Pyrolysis

Table 2 shows the results of swelling ratio, activation energy and volatile yield of untreated, acetone-swelled and mixed acetone/tetralin-swelled of MB coal samples. From the table, it can be seen that the swelling ratios of the coal in acetone and mixed acetone/tetralin are higher than that of tetralin. This observation indicates the interaction of nucleophile in the H-bonding solvent (i.e. acetone) with the reactive sites such as hydroxyl, carboxyl and carbonyl that are presence in the coal forming hydrogen bondings. The increase in solvent-coal interactions enhanced the bonds strength, thus weakened the coal-coal macromolecular interactions, and promotes the swelling process of the coal. Tetralin, which is a non-H-bonding solvent, however, did not exhibit any swelling activity with the swelling ratio value closed to that of untreated coal [6]. Interestingly, when tetralin was mixed with acetone, the swelling ratio of the coal increased to a value of 1.4, which is slightly higher than the pure acetone. This minor increment indicates an additional interaction occurred between the coal macromolecular network and the solvents mixture. The effect of swelling by the mixed solvents seem to weakens the coal macromolecular network rigidity and promotes the diffusion of the solvent mixtures, though the exact mechanism is still not well understood. Further, in order to prove this effect, the solvent pre-swelled and untreated coal samples were subjected to pyrolysis via thermogravimetric analysis and the activation energy of the process was evaluated. The global pyrolysis kinetics for coal that follows the first-order decomposition reaction was used to determine the activation energy of the process [10]. Indeed, the mixed solvent swelled coal exhibits the lowest activation energy with an increased in volatile yield, indicating less energy was required during the pyrolysis process due to the weakening of the coal-coal macromolecular interaction network that occurred during swelling process. Thus, this observation indicates the presence of synergistic effect of the mixed solvent towards swelling activity of the coal that enhanced the lowering of the activation energy with an increased in volatile yield during pyrolysis.

Figure 1 shows the DTG curves of untreated, acetone-swelled and mixed acetone/tetralin-swelled coal during pyrolysis. Apparently, both the pyrolysed acetone and mixed acetone/tetralin-swelled coal samples show the presence of evolution peaks at temperatures ranging from 175 to 395 °C that are due to the releasing of the light molecular weight hydrocarbons [10]. These peaks however, were absence in the untreated coal. Another point of interest is that for the mixed acetone/tetralin-swelled coal sample there appears to be another evolution peaks at high temperature ranging from 500 to 650 °C that are due to the released of heavy hydrocarbons [10], and were not presence apparently in both untreated and acetone pre-swelled coal samples. Hence, these observations further proves that some changes in the coal macrostructure have occurred especially in the mixed solvents swelled coal sample that promotes the released of light and heavy molecular weight hydrocarbons during pyrolysis. Hence, this shows that the swelling pre-treatment on coal would possibly increase the liquefaction performance by increasing coal conversion and product yields (especially percent oil) at less severe conditions.
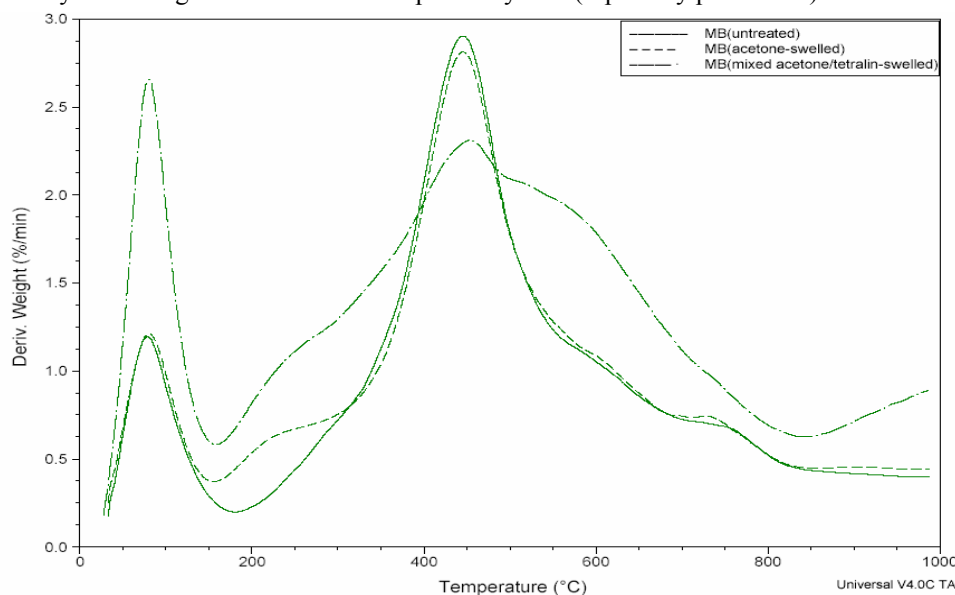
Figure 1: The DTG curves of untreated, acetone-swelled and mixed acetone/tetralin-swelled
of MB coal samples.

Effect of Swelling on Coal Conversion and Oil Yield

Table 3 shows the percent of coal conversion and product yields of liquefaction on the untreated, acetone-swelled and mixed acetone/tetralin-swelled coal samples.

Table 3: Liquefaction results of untreated, acetone- and mixed acetone/tetralin-swelled coal.

Temp. °C	% Coal conversion			% Oil + Gas			% Asphaltene			% Preasphaltene		
	Unt.	Ace.	Mix.	Unt.	Ace.	Mix.	Unt.	Ace.	Mix.	Unt.	Ace.	Mix
360	42	35	-	28	24	-	8	5	-	6	6	-
380	57	43	-	44	29	-	8	3	-	5	11	-
400	66	62	-	50	46	-	10	6	-	6	10	-
420	84	86	86	67	70	78	8	6	1	7	10	7
450	90	83	-	80	75	-		4	-	2	4	-

Unt. = Untreated; Ace. = Acetone-swelled;   Mix. = Mixed acetone/tetralin-swelled.
Liquefaction conditions: 4 MPa, 1:10 coal:solvent, 30 min reaction time and stirred at 500rpm.

Apparently, the results thus far showed that the percent of coal conversion and oil yield obtained during liquefaction of acetone-swelled coal was lower than the untreated coal with preasphaltene predominantly increased at temperature below 400 °C. The fact that as the liquefaction temperature increased at above 350 °C, the coal starts to soften and eventually undergo fragmentation forming preasphaltene and asphaltene [7]. However, with the swelled coal sample, much smaller molecules are being formed due to the weakening of the coal-coal macromolecular interaction as revealed by the DTG curves. The hydrogen donor solvent should cap these smaller radical molecules rapidly in order to prevent repolymerisation reaction. The fact that high formation of preasphaltene suggests that repolymerisation reaction starts to dominate due to the inability of the donor solvent to cap these smaller molecules at temperature below 400 °C. However, as the liquefaction temperature increased beyond 400 °C, a high amount of coal conversion and oil yield being obtained with decreased amount of preasphaltene formation.

Obviously, the effect of mixed solvent swelled coal during liquefaction can be seen by the high percent of oil yield of 78 % at 420 °C, that is higher than that achieved in the acetone- swelled and untreated coal samples. The increase in oil yield corresponds to the decrease in asphaltene and preasphaltene. These observations seem to agree with the pyrolysis which resulting in the lowest activation energy with the greater increased of volatile yield that indicate the high reactivity of the mixed acetone/tetralin-swelled coal. Thus, these phenomenons proved the beneficial effect of mixed solvent-swelled coal in enhancing coal conversion and oil yield prior to liquefaction.

Conclusion

The effect of acetone and mixed acetone/tetralin-swelled on the coal pyrolysis using TGA and the liquefaction products using 1-liter high-pressure high-temperature batch-wise reactor system with tetralin as the hydrogen-donor solvent were studied. The results thus far have shown that the activation energy for the acetone and mixed acetone/tetralin-swelled coal samples exhibit lower values than the untreated coal, indicating less energy is required during the pyrolysis process due to the weakening of the coal-coal macromolecular interaction network. Moreover, liquefaction on the swelled coal samples showed the enhancement of the coal conversion and oil yield at temperature of 420 °C, where the oil yield was greatly increased for mixed acetone/tetralin-swelled with further decreased in asphaltene and preasphaltene, respectively. Thus, these observations proved the beneficial effect of swelling pre-treatment on liquefaction at less severe condition.

References

1. Joseph, J.T., "Liquefaction behaviour of solvent-swollen coals", *Fuel*, vol. 70, pp. 139-144, 1991.
2. Simsek, E.H., "The effect of pre-swelling and/or pre-treatment of some Turkish coals on the supercritical fluid extract yield", *Fuel*, vol. 81, pp. 503-506, 2002.

121

3. Hu, H., Sha, G. and Chen, G., "Effect of solvent swelling on liquefaction of Xinglong coal at less severe conditions", *Fuel*, vol. 68, pp. 33-43, 2000.
4. Artok, L., Davis, A., Mitchell, G.D. and Schobert, H.H., "Swelling pre-treatment of coals for improved catalytic liquefaction", *Fuel*, vol. 71, pp. 981-991, 1992.
5. Shams, K.G., Miller, R.L. and Baldwin, R.M., "Enhancing low severity coal liquefaction reactivity using mild chemical pre-treatment", *Fuel*, vol. 71, pp. 1015-1023, 1992.
6. Abdullah, M.F., Ismail, K. and Ishak, M.A.M., "Investigation of pyrolysis behaviours on solvent swelled Mukah Balingian coal using TGA analysis", *ACGC Chemical Research Commun.*, in print.
7. Ishak, M.A.M., Ismail, K., Abdullah, M.F., Kadir, M.O.A., Mohamed, A.R. and Abdullah, W.H., "Liquefaction studies of low-rank Malaysian coal using high-pressure high-temperature batch-wise reactor system", *Coal Preparation Jour.*, in print.
8. Onal, Y. and Akol, S., "Influence of pre-treatment on solvent-swelling and extraction of some Turkish lignites", *Fuel*, vol. 82, pp. 1297-1304, 2003.
9. ASTM D2974, Annual Book of ASTM Standards, vol. 5.05, *The American Society for Testing and Materials* (ASTM), Philadelphia, PA.
10. Probstein, R.F. and Hicks, R.E., '*Synthetic fuels'*, McGraw-Hill, Inc., 1982.

PENENTUAN KUALITI AIR TASIK KEJURUTERAAN UKM KAMPUS BANGI: KE ARAH SISTEM PENGURUSAN SUMBER AIR BERSEPADU

Mazlin Bin Mokhtar[1], Othman A. Karim[2] dan Irene Lee Pei Ngo[3]

[1]Institut Alam Sekitar dan Pembangunan (LESTARI)
[2]Jabatan Kejuruteraan Awam & Struktur, Fakulti Kejuruteraan
[3]Pusat Pengajian Sains Kimia dan Teknologi Makanan, Fakulti Sains & Teknologi
Universiti Kebangsaan Malaysia
43600 UKM Bangi, Selangor Darul Ehsan, Malaysia

Abstrak

Sistem pengurusan sumber air bersepadu (IWRM) merupakan suatu proses yang mempromosikan pembangunan penyelarasan dan pengurusan air, tanah dan sumber lain yang berkaitan untuk memaksimumkan manfaat ekonomi dan sosial secara seimbang tanpa menjejaskan kelestarian ekosistem. Kajian mengenai kualiti air Tasik Kejuruteraan, UKM Kampus Bangi dijalankan untuk menentukan kualiti air tasik tersebut, membandingkannya dengan nilai Interim Kualiti Air Kebangsaan (INWQS) (JAS, 2001), dan menganggarkan nilai Indeks Kualiti Air berdasarkan enam parameter terpilih. Kajian ini juga bertujuan mengenalpasti sumber dan tahap pencemaran air tasik berkenaan. Kesan hari hujan dan hari kering ke atas kualiti air tersebut juga telah dinilai. Parameter yang diukur adalah pH, suhu, oksigen terlarut (DO), konduktiviti, kekeruhan, jumlah pepejal terampai (TSS), permintaan oksigen biokimia (BOD), permintaan oksigen kimia (COD), nitrogen ammonia (NH$_3$-N), plumbum dan kadmium. Parameter suhu, pH, konduktiviti, oksigen terlarut dan kekeruhan diukur secara *in situ* dengan menggunakan meter yang telah dikalibrasi. Kandungan logam berat ditentukan dengan menggunakan spektrofotometer serapan atom (AAS). Kaedah pensampelan dan analisis dilakukan mengikut garis panduan yang dicadangkan oleh *American Public Health Association* (APHA, 1998). Pada keadaan biasa, kadar aliran masuk bagi air tasik dianggarkan sebanyak 0.057 ± 0.024 m³/s manakala, kadar aliran keluar adalah 0.052 ± 0.018 m³/s. Secara teori, masa mastautin air tasik dengan kedalaman purata tasik (1.5m) dan keluasan (18,000 m²) adalah 62.5 ± 37.6 hari. Jumlah anggaran bagi bahan yang diukur yang berada dalam tasik adalah DO (200.88 ± 28.25 kg), TSS (163.78 ± 18.19 kg), NH$_3$-N (12.65 ± 13.90 kg), BOD (41.90 ± 23.95 kg), COD (1605 ± 75 kg), Pb (9.50 ± 0.90 kg) dan Cd (2.81 ± 0.24 kg). Anggaran jumlah berat bahan yang mengalir ke Sungai Langat setiap hari dari tasik ini adalah TSS (27.81 ± 9.29 kg), NH$_3$-N (2.12 ± 0.71 kg), BOD (7.01 ± 2.34 kg), COD (268.9 ± 89.78 kg), Pb (1.59 ± 0.53 kg) dan Cd (0.47 ± 0.15 kg). Hasil ujian ANOVA dua hala menunjukkan perbezaan yang sangat bererti ($p < 0.001$) antara kepekatan parameter semasa hari hujan dan kering bagi Pb, $p < 0.05$ antara hari hujan dan kering bagi TSS. Perbezaan bererti $p < 0.05$ dicerap bagi data antara stesen bagi parameter suhu, DO dan BOD. Semua stesen pensampelan kajian ini didapati mempunyai kualiti air Kelas II kecuali Stesen S2 yang berada pada Kelas III (sedikit tercemar). Secara keseluruhannya, kualiti air Tasik Kejuruteraan UKM boleh dikategorikan sebagai Kelas II – III. Beberapa langkah yang perlu diambil ke arah sistem pengurusan sumber air bersepadu dalam kampus UKM Bangi bagi mewujudkan kualiti air yang baik, sihat dan harmoni yang selaras dengan tema UKM 'Universiti dalam Taman' telah juga dicadangkan.

Abstract

Integrated Water Resources Management (IWRM) is a process, which promotes the coordinated development and management of water, land and related resources, in order to maximize the resultant economic and social welfare in an equitable manner without compromising the sustainability of vital ecosystem. A study on the water quality of the 'Engineering Lake', UKM Bangi Campus was carried out to determine the water quality, and compare it with the Interim National Water Quality Standard (INWQS) (DOE, 2001), followed by estimation of its Water Quality Index (WQI) based on six selected parameters. The purpose of this study was to identify the possible causes of the water pollution and level of this pollution at the lake. The comparisons of concentration values measured during dry days with those on rainy were performed using suitable statistical methods. Water quality parameters that were measured are pH, temperature, dissolve oxygen (DO), conductivity, turbidity, total suspended solids (TSS), biochemical oxygen demand (BOD), chemical oxygen demand (COD), ammoniacal-nitrogen, lead and cadmium. Temperature, pH, conductivity, dissolved oxygen and turbidity were measured *in situ* by using calibrated meters, whilst metal concentrations were determined by using Atomic Absorption Spectrophotometry

(AAS). Methods of sampling and water analyses were performed according to recommendations that were outlined by the American Public Health Association (APHA, 1998). On normal days, the inflow and the outflow of the lake were estimated to be 0.057 ± 0.024 m³/s inflows and 0.052 ± 0.018 m³/s outflows. The theoretical retention time of the lake water with a mean depth of 1.5 m and area of 18,000 m² was 62.5 ± 37.6 days. On the normal days, the estimated total amounts of materials that were present in the lake were DO (200.88 ± 28.25 kg), TSS (163.78 ± 18.19 kg), NH_3-N (12.65 ± 13.90 kg), BOD (41.90 ± 23.95 kg), COD (1605.58 ± 74.68 kg), Pb (9.50 ± 0.90 kg) and Cd (2.81 ± 0.24 kg). The estimated total amount of polluted materials which flowed into the Langat River daily were TSS (27.81 ± 9.29 kg), NH_3-N (2.12 ± 0.71 kg), BOD (7.01 ± 2.34 kg), COD (268.9 ± 89.78 kg), Pb (1.59 ± 0.53 kg) and Cd (0.47 ± 0.15 kg). The results from two way ANOVA showed that there were significant differences ($p < 0.001$) between rainy days and dry days for Pb. There were also significant differences ($p < 0.05$) between rainy days and dry days in term of TSS. There were significant differences ($p < 0.05$) between stations in terms of temperature, DO and BOD. All sampling stations were categorized as having Class II water that means a reasonably good water quality except S2 which was categorized as a Class III, which means it was slightly polluted. On the overall, the Engineering Lake water of UKM Bangi Campus was categorizes as Class II-III. Some measures of IWRM were suggested for improvement of the lake's water quality and its environment, in achieving a healthy lake ecosystem which is in line with UKM's theme of being a 'University in A Garden'.

Pengenalan

Konsep pembangunan lestari telah dikemukakan oleh *World Commission on Environment and Development (Brundtland Commission)* dalam laporan *Our Common Future* pada tahun 1987 (Bruce, 1997). Pembangunan lestari menekankan pengurusan sumber alam yang terdiri daripada biodiversiti, air, tanah dan sumber lain. Di Malaysia, konsep pembangunan lestari telah dimaktubkan dalam beberapa dasar dan dokumen rasmi kerajaan, seperti Rancangan Jangka Panjang Malaysia Ketiga 2001 – 2010 *("Third Outline Perspective Plan 2001 – 2010"),* yang merangkumi Rancangan Malaysia ke-8 (2001 - 2005) dan Rancangan Malaysia ke-9 (2006 – 2010). Malaysia menyertai Persidangan Pertubuhan Bangsa-Bangsa Bersatu mengenai alam sekitar dan pembangunan (UNCED) di Rio de Janeiro, Brazil pada Jun 1992, bila mana konsep pengurusan air secara bersepadu telah dimajukan untuk memastikan bekalan air tawar dunia adalah mencukupi untuk semua penduduk di semua negara bagi tujuan hidupan seharian dan pembangunan lestari. Dalam *Millenium Summit of the United Nations* di New York (2000), *the International Freshwater Conferences* di Bonn (2001) dan *World Summit on Sustainable Development* di Johannesburg (2002), peserta dari pelbagai kerajaan, NGO dan organisasi telah digalakkan untuk menyatakan iltizam dalam pengurusan air termasuk untuk menghebahkan dan melaksanakan agenda pendekatan Pengurusan Sumber Air Bersepadu ("Integrated Water Resources Management", IWRM) (*World Water Forum 2003*). *Global Water Partnership* (GWP) atau Pakatan Air Sedunia mendefinisikan IWRM sebagai suatu proses yang mempromosikan pembangunan dan pengurusan sumber air, tanah dan sumber lain yang berkaitan untuk memaksimumkan manfaat ekonomi dan sosial secara seimbang tanpa menjejaskan ekosistem lestari (GWP, 2000b).

IWRM boleh dijalankan dalam beberapa skala atau peringkat iaitu kebangsaan, negara, negeri, tempatan dan lembangan sungai. Pengurusan Bersepadu Lembangan Sungai (*Integrated River Basin Management*/ IRBM) merupakan cara pengurusan bersepadu dalam mengatasi pelbagai masalah dan isu sumber air seperti pencemaran air, kekurangan air dan banjir dalam konteks isu guna tanah dan pembangunan di sesebuah lembangan sungai. Lembangan Langat di Semenanjung Malaysia adalah terdiri daripada empat buah daerah, iaitu Hulu Langat, Kuala Langat dan Sepang di Selangor, serta empat mukim di Negeri Sembilan. Lembangan ini mempunyai keluasan kira-kira 2 940 km² dan merupakan suatu pusat perindustrian, pembangunan dan pentadbiran di Malaysia yang merangkumi projek nasional seperti Putrajaya, KLIA dan Koridor Raya Multimedia (MSC) (Mazlin *et al.,* 2004). Sungai Langat ini juga mengalir bersebelahan dengan kawasan UKM Kampus Bangi dan sungai ini juga menerima air luahan dari beberapa saluran dan jasad air tertentu dalam Kampus tersebut. Satu daripada jasad air tersebut adalah "Tasik Kejuruteraan" UKM yang dinamakan sedemikian kerana kedudukannya yang hampir dengan fakulti tersebut. Tasik ini telah dipilih sebagai kawasan kajian memandangkan kualiti airnya yang kelihatan tidak berapa menarik dan juga kerana ia menyumbangkan air luahan kepada Sungai Langat.

Permasalahan Kajian

Pencemaran air telah mula kelihatan berlaku di Tasik Kejuruteraan dan kualiti airnya diandaikan tidak baik berdasarkan pandangan estetik. Antara penyebab pencemaran yang disyaki adalah projek pembinaan Kolej Kediaman Pelajar Kausar dan Kompleks Fakulti Teknologi Sains Maklumat (FTSM) yang melibatkan kerja pembersihan tanah; serta aktiviti perniagaan di kantin dalam bangunan Fakulti Kejuruteraan serta blok-blok makmal di sepanjang saluran menuju ke tasik. Kajian kualiti air perlu dijalankan untuk mengenalpasti sumber

dan tahap pencemaran air tasik dengan menggunakan parameter fizikal dan kimia. Seterusnya, Indeks Kualiti Air (IKA) bagi kualiti air tasik ini telah juga ditentukan.

Objektif Kajian

Objektif kajian ini adalah: (1) mengkaji sistem saliran ke Tasik Kejuruteraan, kampus UKM Bangi; (2) menentukan kualiti air pada hari kering dan hari hujan dan kemudian membandingkannya dengan piawaian Interim Kualiti Air Kebangsaan (INWQS) dan piawaian lain yang sesuai untuk menentukan status pencemaran; (3) memberi cadangan tentang langkah-langkah yang perlu diambil untuk mengurangkan pencemaran air dan mengindahkan tasik bagi menghasilkan suasana sihat dan harmoni selaras dengan tema UKM 'Universiti dalam Taman' dan juga sebagai inisiatif ke arah pengurusan sumber air bersepadu (IWRM) dalam kampus.

Lokasi Kajian

Tasik Kejuruteraan ini sebenarnya telah diubahsuai dari sebuah kawasan paya ke tasik buatan manusia pada tahun 1989. Airnya mengalir dari bukit yang berhutan di hulu ke dalam tasik dan air tasik kemudiannya mengalir ke Sungai Langat. Kawasan sekelilingnya telah dikembangkan menjadi taman rekreasi dengan lorong jalan kaki, pondok dan menawarkan aktiviti mengayak untuk pelajar dan warga kampus. Anggaran keluasan Tasik Kejuruteraan ini adalah kira-kira 1.8 hektar. Kedalamannya secara purata adalah 1.5 m. Jabatan Pengurusan Pembangunan (JPP) UKM bertanggungjawab ke atas pengurusan tasik ini dan ia juga bertanggungjawab memantau dan menjaga kebersihan tasik. Kini, pencemaran air telah mula kelihatan dan kualiti air disyaki menjadi semakin teruk. Nilai estetik di tasik kelihatan menurun saban hari dan pemandangan di tasik tidak menyenangkan mata. Punca pencemaran boleh dibahagi kepada pencemar tentu dan pencemar tidak tentu (Krenkel & Novotny 1980). Di Tasik Kejuruteraan, pencemar tentu yang dikenalpasti termasuklah hakisan permukaan tanah akibat projek pembinaan Kolej Kausar dan longkang Kompleks Fakulti Tenologi dan Sains Maklumat, kantin dan bangunan Fakulti Kejuruteraan. Menurut JPP, semua air buangan samada air dari makmal, tandas atau kantin disalirkan oleh paip pembentungan khas ke tangki kumbahan yang kemudiannya disalirkan ke kolam pengoksidaan kumbahan UKM untuk proses perawatan sebelum ia dialirkan ke Sungai Langat. Air larian hujan dan hakisan kelodak di sekeliling tasik merupakan pencemar tidak tentu. Kajian kualiti air ke atas Tasik Kejuruteraan ini dilakukan di lima lokasi yang telah ditentukan sebagai stesen pensampelan (Jadual 1).

Bahan dan Kaedah

Parameter-parameter kajian

Parameter-parameter yang diukur adalah pH, suhu, oksigen terlarut (DO), konduktiviti, kekeruhan, jumlah pepejal terampai (TSS), permintaan oksigen biokimia (BOD), permintaan oksigen kimia (COD), nitrogen ammonia (NH -N), plumbum dan kadmium. Parameter suhu, pH, konduktiviti, oksigen terlarut dan kekeruhan diukur secara *in situ* dengan menggunakan meter yang telah dikalibrasikan. Kandungan logam ditentukan dengan menggunakan spektrofotometer serapan atom (AAS). Kaedah pengawetan dan penyimpanan sampel sebelum analisis adalah seperti yang disarankan oleh APHA (1998).

Secara ringkas, pengukuran suhu, pH, DO, konduktiviti diukur dengan meter oksigen terlarut model YSI 556. Meter turbiditi 2020 berjenama Lamotte digunakan untuk mengukur kekeruhan. TSS ditentukan dengan kaedah APHA 2540D melalui penurasan dan pengeringan pada 103-105℃. BOD adalah sepertimana saranan Kaedah APHA 5210B kaedah elektrod. COD ditentukan melalui kaedah refluks terbuka APHA 5220B. Nitrogen ammonia diukur dengan kaedah HACH Quick Program 380 (Kaedah Nessler) menggunakan spektrometer HACH DR2000 pada jarak gelombang 425 nm. Halaju aliran air diukur dengan meter aliran elektromagnet model Valeport 801 Ver 3.10.

Jadual 1 : Stesen pensampelan dalam kajian ini.

Stesen	Koordinat	Perihalan Ringkas
1	U 02 55'12.1" T101 46'20.3"	Aliran air sungai dari bukit selepas melalui Fakulti Teknologi dan Sains Maklumat.
2	U 02 55'12.4" T101 46'23.6"	Perangkap lumpur yang berdekatan dengan makmal dan kantin Fakulti Kejuruteraan.
3	U 02 55'24.0" T101 46'24.5"	Kawasan yang menerima aliran air dari longkang bangunan Fakulti Kejuruteraan.
4	U 02 55'28.4" T101 46'20.7"	Di tengah-tengah tasik.
5	U 02 55'28.2" T101 46'17.4"	Kawasan aliran keluar air tasik ke Sungai Langat

Hasil dan Perbincangan

Pengiraan Data Hidrologi

Hasil ukuran keluasan melintang bagi aliran masuk ialah 0.151 m² dan aliran keluar ialah 0.092 m²

Kadar aliran isipadu, Q (m³/s) = V x A   - Persamaan (1)
dimana V = halaju aliran (m/s)
      A = keluasan melintang (m²)

Kadar aliran isipadu masuk, Qin = Vin x A
                    = 0.376 m/s x 0.151 m²
                    = 0.057 ± 0.024 m³/s
Kadar aliran isipadu keluar, Q out = V out x A
                    = 0.567m /s x 0.092 m²
                    = 0.052 ± 0.018 m³/s

Luahan aliran masuk dan keluar, Q = Qin – Qout   - Persamaan (2)
Q = 0.057 m³/s – 0.052 m³/s
   = 5.0 x 10⁻³ ± 0.003 m³/s

Masa mastautin, th = I / Q   - Persamaan (3)
dimana I = isipadu tasik (m³),
Q = Luahan aliran masuk & keluar (m³/s)
Masa mastautin, th   = I/Q
                 =   27,000 m³
                   (5.0 x 10⁻³ m³/s)
                 = 5.4 x 10   s

Jadi, dijangka air tasik berada dalam tasik selama 62.5 ± 37.6 hari.

Bagi pengiraan sesuatu pencemar, purata kepekatan di lima stesen diambilkira :
Jumlah berat, M = C x I   - Persamaan (4)
dimana C = kepekatan sebatian,
      I = isipadu air

Kadar aliran berat, L = C x Qout   - Persamaan (5)

Persamaan (5) boleh digunakan untuk menganggar jumlah pencemar yang mengalir dari Tasik Kejuruteraan ke dalam Sungai Langat.

Parameter-parameter

Nilai purata dan sisihan piawai bagi setiap parameter kajian pada pensampelan hari kering dan hari hujan diringkaskan dalam Jadual 2 dan Jadual 3.

Suhu

Analisis statistik ANOVA dua hala menunjukkan tiada perbezaan yang bererti (p > 0.05) diantara keadaan hari hujan-kering bagi lima stesen dengan P=0.717. Manakala, terdapat perbezaan yang bererti diantara stesen dengan P=0.006. Suhu berada dalam julat 28.00 ± 0.01 C hingga 30.84 ± 1.57 C.

pH

Analisis statistik ANOVA dua hala menunjukkan tiada perbezaan yang bererti (p > 0.10) diantara keadaan hari hujan-kering dengan P=0.148. Tiada perbezaan yang bererti (p > 0.10) antara stesen dengan P=0.913. Nilai pH stesen kajian berada dalam julat 6.06 ± 0.07 hingga 7.57 ± 1.61, iaitu berada pada subkelas IIA. Berdasarkan INWQS (1998), nilai pH yang melebihi julat 6 hingga 9, menunjukkan pencemaran air telah berlaku. Namun menurut APHA (1992), kebiasaannya nilai pH air yang neutral ialah diantara julat 4 hingga 9. Nilai ini adalah merupakan nilai biasa yang menunjukkan kehadiran ion bikarbonat dan karbonat dalam keadaan alkali dan

logam alkali bumi. Nilai pH air semulajadi dipengaruhi oleh bahan organik tanah seperti asid humik, asid tanik, asid uronik dan asid mineral hasil aktiviti tanah (Mokhtar *et al*.,2003)

Konduktiviti
Analisis statistik ANOVA dua hala menunjukkan tiada berbezaan yang bererti (p > 0.10) diantara keadaan hari hujan-kering dengan P=0.339. Tiada perbezaan yang bererti (p > 0.10) antara stesen dengan P=0.712. Julat konduktiviti berada dalam julat 168.33 ± 13.61 µS/cm hingga 207.67 ± 8.14 µS/cm. Menurut Chapman (1992), konduktiviti air permukaan biasanya berada dalam julat 10 µS/cm hingga 1000 µS/cm, tetapi mungkin melebihi nilai julat ini terutamanya dalam air yang tercemar atau sistem saliran yang menerima air larian permukaan. Konduktiviti mengukur bahan bukan organik terlarut yang terion membentuk elektrolit. Konduktiviti dan jumlah pepejal terampai adalah berkadaran terus antara satu sama lain (Mokhtar *et al*., 2003)

Jadual 2 : Nilai purata dan sisihan piawai bagi setiap parameter kajian pada
pensampelan hari kering (1/9/04, 6/9/04, 14/9/04)

Parameter	STESEN				
	1	2	3	4	5
Suhu (^{0}C)	28.00 ± 0.01	29.66 ± 0.67	28.22 ± 0.17	29.91 ± 0.56	30.62 ± 0.30
pH	6.06 ± 0.07	6.64 ± 0.18	6.42 ± 0.18	6.57 ± 0.15	6.84 ± 0.82
Konduktiviti (µS/cm)	205.00 ± 6.56	207.67 ± 0.18	204.00 ± 11.27	173.67 ± 18.50	175.00 ± 19.98
Kekeruhan (NTU)	5.37 ± 0.64	12.70 ± 0.78	7.84 ± 4.46	9.79 ± 1.05	9.78 ± 2.10
TSS (mg/L)	5.83 ± 1.61	6.50 ± 3.12	7.00 ± 5.77	5.67 ± 0.58	5.33 ± 2.57
DO (mg/L)	7.20 ± 0.73	7.58 ± 1.42	5.80 ± 0.65	8.09 ± 1.01	8.53 ± 0.80
DO (%)	92.80 ± 8.36	99.20 ± 20.42	73.47 ± 8.73	105.50 ± 14.08	112.97 ± 11.54
NH_3-N (mg/L)	0.25 ± 0.07	0.21 ± 0.15	0.08 ± 0.03	1.36 ± 2.21	0.44 ± 0.41
BOD (mg/L)	0.92 ± 0.45	2.21 ± 0.92	2.64 ± 2.17	1.50 ± 0.84	0.49 ± 0.37
COD (mg/L)	61.33 ± 8.33	57.33 ± 16.17	62.67 ± 12.86	56.00 ± 27.71	60.00 ± 8.00
Pb (mg/L)	0.36 ± 0.12	0.32 ± 0.04	0.32 ± 0.06	0.40 ± 0.08	0.36 ± 0.10
Cd (mg/L)	0.09 ± 0.02	0.11 ± 0.04	0.11 ± 0.04	0.10 ± 0.03	0.11 ± 0.03

Jadual 3: Nilai purata dan sisihan piawaian bagin setiap parameter kajian pada pensampelan hari hujan
(24/8/04, 21/9/04, 25/11/04)

Parameter	Stesen				
	1	2	3	4	5
Suhu (^{0}C)	28.30 ± 1.42	28.97 ± 2.46	28.08 ± 0.76	29.42 ± 1.57	30.84 ± 1.57
pH	7.05 ± 1.71	7.30 ± 1.77	7.06 ± 1.97	6.96 ± 1.63	7.57 ± 1.61
Konduktiviti (µS/cm)	168.33 ± 13.61	200.00 ± 39.36	175.33 ± 86.29	174.67 ± 23.67	189.33 ± 51.87
Kekeruhan (NTU)	26.10 ± 32.22	192.27±287.48	12.19 ± 14.56	29.53 ± 17.39	28.83 ± 19.72
TSS (mg/L)	20.17 ± 17.02	69.00 ± 92.15	20.83 ± 15.54	18.50 ± 4.77	18.00 ± 12.50
DO (mg/L)	6.82 ± 1.35	6.00 ± 0.92	5.47 ± 1.16	7.20 ± 1.49	7.70 ± 1.45
DO (%)	87.67 ± 16.40	78.70 ± 12.14	70.10 ± 14.22	94.17 ± 21.25	103.90 ± 20.36
NH_3-N (mg/L)	0.49 ± 0.37	1.54 ± 0.85	0.36 ± 0.28	0.41 ± 0.27	0.42 ± 0.28
BOD (mg/L)	0.72 ± 0.72	3.48 ± 2.03	2.69 ± 1.75	2.33 ± 1.42	0.77 ± 0.32
COD (mg/L)	59.73 ± 30.38	59.88 ± 52.90	51.09 ± 36.48	42.87 ± 39.31	64.37 ± 34.27
Pb (mg/L)	0.19 ± 0.11	0.15 ± 0.14	0.14 ± 0.12	0.12 ± 0.10	0.17 ± 0.20
Cd (mg/L)	0.29 ± 0.31	0.09 ± 0.04	0.09 ± 0.02	0.10 ± 0.03	0.10 ± 0.01

Kekeruhan
Analisis statistik ANOVA dua hala menunjukkan tiada perbezaan yang bererti (p > 0.10) diantara keadaan hari hujan-kering dengan P=0.163. Manakala, tiada perbezaan yang bererti (p > 0.10) antara stesen dengan P=0.399. Nilai kekeruhan berada dalam julat 12.19 ± 14.56 NTU hingga 192.27 ± 287.48 NTU. Semua stesen berada pada subkelas I kecuali S2 yang melampaui paras maksimum 50 NTU yang disarankan oleh subkelas IIB. Stesen S2

adalah paling keruh (192.27 ± 287.48 NTU) pada hari hujan kerana merupakan perangkap lumpur yang memerangkap sedimen dari projek pembinaan Kolej Kausar dan Kompleks FTSM.

TSS
Analisis statistik ANOVA dua hala menunjukkan terdapat perbezaan yang bererti ($p < 0.05$) diantara keadaan hari hujan-kering dengan P=0.049. Manakala, tiada perbezaan yang bererti antara stesen dengan P=0.527. TSS adalah lebih tinggi pada hari hujan kerana air larian permukaan sewaktu hujan mempunyai daya hakisan yang kuat dan mengakibatkan kadar hakisan tanah yang kuat dan menyumbangkan kepada peningkatan pepejal terampai di kawasan tanah rata terutamanya yang terdedah akibat proses pembangunan. Nilai TSS berada dalam julat 5.33 ± 2.57mg/L hingga 69.00 ± 92.15 mg/L. Pada hari kering, semua stesen terletak pada subkelas I. Manakala pada hari hujan, semua stesen dikategorikan sebagai subkelas I kecuali S2 berada pada subkelas III. Stesen S2 mempunyai TSS yang paling tinggi (69.00 ± 92.15 mg/L) pada hari hujan kerana merupakan perangkap lumpur yang memerangkap sedimen dari projek pembinaan Kolej Kausar dan Kompleks FTSM. Pada keadaan normal, jumlah berat TSS dalam tasik adalah 163.78 ± 18.19 kg. Anggaran jumlah pepejal terampai yang mengalir masuk ke Sungai Langat adalah 27.81 ± 9.29 kg setiap hari.

Oksigen Terlarut
Analisis statistik ANOVA dua hala menunjukkan tiada perbezaan yang bererti ($p > 0.05$) diantara keadaan hari hujan-kering dengan P=0.068. Manakala, terdapat perbezaan yang bererti antara stesen dengan P=0.014. DO berada dalam julat 5.47 ± 1.16 mg/L hingga 8.53 ± 0.80 mg/L. Pada hari kering, semua stesen berada pada subkelas I kecuali S3 berada pada subkelas IIA. Pada hari hujan, S4 dan S5 berada pada subkelas I manakala S1, S2, S3 berada pada subkelas IIA. S3 mempunyai nilai DO yang paling rendah (5.47 ± 1.16 kg) kerana kehadiran bahan organik yang tinggi di S3. Bakteria menggunakan oksigen terlarut semasa proses penguraian bahan organik tersebut. Pada keadaan normal, dianggarkan 200.88 ± 28.25 kg oksigen terlarut berada dalam air tasik.

Nitrogen Ammonia
Analisis statistik ANOVA dua hala menunjukkan tiada perbezaan yang bererti ($p > 0.10$) diantara keadaan hari hujan-kering dengan P=0.545. Tiada perbezaan yang bererti ($p > 0.10$) diantara stesen dengan P=0.476. Nilai nitrogen ammonia berada dalam julat 0.08 ± 0.03 mg/L hingga 1.54 ± 0.85 mg/L. Pada hari kering, Stesen S3 terletak dalam subkelas I; S2 dan S3 berada pada subkelas IIA, manakala S5 terletak pada subkelas III dan S4 terletak pada subkelas IV. Pada hari hujan, Stesen S1, S3, S4 dan S5 dikategorikan sebagai subkelas III dan S2 terletak pada subkelas IV. Ini mungkin disebabkan air kumbahan domestik yang dilepaskan ke dalam Tasik Kejuruteraan dan pembuangan air sisa makanan dari kantin. Menurut Jabatan Pengurusan Pembangunan (JPP), semua air buangan sama ada dalam makmal dan tandas disalirkan oleh paip pembentungan dalam sistem pembentungan ke kolam pengoksidaan kumbahan UKM untuk proses perawatan sebelum ia dialirkan ke Sungai Langat, namun dijangkakan terdapat juga luahan air buangan yang disalirkan ke dalam longkang yang mengalir ke dalam tasik kajian. Pada keadaan normal, dianggarkan 12.65 ± 13.90 kg nitrogen ammonia berada dalam tasik. Anggaran jumlah nitrogen ammonia yang mengalir masuk ke Sungai Langat adalah 2.12 ± 0.71 kg setiap hari.

Permintaan Oksigen Biokimia (BOD)
Analisis statistik ANOVA dua hala menunjukkan tiada perbezaan yang bererti ($p > 0.10$) diantara keadaan hari hujan-kering dengan P=0.354; manakala, terdapat perbezaan yang bererti antara stesen dengan P=0.018. BOD berada dalam julat 0.49 ± 0.37 mg/L hingga 3.48 ± 2.03 mg/L. Pada hari kering, S1 dan S5 terletak pada subkelas I manakala S2, S3 dan S4 berada pada subkelas IIA. Pada hari hujan, S1 dan S5 terletak pada subkelas I, S3 dan S4 berada pada subkelas IIA, manakala S2 berada pada subkelas III. Stesen 2 mempunyai nilai BOD yang paling tinggi, iaitu 3.48 ± 2.03 mg/L sewaktu hari hujan. Ini mungkin kerana stesen ini terletak berdekatan dengan bengkel fakulti kejuruteraan. Kawasan bengkel ini mungkin menyebabkan saliran air buangan berjaya masuk ke dalam longkang pada hari hujan yang mengandungi bahan berorganik tinggi yang boleh meningkatkan paras kepekatan BOD dalam sistem air. Pada keadaan normal, jumlah berat BOD yang dianggarkan hadir dalam tasik adalah 41.90 ± 23.95 kg. Anggaran BOD yang mengalir masuk ke Sungai Langat adalah 7.01 ± 2.34 kg setiap hari.

Permintaan Oksigen Kimia (COD)
Analisis statistik ANOVA dua hala menunjukkan tiada perbezaan yang bererti ($p > 0.10$) diantara keadaan hari hujan-kering dengan P=0.729. Tiada perbezaan yang bererti ($p > 0.10$) antara stesen dengan P=0.955. Secara keseluruhan, nilai COD adalah tinggi, iaitu dalam kategori subkelas IV (51 mg/L hingga 100 mg/L) berdasarkan

INQWS disebabkan kehadiran bahan organik dan bahan bukan organik yang banyak dalam tasik mungkin disebabkan air larian sisa makanan dari kantin dan air sisa buangan dari makmal dan bengkel fakulti. Menurut JPP, semua air buangan sama ada air dalam makmal dan tandas disalirkan oleh paip pembentungan dalam sistem pembentungan ke kolam pengoksidaan kumbahan UKM untuk proses perawatan sebelum ia dialirkan ke Sungai Langat, namun terdapat kemungkinan air sisa ini juga mengalir dalam saluran longkang dan mengikut air larian sewaktu hari hujan. Nilai COD yang tinggi menunjukkan pembuangan air sisa yang mungkin dialirkan secara langsung atau tidak langsung dari kawasan bangunan fakulti. Pada keadaan normal, dianggarkan air tasik mengandungi jumlah berat COD sebanyak 1605.58 ± 74.68 kg. Anggaran COD yang mengalir masuk ke Sungai Langat adalah 268.90 ± 89.78 kg setiap hari. Nilai ini adalah adalah amat tinggi dan memberikan beban terhadap kualiti air Sungai Langat yang semakin tercemar.

Plumbum
Analisis statistik ANOVA dua hala menunjukkan terdapat perbezaan yang sangat bererti ($p < 0.001$) diantara keadaan hari hujan-kering dengan P=0.001. Julat pB ialah 0.32 ± 0.06 mg/L hingga 0.40 ± 0.08 mg/L sewaktu hari kering manakala julatnya pada hari hujan adalah 0.12 ± 0.10 mg/L hindda 0.19 ± 0.11 mg/L. Nilai pB adalah rendah semasa hujan disebabkan proses pencairan air tasik. Tiada perbezaan yang bererti antara stesen dengan P=0.345 hasil ujian ANOVA. Secara keseluruhan, nilai Pb adalah amat tinggi dan melebihi had piawaian JAS, iaitu 0.05 mg/L. Kebanyakan plumbum yang dibebaskan ke atmosfera berpunca daripada bahan api kenderaan bermotor yang mengandungi bahan kimia antiketuk, tetraetil plumbum, $(C \ H \ )\ Pb$. Plumbum yang termendap di tempat letak kereta dan jalanraya boleh dibawa oleh air larian permukaan yang mengalir ke dalam tasik. Menurut Camp dan Meserve (1974), berdasarkan pencemaran yang diakibatkan daripada kawasan bandar, terdapat peningkatan masalah pencemaran logam berat semasa berlakunya air larian permukaan di kawasan bandar. Menurut Spliethoff dan Hemond (1996), kewujudan plumbum bukan sahaja boleh dicerap di kawasan berkepadatan dengan kenderaan, tetapi juga dalam atmosfera yang turun dengan air hujan dan diangkut ke sedimen akuatik dengan berkesan berbanding dari permukaan kawasan pertanian. Pada keadaan normal, dianggarkan terdapat kandungan Pb sebanyak 9.50 ± 0.90 kg. Anggaran jumlah Pb yang mengalir masuk ke Sungai Langat adalah 1.59 ± 0.53 kg setiap hari. Nilai ini adalah amat tinggi kerana logam berat ini amat toksik kepada manusia walaupun dalam kuantiti kecil.

Kadmium
Analisis statistik ANOVA dua hala menunjukkan tiada perbezaan yang bererti ($p > 0.10$) di antara keadaan hari hujan-kering dengan P=0.404. TIada perbezaan yang bererti ($p > .010$) antara stesen dengan P=0.931. Julat Cd ialah 0.09 ± 0.02 mg/L hingga 0.11 ± 0.04 mg/L. Nilai kepekatan Cd adalah amat tinggi dan melebihi had piawai JAS, iaitu 0.01 mg/L. Ini mungkin disebabkan kehadiran Cd dalam debu dan termendap di tasik. Kewujudan Cd dalam atmosfera biasanya berpunca dari pembakaran bahan api dalam keadaan bermotor, kegiatan perindustrian dan aktiviti pembinaan yang amat pesat di sekitar lembangan. Pada keadaan normal, kandungan Cd dalam tasik dianggarkan 2.81 ± 0.24 kg. Anggaran jumlah Cd yang mengalir masuk ke Sungai Langat adalah 0.47 ± 0.15 kg setiap hari. Nilai ini adalah tinggi dan membahayakan hidupan jika ia terkumpul dalam tisu badan.

Indeks Kualiti Air (IKA)
Jadual 4 menunjukkan nilai IKA secara purata bagi hari hujan dan hari kering di stesen kajian ini.

Jadual 4 : Nilai IKA secara purata di stesen kajian ini

Stesen	IKA	Pengelasan	Status
1.	81.32 ± 3.33	(II)	Baik
2.	72.85 ± 2.45	(III)	Sedikit tercemar
3.	81.22 ± 0.02	(II)	Baik
4.	81.99 ± 3.24	(II)	Baik
5.	82.50 ± 2.62	(II)	Baik

Semua stesen pensampelan berada pada Kelas II, iaitu mempunyai kualiti air yang baik kecuali stesen S2 dikategorikan sebagai Kelas III, iaitu sedikit tercemar dan memerlukan rawatan ekstensif. Secara keseluruhannya, Tasik Kejuruteraan dikategorikan sebagai Kelas II-III, iaitu merupakan bekalan air yang memerlukan rawatan konvensional dan membenarkan kegunaannya untuk aktiviti rekreasi yang melibatkan

sentuhan. Hujan mempengaruhi kualiti air Tasik Kejuruteraan, terutamanya pada musim tengkujuh, yang menyebabkan nilai bagi parameter TSS meningkat dengan banyak dan menyebabkan air tasik kelihatan keruh dan berwarna coklat.

Cadangan

Berikut merupakan cadangan tentang langkah-langkah yang perlu diambil untuk menuju ke arah IWRM dalam kampus bagi menghasilkan suasana ekosistem sihat dan harmoni selaras dengan tema UKM 'Universiti dalam Taman'. Di peringkat kampus, Pembuatan Keputusan Kolaboratif atau 'Collaborative Decision Making' atau CDM (Mazlin *et al*. 2004b) sangat digalakkan sebagai inisiatif bersama pelbagai pihak berkepentingan termasuk pihak pengurusan tertinggi universiti yang terdiri daripada Naib Canselor, pihak pengurusan professional dan eksekutif seperti jurutera dan peringkat lain merangkumi warga universiti yang terdiri daripada pengajar, pelajar dan kakitangan sokongan serta pengguna lain seperti kontraktor projek bertujuan untuk memperbaiki sistem pengurusan sumber air yang sedia ada. CDM menggalakkan proses perkongsian dan pertukaran maklumat di antara pelbagai pihak, dan secara tidak langsung turut memperbaiki alat sokongan membuat keputusan. Orang ramai yang memasuki kampus seperti ibu bapa pelajar dan orang yang menggunakan kemudahan universiti juga harus didedahkan tentang konsep CDM dan IWRM.

Pihak pengurusan universiti bertanggungjawab membuat dasar dan peraturan, menetapkan mesyuarat bersama eksekutif dan menggalakkan proses berkongsi data dan maklumat, serta cara menangani isu bersama. Jurutera atau saintis berperanan dalam pemonitoran kualiti air.Pengajar perlu menerapkan konsep IWRM kepada setiap pelajar. Kakitangan sokongan mesti juga terlibat membantu mengawal pelepasan sisa secara tidak bertanggungjawab. Pelajar harus menjaga kebersihan tasik seperti tidak membuang sampah ke dalam tasik manakala kontraktor bertanggungjawab dalam pengaliran air buangan berkelodak dan mengandungi pelbagai bahan buangan lain serta juga mereka mengambil inisiatif untuk menjamin kebersihan air tasik.

Selain itu, dana kewangan dan sumber manusia yang berpatutan juga perlu disediakan oleh pihak pengurusan universiti, bermula dengan menerapkan konsep IWRM dan CDM kepada golongan staf sedia ada. Kakitangan di Jabatan Pengurusan Pembangunan khususnya perlu didedahkan dengan konsep tersebut agar dapat mengurus tasik ini dengan baik. Daya tampung bagi bahan pencemar dalam tasik harus dinilai oleh pihak jurutera. Jenis spesies hidupan yang ada di dalam tasik perlu diketahui melalui kajian masa depan. Pangkalan data harus dibina dan dikongsi bersama oleh semua pihak berkepentingan dalam universiti dan masyarakat yang berminat.

Kesimpulan

Sistem saliran air ke Tasik Kejuruteraan telah dikaji dan menunjukkan bahawa parameter kekeruhan di S2 melampaui paras maksimum 50 NTU yang disarankan oleh subkelas IIB bagi INWQS. Jumlah TSS di S2 tergolong dalam subkelas III pada hari hujan. Parameter NH -N di S5 dan S4 telah melebihi paras maksimum subkelas IIB pada hari kering manakala semua stesen telah melebihi paras maksimum subkelas IIB pada hari hujan. Kandungan BOD di S2 tergolong dalam subkelas III pada hari hujan. NIlai COD adalah tinggi, iaitu dalam kategori subkelas IV. Nilai kepekatan Pb dan Cd adalah amat tinggi dan masing-masing melebihi had piawaian JAS, iaitu 0.05 mg/L dan 0.01 mg/L. Tasik Kejuruteraan dikategorikan dalam Kelas II-III menurut pengkelasan INWQS. Analisis ANOVA dan kolerasi telah dilakukan. Beberapa langkah untuk memperbaiki kualiti air dan keadaan saliran tasik serta sistem sumber air di kampus telah juga dicadangkan.

Rujukan

1. AHPA.AWWA.WEF. 1998. *Standard Methods for the Examination of Water and Wastewater* Ed.20, American Public Health Association, Washington.
2. Bruce Mitcell, 1997. *Resource and Environmental Management*. England. Wesley Longman Limited.
3. Camp, T.R. & Meserve, R.L. 1974. *Water and its impurities*. Ed. Ke 2. Stroudsburd: Dowden Hutchinson & Ross, Inc.
4. DID. 2000. *Urban Stormwater Management Manual for Malaysia (Manual Saliran Mesra Alam Malaysia).* Vol 5: Runoff Estimation. KL.
5. DID. 2000. *Urban Stormwater Management Manual for Malaysia (Manual Saliran Mesra Alam Malaysia).* Vol 8: Retention. KL.
6. Global Water Partnership, 2000b. *Integrated water resources management*. TAC Background papers, Nomer 4, Stockholm, Sweden.
7. Mazlin Mokhtar, Mohd. Talib Latif, Lee Yook Heng. 2003. Kimia Air. KL. Utusan Publications & Distributors Sdn Bhd.
8. Mazlin b. Mokhtar, Shaharudin Idrus, Sarah Aziz. 2004. Kesihatan Ekosistem Lembangan Langat. *Prosiding Simposium Penyelidikan Ekosistem Lembangan Langat 2003*, Penerbit Lestari, UKM.

9. Mazlin b. Mokhtar, Rahmah Elfithri and Abdul Hadi Harman Shah. 2004b. "Collaborative Decision Making as a Best Practice in Integrated Water Resources Management: A Case Study on Langat Basin, Malaysia". Proceedings (Technical Papers), First Southeast Asia Water Forum, 17-21 November 2003, Chiang Mai, Thailand, Volume 2: pp. 333-354. ISBN 974-241-776-8.

10. *World Water Forum 2003* (atas talian) http://www.water-forum3.com (21 Oktober 2004).

11. Spliethoff, H.M. & Hemond, H.F. 1996. History of toxic dischange to surface waters of the Aberjona Watershed. *Journal of Environmental Science & Technology* 30 (1): 121-127.

SQUARE WAVE CATHODIC STRIPPING VOLTAMMETRIC TECHNIQUE FOR DETERMINATION OF AFLATOXIN B1 IN GROUND NUT SAMPLE

Mohamad Hadzri Yaacob[1], Abdull Rahim Hj. Mohd. Yusoff[2] and Rahmalan Ahamad[2]

1*School of Health Sciences, USM, 16150 Kubang Krian, Kelantan, Malaysia*
2*Chemistry Dept., Faculty of Sciences, UTM, 81310 Skudai, Johor, Malaysia*

Abstract

An electroanalytical method has been developed for the detection and determination of 2,3,6a,9a-tetrahydro-4-methoxycyclo penta[c] furo[3',2':4,5] furo [2,3-*h*][l] benzopyran-1,11-dione (aflatoxin B1, AFB1) by a square wave cathodic stripping voltammetric (SWSV) technique on a hanging mercury drop electrode (HMDE) in aqueous solution with Britton-Robinson Buffer (BRB) at pH 9.0 as the supporting electrolyte. Effect of instrumental parameters such as accumulation potential (E_{acc}), accumulation time (t_{acc}), scan rate (v), square wave frequency, step potential and pulse amplitude were examined. The best condition were found to be E_{acc} of -0.8 V, t_{acc} of 100 s, v of 3750 mVs^{-1}, frequency of 125 Hz, voltage step of 30 mV and pulse amplitude of 50 mV. Calibration curve was linear in the range of 0.01 to 0.15 uM with a detection limit of 0.125 x 10^{-8} M. Relative standard deviation for a replicate measurement of AFB1 (n = 5) with a concentration of 0.01 μM was 0.83% with a peak potential of -1.30 V (against Ag/AgCl). The recovery values obtained in spiked ground nut elute sample were 94.00 ± 0.67 % for 3.0 ppb, 91.22 ± 1.56 % for 9 ppb and 92.56 ± 2.00 % for 15.0 ppb of AFB1. The method was applied for the determination of the AFB1 in ground nut samples after extraction and clean-up steps. The results were compared with that obtained by high performance liquid chromatography (HPLC) technique.

Abstrak

Satu kaedah elektroanalisis telah dibangunkan untuk mengesan dan menentukan 2,3,6a,9a-tetrahydro-4-methoxycyclo penta[c] furo[3',2':4,5] furo [2,3-*h*][l] benzopyran-1,11-dione (aflatoxin B1, AFB1) menggunakan teknik voltammetri perlucutan katodik denyut pembeza di atas elektrod titisan raksa tergantung (HMDE) di dalam larutan akuas dengan larutan penimbal Britton-Robinson (BRB) pada pH 9.0 bertindak sebagai larutan penyokong. Kesan parameter peralatan seperti keupayaan pengumpulan (E_{acc}), masa pengumpulan (t_{acc}), kadar imbasan (v), frekuensi gelombang bersegi, kenaikan keupayaan dan amplitud denyut telah dikaji. Keadaan terbaik yang diperolehi adalah E_{acc}; -0.8 V, t_{acc}; 100 s, v; 3750 mV/s, frekuensi; 125 Hz, kenaikan keupayaan; 30 mV dan amplitud denyut; 50 mV. Keluk kalibrasi adalah linear pada julat di antara 0.01 ke 0.15 μM dengan had pengesan pada 0.125 x 10^{-8} M. Sisihan piawai relatif untuk 5 kali pengukuran AFB1 dengan kepekatan 0.01uM ialah 0.83 %. Nilai perolehan semula di dalam larutan elusi sampel kacang yang disuntik dengan 3.0 ppb, 9 ppb dan 15.0 ppb AFB1 adalah 94.00 ± 0.67 %, 91.22 ± 1.56 % dan 92.56 ± 2.00 % masing-masingnya. Kaedah ini telah digunakan untuk menentukan kandungan AFB1 di dalam sampel kacang tanah selepas proses pengekstraksian dan pembersihan dijalankan. Keputusan yang diperolehi telah dibanding dengan keputusan dari kaedah kromatografi cecair berprestasi tinggi.

Introduction

Aflatoxins (AF), the mycotoxin produced mainly by *Aspergillus flavus* and *parasiticus* display strong carcinogenicity [1]. They are dangerous food contaminants and represent a worldwide threat to public health. AFB1, B2, G1 and G2 and their metabolites M1 and M2 are the most common, and of these, AFB1 and AFG1 are observed most frequently in food [2]. Research has shown that AFB1 (Figure 1) exhibits the most toxic [3] with the order of toxicity AFB1 > AFG1 > AFB2 > AFG2. This indicates that the terminal furan moiety of AFB1 is a critical point for determining the degree of biological activity of this group of mycotoxins [4]. Many countries including Malaysia have stringent regulatory demands on the level of aflatoxins permitted in imported and traded commodities.
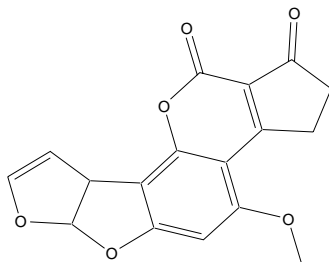
Figure 1: Chemical structure of AFB1

One of the foodstuffs with the most occurrence of AFB1 is ground nut. In Malaysia, the AFB1 level in peanut is regulated with maximum level that cannot be greater than 15 ppb [5]. Several analytical techniques for quantitative determination of the AFB1 in ground nut have been proposed, such as thin layer chromatograhpy [6], high performance liquid chromatography [7-9] and an enzyme-linked immunosorbent assay, ELISA [10], All these methods, however, require specialist equipment operated by skilled personnel and expensive instruments and high maintenance cost [11].

Due to all these reasons, a voltammetric technique which is fast, accurate and require low cost equipment [12,13] is proposed. A square wave cathodic stripping which is presented in this paper is one of the voltammetric technique that in particular, has a several advantages compared to other voltammetric technique such as high speed, increased analytical sensitivity and relative insensitivity to the presence of dissolved oxygen [14]. Previous experiment using cyclic voltammetric technique showed that AFB1 reduced at mercury electrode and the reaction is totally irreversible [15]. This work discusses the development of SWSV method for determination of AFB1 at trace levels and to determine this aflatoxin in ground nut samples.

Experiment

Apparatus
Square-wave voltammograms were obtained with Metrohm 693 VA Processor coupled with a Metrohm 694 VA stand. Three electrode system consisted of a hanging mercury drop electrode (HMDE) was used as the working electrode, Ag/AgCl/3 M KCl reference electrode and a platinum wire auxiliary electrode. A 20 ml capacity measuring cell was used for placing supporting electrolyte and sample analytes. All measurements were carried out at room temperature. All pH measurements were made with Cyberscan pH meter, calibrated with standard buffers at room temperature.

Reagents
AFB1 standard (1mg per bottle) was purchased from Sigma Co. and was used without further purification. Stock solution (10 ppm or 3.21×10^{-5} M) in benzene:acetonitrile (98:2) was prepared and stored in the dark at 14 ^{o}C. The diluted solution was prepared daily by using certain volume of stock solution, degassed by nitrogen until dryness and redissolved in Britton-Robinson buffer (BRB) solution at pH 9.0. Britton-Robinson buffer solutions (prepared from a stock solution 0.04 M phosphoric (Merck), boric (Merck) and acetic (Merck) acids; and by adding sodium hydroxide (Merck) 1.0 M up to pH of 9.0). All solutions were prepared in double distilled dionised water ($\sim 18M \Omega$ cm). All chemicals were of analytical grade reagents.

Procedure
For voltammetric experiments, 10 ml of Britton-Robinson buffer solution with pH 9.0 was placed in a voltammetric cell, through which a nitrogen stream was passed for 600 s before recording the voltammogram. The selected E_{acc} = - 800 mV was applied during the t_{acc} = 100 s while the solution was kept under stirring. After the accumulation time had elapsed, stirring was stopped and the selected accumulation potential was kept on mercury drop for a rest time (t_r = 10 s), after which a potential scan was performed between -1.00 as initial potential (E_i) and completed at -1.400 V as final potential (E_f) by SWSV technique.

Procedure for the determination in ground nut samples
AFB1 was extracted according to the standard procedure developed by Chemistry Department, Penang Branch, Ministry Of Science, Technology and Innovation, Malaysia [16]. 1ml of the final solution from extraction and

clean-up steps in chloroform was pipetted into an amber bottle, degassed with nitrogen and redissolved in 1ml of BRB solution. 200 μl of this solution was spiked into 10 ml supporting electrolyte in volumetric cell. The general procedure was then applied and voltammogram of sample was recorded. This experiment was repeated with standard additions of 10 ppb of AFB1.

Results and Discussion

Using previous differential pulse stripping voltammetry (DPCSV) optimum parameters [17], SWSV was run to determine 0.1 μM AFB1 in BRB pH 9.0. It gave a single reduction signal with peak height (I_p) of 250 nA at peak potential (E_p) of -1.26 V (against Ag/AgCl). The SWS voltammograms showed improved I_p compared to that obtained bt DPCSV where the I_p was increased almost 4 times as shown in Figure 2.

Cyclic voltammogram of AFB1 in BRB pH 9.0, shown in Figure 3 produced only a cathodic peak that indicates the non-reversibility of the electrode process [18].
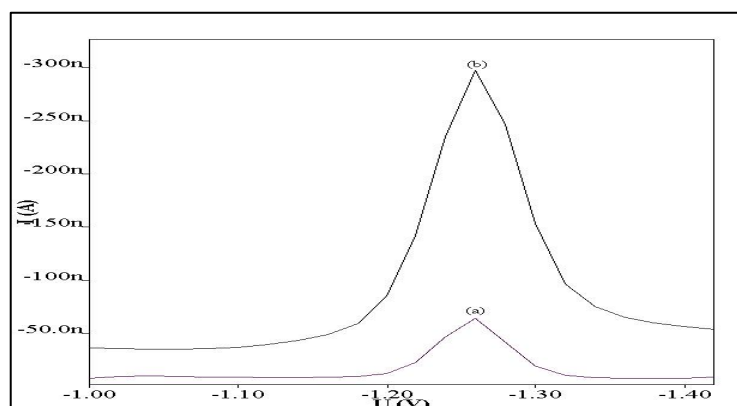
Figure 2: Voltammograms of 0.1 uM AFB1 obtained by (a) DPCSV and (b) SWSV techniques. Experimental condition; for DPCSV: E_i = -1.0 V, E_f = -1.4 V, E_{acc} = -0.6 V, t_{acc} = 80 s, υ = 50 mV/s and pulse amplitude = 80 mV and for SWSV: E_i = -1.0 V, E_f = -1.4 V, E_{acc} = -0.6 V, t_{acc} = 80 s, frequency = 50 Hz, voltage step = 0.02, amplitude = 50 mV and υ = 1000 mV/s.
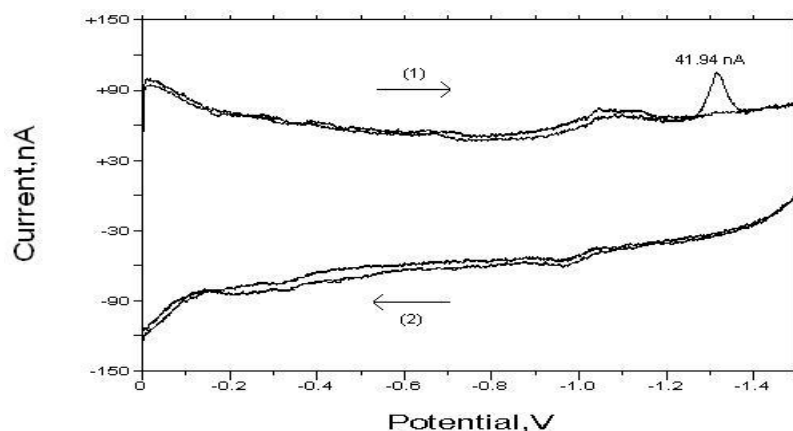
Figure 3: Cyclic voltammogram of AFB1 in BRB pH 9.0. Experimental conditions: E_i = 0, E_{low} = -1.5 V, E_{high} = 0 and scan rate = 200 mV/s.

The effect of the pH of the BRB on the stripping was studied in a pH range of 6 – 13 (Fig. 4). The I_p increased slowly with increasing pH up to 8.0 followed with a sharp increase for pH 8.0 to 9.0, then decreases at pH 10.0 and continuously decreasing at pH 10 – 13. Thus pH 9.0 was chosen for the analysis. This result is in agreement with that found by Smyth *et al.* (1979) when they performed polarographic study of AFB1 [19].
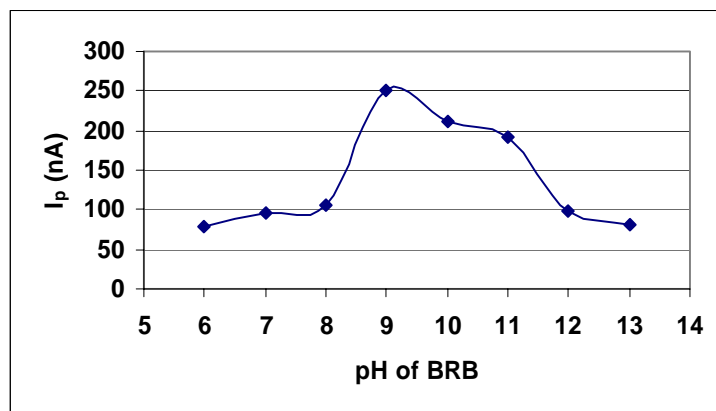
Figure 4: Influence of pH of BRB on the I_p of 0.10 μM AFB1 using SWSV technique.
The instrumental parameters are the same as in Figure 2.0.

Figure 5 shows a dependence of the E_p on pH. Shifting of the E_p towards the negative direction at higher pH implies that the reduction process takes up hydrogen ions [20]. A double bond in the aromatic ring conjugated with ketone group, in general, undergoes a reduction at mercury electrode. The suggested mechanism of this reaction in BRB pH 9.0 is illustrated in Figure 6 as reported by Smyth *et al.* (1979) [19].
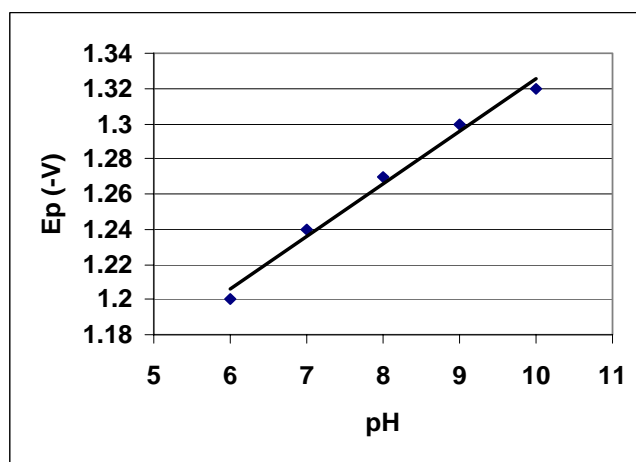
Figure 5: Relationship between E_p of AFB1 with pH of BRB
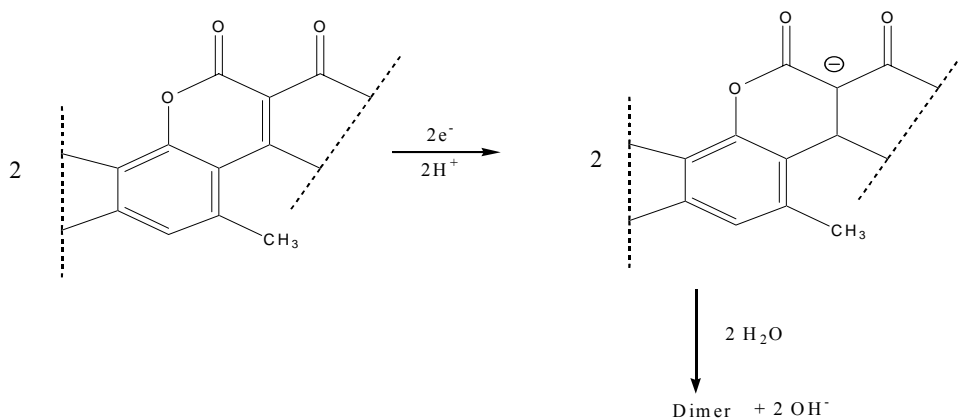
Figure 6: Mechanism for reduction of AFB1 at mercury electrode in BRB pH 9.0

Optimisation of condition for the stripping analysis

The voltammetric determination of analytes at trace levels normally involves very small current response. For that reason it is important to optimise all those parameters which may have an influence on the measured current. The effect of E_i , E_{acc} , t_{acc}, frequency, voltage step and amplitude were studied. Square-wave voltammetric technique was used with stirring. For this study, 1.0×10^{-7} M of AFB1 was spiked into the supporting electrolyte.

A study of the influence of E_i showing a peak height (I_p) was obtained for E_i = -1.0 V (Figure 7). The I_p was slowly decreased for E_i more negative than -1.0 V. This value was chosen for subsequent studies for further optimisation steps. The influence of E_{acc} to I_p of AFB1 was investigated where the E_{acc} was varied between 0 to -1.4 V. The maximum value of I_p obtained at -0.8 V (366 nA) is as shown in Figure 8. This value was selected for subsequent experiments.

The dependence of I_p on t_{acc} was studied. The effect of t_{acc} on the I_p was studied where t_{acc} was varied from 0 to 160 s. The result is shown in Figure 9 which reveals that the relationship is linear up to 100s (y = 3.8557x + 21.383 (n=6) with R^2 = 0.9936), then it increases rather slowly leveling off at about 140 s. At 160 s, the I_p decreases, which may be due to the electrode saturation [21]. Thus, 100 s was chosen as the optimum t_{acc} for the pre-concentration prior to stripping.
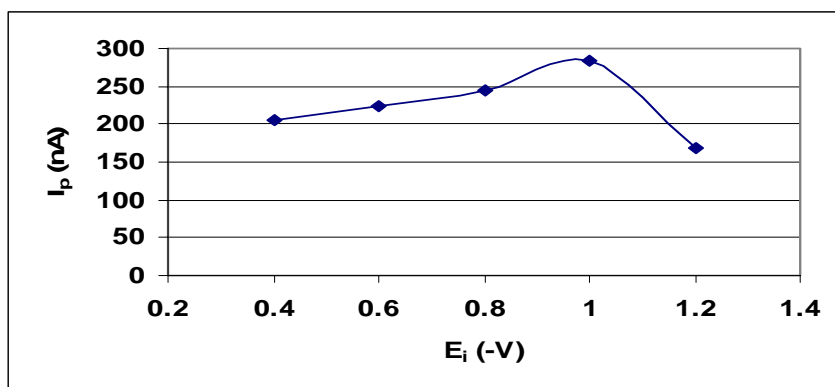
Figure 7: Effect of E_i on the I_p of 0.1 µM AFB1 in BRB pH 9.0
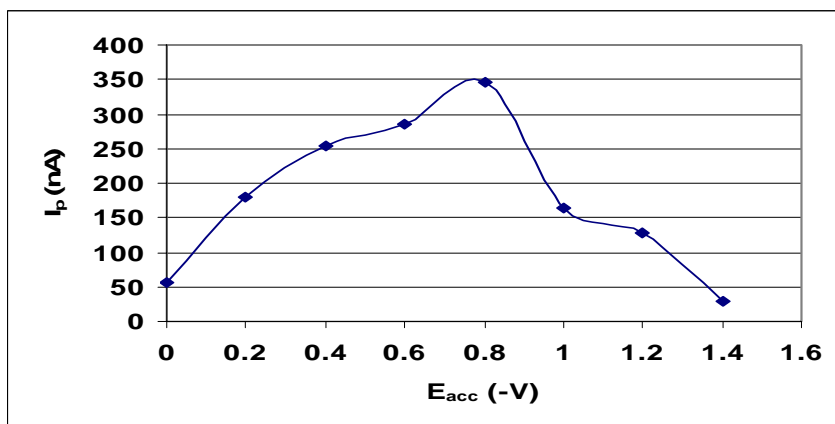
Figure 8: Effect of E_{acc} on the I_p of 0.1 µM AFB1 in BRB pH 9.0
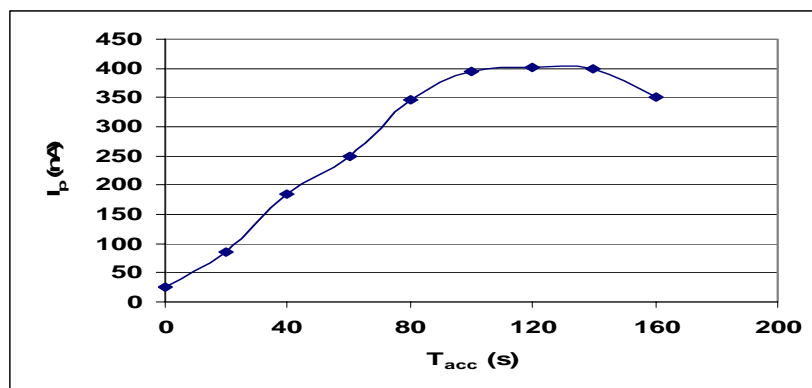
Figure 9: Effect of t_{acc} on the I_p of 0.1 µM AFB1 in BRB pH 9.0

For other instrumental condition such as square wave frequency, step potential and pulse amplitude were examined, varying one of them and maintaining the others constant. The variables were 25 to 125 Hz for the frequency, 0.01 to 0.04 for the voltage step and 25 to 100 mV for pulse amplitude. Generally, the I_p increases by increasing all of these instrumental parameters [22]. At higher potential values the peak width increases while at higher frequency values the current background increases. Finally, the condition selected were 125 Hz for frequency, 0.03 V for voltage step and 50 mV for pulse amplitude (Figs. 10 to 12). Under optimised parameters, I_p of AFB1 was 956 nA which is 16 times higher compared to that obtained by DPCSV. Figure 13 shows voltammograms of 0.1 µM AFB1 obtained by SWSV and DPCSV techniques.

Voltammetric determination of AFB1 and analytical characteristics of the method
Using the selected conditions already mentioned, a study was made on the relationship between I_p and concentration. A linear relationship was observed in the concentration range of 0.01 to 0.15 µM as shown in Figure 14. Limit of detection (LOD) was 0.389 ppb (0.125 x 10^{-8} M) which was determined by standard addition of low concentration of AFB1 until a sample response that is significantly different from blank was obtained[23]. Relative standard deviation (RSD) of the analytical signals at several measurement (n=5) of 0.10 µM was 0.83%.
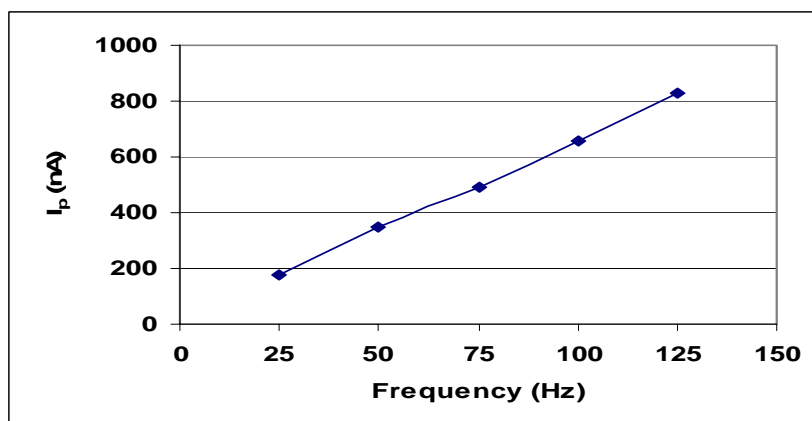
Figure 10: Dependence of the I_p of AFB1 on SWSV frequency
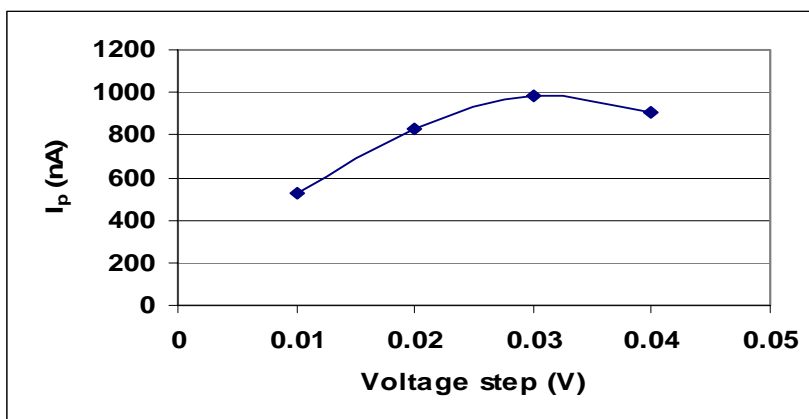
Figure 11: Dependence of the I_p of AFB1 on SWSV voltage step
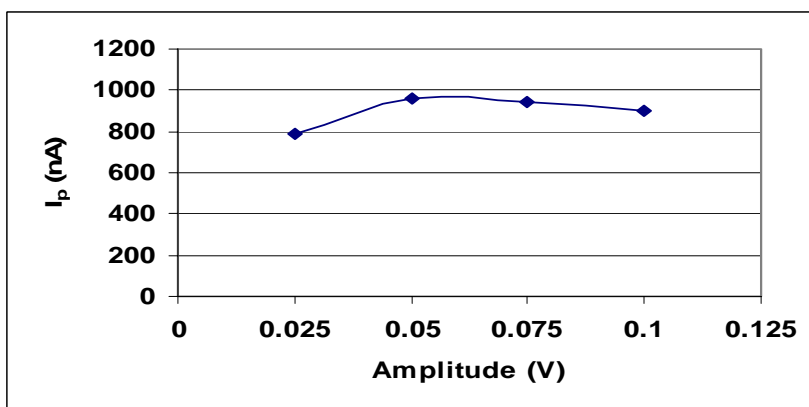
Figure 12: Dependence of the I_p of AFB1 on SWSV pulse amplitude
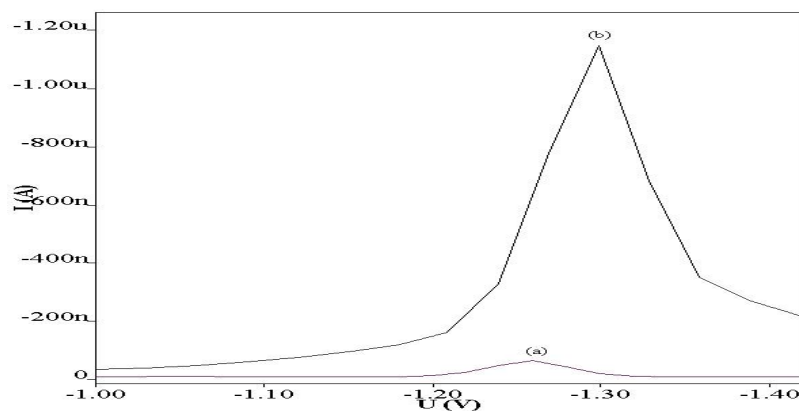
Figure 13: Voltammograms of AFB1 obtained by (a) DPCSV and (b) SWSV techniques in BRB pH 9.0.
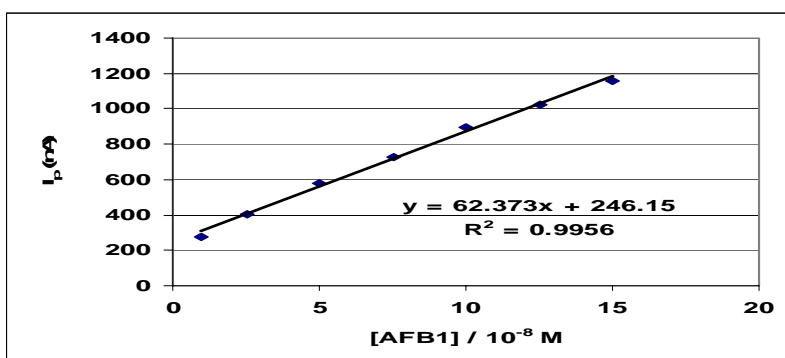
Figure 14   Calibration plot of AFB1 in BRB pH 9.0 obtained by SWSV technique.

Determination of AFB1 in ground nut samples

The proposed method was applied to the analysis of the AFB1 in ground nut samples. Recovery studies were performed by spiked with difference concentration levels of AFB1 standard into eluate of ground nut sample. In this case the concentrations used were 3 ppb (0.963×10^{-8} M), 9 ppb (2.889×10^{-8} M) and 15 ppb (4.815×10^{-8} M). The results of these studies are shown in Table 1. For the analysis of AFB1 in ground nut samples, the standard addition method was used in order to eliminate the matrix effects. Figure 15 shows voltammograms of real sample together with spiked AFB1 standard. Table 2 listed the content of AFB1 in 6 samples obtained by the proposed technique compared with that obtained by HPLC. The results show that there is no significant different of AFB1 content obtained by both techniques.

Table 1: Percent recovery of AFB1 spiked in real samples (n=3)

Amount added (ppb)	Amount found (ppb)	Recovery (%) n=3
3.00	2.82 ± 0.02	94.00 ± 0.67
9.00	8.21 ± 0.14	91.22 ± 1.56
15.00	13.88 ± 0.30	92.53 ± 2.00
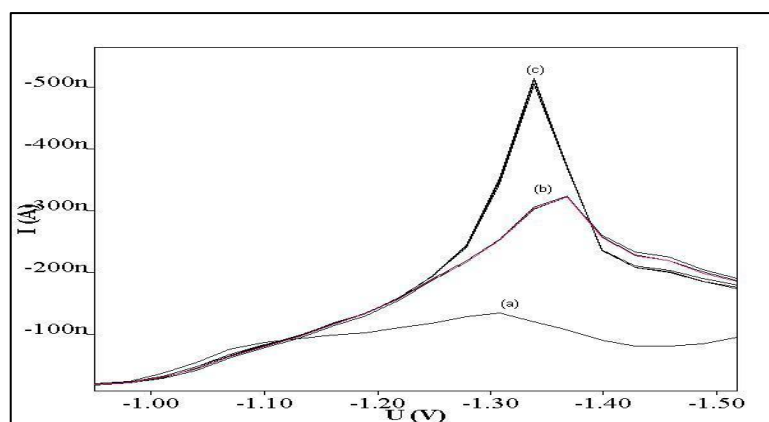
Figure 15: SWS voltammograms of real sample (b) and spiked AFB1 (c) obtained in BRB pH 9.0 as the supporting electrolyte (a)

139

Table 2: AFB1 content in ground nut samples by proposed technique compared with those obtained by HPLC.

No of sample	AFB1 content in real sample	
	By SWSV	By HPLC
1	ND	ND
2	ND	ND
3	ND	ND
4	9.21	8.25
5	13.92	14.34
6	36.00	36.00

Conclusion

A SWSV technique was successfully developed for the determination of AFB1 in ground nut as an alternative method for determination of AFB1 which is sensitive, accurate and fast technique. The results are not significantly different with that obtained by accepted technique used for routine analysis of AFB1.

Acknowledgement

References

1. Akiyama, H. Goda, Y. Tanaka, T and Toyoda, M. 2001. Determination of aflatoxins B1, B2, G1 and G2 in spices using a multifunctional column clean-up. *J. Chromatogr. A.* 932: 153-157.
2. Yoruglu, T, Oruc, H.H. and Tayar, M. 2005. Aflatoxin M1 levels in cheese samples from some provinces of Turkey. *Food Control* 16(10): 883-895.
3. World Health Organisation in: IARC Monograph on the evaluation of carcinogenic risk to human, WHO, Lyon, 1987.
4. Hall, A.J., Wild, C.P in: Eaton, D.L., Groopman, J.D. (Eds) 1994. The toxicology of aflatoxins: human health, veterinary and agricultural significance. Academic, New York.
5. Malaysian Food Act 1983. Act No 281, Reviewed 2002, Food Quality Control Dept, Ministry of Health, Malaysia.
6. Bicking,M.K.L., Kniseley, R.N and Svec, H.J. 1983. Coupled-Column for quantitating low levels of aflatoxins. *J. Assoc. Off. Anal. Chem.* 66: 905-908.
7. Beebe, B.M. 1978. Reverse phase high pressure liquid chromatographic determination of aflatoxins in foods." *J. Assoc. Off. Anal. Chem.* 81: 1347-1352.
8. Cepeda, A., Franco, C.M., Fente, C.A., Vazquez, B.I., Rodriguez, J.L., Prognon, P. and Mahuzier, G. 1996. Postcolumn excitation of aflatoxins using cyclodextrins in liquid chromatography for food analysis. *J. Off. Chrom. A* 721: 69-74.
9. Garner, R.C., Whattam, M.M., Taylor, P.J.L. and Stow, M.W 1993. Analysis of United Kingdom purchased spices for aflatoxins using immunoaffinity column clean up procedure followed up by high-performance liquid chromatographic analysis and post-column derivatization with pyridium bromide perbromide" *J. Chromatogr* 648: 485-490
10. Beaver, R.W., James, M.A. and Lin ,T.Y. 1991. ELISA-based screening test with liquid chromatography for the determination of aflatoxin in corn. *J. Assoc.Off. Anal. Chem* , 74: 827 – 829
11. Garden, S.R. and Strachan, N.J.C. 2001. Novel colorimetric immunoassay for the detection of aflatoxin B1 *Anal. Chim. Acta* 444: 187-191.
12. Braitina, Kh. Z., Malakhova, N.A. and Stojko, Y. 2000. Stripping voltammetry in environmental and food analysis" *Fresenius J Anal. Chem.* 368: 307-325
13. Skrzypek, S., Ciesielski, W., Sokolowski, A., Yilmaz, S. and Kazmierczak, D. 2005. Square wave adsorption stripping voltammetric determination of famotidine in urine. *Talanta*, 66(5): 1146-1151
14. Economou, A., Bolis, S.D., Efstathiou, C.E. and Volikakis, G.J 2002. A virtual electrochemical instrument for square wave voltammetry". *Anal. Chim. Act.* 467: 179-188.
15. Yaacob, M.H., Mohd Yusoff, A.R. and Ahmad, R. 2003. Cyclic voltammetry of AFB2 at the mercury electrode. Simposium Kimia Malaysia ke 13 (SKAM-13), 9 – 11th September 2003, Kucing, Sarawak, Malaysia.
16. Standard procedure for determination of aflatoxins 2000. Chemistry Dept. Penang Branch, Ministry of Science, Technology and Innovation (MOSTI), Malaysia – unpublished report.
17. Yaacob, M.H., Mohd Yusoff, A.R. and Ahamad, R. 2005. Determination of the aflatoxin B1 in ground nut by differential pulse cathodic stripping voltammetry technique. 2nd National Seminar On Chemistry, 14th April 2005, Universiti Sumatera Utara, Medan, Indonesia.

18.   Rodriguez, J., Berzas, J.J., Casteneda, G. and Rodriguez, N. 2005. Voltammetric determination of Imatinib (Gleevec) and its main metabolite using square-wave and adsorptive stripping square-wave techniques in urine samples. *Talanta*. 66: 202-209.

19.   Smyth, M. R., Lawellin, D. W. and Osteryoung, J.G. 1979. Polarographic study of Aflatoxin B1, B2, G1 and G2: Application of differential pulse polarography to the determination of Aflatoxin B1 in various foodstuffs" *Analyst.* 104: 73-78

20.   Sun, N., Mo, W-M., Shen, Z-L. and Hu, B-X. 2005. Adsorptive stripping voltammetric technique for the rapid determination of tobramycin on the hanging mercury electrode. *J Pharm. Biomed. Anal.* 38(2): 256-262

21.   Wang J. 1994. Analytical electrochemistry. VCH Publisher, USA.

22.   Komorsky-Lovric, S., Lovric, M. and Branica, M. 1992. Peak current-frequency relationship in adsorptive stripping square-wave voltammetry. *J Electroanal Chem.* 335(1-2):. 297-308.

23.   Barek, J. , Fogg, A. G., Muck, A. and Zima, J. 2001. Polarography and Voltammetry at Mercury Electrodes. *Critical Reviews In Analytical Chemistry*, 31: 291-309

PERLAKUAN ISOTOP URANIUM DI PERAIRAN PANTAI TIMUR SEMENANJUNG MALAYSIA: PENENTUAN NISBAH KEAKTIFAN ^{234}U/^{238}U

Zal U'yun Wan Mahmood, Zaharudin Ahmad, Abd. Kadir Ishak, Yii Mei Wo, Norfaizal Mohamed, Jalal Sharib @ Sarip, Kamarozaman Ishak, Azlina Shafie

Kumpulan Radiokimia dan Alam Sekitar Bahagian Teknologi Industri
Agensi Nuklear Malaysia,Bangi, 43000 Kajang, Malaysia

Kata kunci: Uranium; sekitaran marin; perairan Pantai Timur Semenanjung Malaysia; sedimen; air laut

Abstrak

Penentuan keaktifan isotop uranium dan taburannya di dalam sampel air laut dan sedimen permukaan di sepanjang pesisiran perairan Pantai Timur Semenanjung Malaysia telah dilakukan dengan menggunakan sistem pembilang spektrometri alfa. Persampelan kedua-dua air laut dan sedimen bagi kajian ini telah dijalankan pada bulan Ogos, 2003 di beberapa lokasi terpilih dan ia merupakan sebahagian daripada projek Pembangunan Data Asas Keradioaktifan Marin di Malaysia. Keputusan kajian menunjukkan taburan radionuklid uranium (^{234}U dan ^{238}U) dalam sampel air laut dan sedimen permukaan tidak konsisten di mana keaktifannya berubah-ubah mengikut lokasi persampelan. Secara umum, julat keaktifan ^{234}U dan ^{238}U yang diukur di dalam sampel air laut masing-masing adalah 2.94 – 45.80 dan 2.12 – 38.10 Bq.m^{-3}, manakala julatnya di dalam sampel sedimen permukaan masing-masing adalah 28.00 – 60.05 dan 25.15 – 55.15 Bq.kg^{-1} berat kering. Secara umumnya di semua lokasi persampelan, nisbah keaktifan ^{234}U/^{238}U adalah hampir seragam dalam julat 1.08 – 1.39 untuk sampel air laut dan 1.01 – 1.12 untuk sampel sedimen permukaan. Nisbah yang diperolehi ini adalah hampir sama dengan sumber-sumber penerbitan terdahulu.

Abstract

The determination of uranium isotopes activity concentration and their distributions in the seawater and surface sediment along the coastal area of the East Coast of Malaysia Peninsular have been performed using alpha spectrometry counting system. The sampling of both seawater and surface sediment for this study was carried out in August 2003 as part of the Marine Radioactivity Database Development Project for Malaysia. This results show that the distribution of uranium radionuclides (^{234}U and ^{238}U) in seawater and surface sediment is not consistent, their activities are fluctuated depending on the sampling locations. Generally, the ^{234}U and ^{238}U activities measured in the seawater are in the range of 2.94 – 45.80 and 2.12 – 38.10 Bq.m^{-3}, respectively, whilst in the surface sediment they are in the range of 28.00 – 60.05 and 25.15 – 55.15 Bq.kg^{-1} dry weight, respectively. In general, the activity ratios of ^{234}U/^{238}U at all sampling locations are nearly uniform in the range of 1.08 – 1.39 for seawater and 1.01 – 1.12 for surface sediment. These ratios are comparable with those found in published literatures.

Pendahuluan

Uranium ialah unsur radioaktif yang terbentuk secara tabii dan merupakan pemancar alfa. Ia mempunyai tiga isotop utama iaitu ^{234}U (anak ^{238}U, $t_{1/2}$: 2.45 x 10^5 tahun), ^{235}U ($t_{1/2}$: 7.04 x 10^8 tahun) dan ^{238}U ($t_{1/2}$: 4.47 x 10^9 tahun) [1]. Kelimpahan isotop bagi ^{234}U, ^{235}U dan ^{238}U adalah masing-masing 0.0058, 0.721 dan 99.28 % [2]. Di persekitaran marin terdapat pelbagai radionuklid yang terhasil daripada siri pereputan isotop uranium dan ia boleh dikelaskan kepada dua kumpulan iaitu: (i) radionuklid yang terlarut secara stabil dalam air laut, (ii) radionuklid partikel reaktif yang disingkirkan daripada air laut melalui proses penjerapan, pemendakan atau biologikal. Dalam hal ini, radioisotop uranium (^{234}U, ^{235}U dan ^{238}U) dikelaskan di bawah kumpulan (ii) [3].

Pengetahuan terhadap perlakuan geokimia uranium di dalam sistem marin masih lagi di peringkat yang rendah. Begitu juga, perlakuan uranium di zon persisiran dan khususnya semasa percampuran muara, tidak begitu difahami. Kepekatan uranium di persisiran adalah berubah-ubah dan berkait rapat dengan kepelbagaian kepekatan semulajadi uranium di dalam sungai yang memasuki zon persisiran. Taburan uranium di dalam larutan adalah sangat penting kerana ia menghasilkan radionuklid partikel reaktif seperti ^{234}Th, ^{231}Pa dan ^{230}Th [3].

Penentuan keaktifan radionuklid daripada siri reputan raadionuklid uranium di dalam tanah, air dan partikulat terampai di sepanjang sungai – muara – persisiran pantai dan seterusnya ke marin, akibat daripada proses pencuacaan (seperti luluhawa, perubahan suhu) dan mekanisma pengangkutan radionuklid tersebut dari darat ke sistem marin, dapat memberi maklumat mengenai taburan dan perlakuannya [3 - 7]. Sementara itu, pengetahuan tentang nisbah sesuatu radionuklid boleh memberi maklumat yang berkaitan dengan sesuatu sistem tabii tersebut [8]. Kepekatan dan nisbah isotop siri reputan uranium di dalam air sungai dan sedimen merupakan parameter yang sangat penting dan ia diperlukan untuk membentuk keseimbangan geokimia bagi unsurtersebut [4]. Menurut Fujikawa et al. [1], ^{234}U dan ^{238}U yang berda di dalam suatu sistem tertutup akan mencapai keseimbangan sekular apabila nisbah (^{234}U/^{238}U) adalah bersamaan 1.0. Sebaliknya ia didapati berubah-ubah disebabkan oleh keadaan asal geografi tabii yang berbeza seperti kebanyakan air, tanah, dan sedimen. Perubahan ini adalah disebabkan oleh beberapa mekanisma seperti berlakunya proses larutlesap yang berlebihan terhadap ^{234}U daripada fasa pepejal berbanding dengan ^{238}U, kesan kerosakan sinaran ke atas kekisi kristal semasa penyepaian alfa ^{238}U, pengoksidaan ^{234}U tetravalen tak larut kepada ^{234}U heksavalen yang larut semasa penyepaian dan sentakan alfa bagi ^{234}Th (dan juga anaknya ^{234}U) ke dalam fasa larutan dan pergerakan ^{234}U itu sendiri.

Nisbah keaktifan isotop uranium ^{234}U dan ^{238}U di dalam air laut didapati tidak berada di dalam keseimbangan sekular sebagaimana organisma marin. Seperti yang dilaporkan oleh Sugimura dan Mayeda [2], kebanyakan penulis mengatakan lebih kurang 25% kepekatan uranium di dalam air laut tersebar mengikut lokasi dan kedalaman dan ia berperanan di dalam beberapa aktiviti biologi di dalam lautan.

Kajian ke atas radionuklid hasil daripada siri reputan uranium di dalam sekitaran marin telah banyak dijalankan di seluruh dunia terutamanya di negara maju sejak beberapa dekad yang lalu. Umumnya kajian itu bertujuan untuk mendapatkan kefahaman mengenai proses dan fenomena oseanografik unutkpengurusan marin yang lebih baik. Di negara-negara yang sedang membangun seperti Malaysia, penyelidikan di dalam bidang ini menjadi semakin penting untuk melindungi sekitaran marin dan muara-muara sungai daripada pencemaran daratan serta kesan-kesan antropogenik lain terhadap ekosistem marin dan akuatik khasnya daripada perlepasan bahan buangan radioaktif [9]. Sehubungan itu, penentuan keaktifan isotop uranium dan taburannya di dalam sampel air laut dan sedimen permukaan di sepanjang pesisiran perairan Pantai Timur Semenanjung Malaysia telah dilakukan dengan menggunakan sistem pembilang spektrometri alfa. Persampelan air laut dan sedimen bagi kajian ini telah dijalankan pada bulan Ogos, 2003 di beberapa lokasi terpilih dan ia merupakan sebahagian daripada projek Pembangunan Data Asas Keradioaktifan Marin di Malaysia. Kajian ini adalah bertujuan untuk melihat perlakuan, taburan dan mengenalpasti punca kehadiran uranium dalam sistem perairan marin.

Eksperimen

Kawasan kajian adalah meliputi laut dalam dan persisiran pantai di sepanjang perairan Pantai Timur Semenanjung Malaysia. Sebanyak tiga stesen persampelan laut dalam dan sepuluh stesen persampelan persisiran pantai telah dipilih bermula dari Kota Bharu di Kelantan hingga ke Tanjung Datok di Johor. Stesen-stesen laut dalam yang dipilih terletak kira-kira 50-60 batu nautika dari daratan pada kedalaman air 35-65m manakala stesen-stesen persisiran pantai pula terletak di antara 2-3 batu nautika dari daratan pada kedalaman air 8-15m. Kebanyakan stesen persisiran pantai mengadap ke kuala sungai-sungai utama bagi mendapatkan input maksimum radionuklid tabii yang berpunca dari daratan. Sampel air laut telah diambil di setiap stesen persampelan laut dalam dan persisiran pantai manakala sampel sedimen permukaan hanya diambil di stesen persisiran pantai sahaja. Lokasi stesen persampelan di kawasan kajian ditunjukkan dalam Rajah 1. EC01 – EC05 adalah stesen laut dalam manakala EC06 – EC15 adalah stesen persisiran pantai.
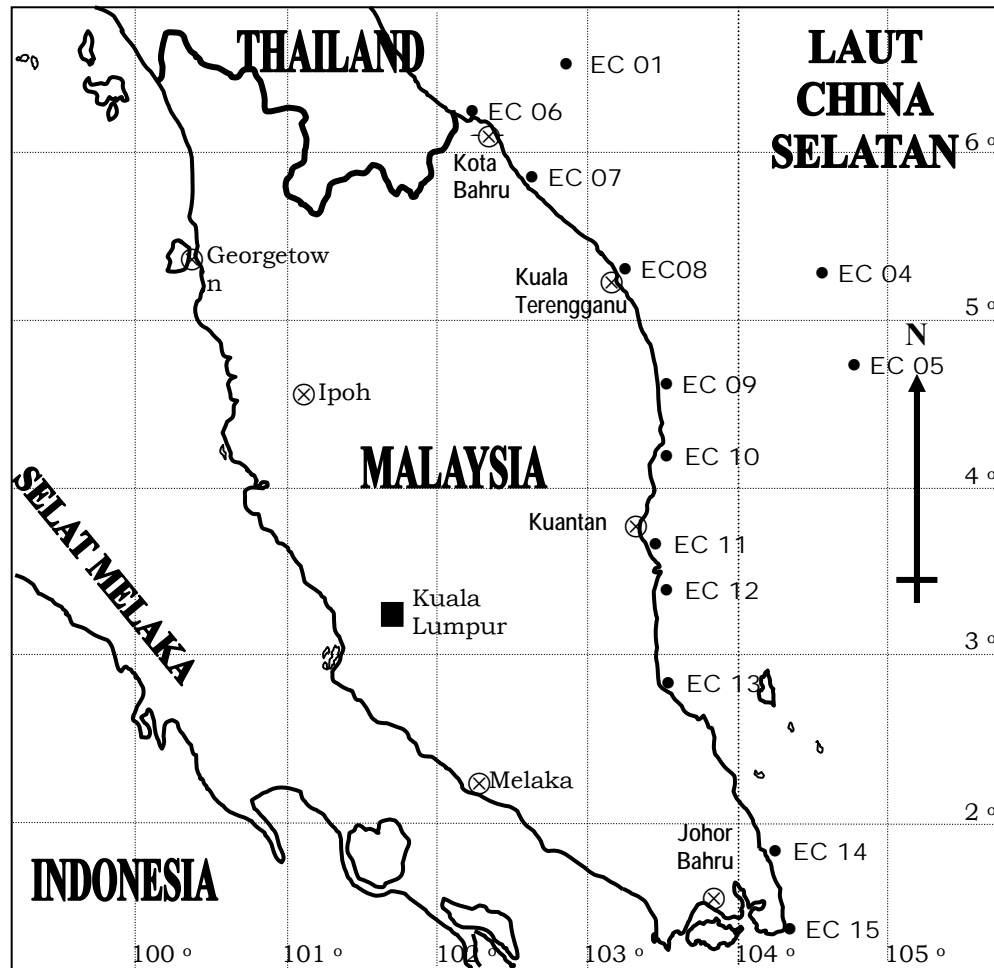
Rajah 1: Peta menunjukkan lokasi stesen persampelan di perairan Pantai Timur Semenanjung Malaysia.

Di dalam kajian ini, sampel air laut telah diambil pada kedalaman 2.5 - 5m dari permukaan laut dengan menggunakan 'Grunfos submersible pump'. Sebanyak 230 L air laut di pam ke dalam bekas plastik 250 L. Seterusnya proses pengasidan dan penambahan penyurih (^{232}U) yang diketahui keaktifannya dan proses pemendakan dilakukan ke atas air laut tersebut di lapangan. Setelah sampel dibawa ke makmal, proses pemelarutan mendakan dan pemendakan semula dilakukan dengan menggunakan HCl dan NH_4OH.

Sampel sedimen persisiran pantai pula telah diambil dari tiga lokasi (sub-stesen) yang jaraknya satu batu nautika antara satu sama lain di setiap stesen dengan menggunakan 'Ponar grab sampler'. Sampel tersebut kemudian dimasukkan ke dalam bekas polietilena yang telah dibersihkan, sebelum ianya dikeringkan di makmal. Sampel sedimen dikeringkan di dalam ketuhar pada suhu 60°C untuk tempoh 72 jam. Sampel yang telah kering ditimbang, dan dihancurkan untuk mendapatkan sampel yang halus dan homogen. Kaedah pencernaan menggunakan asid HNO_3, $HClO_4$ dan HCl pekat dilakukan ke atas sampel-sampel sedimen yang telah ditambahkan dengan penyurih ^{232}U yang diketahui keaktifannya.

Kaedah pemisahan radiokimia seperti yang disyorkan oleh beberapa penyelidik terdahulu [10 - 13] dengan beberapa modifikasi yang melibatkan proses pengekstrakan dengan pelarut organik, turus penukar ion dan penulenan dilakukan ke atas kedua-dua mendakan sampel air laut dan sedimen. Ia melibatkan proses pengekstrakan dengan pelarut organik, turus resin penukar ion dan proses penulenan. Akhirnya, proses pemendapan elektro uranium dilakukan ke atas keluli tanpa karat selama sejam.

Penentuan keaktifan ^{234}U dan ^{238}U di dalam sampel telah dilakukan dengan menggunakan sistem spektrometri alfa EG&G ORTEC dan CANBERRA. Proses pembilangan ke atas keluli tanpa karat dilakukan selama 3 hari. Keputusan untuk sampel sedimen dilaporkan berdasarkan nilai purata data yang bersesuaian bagi ketiga-tiga lokasi di setiap stesen berkenaan.

<div align="center">

Keputusan dan Perbincangan
</div>

Perlakuan radionuklid ^{234}U dan ^{238}U di dalam sampel air laut

Secara keseluruhannya, keaktifan ^{234}U dan ^{238}U di semua stesen persampelan bertabur secara tidak seragam (Jadual 1) dengan julat keaktifan yang diukur di dalam sampel air laut adalah masing-masing 2.94 – 45.80 dan 2.12 – 38.10 Bq.m^{-3}. Ketidakseragaman bukan saja bergantung kepada kedudukan sesuatu stesen itu, malahan juga bergantung kepada perbezaan kawasan samada di laut dalam atau di persisiran pantai. Julat keaktifan radionuklid tersebut yang ditunjukkan di kawasan laut dalam adalah 2.94 – 8.69 dan 2.12 – 8.08 Bq.m^{-3} dan di kawasan persisiran pantai pula adalah 4.03 – 45.80 dan 3.76 – 38.10 Bq.m^{-3}. Merujuk kepada julat tersebut, catatan aras keaktifannya yang tertinggi dikesan bagi laut dalam ialah Stesen Desaru dan persisiran pantai pula ialah di sekitar muara Sungai Pahang/Pekan. Sebaliknya nilai terendah dikesan di sekitar Pulau Tioman (kawasan laut dalam) dan muara Sungai Kelantan/Kuala Besar (kawasan persisiran pantai).

Jadual 1: Keaktifan ^{234}U dan ^{238}U di dalam sampel air laut di kawasan laut dalam dan persisiran pantai di perairan Pantai Timur Semenanjung Malaysia

Stesen Persampelan	Keaktifan Spesifik (Bq/m^3)		^{234}U/^{238}U
	^{234}U	^{238}U	
Kota Bharu (EC 01)	4.34 ± 0.32	3.68 ± 0.27	1.18 ± 0.25
Pulau Tioman (EC 04)	2.94 ± 0.22	2.12 ± 0.17	1.39 ± 0.24
Desaru (EC 05)	8.69 ± 0.64	8.08 ± 0.59	1.08 ± 0.32
Muara Sungai Kelantan/K. Besar (EC 06)	4.03 ± 0.29	3.76 ± 0.29	1.07 ± 0.22
Muara Sungai Besut (EC 07)	6.22 ± 0.46	4.73 ± 0.34	1.32 ± 0.32
Kuala Terengganu (EC 08)	22.70 ± 1.66	17.62 ± 0.15	1.29 ± 0.45
Muara Sungai Dungun (EC 09)	9.00 ± 0.66	8.22 ± 0.60	1.10± 0.33
Muara Sungai Kemaman (EC 10)	8.50 ± 0.62	6.97 ± 0.51	1.22 ± 0.35
Muara Sungai Kuantan (EC 11)	7.22 ± 0.53	6.33 ± 0.46	1.14 ± 0.31
Muara Sungai Pahang/Pekan (EC 12)	45.80 ± 3.35	38.10 ± 2.79	1.20 ± 0.80
Muara Sungai Rompin (EC 13)	32.80 ± 2.40	29.30 ± 2.14	1.12 ± 0.64
Muara Sungai Sedili Besar (EC 14)	17.40 ± 1.24	15.30 ± 1.11	1.14 ± 0.47
Tanjung Datok (EC 15)	7.02 ± 0.51	6.24 ± 0.46	1.13 ± 0.30

Fenomena perubahan taburan radionuklid ini dipercayai dipengaruhi oleh beberapa faktor seperti sifat kimia dan fizikal radionuklid berkenaan, pengdepositan, pemindahan dan pengangkutan. Bagi stesen yang mencatatkan aras keaktifan U yang tertinggi (> 20 Bq.m^{-3}) pula mungkin disebabkan oleh kesan arus pasang surut. Persampelan di sesetengah stesen berkenaan dilakukan semasa air sedang surut di mana sampel air permukaan mengandungi kandungan sedimen terampai yang tinggi dari luahan sungai berdekatan. Fenomena perubahan taburan radionuklid ini dipercayai dipengaruhi oleh beberapa faktor seperti sifat kimia dan fizikal radionuklid berkenaan, pengdepositan, pemindahan dan pengangkutan. Bagi stesen yang mencatatkan aras keaktifan U yang tertinggi (> 20 Bq.m^{-3}) pula mungkin disebabkan oleh kesan arus pasang surut. Persampelan di sesetengah stesen berkenaan dilakukan semasa air sedang surut di mana sampel air permukaan mengandungi kandungan sedimen terampai yang tinggi dari luahan sungai bedekatan.

Secara umumnya, didapati aras keaktifan ^{234}U dan ^{238}U di dalam air laut yang diambil di kawasan persisiran atau muara adalah tinggi jika dibandingkan dengan kawasan laut dalam. Keadaan ini disokong oleh kenyataan Cochran [3] yang melaporkan bahawa keaktifan U di zon persisiran utara-barat pasifik adalah tersangat tinggi jika dibandingkan dengan laut terbuka. Menurut beliau, perlakuan U di dalam zon persisiran semasa percampuran muara kurang difahami. Keaktifan U di dalam air laut di persisiran dan di luar persisiran pantai adalah berbeza dan keadaan ini boleh dikaitkan dengan perubahan semulajadi terhadap keaktifan U di dalam sungai yang memasuki zon persisiran.

Didapati muara Sungai Pahang/Pekan dan muara Sungai Rompin mempamirkan keaktifan [234]U dan [238]U yang tinggi berbanding dengan muara-muara lain. Peningkatan keaktifan uranium di sesetengah muara adalah disebabkan oleh penurunan aras pH yang berpunca daripada percampuran air laut yang melimpah masuk ke kawasan tersebut. Menurut Cochran [3], [234]U dan [238]U akan terlarut semasa proses luluhawa kimia dan membentuk spesies karbonat uranil yang stabil dalam persekitaran muara yang mempunyai pH 6 atau lebih. Manakala, Scott [4] pula menyatakan bahawa fenomena ini berlaku adalah disebabkan oleh U di kaut dari larutan oleh pemendapan sebatian humik di dalam kawasan saliniti yang berjulat rendah seperti muara sungai. Juga, +perpindahan partikel dari sungai ke laut mungkin membantu nyahjerapan U kerana pertambahan pH. Kenyataan ini disokong oleh laporan yang telah dibuat oleh Rodriguez-Alvarez dan Sanchez [12] yang menyatakan aras keaktifan [234]U bertambah bila nilai pH air menyusut atau disebaliknya. Menurut beliau lagi, pertambahan keaktifan [234]U juga akibat dari kesan peningkatan paras saliniti di kawasan muara yang berpunca dari percampuran air sungai dengan air laut yang menyebabkan berlakunya proses nyahjerapan radionuklid tersebut dari sedimen di kawasan tersebut. Perlakuan yang sama juga berlaku di muara Sungai Jucar-Cabriel dan Sungai Guadalquivir di Spain dan sungai-sungai lain seperti Sungai Forth di United Kingdom [12]. Walau bagaimanapun hubungan di antara keaktifan dan pH hanya dijumpai untuk [234]U sahaja dan bukan untuk [238]U.

Pada umumnnya, nisbah keaktifan [234]U/[238]U di dalam air laut di kawasan laut dalam dan persisiran pantai didapati masing-masing dalam julat 1.08 – 1.39 dan 1.07 – 1.32. Nisbah keaktifan yang diperolehi di kebanyakan lokasi dengan nilai purata masing-masing 1.22 dan 1.17 adalah setanding dengan sumber-sumber penerbitan yang lain yang mendapati nisbahnya lebih besar dari uniti iaitu 1.15 [3,11&13]. Merujuk kepada julat-julat tersebut, jelaslah ia menyimpang dari keseimbangan sekular ([234]U/[238]U=1). Keadaan ini menunjukkan kandungan [234]U melebihi kandungan [238]U di dalam air akibat kesan pertambahan kemasukan [234]U semasa air pasang. Menurut Rodriguez-Alvarez & Sanchez [12], fenomena ini terjadi kerana di kawasan tersebut terdapat proses-proses kompleks yang terlibat di dalam perlakuan tersebut. Pengurangan [238]U juga berlaku akibat daripada pencairan dan penyebaran ke atas pengkayaan radionuklid antropogenik oleh aliran pasang surut [14]. Begitu juga di muara, nisbah keaktifan [234]U/[238]U adalah lebih dari nilai uniti, yang menunjukkan terdapat hubungan di antara pH dan keaktifan [234]U yang mana ia boleh diterangkan dengan menganggapkan nilai pH yang rendah akan menggalakkan proses larutlesap [234]U dari kedudukan kristal yang tidak teratur dan mengurangkan serapan [234]Th dan [234]U oleh partikel sedimen [12].

Perlakuan radionuklid [234]U dan [238]U di dalam sampel sedimen permukaan di persisiran pantai
Keputusan kajian ini mendapati profil taburan radionuklid [234]U dan [238]U yang dicerap di dalam sampel sedimen permukaan persisiran pantai yang diambil dari 10 stesen persampelan adalah tidak seragam, di mana keaktifannya berubah-ubah mengikut lokasi stesen seperti yang ditunjukkan dalam Jadual 2. Secara keseluruhannya, keaktifan radionuklid [234]U dan [238]U masing-masing adalah dalam julat 28.00 – 60.05 dan 25.15 – 55.15 Bq.kg^{-1} berat kering. Merujuk kepada julat tersebut, catatan aras keaktifan tertinggi dikesan ialah di sekitaran muara Sungai Kelantan dan sebaliknya terendah di sekitaran muara Sungai Kuantan. Di beberapa muara seperti muara Sungai Kelantan, Sungai Pahang dan Sungai Rompin didapati aras keaktifannya agak tinggi iaitu melebihi 45 Bq.kg^{-1} berat kering hingga 60 Bq.kg^{-1} berat kering. Keadaan ini berlaku kerana muara-muara tersebut sentiasa menerima input sedimen dari daratan dan ianya adalah sungai-sungai besar di mana aliran air dan sedimen terampai sampai lebih jauh ke tengah laut [15].

Keaktifan [234]U adalah lebih tinggi berbanding dengan [238]U, disebabkan oleh sifat siri pereputan masing-masing, di mana [234]U mempunyai separa hayat ($t_{1/2}$) yang lebih pendek, dengan itu ia cepat dijana semula berbanding dengan [238]U. Kenyataan ini disokong oleh laporan yang telah dibuat oleh Keating et al. [14] yang menyatakan tiada pertambahan keaktifan hasil daripada pereputan [238]U secara *in-situ* kerana mempunyai $t_{1/2}$ yang amat panjang.

Seterusnya tiada hubungan korelasi secara statistik di antara aras keaktifan [234]U (R=0.08) dan [238]U (R=0.12) di dalam sedimen dengan kedalaman air. Ini menunjukkan bahawa, kedalaman air tidak mempengaruhi atau menghalang pergerakan radionuklid tersebut dari permukaan air ke dalam sedimen. Dengan kata lain, kewujudan [234]U di stesen kajian adalah hasil daripada pereputan induknya, [238]U. Bagi sesetengah stesen pula, didapati aras keaktifan [234]U adalah tinggi dan keadaan ini berkemungkinan berpunca dari perbezaan input daratan dan sungai.

Jadual 2: Keaktifan ^{234}U dan ^{238}U di dalam sampel sedimen persisiran pantai di perairan Pantai Timur Semenanjung Malaysia

Stesen Persampelan	Keaktifan Spesifik (Bq/kg berat kering)		^{234}U/^{238}U
	^{234}U	^{238}U	
Muara Sungai Kelantan/K. Besar (EC 06)	60.05 ± 4.38	55.15 ± 4.04	1.09 ± 0.85
Muara Sungai Besut (EC 07)	39.25 ± 2.87	39.05 ± 2.86	1.01 ± 0.65
Kuala Terengganu (EC 08)	29.27 ± 2.14	28.17 ± 2.36	1.04 ± 0.62
Muara Sungai Dungun (EC 09)	34.33 ± 2.51	30.78 ± 2.25	1.12 ± 0.66
Muara Sungai Kemaman (EC 10)	32.90 ± 2.40	29.57 ± 2.16	1.11 ± 0.64
Muara Sungai Kuantan (EC 11)	28.00 ± 2.05	25.15 ± 1.84	1.11 ± 0.60
Muara Sungai Pahang/Pekan (EC 12)	54.97 ± 4.01	52.00 ± 3.79	1.06 ± 0.80
Muara Sungai Rompin (EC 13)	50.70 ± 3.70	47.53 ± 3.48	1.07 ± 0.78
Muara Sungai Sedili Besar (EC 14)	28.73 ± 2.10	25.57 ± 1.87	1.12 ± 0.60
Tanjung Datok (EC 15)	35.80 ± 2.55	32.63 ± 2.38	1.10 ± 0.66

Nisbah keaktifan ^{234}U/^{238}U di dalam sedimen adalah dalam julat 1.01 – 1.12 (Jadual 2). Nilai purata nisbah keaktifan 1.08 adalah setanding dengan laporan yang ditulis oleh Balakrishna et al. [13]. Merujuk kepada julat-julat tersebut, jelaslah ia menyimpang daripada keseimbangan sekular. Di dapati hanya stesen muara sungai Besut dan Kuala Terengganu sahaja yang boleh dikatakan telah mencapai keseimbangan sekular di antara ^{234}U dan ^{238}U (^{234}U/^{238}U = 1.01 & 1.04), manakala stesen-stesen lain pula menunjukkan ^{234}U/^{238}U > 1. Nisbah keaktifan ^{234}U/^{238}U adalah tinggi dari uniti di semua muara dan persisiran pantai telah disokong oleh laporan Keating et al [14] yang menyatakan pengkayaan ^{234}U berlaku semasa proses lulohawa dan pengangkutan. Ia juga disebabkan oleh pertambahan secara relatif kadar larutlesap ^{234}U berbanding dengan kadar ^{238}U yang mengakibatkan lebih banyak ^{234}U terdapat di situ [16]. Selain itu, ketinggian nisbah yang diukur juga disebabkan oleh gangguan daripada ^{237}Np yang mempunyai tenaga penyepaian yang hampir sama dengan ^{234}U [17].

Perlakuan ^{234}U , ^{238}U dan nisbah keaktifan ^{234}U /^{238}U di dalam air laut dan sedimen
Secara umumnya keaktifan kedua-dua radionuklid tersebut adalah tinggi secara relatif di dalam sedimen permukaan di persisiran pantai jika dibandingkan dengan keaktifannya di dalam air laut di kawasan laut dalam dan persisiran pantai. Keadaan ini disokong oleh kenyataan Yu et al. [10] yang menyatakan bahawa pecahan yang besar bagi uranium autigenik (secara *in-situ*) akan disalurkan kepada sedimen melalui dua proses: i) pengukuhan biogenik U di dalam turus air dan U dikaut oleh mikroorganisma dan ii) pemendakan U di antara permukaan air-sedimen, di mana kadar bahan organik reaktif yang tinggi akan meningkatkan aktiviti bakteria seterusnya menyebabkan U terperangkap di dalam sedimen samada secara langsung atau tidak langsung.

Purata bagi nisbah keaktifan ^{234}U/^{238}U di dalam air laut di kawasan laut dalam, persisiran pantai dan sedimen permukaan persisiran pantai adalah masing-masing 1.22, 1.17 dan 1.08 (Rajah 2).   Menurut kajian lepas, nisbah keaktifan ^{234}U/^{238}U di dalam air laut adalah dalam julat 1.02 – 1.20 dengan purata 1.14 [2] dan 1.19 di dalam sedimen dari kawasan tropika [18]. Di dalam sedimen, kebanyakan uranium berasal daripada air laut, oleh itu nisbah keaktifan ^{234}U/^{238}U sepatutnya menghampiri nilai nisbah bagi air. Kadar pengumpulan uranium autigenik mempunyai kaitan dengan nisbah keaktifan ^{234}U/^{238}U daripada jumlah uranium di dalam sedimen. Di antara proses yang menyebabkan pengumpulan uranium dikebanyakan sedimen yang telah dinyatakan oleh Andersson et al. [19] ialah pengambilan aktif uranium secara biologi oleh plankton, serapan uranium terlarut secara kimia oleh partikel organik, dan proses penurunan dan pemendakan di dasar. Nisbah yang dipamerkan oleh air laut di persisiran pantai menunjukkan sumber ^{234}U adalah mungkin berpunca daripada input sungai atau daratan. Di samping itu, sedimen juga memberi sumbangan radionuklid tersebut kepada air atau disebaliknya. Walaupun hubungan korelasi yang ditunjukkan antara keaktifan ^{234}U dan ^{238}U di dalam air dan sedimen permukaan di persisiran pantai adalah sederhana iaitu ^{234}U (R= 0.40) dan ^{238}U (R=0.34), tetapi sekurang-kurangnya ia menyokong kenyataan di atas.
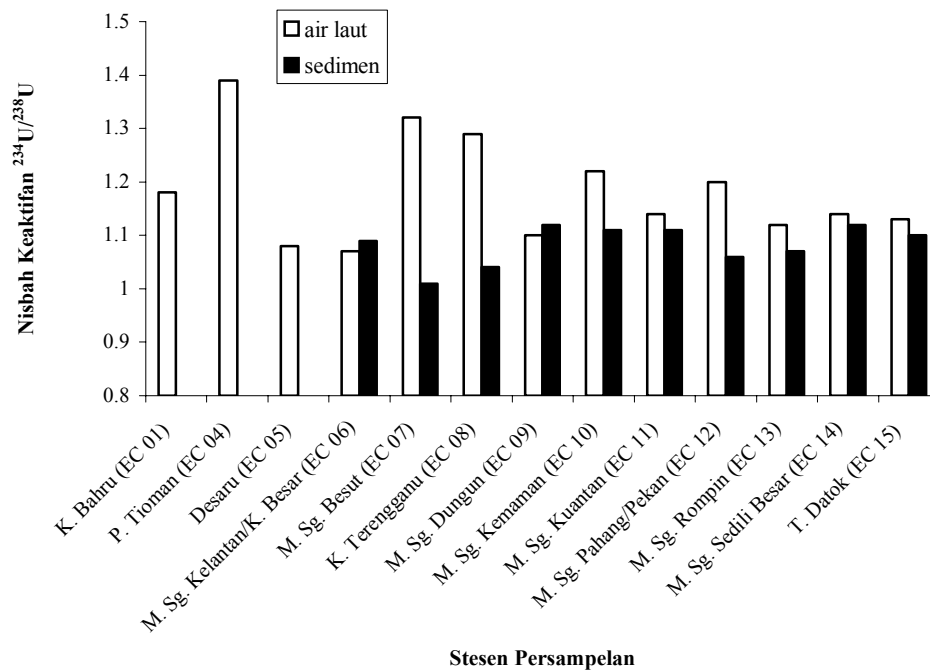
Rajah 4: Taburan nisbah keaktifan ^{234}U/^{238}U di dalam sampel air laut (laut dalam dan persisiran pantai)
dan sedimen permukaan di perairan Pantai Timur Semenanjung Malaysia

Kesimpulan

Kajian ke atas perlakuan isotop U (radionuklid ^{234}U dan ^{238}U) di dalam air laut (laut dalam dan persisiran pantai) dan sedimen persisiran di perairan Pantai Timur Semenanjung Malaysia, mendapati profil perlakuan dan taburan isotop ini adalah berbeza-beza mengikut jenis isotop dan lokasi persampelan. Dalam kajian ini, secara umumnya julat keaktifan masing-masing ^{234}U dan ^{238}U yang diukur dalam sampel air laut permukaan masing-masing adalah 2.94 – 45.80 dan 2.12 – 38.10 Bq/m^3, manakala di dalam sampel sedimen permukaan masing-masing adalah 28.00 – 60.05 dan 25.15 – 55.15 Bq/kg berat kering.

Di semua lokasi persampelan, nisbah keaktifan ^{234}U/^{238}U adalah hampir seragam dalam julat 1.07 – 1.39 untuk sampel air laut dan 1.01 – 1.12 untuk sampel sedimen permukaan. Nisbah yang diperolehi ini adalah setanding dengan sumber-sumber penerbitan terdahulu.

Keputusan kajian, mendapati aras keaktifan ^{234}U dan ^{238}U di dalam sampel sedimen persisiran pantai dan air laut permukaan yang ditunjukkan di sesetengah stesen persampelan yang dikaji boleh dikatakan tinggi yang disebabkan oleh beberapa faktor sekitaran yang mempengaruhinya seperti yang telah dibincangkan. Dalam hal yang demikian, ia boleh mengukuhkan lagi bukti-bukti yang membolehkan kita membuat andaian bahawa stesen persampelan tersebut adalah sangat aktif secara fizik, kimia dan biologi.

Rujukan

1. Fujikawa, Y., Fukui, M., Sugahara, M., Ikeda, E. & Shimada, M. 2005. Variation in uranium isotopic ratios $^{234}U/^{238}U$ and ^{238}U/total-U in Japanese soil and water samples-application to environmental monitoring. Sumber dari laman web http://www.irpa.net/irpa10/ cdrom/00809.pdf. Tarikh akses: 14/06/2005.

2. Sugimura, Y. & Mayeda, M. 1980. The uranium content and the activity ratio $^{234}U/^{238}U$ in sea water in the Pacific Ocean. In D.G. Edward, Y. Horibe & K. Saruhashi (Eds.), *Isotope Marine Chemistry* (pp. 211–246). Uchida Rokakuho Publishing Co., Ltd., Japan.

3. Cochran, J. K. 1982. The oceanic chemistry of U- and Th-siries nuclides. In. M. Ivanovich & R. S. Harmon (Eds.), Uranium siries desequilibrium: Applications to environmental problems (pp. 384 – 430). Clarendon Press, Oxford.

4. Scott, M.R. 1982. The chemistry of U and Th-siries nuclides in rivers. In. M. Ivanovich & R. S. Harmon (Eds.), Uranium siries desequilibrium: Applications to environmental problems (pp. 181– 202). Clarendon Press, Oxford.

5. Borole, D. V., Krishnaswami, S. & Somayajulu, B. L. K. 1982. Uranium isotopes in rivers, estuaries and adjacent coastal sediments of Western India: Their weathering, transport and oceanic budget. *Geochimica et Cosmochimica Acta **46**:125 – 137*.

6. Sarin, M. M., Krishnaswami, S., Somayajulu, B. L. K. & Moore, W. S. 1990. Chemistry of uranium, thorium and radium isotopes in the Ganga-Brahmaputra river system: Weathering processes and fluxes to the Bay of Bengal. *Geochimica et Cosmochimica Acta **54**:1387 – 1396*.

7. Palmer, M. R., & Edmond, J. M. 1993. Uranium in river water. *Geochimica et Cosmochimica Acta **57**:4947 – 4955*.

8. Uchida, S., Garcia-Tenorio, R., Tagami, K. & Garcia-Leon, M. 2000. Determination of U isotopic ratios in environmental samples y ICP-MS. *J. Anal. At. Spectrom., **15**: 889 – 892*.

9. Sam, A.K., Ahamed, M.M.O., El Khangi, F.A., El Nigumi, Y.O. & Holm, E. 1998. Radioactivity levels in the Red Sea Coastal Environment of Sudan. *Mar. Poll. Bull.* **36**(1): 19 – 26.

10. Yu, E. F., Liang, C. H. & Chen, M. T. 1999. Authigenic uranium in marine sediments of the Benguela current upwelling region during the last glacial period. *TAO, **10**: 201 – 214*.

11. Moore, W. S. 1967. Amazon and Mississippi river concentrations of uranium, thorium and radium isotopes. *Earth and Planetary Science Letters **2***: 231–234.

12. Rodriguez-Alvarez, M. J. & Sanchez, F. 1995. Behavior of uranium along Jucar River (Eastern Spain): Determination of $^{234}U/^{238}U$ and $^{235}U/^{238}U$ ratios. *J. Radioanal. Nucl. Chem, Articles, **190***: 113 –120.

13. Balakrishna, K., Shankar, R., Sarin, M. M. & Manjunatha, B. R. 2001. Distribution of U-Th nuclides in the riverine and coastal environments of the tropical southwest coast of India. *J. Environ. Radioact., **57**: 21 – 33*.

14. Keating, G. E., McCarteney, M. & Davidson, C. M. 1996. Investigation of the technological enhancement of natural decay series radionuclides by the manufacture of phosphates on the Cumbrian coast. *J. Environ. Radioact., **32**(1-2): 53 – 66*.

15. Zal U'yun Wan Mahmood, Zaharudin Ahmad, Abd Kadir Ishak, Yii Mei Wo, Norfaizal Mohamed, Jalal Sharib, Kamarozaman Ishak, Khairul Nizam Razali & Maziah Mahmud. 2004. Kajian awal ke atas taburan radionuklid tabii di perairan Pantai Timur Semenanjung Malaysia. Pembentangan Lisan di SKAM 17, 2004, Kuantan, Pahang.

16. Osmond, J. K. & Cowart, J. B. 1982. Ground water. In. M. Ivanovich & R. S. Harmon (Eds.), Uranium siries desequilibrium: Applications to environmental problems (pp. 202 – 245). Clarendon Press, Oxford.

17. Assinder, D. J., Mudge, S. M. d& Bourne, G. S. 1997. Radiological assessment of the Ribble Estuary-1. Distribution of radionuclides in surface sediments. *J. Environ. Radioactivity, 36(1), p: 1-19*.

18. Khairul Nizam Mohd Ramli. 2005. Perubahan aktiviti ^{234}U, ^{238}U dan nisbah $^{234}U/^{238}U$ di kawasan persisiran pantai Kuala Selangor, Selangor. Tesis Ijazah Sarjana Sains, Universiti Kebangsaan Malaysia.

19. Andersson, R.F., Fleisher, M. Q. & Lehurary, A. P. 1989. Concentration, oxidation state and particulate flux of uranium in the Black Sea. *Geochimica et Cosmochimica Acta, **53**: 2215-2224*.

ASSESSMENT OF NATURAL RADIOACTIVITY IN WATER AND SEDIMENT FROM AMANG (TIN TAILING) PROCESSING PONDS

Mohsen Nasirian, Ismail Bahari, and Pauzi Abdullah

Faculty of Science and Technology, Universiti Kebangsaan Malaysia, 43600, Bangi, Selangor, Malaysia

Keywords: Amang processing, natural radionuclides, uranium-238, Thorium-232, gamma spectrometry

Abstract
Gamma spectroscopy was performed to determine the concentrations of uranium-238 and thorium-232 concentrations in the environment as a consequence of amang processing. In this study 33 water samples and 26 sediment samples were collected from 7 amang processing areas. The concentrations of uranium-238 and thorium-232 were determined by direct counting using a hyper pure germanium (HPGe) detector inter phased with a multi channel analyzer (MCA) . Results showed that the maximum mass and activity concentrations of uranium in water samples were 6.64 ppm and 78.53 Bql^{-1} respectively, while in sediment samples were 69.75 mgkg^{-1} and 860.57 Bqkg^{-1} respectively. The maximum mass and activity concentrations of thorium in water samples were 1.71 ppm and 6.90 Bql^{-1}, while in sediment samples were 157.73 mgkg^{-1} and 637.61 Bqkg^{-1} respectively. Concentrations of uranium-238 and thorium-232 in sediment samples were higher than concentrations of uranium-238 and thorium-232 in water samples, and this may be attributed to insolubility of these radionuclides in water. The concentrations of both radionuclides were higher in sediments collected from ponds involved in the close water recycle system compared to those ponds involved in the open water system. Results also showed that the concentrations of these radionuclides were higher than background indicating that amang processing activity has enhanced the natural radionuclides contents in water and sediment.

Introduction:
Tin mining has been a major activity of Malaysia since 1848. Up till 1980, Malaysia contributed 30.7 % of the world's produce of tin. However her contribution to the world's tin dropped sharply since 1983. By 1996 Malaysia's contributed only 3.9 % and by then there were only 63 mines in operation (Malaysian Department of Mines, 1997). With the drop in tin production and the cost of world's tin, attention shifted toward processing amang (a tin by product) for valuable minerals [1]. Amang is a local (Malaysian) slang word used by the tin mining community to describe tin tailing consisting of a mixture of tin ore, sand and minerals initially discarded by tin miners [5, 16]. Amang or by- product of tin minerals reprocessing, has been found to contain valuable minerals such as ilmenite, zircon, monazite, xenotime, columbite and struvirite that has high demand in production industry [2]. Studies done by the Atomic Energy Licensing Board have shown that the uranium and thorium concentrations vary in monazite, xenotime and ilmenite respectively [3]. Valuable minerals such as monazite ([Ce,La,Y,Th]PO$_4$) are radioactive because they contain naturally occurring thorium. Zircon becomes radioactive when cations, such as Zr^{+4}, are replaced with uranium or thorium [2, 14]. Other minerals may be contaminated with minerals that are radioactive. Amang consists of natural occurring radioactive materials (NORM) such as ^{238}U and ^{232}Th that are technologically enhanced natural occurring radioactive materials (TENORM) during the mining and amang processing activities. Amang which consists of heavy metals is the reason why the mining of tin is blamed for upsetting the ecosystem. Beside the obvious scaring of large and beautiful landscape and turning it into barren lands, tin mining together with amang processing have also been blamed for changing concentration distribution of elements in the ecosystem, namely the distribution of heavy metals as well as NORM in soil and water [15].

In amang processing, separation and concentration of valuable minerals are based on three physical properties, i.e. different specific gravities, magnetic and electrostatic properties. In this process, large volume of water is used in wet gravity separation process and has become a potential source of environmental pollution depending how the water is managed**.** The water may be released directly into the environment (open water management system) or recycle (close water management system). Such activities have been associated with giving rise to radiological environmental problems [16]. The risk of such problem is high due to the fact that legally, amang

plants in Malaysia are categorized as small amang factory and is exempted from licensing by the Atomic Energy Licensing Board (small amang factory) Order 1994 [4].

In Malaysia, there are 113,700 hectares (281,000 acres) of former mining land and 14.4 percent of it is in the form of water pond, used extensively for aqua culture. About four percent has been turned into food production areas, when tin mining collapsed in the 1980s [6].

Using energy dispersive X-ray fluorescence (EDXRF) A.F.Oluwole [10] measured the concentrations of radionuclides and toxic heavy metals in the soil around a lead/tin smelter and also air particulate and mining wastes collected from some tin mines and a tin mill. The concentrations of thorium and uranium reported ranged between 0.01 - 2.94 % and 0.002 - 0.11% in the tailing and between 2.25 - 9.09% and 0.25 - 5.65% in the monazites respectively. Studies by Hu [12] and Kandaiya have also shown the presence of naturally occurring radionuclides in the valuable minerals of amang. Ismail B. [15, 16] reported that amang processing reduces the pH of water and radionuclides contaminates the water and consequently decrease quality of water.

Materials and Methods
Sampling location:
Seven different amang processing plants employing three kinds of water management systems (i.e. open water system, close water natural and close water man made systems) were chosen for this study. Thirty three water samples and 26 sediment samples were taken from seven amang plants. All water and sediment samples were taken from Selangor and Perak State in Malaysia. Hand made water sampler was used for taking water sample from surface level (top), mid and bottom levels of the lakes and ponds. If the depth of pond was less than three meters, only one water sample from top was taken, if the depth was more than three meter and less than four meter, two water samples from top and bottom were taken. If the depth of the lake was more than four meters, three water samples (top, middle and bottom levels) were taken. Water samples were collected and stored in extra clean polyethylene bottle. Water samples collected were labeled as $S_X L_Y$, where S indicates sampling station and L indicates depth at which the water samples were collected. X represents station number from 1-18, and y represents depth of the water samples from 1-3. For example water sample $S_1 L_1$ means station number 1 and top level of water.

Twenty six sediment samples were collected from two different amang processing plants employing close water natural system. Sediment samples were collected in special PVC container. Sediment sampler model Ejkelkamp with PVC transparent tubes (60,100,150 cm length and 63 mm diameter) was used for taking the sediment samples. Sediment samples collected were labeled as $S_X L_Y$. Where S indicates sampling station and L indicates depth at which the sediment samples were collected.

Treatment of samples:
The determination of uranium-238 and thorium-232 concentrations in water samples were based on 2000 ml of water samples collected and subsequently evaporated to 200 ml and stored, capped and sealed in Merinelli containers. In sediment samples, large stones and other objects were removed, then were dried in oven at 105ºC for 24 hours to constant mass, then sieved through mesh 500 μm. All sediment samples were weighed and sealed in Merinelli containers. All water and sediment samples were kept for at least four weeks before counting in order to allow the in-growth of uranium and thorium decay products and achievement of secular equilibrium for ^{238}U and ^{232}Th with their respective progenies.

Gamma spectroscopy:
A stand-alone high-resolution gamma spectrometric system was used for the measurement of the energy spectrum of the emitted gamma rays in the energy range between 50 keV and 3000 keV [12]. The gamma spectroscopy system consists of the high purity germanium (HPGe) detector from Oxford Company with an efficiency of 15%. Detector model number is CNVDS30 with crystal characteristics of diameter 45.3 MM, length 47.3 mm, active volume 75 and germanium dead layer thickness 0.3 microns and detector to window distance less than or equal to 5 mm. The end cap outside diameter is 76-mm aluminum 1 mm thick. The spectra were fed through the Amplifier Canbera Model 2020 to the multi channel analyzer with two analog to digital converters and the memory containing 8192 channels. The multi channel analyzer was directly connected to a personal computer where the spectra were processed and stored. In this system bias supply is from Ortec Company. The detector was mounted on a cryostat which was dipped in to a 30 liters dewar filled with liquid

nitrogen. The detector was surrounded by a cylindrical shield consisting of lead with thickness of 5 cm, which provides an efficient suppression of background gamma radiation present at laboratory site. Soil-IAEA-375 was used as standard reference for sediment samples and uranium and thorium mix stock standard solutions were used as standard reference for water samples.

Analysis and Instrumentation:
Gamma spectroscopy was used to determine the concentrations of uranium-238 and thorium-232 in water and sediment samples. Water sample was put into the shielded HPGe detector and the activity concentration present was counted for 86400 seconds (24 hours), while sediment samples were counted for 43200 seconds (12 hours). Prior to the sample measurement, the environmental gamma background at the laboratory site was determined using a blank Merinelli under identical measurement conditions. The laboratory background reading was averaged from four readings taken.

Based on the measured gamma ray photo peaks, emitted by specific radio nuclides in the thorium-232 and uranium-238 decay series, their radiological concentrations in samples collected can be determined. Calculations relied on establishment of secular equilibrium in the samples, due to the much smaller lifetime of daughter radionuclides in the decay series of thorium-232 and uranium-238. More specifically, the thorium-232 concentration was determined from the concentrations of Tl -208 in the samples, and the concentration of U-238 was determined from concentrations of the Bi-214 decay products.

Energy 1120.3 keV belonging to radionuclide Bi-214 was used for measuring mass concentration and activity of uranium-238 in water samples. Energy 2614.4 keV belonging to radionuclide Tl-208 was used for measuring concentration and activity thorium-232 in water samples. Energy 609.3 keV belong to radionuclide Bi-214 was used for measuring mass concentration and activity of uranium-238 in sediment samples. Energy 2614.4 keV belonging to radionuclide Tl-208 was used for measuring mass concentration and activity concentrations of Th-232 in sediment samples. The mass and activity concentrations of radionuclides were obtained using related formula [3].

Results and Discussion:

Before detail discussion was made in this study, the overall finding of this study was prepared first. Figures 1 and 2 show the mass and activity concentrations of uranium-238 and thorium-232 in water samples. S1- S16 are water sampling stations in different amang ponds, S17 and S18 are water sampling stations along a river (S17 being upstream and S18 down stream). L1, L2 and L3 are different depth where water samples were taken. L1 being near the surface and L3 being near the bottom. Figures 3 and 4 show the mass and activity concentrations of uranium and thorium respectively in sediment samples in amang plant number 1. Figures 5 and 6 show the mass and activity concentrations of uranium and thorium in sediment samples in amang plant number 2. Amang plants number 1 and 2 represent two different amang plants. S1-S4 are sediment sampling stations around the ponds, and L1-L4 are the sediment layer (L1 means top sediment layer and L4 means bottom sediment layer).

Figures 1 and 2 show the mass and activity concentrations of uranium-238 and thorium-232 in water samples respectively. Maximum mass concentration of uranium in water samples was 6.64 ppm and maximum activity concentration was 78.53 Bql^{-1} belonging to sample taken at station 8 (ie. S8L1). Maximum mass and activity concentrations of thorium-232 in water samples were 1.71 ppm and 6.90 Bql^{-1} respectively. These readings were recorded in station 15 (ie. S15-L1).

Figures 3 and 4 show the mean mass and activity concentrations of uranium-238 and thorium-232 in sediment samples in amang plant number 1 respectively. Maximum mass concentration of uranium-238 in sediment samples was 69.75 mg/kg and maximum activity concentration was 860.57 Bqkg^{-1} . These readings were recorded at station 3 (ie. S3L1). Maximum mass concentration of thorium-232 in sediment samples in amang plant 1 was 157.73 mgkg^{-1} and maximum activity concentration was 637.61 Bqkg^{-1}, recorded at station 2 (S2L1).

Figures 5 and 6 show the mass and activity concentrations of uranium-238 and thorium-232 in sediment samples sampled at amang plant number 2. Maximum mass concentration of uranium-238 in sediment samples was 27.59 mgkg^{-1} and maximum activity concentration was 340.40 Bqkg^{-1}, these values were observed in station 1 (S1L1). The maximum of mean mass concentration of thorium in sediment samples in amang plant 2 was 150.8 mgkg^{-1} and maximum activity concentration was 609.60 Bqk^{-1}g. These readings were recorded at station 1 (S1L1).

Table 1 shows the summary and statistical calculations of data collected from all water and sediment samples. Results from Table 1 shows that the mean concentration of uranium-238 in water samples was 4.34 ± 1.58 ppm and with a range 0.12 - 6.64 ppm. The results also shows that the mean concentration of thorium-232 in water samples was 0.37 ± 0.37 ppm with a range between 0.01 – 1.71 ppm. Mean maximum concentrations of uranium-238 and also thorium-232 were observed in stations 8 (S8-L1) and station 15 (S15-L1) respectively. Both stations were close to water discharge point of the plant and involved with the amang plant using the close water management system

Results from Table 1 shows that the mean concentration of uranium-238 in the sediment samples in amang plant 1 was 18.00 ± 17.55 mgkg^{-1} and the range was between 6.82 - 69.75 mgkg^{-1}. The mean concentration of thorium-232 in sediment samples taken from amang plant 1 was 62.05 ± 39.34 mgkg^{-1} and the range was between 26.00 – 157.73 mgkg^{-1}. Maximum mean concentrations of uranium-238 and also thorium-232 were observed in stations 3 (S3-L1) and 2 (S2-L1) respectively. These two stations were close to water discharge point, and where the water management in these amang plants is close water system type.

Table 1 also shows the statistical calculations of uranium-238 and thorium-232 in the sediment samples taken from amang plant 2. The mean concentration of uranium in sediment samples in amang plant 2 was 9.62 ± 6.47 mgkg^{-1} and was in the range 4.96-27.95 mg-1^{kg}. The mean concentration of thorium-232 in sediment samples in amang plant 2 was 40.49 ± 39.41 mgkg^{-1} and was in the range 11.92 - 150.80 mgkg^{-1}. Maximum mean concentrations of uranium-238 and also thorium-232 were observed in station 1 (S1-L1), i.e. discharge point in this amang plant, where the management system in this amang plant is close water system type.

Table 2 shows statistical calculations and activity concentrations of uranium-238 and thorium-232 in water collected from seven amang plants highlighting the different water samples collected at point of discharge and those collected elsewhere. This table shows their mean, $\pm$ standard error mean, median, range and standard deviation. Based on these results the highest uranium-238 and thorium-232 in all amang plants were recorded near or at the point of water discharge (except amang plant 5). The median concentrations of uranium-238 in discharge points were 56.53, 64.93, 71.55, 20.40, 64.00, 54.61and 7.62 Bql^{-1} respectively and for thorium-232 were 1.19, 1.39, 2.55, 1.33, 1.46, 6.9 and 0.12 Bql^{-1} respectively. It should be mentioned that near station S3 in amang plant 5, there were several mounds and valuable minerals next to the point where rainfall could have washed down these minerals and carry them into the pond.
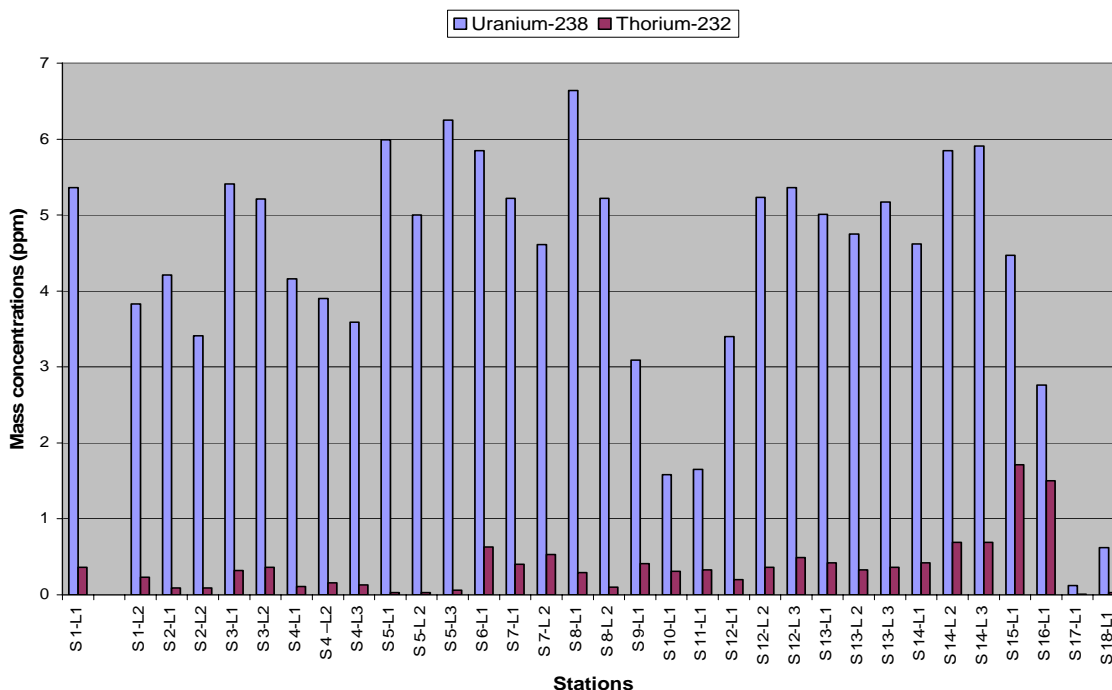
Figure 1. Mass concentrations of U-238 and Th-232 in water samples
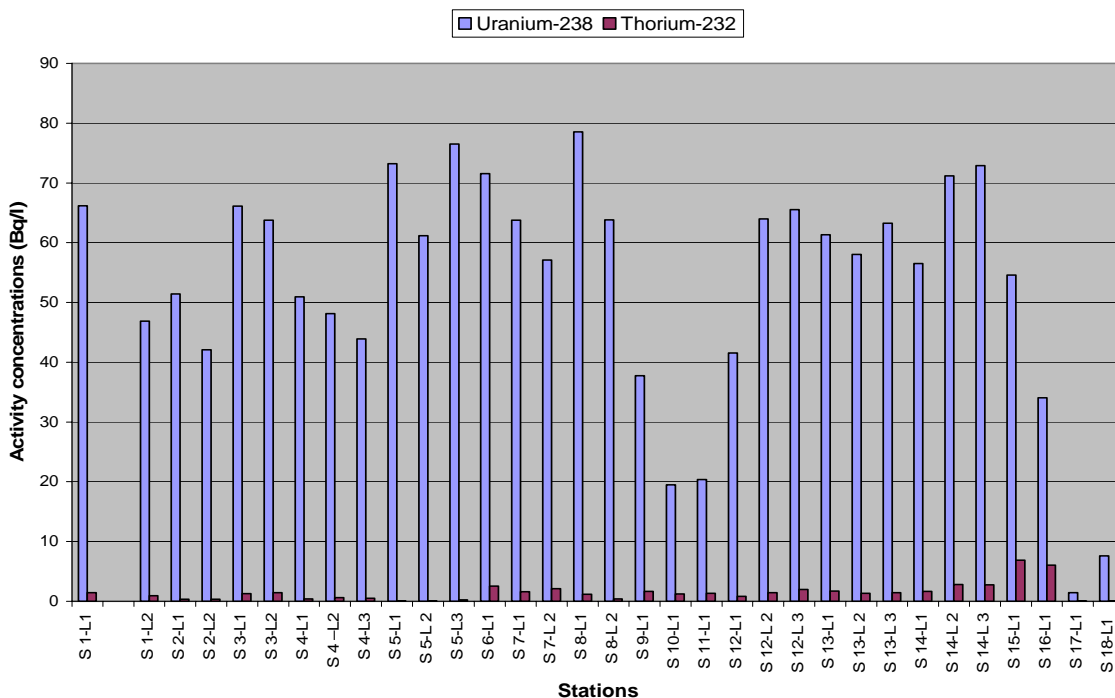
Figure 2**.** Activity concentrations of U-238 and Th-232 in water samples
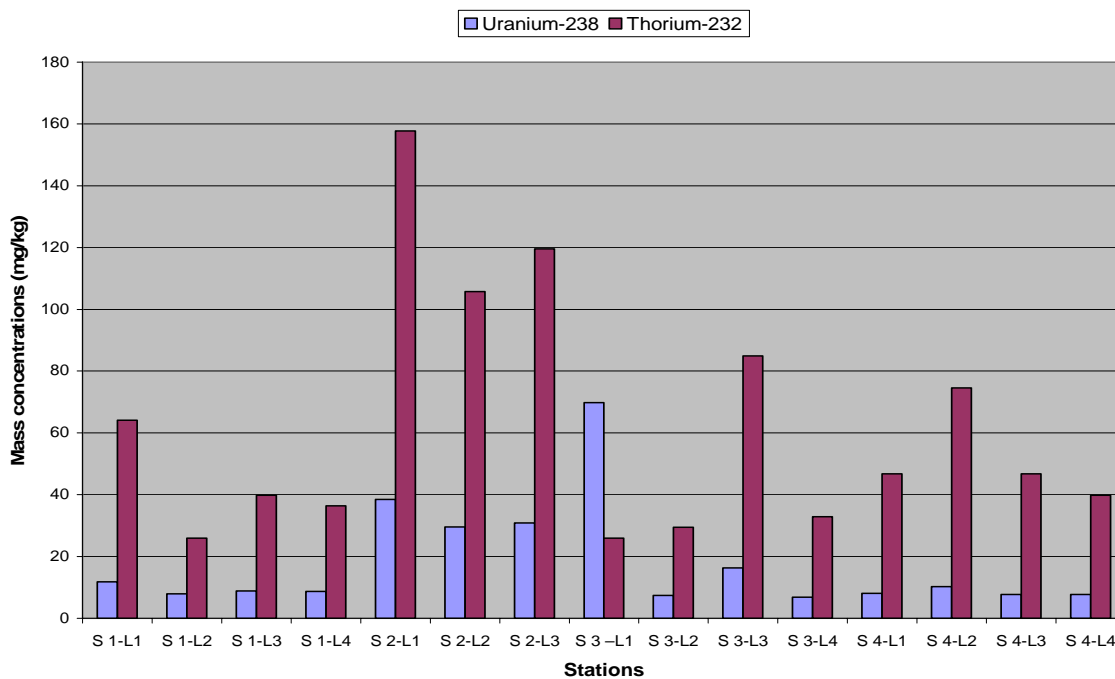
Figure 3. Mass concentrations of U-238 and Th-232 in sediment sample (amang plant 1)
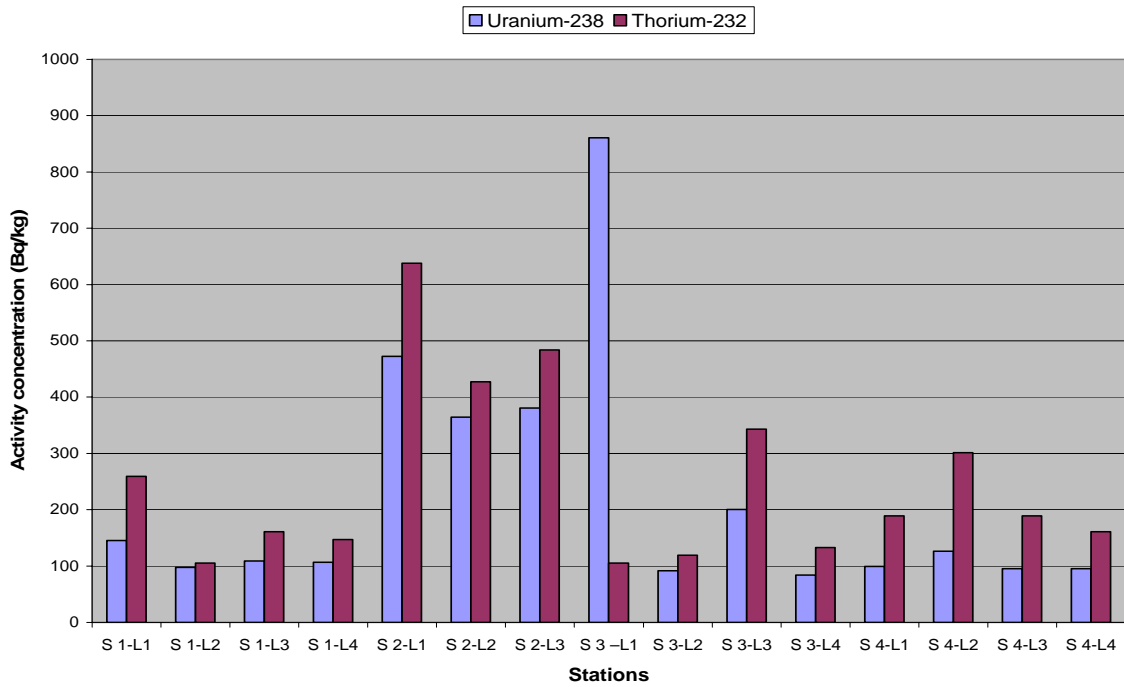
Figure 4. Activity concentrations of U-238 and Th-232 in sediment samples (amang plant 1)
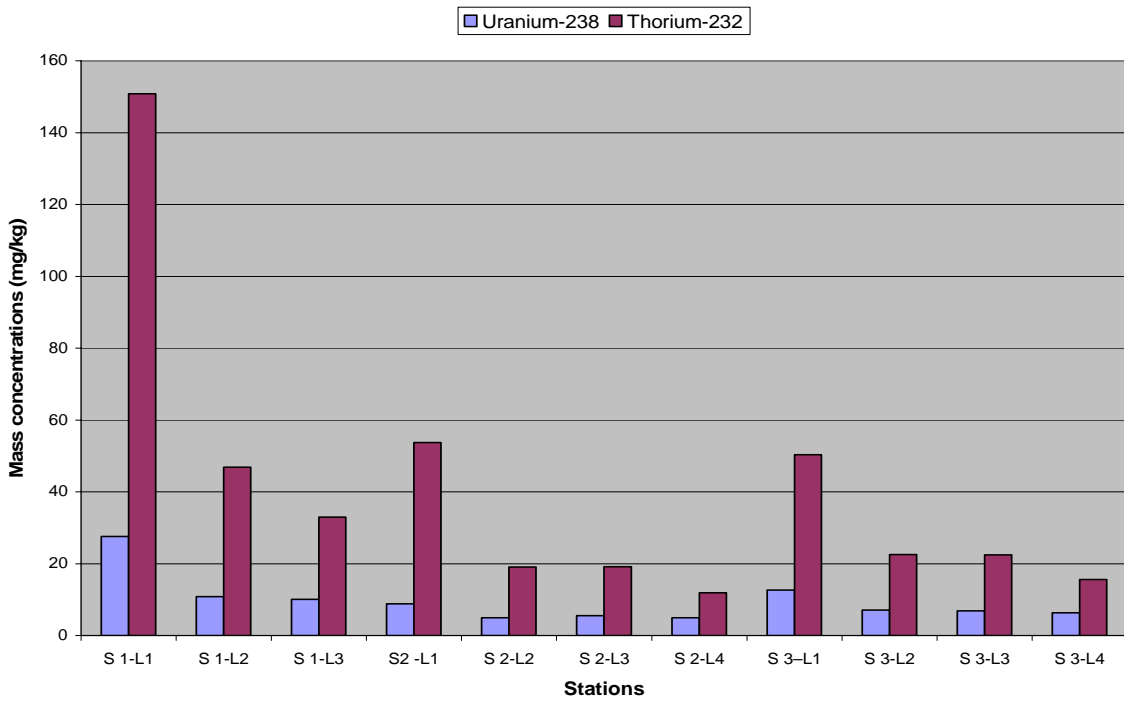
Figure 5. Mass concentrations of U-238 and Th-232 in sediment samples (amang plant 2)

155
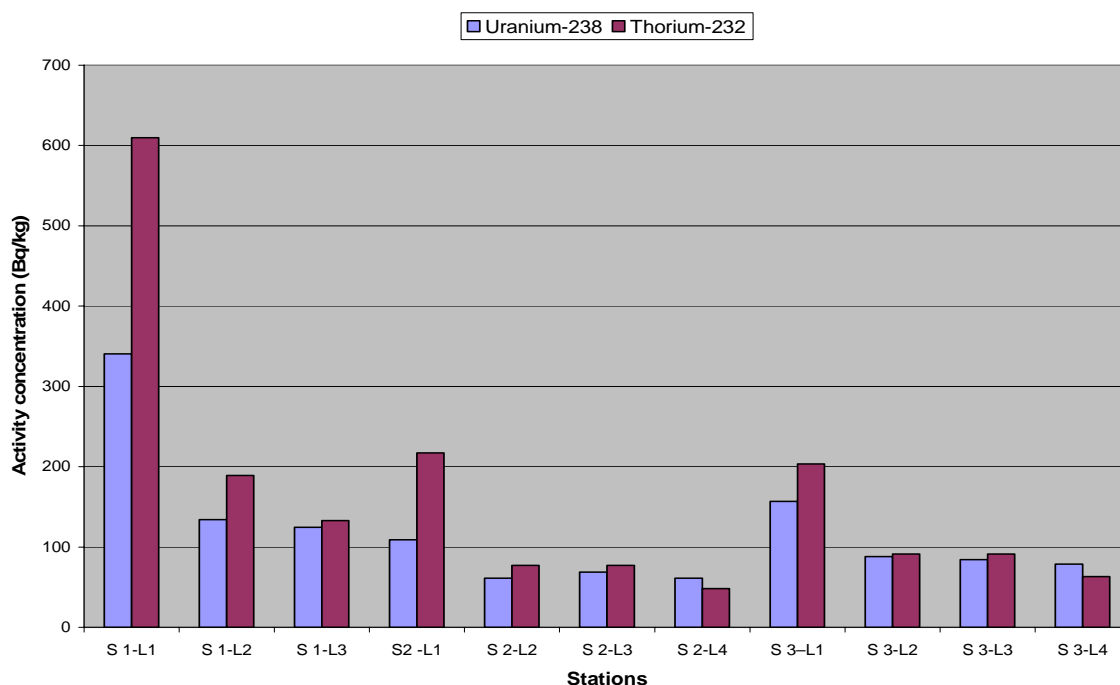
Figure 6. Activity concentrations of U-238 and Th-232 in sediment samples (amang plant 2)

Table 1. Statistical calculations of water and sediment samples

Sample	Sample size	Mean	Std error of mean	Lower 95% Conf limit	Upper 95% conf limit	Minimum	Media (50 percentile)	Maximum
U in Water sample	33	4.34 ppm	0.275	3.785	4.909	0.12 ppm	4.750 ppm	6.64 ppm
Th in water sample	33	0.37 ppm	0.064	0.231	0.501	0.01 ppm	0.331 ppm	1.71 ppm
U in Sediment sample (amang plant 1)	15	18.00 mg/kg	4.533	8.285	27.730	6.82 mg/kg	8.84 mg/kg	69.75 mg/kg
Th in sediment sample (amang plant 1)	15	62.05 mg/kg	10.159	40.261	83.844	26.00 mg/kg	46.80 mg/kg	157.73 mg/kg
U in sediment Sample (amang plant 2)	11	9.62 mg/kg	1.952	5.275	13.975	4.96 mg/kg	7.13 mg/kg	27.59 mg/kg
Th in sediment sample (amang plant 2)	11	40.49 mg/kg	11.882	12.024	66.970	11.920 mg/kg	22.57 mg/kg	150.80 mg/kg

Table 2. Activity concentrations of ^{238}U and ^{232}Th in water collected from 7 amang plant.

Amang Plants/Sample	Uranium-238				Thorium-232			
	Mean ± sem (Bq/L)	Median (Bq/L)	Range (Bq/L)	St. dev.	Mean ± sem (Bq/L)	Median (Bq/L)	Range (Bq/L)	St. dev.
Plant 1								
S1-Point of discharge	56.53±9.645	56.53	46.88-66.17	13.64	1.19±0.27	1.19	0.92-1.46	0.38
S2	46.74±4.680	46.74	42.06-51.42	6.62	0.37±0.15	0.37	0.35-0.38	0.21
Plant 2								
S1-Point of discharge	64.93±1.18	64.93	63.75-66.10	1.66	1.39±0.09	1.39	1.3-1.47	0.12
S2	47.64±2.05	48.11	43.88-50.92	3.54	0.532±0.6	0.51	0.43-0.63	0.10
S3	70.28±4.67	73.21	61.14-76.48	8.09	0.16±0.04	0.12	0.12-0.24	0.07
Plant 3 (pond 1)								
S1-Point of discharge	71.55	71.55	71.55	0.00	2.55	2.55	2.55	0.00
S2	60.44±3.33	60.44	57.11-63.77	4.71	1.89±0.28	1.89	1.61-2.16	0.39
S3	71.17±7.36	71.17	63.82-78.53	10.40	0.8±0.39	0.80	0.41-1.19	0.55
Plant 3 (pond-2)	37.75	37.75	37.75	0.00	1.65	1.65	1.65	0.00
Plant 4								
S1-Point of discharge	20.40	20.40	20.40	0.00	1.33	1.33	1.33	0.00
S2	1952	19.52	19.52	0.00	1.27	1.27	1.27	0.00
Plant 5								
S1-Point of discharge	57.03±7.75	64.00	41.56-65.40	13.42	1.42±0.33	1.46	0.82-1.97	0.58
S2	60.866±1.52	61.31	58.04-63.25	2.63	1.50±0.10	1.47	1.34-1.70	0.18
S3	66.87±5.19	5.19	56.53-72.90	9.0	2.42±0.37	2.77	1.69-2.81	0.64
Plant 6								
S1-Point of discharge	54.61	54.61	54.61	0.00	6.9	6.9	6.9	0.00
S2	34.05	34.05	34.05	0.00	6.07	6.07	6.07	0.00
Plant 7								
S1-Down stream	7.62±	7.62	7.62	0.00	0.12	0.12	0.12	0.00
S2-Up stream	1.48±	1.48	1.48	0.00	0.03	0.03	0.03	0.00

S1-S3 are sampling station, **Sem:** Standard error mean and **St.D:** Standard deviation

The higher uranium-238 and thorium-232 concentrations in water samples collected at down stream relative to upstream, suggested that amang processing enhances their concentrations. In the case of plants employing close water system, such enhancement is expected with every recycling process.

The enhancement of NORM in water may also be attributed to the acidity of the recycling water. Such acidity is caused by the acidic nature of amang [16]. Acid conditions caused the radionuclides to dissolved in water.

Another finding from this study is that, the mean mass and activity concentrations of thorium-232 in all sediment samples (amang plants 1 and 2) were higher than the mass and activity concentrations of uranium-238 in sediment samples (Table 1). However this was the opposite in water samples.

Results from this also showed that average concentrations of uranium-238 and thorium-232 in both water and sediment samples were higher than those measured from areas that were not involved in amang processing or tin mining activities. According to R.M.R. Almedia [6], natural uranium-238 concentration in ground water range from 0.1 to 10 ppb, while in this study the mean maximum concentration in water sample reported was 6.64 ppm (in S8-L1), or 6600 times more than the maximum concentration of uranium-238 in natural ground water. Natural uranium is the only radioactive substance for which chemical toxicity is the limiting factor in risk assessment the maximum contaminant level for uranium is 20 μgl^{-1} [6]. As mentioned mean concentration of uranium-238 in amang water samples was 4.34 ppm, it means the average concentration of uranium in amang water samples was around 220 times more than maximum contamination level of uranium. A. Martin Sanchez [18] reported low concentration of uranium series in water samples in Extramadura (Spain), ranging from 0.024 to 2.69 ppb and most of them were below 1.0 ppb. Likewise the uranium concentration of Slovenian spas area ranged from 0.2 to 2.7 ppb [Kobal, 9]. According to Boyle (1982) the mass concentration of thorium in natural water is around 0.005 – 0.5 ppb. In this study the concentration of thorium-232 in water samples ranged from 0.03 – 1.7 ppm. The maximum mean concentration of thorium-232 in water taken at station S15-L1 was 3400 times higher than those reported by Boyle in ground water. I. G. E. Ibeanu [8], showed that the measured concentration levels of uranium and thorium in tin tailing samples and the measured dose rates in Nigeria were found to be elevated with values up to approximately 100 times above background levels of control soils.

Higher concentrations of uranium-238 and thorium-232 in sediment relative to water observed in this study supported other earlier reports [15, 16]. Higher concentrations of both radionuclides in sediment is attributed to the insolubility of minerals bearing radionuclide in this water, such minerals include monazite, zircon and ilmenite.

Ismail *et al*. [15, 16] and Redzuwan *et al*. [2] carried out similar studies in Perak and Selangor in Malaysia respectively. Ismail *et al* reported uranium-238 and torium-232 mass concentrations ranging from 6.93- 11.45 $mgkg^{-1}$ and 27.72-120.88 $mgkg^{-1}$ respectively. Redzuwan reported activity concentrations of uranium-238 and thorium-232 ranging from 6.27-435.95 $Bqkg^{-1}$ and 12.90-301.59 $Bqk^{-1}g$ respectively. Our finding were in correlations with those of Ismail *et al*. and Redzuwan *et al*. in both the mass and activity concentration of both radionuclides and their differences between uranium-238 and thorium-232.

Conclusion:

Gamma ray spectrometry definitely appeared to be a useful and sensitive method for obtaining actual information on radionuclides in the environments. A total of 33 water samples and 26 sediment samples taken from amang processing plants$^/$ river and ponds where analyzed for uranium-238 and thorium-232 concentrations. Results further confirm other earlier limited studies that amang processing enhances NORM into TENORM. Concentrations of uranium-232 were higher in water than thorium-232.However it was the opposite in sediment. Overall uranium-238 and thorium-232 concentrations were higher in sediment than water indicating the insolubility of these NORM in water and suggesting that they remained in mineral form in the sediment.

Acknowledgment:

References

1. Ismail, B.Y., Othman, M. Soong, H. F., (2000) "Effect of tin dredging on the environmental concentrations of arsenic, chromium and radium-226 in soil and water", *J. Sains nuklear Malaysia*, Vol 18, No1.
2. Redzuwan Yahaya, Ismail Bahari , Amran Ab. Majid, Muhamad Samudi Yasir, Lin Cheng lee, (2002) "The impact of amang processing activity on the water quality and sediment of open water system", 15th Analytical chemistry symposium, Penang, Malaysia.
3. AELB. (1991) "Radiological hazards assessment at mineral processing plants in Malaysia " Atomic energy Licensing Board of Malaysia, LEM/LST/16/pind. 1.
4. M.J. azlina, B.Ismail, M. Samudi Yasir, Syed Hakimi Sakuma, M.K. Khairuddin, (2003)   "Radiological impact assessment of radioactive minerals of amang and ilmenite on future land use using RESRAD computer code, " *J. of Applied radiation and isotopes,* 58, 413-419 .
5. M.J.Azlina , B.Ismail , M. Samudi Yasir , Taiman , K. (2001) "Work activity , radiation dosimeters and external dose measurement in amang processing plant, *j. sains nuclear Malaysia* , vol.19, no 1&2 ,31-39 .
6. R. M.R. Alemedia, D.C. Lauria, A. C. Ferreira, O. Sracek, (2004) " Ground water radon, radium and uranium concentrations in Regiao dos Lagos, Rio de Janerio State, Brazil", *J. of environmental radioactivity,* 73, p. 323-334.
7. J. Al-Jundi, E.Werner, P. Rot, V. Hollriegl, I. Wendler, P.Schramel, (2004) "Thorium and uranium in human urine" , *J. of environmental radioactivity*, 71, p. 61-70.
8. I. G. E. Ibeanu, (2002) "Tin mining and processing in Nigeria: Cause for concern" , *J. of environmental radioactivity*, Vol, 64, Issue 1, P.59-66.
9. Mantazul I, Chowdhury, M. N. Alam, S.K.S.hazari, (1999) "Distribution of radio nuclides in the river sediments and coastal soils of Chttagong , Bangladesh and evaluation of the radiation hazard", *J. Applied radiation and isotopes,* 51, P. 747-755.
10. Mohd Tadza Abdul Rahim, Shamsulbahrin Ludin , Mohd Yusof Harun , Amran Kamarudin , Abdul hamid Latip , Mohd Azwar Hashim , (21-22 June,1994) "Radiological assessment at mineral processing plants in Malaysia " , Radiological hazards in the tin mining and heavy mineral processing , seminar*, Ipoh, Malaysia.
11. W.W.S.Yim, (Aug 1976) "Heavy metals accumulation in estuarine sediments in a historical mining of Cornwall " , M*arine pollution Bulletin* , Vol 7, issue 8, p. 147-150 .
12. Michalis Tzortzis, Haralabos Tsertos, Stelious Christofides, George Christodoulides, (2003)   "Gamma radiation measurement and dose rates in commercially – used natural tiling rocks (granites)", *J. of environmental radioactivity*, 70, p. 223-235.
13. Hu, S.J., Kandaiya, (1985) " Radium 226 and Th 232 concentration ", *J. Health physics*, 49, p. 1003-1007 .
14. Ismail B., Mokhtar M.B. , tan B.H., (1999), " Impact of amang processing on the water quality of an immediate water body : A case of a recycling water system ", *sci. int* . (lahore) 11(1), p 1-4. 19
15. Ismail Bahari, Redzuwan Yahaya , Muhamad Samudi Yasir , Amran Ab. Majid, Lin cheng Lee, (2003) " The impact of open water management system in amang processing on the water quality and ^{238}U and ^{232}Th activity concentration in sediment and water " , *J. of Biological science*, 3(11), p. 1063-1069.
16. B.Ismail , M.S. Yasir, Y. Redzuwan , A.M.Amran, (2003) "Radiological environmental risk associated with different water management system in amang processing in Malaysia" , *Pakistan j. of biological science,* 6 (17), September, p. 1544-1547 .
17. D.Malczewski, L. Teper, J.Dorda, (2004) "Assessment of natural and anthropogenic radioactivity levels in rocks and soils in the environs of Swieradow Zdroj in Sudetes , Poland , by in situ gamma – ray spectrometry", *J. of environmental radioactivity*, 73, P. 233-245.
18. A. Martin Sanchez, F. Vera Tome R. M. Orantos Quintana, V. Gomes Escobar, M. Jurado Vargas, (1995) "Gamma and alpha spectrometry for natural radioactive nuclides in the Spa waters of Extramadua-Spain" *J. of environmental radioactivity*, Vol 28, No. 2, p. 209-220.

AKTIVITI ^{226}Ra DAN ^{228}Ra PADA PERMUKAAN SEDIMEN BAGAN LALANG, SELANGOR

Che Abd Rahim Mohamed[1], Zaharuddin Ahmad[2] dan Nioo Siew Yew[2]

[1]*Pusat Pengajian Sains Sekitaran Dan Sumber Alam, Fakulti Sains Dan Teknologi, Universiti Kebangsaan Malaysia, 43600 Bangi, Selangor, Malaysia*
[2]*Agensi Nuklear Malaysia, Bangi, 43000 Kajang, Selangor, Malaysia*

Key words: ^{226}Ra, ^{228}Ra, sediment

Abstrak

Sebanyak enam stesen sampel sedimen telah dipilih di Sungai Sepang Kecil, Selangor pada bulan Mac, September dan Oktober 2004. Hasil kajian mendapati bahawa terdapat perbezaan yang bererti antara masa persampelan bagi aktiviti ^{226}Ra dan ^{228}Ra (P < 0.01). Purata aktiviti pada bulan Mac mencatatkan nilai tertinggi, iaitu masing-masing dengan aktiviti 161.30 Bq kg^{-1} dan 466.88 Bq kg^{-1} bagi ^{226}Ra dan ^{228}Ra. Manakala aktiviti isotop radium pada bulan September dan Oktober pula masing-masing mencatatkan nilai purata 24.77 Bq kg^{-1} dan 69.22 Bq kg^{-1} bagi ^{226}Ra serta 73.13 Bq kg^{-1} dan 1284.58 Bq kg^{-1} bagi ^{228}Ra. Kesan Monsun Timur Laut mungkin merupakan faktor yang mendorong aktiviti isotop radium yang lebih tinggi ketika persampelan bulan Mac. Hasil kajian memperolehi bahawa sedimen di Bagan Lalang adalah jenis berpasir dan mempunyai variasi saiz yang terhad. Di samping itu, didapati bahawa isotop radium adalah lebih terjerap dengan sedimen yang bersaiz antara 63 – 125 µm yang biasanya mengandungi kandungan feldspar alkali yang tinggi.

Abstract

Six stations had selected from Sungai Sepang Kechil, Selangor during Mac, September and October 2004 for sediment analysis. The results showed a significant difference among the ^{226}Ra and ^{228}Ra activities (P < 0.01) with sampling period. The highest activities of ^{226}Ra and ^{228}Ra have obtained during the sampling on Mac, which show the average activities 161.30 Bq kg^{-1} and 466.88 Bq kg^{-1}, respectively. Meanwhile, ^{226}Ra activities obtained on September and October are in the average of 24.77 Bq kg^{-1} and 69.22 Bq kg^{-1}, respectively. Average activities of ^{228}Ra are 73.13 Bq kg^{-1} and 1284.58 Bq kg^{-1}, respectively for September and October. Northeast Monsoon effect might cause the higher activities of radium isotopes during sampling on Mac. Sediments from Bagan Lalang are sandy type with a limited size variation. Furthermore, radium isotopes are more adsorbed on the particles sediments between size 63 – 125 µm, which usually rich in alkaline feldspar.

Pegenalan

Sifat radiologi isotop radium yang membahayakan kesihatan awam merupakan salah satu faktor ia sering kali dikaji oleh para saintis. Di samping itu, setengah hayat isotop radium semulajadi (^{223}Ra, ^{224}Ra, ^{226}Ra dan ^{228}Ra) yang berbeza dari beberapa hari hingga 1600 tahun mencetuskan ia sesuai digunakan sebagai penyurih semulajadi dalam pelbagai bidang seperti proses percampuran dalam sistem akues serta kajian kronologi dalam lautan dan tasik [1].

Selain itu, hubungan antara isotop-isotop radium juga sesuai untuk mengkaji fluks dan kadar percampuran air daripada daratan dengan air laut dan estuari serta menyiasat pertukaran antara air bawah tanah dengan air permukaan [2, 3]. Manakala perubahan pekali jerapan (adsorption coefficient) di antara radium dengan air tawar dan air masin telah mengakibatkan radium terikat kuat dengan butiran sedimen dalam air tawar, malah cenderung terlarut dalam air masin. Keadaan ini disebabkan oleh radium lebih cenderung terjerap dalam bahan terampai dengan kekuatan ionik meningkatkan dan kepekatan partikel menurun. Oleh yang demikian, keterlarutan radium adalah lebih tinggi di kawasan estuari dan persisir pantai [4]. Tujuan kajian ini dilakukan adalah untuk melihat taburan aktiviti isotop ^{226}Ra dan ^{228}Ra di permukaan sedimen kawasan Bagan Lalang, Selangor serta mengkaji kesan saiz partikel terhadap isotop radium.

Bahan dan Kaedah

Lokasi kajian dan persampelan

Pantai Bagan Lalang terletak berdekatan dengan kawasan Lembah Kelang dan diperkenalkan oleh Kerajaan Selangor pada tahun 1990-an [5]. Projek "Sepang Gold Coast" dan "Sepang Water City" yang diperkenalkan oleh Permodalan Negeri Selangor Berhad (PNSB) dijangka akan menggunakan tanah seluas 4621 ekar, iaitu pinggir Sungai Sepang Kecil dan Sungai Sepang Besar serta pinggir pantai Bagan Lalang hingga ke Tanjung Sepat [6]. Oleh yang demikian, salah satu sebab kajian ini dilakukan di Sungai Sepang Kecil adalah untuk menghasilkan satu data pangkalan sebelum ia diperbangunkan.

Sebanyak tiga kali persampelan (Jadual 1) dijalankan di enam stesen yang ditentukan seperti yang ditunjukkan dalam Rajah 1 dan Jadual 1. Sungai Sepang Kecil dipilih sebagai kawasan kajian kerana ia dapat memaparkan sistem aliran yang membezakan antara air payau dengan air laut.

Jadual 1. Stesen-stesen persampelan sedimen di sekitar Sungai Sepang Kecil, Bagan Lalang.

Stesen	Kod	Latitud (U)	Longitud (T)
1	BL1	02°36'55''	101°41'07''
2	BL2	02°36'35''	101°40'20''
3	BL3	02°36'30''	101°39'19''
4	BL4	02°36'05''	101°38'05''
5	BL5	02°36'11''	101°36'56''
6	BL6	02°36'06''	101°35'38''

Sampel sedimen permukaan dasar laut diambil pada setiap stesen kajian dengan *Ponar Grab*. pH setiap sampel diukur dengan pH meter (model 210Aplus, *Thermo Orion*) di lapangan. Seterusnya, sampel sedimen disimpan dalam beg plastik dan dibawa ke makmal untuk analisis lanjutan.

Analisis kajian

Ketika di makmal, sampel sedimen dikeringkan dengan ketuhar pada suhu 60°C. Porositi (Φ) sampel sedimen dicatatkan. Seterusnya ketumpatan sedimen dikira dengan menggunakan persamaan 1(7)
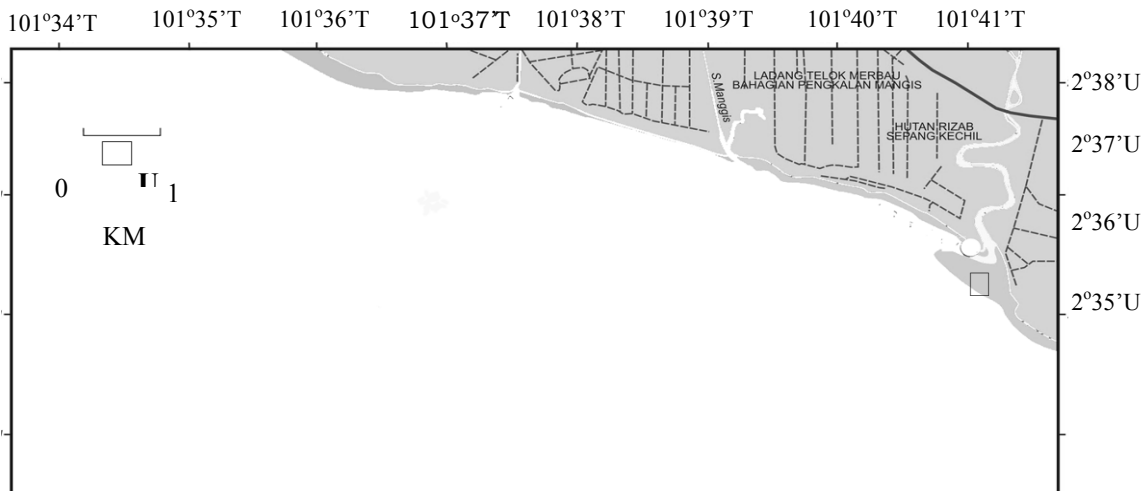
Rajah 1. Stesen kajian di Bagan Lalang, Selangor

$$\text{Ketumpatan sedimen } \rho_S = \frac{2.6}{1 - \Phi} \qquad (1)$$

Seterusnya, sampel sedimen kering ditumbuk dengan menggunakan mortar dan diayak dengan pengayak elektronik bagi menentukan partikel saiz sedimen. Diameter (*d*) sampel sedimen yang bersaiz: $125 < d < 250$ μm, $63 < d < 125$ μm dan $d < 63$ μm disimpan untuk analisis yang seterusnya. Pengelasan partikel sedimen dilakukan

menggunakan skala Wentworth. Skala ini digunakan secara meluas dan partikel saiz sedimen ditukar kepada unit phi (Ø) (8).

$$\Phi = - \log_2 mm \qquad (2)$$

Pengukuran statistik yang lazim digunakan dalam skala Wentworth adalah:

$$\text{Purata } \overline{x} = \frac{\Phi16 + \Phi50 + \Phi84}{3} \qquad (3)$$

$$\text{Ralat } \sigma = \frac{\Phi84 - \Phi16}{4} + \frac{\Phi95 - \Phi5}{6.6} \qquad (4)$$

$$\text{Skewness (sk)} = \frac{\Phi16 + \Phi84 - 2\Phi50}{2(\Phi84 - \Phi16)} + \frac{\Phi5 + \Phi95 - 2\Phi50}{2(\Phi95 - \Phi5)} \qquad (5)$$

Sampel sedimen kering dicerna dengan asid hidroklorik. Lebih kurang 1 g sampel sedimen dimasukkan ke dalam bikar kaca bersama dengan 1 ml pembawa Ba^{2+} dan 20 ml 8 M asid hidroklorik ditambahkan. Campuran ini ditutup dengan penutup kaca dan dipanaskan atas piring pemanas selama 2 – 3 jam. Seterusnya, hasil hadaman dibiar sejuk dan dituras dengan kertas turas yang berdiameter 47 mm dengan saiz liang 0.45 µm (G/FC filter, Whatman). Hasil turasan dikeringkan atas piring panas. Bahan yang tertinggal dalam bikar dilarutkan dengan lebih kurang 50 ml asid perklorik 1% untuk proses penulenan radium.

Radium ditulenkan dengan menggunakan turus pemisah kation AG 50W-X4 Resin (200-400 mesh, Bio-rad). Di mana sampel (≈ 50 ml) dialir dalam turus pemisah kation untuk penulenan. Kemudiannya, 200 ml asid hidroklorik 1.5 M dialirkan melalui turus. Efluen disimpan dalam bikar dan dikeringkan atas plat pemanas. Hasil pengeringan dilarutkan dengan asid nitrik 0.5 M (≈ 100 ml). Seterusnya, 2 ml asid sulfurik pekat ditambahkan. Mendakan barium sulfat ($BaSO_4$) yang terbentuk dituraskan dengan mengguna kertas turas berdiameter 25 mm (GF/C, Whatman). Berat bersih $BaSO_4$ dicatatkan untuk mendapatkan perolehan semula kimia sampel. Seterusnya, $BaSO_4$ diletakkan atas disk *stainless steel* dan dilabut dengan kertas plastik. Disk yang disiap balut dibilang dengan Spektrometer Gross Alfa/Beta (model LB5100-W, Tennelec) setelah keseimbangan sekular radium dengan anak-anaknya dapat dicapai (dibiarkan selama tiga bulan).

Hasil dan Perbincangan

Taburan isotop radium pada permukaan sedimen

Rajah 2 menunjukkan taburan isotop radium pada permukaan sedimen di Bagan Lalang. Stesen 4 terletak pada mulut muara sungai mencatatkan aktiviti ^{226}Ra dan ^{228}Ra tertinggi pada bulan September dan Oktober. Hal sedemikian mungkin disebabkan oleh pengumpulan partikel sedimen yang dibawa dari sungai (semasa air surut) serta laut (semasa air pasang). Partikel sedimen yang terkumpul mungkin mengalami penjanaan semula dan mengakibatkan aktiviti radium pada permukaan sedimen yang tinggi di Stesen 4. Oleh sebab ^{228}Ra mempunyai setengah hayat yang pendek (5.75 tahun), jadi penjanaan semula bagi aktiviti ^{228}Ra adalah lebih cepat ($\cong$ 280 kali) berbanding ^{226}Ra. Maka, nisbah aktiviti $^{228}Ra/^{226}Ra$ di Stesen 4 juga tinggi, iaitu lebih kurang lima.

Manakala taburan aktiviti isotop radium pada permukaan sedimen pada bulan Mac 2004 adalah hampir sekata, kecuali aktiviti ^{228}Ra yang abnormal (870 Bq kg^{-1}) di Stesen 6. Faktor yang menyumbangkan aktiviti ^{228}Ra yang tinggi di Stesen 6 adalah tidak jelas.

Aktiviti isotop 226Ra dan 228Ra (P < 0.01) pada permukaan sedimen pula menunjukkan perbezaan yang sangat bererti dengan masa persampelan. Rajah 3 memaparkan taburan aktiviti isotop radium pada permukaan sedimen mengikut masa peersampelan. Hasil kajian mendapati bahawa purata aktiviti 226Ra dan 228Ra adalah maksimum pada persampelan bulan Mac, iaitu masing-masing dengan purata aktiviti 161.30 Bq kg-1 dan 466.88 Bq kg-1. Manakala aktiviti isotop radium pada bulan September dan Oktober adalah lebih rendah, iaitu dengan masing - masing mencatatkan nilai purata 24.77 Bq kg^{-1} dan 69.22 Bq kg^{-1} bagi ^{226}Ra serta 73.17 Bq kg^{-1} dan 184.58 Bq kg^{-1} bagi ^{228}Ra.
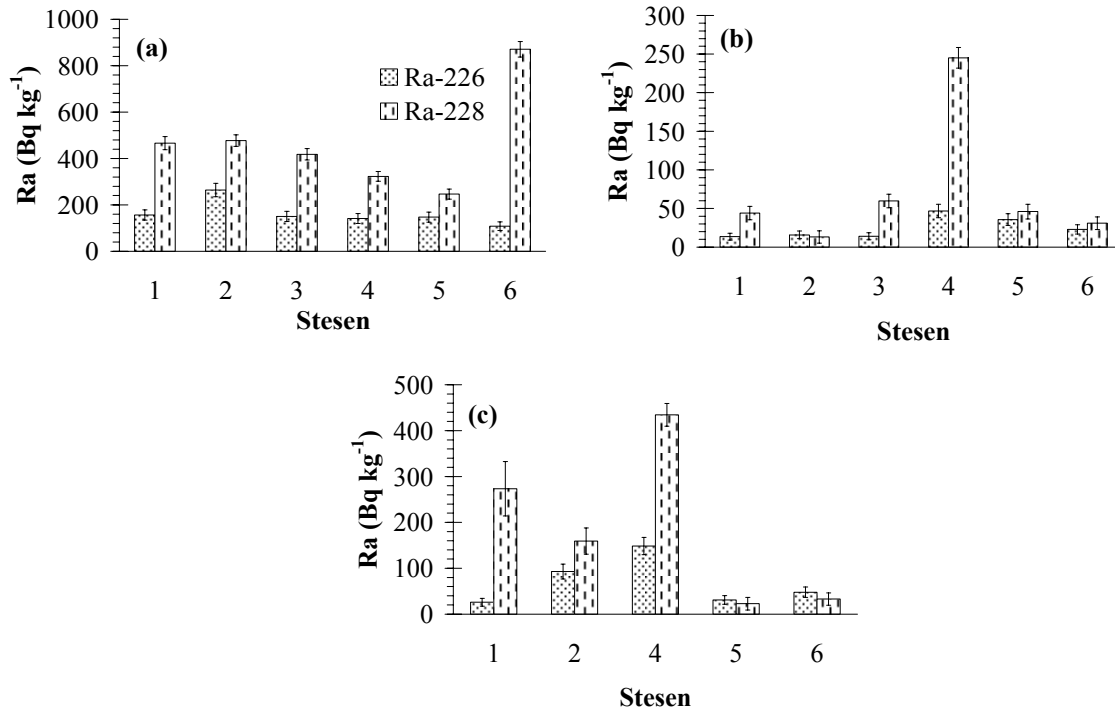
Rajah 2. Taburan ^{226}Ra dan ^{228}Ra pada permukaan sedimen ketika persampelan bulan (a) Mac, (b) September, dan (c) Oktober.
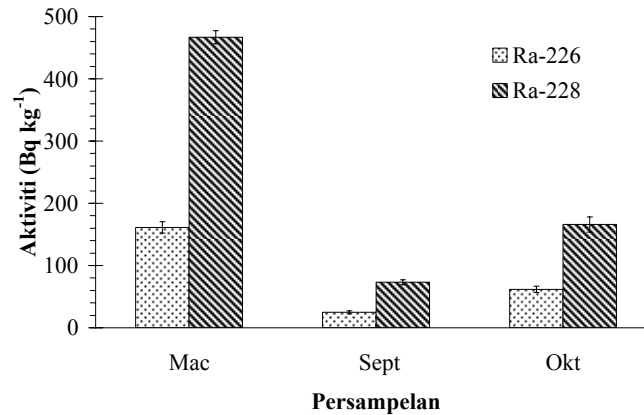
Rajah 3 Purata aktiviti ^{226}Ra dan ^{228}Ra pada permukaan sedimen mengikut masa persampelan.

Pantai barat Semenanjung Malaysia mengalami musim hujan ketika Monsun Timur Laut (Mac). Partikel sedimen dari daratan dan sungai turut dibawa oleh air hujan ke estuari dan lautan. Justeru itu, terdapat input tambahan bagi aktiviti isotop radium pada permukaan sedimen. Jadi, aktiviti isotop radium pada bulan Mac adalah lebih tinggi berbanding dengan persampelanpada bulan September dan Oktober.

Kesan partikel saiz sedimen terhadap isotop radium
Jadual 2 menunjukkan partikel saiz dan jenis sedimen bagi ketiga-tiga persampelan. Secara keseluruhannya, permukaan sedimen Bagan Lalang dikelaskan dalam kumpulan pasir. Purata saiz sedimen ($\overline{x}$) adalah daripada saiz -0.83Ø (pasir sangat kasar) hingga 3.12 Ø (pasir sangat halus). Ralat partikel sedimen (σ) yang besar merujuk kepada pengelasan sedimen Bagan Lalang adalah kurang baik, iaitu variasi partikel saiz sedimen yang diangkut atau termendak adalah kurang.

Jadual 2 Pengelasan sedimen di Bagan Lalang.

Stesen	Purata saiz ($\overline{X}$), Φ	Ralat (σ)	Skew (*sk*)	Porositi (Φ)	pH	Kelas sedimen
			Mac			
1	1.95	0.84	0.18	0.41	9.51	Pasir sederhana
2	2.18	1.44	-0.16	0.52	8.65	Pasir halus
3	2.13	0.64	0.07	0.74	8.76	Pasir halus
4	-0.60	1.23	-0.39	0.83	8.36	Pasir sangat kasar
5	0.26	0.63	-0.32	0.81	5.58	Pasir kasar
6	-0.43	0.60	-0.19	0.84	4.11	Pasir sangat kasar
			September			
1	1.91	1.98	-0.23	0.54	7.06	Pasir sederhana
2	1.67	0.54	-0.17	0.76	7.18	Pasir sederhana
3	0.32	0.61	0.19	0.81	7.58	Pasir kasar
4	-0.83	0.90	0.21	0.77	7.54	Pasir sangat kasar
5	-0.28	0.90	-0.28	0.81	7.98	Pasir sangat kasar
6	-0.54	0.85	0.55	0.83	7.94	Pasir sangat kasar
			Oktober			
1	1.169	1.85	0.39	0.29	6.72	Pasir sederhana
2	1.09	2.20	0.05	0.39	7.22	Pasir sederhana
4	-0.67	1.29	-0.11	0.78	7.60	Pasir sangat kasar
5	-0.54	1.20	0.02	0.84	7.73	Pasir sangat kasar
6	0.01	0.75	-0.18	0.81	7.83	Pasir kasar

Nilai skewness (*sk*) pula digunakan sebagai penunjuk bagi sejarah taburan partikel saiz sedimen. Sampel yang mempunyai nilai *sk* yang positif menunjukkan bahawa stesen tersebut mengandungi lebihan partikel yang halus. Sumber kemasukan partikel halus ini mungkin disebabkan oleh peningkatannya partikel halus yang termendak ataupun partikel yang kasar telah terpindah daripada stesen tersebut. Manakala bagi sampel yang mempunyai nilai *sk* yang negatif merujuk kepada pemendakan partikel kasar telah berlaku di kawasan tersebut. Faktor yang mendorong kepada perubahan nilai sk adalah angin dan kesan ombak (8).
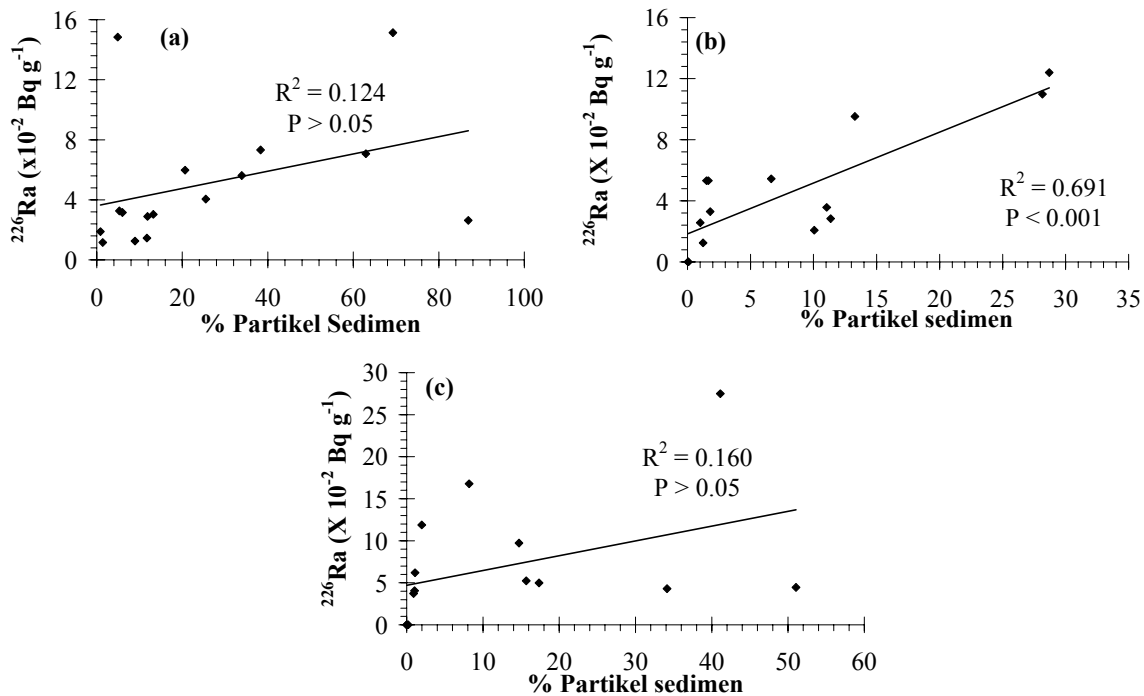
Rajah 4: Kolerasi aktiviti ^{226}Ra dalam sedimen Bagan Lalang dengan peratusan partikel sedimen dengan saiz partikel (a) +2<Ø<+3, (b) +3<Ø<+ 4, dan (c) Ø>+4.

Rajah 4 dan 5 memaparkan kesan saiz partikel terhadap isotop radium. Hasil kajian mendapati bahawa aktiviti [226]Ra ($P < 0.01$) dan [228]Ra ($P < 0.05$) lebih terjerap dalam partikel sedimen bersaiz +3<Ø<+ 4 (63-125μm). Menurut Zhang et al (9), logam alkali bumi, iaitu barium dan strontium (mempunyai sifat yang menghampiri dengan radium) juga menunjukkan kolerasi possitif degan partikel saiz yang lebih kasar. Keadaan ini mungkin disebabkan oleh feldspar alkali yang biasanya wujud dalam partikel yang lebih kasar mengandungi unsur barium, strontium, rubidium dan cesium yang tinggi (10).
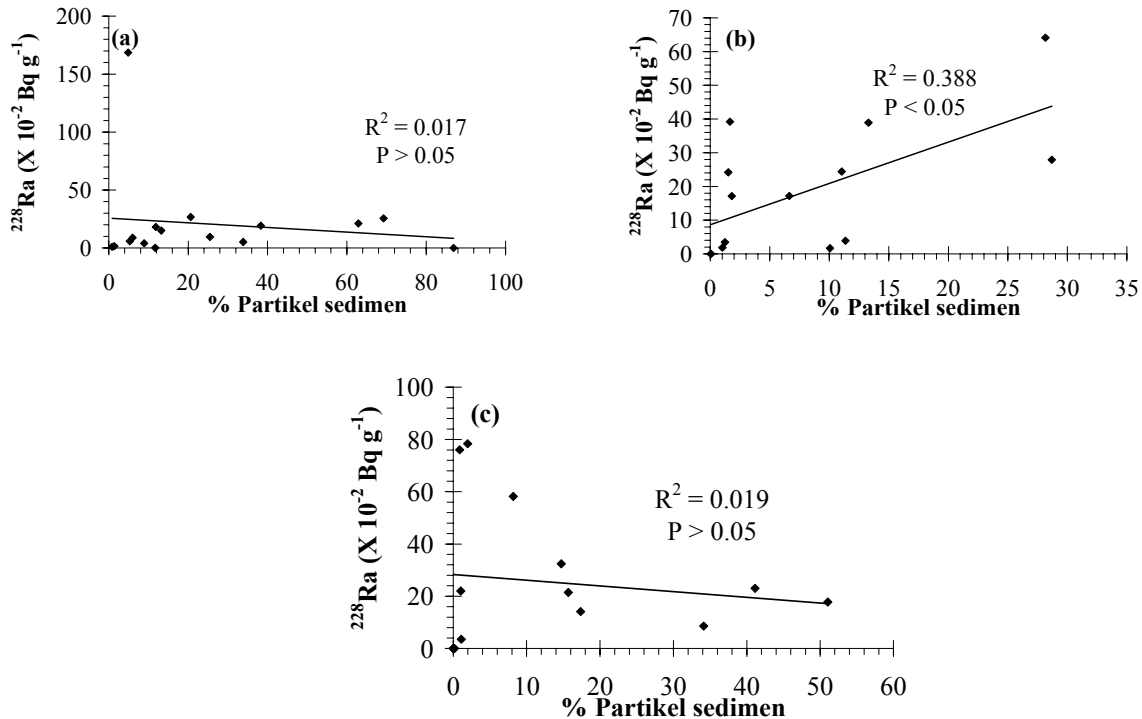
Rajah 5. Kolerasi aktiviti [228]Ra dalam sedimen Bagan Lalang dengan peratusan partikel sedimen dengan saiz partikel (a) +2<Ø<+3, (b) +3<Ø<+ 4, dan (c) Ø >+4.

Kesimpulan

Secara kesimpulannya, aktiviti isotop radium pada permukaan sedimen adalah lebih tinggi ketika musim hujan. Air hujan merupakan agen pembawa partikel sedimen yang mengandungi isotop radium dari daratan dan sungai ke estuari dan lautan. Sampel sedimen di Bagan Lalang dikelaskan sebagai jenis berpasir dengan mengandungi variasi saiz yang kurang. Di samping itu, aktiviti isotop radium juga boleh disimpulkan bahawa ia lebih terjerap dalam partikel yang bersaiz 63 – 125 μm yang biasanya mengandungi kandungan feldspar alkali yang tinggi.

Penghargaan

Rujukan

1. Kim, Y.J., Kim, C.K., Kim, C.S., Yun, J.Y., Rho, B.H. 1999. Determination of [226]Ra in environmental samples using high-resolution inductively coupled plasma mass spectrometry. *J. Radioanal. Nucl. Chem.* **240**: 613-618.
2. Nour, S., El-Sharkawy, A., Burnett, W.C., Horwitz, E.P. 2004. Radium-228 determination of natural waters via concentration on manganese dioxide and separation using Diphonix ion exchange resin. *Appl. Radiat. Isot.* **61**: 1173-1178.
3. Eikenberg, J., Tricca, A., Vezzu, G., Stille, P., Bajo, S., Ruethi, M. 2001. [228]Ra/[226]Ra/[224]Ra and [87]Sr/[86]Sr isotope relationships for determining interactions between ground and river water in the upper Rhine Valley. *J. Environ. Radioact.* **54**: 133-162.
4. Rama, Moore, W.S. 1996. Using the radium quartet to estimate water exchange and ground water input in salt marshes. *Geochim. Cosmochim. Act*. **60**: 4645-4652.
5. Dharmender, S. 2003. Rare sights at Bagan Lalang. http://www.allmalaysia.info/news/story. (17 Januari 2005).
6. Sepang Gold Coast dan Sepang Water City. (atas talian) http://www.pnsb.com.my/n_jan03.htm. (17 Januari 2005).
7. DiToro, D.M. 1999. *Sediment Flux Modelling*. New York: John Wiley & Sons.

8. Pethick, J. 1984. *An introduction to coastal geomorphology*. London: Edward Arnold.
9. Zhang, C., Wang, L., Li, G., Dong, S., Yang, J., Wang, X. 2002. Grain size effect on multi-element concentrations in sediments from the intertidal flats of Bohai Bay, China. *Appl. Geochem.* **17**: 59-68.
10. Gotze, J. 1998. Geochemistry and provenance of the Atlendrof feldspathic sandstone in the Middle Bunter of the Thuringian basin (Germany). *Chemical Geol.* **150**: 43-61.

ANALISIS UNSUR DAN KERADIOAKTIFAN DALAM SAMPEL SEDIMEN TASIK CHINI, PAHANG DARUL MAKMUR

Amran Ab.Majid*, Siti Rahimah Umar, Redzuwan Yahaya, Muhamad Samudi Yasir
dan Mohd Suhaimi Othman

Program Sains Nuklear, Fakulti Sains dan Teknologi, Universiti Kebangsaan Malaysia,
43600 Bangi, Selangor Darul Ehsan

Abstrak

Kajian taburan unsur dan keradioakifan dalam sampel sedimen dari 12 lokasi Tasik Chini telah dilakukan menggunakan teknik spektrometri gama dan analisis pendarfluor sinar-X (XRF). Sebanyak dua belas unsur surih iaitu As, Ba, Co, Cr, Cu, Ni, Pb, Rb, Sr, V, Zn, Zr, tiga unsur radionuklid tabii iaitu ^{40}K, ^{238}U, ^{232}Th dan satu unsur radionuklid buatan iaitu ^{137}Cs telah dapat dikesan dalam sampel sedimen. Keputusan yang diperolehi menunjukkan nilai kepekatan unsur surih adalah berbeza mengikut lokasi persampelan dan ketiga-tiga radionuklid tabii menunjukkan hampir semua stesen mempunyai kepekatan melebihi had purata dunia dalam tanah. Radionuklid ^{137}Cs telah ditemui di lima stesen tetapi secara kualitatif sahaja. Secara umumnya, kepekatan unsur di setiap stesen berkait rapat dengan aktiviti yang terdapat di stesen masing-masing. Kajian menunjukkan bahawa stesen Laut Jemberau yang terletak berhampiran dengan bekas kawasan perlombongan dan pelbagai gunatanah menunjukkan lokasi yang mengandungi kepekatan unsur As, Co, Cr, Cu, Pb, V dan Zn tertinggi berbanding lokasi lain.

Pengenalan

Tasik Chini merupakan tasik semulajadi yang kedua terbesar di Malaysia, di mana ia berada dalam persekitaran asal. Ianya terletak di Mukin Penyur, Pekan, Pahang Darul Makmur pada kedudukan 3°26'-102°55'. Jaraknya dari Kuantan adalah lebih kurang 100 km. Tasik Chini merupakan tasik yang berpola dendritik (berbentuk ranting) dengan keluasan 150 hektar atau 12 km^2. Sekitaran Tasik Chini ini dikelilingi oleh hutan tropika. Namun kebanyakan kawasan telah dibalak dan kini ia telah menjadi hutan sekunder dan terdapat juga banyak berlakunya gunatanah di kawasan sekitar Tasik Chini seperti sebagai pusat pelancongan dan pertanian komersil. Malahan terdapat juga bekas kawasan perlombongan di sekitar Tasik Chini. Tasik Chini dijadikan lokasi kajian kerana ia merupakan tasik semulajadi yang menjadi kawasan penempatan penduduk orang asli di mana kawasan tersebut menjadi sumber bekalan air [1,2]. Oleh yang demikian, terdapat satu inisiatif untuk mengkaji kesan aktiviti yang berlaku ini dengan menganalisis unsur dan keradioaktifan di kawasan sekitar Tasik Chini. Ia bertujuan melihat samada pembangunan yang dijalankan ini boleh mengakibatkan pencemaran di kawasan sekitar Tasik Chini ataupun tidak. Jadi dengan menganalisis sedimen dapat memberi gambaran tahap pencemaran air yang boleh mengakibatkan pencemaran logam berat dan dapat mengkaji perkaitan antara kepekatan unsur dengan lokasi persampelan. Sedimen merupakan dasar atau tapak bagi sesebuah tasik di mana ia merupakan perhentian terakhir unsur dan radionuklid serta pemberi "maklumat" terbaik mengenai lokasi kajian. Dalam kajian ini, sedimen Tasik Chini dari pelbagai lokasi telah dianalisis kandungan unsur dan keradioaktifannya menggunakan dua teknik analisis iaitu analisis pendarfluor sinar-X (XRF) dan spektroskopi sinar gama.

Eksperimen

Lokasi Kajian

Sebanyak 15 sampel sedimen telah diambil dari 12 lokasi persampelan di sekitar Tasik Chini pada bulan Mei 2004 seperti yang ditunjukkan dalam Rajah 1.

Pengumpulan Sampel

Sampel sedimen di setiap stesen diambil menggunakan pensampel sediment secara kaut (Ekman). Alat pensampel sediment diturunkan perlahan-lahan menggunakan tali dari bot dengan mulut pengautnya terbuka. Apabila sampai di dasar tasik, satu alat penghentak dilurutkan turun melalui tali dan menyebabkan mulut pengaut ini tertutup dan memerangkap sedimen di dasar.
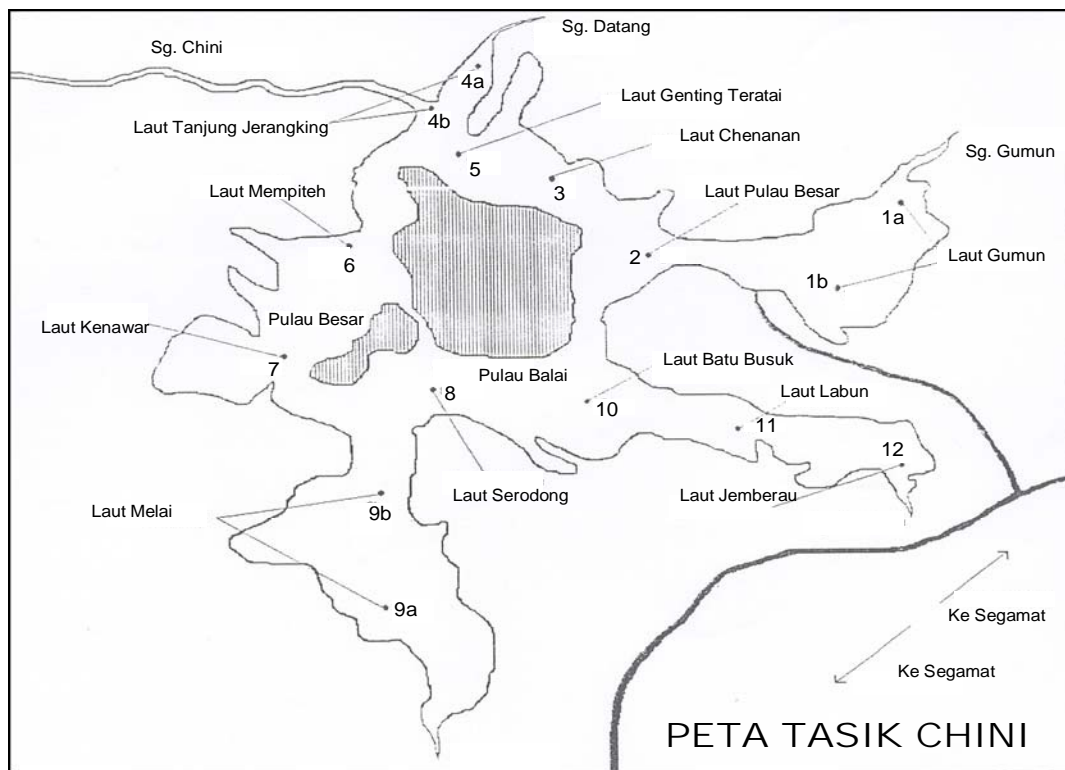
Rajah 1: Peta lokasi persampelan sediment Tasik Chini

Penyediaan dan Rawatan Sampel.

Semua sampel dimasukkan ke dalam dulang dan dibersihkan dari bendasing yang nyata dan berat basahnya dicatat. Sampel sediment kemudian dikeringkan pada suhu 105°C semalaman. Setelah sampel sejuk berat keringnya ditentukan. Sampel kemudiaannya dihancurkan dengan menggunakan mortar dan ditapis menggunakan penapis bersaiz 0.5 mm.

Penyediaan Sampel untuk Teknik Pendarfluor Sinar-X

Semua sampel sedimen yang telah dihancurkan dan ditapis, perlu ditumbuk halus dan dihomogenkan. Sebanyak 1.00 g sampel sedimen dimasukkan ke dalam radas pembuat pelet dengan ditambahkan asid borik sebanyak 6.00 g sebagai pengikat pelet. Setelah itu, sampel bersama asid borik yang dicampurkan tadi diberi tekanan sebanyak 5 tons dan 15 tons untuk mendapatkan palet tertekan yang baik. Pada bahagian belakang palet dilabelkan mengikut stesen masing-masing. Palet seterusnya dimasukkan ke dalam alat pendarfluor sinar-X iaitu Spektrometer PW 1480 (Philips) untuk dianalisis kandungan unsurnya. Bahan piawai yang digunakan adalah basalt.

Penyediaan Sampel untuk Teknik Analisis Keradioaktifan.

Sebanyak 15 sampel yang diketahui berat masing-masing dimasukkan ke dalam botol pembilang kedap udara dan disimpan selama 30 hari bagi mencapai keseimbangan sekular. Analisis keradioaktifan dalam sampel sedimen ditentukan dengan menggunakan sistem spektrometri gama yang terdiri daripada pembilang gama HPGe (Tennelec) dan penganalisis multisalurann berasaskan komputer peribadi untuk analisis keradioaktifan. Kandungan keradioaktifan dalam sampel ditentukan secara kaedah bandingan menggunakan Bahan Rujukan Piawai (SRM) *Soil*-375 (IAEA) sebagai piawai. Masa pembilang sampel dan piawai adalah selama 12 jam.

Hasil Dan Perbincangan

Keputusan Analisis Unsur

Keputusan analisis kandungan unsur dalam sampel sedimen Tasik Chini menggunakan teknik pendarfluor sinar-X ditunjukkan dalam Jadual 1. Daripada keputusan analisis, sebanyak 12 unsur telah dikesan dalam sampel sedimen Tasik Chini yang terdiri daripada As, Ba, Co, Cr, Cu, Ni, Pb, Rb, Sr, V, Zn dan Zr.

Jadual 1 : Keputusan analisis unsur bagi setiap stesen persampelan

	Stesen	Kepekatan (ppm)											
		As	Ba	Co	Cr	Cu	Ni	Pb	Rb	Sr	V	Zn	Zr
1a	Laut Gumun	21	571	20	92	43	125	67	119	75	134	326	226
1b	Laut Gumun	14	888	26	87	57	128	50	136	18	134	1145	290
2	Laut Pulau Balai	15	557	LOD	90	60	157	76	132	101	130	147	208
3	Laut Chenanan	13	553	LOD	99	66	78	65	105	59	142	260	190
4a	L. Tanjung Jerangking	12	714	22	95	11	143	48	128	99	139	693	225
4b	Laut Tanjung Jerangkin	17	603	26	87	44	149	39	133	100	130	329	235
5	Laut Genting Teratai	15	630	LOD	96	60	101	38	119	78	127	321	201
6	Laut Mempiteh	13	714	15	96	60	141	44	131	93	147	645	227
7	Laut Senawar	11	824	26	96	20	189	37	138	113	126	655	249
8	Laut Serodong	13	944	24	98	49	145	46	129	98	148	948	274
9a	Laut Melai	17	582	LOD	85	68	186	56	149	127	117	488	230
9b	Laut Melai	15	831	35	82	LOD	151	61	120	88	117	1130	284
10	Laut Batu Busuk	13	651	25	83	55	146	83	131	92	105	1097	211
11	Laut Labun	18	555	8	87	54	193	59	146	104	93	1032	209
12	Laut Jemberau	50	782	46	113	68	67	156	109	23	156	1679	221
	Min	17±10	693 ±132	18±14	92±8	48±21	140±37	62±30	128±2	85±31	130±17	726±434	232±0
	Had pengesan (LOD)	0.5	2	1	2	1	1	1	0.5	0.5	1	1	0.5

LOD – di bawah had pengesanan

Keputusan kajian menunjukkan bahawa setiap unsur mempunyai kepekatan yang berbeza bagi setiap lokasi persampelan. Secara amnya keputusan mendapati Laut Jemberau mempunyai kepekatan yang paling tinggi bagi unsur As, Co, Cr, Cu, Pb, V dan Zn dengan kepekatan masing-masing unsure sebesar 50, 46, 113, 68, 156, 156 dan 1679 ppm. Dua bekas lombong besi dan barit serta kedudukanyan yang berdekatan dengan Laut Gumun dan terdapatnya kawasan pelancongan Tasik Chini, pembukaan FELDA, penempatan dan yang terbaru ialah Pusat Latihan Khidmat Negara dipercayai menyumbang terhadap kandungan unsur yang tinggi ini. Hal ini menunjukkan sememangnya perlombongan dan pembangunan yang terdapat di sekitar lokasi persampelan mempengaruhi kepekatan unsur dan keputusan ini mempamerkan sedimen boleh bertindak sebagai sinki kepada pencemaran akuatik sebagaimana yang dilaporkan oleh Mouhi et.al [3].

Kajian para penyelidik Kanada di Tasik Killarney, Canada mendapati sampel dari kawasan perindustrian mempunyai unsur-unsur kadmium, kuprum, plumbum, nikel dan zink manakala pada kawasan yang masih lagi terpelihara terdapat unsur-unsur ferum, mangan, arsenik dan kobalt [4]. Kajian lain pula melaporkan arsenik biasanya ditemui dalam sedimen tasik dengan kepekatan 1-15 ppm [5]. Menurut Fytianos dan Laurantou [6] dalam kajiannya terhadap sampel sedimen di Tasik Volvi dan Koronia di Greece terdapat tujuh unsur yang dapat dikesan iaitu kadmium, plumbum, kromium, kuprum, mangan, zink dan ferum. Sampel ini diambil di dua keadaan cuaca yang berbeza dan kedua-dua tasik ini merupakan tasik yang masih belum tercemar.

Krumgalz dan Fainshtein (1991) [7] pula melaporkan sedimen bagi kawasan Haifa Bay yang berdekatan dengan kawasan perindustrian dan perbandaran menunjukkan terdapat pengumpulan merkuri, plumbum, zink, kadmium, ferum dan kuprum. Kuprum, zink, plumbum dan kadmium juga ditemui dalam sedimen Kenyan Coast. Kajian oleh Mouhi et.al [3] juga mendapati kawasan persampelan sediment Makupa yang berdekatan dengan kawasan perindustrian dan pelupusan sampah tinggi kandungan unsur. Sebagai contoh mereka mendapati kepekatan (ppm) masing-masing kupram, zink, plumbum dan kadmium adalah setinggi 102.0 ± 46.0, 1017.0 ± 840.0, 103.0 ± 35.8, dan 51.0 ± 14.3 manakala kepekatan (ppm) unsur kawasan Port Reitz Creek yang kurang tercemar adalah kuprum, 21.6 ± 7.1; zink, 57.1 ± 17.9; plumbum, 26.2 ± 11.6 dan kadmium, 1.38 ± 14.3.

Menurut Kamaruzzaman et. al (2004) [8], kepekatan logam berat dalam sedimen dipengaruhi oleh pelbagai faktor seperti ciri sedimen, jenis, kualiti bahan organik dan saiz partikel sedimen itu sendiri. Kajian oleh Suhaimi-Othman & Tan (2004) [9] pula mendapati saiz butiran sedimen memainkan peranan penting dalam menentukan keupayaan sedimen menjerap logam di mana pengurangan saiz sedimen didapati meningkatkan keupayaan memerangkap logam.

Analisis keradioaktifan tabii
Selain kandungan unsur, analisis keradioaktifan juga telah ditentukan menggunakan spektrometri gama seperti yang diberikan dalam Jadual 2. Keputusan analisis menunjukkan kepekatan radionuklid tabii bagi masing-masing uranium-238, torium-232 dan kalium-40 pada hampir semua stesen mencatatkan bacaan melebihi had purata dunia.

Jadual 2: Kepekatan radionuklid tabii sampel sedimen Tasik Chini

| Stesen | Kepekatan radionuklid | | | | | Nisbah |
	K-40 (Bq/kg)	Th-232 (Bq/kg)	Th-232 (ppm)	U-238 (Bq/kg)	U-238 (ppm)	Th:U
Laut Gumun: 1a	599	126.8	32.0	215.6	16.0	2 : 1
Laut Gumun: 1b	757	109.8	28.0	130.7	10.0	3 : 1
L. Pulai Balai: 2	549	189.7	48.0	225.8	17.0	3 : 1
Laut Chenanam: 3	674	206.7	52.0	268.4	20.0	3 : 1
L. Tanj. Jerangking: 4a	713	139.3	35.0	142.1	11.0	3 : 1
L. Tanj. Jerangking:4b	594	143.7	36.0	114.0	9.0	4 : 1
L. Genting Teratai: 5	690	178.8	45.0	170.2	13.0	4 : 1
Laut Mempiteh: 6	656	152.2	39.0	135.9	10.0	4 : 1
LautKenawar: 7	760	152.1	39.0	90.5	7.0	6 : 1
Laut Serodong: 8	818	105.9	27.0	151.3	12.0	2 : 1
Laut Melai: 9a	537	160.3	41.0	54.5	4.0	10 : 1
Laut Melai: 9b	741	170.5	27.0	153.5	12.0	2 : 1
L. Batu Busuk: 10	435	168.3	43.0	400.5	31.0	1 : 1
Laut Labun: 11	475	221.4	56.0	292.8	22.0	3 : 1
Laut Jemberau: 12	277	178.8	45.0	319.3	24.0	2 : 1
Min	618.3 ± 1454	160.3 ± 32.8	39.5 ± 8.9	191.0 ± 94.7	14.5 ± 7.2	3:1
UNSCEAR (tanah) [14].	400	-	6.3	-	2.0	3:1

Kajian menunjukkan purata kepekatan uranium-238 adalah 191.0 ± 94.7 Bq/kg (14.5 ± 7.2 ppm) manakala bagi torium-232 pula ialah 160.3 ± 32.8 Bq/kg (39.5 ± 8.9 ppm) iaitu 5 atau 6 kali lebih tinggi berbanding kepekatan purata dunia. Walau pun kepekatan Th-232 dan U-238 lebih tinggi, tetapi nisbah Th:U masih lagi 3:1. Ini menunjukkan pertambahan U-238 dan Th-232 berpunca dari sumber tabii. Bagi kawasan kajian Tasek Chini

ini, aktiviti perlombongan serta jenis batuan yang terdapat di sini dijangka banyak mempengaruhi nilai keradioaktifan tabii yang tinggi ini. Peningkatan kepekatan uranium-238, torium-232 dan kalium-40 di kerak bumi secara umumnya semakin tinggi apabila kandungan SiO_2 dan K_2O dalam kerak bumi semakin tinggi [10,11].

Keputusan kajian ini juga mendapati radionuklid buatan manusia iaitu Cs-137 di lima stesen secara kualitatif iaitu Laut Gumun (1a,1b), Laut Mempiteh (6), Laut Melai (9b) dan Laut Labun (11). Radionuklid buatan Cs-137 memang boleh ditemui dalam sampel yang tidak terganggu kerana ianya berpunca dari radionuklid guguran. Kajian oleh Muhamad Omar [12] melaporkan kehadiran Cs-137 antara 0.2 – 10.0 Bg/kg bagi beberapa sampel tanah di Malaysia.

Kesimpulan

Kajian penentuan unsur dalam sampel sedimen Tasik Chini menggunakan teknik pendarfluor sinar-X telah dapat mengesan 12 unsur. Unsur-unsur tersebut ialah As, Ba, Co, Cr, Cu, Ni, Pb, Rb, Sr, V, Zn dan Zr. Kesemua unsur ini mempunyai kepekatan yang berbeza di setiap lokasi kajian iaitu As (11-50 ppm), Ba (553-944 ppm), Co (8-46 ppm), Cr (82-113 ppm), Cu (11-68 ppm), Ni (67-193 ppm), Pb (37-156 ppm), Rb (105-149 ppm), Sr (18-127 ppm), V (93-156 ppm), Zn (147-1679 ppm) dan Zr (190-290 ppm). Walaupun persekitaran Tasik Chini dikatakan masih lagi terpelihara, namun terdapat juga kepekatan unsur yang tinggi terutamanya di Laut Jemberau. Sebanyak tujuh jenis unsur di laut ini mempunyai kepekatan paling tinggi jika dibandingkan dengan lokasi kajian yang lain. Unsur tersebut ialah As (50 ppm), Co (46 ppm), Cr (113 ppm), Cu (68 ppm), Pb (156 ppm), V (156 ppm) dan Zn (1679 ppm). Kawasan Laut Jemberau ini dikelilingi oleh banyak aktiviti manusia seperti berdekatan dengan kawasan carigali barit (mineral) pembalakan dan pembukaan tanah untuk pembinaan FELDA dan kawasan rekreasi serta berdekatan dengan kawasan pelancongan Tasik Chini di Laut Gumun dan lombong besi di bahagian selatan Laut Jemberau.

Hasil kajian juga menunjukkan bahawa kepekatan radionuklid tabii uranium-238, torium-232 dan kalium-40 dalam sediment Tasik Chini melebihi nilai purata kepekatan dunia tetapi bersumberkan secara tabii. Selain itu radionuklid guguran Cs-137 turut ditemui di lima lokasi kajian secara kualitatif sahaja.

Rujukan

1. ERINCO. 1992. *Kuala Sungai Chini Gateway Development Plan Vol 1*. Petaling Jaya: ERINCO.
2. ERINCO. 1993. *Tasik Chini Eco Tourism Development Study Environment Impact Assesment Vol II*. Petaling Jaya: ERINCO.
3. Muohi, A.W., Mavuti, K.M., Omondi, J.G. & Onyari, J.M. 2003. Heavy metals in sediments from Makupa and Port-Reitz Creek systems: Kenyan Coast. *Environment International*. **28**: 639-647.
4. Nelson, B., Chen, Y.W., Gunn, J. M. and Dixit, S.S. 2004. Sediment Trace Metal Profiles in Lakes of Killarney Park, Canada from Regional to Continental Influence.
5. Lollar, B. S. 2004. *Treatise on Geochemistry Environmental Geochemistry*. Ed. ke-9.Oxford: Elsevier Pergamon.
6. Fytianos, K. & Lourantou, A. 2004. Speciation of elements in sediment samples collected at lakes Volvi and Koronia, N.Greece. *Environment International*. **30**(1):11-17.
7. Krumgalz, B. S. & Fainshtein, G. 1991. Trace Metal and Organic Matter in Nearshore Sediment Cores from the Eastern Mediterranean (Haifa Bay of Israel). *Marine Environmental Research*. **31**: 1-15.
8. Kamaruzzaman, B. Y., Ong, M. C. & Willison, K. Y. S. 2004. *Taburan Kepekatan Elemen-elemen Kimia di dalam Teras Sedimen di Hutan Paya Bakau Paka, Terengganu.* Prosiding Simposium Kimia Analisis Malaysia Ke 17.
9. Suhaimi-Othman, M. & Tan, B. F. 2004. *Kajian Kandungan Logam Berat (Cu, Cd, Zn dan Pb) di dalam Air, Sedimen dan Udang Air Tawar Macrobrachium Ianchesteri di Sungai Langat.* Prosiding Simposium Kimia Analisis Malaysia Ke 17.
10. International Atomic Energy Agency (IAEA). 1990. *The Use of Gamma Ray Data To Define The Natural Radiation In Environment.* IAEA-TECDOC_566, Vienna: IAEA.
11. Khursyid Alam Butt, Amanat Ali & Aziz Ahmad Qureshi. 1998. Estimation of Environmental Gama Background Radiation Levels in Pakistan. *Health Physics*. **75**(1): 63-66.
12. Muhamat Omar (1991), Environmental Radiation and Its Relation with Man. *Nuclear Buletin of Malaysia*. **1**(2). 16-18.

KANDUNGAN LOGAM BERAT DAN RADIONUKLID TABII DALAM IKAN, AIR, TUMBUHAN DAN SEDIMEN DI BEKAS TASIK LOMBONG

Muhamad Samudi Yasir, Norlaili bt Ahmad Kabir, Redzuwan Yahaya & Amran Ab Majid

Pusat Pengajian Fizik Gunaan, Fakulti Sains dan Teknologi, Universiti Kebangsaan Malaysia, 43600 Bangi, Selangor.

Abstrak

Tasik bekas lombong bijih timah di Malaysia kini giat ditebusguna untuk kegiatan pertanian, akuakultur, kawasan rekreasi atau dijadikan sebagai kawasan perumahan dan perindustrian. Kesan aktiviti perlombongan boleh menyebabkan peningkatan kepekatan atau pengkayaan radionuklid tabii dan logam berat terhadap ekosistem. Maka, kajian telah dilakukan untuk menentukan kandungan radionuklid tabii dan 12 unsur logam berat (Hf, Zr, Mn, Cu, Zn, As, Cd, Sn, Sb, Ba, Hg dan Pb) di dalam ikan, air, tumbuhan dan sedimen di tiga tasik bekas lombong sekitar Puchong dan Sepang, Selangor Darul Ehsan. Analisis dilakukan menggunakan ICP-MS. Secara keseluruhannya kepekatan logam berat adalah tinggi dalam sedimen serta tumbuhan berbanding dengan dalam ikan dan air. Barium mencatatkan kepekatan yang tinggi dikesan di dalam sedimen dan air, manakala zink dan mangan paling tinggi dikesan masing-masing dalam ikan dan tumbuhan. Kesemua unsur logam berat dalam ikan berada di bawah paras maksimum cemaran logam yang dibenarkan oleh Akta Makanan (Akta 281) dan Peraturan-Peraturan 1983 kecuali bagi kepekatan merkuri bagi ikan di lombong kedua iaitu 0.53 ± 0.20 mg/kg) yang melebihi had yang dibenarkan iaitu 0.5 mg/kg. Aktiviti radionuklid thorium (Th-232) dan uranium (U-238) dalam sedimen adalah tinggi berbanding dalam ikan, air dan tumbuhan dengan masing-masing berada dalam julat (30.76 ± 2.71 – 35.34 ± 0.27 Bq/kg) dan (9.37 ± 2.30 - 26.32 ± 3.01 Bq/kg). Manakala aktiviti kalium (K-40) dalam tumbuhan dan ikan didapati lebih tinggi berbanding di dalam air dan sedimen.

Abstract

Malaysia aggressively reclaimed most of their disused tin-mining pool especially for agricultural activities, freshwater fish farming area, recreational area, houses area and even as an industrial area. Past mining activities might induced the concentration of naturally occurring radionuclide (NORM) and heavy metal at the disused tin-mining pool ecosystem. A study has been conducted on the status of heavy metal (Hf, Zr, Mn, Cu, Zn, As, Cd, Sn, Sb, Ba, Hg and Pb) concentration and naturally occurring radionuclide activity in fish, water, plants and sediments at three different disused tin-mining pool near by Sepang and Puchong, Selangor Darul Ehsan. Sample of fish, water, plant and sediment being analyze using ICP-MS. The concentrations of heavy metal in sediment and plant are higher than its concentrations in fish and followed by water. The highest concentration of heavy metal in sediment and water is barium, whereas the highest concentration of heavy metal in fish and plant is zinc and manganese. The result also showed that only mercury level in fish collected in second disused tin-mining pool (0.53 ± 0.20 mg/kg) is exceed the maximum limit (0.5 mg/kg) prescribe by the Malaysian Food Act (Act 281). The activity of U-238 and Th-232 in sediment was found to be relatively higher than its activity in fish, plant or water (30.76 ± 2.71 – 35.34 ± 0.27 Bq/kg) and (9.37 ± 2.30 -18.86 ± 2.60 Bq/kg). The determination of K-40 activity showed that it is highly contained in plant and fish than in sediment or water.

Pendahuluan

Malaysia satu ketika dahulu merupakan salah sebuah negara pengeluar utama timah dunia. Malah pembangunan Lembah Kelang dan Lembah Kinta mempunyai kaitan yang rapat dengan penemuan timah. Walaupun kini tidak banyak lagi lombong timah yang masih aktif beroperasi, ujud pula industri sampingan seperti pengekstrakan pelbagai mineral berharga dari amang (zirkon, ilmenit dan struverit). Salah satu peninggalan industri perlombongan timah ialah bekas tasik lombong yang dikategorikan sebagai tasik buatan. Kini tasik dan kawasan bekas lombong ini telah banyak ditebus guna untuk dimajukan sebagai kawasan perumahan dan perindustrian, ditanami rumput untuk tujuan penternakan, akuakultur atau pun dijadikan kawasan rekreasi (Amran Ab Majid *et al*. [1]). Selain bijih timah, perlombongan turut sama mengeluarkan pelbagai jenis mineral lain dari perut bumi. Sekiranya mineral sampingan ini terdiri daripada logam berat, dikhuatiri sisanya masih tertinggal di kawasan bekas lombong yang kini telah dijadikan kawasan pertanian, perternakan ataupun akuakultur. Bagi tujuan

172

akuakultur, proses bioakumulasi logam berat boleh terjadi yang akhirnya berkemungkinan memasuki rantai makanan ekosistem bekas lombong tersebut. Oleh itu, ikan yang merupakan sebahagian daripada komponen rantai makanan dalam ekosistem tasik ini mungkin akan turut tercemar dengan sisa logam berat tersebut. Keadaan yang sama mungkin juga berlaku kepada radionuklid tabii seperti U-238, Th-232 dan K-40. Kemasukan logam berat dan radionuklid tabii dalam rantai makanan ini akan akhirnya sampai kepada manusia yang memungkinkan pemakannya menghadapi resiko kesihatan.

Oleh yang demikian objektif utama kajian ini adalah untuk menentukan aras kandungan logam berat dan radionuklid tabii dalam ikan di tasik bekas lombong serta hubungkaitnya dengan kandungan pada sediment, air dan tumbuhan.

Bahan dan kaedah

Kawasan kajian
Tiga buah tasik bekas lombong (L1, L2 dan L3) yang dijadikan kawasan kajian terletak di kawasan Puchong (Rajah 1). Ketiga-tiga tasik ini telah ditebusguna dan dijadikan kawasan ternakan akuakultur.

Sampel kajian.
Sampel ikan yang diguna adalah Ikan Keli Kayu (*Clarias batrachus*), Ikan Patin (*Pangasius sutchi*), Ikan Tilapia (*Oreochromiis mussambics*), ikan dari famili Lidae seperti Ikan Toman (*Ophiocehalus micropeltes*) dan Ikan Haruan (*Ophiocehalus striatus*), Ikan Tilapia (*Oreochromiis Mussambics)* atau Ikan Belida (*Notopterus notopterus*)). Ikan ini ditangkap menggunakan jaring yang dipasang semalaman.

Sama sebagaimana sampel ikan, sampel air (4L) juga diambil daripada tiga lokasi pada ketiga-tiga tasik. Asid nitrik dititiskan kepada setiap sampel air yang diambil mengelak pertumbuhan mikrob dan menghalang unsur daripada sampel air melekat pada dinding botol plastik yang diguna. Parameter air turut diambil yang meliputi parameter fizikal (suhu, pH, konduktiviti, saliniti dan oksigen terlarut).

Tumbuhan yang diambil bergantung kepada kehadiran pada setiap lokasi. Ianya terdiri dari *Eichhornia crassipes*, *Eragrostis atrovirens, Pennisetum puerperiu*, *Panicum repen, Pennisetum polystachion, Melampodium divaricatu* dan *Brachiaria mufica*.

Sedimen
Sedimen diambil menggunakan penceduk plastik dan dimasukkan ke dalam beg plastik yang telah dilabel.

Perawatan dan analisis sampel
Sampel ikan yang diambil dibasuh menggunakan air suling dan disiang untuk mengasingkan kepala, isi perut, insang dan tisu daging ikan. Setelah dicuci menggunakan air suling, tisu daging ikan yang diketahui beratnya dikeringkan menggunakan ketuhar pada suhu 80°C sehingga beratnya menjadi malar. Sampel kering ini kemudiannya dikisar sekali lagi untuk mendapatkannya butiran halus sekitar 500 μm. Sebanyak 400 mg sampel kemudiannya dicampurkan dengan 3.0 ml asid nitrik, 3.0 ml asid hidroklorik dan 0.5 mL asid peroksida. Campuran dihazam menggunakan kemudahan multigelombang selama dua jam sehingga membentuk larutan jernih. Larutan sampel yang terhasil kemudiannya dituras dan ditambah air suling sehingga isipadu larutan sampel mencecah 100 mL sebelum ditentukan kandungan logamnya berat menggunakan peralatan ICP-MS.

Sampel air yang telah diambil itu dibersihkan daripada kotoran dengan cara menapisnya menggunakan penapis membran plasma. Sampel air yang digunakan untuk penentuan keradioaktifan tabii dan logam berat di dalam kajian ini disediakan di dalam dua bentuk iaitu sampel air yang dipekatkan dan yang tidak dipekatkan.
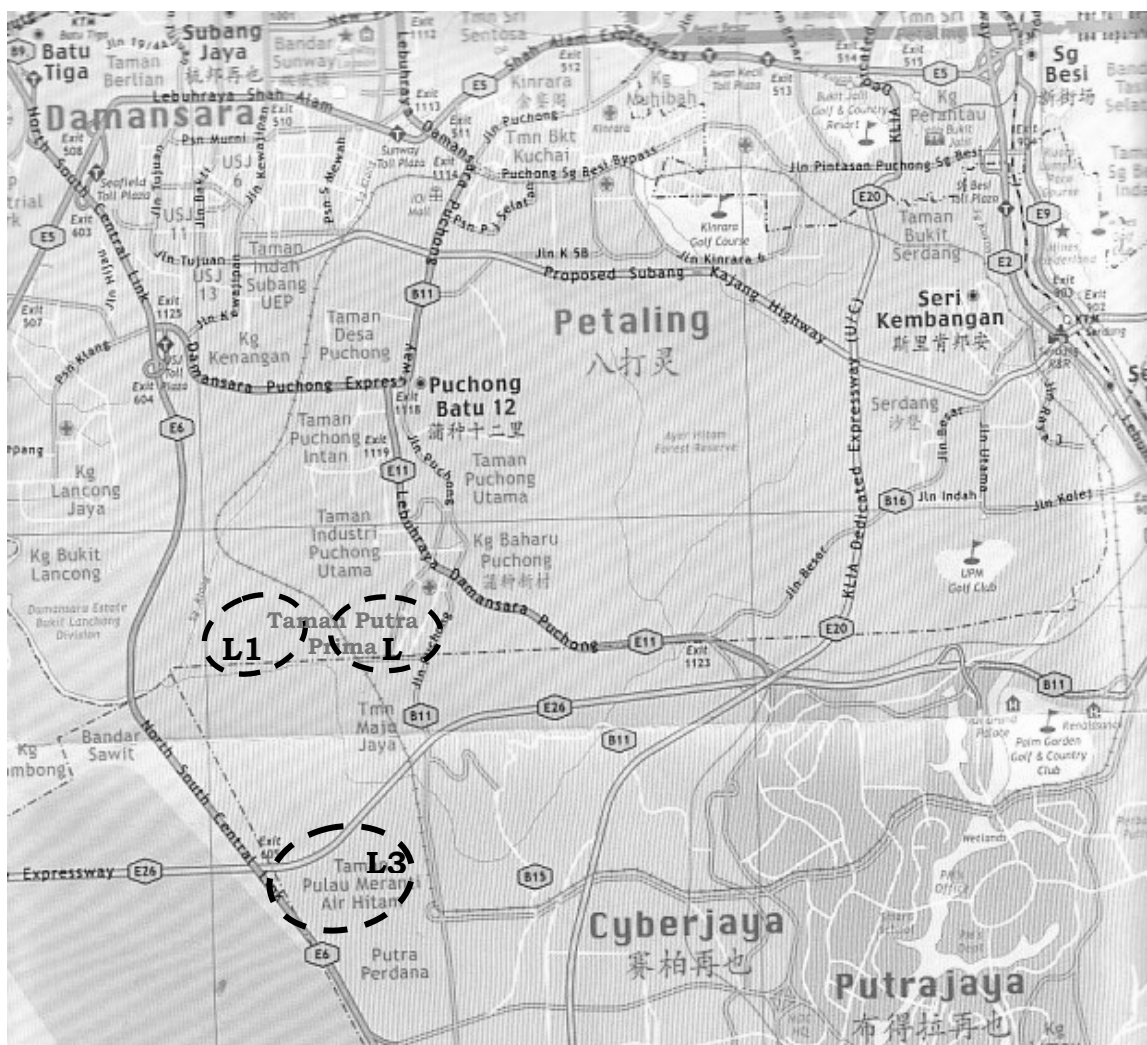
L1, L2 dan L3 Tasik bekas lombong.

Rajah1 Lokasi tasik kajian

Penyediaan sampel air yang tidak melalui proses pemekatan ialah dengan cara menuras sampel air yang telah dibersihkan menggunakan membran plasma menggunakan kertas turas sehingga isipadunya mencapai 100 mL.

Tumbuhan

Sampel tumbuhan itu dibasuh menggunakan air suling untuk menghilangkan kotoran yang melekat. Tumbuhan kemudiannya dibilas menggunakan air suling sekali lagi. Berat basah tumbuhan yang telah bersihkan dicatatkan. Keseluruhan tumbuhan (akar, daun dan batang) kemudiannya dikeringkan menggunakan ketuhar pada suhu 105°C sehingga beratnya menjadi malar. Sampel kering ini kemudiannya dikisar menggunakan pengisar untuk mendapatkan butiran halus sekitar 500 μm. Sebanyak 400 mg butiran halus seterusnya dicampur dengan asid nitrik (3.0 mL), asid hidroklorik (0.5 mL) dan asid peroksida   (9.0 mL). Campuran dihazamkan menggunakan kemudahan multigelombang selama dua jam sehingga membentuk larutan jernih. Larutan sampel yang terhasil dari proses penghadaman itu kemudiannya dituras dan air suling ditambah sehingga isipadu larutan sampel mencecah 250 mL.

Sampel sedimen itu dibersihkan daripada kotoran dengan membuang semua akar tumbuhan dan bendasing lain. Berat basah sedimen yang telah dibersihkan dicatatkan. Sampel sedimen kemudiannya dikeringkan menggunakan ketuhar pada suhu 105ºC sehingga berat menjadi malar. Sampel kering ini seterusnya dikisar untuk mendapatkannya butiran halus sekitar 500 μm.

Sebanyak 300 mg butiran halus sedimen dicampurkan dengan asid nitrik (5.0 mL), asid hidroklorik (2.0 mL) dan asid peroksida (0.5 ml) dan asid fluorida (3.0 mL). Campuran seterusnya dihazamkan menggunakan kemudahan multigelombang selama dua jam sehingga membventuk larutan jernih. Larutan sampel yang terhasil dari proses penghadaman itu kemudiannya dituras dan air suling ditambah sehingga isipadu larutan sampel mencecah 100 mL.

Analisis sampel
Sampel yang telah disediakan dalam bentuk larutan dianalisis menggunakan Spektrometer Jisim Gandingan Plasma Teraruh (ICP-MS) yang telah dikalibrasi menggunakan piawai (*SRM MA-A-2 (TM) Fish Flesh Homogenate*), piawai tumbuhan (*SRM 1572 Citrus Leave*) dan larutan *Perkin Elmer Pure Atomic Spectroscopy Standard.*

Analisis data
Bagi penentuan kepekatan logam berat, setiap data yang diperolehi dikira semula kepada berat asal sampel dan dinyatakan dalam unit mg/kg atau mg/L.

Manakala aktiviti radionuklid tabii (Bq/kg) pula boleh ditentukan menggunakan rumus:

$$\frac{dN}{dt} = \frac{\lambda\theta\,wN_A}{WM}$$

dengan;

θ	= Kelimpahan tabii radionuklid tabii di dalam semesta
w	= Berat radionuklid tabii di dalam sampel
N_A	= Nombor Avogadro
M	= Berat molekul radionuklid tabii
W	= Berat sampel

Hasil dan perbincangan

Parameter fizikal
Jadual 1 menunjukkan bacaan pelbagai parameter fizikal lombong kajian. Oksigen terlarut yang diukur *in situ* menunjukkan nilainya berada di antara 7.0 -7.6 mg/l. Kandungan oksigen ini dipengaruhi oleh pelbagai faktor seperti proses pernafasan haiwan akuatik, forosintesis tumbuhan akuatik serta pengoksidaan yang berlaku di bawah permukaan air (Elbering et al. [2]). Air tasik bekas lombong biasanya bersifat asid (Muhamad Samudi Yasir et al. [3]). Sungguhpun begitu hasil kajian ini menunjukkan sebaliknya, iaitu sedikit beralkali. Ini mungkin disebabkan oleh faktor masa, iaitu telah melebihi 15 tahun berhenti beroperasi. Kajian yang dilakukan di Sepanyol juga menunjukkan sifat kealkalian pada air tasik bekas lombong (Riba *et al.* [4]).

Nilai konduktiviti menggambarkan kandungan kation dan anion yang terlarut dalam air tasik. Hasil kajian mendapati nilainya berada pada julat 278 – 386 µS/cm bagi ketiga-tiga tasik.

Jadual 1. Pelbagai parameter air dan sedimen tasik

Parameter	Tasik 1 (L1)	Tasik 2 (L2)	Tasik 3 (L3)
Oksigen terlarut (mg/L)	7.0	7.4	7.6
Nilai pH			
a.air	7.21	7.47	7.92
b.sedimen	7.34	6.80	6.97
Suhu (^{o}C)	30.6	30.0	32,3
Konduktiviti (µS/cm)	386	385	278

Logam berat
Logam berat yang ditentukan dalam setiap sampel ialah mangan, kuprum, zink, arsenik, kadmium, stanum, antimoni, barium, merkuri, plumbum, zirkonium dan hafnium. Hasil kajian mendapati Zn dan Cu merupakan logam berat yang paling banyak terkandung dalam tisu daging ikan dengan masing-masing dalam julat (0.50 - 3.81 mg/kg) dan (0.50 - 2.27 mg/kg). Kepekatan tinggi kedua-dua logam ini berbanding logam lain mungkin

disebabkan kedua-duanya merupakan sebahagian daripada nutrien utama yang diambil oleh ikan untuk hidup. Selain daripada itu, kajian yang dijalankan oleh Papagiannis et al. [5] mendapati hubungan yang rapat di antara kandungan Zn dan Cu di dalam ikan dan zooplankton di dalam ekosistem tasik. Oleh yang demikian, Zn dan Cu yang terkandung di dalam ikan ini mungkin di ambil secara tidak langsung melalui makanan yang di ambil oleh ikan tersebut. Nilai kepekatan logam berat yang diperolehi ini tidak melebihi tahap maksimum yang dibenarkan dalam Akta Makanan 1983 (Akta 281)[6] iaitu 30 mg/kg dan 100 mg/kg untuk masing-masing Cu dan Zn. Walau bagaimanapun kandungan Hg pada L2 (0.53 mg/kg) adalah 0.05 mg/kg melebihi takat maksimum yang dibenarkan. Oleh itu bolehlah disimpulkan bahawa tasik yang tercemar dengan logam berat akibat aktiviti perlombongan tidak semestinya akan menyebabkan peningkatan kepekatan kesemua logam berat di dalam tasik terhadap yang hidup akuatik di dalamnya.

Secara amnya kandungan logam berat dalam air adalah lebih rendah berbanding dengan sedimen dan tumbuhan kecuali barium yang mana kandungannya berada dalam julat 7.78 ± 1.80 hingga 27.67 ± 2.25 μg/l (Jadual 2). Barium terdiri daripada logam alkali yang mudah ditemui di dalam perut bumi. Proses perlombongan menyebabkan sebahagian besar logam yang terkandung dalam perut bumi dikeluarkan yang akhirnya menyebabkan kandungannya tinggi pada tasik bekas lombong.

Logam berat tertinggi yang dikesan pada tumbuhan adalah mangan iaitu 19.05 ± 8.10 mg/kg di tasik L2, diikuti oleh barium (7.66 ± 0.66 mg/kg) juga di L2. Kajian yang dilakukan di kawasan tasik bekas lombong arang batu di Poland oleh Samecka dan Kempers [7] mendapati kandungan Mn amat tinggi ($1142 - 2116$ mg/kg) diikuti oleh Zn, Ba dan Pb. Hasil kajian ini didapati tidak mengikut corak tersebut. Ini disebabkan oleh perbezaan jenis mineral yang pernah dilombong.

Kandungan Ba juga didapati tertinggi berbanding logam berat lain dalam sedimen, diikuti oleh Pb dan Cu. Terdapat persamaan antara kepekatan Cu dalam sedimen dengan kepekatan Cu dalam tumbuhan di mana kepekatannya adalah paling tinggi di L1, di ikuti oleh L3 dan L2. Corak ini sama dengan nilai pH sedimen (Jadual 1). Ini mungkin disebabkan pada pH tinggi, Cu dalam sedimen dapat diambil oleh tumbuhan yang berada berdekatan berbanding pada keadaan pH rendah. Kandungan Cu di dalam sedimen mungkin meresap melalui air bawah tanah dan akhirnya diambil oleh akar tumbuhan. Kepekatan Hf dan Hg pula adalah paling tinggi di L3 dan diikuti oleh L2 dan L1. Kepekatan Hf dan Hg yang tinggi turut dikesan pada ikan dari tasik berkaitan. Oleh yang demikian pencemaran logam Hg dan Hf boleh menyebabkan pemekatan dan akhirnya memasuki rantai pemakanan akuatik.

Radionuklid tabii
Kandungan radionuklid tabii U-238, Th-232 dan K-40 ditunjukkan dalam Jadual 3. Hanya K-40 yang dapat dikesan pada sampel ikan, air, tumbuhan dan sedimen dari ketiga-tiga tasik. Radionuklid U-238 dan Th-232 hanya terdapat pada sampel sedimen.

Jadual 2 Kepekatan logam berat di dalam ikan, sedimen, air dan tumbuhan

Unsur	Kandungan logam berat dalam sampel (mg/kg) basah atau ug/L (air)											
	L1				L2				L3			
	Ikan	Sedimen	Air	tumbuhan	Ikan	Sedimen	Air	tumbuhan	Ikan	Sedimen	Air	tumbuhan
Mn	0.08 ± 0.03	2.2 ± 0.85	0.00	3.92 ± 2.58	0.07 ± 0.01	2.63 ± 0.02	0.00	19.05 ± 8.10	0.06 ± 0.01	0.00	0.00	8.63 ± 5.56
Cu	0.50 ± 0.02	2.47 ± 1.29	1.00 ± 0.01	5.97 ± 1.33	2.27 ± 0.48	1.0 ± 0.51	1.00 ± 0.01	1.79 ± 0.03	0.13 ± 0.01	2.28 ± 2.22	1.00 ± 0.01	2.49 ± 1.16
Zn	0.50 ± 0.10	0.40 ± 0.21	0.88 ± 0.02	4.09 ± 0.67	3.81 ± 2.91	0.38 ± 0.01	13.5 ± 2.65	0.75 ± 0.24	0.65 ± 0.21	0.51 ± 0.30	7.73 ± 1.03	1.38 ± 0.54
As	0.11 ± 0.01	0.34 ± 0.20	2.83 ± 0.29	0.00	0.07 ± 0.01	0.32 ± 0.11	2.25 ± 0.29	0.00	0.06 ± 0.01	0.35 ± 0.14	0.00	0.00
Cd	0.00	0.00	0.00	0.00	0.00	0.00	0.00	0.00	0.07 ± 0.01	0.00	0.00	0.00
Sn	0.00	0.00	0.00	0.00	0.00	0.00	0.00	0.00	0.00	0.00	0.00	0.00
Sb	0.00	0.00	0.00	0.00	0.00	0.00	0.00	0.00	0.00	0.00	0.00	0.00
Ba	0.00	14.78 ± 5.30	27.7 ± 2.25	4.52 ± 2.50	0.11 ± 0.03	45.10 ± 9.26	25.0 ± 0.29	7.66 ± 0.66	0.13 ± 0.03	13.08 ± 4.20	7.78 ± 1.80	3.32 ± 1.19
Hg	0.17 ± 0.01	0.20 ± 0.10	0.00	0.00	0.53 ± 0.20	0.33 ± 0.10	0.00	0.00	0.11 ± 0.02	0.60 ± 0.13	0.00	0.00
Pb	0.00	6.09 ± 0.73	1.00 ± 0.01	2.26 ± 0.25	0.00	13.55 ± 1.67	1.05 ± 0.01	0.00	0.00	3.57 ± 0.56	0.00	0.68
Zr	0.00	0.33 ± 0.12	0.00	0.00	0.00	0.53 ± 0.20	0.00	0.00	0.12 ± 0.01	0.52 ± 0.16	0.00	0.00
Hf	0.00	0.72 ± 0.06	2.83 ± 0.29	0.00	0.00	1.40 ± 0.31	3.00 ± 0.01	0.00	0.14 ± 0.02	1.65 ± 0.56	0.00	0.00

Terdapat dua laluan utama yang membolehkan ikan di tasik bekas lombong dicemari oleh K-40, iaitu melalui deposisi permukaan ataupun melalui rantai pemakanan ikan tersebut. Deposisi permukaan boleh berlaku apabila terdapat pemindahan unsur kalium daripada komponen ekosistem tasik seperti sedimen dan tumbuhan. Aktiviti perlombongan dijangka meningkatkan kandungan pelbagai radionuklid tabii di kawasan sekitarnya. Kajian ini menunjukkan walaupun ketiga-tiga radionuklid tersebut terdapat pada sediment, hanya K-40 yang dapat dikesan pada tumbuhan dan ikan. Penyebaran unsur K-40, Th-232 dan U-238 dalam ekosistem akuatik boleh berlaku melalui ampaian pepejal yang seterusnya membabitkan komponen akuatik lain seperti plankton, herbivor, karnivor serta omnivor yang terdapat dalam sistem akuatik tersebut. Ketiadaan U-238 dan Th-232 dikesan pada tumbuhan adalah disebabkan unsur tersebut diikat kuat oleh komposisi tanah dan sukar di ambil oleh tumbuhan. Selain daripada itu, tumbuhan juga tidak mengambil uranium dan thorium sebagai unsur nutrien. Kajian sebelum ini mendapati kandungan radionuklid tabii U-238 dan Th-232 dalam sampel tanah di kawasan lombong aktif adalah masing-masing 3.75 Bq/kg dan 10.51 Bq/kg (Muhamad Samudi Yasir et al.[8]), manakala kandungan dalam sistem air kawasan lombong aktif pula adalah antara 26.3 – 36.2 Bq/L (Th-232) dan 26.8 – 35.4 Bq/L (U-238) (Ismail et al. [9]. Oleh yang demikian kandungan radionuklid tabii dalam semua sampel yang di ambil adalah lebih rendah dari hasil kajian sebelumnya.

Jadual 3. Kandungan radionuklid tabii dalam ikan, air, tumbuhan dan sedimen.

	Kandungan radionuklid tabii (Bq/kg atau Bq/L)		
	Tasik 1	Tasik 2	Tasik 3
Ikan			
K-40	7.78E-02 ± 0.01	7.34E-02 ± 0.01	6.52E-02 ± .01
Th-232	0	0	0
U-238	0	0	0
Air			
K-40	1.11E-03 ± 0.00	1.07E-03 ± 0.00	1.23E-03 ± 0.00
Th-232	0	0	0
U-238	36.72	36.72	0
Tumbuhan			
K-40	0.09 ± 0.05	1.12E-03 ± 0.00	0.10 ± 0.04
Th-232	0	0	0
U-238	0	0	0
Sedimen			
K-40	1.57E-04 ± 4.48E-05	4.24E-04 ± 1.47E-04	9.44E-05 ± 5.40E-06
Th-232	30.76 ± 2.71	35.34 ± 0.27	34.06 ± 11.85
U-238	18.86 ± 2.60	26.32 ± 3.01	9.37 ± 2.30

Aktiviti U-238 dan Th-232 bagi sedimen di L1, L2 dan L3 adalah relatif lebih tinggi berbanding aktivitinya di dalam tisu daging ikan, air dan tumbuhan. Tetapi aktiviti K-40 bagi sedimen di L1, L2 dan L3 adalah relatif lebih rendah berbanding aktivitinya di dalam tisu daging ikan. Fenomena ini mungkin terjadi kerana faktor kedudukan tropik ikan yang tinggi menyebabkan berlaku pemekatan K-40 dalam jumlah yang banyak.

Kesimpulan

Hasil kajian ini mendapati walaupun ekosistem tasik bekas lombong mengandungi pelbagai logam berat dan radionuklid tabii, kandungannya kebanyakan logam berat dalam ikan adalah rendah dan berada di bawah aras maksimum yang dibenarkan dalam Akta Makanan (1983). Oleh yang demikian dari sudut pencemaran logam berat dan radionuklid tabii kawasan tasik bekas lombong ini berpotensi untuk dimajukan sebagai kawasan ternakan akuakultur.

Penghargaan

Rujukan

1. Amran Ab Majid, Muhamad Samudi Yasir, Redzuwan Yahaya. 2004. "Taboran Radionuklid Tabii (NORM) dan Kaitannya dengan Aktiviti Pembangunan di Negeri Selangor". Dalam: *Indicator of Sustainable Development: Assessing Changes in Environmental Conditions*. A. Latiff et al. (ed), Institute For Environment and Development (LESTARI), Universiti Kebangsaan Malaysia, ISBN 983-9444-58-1, 213 – 225.
2. Elbering B., Knudsen K.L, Kristensen P.H dan Asmund G., 2004.   "Appliying foramineral stratigraphy contaminationand mining impact in a fiord in West Greenland". *Marine Enviromental Research* 55 *3*: 235-256.
3. Muhamad Samudi Yasir, Ismail Bahari, Sahibin A.R., Dahlia Suriati Abd Rahim and Halim Abd Rahman, 2001. "The Concentration of Natural Radiobuclides and Heavy Metals in Soils From A Tin-Mining and Its Surrounding Area". *J. Sains Nuklear Malaysia*, *19*: 50 – 56.
4. Riba I., Conradi M., Forja J.M. dan Delvalls T.A. 2004. "Sediment Quality in the Guadalquivir Estury: Lethal Effect Associated with the Azhalcollar Mining Spil". *Marine Poll. Bull.*. 48 *1*:144-152.
5. Papagiannis I, Kagalov I., Leonardos J., Petridis D. dan Kalfakou V. 2004. "Copper and Zink in Four Freshwater Fish Species from Lake Pamvotis (Greece)". *J. Environ. Intl*. 30 (3) :257-362.
6. Akta Makanan 1983. MDC, Kuala Lumpur.
7. Samecka C. dan Kempers. 2004. "Consentrations of heavy metal and plant nutrients in water, sediments and aquatic macrophytes of anthropogenic lakes (former open cut brown coal mines) differing in stage of acidification". *Environ. Intel*. 281 :87-98
8. Muhamad Samudi Yasir, Amran Ab Majid dan Redzuwan Yahaya, 2005. "Kandungan Radionuklid Tabii Dalam Sampel Amang, Tanah dan Air di Sekitar Kawasan Industri Perlombongan Di Dengkil Selangor". Proceeding of The 6th ITB-UKM Joint Seminar on Chemistry, 17 – 18 May, Bali Indonesia. ISBN: 983-29766-38-7653 - 658.
9. B. Ismail, M.S. Yasir, Y. Redzuwan and A.M. Amran, 2003. "Radiological Environmental Risk Associated with Different Water Management System in Amang Processing in Malaysia". *Pakistan J. Biol. Sci.. 6:* 1544 – 1547.

VALIDATION OF Ra-226 AND K-40 MEASUREMENT IN ENVIRONMENTAL SAMPLES USING GAMMA SPECTROMETRY SYSTEM

Yii Mei Wo and Zaharudin Ahmad

Industrial Technology Division
Agensi Nuklear Malaysia
Bangi, 43000 KAJANG, MALAYSIA

Keywords: Ra-226, K-40, Method Validation, Gamma Spectrometry System

Abstract

Mineral and natural resources usually contains long half-life natural radionuclides (such as U-238, Th-232 and K-40) and had been greatly exploited for different utilizations. When these materials are processed, their concentration become higher in the wastes. Since all these radionuclides have a very long half-life, when concerning about the safety of members of public, it became a requirement by regulation under the Atomic Energy Licensing Act (Act 304) to control the limits of discharge. Both U-232 and Th-228 are less soluble and less mobile compared to their decay daughter products (such as Ra-226 for U-238 and Ra-228 for Th-232). Therefore the determination of these soluble radionuclides, i.e. Ra-226, Ra-228 and K-40 in the environmental samples becomes more important due to their high mobility and solubility. Gamma Spectrometry System was used in the measurement of radium isotopes and K-40, because it is one of the easiest methods to be performed. This measuring method must be validated for several parameters include specificity, precision (repeatability), bias (accuracy), linearity, range, detection limit, robustness and ruggedness in order to ensure it fits for the purpose. This work summarizes how these parameters were fulfilled for this analytical method using several types of certified reference materials. The same validation method would be considered workable on Ra-228 as well, since both Ra-226 and Ra-228 are isotopic, thus have similar physical and chemical properties.

Introduction

For the past few decades, there has been an increasing interest in radionuclides present in the environment and their possible effect, either acute or chronic, on human health [1]. These radionuclides can be transported across long distances from their source of emission, removed from the atmosphere, then move into the biosphere and hydrosphere where finally will affect the human population by several pathways. Among these, one of them is from the radionuclides that present naturally in the environment [2].

Mineral and natural resources had been greatly exploited for different uses. Usually, these materials contain natural radionuclides such as from the uranium and thorium series, and K-40, which were known as the Natural Occurring Radioactive Material (NORM). When the NORM is processed, the concentration for these radionuclides became higher in the wastes [3]. Since all these radionuclides have a very long half-life, when concerning about the public safety, it became an urge by regulation under the Atomic Energy Licensing Act (Act 304) to control the limits of discharge.

Naturally, in the earth cluster, majority of uranium presents as U-238 and thorium presents as Th-232. Both uranium and thorium are less soluble and less mobile compared to their decay daughter products (such as Ra-226 for U-238 and Ra-228 for Th-232). Therefore the determination of these soluble radionuclides, i.e. Ra-226, Ra-228 and K-40 in the environmental samples become more important because of their high mobile ability and solubility.

Gamma Spectrometry is one of the most widely used nuclear instrumentations in determining the activity concentration of Ra-226, Ra-228 and K-40 inside a sample. This is because no chemical treatments and no complicated sample preparation techniques were required during the measurement and the samples usually were not being destructed after the analysis. Basically, the instrument needs to be calibrated for the energy and efficiency prior to a measurement. After calibration, Ra-226, Ra-228 and K-40 inside a sample can be measured

179

either directly or let it be in secular equilibrium with its daughter products. K-40 can be detected easily at its own energy line at 1460.83 keV. While, Ra-226 and Ra-228 are detected using the equilibrium daughters' energy lines, i.e. Pb-214 (295.22 keV and 351.93 keV) and Bi-214 (609.31 keV) for Ra-226 and Ac-228 (911.20 keV) for Ra-228 [4]. Usually, all solid samples were directly packed homogenously into the container as its original form. When necessary, the sample was crushed or cut into small pieces to have more samples to be put inside the container. On the other hand, for the water samples, large volume of water (1-10 litres) was pre-concentrated in order to have a higher activity inside the container.

In order to ensure that this method is able to give a representative result for the Ra-226 and K-40, the method was first validated using some traceable and certified material. Certified reference material was used in most of the test in order to reduce the systematic errors that could arise from the complicated sample preparations. Method validation is a prerequisite for a laboratory going for accreditation to international standards. The parameters required for method validation of an analytical method include specificity, precision (repeatability), bias (accuracy), linearity, range, detection limit, robustness and ruggedness [5-7].

Experimental

Preparation and counting of standards, samples and certified reference material

All standards, samples and certified reference material were prepared in a same size container to obtain the similar counting geometry. The high-purity germanium (HPGe) detector was calibrated by using a prepared commercial gamma multinuclides standard that is traceable to NIST. The energy and efficiency calibration were then be validated by using the Certified Reference Material, CRM, (IAEA, Soil-6) present in the same counting geometry. All the samples (including standard) were counted directly in the system with a suitable counting time. Data was collected through counting different types of certified reference material and also from some prepared samples, by using standard source solution for Ra-226 that is traceable to NIST. K-40 solution was prepared from the 99.5% purity Potassium Dichromate that supplied by the May & Baker Ltd. All the data was used to calculate the specificity, precision (repeatability), bias (accuracy), linearity, range, detection limit, robustness and ruggedness.

Specificity

Specificity is the ability of an analytical method to distinguish the analyte to be measured (hence Ra-226 and K-40) from other substances present in the sample. Specificity is necessary to assure the accuracy of the measurement and the quality of the analysis results. The specificity of the instrument can be determined by counting the SRM IAEA-326, which contains both Ra-226 and K-40 radionuclides. The interested radionuclides shall appear at the expected energy line to prove the specificity of the technique.

Precision/Repeatability

Precision is a measure of the degree of repeatability for a test or measurement method under normal conditions. It is usually expressed as the standard deviation(s) or the percent relative standard deviation (RSD) for a statistically significant number of samples. Precision depends only on the distribution of random errors but is not associated with the true value. To check the precision of this method, it was determined by calculating the percent of RSD for at least seven measurement results from this method [7].

Bias/Accuracy

Accuracy (mostly caused by systematic errors) is the closeness of the samples true content of a specific analyte with the average result from several measurements. The accuracy of a measurement method shall be determined by comparing the arithmetic mean (average) of at least seven measurement results [7] obtained from this specific method with the known value (activity or concentration) of the standard reference source containing the specific analyte. In this work, a certified reference material (Soil-6) will be used to serve this purpose. To achieve this target, the U score value shall be calculated by using the equation below.

$$U_{score} = \frac{\left|\overline{x}_{lab} - u_{CRM}\right|}{\sqrt{Unc_{CRM}^{2} + Unc_{lab}^{2}}} \quad (1)$$

where x_{lab} is the mean value from measurement; u_{CRM} is the certified value, Unc_{CRM} and Unc_{lab} is the standard deviation for the certified value and analytical value respectively.

The calculated U score value shall not be greater than 1.5 to prove that the method is not bias [8].

The accuracy of the analytical measurement can also be estimated via a statistical equation known as z-core defined as below:

$$z = \left| \frac{x_i - x_{ref}}{\sigma_i^{\,2} - \sigma_{ref}^{\,2}} \right| \qquad (2)$$

where x_i is the measured value of analytes in control sample

σ_I is the standard deviation of the sample

x_{ref} is reference value or certified value of the control sample

σ_{ref} is the standard deviation of the control sample

Hence the classification of accuracy can be based on the basis of z-scores:

if $z < 2$, the quality of measurement is satisfactory

if $2 < z < 3$, the quality of measurement is questionable, and

if $z > 3$, the quality of measurement is poor thus require further analysis

The certified value of the Ra-226 in the certified reference material, Soil-6, is 79.92 Bq/kg with the 95% confidence level within 69.56 to 93.42 Bq/kg. Whilst, the certified value of the K-40 in the certified reference material, IAEA-326, is 580 Bq/kg with the 95% confidence level within 571 to 589 Bq/kg.

Linearity and Working Range
Linearity is the ability of the method to elicit test results that are directly proportional to radionuclide activity within a given range. Linearity is usually reported as the variance of the slope of the linear regression of a standard curve. Measurements shall be made with the method for the range of standard or reference concentrations available to the laboratory (from background concentrations to the highest concentration available in standard). The measurement points shall be graphed and the variance of the linear fit shall be calculated. The range shall be expressed in the same unit (such as Bq/kg) as the test results obtained with the method. The gamma-ray spectrometry used with the test methods at the laboratory have been shown by the instrument vendors to be linear over the entire range of measurements possible at the laboratory. The linearity of the analyte measurement was carry out by preparing a series of different radioactivity from NIST traceable Ra-226 and pure $K_2Cr_2O_7$ for K-40.

Limit of Detection
The detection limit (DL) is an estimation of the minimum activity or concentration that can be measured with a specific level of confidence. The type of detection limits used at the laboratory was calculated based on the Currie Limit equation. The minimum detectable activity (MDA) is generated and reported for sample with calculated activity lower than MDA.

$$MDA = 1.645 \times \sqrt{\frac{Background\ \ counts}{Live\ \ time(s)}} \qquad (3)$$

Robustness
Robustness is a measure of the sensitivity of an analytical method in the presence of minor deviations in the experimental conditions of the method. This can be done by having different operators to analyse the same reference material [7].

Ruggedness/Reproducibility
Ruggedness is a more measure of the method performance under variations of condition more severe than determine for robustness. Ruggedness is a measure of how effectively the method performs under less-than-ideal laboratory conditions. The ruggedness of the method was determined from the analysing data of the same reference material using several different equipments [7].

Results and Discussion

Specificity
Since the SRM IAEA-326 contains both Ra-226 and K-40, the measured results from this sample are used to study the specificity for the method. Ra-226 is determined through its daughter energy line, i.e. Pb-214 (295.22 keV and 351.93 keV) and Bi-214 (609.31 keV). Meanwhile, the K-40 is identified through its energy line at 1460.83 keV. All the energy lines used were suggested values [4]. From the experiment, both Ra-226 and K-40 could still be identified easily at the suggested energy lines. This shows that the method was able to specify both radionuclides at it particular energy line with a little variance in energy. Table 1 below summarised the energy line measured by the counting system to identify both the Ra-226 and K-40 for several measurements.

Table 1. Ra-226 and K-40 energy lines for several measurements

No of Measurement	*Ra-226*			K-40
	Peak 1	Peak 2	Peak 3	
Measurement 1	295.11	351.86	609.25	1460.40
Measurement 2	295.11	351.86	609.12	1460.52
Measurement 3	295.11	351.74	609.12	1460.15
Measurement 4	295.24	351.86	609.00	1460.27
Measurement 5	295.11	351.86	609.12	1460.40
Measurement 6	295.24	351.86	609.00	1460.02
Measurement 7	295.11	351.86	609.12	1460.40
Measurement 8	295.24	351.86	609.25	1460.52

The slight different in the energy line could be due to the stability of the electronic components for the system [9]. However, this slight different in the peak energy (less than 1 keV) is meaningless when compared to the whole working range of the system beginning from 40 to 2000 keV. Therefore, from this method, the radionuclides of Ra-226 and K-40 can be identified easily using the gamma spectrometry.

Precision/Repeatability
The CRM Soil-6 had been used to check Ra-226 while CRM IAEA-326 was used to check K-40 in order to determine the precision of the method. The CRM Soil-6 was used to check the Ra-226 because the activity is higher when compared to the CRM IAEA-326 and the activity is also close to the background level of Malaysia [10]. Therefore this value is more suitable to be used when dealing with environmental samples. The average value reported was 84.83 ± 5.25 Bq/kg and 559.7 ± 47.4 Bq/kg, for Ra-226 and K-40 respectively. The counting results on both CRM were shown in the following control charts (Figure 1 and 2) with horizontal lines indicating the acceptance limit (mean ± 1σ), warning limit (mean ± 2σ), and action limit (mean ± 3σ) respectively. From the control charts, the changes of counting results over time would be monitored and proper corrective action will be taken if the counting results depart from the acceptable range. From the accumulated results, 72.7 % % for Ra-226 and 87.5% for K-40 of the results falls within the acceptable limit (mean ± 1σ) while about 96.4 % of the Ra-226 in Soil-6 and all K-40 for IAEA-326 falls within the warning limit (mean ± 2σ). The precision expressed in the relative standard deviation (RSD) of this analysis was 6.2% and 8.5 % for Ra-226 and K-40 respectively. Generally, the precision for this method is considered to be fairly good.

Ra-226 in Soil 6
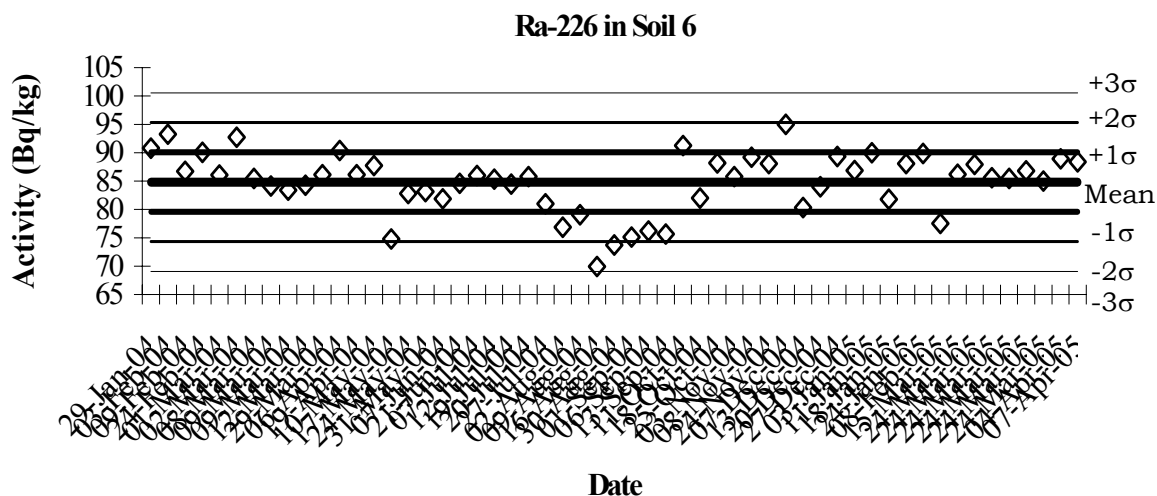
Figure 1. Control Chart of Soil-6 analysis for Ra-226

K-40 in IAEA-326
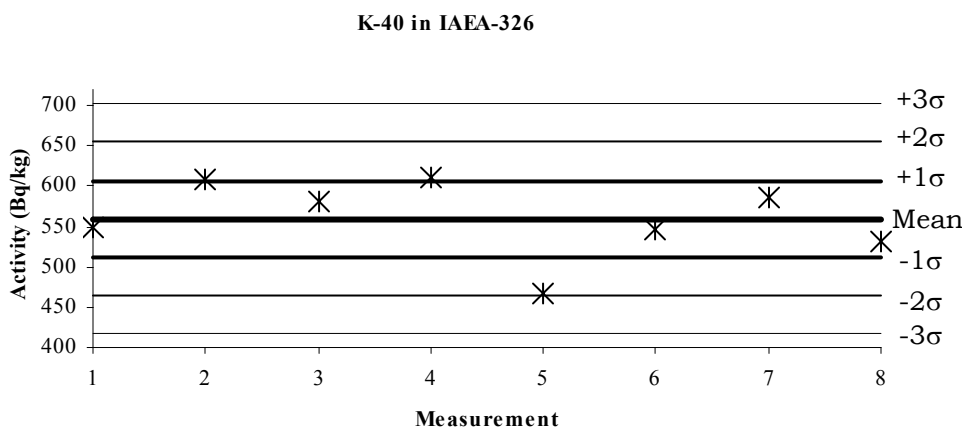
Figure 2. Control Chart of IAEA-326 analysis for K-40

Bias/Accuracy
Bias is calculated based on the U score between the experimental values (the same data obtained from Figure 1 and Figure 2 above) and the CRM's certified value. From the measurements data, the calculated U score is found to be 0.62 and 0.43 for Ra-226 and K-40 respectively, which means that there is no significant bias in this method [8]. However, if there is a possibility of occurring bias, correction from the bias can be made by applying a correction factor in the equation when calculating the activity for the Ra-226 or K-40 in a sample. The calculated Z score is found to be 0.60 and 0.01 for Ra-226 and K-40 respectively, showing that the accuracy of the measurement is satisfactory.

Linearity and Working Range
The results of the linearity tests were shown in Figure 3 below, which indicating a strong linear correlation between the measured activities for Ra-226 and K-40 and the amount of standard added. The correlation coefficient found to be 0.9970 and 0.9796 for Ra-226 and K-40 respectively. Since the figure indicating a good linearity, the figure can be extrapolates towards minimum and maximum to extend the working range. Slight deviation for the linearity of K-40 could be probably due to disturbance from the natural potassium present in the distill water used. The minimum working range for this method will be at it's detection limit. Meanwhile the

upper working range was considered happen when the activity inside the sample causes detector of the system have a high dead time, such as 20 % and above. At such situation, the distance between the sample and the detector will be increased to reduce the dead time. New calibration will be established for the system prior to a measurement of sample.
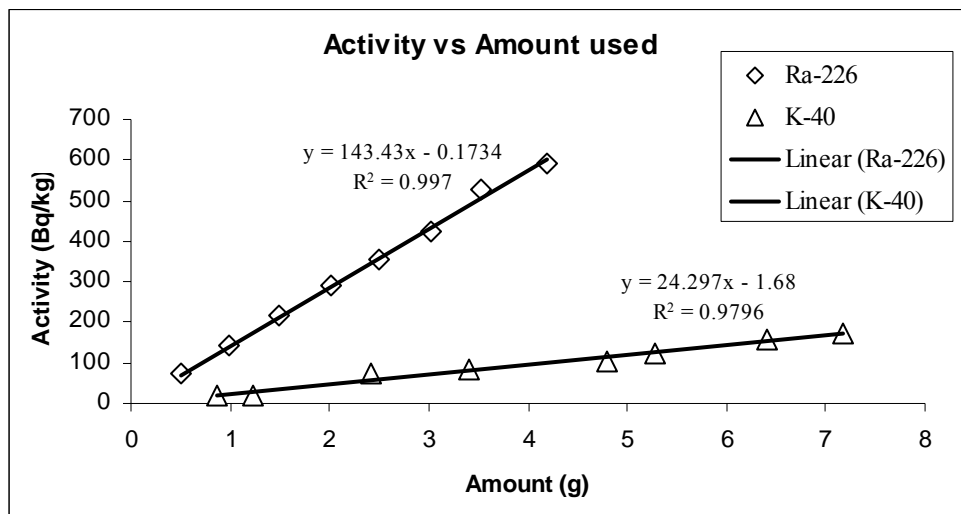
Figure 3. Linearity test of Ra-226 and K-40 showing relation between
added standard and measured activity.

Limit of Detection
Detection limit is not the minimum amount ever to be detected inside the sample. It is proportional to the square root of background and thus also proportional to the square root of the measurement time. For the activity measurement, the limit of detection usually been expressed as the minimum detectable activity (MDA). However, this value is very much depending on background counts, counting time, detector efficiency, emission probability and the gamma-ray energy [11-12]. If a lower limit of detection value is needed, usually a very long counting time (2-3 days) will be required. This is only necessary when dealing with samples for research purpose. Basically a brand new counting system will be able to achieve a lower MDA value. When the detector getting older, the MDA value will start to increase. In such case, the MDA of the measurement was determined by counting a distilled water sample for more than 60 hours. The values are found to be 0.09 Bq/kg and 0.19 Bq/kg for Cs-137 and Ra-226 when using a new counting system (shelf life < 1 year) compared to 0.84 Bq/kg and 2.43 Bq/kg for Cs-137 and Ra-226 for an old counting system (shelf life > 15 years).

The Soil-6 was also be counted at different counting time range of 15 minutes, 30 minutes, 1 hour, 2 hours, 4 hours, 8 hours and 16 hours to find the minimum counting time that can still produce quantitative results. Experimental results (range from 76.97 to 89.12 Bq/kg) show that the minimum counting time of 30 minutes is sufficient enough to enable the spectrometry system to detect Ra-226 quantitatively and the measured value was also closed to the certified value. The same behaviour is found when counting Cs-137 in food samples. Therefore, as a whole, all samples shall be counted for at least 30 minutes to obtain representable results.

Robustness
Robustness of the method was determined by replicate measuring of the CRM Soil-6 by several different operators using the same instrument. The results of the measurement were summarised as in the table 2. From this table, we found that the mean value for the measurement is very close to each other, showing the high precision among the operators. The RSD from the three operators are below 7%. The robustness of the method was checked, by performing the student t-test [13] using the above data. The calculated t value is found to be less than the t critical value, at 95% confidence level when comparing the sets of data. This means that the slight different among the measurement results arose can still be tolerance. No similar experiments had been conducted for the K-40. However, since the Ra-226 can produce robust results, the K-40 will considers being robust if both radionuclides are present in the environmental samples. The calculated Z score value is 0.36, 1.85 and 1.98 for operator 1, 2 and 3, respectively. This score indicates that the precision of the measurement carried out by the respective operator is still within the satisfactory level.

Table 2. Ra-226 measurement data for three different operators

Operator	1	2	3	Operator	1	2	3
Reading 1	90.78	90.08	90.37	Reading 13	84.97	69.95	75.67
Reading 2	93.24	86.08	86.11	Reading 14	88.40	88.04	91.24
Reading 3	86.74	92.75	87.74	Reading 15	-	95.00	81.99
Reading 4	83.40	85.46	74.81	Reading 16	-	89.99	88.23
Reading 5	84.27	84.11	82.82	Reading 17	-	88.95	85.83
Reading 6	88.06	86.15	83.16	Reading 18	-	-	89.19
Reading 7	77.56	85.99	81.85	Reading 19	-	-	80.36
Reading 8	86.21	85.35	84.58	Reading 20	-	-	83.97
Reading 9	87.95	84.45	79.05	Reading 21	-	-	89.36
Reading 10	85.62	85.79	73.72	Reading 22	-	-	86.85
Reading 11	85.46	81.03	75.15	Reading 23	-	-	81.78
Reading 12	86.83	76.84	76.18	Reading 24	-	-	89.87
				Mean	**86.39**	**85.65**	**83.33**
				Std. Dev.	**3.62**	**5.82**	**5.41**
				Rel. Std Dev.	**4.19**	**6.80**	**6.49**
				Z-score	**0.36**	**1.85**	**1.98**

Ruggedness/Reproducibility

The certified value for the Ra-226 in the Soil-6 and K-40 in the SRM IAEA-326 was the average results obtained from the inter laboratories comparison organized by the IAEA which involves the usage of various method and equipments. In other words, the certified value is an acceptable value internationally. Therefore, if the laboratory is able to measure the activity for Ra-226 and K-40 that close to the certified value, it shows that the reproducibility ability of the laboratory. Since the activities measured for both Ra-226 and K-40 were close to the certified value, the reproducibility for this method is therefore no doubtful. Moreover, the results from the ANOVA statistical test performed using the sets of data in table 2 above found that the probability of this result, assuming the null hypothesis, is 0.165. This shows that the results were not significant ($P > 0.05$) and therefore the probability of the result occurring by chance is high [13].

Since both Ra-226 and Ra-228 are isotopes that carry the similar chemical behaviour, the use of Ra-226 to validate the measurement method above shall also be representative for Ra-228 as well.

Conclucions

The method used in the measurement was found to be fairly good to measure the activity of radium isotopes and K-40 in the environmental samples. There is no doubt for the system (this method) to sense the present of Ra-226 and K-40 inside a sample. The precision of the method is found to be fairly good, with the RSD value less than 10% and the calculated z-score values are less than 2, indicate that the precision of the measurement is still within the satisfactory level. The average value obtained for the CRM is close to the certified value with the U score value less than 1 showing no significant bias of this method. Also, a wide linearity range was observed showing that the ability of the system to work from the minimum detectable activity till it maximum range. Minimum counting time of 30 minutes is found to be sufficient enough to enable the spectrometry system to detect Ra-226 quantitatively. Meanwhile, the MDA values are found ranging from 0.19 to 2.43 Bq/kg for several different counting systems. The method validation has also demonstrated that, this measuring technique is robust and rugged. Overall, this analytical technique is able to produce quality and reliable analytical result for measuring of radium isotopes and K-40 in the samples.

Rujukan

1. Povinec P. P., 1994. Sources of Radioactivity in the Marine Environment and their Relative Contributions to Overall Dose Assessment from Marine Radioactivity. IAEA-MEL-R2/94.
2. Instituto de Pesquisas Energeticas e Nucleares, 1998-1999. Progress Report. Brazil. 87.
3. Malaysian Institute for Nuclear Technology Research, 2002. Radiation Safety, Second Edition. Malaysia. 341.
4. Lawrence Berkeley National Laboratory, 1999. Source from "The Lund/LBNL Nuclear Data Search Version 2.0, February 1999" website http://nucleardata.nuclear.lu.se/nucleardata /toi/.. Accessed on 21 March 2005.
5. Department of Standards Malaysia, 1999. ISO/IEC 17025: General Requirements for The Competence of Testing and Calibration Laboratories. Malaysia. 16.
6. Ellison, S.L.R., Rosslein, M. and Williams, A., 2000.   EURACHEM, Quantifying Uncertainty in Analytical Measurement, Second Edition. UK.
7. National Association of Testing Authorities, 1997. Format and Content of Test Methods and Procedures for Validation and Verification of Chemical Test Methods*.,* Technical note. ISBN 0947289151. Australia.
8. Peter, V., 2003. Method Validation, 4th Regional Training Course on QA/QC of Nuclear Analytical Techniques. 20-24 October 2003. KAERI, Taejon, Korea.
9. Yii, M. W., Zaharudin, A., and Kamarozaman, I., 2003. The Effect Of Surrounding Conditions On The Radioactivities Measurement Using Gamma Spectrometry System. In MTC Proceeding. 22-24 July 2003. MINT, Malaysia.
10. Omar, M., Ibrahim, M. Y., Hassan, A., Lau, H.M., and Ahmad, Z., 1990. Enhanced Radium Level in Tin Mining Areas in Malaysia. In: Proceedings of an International Conference on High Levels of Natural Radiation. M. Sohrabi, J.U. Ahmad and S. A. Durrani (editors). 3-7 Nov 1990. Ramsar, Islamic Republic of Iran. 191-195.
11. Debertin, K. and Helmer, R. G., 1988. Gamma and X-Ray Spectrometry with Semiconductor Detectors. Elservier Science. The Netherlands. 399.
12. Dovlete, C. and Povinec, P.P., 2002. Quantification of Uncertainty in Gamma Spectrometric Analysis of Environmental samples. 2nd Regional Training Course on QA/QC of Nuclear Analytical Techniques. 12-16 August 2002. Kuala Lumpur.
13. LGC Limited, 2001. Method Validation Training Course. 3-5 December 2001. SCK•CEN, Mol, Belgium.

ANALYSIS OF PM$_{10}$ IN KUALA TERENGGANU BY INSTRUMENTAL NEUTRON ACTIVATION ANALYSIS

Norhayati Mohd Tahir[1*], Poh Seng Chee[1], Suhaimi Hamzah[2], Khalik Hj Wood[2], Shamsiah Abd. Rahman[2], Wee Boon Siong[2], Suhaimi Elias[2] and Nazaratul Ashifa Abdullah Salim[2].

[1]*Department of Chemical Sciences, Faculty of Science and Technology, Universiti Malaysia Terengganu, 21030 Kuala Terengganu, Terengganu*
[2]*Pusat Nuklear Negara, Bangi 4300 Kajang, Selangor*

Key words: airborne particulate matter, trace elements, PM$_{10}$, INAA, Kuala Terengganu

Abstract

Instrumental neutron activation analysis was used for the determination of trace elements in airborne particulate matter (PM$_{10}$) for air pollution monitoring. For the collection of air samples, the PM$_{10}$ high volume sampler unit and Whatman 41 cellulose filter papers were employed. Samples were collected at 13 selected sampling sites covering areas in the city center, inner and outer city of Kuala Terengganu during the month of March 2005. The average PM10 was 69.64 µgm^{-3}, 83.58 µgm^{-3} and 72.22 µgm^{-3} for sampling stations located in the city center, inner and outer city of Kuala Terengganu, respectively. It was found that the mass of air particles in the study area was higher compared to Bangi and Kuala Lumpur. Chemical analysis of selected elements (Al, Fe, Cu, Pb, V, Mn, Zn, Cr, As Cd), ionic species (Na$^+$, SO$_4^{2-}$, Cl$^-$, NH$_4^+$, Mg^{2+}, K$^+$, Ca^{2+}) and some rare earth elements (REE) were included in this study. In general, most of the average concentration of trace elements in the city center sampling stations was generally higher than the inner and outer city sampling stations. The concentrations of trace elements in sampling stations follow the general trend of Al>Fe>Zn>Cu>Mn>Pb>V>Cr>As>Ni>Cd. The elements concentration ranged from 680-2119 ngm^{-3}, 170-1132 ngm^{-3}, 8.13-122.4 ngm^{-3}, 8.48-77.3 ngm^{-3}, 7.68-14.4 ngm^{-3}, 1-90.4 ngm^{-3}, 1.47-3.25 ngm^{-3}, 1.43-5.03 ngm^{-3}, 1.15-4.45 ngm^{-3}, 0.24-3.75 ngm^{-3} and 0.28-1.36 ngm^{-3}, respectively.

Abstrak

Kajian kualiti udara telah dijalankan melalui penentuan paras kepekatan beberapa logam dalam habuk halus (PM10) dengan kaedah pengaktifan neutron (NAA). Pensampel isipadu tinggi PM10 yang dilengkapi kertas turas selulosa jenis Whatman 41 telah digunakan untuk menentukan kandungan zarahan terampai udara. Sebanyak 13 lokasi pensampelan telah di pilih merangkumi pusat bandar, luar pusat bandar dan pinggir bandar Kuala Terengganu. Purata kepekatan habuk halus (PM10) yang diperolehi adalah 69.64 µg m^{-3}, 83.58µg m^{-3} dan 72.22 µg m^{-3} pada ketiga-tiga lokasi pensampelan tersebut. Kepekatan habuk halus (PM10) yang dicatat di ketiga lokasi ini adalah lebih tinggi berbanding dengan Bandar Bangi dan Kuala Lumpur. Kandungan kepekatan logam (Al, Fe, Cu, Pb, V Mn, Zn, Cr, As Cd dan REE), cation dan anion (Na$^+$, SO$_4^{2-}$, Cl$^-$, NH$_4^+$, Mg^{2+}, K$^+$, Ca^{2+}) dalam habuk halus (PM10) telah dikaji. Secara amnya, turutan logam dalam habuk halus (PM10) adalah seperti berikut Al>Fe> Zn>Cu>Mn >Pb>V>Cr>As>Ni>Cd dan julat kepekatan masing-masing adalah seperti berikut 680-2119 ng/m^3, 170-1132 ngm^{-3}, 8.13-122.4 ngm^{-3}, 8.48-77.3 ngm^{-3}, 7.68-14.4 ngm^{-3}, 1-90.4 ngm^{-3}, 1.47-3.25 ngm^{-3}, 1.43-5.03 ngm^{-3}, 1.15-4.45 ngm^{-3}, 0.24-3.75 ngm^{-3} dan 0.28-1.36 ngm^{-3}.

Introduction

The effects of atmospheric particulate matters on environment and human health have been of great global concern. Many epidemiological studies [1,2,3] have established an association between the particle concentration in the atmospheric and adverse effects on health; the PM10 fraction (diameter < 10 µm), and particularly the PM2.5 fraction (diameter < 2.5 µm) are known to be the primary cause of COPD (Chronic Obstructive Pulmonary Disease), asthma exacerbation, respiratory symptoms, morbidity and mortality, decrement in lung function and possible risk of lung cancer.

Atmospheric aerosol found in urban areas represent a mixture of primary particles emitted from various sources (e.g. vehicles exhausts, coal-fired power plants, oil refineries, forest fires, industrial emission, sea spear, volcano eruption etc) and secondary particles from aerosols formed by chemical reactions [4,5]. The morphology and composition of these particles may change through several processes, including vapor condensation, evaporation and coagulation. The final 'products' usually vary according to origin, chemical composition and physical properties, leading to particular deposition patterns in the human respiratory system. For this reason, intensive

efforts to control pollution sources and to examine contamination levels through the analysis of various air pollution parameters are being followed up all around the region.

Mass concentrations of PM10 in the ambient air are usually less than 0.1 mgm^{-3} as and may contain elements at low concentration range (ngg^{-1}). In order to get good results, the methods of analyzing these elements need to be sensitive and precise, and also be able to identify multielements simultaneously because of the diversity of elements in the samples. Generally, these requirements could not be satisfied by conventional techniques (ICP-AES, and AAS) in a single chemical analysis. However, instrumental neutron activation analysis (INAA) using thermal neutrons in a nuclear reactor as an irradiation source, and high-resolution semiconductor detectors as measuring equipment, is one of the most suitable methods for satisfying the above mentioned requirements. INAA for airborne particulate matter can analyze up to μgg^{-1} ~ ngg^{-1} level of concentrations for 30~40 trace elements simultaneously [6,7,8].

Previous study conducted by Poh [9] on TSP levels in Kuala Terengganu has shown moderate particulate matter concentrations (17.2-148μgm^{-13}) in different areas. However, to the best of the authors' knowledge, there have been very little studies on the chemical characterization in PM10 fraction in Terengganu. The main objective of this study was to determine the distribution characteristics of trace elements in a rapidly urbanized area around Kuala Terengganu. Using appropriate statistical analysis such as correlation and enrichment factor analysis, attempt will be made to identify and apportion source(s) of these particulate matters in an effort to provide some baseline data on air quality for Kuala Terengganu for future references.

Experimental

Study Sites and Location
Kuala Terengganu is the capital of state Terengganu and located in the eastern part of Penisular Malaysia. The area of the capital is 605.28 km^2 with a population of 360,708 people, which accounts for about 35% of the total state population. Samples were taken during March 2005, aerosol samples were collected in 13 sampling stations representing town center (4 station), inner (5 station) and outer city (4 station). Figure 1 illustrated the map off sampling location. Particles with an aerodynamic diameter smaller than 10 μm (PM10) were collected on 8'x10' cellulose membrane filters exposed for 24 hours using PM10 high-volume samplers (Environmental Tisch, USA) at the average flow rate of 1.13 m^{3}min^{-1}. Filters were pre-weighed and then dried in a desiccator for at least 24 hours after being exposed to air.

PM10 and Elemental Concentration
The mass of particulate matter on filters were determined by gravimetric method using a microbalance to an accuracy of ±0.0001g. The chemical analysis was done for soluble ionic species such as Cl$^-$, SO$_4^{2-}$, Na$^+$, NH$_4^+$, K$^+$, Mg^{2+}, and Ca^{2+} and metallic elements such as Al, Fe, Zn, Mn, As, Cr, Cd, Pb, Co, Sb, Th, Cs, Sm, Sc and Eu. For ionic species analysis, portion of filters (5cm in diameter) were placed in 25ml pp centrifuge tube and sonicate for 60 minutes in the ultrasonic bath. The sonic bath temperatures were maintained within 27°C. After removing from the sonic bath, the tubes were continuously shaken for 12 hours. The water extracted ionic species were determined using ion chromatography (DX120, Dionex). Most of the elemental concentrations in particles were determined by INAA. The filter samples were cut into a portion of 5cm in diameter then folded into clean polyethylene vials. Together with the standards, vessel and filter blanks were irradiated in MINT Triga reactor. Both short and long irradiation programs were used for the analysis. In short irradiation program, samples were irradiated individually using a pneumatic transfer system (Rabbit). Samples were counted for 5 minutes and subsequently for 30 minutes on PC based gamma spectrometer systems. For measurement of elements that produced long-lived radionuclides (6 hour irradiation) after 2 weeks of cooling period, the samples were also counted for 1 hour on gamma spectrometer systems. The elemental concentrations were calculated based on comparative method. Standard references material NIST SRM1648 Urban Particulate Matter and IAEA CRM SL-1 Lake Sediment were analysed flowing thesame procedures in every batch of irradiation for quality assurance and quality control purposes. In this work, Pb and Cd determination were unpractical using INAA. Since Cd and Pb are key element for sources apportionment, acid digestion couple with ICP-AES method suggested by Poh [9] was used .
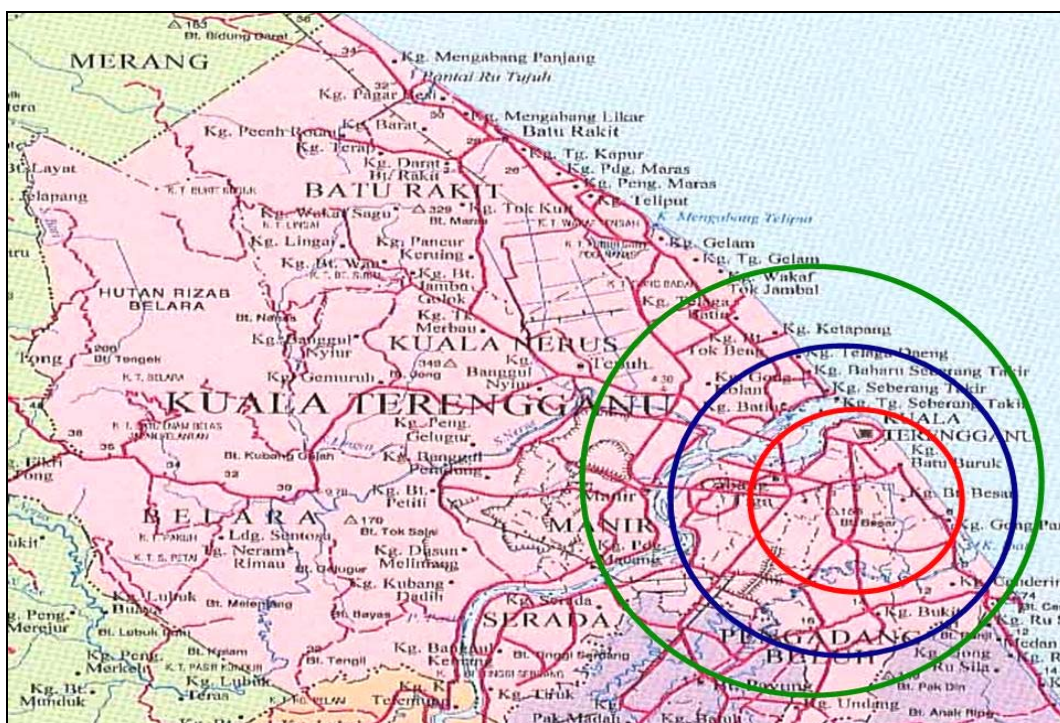
Figure 1. Map of Kuala Terengganu and sampling zones; (red-town center, blue-inner city, green-outer city).

Results and Discussion

Recoveries of the elements in SRM and CRM

Table 1 shows the results of the recovery study using NIST 1648 (Urban Particulate Matter) and IAEA CRM (SL-1 Lake Sediment). Briefly, most of the elements recoveries were within 80-120%. In the INAA analysis of PM10 samples, some elements like Fe, Zn, Mn, As, Cr, Co, La, Sb, Th, Cs, Sm, Sc and Eu were mostly detected in samples. However it was not easy to determine Na, K, Ti, V, Mg, Cl and Al in most of the samples as the sensitivities for these elements were not good. Especially the essential elements (Ca, Na, K, Mg, Cl), the accuracy of recoveries test were far to further from the recommended errors, 15%. For Al, Ti and V samples always lost count in gamma detector due to very short half-life radionuclides. Besides, some of the key elements like Pb and Cd were not determined because of unpractical determination using INAA or most of the recoveries results were too bad in many samples. In order to improve accuracies and uncertainties, cations (NH_4^+, K^+, Na^+, Mg^{2+} and Ca^{2+}), and anions (Cl^- and SO_4^{2-}) were determined by Ion Chromatography (DX 120) and INAA unpractical elements (Pb and Cd) and other poor recoveries elements was determined by more sensitive instruments, ICP-OES (Pb, Cd and others elements).

PM10 and Elementals concentration

Table 2 and Figure 2 illustrated average mass concentrations of PM10 in this study. Highest mean concentration was observed at inner city with value of 83.58 μgm^{-3} followed by outer city with mean value of 72.22 μgm^{-3}. Surprisingly town center poses the lowest concentration (69.64μgm^{-3}); the town center zone was associated with relatively high population and traffic density. It was found that the mass of air particles in the study area was higher compared to Bangi (63.6±26.4 μgm^{-3}) and Kuala Lumpur (55.4±30.3 μgm^{-3})[14].The high mass concentrations of inner city are caused by high value obtained from the fifth monitoring stations called *Losong*. During the sampling period, we managed to observe major soil excavation and building demolishing activities at about 3 km radius from *Losong* monitoring station. This contributed significantly to the increase in the mass concentration. The range of mass concentration in outer city (suburban residential areas) were relatively small compared to others. The free flow of air and totally no tall obstruction (buildings, trees and vehicles) around the monitoring stations make it an ideal criteria to collect air samples. All the PM10 values obtained were still well below the recommended Malaysia guideline for PM10 (mean of 24-hour measurement = 150 μgm^{-3}).

Table 3 presents the concentration of the measured elements and ionic species in PM10 in the three zones during to entire sampling period. The concentration levels between each zone are given in term of average mean and

range of the value. In general, most of the average concentration of trace elements in the city center sampling stations was generally higher than the inner and outer city sampling stations. The concentrations of trace elements in sampling stations follow the general trend of Al>Fe> Zn>Cu>Mn>Pb>V>Cr>As>Ni>Cd. The elements concentration ranged from 680-2119 ngm^{-3}, 170-1132 ng m^{-3}, 8.13-122.4 ngm^{-3}, 8.48-77.3 ngm^{-3}, 7.68-14.4 ngm^{-3}, 1-90.4 ngm^{-3}, 1.47-3.25 ngm^{-3}, 1.43-5.03 ngm^{-3}, 1.15-4.45 ngm^{-3}, 0.24-3.75 ngm^{-3} and 0.28-1.36 ngm^{-3}, respectively. For outer city, the concentration of REE showed the trend of La>Sb>Th>Cs>Sm>Sc>Eu, whereas in inner city and town center followed the trends of Sb>La>Th>Cs>Sc>Sm>Eu.

In general, the average of the concentration of ionic species follows the trend of Na$^+$>SO$_4$$^{2-}$>Cl$^-$,>NH$_4$$^+$>Mg^{2+}>K$^+$>Ca^{2+}. High loading of Na$^+$,Mg^{2+} and Cl$^-$ species in samples were found in inner city zones. Whereas, higher concentration of NH$_4$$^+$, K$^+$ and SO$_4$$^{2-}$ species were found in outer city aerosol samples. The average and range of species ionic concentration are given in Table 3. The high loadings of Na$^+$, Mg^{2+} and Cl$^-$ in inner city were most probably generated from sea breeze. Correlation analysis indicated there was no clear correlation between these species in data combined from the three zones (Table 4) due to large variation in the analysis results for some ionic species in three different zones. However, the plot of Na against Mg^{2+} and Cl$^-$ (Fig. 3) within inner city samples only show some trends of better correlation (Cl$^-$, r = 0.995; Mg^{2+}, r = 0.999) which might explain the role of sea breeze as major sources for Na$^+$, Mg^{2+} and Cl$^-$ in inner city.

Table 1. Recoveries results of certified/standard references material (INAA method)

Element	SRM 1648			CRM SL 1		
	Certified Value	Obtained Value	Recovery (%)	Certified Value	Obtained Value	Recovery (%)
Al	34200	30882	90.3	89000	77990	87.63
Mn	786	694	88.4	3460	3699	106.93
Fe	39100	36722	93.92	67400	58253	86.43
As	115	110	95.76	27.5	28.7	104.47
Cr	403	349	86.68	104	120	115.56
Co	609	579	95.10	19.8	20.8	105.15
Zn	4760	3839	80.66	223	276.5	123.97
Eu	0.8	0.73	92	1.6	1.72	108
Sm	4.4	3.73	85.5	9.25	7.80	84.42
Th	7.4	6.75	91.31	14	15.02	107.32
Sc	7	6.22	88.91	17.3	19.03	110.21
La	42	39.44	93.92	52.6	60.67	115.36
Ce	55	53.43	97.16	117	120.40	102.91
Sb	45	40.62	90.28	1.31	1.45	110.76

Table 2**.** PM10 range and average within 3 different sections

Site	Average (range)
Town center	69.64 (58.37-83.06)
Inner city	83.58 (52.91-134)
Outer city	72.22 (70.02-73.25)

| Element	Outer City (ng/m^3)	Inter City (ng/m^3)	Town Center (ng/m^3)
Na^+	18366 (5708-41262)	35094 (1063-64518)	15526 (2175-30417)
NH_4^+	5184 (1571-9393)	4461 (3863-5099)	3660 (2935-4378)
K^+	1881 (1418-2211)	1484 (592-2594)	1758 (944-3243)
Mg^{2+}	2574 (727-4507)	2243 (216-7176)	1784(335-3461)
Ca^{2+}	1527 (903-2069)	1160 (441-2671)	1764 (731-2760)
Cl^-	5393 (2898-8678)	7717 (475-21453)	6298 (2213-10409)
SO_4^{2-}	10960 (5115-17065)	9477 (3055-15282)	9872 (6982-13555)
Al	780 (680-2119)	630 (510-1520)	1020 (950-1380)
Fe	430 (170-650)	660 (360-1040)	690 (570-1132)
As	1.09 (1.32-4.45)	1.53 (1.15-2.35)	1.70 (1.57-2.93)
Pb	3.973 (1.00-7.35)	25.34 (3.61-51.3)	55.45 (53.6-90.4)
Cd	0.329 (0.28-0.39)	0.563 (0.24-1.07)	0.843 (0.25-1.36)
Ni	1.003 (0.24-2.05)	0.959 (0.48-1.39)	1.715 (0.49-3.75)
V	2.362 (1.47-2.89)	2.391 (1.83-2.73)	2.376 (1.91-3.25)
Cu	30.67 (8.48-41.0)	39.72 (20.2-77.3)	43.85 (22.4-66.5)
Zn	16.14 (8.13-42.8)	59.34 (14.6-88.2)	72.36 (7.34-122.4)
Cr	1.30 (1.43-2.20)	1.32 (1.73-2.97)	2.65 (1.67-5.03)
Mn	8.29 (7.68-8.89)	9.89 (7.78-11.5)	11.2 (8.45-14.4)
Cs	0.29 (0.28-0.30)	0.23 (0.11-0.28)	0.19 (0.13-0.44)
Sb	1.41 (0.45-2.58)	1.79 (1.21-3.06)	1.96 (0.89-3.51)
Sc	0.14 (0.04-0.20)	0.18 (0.09-0.31)	0.19 (0.06-0.32)
La	2.04 (1.72-4.04)	1.67 (0.89-2.27)	1.56 (1.12-2.29)
Sm	0.21 (0.18-0.23)	0.14 (0.09-0.18)	0.14 (0.10-0.12)
Th	0.47 (0.37-0.57)	0.51 (0.20-0.77)	0.45 (0.23-0.85)
Eu	0.063 (0.055-0.086)	0.095 (0.071-0.147)	0.087 (0.089-0.153)
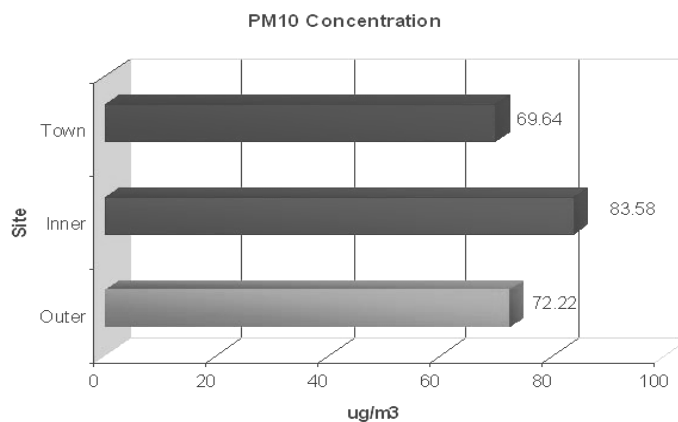
Figure 2. PM10 comparisons within 3 sections

Table 3. The range of concentration and mean value of elements and ionic species in PM10
Table 4. Correlation analysis of ionic species and element data combined from 3 sampling zones (n=13)

* Correlation is significant at the 0.05 level (2-tailed).

191

	Na	Cl	NH4	K	SO4	Al	Cd	Cu	Ni	Pb	Ti	V	Zn	As	Fe	Cr
Na	1	-0.227	-0.553	-0.217	-0.124	-0.064	0.076	0.229	-0.133	-0.064	0.076	0.229	-0.133	0.685(*)	0.173	-0.334
Cl	-0.227	1	0.130	0.276	0.325	0.074	0.061	0.478	0.134	0.074	0.061	0.478	0.134	0.264	-0.057	0.185
NH4	-0.553	0.130	1	-0.081	0.070	-0.311	-0.009	0.141	0.122	-0.311	-0.009	0.141	0.122	-0.084	0.080	0.191
K	-0.217	0.276	-0.081	1	0.619(*)	0.855(**)	0.441	0.379	0.737(**)	0.855(**)	0.441	0.379	0.737(**)	0.127	-0.191	-0.498
SO4	-0.124	0.325	0.070	0.619(*)	1	0.696(*)	0.565	0.631(*)	0.568(*)	0.696(*)	0.565	0.631(*)	0.568(*)	0.300	-0.351	-0.328
Al	-0.084	0.074	-0.311	0.855(**)	0.696(*)	1	0.327	0.424	0.786(**)	0.795(**)	0.327	0.424	0.786(**)	0.597	-0.030	-0.752
Cd	0.076	0.061	-0.009	0.441	0.565	0.327	1	0.393	0.540	0.327	0.789(**)	0.393	0.540	0.190	-0.428	-0.347
Cu	0.229	0.478	0.141	0.379	0.631(*)	0.424	0.393	1	0.194	0.424	0.393	0.847(**)	0.194	0.758(*)	-0.260	-0.507
Ni	-0.133	0.134	0.122	0.737(**)	0.568(*)	0.786(**)	0.540	0.194	1	0.786(**)	0.540	0.194	0.687(**)	0.044	-0.032	-0.336
Pb	-0.064	0.074	-0.311	0.855(**)	0.696(*)	0.795(**)	0.327	0.424	0.786(**)	1	0.327	0.424	0.786(**)	0.597	-0.030	-0.752
Ti	0.076	0.061	-0.009	0.441	0.565	0.327	0.789(**)	0.393	0.540	0.327	1	0.393	0.540	0.190	-0.428	-0.347
V	0.229	0.478	0.141	0.379	0.631(*)	0.424	0.393	0.847(**)	0.194	0.424	0.393	1	0.194	0.758(*)	-0.260	-0.507
Zn	-0.133	0.134	0.122	0.737(**)	0.568(*)	0.786(**)	0.540	0.194	0.786(**)	0.786(**)	0.540	0.194	1	0.044	-0.032	-0.336
As	0.685(*)	0.264	-0.084	0.127	0.300	0.597	0.190	0.758(*)	0.044	0.597	0.190	0.758(*)	0.044	1	0.418	-0.227
Fe	0.173	-0.057	0.080	-0.191	-0.351	-0.030	-0.428	-0.260	-0.032	-0.030	-0.428	-0.260	-0.032	0.418	1	0.587
Cr	-0.334	0.185	0.191	-0.498	-0.328	-0.752	-0.347	-0.507	-0.336	-0.752	-0.347	-0.507	-0.336	-0.227	0.587	1

**

Correlation is significant at the 0.01 level (2-tailed).
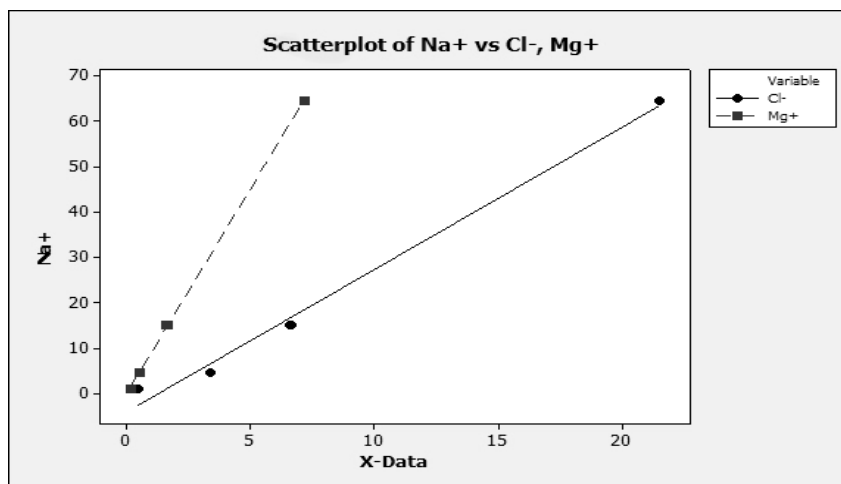
Figure 3. The plot of Na against Mg^{2+} and Cl^-

Enrichment Factor

The enrichment factor method has commonly been used as a tool to evaluate the strength of enrichment or depletion, relative to specific sources. The enrichment factor for any element X relative to control/unpolluted references material is defined by

$$EF_X = \frac{(X/Y)_{air}}{(X/Y)_{control}}$$

Where EF_X is the enrichment factor of X, Y is a reference element for crustal material and $(X/Y)_{air}$ is the concentration ratio of X to Y in the samples and $(X/Y)_{control}$ is the same ratio in control/unpolluted references material. If EF_X approached unity, crustal soils are likely the predominant sources for element X[10]. In this study, the $(X/Y)_{control}$, ratio calculation for each elements was based on samples collected from a rural area call *Manir* (one of the sampling station in outer city). Al is normally use as references element since it can be accurately measured by a number of analytical method and abundance in the earth crusts [11].

Figure 4. Enrichment factors of selected trace elements relatively to Al for the PM10 samples at three locations.

Figure 4 indicates that the enrichment factors of all elements except La and Sm in town center are higher than those in inner and outer city. The rapid urbanization activities in Kuala Terengganu explains for the high elements loading to ambient atmospheric. The enrichment factor for Cd, Cr, Ni, Ti, Pb and Zn in town center exhibited at l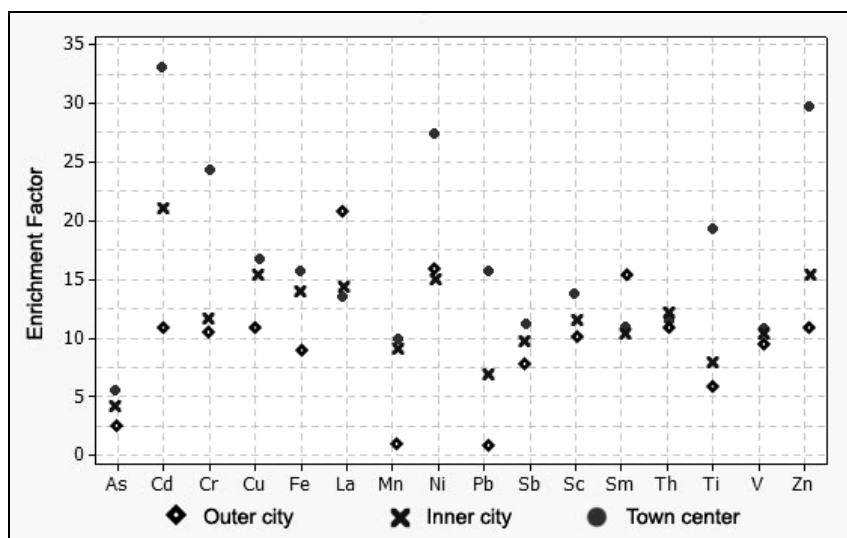east 10 times higher than other places. The strong correlation (Table 4) between Pb, Zn, Ni and SO_4^{2-} ($r \geq 0.696$) explained these elements may originate from traffic emission sources. Cadmium, Pb, Cr, Ti and Zn probably emitted on atmospheric as part of brake dust, road paint, diesel exhaust particles, road construction materials, or car catalyst materials [12]. Whereas Ni, which are frequently associated with fuel burning, can be easily attributed to emissions from the petrochemical combustion such as vehicle gasoline. According to Chiarenzelli *et al.*[13] rare earth elements may be useful as reference elements in environmental studies due to its transport in the particulate phase, lack of significant anthropogenic sources, coherent group geochemistry, generally robust concentrations, and upper crustal signatures. For REE except La, most of the enrichment factors were below 15 and close to each study zones. This indicates the REE may appear to be of soils origin.

Conclusion

Highest mean PM10 concentration was observed in inner city with value of 83.58 μgm^{-3} followed by outer city with mean value of 72.22 μgm^{-3} and town center, 69.64μgm^{-3}. The Al, Fe, Cu, Zn, Mn, Pb, V, Cr, As, Ni, Cd, Cs, Sb, Sc, La, Sm, Th and Eu concentration ranged from 680-2119 ngm^{-3}, 170-1132 ngm^{-3}, 8.13-122.4 ngm^{-3}, 7.68-14.4 ngm^{-3}, 1-90.4 ngm^{-3}, 1.47-3.25 ngm^{-3}, 1.43-5.03 ngm^{-3}, 1.15-4.45 ngm^{-3}, 0.24-3.75 ngm^{-3} and 0.28-1.36 ngm^{-3}, 0.11-0.44 ngm^{-3}, 0.0.45-3.51 ngm^{-3}, 0.04-0.32 ngm^{-3}, 0.89-4.40 ngm^{-3}, 0.09-0.23 ngm^{-3}, 0.2-0.85 ngm^{-3} and 0.05-0.153 ngm^{-3}, respectively. For ionic species, all the three locations follow a similar trends of $Na^+ > SO_4^{2-} > Cl^-, > NH_4^+ > Mg^{2+} > K^+ > Ca^{2+}$. The high loadings of Na^+, Mg^{2+} and Cl^- in inner city were most probably generated from sea breeze. Finally, enrichment factors for Cd, Cr, Ni, Ti, Pb and Zn indicate that these elements may origin from traffic emission sources and REE may appear to be of soils origin.

References
1. Jalaludin B., O'Toole B.I., Leeder S.R. (2004). "Acute effects of urban ambient air pollution on respiratory symptoms, asthma medication use, and doctor visits for asthma in a cohort of Australian children" *J. Environmental Research, A.* 95, 34-32.
2. Kappos A.D., Bruckmann P., Eikmann T., Englert N., Heinrich U., Höppe P., Koch E., Krause G.H.M., Kreyling W.G., Rauchfuss K. (*2004). "Health effects of particles in ambient air" *International Journal of Hygiene and Environmental Health A.* 4, 399-407.
3. Desqueyroux H., Pujet J.C., Prosper M., Squinazi F., Momas I. (2002). "Short-Term Effects of Low-Level Air Pollution on Respiratory Health of Adults Suffering from Moderate to Severe Asthma**"** *J. Environmental Research A.* 89, 29-37.

4. Salma I., Chi X.G., Maenhaut W. (2004) "Elemental and organic carbon in urban canyon and background environments in Budapest, Hungary**"** *J. Atmospheric Environment, A.* 38, 27-36.
5. Pun B.K. and Seigneur C. (1999). "Understanding particulate matter formation in the California San Joaquin Valley: conceptual model and data needs" *J. Atmospheric Environment, A.*33- 29, 4865-4875.
6. Rizzio E., Giaveri G., Arginelli D., Gini L., Profumo A., Gallorini M. (1999). "Trace elements total content and particle sizes distribution in the air particulate matter of a rural-residential area in north Italy investigated by instrumental neutron activation analysis" *J. The Science of The Total Environment, A.* 226-1, 47-56.
7. Freitas M.C., Almeida S.M., Reis M.A., Oliveira O.R. (2003). "Monitoring trace elements by nuclear techniques in PM10 and PM2.5" *J. Nuclear Instruments and Methods in Physics Research Section A, A.* 505-1, 430-434.
8. Alemón E., Herrera L., Ortiz E., Longoria L.C. (2004). "Instrumental nuclear activation analysis (INAA) characterization of environmental air filter samples" *J. Applied Radiation and Isotopes A.*60-6, 815-823.
9. Poh S.C. (2004). "Determination of heavy metals in airborne particulate matter in Kuala Terenggu, Malaysia" *Bsc Environmental Analytical Chemistry, FST*, KUSTEM; 88p.
10. Gao Y., Nelson E.D., Field M.P., Ding Q., Li H., Sherrell R.M., Gigliotti C.L., Van Ry D.A., Glenn T.R., Eisenreich S.J. (2002). "Characterization of atmospheric trace elements on PM2.5 particulate matter over the New York–New Jersey harbor estuary" *J. Atmospheric Environment A.*36, 1077–1086.
11. Chester R., Nimmo M., Corcoran P.A. (1997). "Rain water-aerosol trace metal relationship at Cap Ferrat: A costal site in the western Mediterranean" *J. Marine Chemistry A.*58, 293-312.
12. Kim K.W., Myung J.H., Ahn J.S., Chon H.T. (1998) "Heavy metal contamination in dusts and stream sediments in the Taejon area, Korea" *J. Geochemical Exploration A.* 64, 409- 419.
13. Chiarenzelli J., Aspler L., Dunn C., Cousens B., Ozarko D., Powis K. (2002). "Multi-element and rare earth element composition of lichens, mosses, and vascular plants from the Central Barrenlands, Nunavut, Canada" *J. Applied Geochemistry, V.* 16- 2, 245-270.
14. Suhaimi Hamzah M., Shamsiah A.R., Mohd Khalid M., Khalik W. (2001). "Characterisation of Air Particulate Matter in Klang Valley by NAA technique*". Seminar RND 2000, MINT*.

AN ASSESSMENT OF ABSORBED DOSE AND RADIATION HAZARD INDEX FROM NATURAL RADIOACTIVITY

Masitah Alias[1], Zaini Hamzah[1], Ahmad Saat[1], Mohamat Omar[2] and Abdul Khalik Wood[2]

[1]Faculty of Applied Sciences, Universiti Teknologi MARA, 40450 Shah Alam, Selangor Darul Ehsan
[2]Malaysian Institute for Nuclear Technology Research, 43000, Bangi, Selangor Darul Ehsan.
e-mail: ellyaa@yahoo.com

Abstract

Naturally occurring radionuclides such as ^{40}K, ^{226}Ra and ^{228}Ra which emit gamma radiation through their decaying process could reach the human in vicinity. The study area was chosen for its variety of surface conditions such as slope, flat land catchments and also forest area, which is used as a reference place. Soil samples were collected using hand auger, and the sampling positions were determined using a Global Positioning System (GPS). The amount of radioactivity concentration of these radionuclides is the important factor in assessing whether it is harmful or otherwise. In this study, the surface doses rate measurements were done in-situ using dose rate meter, and the radioactivity concentration levels were done by counting the soil samples using gamma spectrometer with HPGe detector in the laboratory. The amount of uranium, thorium and potassium in soil were determined using neutron activation analysis (NAA) technique. The results show a reasonably low radiation absorb dose and radiation hazard index, which is a good indication for the farmers to work in the area.

Abstrak

Radionuklida semulajadi seperti ^{40}K, ^{226}Ra dan ^{228}Ra yang memancarkan sinar gama melalui proses pereputannya boleh mengenai manusia yang berhampirannya. Kawasan kajian ini telah dipilih berdasarkan keadaan permukaan tanah yang berbeza seperti tanah rata, cerun, dan kawasan rendah yang berpaya serta kawasan hutan untuk dijadikan kawasan rujukan. Sampel tanah telah dipungut menggunakan auger dan lokasi pensampelan ditentukan dengan menggunakan sistem penempatan global (GPS). Jumlah kepekatan radioaktiviti dari radionuklida ini adalah faktor penting bagi menentukan samada ianya berbahaya atau tidak. Dalam kajian ini, pengukuran radioaktiviti dalam makmal dilakukan dengan membilang sampel tanah menggunakan spektrometer gama dilengkapkan dengan pengesan HPGe. Jumlah uranium, thorium dan kalium di dalam tanah ditentukan dengan teknik analisis pengaktifan neutron. Hasil kajian menunjukkan kadar serapan dan indeks radiasi berbahaya yang agak rendah yang menunjukkan indikasi yang baik untuk petani yang bekerja di kawasan tersebut.

Introduction

Over 60 radionuclides (radioactive elements) can be found in nature, and they can be placed in three general categories i.e. Primordial - formed before the creation of the Earth, Cosmogenic - formed as a result of cosmic ray interactions, and Human Produced - enhanced or formed due to human actions (minor amounts compared to natural). Radionuclides are found naturally in air, water and soil. They are even found in us, being that we are products of our environment. Every day, we ingest and inhale radionuclides in our air, food and the water. Natural radioactivity is common in the rocks and soil that makes up our planet, in water and oceans, and in our building materials and homes. There is nowhere on Earth that we can not find natural radioactivity [1].

Some radioactive nuclides are detectable in soil. They belong to the natural radionuclides like the members of the uranium and thorium decay series. More specifically, natural environment radioactivity and the associated external exposure due to gamma radiation depend primarily on the geological and geographical conditions, and appear at different levels in the soils of each region in the world [2,3]. The specific levels of terrestrial environmental radiation are related to the geological composition of each lithologically separated area, and to the content of the rock from which the soils originated in each area in the radioactive elements of thorium (Th), uranium (U) and potassium (K). It is well known, for instance, that igneous rocks of granitic composition are strongly enriched in Th and U (on average 15 μgg^{-1} of Th and 5 μgg^{-1} of U), as compared to rocks of basaltic or ultramafic composition (< 1μgg^{-1} of U) [2,9,10]. For that reason, higher radiation levels are associated with igneous rock and lower level with sedimentary rocks. There are exceptions, however, as some shales and phosphate rocks have relatively high content of those radionuclides [2,3].

Uranium minerals are chemically weathered to soluble U(VI) complexes and carried by river water downstream to the oceans, while the primary mode for transport of thorium from the continents to the oceans follow the detrital phase [4,5]. The residence time for thorium in sea water is only approximately 300-350 years. Uranium remains soluble in the sea (as carbonate and other complexes) and has a residence time in sea water of some 500 000 years [6].

Precipitation of uranium can occur easily by reduction to insoluble U(IV). Thus, environments in which carbonaceous and bituminous shales form are particularly favourable for U removal by reduction of U(VI) to U(IV). Lignites are also enriched in uranium, some as U(IV), as expected, and some as U(VI) because the latter form can easily be scavenged by 'coaly' material without reduction. This accounts, in part, for the high U content of such rock. In the case of phosphotic rocks, co-precipitation of U(IV) with Ca^{2+} is likely owing to their very similar ionic radii, but the exact mechanism for the reduction of U(VI) to U(IV) in these rocks is not known [6].

Th/U ratio in nature varies widely. In rocks from which U has been removed, high Th/U ratio results; conversely, in rocks precipitated under chemically reducing environments far from suspected rock source, U is enriched over thorium. Thus, above average Th/U ratios are observed in continental sediments, especially in laterites and other residual deposits. Low Th/U ratios are found in chemically precipitated marine sedimentary rock, such as evaporate sand, limestone, and extremely low Th/U ratios are found in carbonaceous rock . [6].

Human beings have always been exposed to natural radiations from their surrounding. The exposure to ionizing radiations from natural sources occurs because of naturally occurring radioactive elements in the soil and rocks, cosmic rays entering the earth's atmosphere from outer space and the internal exposure from radioactive elements through food, water and air. Therefore the assessment of gamma radiation dose from natural sources is of particular importance as natural radiation is the largest contributor to the external dose of the world population [7].

The objectives of this research project are to determine the radioactivity concentrations of ^{40}K, ^{226}Ra and ^{228}Ra in top soil and depth soil samples, to measure the surface radiation dose rate, to determine the concentration of uranium, thorium and potassium in topsoil samples, to evaluate the level of radioactivity concentrations and their relation with soil texture, physical and chemical properties of soil, and to estimate the radiation absorbed dose, effective annual dose, radium equivalent activity and radiation hazard index from the radioactivity measured in the study area.

Experimental

Sampling and Sample Preparation
The sampling area was an oil palm area located at Jengka 15, Pahang, Malaysia. The sampling technique was in accordance of the California Standard Operating Procedure [8]. The sampling was done in a zig-zag pattern comprising 50 sampling points for topsoil (up to 6cm) and 7 points for depth profile (up to 20 cm). From each point, five representative samples were collected at equal distance along the 1 m circumference around the point. This will improve the representative homogeneity of sample from each sampling point. The distance between each point was about 40 meters. The position and elevation of each sampling points was determined using a global positioning system (GPS). Soil samples were taken to the lab and cleaned from plant roots and other foreign materials. Samples were dried in an oven at 60°C or air dried for a few days. Samples were grounded and sieved using 2 mm sieve to get the homogeneous samples. About 400 g of dry sample was weighed into a plastic container, capped, sealed and then labeled.

Measurement of Activity Concentrations of Radionuclides in Top Soils: ^{40}K, ^{226}Ra, and ^{228}Ra.
The samples were kept at room temperature for three weeks to allow the natural radionuclides to achieve equilibrium. A same amount of IAEA (soil-6) prepared in the same manner was used as standard reference material. The measurements were made using a gamma ray HPGe counting system calibrated using ^{57}Co, ^{137}Cs, ^{133}Ba, ^{85}Sr, ^{54}Mn, ^{88}Y and ^{65}Zn for two hours. Counting efficiency of the counting system used was determined previously for all of its counting geometry. The measurements were carried out using facilities in Malaysian Nuclear Agency, Bangi. The radionuclides were identified according to their individual photo peak which are energy peaks 295, 352 and 609 keV used to determine ^{226}Ra. Energy peak 911 keV was used to determine ^{228}Ra

while 1462 keV was used to determine ^{40}K. The concentration of the individual radionuclide was calculated by using the following formula:

$$W_S = \frac{M_p \times A_S \times W_p}{M_S \times A_p} \qquad \text{where}$$

W_s;   the concentration of the radionuclides in sample (Bq/kg)
W_p;   the concentration of the radionuclides in standard (Bq/kg)
M_s ;   the weight of the sample (g),
M_p ;   the weight of the standard (g)
A_s ;   the counting of the samples (cps); and,
A_p;   the counting of the standard (cps)

Surface Dose Rate
The surface doses rate were measured in-situ at each sampling point using LUDLUM rate meter. The detector was placed 1 meter above the ground when taking the reading. The meter was pre calibrated before taking it to the field.

Results and Discussion

Radionuclides Activity Concentrations
Table1 lists the radionuclide activity concentrations for ^{40}K, ^{226}Ra and ^{228}Ra in forest, flat, slope and catchments area. 50 samples were analyzed and it gives the means activity concentrations of ^{40}K, ^{226}Ra and ^{228}Ra.

Table 1: Radionuclides (^{40}K, ^{226}Ra, and ^{228}Ra) activity concentrations in top soils

Sample Code	North	South	^{40}K (Bq/kg)	^{226}Ra (Bq/kg)	^{228} Ra (Bq/kg)
			Forest Area		
F_RSP_1	03⁰44.362'	102⁰34.000'	45.9 ± 11.9	16.9 ± 9.6	37.1 ± 3.7
F_RSP_2	03⁰44.386'	102⁰33.967'	217.6 ± 36.5	18.3 ± 5.7	26.7 ± 2.3
F_RSP_3	03⁰44.350'	102⁰33.968'	55.3 ± 17.1	12.6 ± 7.9	28.8 ± 2.7
F_RSP_4	03⁰44.349'	102⁰33.975'	124.8 ± 21.4	23.8 ± 5.4	31.5 ± 2.2
F_RSP_5	03⁰44.348'	102⁰33.980'	89.7 ± 18.7	23.0 ± 1.1	42.0 ± 3.9
F_RSP_6	03⁰44.355'	102⁰33.990'	152.4 ± 20.2	25.2 ± 1.2	33.9 ± 2.4
F_RSP_7	03⁰44.361'	102⁰34.003'	234.5 ± 29.6	24.3 ± 1.3	35.2 ± 3.6
F_RSP_8	03⁰44.339'	102⁰33.993'	87.1 ± 13.3	23 ± 0.6	35.5 ± 2.2
	Range		45.9 - 234.5	12.6 - 25.2	26.7 - 42.0
	Mean		125.9 ± 21.1	20.9 ± 4.1	33.8 ± 2.9
			Flat Area		
F_1CLSP_1	03⁰44.350'	102⁰33.909'	45.9 ± 11.9	10.5 ± 0.7	16.3 ± 2.3
F_1CLSP_2	03⁰44.402'	102⁰33.806'	68.4 ± 14.0	19.8 ± 1.0	24.9 ± 2.4
F_1CLSP_3	03⁰44.401'	102⁰33.790'	45.4 ± 11.8	10.1 ± 0.8	12.0 ± 2.4
F_1CLSP_4	03⁰44.391'	102⁰33.874'	61.8 ± 11.9	19.2 ± 0.9	26.1 ± 2.8
F_1CLSP_5	03⁰44.380'	102⁰33.822'	46.3 ± 7.5	10.7 ± 0.7	15.8 ± 2.4
F_1CLSP_6	03⁰44.396'	102⁰33.816'	156.6 ± 17.3	29.3 ± 0.8	39.1 ± 2.9
	Range		45.4 - 156.6	10.1 - 29.3	12.0 -39.1
	Mean		70.7 ± 12.4	16.6 ± 0.8	22.4 ± 2.5
			Flat Area		
F_2CLSP_1	03044.371'	102033.897'	44.8 ± 8.6	16.3 ± 0.4	29.8 ± 2.6
F_2CLSP_2	03044.365'	102033.903'	42.2 ± 9.3	12.6 ± 0.9	20.9 ± 2 .8
F_2CLSP_3	03044.356'	102033.917'	84.0 ± 10.6	14.7 ± 0.8	27.9 ± 3.0
F_2CLSP_4	03044.359'	102033.902'	46.2 ± 11.1	19.1 ± 1.0	29.1 ± 3.4
F_2CLSP_5	03044.385'	102033.880'	59.9 ± 7.2	16.1 ± 0.4	21.7 ± 1.3
F_2CLSP_6	03⁰44.380'	102⁰33.904'	23.9 ± 6.1	31.6 ± 0.7	34.0 ± 2.1
F_7CLSP_7	03⁰44.362'	102⁰33.896'	98.4 ± 13.6	16.8 ± 1.0	29.8 ± 3.3
F_2CLSP_8	03⁰44.364'	102⁰33.881'	29.8 ± 10.2	15.2 ± 1.0	22.7 ± 3.0
F_2CLSP_9	03⁰44.381'	102⁰33.886'	70.0 ± 12.2	18.9 ± 1.0	26.3 ± 2.1
	Range		23.9 - 98.4	12.6 - 31.6	21.7 – 34.0
	Mean		55.5 ± 10.9	17.9 ± 0.8	26.9 ± 2.6

Table 1: Radionuclides (^{40}K, ^{226}Ra, and ^{228}Ra) activity concentrations in top soils (cont'd)

Sample Code	North	South	^{40}K (Bq/kg)	^{226}Ra (Bq/kg)	^{228}Ra (Bq/kg)
			Slope Area		
S_1CLSP_1	$03^044.380$'	$102^033.771$'	50.4 ± 16.2	23.5 ± 2.2	32.8 ± 5.3
S_1CLSP_2	$03^044.361$'	$102^033.785$'	69.7 ± 14.4	30.3 ± 1.8	27.5 ± 5.4
S_1CLSP_3	$03^044.367$'	$102^033.809$'	51.2 ± 17.8	22.2 ± 2.3	42.8 ± 4.5
S_1CLSP_4	$03^044.392$'	$102^033.775$'	49.8 ± 17.5	20.6 ± 2.1	32.8 ± 6.0
S_1CLSP_5	$03^044.381$'	$102^033.791$'	108.3 ± 15.5	21.3 ± 1.1	25.7 ± 2.9
S_1CLSP_6	$03^044.362$'	$102^033.771$'	108.4 ± 15.2	21.2 ± 1.0	25.6 ± 2.9
S_1CLSP_7	$03^044.330$'	$102^033.871$'	48.9 ± 6.6	15.8 ± 0.4	22.0 ± 1.3
S_1CLSP_8	$03^044.321$'	$102^033.852$'	71.0 ± 14.8	16.6 ± 1.0	17.6 ± 2.5
S_1CLSP_9	$03^044.336$'	$102^033.771$'	52.1 ± 5.5	16.3 ± 0.3	25.2 ± 1.3
S_1CLSP_{10}	$03^044.330$'	$102^033.820$'	102.3 ± 23.7	36.5 ± 2.4	41.3 ± 5.3
S_1CLSP_{11}	$03^044.330$'	$102^033.897$'	11.3 ± 1.3	14.8 ± 1.8	20.0 ± 4.3
S_1CLSP_{12}	$03^044.327$'	$102^033.859$'	51.8 ± 6.0	11.3 ± 0.3	17.8 ± 1.2
S_1CLSP_{13}	$03^044.351$'	$102^033.916$'	34.7 ± 9.6	11.7 ± 0.8	18.9 ± 2.1
S_1CLSP_{14}	$03^044.375$'	$102^033.771$'	50.5 ± 11.2	19.6 ± 1.5	29.1 ± 3.4
	Range		11.3 - 108.4	11.3 – 36.5	17.8 – 42.8
	Mean		61.5 ± 12.5	20.1 ± 1.4	27.1 ± 3.5
S_2CLSP_1	$03^044.321$'	$102^033.925$'	52.1 ± 13.1	14.0 ± 1.0	22.8 ± 2.9
S_2CLSP_2	$03^044.325$'	$102^033.942$'	78.3 ± 11.5	18.7 ± 11.5	27.5 ± 3.4
S_2CLSP_3	$03^044.344$'	$102^033.945$'	126.4 ± 12.4	18.7 ± 0.5	18.7 ± 1.7
S_2CLSP_4	$03^044.358$'	$102^033.940$'	72.4 ± 13.1	16.5 ± 0.9	16.5 ± 0.9
S_2CLSP_5	$03^044.326$'	$102^033.904$'	14.2 ± 6.7	18.0 ± 0.8	28.6 ± 1.8
S_2CLSP_6	$03^044.343$'	$102^033.880$'	59.1 ± 19.2	35.3 ± 2.2	38.2 ± 4.6
S_2CLSP_7	$03^044.334$'	$102^033.925$'	32.0 ± 8.0	10.5 ± 0.7	11.4 ± 1.2
S_2CLSP_8	$03^044.338$'	$102^033.909$'	60.5 ± 12.5	18.9 ± 1.1	32.5 ± 3.6
	Range		32.0 – 126.4	14.0 – 35.3	11.4 – 38.2
	Mean		61.9 ± 12.8	18.8 ± 1.7	24.5 ± 3.1
			Catchment area		
$W1_1CLSP_1$	$03^044.278$'	$102^033.839$'	258.5 ± 29.6	16.2 ± 1.1	35.5 ± 28.2
W_1CLSP_2	$03^044.255$'	$102^033.906$'	300.3 ± 32.4	16.2 ± 0.8	38.9 ± 4.0
W_1CLSP_3	$03^044.366$'	$102^033.857$'	383.8 ± 41.4	19.7 ± 1.1	36.2 ± 4.2
W_1CLSP_4	$03^044.349$'	$102^033.924$'	165.4 ± 18.4	16.2 ± 0.8	27.3 ± 26.0
W_1CLSP_5	$03^044.373$'	$102^033.771$'	107.2 ± 13.4	42.0 ± 1.5	44.9 ± 3.7
	Range		107.2 - 383.8	16.2 - 42.0	27.3 - 44.9
	Mean		243.0 ± 27.0	22.1 ± 1.1	36.6 ± 13.2

The mean activity concentrations of ^{40}K are 125.9 ± 21.1, 70.7 ± 12.4, 55.5 ± 10.9, 61.5 ± 12.5, 61.9 ± 12.8, and 243.0 ± 27.0 Bqkg^{-1} for forest, flat 1 , flat 2, slope 1, slope 2 and catchment areas respectively. The mean activity concentrations of ^{226}Ra are 20.9 ± 4.1, 16.6 ± 0.8, 17.9 ± 0.8, 20.1 ± 1.4, 18.8 ± 1.7, and 22.1 ± 1.1 Bqkg^{-1} for forest, flat 1, flat 2, slope 1, slope 2 and catchments areas respectively. The mean activity concentrations of ^{228}Ra are 33.8 ± 2.9, 22.4 ± 2.5, 26.9 ± 2.6, 27.1 ± 3.5, 24.5 ± 3.1, and 36.6 ± 13.2 Bqkg^{-1} for forest, flat 1 , flat 2, slope 1, slope 2 and catchments areas respectively.

Figure 1 below, summarizes the means activity concentrations for ^{40}K, ^{226}Ra and ^{228}Ra in top soil samples. It shows the accumulation effect of the activity concentrations in the catchment area. This could be due to run off activities in the area where the amount of rainfall in the area is more than 300 mm per year.

Surface Dose Rate
Table 2 lists the ratio of ^{226}Ra/^{228}Ra activity concentration, surface dose rate and radium equivalent, Ra$_{eq}$ for top soil samples. The ratio of ^{226}Ra/^{228}Ra concentration activities is less than 1 because the concentration activity of ^{226}Ra in soil is less than concentration activity of ^{228}Ra. In other word, the concentration of uranium in soil is less then thorium, since uranium and thorium are the parent of ^{226}Ra and ^{228}Ra respectively.
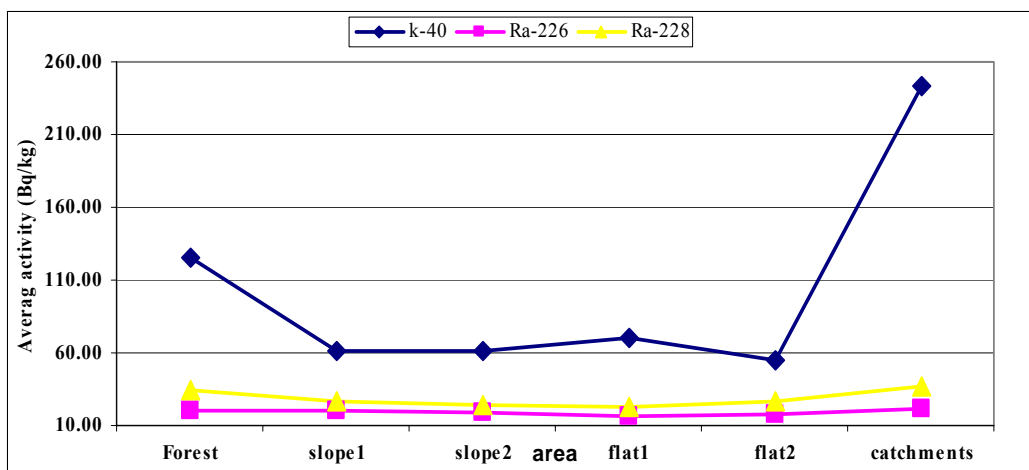
Figure 1. Means activity concentration for ^{40}K, ^{226}Ra and ^{228}Ra in top soil samples

Radium equivalent is defined as,

$$Ra_{eq} = C_{Ra} + 1.43C_{Th} + 0.07C_K$$

where C_{Ra}, C_{Th} and C_K are the activity concentrations of ^{226}Ra, ^{232}Th and ^{40}K in Bq/kg, respectively. While defining Ra_{eq} activity, it has been assumed that 370 Bqkg^{-1}, ^{226}Ra or 259 Bqkg^{-1} ^{232}Th or 4810 Bqkg^{-1} ^{40}K produce the same gamma rate to compare the specific activity of materials containing different amounts of ^{226}Ra, ^{228}Ra and ^{40}K.

Table 2. The ratio $^{226}Ra/^{228}Ra$, Surface dose rate and Radium equivalent activity

Code Sample	Ratio $^{226}Ra/^{228}Ra$	Surface Dose Rate (µSv/hr)	Ra_{eq} activity (Bq/kg)
		Forest	
F_RSP_1	0.46	0.224	73.17
F_RSP_2	0.68	0.191	71.71
F_RSP_3	0.43	0.159	57.66
F_RSP_4	0.75	0.107	77.58
F_RSP_5	0.55	0.204	89.34
F_RSP_6	0.74	0.161	84.35
F_RSP_7	0.69	0.118	91.05
F_RSP_8	0.65	0.114	79.86
Range		0.107 – 0.224	57.7-91.1
Mean		0.160	78.1
		Flat area	
F_1CLSP_1	0.64	0.084	37.02
F_1CLSP_2	0.80	0.176	60.20
F_1CLSP_3	0.84	0.057	30.44
F_1CLSP_4	0.74	0.160	60.85
F_1CLSP_5	0.68	0.125	36.54
F_1CLSP_6	0.75	0.188	96.18
Range		0.057-0.188	30.44 – 96.18
Mean		0.132	53.5
F_2CLSP_1	0.55	0.135	62.05
F_2CLSP_2	0.60	0.139	45.44
F_2CLSP_3	0.53	0.105	60.48
F_2CLSP_4	0.66	0.124	63.95
F_2CLSP_5	0.74	0.117	51.32
F_2CLSP_6	0.93	0.127	81.89
F_7CLSP_7	0.56	0.101	66.30
F_2CLSP_8	0.67	0.129	49.75
F_2CLSP_9	0.72	0.125	61.41
Range		0.101-0.139	45.44 - 81.89
Mean		0.122	60.3

Code Sample	Ratio $^{226}Ra/^{228}Ra$	Surface Dose Rate (μSv/hr)	Ra_{eq} activity (Bq/kg)
		Slope area	
S_1CLSP_1	0.72	0.100	73.93
S_1CLSP_2	0.91	0.106	74.50
S_1CLSP_3	0.52	0.156	86.99
S_1CLSP_4	0.63	0.099	70.99
S_1CLSP_5	0.83	0.152	65.63
S_1CLSP_6	0.83	0.099	65.40
S_1CLSP_7	0.71	0.100	50.68
S_1CLSP_8	0.94	0.112	46.74
S_1CLSP_9	0.65	0.190	55.98
S_1CLSP_{10}	0.88	0.105	102.72
S_1CLSP_{11}	0.74	0.100	44.19
S_1CLSP_{12}	0.64	0.121	40.38
S_1CLSP_{13}	0.62	0.172	41.16
S_1CLSP_{14}	0.67	0.137	64.8
Range		0.099-0.190	41.16-102.72
Mean		0.125	63.15
S_2CLSP_1	0.62	0.132	50.25
S_2CLSP_2	0.68	0.129	63.51
S_2CLSP_3	0.56	0.100	54.29
S_2CLSP_4	0.79	0.130	45.16
S_2CLSP_5	0.63	0.200	59.89
S_2CLSP_6	0.92	0.132	94.06
S_2CLSP_7	0.92	0.098	29.04
S_2CLSP_8	0.58	0.195	69.61
Range		0.098 – 0.200	29.04-94.06
Mean		0.140	58.2
		Catchments area	
$W1_1CLSP_1$	0.46	0.130	85.06
W_1CLSP_2	0.42	0.115	92.85
W_1CLSP_3	0.54	0.130	98.33
W_1CLSP_4	0.59	0.136	66.82
W_1CLSP_5	0.94	0.102	113.71
Range		0.102 – 0.136	66.8 - 113.7
Mean		0.123	91.4

The mean surface does rate for various sections in the area are 0.160, 0.132, 0.122, 0.125, 0.140, and 0.123 μSvhr^{-1} for forest, flat 1, flat 2, slope 1, slope 2, and catchment areas respectively. The mean radium equivalent Ra_{eq} are 78.1, 53.5, 60.3, 63.15, 58.2, and 91.4 Bqkg^{-1} for forest, flat 1, flat 2, slope 1, slope 2, and catchment areas respectively. Figure 2 below shows the radium equivalent activity in Bqkg^{-1} for various sections in the study area. The catchment area shows an enrichment of activity, since it is the low land and it is collecting all the eroded soil carried by the run off water. Therefore, the radionuclides tend to accumulate in the catchment area giving the highest radium equivalent activity.
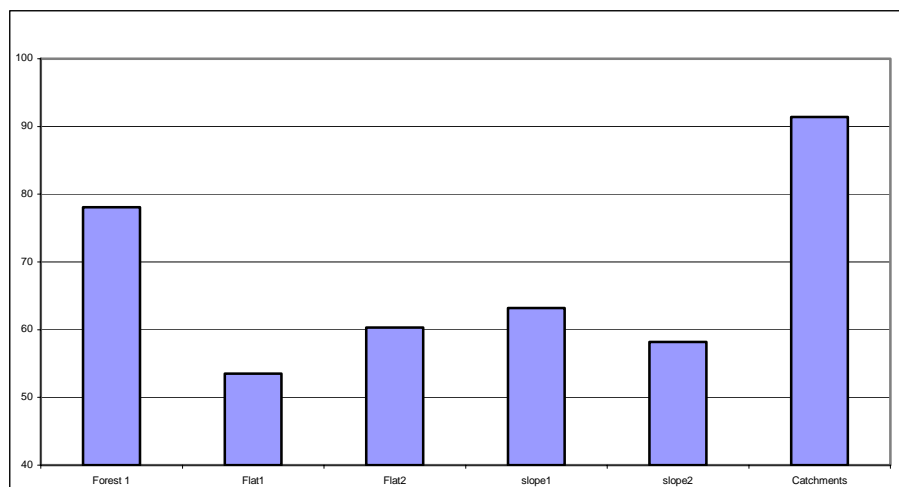
Figure 2:. Radium equivalent activity in Bq/kg for various sections in the study area

Absorbed Dose Rate ,Annual Effective Dose and External Hazard Index

Table 3 lists the air absorbed dose rate, external hazard index H_{ex} and annual effective dose for various sections in the study area. The outdoor air-absorbed dose rates due to terrestrial gamma rays at 1 m above the ground were calculated from ^{226}Ra, ^{232}Th and ^{40}K concentration values in soil assuming that the other radionuclides, such as ^{137}Cs, ^{90}Sr and ^{235}U decay series can be neglected as they contribute very little to the total dose from environmental background [11,12,13]. The conversion factors used to calculate the absorbed dose rates is given as [14].

$$D = 0.461C_{Ra} + 0.623C_{Th} + 0.0414C_K$$

In the above conversions, it is assumed that all the decay products of ^{226}Ra and ^{232}Th are in radioactive equilibrium with their precursors. The mean air absorbed dose rate are 35.34, 25.76, 27.44, 42.41 nGyhr^{-1} for forest, flats, slopes, and catchments areas respectively.

Annual Effective Dose

To estimate the annual effective dose, account must be taken of to the conversion coefficient from absorbed dose in air to effective dose and the indoor occupancy factor. Using the dose rate data obtained from the concentration values of natural radionuclides in soil, adopting the conversion factor of 0.7 Sv/Gy absorbed dose in air to effective dose received by adults and considering that people on the average, spent 20% of their time outdoors, the annual effective doses are calculated [15]. The mean annual effective doses are 1.19 x 10^{-7}, 0.78 x 10^{-7}, 0.88 x 10^{-7}, 1.42 x 10^{-7} Sv for forest, flats, slopes, and catchment areas respectively.

External Hazard Index (H_{ex}) is defined as;

$$H_{ex} = C_{Ra}/370 + C_{Th}/259 + C_K/4810$$

where C_{Ra}, C_{Th} and C_K are the activity concentrations of ^{226}Ra, ^{232}Th and ^{40}K in Bqkg^{-1}, respectively . The value of this index must be less than unity in order to keep the radiation hazard to be insignificant. This is the radiation exposure due to the radioactivity from a construction material, limited to 1.5 mGyyr^{-1}. The maximum values of H_{ex} equal to unity corresponds to the upper limit of Ra$_{eq}$ (370 Bqkg^{-1}) [16].

The mean external radiation hazard index H_{ex} are 0.21, 0.16, 0.17, and 0.25 for forest, flats, slopes, and catchment areas respectively. The mean air absorbed dose rate is lower than the UNCEAR value i.e. 92 nGyyr^{-1}. The mean annual effective dose is also lower than the UNCEAR value i.e. 0.07 mSv. The external radiation hazard index is less then 1, which means it is safe for human to carry out their activities in the area.

201

Table 3: Air absorbed dose rate, external hazard index and annual effective dose for forest area

Code Sample	Absorbed dose rate (nGy/hr)				External hazard index (H_{ex})	Annual effective dose (10^{-7}Sv)
	^{40}K	^{226}Ra	^{228}Ra	Total		
Forest area						
F_RSP_1	1.91	7.81	22.41	32.13	0.20	1.08
F_RSP_2	9.07	8.45	16.13	33.66	0.20	1.13
F_RSP_3	2.31	5.82	17.40	25.52	0.16	0.86
F_RSP_4	5.20	11.00	19.03	35.23	0.21	1.18
F_RSP_5	3.74	10.63	25.37	39.73	0.24	1.34
F_RSP_6	6.36	11.64	20.48	38.47	0.23	1.29
F_RSP_7	9.78	11.23	21.26	42.27	0.25	1.42
F_RSP_8	3.63	10.63	21.44	35.70	0.22	1.20
Range	1.91 - 9.78	5.82 - 1.64	16.13 - 25.37	25.52 - 42.27	0.20 - 0.25	0.86 - 1.19
Mean	5.25	9.65	20.44	35.34	0.21	1.19
Flat area						
F_1CLSP_1	1.91	4.85	9.85	16.61	0.10	0.59
F_1CLSP_2	2.85	9.15	15.04	27.04	0.16	0.91
F_1CLSP_3	1.89	4.67	7.25	13.81	0.08	0.50
F_1CLSP_4	2.58	8.87	15.76	27.21	0.17	0.91
F_1CLSP_5	1.93	4.94	9.54	16.42	0.10	0.55
F_1CLSP_6	6.53	13.54	23.62	43.68	0.26	1.47
F_2CLSP_1	1.87	7.53	18.00	27.40	0.17	0.92
F_2CLSP_2	1.76	5.82	12.62	20.20	0.12	0.68
F_2CLSP_3	3.50	6.79	16.85	27.15	0.16	0.91
F_2CLSP_4	1.93	8.82	17.58	28.33	0.17	0.95
F_2CLSP_5	2.50	7.44	13.11	23.04	0.14	0.77
F_2CLSP_6	1.00	14.60	20.54	36.13	0.22	0.12
F_7CLSP_7	4.10	7.76	18.00	29.86	0.18	1.00
F_2CLSP_8	1.24	7.02	13.71	21.98	0.13	0.74
F_2CLSP_9	2.92	8.73	15.89	27.54	0.17	0.92
Range	1.00 - 6.53	4.85 - 4.60	9.54 - 23.62	13.81 - 36.13	0.10 - 0.26	0.50 - 0.80
Mean	2.57	8.04	15.16	25.76	0.16	0.78
Slope area						
S_1CLSP_1	2.10	10.86	19.81	32.77	0.20	1.10
S_1CLSP_2	2.91	14.00	16.61	33.52	0.20	1.13
S_1CLSP_3	2.14	10.26	25.85	38.24	0.24	1.28
S_1CLSP_4	2.08	9.52	19.81	31.41	0.19	1.06
S_1CLSP_5	4.52	9.84	15.52	29.88	0.18	1.00
S_1CLSP_6	4.52	9.79	15.46	29.78	0.18	1.00
S_1CLSP_7	2.04	7.30	13.29	22.63	0.14	0.76
S_1CLSP_8	2.96	7.67	10.63	21.26	0.13	0.71
S_1CLSP_9	2.17	7.53	15.22	24.92	0.15	0.83
S_1CLSP_{10}	4.27	16.86	24.95	46.07	0.28	1.55
S_1CLSP_{11}	0.47	6.84	12.08	19.39	0.12	0.65
S_1CLSP_{12}	2.16	5.22	10.75	18.13	0.11	0.61
S_1CLSP_{13}	1.45	5.41	11.42	18.27	0.11	0.61
S_1CLSP_{14}	2.11	9.06	17.58	28.74	0.18	0.97
S_2CLSP_1	2.17	6.47	13.77	22.41	0.14	0.75
S_2CLSP_2	3.27	8.64	16.61	28.51	0.17	0.96
S_2CLSP_3	5.27	8.64	11.29	25.21	0.15	0.84
S_2CLSP_4	3.02	7.62	9.97	20.61	0.12	0.69
S_2CLSP_5	0.59	8.32	17.27	26.18	0.16	0.88
S_2CLSP_6	2.46	16.31	23.07	41.85	0.26	1.41
S_2CLSP_7	1.33	4.85	6.89	13.07	0.08	0.44
S_2CLSP_8	2.52	8.73	19.63	30.88	0.19	1.04
Range	0.47 - 5.27	4.85 - 6.86	6.89 - 25.85	18.13 - 46.07	0.11 - 0.28	0.44 - 0.92
Mean	2.57	9.08	15.79	27.44	0.17	0.88
Catchments area						
$W1_1CLSP_1$	10.78	7.48	21.44	39.71	0.23	1.33
W_1CLSP_2	12.52	7.48	23.50	43.50	0.26	1.46
W_1CLSP_3	16.00	9.10	21.86	46.97	0.27	1.58
W_1CLSP_4	6.90	7.48	16.49	30.87	0.18	1.04
W_1CLSP_5	4.47	19.40	27.12	50.99	0.31	1.71
Range	6.90 - 6.00	7.48 - 9.40	16.49 - 27.12	30.87 - 46-.97	0.18 - 0.27	1.04 - 1.58
Mean	10.13	10.19	22.08	42.41	0.25	1.42

Figure 3 below shows the surface dose rate in uSvhr^{-1}, annual effective dose ($\times 10^{-7}$) in Sv, absorbed dose rate in uSv/hr, and external hazard index. The is a common trend where the highest values are from the catchments area.
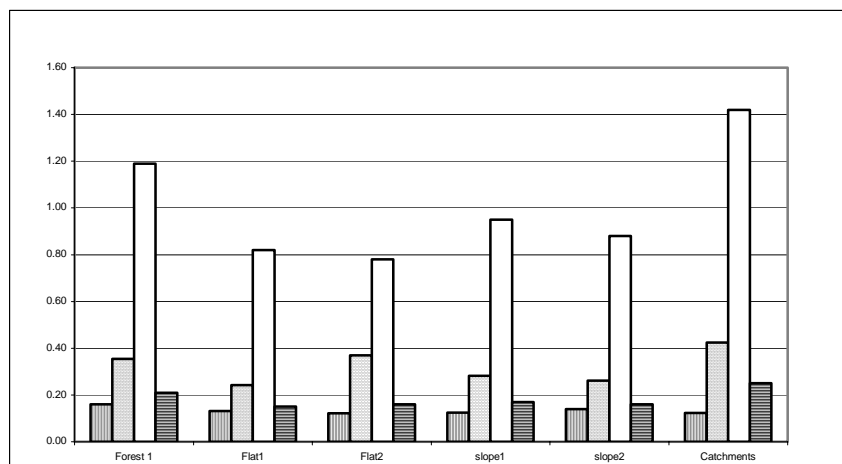

Figure 3. Surface dose rate ▯ annual effective dose ▯ , absorbed dose rate, ▯ and

external hazards index, ▯ for various sections in the study area.

In short, the activity concentrations of natural radionuclides in top soil, ^{40}K, ^{226}Ra and ^{228}Ra vary in a different sections in the study area depending on the condition of the surface area of the soils. The amount of rain in the area influences very much the movement of these radionuclides which finally settles down in the catchment area. The trend shows in Figure 3 supported this statement.

Conclusion

From this study, the mean value of air absorbed dose and annual effective dose are lower than UNCEAR values. The external radiation hazard index is less than 1. These are an indication that the area is safe for the human activity.

References

1. Radiation Information Network Michigan University 2000. Radioactivity in nature, Retrieved May 30, 2005 from http://www.physics.isu.edu/radinf/natural.html
2. Tzortzis M., Svoukis E. & Tsertos H. 2001. A comprehensive study of natural gamma radioactivity levels and associated dose rates from surface soils in cyprus. *J. Radiant Prot Dosim*. 109: 217-224.
3. United Nations Scientific Committee of the Effect of Atomic Radiation (UNSCEAR) 2000. Sources and Effects of Ionizing Radiation. *Report on General Assembly, United Nations New York*.
4. Moore, W.S., Krishnaswami,S. 1972. Thorium: element and geochemistry. *The Encyclopedia of Earth Sciences Series*, Vol. IVA: 1183-1189
5. Haglund D.S. 2004. Uranium: element and geochemistry. The Encyclopedia of Earth Sciences Series, Vol. IVA: 1215 – 1222.
6. Brookins D.G. 1984. Geochemical, aspects of radioactive waste disposal, *Springer-Verlag, Berlin*, 23-27.
   United Nations Scientific Committee on the Effects of Atomic Radiation (UNCEAR) 1998. Sources, effects and risks of ionizing radiation, *Report, UN, New York*.
7. Standard Operating Procedure to surface and subsurface soil sampling. FSSO 002.00 (California SOP) 1999.
9. Faure G. 1986. Principles of Isotopes Geology. (2nd ed.): John Wiley & Son.

10. Menager M. T, Health M. J, Ivanovich M, Montjotin C., Barillon C. R, Camp J., Hasler SE. 1993. Migration of uranium-mineralised fractures into the rock matrix in granite: implications for radionuclide transport around a radioactive waste repository, *Radiochimica Acta* 66(7): 44-83.
11. Kocher, D.C., & Sjoreen, A.L. 1985. Dose-rate conversion factors for external exposure to photon emitters in soil. *Health Physics* 48: 193-205.
12. Jacob, P., Paretzke, H. G.,Rosenbaum, H., Zanki, M. 1986. Effective dose equivalents for photon exposure from plane sources on the ground. *Radiant. Prot. Dosim.* 14: 299-310.
13. Leung, K.C., Lau, S.Y., Poon, C.B. 1990. Gamma radiation dose from radionuclides in Hong Kong soil. *J. Environ. Radioactive* 11: 279-290
14. United Nations Scientific Committee on the Effects of Atomic Radiation (UNCEAR) 1993. Sources, effects and risks of ionizing radiation. *Report, UN, New York.*
15. Human Health Fact Sheet 2001. Potassium-40. Retrieved December 11, 2004 from http://www.oversight.state:id/or-library/contaminat-Fact-sheets/potassium.
16. Beretka, J., & Mathew, P.J. 1995. Natural radioactivity of Australian building materials, industrial wastes and by-products. *Health Physics* 48: 87-95.

KAJIAN PENGOPTIMUMAN TINDAK BALAS HIDROLISIS MINYAK KACANG SOYA

Hasnisa binti Hashim dan Jumat Salimon

Program Oleokimia, Pusat Pengajian Sains Kimia dan Teknologi Makanan, Fakulti Sains dan Teknologi, Universiti Kebangsaan Malaysia, 43600 Bangi, Selangor, Malaysia

Abstrak

Pengoptimuman tindak balas hidrolisis minyak kacang soya telah dilakukan. Kesan kepekatan larutan bes kalium hidroksida (KOH) dan natrium hidroksida (NaOH) dalam kehadiran etanol ke atas nilai keasidan minyak telah dikaji. Kepekatan alkali, masa tindak balas dan faktor suhu telah dikaji ketika pengoptimuman tindak balas hidrolisis atau tindak balas saponifikasi. Larutan KOH 1 M menunjukkan ciri-ciri tindak balas hidrolisis yang lebih baik berbanding dengan NaOH 1 M di mana nilai keasidan minyak selepas tindak balas hidrolisis adalah 226.8mg/g dan NaOH 225.4mg/g masing-masing dalam keadaan tindak balas yang sama. Keadaan optimum tindak balas hidrolisis bagi minyak kacang soya terjadi pada suhu 60°C dalam masa 30 minit (KOH 1 M dalam kehadiran etanol). Komposisi asid lemak bagi minyak kacang soya sebelum dan selepas hidrolisis ditentukan dengan menggunakan kromatografi gas.
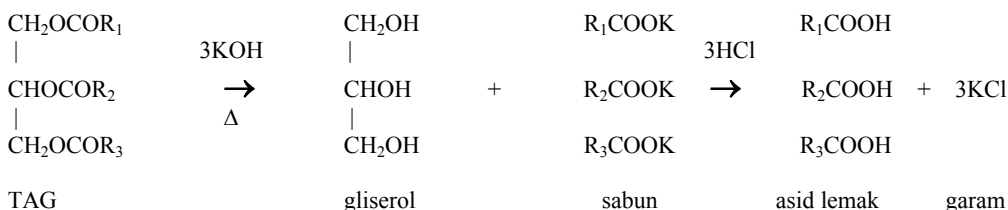
Abstract

The hydrolysis reaction of soybean oil was optimized. The concentration effect of ethanolic alkaline solution (KOH and NaOH) to the oil acidity was studied. The alkaline concentrations, reaction time and temperature factors was investigated during the optimization of the hydrolysis or saponification reaction. KOH solution of 1 M showed a good saponification activity which resulted oil acid value of 226.8 mg/g compared to NaOH solution with acid value of 225.4 mg/g for the same reaction. The optimum saponification reaction of soybean oil occured at 60 °C in 30 minutes by using ethanolic KOH 1 M with acid value of 229.6 mg/g. Composition of free fatty acid before and after hydrolysis were dertermined by using gas chromatography.

Pengenalan

Kacang soya atau nama saintifiknya *Glycine max* (L.) Merrill berasal dari timur laut Asia dan mula diperkenalkan di Amerika Syarikat pada tahun 1765. Kini kacang soya merupakan hasil tanaman kedua terpenting di Amerika Syarikat selain jagung [1] dan satu per empat bekalan minyak masak dunia adalah minyak kacang soya. Minyak tersebut digunakan untuk menghasilkan kebanyakan produk makanan seperti minyak masak, sos salad, lelemak dan marjerin. Minyak kacang soya merupakan minyak hasil tanaman terbesar di dunia di mana 13 juta tan minyak dihasilkan setiap tahun. Minyak ini mendapat permintaan tinggi di pasaran disebabkan oleh kandungan minyak dan protein yang tinggi [2]. Selain daripada kandungan protein yang tinggi, ia juga mengandungi kandungan lemak tepu yang rendah (15%) dan lemak tak tepu yang tinggi (61% poli tak tepu dan 24% mono tak tepu). Dua daripada asid lemak poli tak tepu dalam minyak ini dikenali sebagai asid lemak perlu (EFA) iaitu asid linoleik dan linolenik yang tidak dihasilkan oleh badan manusia tetapi perlu diambil dari sumber makanan [3]. EFA memainkan peranan penting dalam mengekalkan kesihatan manusia, menyalurkan tenaga ke seluruh sistem badan, dalam penghantaran oksigen dan penghasilan hemoglobin. EFA juga dapat menurunkan lipoprotein berketumpatan rendah (LDL) iaitu kolesterol yang tidak baik yang boleh menyebabkan penyakit jantung [4].

Minyak dan lemak terdiri daripada triasilgliserol (TAG), hidrokarbon, tokoferol (vitamin E), fosfolipid, sterol dan lain-lain. Triasilgliserol merupakan komponen utama dalam minyak dan lemak. TAG terdiri daripada ester gliserol dan asid lemak. Asid lemak mempunyai rantai hidrokarbon yang panjang, lurus serta rantai alkil tepu mahupun tak tepu dengan kumpulan karboksil terikat pada satu hujungnya. Penambahan alkali membolehkan tindak balas esterifikasi berbalik semula, menyebabkan asid lemak dan alkali bergabung dan membentuk sabun [5].

Saponifikasi minyak dan lemak merupakan proses unit heterogenus yang penting di mana ia bukan sahaja digunakan dalam penyediaan sabun tetapi ia turut digunakan dalam penyediaan garam asid lemak dengan menggunakan larutan aqueus alkali beretanol [6]. Proses saponifikasi penting dalam mengasingkan asid lemak dari TAG. Saponifikasi adalah proses hidrolisis beralkali ester asid lemak di mana tindak balas ini memerlukan mangkin alkali kuat dan pemanasan. Alkali beralkohol ini berfungsi sebagai mangkin dalam pemutusan ikatan kovalen TAG untuk membentuk garam asid lemak. Seterusnya peneutralan menggunakan asid dijalankan bagi membentuk asid lemak dan larutan garam. Tindak balas yang berlaku ditunjukan dalam Rajah 1.

$$
\begin{array}{llllll}
CH_2OCOR_1 & & CH_2OH & R_1COOK & R_1COOH & \\
| & 3KOH & | & & 3HCl & \\
CHOCOR_2 & \rightarrow & CHOH \quad + & R_2COOK \rightarrow & R_2COOH \quad + \quad 3KCl \\
| & \Delta & | & & \\
CH_2OCOR_3 & & CH_2OH & R_3COOK & R_3COOH & \\
\end{array}
$$

TAG   gliserol   sabun   asid lemak   garam

Rajah 1 : Tindak balas saponifikasi

Asid lemak yang terhasil dari tindak balas di atas boleh digunakan dalam pelbagai penyediaan bahan-bahan oleokimia yang berasaskan minyak dan lemak. Penggunaan asid lemak dalam proses pengubahsuaian sifat minyak contohnya pengkayaan asid lemak poli tak tepu ke dalam minyak sawit adalah satu contoh penggunaannya. Untuk mendapatkan sumber asid lemak poli tak tepu dari minyak kacang soya contohnya, proses hidrolisis perlu dioptimumkan.

Kajian ini dijalankan bagi mengkaji faktor yang mempengaruhi proses hidrolisis minyak kacang soya dan seterusnya mendapatkan keadaan optimum tindak balas hidrolisis. Beberapa siri kepekatan larutan KOH dan NaOH, suhu tindak balas dan tempoh tindak balas dikaji bagi mendapatkan tindak balas saponifikasi atau hidrolisis yang optimum. Komposisi asid lemak minyak kacang soya dianalisis sebelum dan selepas hidrolisis menggunakan kromatografi gas.

Eksperimen
Bahan
Minyak kacang soya (nilai saponifikasi, 190) gred komersial digunakan. KOH, NaOH, Na_2SO_4 kontang, HCl, dietil eter dan etanol 95 % yang digunakan merupakan bahan kimia gred analitikal. Nilai saponifikasi minyak ditentukan menggunakan carakerja dalam PORIM Test Method [7].

Saponifikasi/Hidrolisis
20.00 g minyak kacang soya disaponifikasikan menggunakan 100 mL KOH 1 M (95 % EtOH) pada suhu (62 ± 2) °C selama satu jam sambil dilalukan gas nitrogen (N_2). Kemudian 50 mL air suling ditambah ke dalam campuran saponifikasi dan bahan tak tersaponifikasi dipisahkan menggunakan pelarut heksana (2 x 70mL) dan dibuang. Lapisan akueus yang mengandungi bahan saponifikasi diasidkan kepada pH=1.0 dengan HCl 3 N. Campuran ini dipindahkan ke dalam corong pemisah dan asid lemak bebas diekstrak menggunakan 50mL heksana. Lapisan heksana yang mengandungi asid lemak bebas dikeringkan menggunakan natrium sulfat (Na_2SO_4) kontang. Pelarut diasingkan menggunakan 'rotary evaporator' pada suhu 40 °C. Asid lemak bebas yang diperolehi disimpan pada suhu -20 °C [8].

Nilai Asid
5.0 g sampel ditambah dengan 50 mL pelarut dietil eter:etanol (1:1) dan 2 mL larutan penunjuk fenolftalein 1 %. Setelah dibiarkan selama 15 minit campuran tersebut dititratkan dengan KOH 0.05 M sehingga larutan berubah menjadi merah jambu kekal selama 30 saat.

Analisis Gas Kromatografi
Komposisi asid lemak yang terdapat di dalam minyak dan lemak ditentukan menggunakan kaedah kromatografi gas [7]. Asid-asid lemak perlu ditukarkan kepada ester metil asid lemak (FAME) untuk menurunkan suhu didihnya dan kemudian dianalisis menggunakan kromatografi gas (GC). Pengenalan suatu asid lemak dilakukan dengan membandingkan profil ester metil asid lemak daripada beberapa sumber minyak (sampel minyak)

terhadap profil ester metil asid lemak piawai (C18:1, C18:2, C18:3). Proses pemetilan dilakukan dengan memasukkan 1 ml pelarut heksana ke dalam 0.1 ml sampel minyak. Kemudian 1 ml natrium metoksida (NaOCH$_3$) ditambah ke dalam larutan minyak dan dikacau dengan kuat menggunakan alat pengaduk Vortek selama 10 saat. Larutan dibiarkan selama 10 minit untuk memisahkan larutan jernih metil ester asid lemak. 1.0 μl lapisan FAME di bahagian atas disuntik ke dalam kromatografi gas (Shimadzu, Model GC-17A) yang dilengkapi dengan turus kapilari polar (bpx-70, 0.25 mm × 30 mm × 0.25μm) dan pengesan pengionan nyala (FID). Suhu penyuntik dan pengesan ditetapkan pada 250°C dan 280 °C masing-masing. Kadar alir gas nitrogen adalah 0.3 ml min^{-1} [7].

Bagi sampel selepas hidrolisis pula, 0.1 ml asid lemak ditambah dengan 1 ml 0.2 M HCl (metanol kering) dan dipanaskan dalam air bersuhu 60 °C selama 4 jam. Kemudian 0.2 ml air suling dan 1 ml heksana ditambah. Lapisan heksana diasingkan dan dikeringkan menggunakan Na$_2$SO$_4$ kontang. FAME disuntik ke dalam GC.

Hasil dan Perbincangan

Bagi mengikuti perjalanan tindak balas hidrolisis, nilai keasidan perlu ditentukan. Hasil tindak balas hidrolisis minyak adalah asid-asid lemak yang terus memberikan nilai kemasaman atau keasidan minyak asid. Nilai keasidan hasil saponifikasi menggunakan mangkin alkali dengan kepekatan berbeza (suhu dan tempoh tindak balas ditetapkan iaitu 60 °C dan 60 minit) ditunjukkan dalam Jadual 1. Larutan KOH 1 M dengan kehadiran etanol (EtOH) menunjukkan nilai asid yang tinggi iaitu 226.8 mg g^{-1} berbanding KOH aqueus dan NaOH (dengan dan tanpa kehadiran EtOH) masing-masing memberikan nilai asid yang rendah iaitu 8.4 mg g^{-1}, 225.4 mg g^{-1} dan 16.8 mg g^{-1}. KOH menunjukkan kesan pemangkinan saponifikasi yang baik disebabkan sifat kalium yang lebih reaktif dan mudah membentuk garam asid lemak berbanding Na, sifat bes hidroksida yang kuat dan kestabilan yang baik[9].

Jadual 1 : Nilai keasidan larutan hasil saponifikasi menggunakan larutan aqueus alkali

Kepekatan (M)	Nilai Keasidan (mg/g)			
	KOH	KOH (EtOH)	NaOH	NaOH (EtOH)
1.0	8.4 ± 0.1	226.8 ± 0.1	16.8 ± 0.1	225.4 ± 0.0
2.0	15.4 ± 0.1	225.4 ± 0.0	15.4 ± 0.1	219.8 ± 0.1
3.0	39.2 ± 0.0	225.4 ± 0.0	25.2 ± 0.1	219.8 ± 0.1

*suhu 60°C dan tempoh tindak balas 60 minit.

Jadual 2 : Nilai keasidan larutan hasil saponifikasi menggunakan larutan KOH dengan tempoh tindak balas berbeza

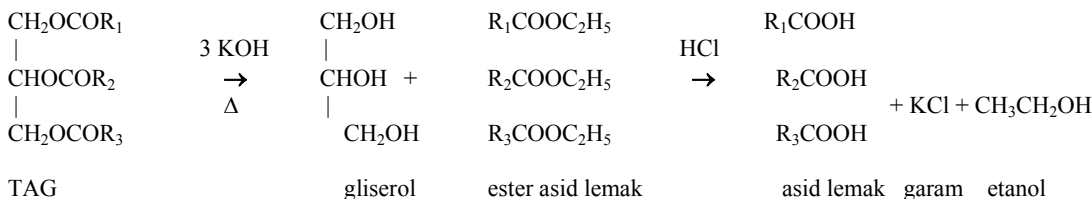| Masa (minit)	Nilai asid (mg/g)
30	229.6 ± 0.1
60	226.8 ± 0.1
90	226.8 ± 0.1

* suhu 60°C.

Jadual 3 : Nilai keasidan larutan hasil saponifikasi menggunakan larutan KOH dengan suhu tindak balas berbeza

Suhu Tindak Balas (°C)	Nilai Asid (mg/g)
30	191.8 ± 0.0
40	197.4 ± 0.1
50	218.4 ± 0.1
60	229.6 ± 0.1
70	243.6 ± 0.1
80	250.6 ± 0.0

Etanol (EtOH) bertindak sebagai medium perantaraan bes dan membantu mempercepatkan proses hidrolisis di mana EtOH merupakan pelarut yang kurang polar berbanding air. Alkali dengan kehadiran etanol dapat memutuskan ikatan-ikatan TAG dan membentuk asid lemak dalam masa yang singkat berbanding alkali aqueus yang memerlukan proses saponifikasi yang sangat lama untuk memutuskan ikatan-ikatan TAG. KOH/NaOH dalam etanol akan membentuk kalium etoksida atau natrium etoksida yang berfungsi sebagai mangkin dalam proses saponifikasi manakala KOH/NaOH dalam aqueus hanya membentuk ion K$^+$/Na$^+$ dan OH$^-$. TAG mempunyai berat molekul yang tinggi dan takat didih yang tinggi. Ini menunjukkan suhu yang tinggi diperlukan untuk memutuskan ikatan-ikatan TAG. Oleh itu, tindak balas hidrolisis menggunakan larutan aqueus KOH memerlukan suhu yang tinggi dan masa tindak balas yang lama untuk memutuskan semua ikatan-ikatan TAG

bagi membentuk asid lemak. Kalium etoksida yang terhasil daripada tindak balas KOH dan EtOH pula bertindak sebagai pembentuk ester bagi menurunkan takat didih yang diperlukan. Tindak balas hidrolisis minyak menggunakan larutan KOH dalam EtOH ditunjukkan dalam Rajah 2. Ester etil asid lemak mempunyai takat didih yang lebih rendah berbanding asid lemak (mempunyai kumpulan karboksil). Suhu yang diperlukan untuk memutuskan ikatan ester adalah 60-65°C [10].

$$
\begin{array}{cccccc}
CH_2OCOR_1 & & CH_2OH & R_1COOC_2H_5 & & R_1COOH \\
| & 3\ KOH & | & & HCl & \\
CHOCOR_2 & \rightarrow & CHOH\ + & R_2COOC_2H_5 & \rightarrow & R_2COOH \\
| & \Delta & | & & & \qquad + KCl + CH_3CH_2OH \\
CH_2OCOR_3 & & CH_2OH & R_3COOC_2H_5 & & R_3COOH \\
\end{array}
$$

TAG   gliserol   ester asid lemak   asid lemak garam   etanol

Rajah 2 : Tindak balas hidrolisis minyak

Penggunaan KOH adalah lebih baik daripada NaOH kerana garam kalium bagi asid karboksilik pada amnya lebih larut dalam air berbanding garam natrium [10]. Natrium dan kalium merupakan unsur dalam kumpulan I Jadual Berkala. Kereaktifan unsur-unsur bertambah dari atas ke bawah kumpulan. Ciri elektropositif bertambah dari atas ke bawah iaitu pertambahan kecenderungan pembentukan ion positif, K^+. Ini kerana semakin besar saiz atom semakin jauh elektron valensi daripada nukleus dan semakin mudah dikeluarkan. Ini dapat dilihat daripada tenaga pengionan pertama unsur-unsur ini di mana tenaga pengionan Na dan K masing-masing ialah 496 dan 419 kJ mol^{-1} [11]. Dari segi kekuatan bes hidroksida pula, sifat bes hidroksida unsur-unsur kumpulan I bertambah semakin ke bawah kumpulan. Ini menunjukkan KOH memberikan sifat bes hidroksida yang lebih kuat berbanding NaOH [11]. Dalam proses pembuatan sabun pula, KOH merupakan alkali yang biasa dipilih disebabkan kestabilannya yang baik dan sabun yang terbentuk lebih lembut berbanding penggunaan alkali NaOH [9].

Jadual 2 dan 3 pula menunjukkan kesan suhu dan masa tindak balas terhadap proses hidrolisis. Proses hidrolisis yang terjadi dalam tempoh 30, 60 dan 90 minit memberikan nilai keasidan masing-masing ialah 229.6 mg g^{-1} dan 226.8 mg g^{-1}. Ini menunjukkan masa tindak balas tidak mempengaruhi tindak balas hidrolisis. 30 minit diperlukan untuk menjalankan proses hidrolisis dengan berkesan. Proses saponifikasi yang optimum dapat dicapai pada suhu 60°C dalam tempoh 30 minit di mana nilai asid yang diperolehi adalah 229.6 mg g^{-1}. Suhu yang diperlukan untuk memutuskan ikatan ester adalah 60-65°C [10]. Nilai asid semakin meningkat terhadap suhu. Walau bagaimanapun suhu yang terlalu tinggi boleh mengakibatkan proses pengoksidaan TAG. Minyak kacang soya merupakan minyak yang kurang stabil disebabkan bilangan ikatan ganda dua yang tinggi. Ikatan ganda dua kurang stabil dan cenderung mengalami pengoksidaan. Oleh itu suhu optimum yang dicadangkan ialah 60°C.

Komposisi asid lemak dalam minyak kacang soya sebelum dan selepas proses hidrolisis ditunjukkan dalam Jadual 4. Kandungan asid lemak dalam minyak (sebelum hidrolisis) dan kandungan asid lemak bebas (selepas hidrolisis) tidak menunjukkan perbezaan yang ketara. Ini menunjukkan proses hidrolisis telah berlaku dengan jayanya pada keadaan optimum.

Jadual 4 : Komposisi asid lemak dalam minyak kacang soya (sebelum) dan asid lemak bebas (selepas proses hidrolisis).

Asid lemak	Sebelum Hidrolisis	Selepas Hidrolisis
Miristik	0.32	0.32
Palmitik	11.86	11.79
Palmitoleik	0.11	0.12
Stearik	4.37	4.08
Oleik	23.05	23.05
Linoleik	53.24	53.45
Linolenik	6.31	6.38
Arakidik	0.41	0.44
Behenik	0.35	0.38

Kesimpulan

Hasil kajian menunjukkan larutan KOH dalam keadaan beretanol dapat memberikan tindak balas hidrolisis minyak kacang soya yang lebih baik daripada larutan NaOH pada keadaan yang sama. Keadaan optimum tindak balas hidrolisis bagi minyak kacang soya didapati terjadi pada suhu 60°C dalam masa 30 minit dengan menggunakan mangkin larutan KOH 1 M dalam kehadiran etanol.

Penghargaan

Rujukan

1. Comptonis. (1995). Comptonis Interactive Encyclopedia. Comptonis New Media.
2. O'Brien, R. (1998). *Fats and Oils Formulating and Processing for Applications*. Lancaster: Technomic Publishing Co. Inc.
3. Lai, J.C.Y. (2002). Unravelling The Perplexity of Fatty Acids : Ω-3. Symbiosis, Jun : 18-19
4. Jamaludin Mohamed & Khairul Osman. 2003. *Siri Mengenal Nutrien Lemak.* Kuala Lumpur: Dewan Bahasa dan Pustaka.
5. Jumat Salimon & Mamot Said. (2004). *Eksperimen Kimia Analisis Minyak & Lemak II.* Bangi: Universiti Kebangsaan Malaysia.
6. Bhatkhande, B.S. & Samant, S.D. (1998). Ultrasound assisted PTC catalyzed saponification of vegetable oils using aqueous alkali. *Ultrasonics Sonochemistry*. **5**: 7-12.
7. *PORIM Test Method*. (1995). Bandar Baru Bangi: Palm Oil Research Institute of Malaysia.
8. Gamez-Meza, N., Noreiga-Rodriguez, J.A., Medina-Juarez, L.A., Ortega-Garcia, J., Monroy-Rivera, J., Toro-Vazquez, F.J., Garcia, H.S. & Angulo-Guerrero, O. 2003. Concentration of eicosapentaenoic acid and docosahexaenoic acid from fish oil by hydrolysis and urea complexation. *Food Research International*. **36**: 721-727.
9. Hamner, R. (2005). www.realhandmadesoap.com (12 Ogos 2005).
10. McMurry, J. (2004). *Organic Chemistry*. 6. Amerika Syarikat: Brooks-Cole-Thomson Learning.
11. Housecroft, C.E. & Sharpe, A.G. (2005). *Inorganic Chemistry*. 2. England: Pearson Prentice Hall.

CLASSIFICATION OF CHILLI SAUCES: MULTIVARIATE PATTERN RECOGNITION USING SELECTED GCMS RETENTION TIME PEAKS OF CHILLI SAUCE SAMPLES

Low Kah Hin*[1], Sharifuddin M. Zain[1], Mohd. Radzi Abas[1], Mustafa Ali Mohd[2].

[1]Department of Chemistry, Faculty of Science, University Malaya, 50603, Kuala Lumpur, Malaysia
[2]Shimadzu-UMMC Centre for Xenobiotics Studies, University of Malaya Medical Centre,University Malaya, 50603, Kuala Lumpur, Malaysia

Abstract
As a preliminary work on the possibility of separating classes of chili sauces based on taste or customer preferences, organic compounds from different kinds of chili sauces of various brands were separated and analyzed by gas chromatography/mass spectrometry (GC/MS). It was found that these organic compounds do form a basis for separation of different types of sauces. The similarity and dissimilarity of chromatograms due to the organic composition of the chili sauces were explored by multivariate pattern recognition techniques based on cluster analysis (CA) and principal component analysis (PCA). Both CA and PCA results exhibit four linearly separable classes, namely general sauces, hot sauces, sauces with benzoic acid and sauces with garlic. It was concluded that by using chosen retention peaks in the chromatograms of various sauce samples as multivariate features, CA and PCA can be successfully used to reveal the natural clusters existing in chili sauces according to their organic composition.

Introduction
Originally, chilli sauces were produced at home. Today, this practice still preservere but most chilli sauces available nowadays are mass manufactured in factories. Today, much effort is spent to ensure that mass manufactured sauces resemble as close as possible home made ones. Some brands do this better than others. The ingredients used in chilli sauces are very similar to those used in tomato ketchup. However, the methods of preparation and the amount of the ingredients used may vary considerably. The primary ingredients in chili sauce are red tomatoes and chilies. The usual sweetener is sugar (sucrose). The proportions of the various spice ingredients are not standardized between manufacturers [1].

Humans are very good at perceiving similarities and differences between objects of different shapes. The goal of pattern recognition in analytical chemistry is finding similarities and differences between chemical samples based on measurements made on the sample [2]. Therefore, pattern recognition appears to be a useful tool to authenticate foodstuffs according to their quality/variety/brand, when a set of samples whose classification is known a priori is available.

This study initially involved data collection via instrumental analysis, basically GC/MS. By using only chromatographic techniques, we able to separate the chemical compounds in the sauces, which are mainly capsaicinoid compounds, the pungent principle of capsicum fruits, benzoic acid which is a preservative, and other compounds due to the ingredients of the sauce.

Capsaicinoid compounds are a group of pungent compounds found mostly in capsicum fruits - the main components are acid amides of vanillylamine and $C_9 - C_{11}$ branched-chain fatty acids. There are five naturally occurring capsaicinoids, which have been reported, namely capsaicin, nordihydrocapsaicin, dihydrocapsaicin, homocapsaicin and homodihydrocapsaicin. Of these, capsaicin and dihydrocapsaicin are the major compounds of most capsicum species. Therefore these compounds have been considered as major indicators of chili product quality [3].

Techniques using GC/MS provide accurate and efficient analysis of content and type of capsaicinoids present in a chili sauce sample. These results are probably the major factors in determining the qualities/variety/brand of those sauces, and are the most important parameters used in this statistical study.

In this work, different multivariate chemometric methods been employed in the exploration; this primarily involve the use of cluster analysis (CA) and principal component analysis (PCA). Cluster analysis, which involving the search for natural grouping among samples is a preliminary way to study data sets and to discover the structure residing in them. PCA is used to transform the original data matrix ($X_{n \times m}$) into a product of two matrices, once which contains information about the objects (Scores matrix, $S_{n \times m}$) and the other about the variables (Loadings matrix, $L_{n \times m}$) [4]. PCA enables one to study data structure in reduced dimensions.

Experimental

Sample preparation
About 1 mL of sauce was weighed and extracted with 5 mL dichloromethane in a vial for overnight. Then 1 mL of sauce extracts was drawn and filtered using a 0.4μm nylon filter membrane with a syringe filter into a small glass vial. The filtrate was dried under nitrogen gas, and reconstituted with 200 μL of chloroform and was later used for a GC/MS analysis with injection volume of 1 μL.

GC/MS analysis
Samples were assayed using a Gas Chromatograph (Shimadzu GC-17A) with a Mass Spectrometer (Shimadzu QP-5000). A 30 m × 0.247 mm × 0.25 μm capillary column, with a stationary phase of (5% - phenyl) – methyl polysiloxane (J & W Scientific, DB-5), was used. For analysis, the initial temperature was 60°C held for 1 min. The temperature was increased from 60 to 280°C at the rate of 10°C/min and held at 280°C for 22 min. The total run time was 38 min. The injection volume was 1.0 μL and the total flow of carrier gas was 39.5 mL/min helium.

Data processing
Data preprocessing is a very important part of any chemometric data analysis project. It consist of whatever mathematical manipulation of data prior to primary analysis. From the obtained GC profiles, 12 marked peaks were considered as the multivariate variables. They are the compounds eluting at retention times, 7.6 (1), 9.2 (2), 12.2 (3), 17.0 (4), 19.2 (5), 19.5 (6), 21.0 (7), 21.2 (8), 24.4 (9), 25.4 (10), 25.7 (11), and 36.9 (12) minutes. These peaks were examined for their mass spectra and identification of these peaks were attempted. The peaks' area per weight of sample were preprocessed, then arranged the in an X-matrix (201 x 12). The values of each row represent the measurement of different variable for each sample, and the values of each column represent the measurement of different samples for a particular variable. Each replicate was treated as an individual sample in the data matrix, which then undergo CA and PCA. All these were done by combination of several statistical software packages such a Microsoft® Excel, Teach/Me®-Data Analysis, JMP® and JMP IN®.
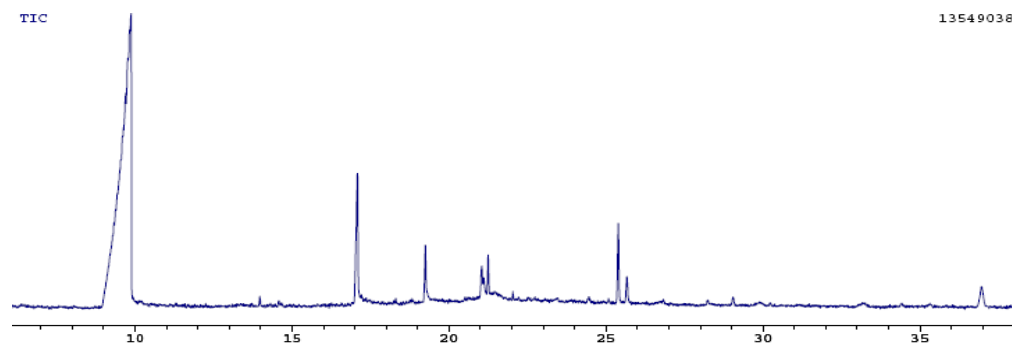

Figure 1: Typical GC/MS chromatogram of a chili sauce extract.

Table 1: Peak areas at particular retention times for a part of sauce samples

Retention Time	GCS0036 S01a	GCS0035 S01b	GCS0035S01c	GCS0035 S02a	GCS0035 S02b
7.5	782155	1387435	1613369	801396	968122
9.2	0	0	0	0	0
12.2	186056	597293	819216	386139	385629
17.0	28568683	23716034	37251905	18332483	14260443
19.2	12228225	6519874	11069449	4543486	3855149
19.5	0	0	0	0	0
21.0	5353903	4026651	6242748	923887	1528811
21.2	9774055	10841376	14612206	8586443	9105060
24.4	1426550	1902577	2076992	1914108	1396709
25.4	10714811	13662227	19084453	10339062	11473199
25.7	6485459	8002463	11712994	6540138	7115043
36.9	2731411	4064320	6083270	2461134	2353073

In this work, CA was applied to the autoscaled data, the sample were calculated on the basis of Euclidean distances, while Ward hierarchical agglomerative method was used to establish the clusters. Next, PCA was performed on the unscaled data, used to provide data structure in a reduced dimension, retaining the maximum amount of variability present in the data.

Results and discussion

Mass spectra analysis

From the total ion chromatograms of chili sauces extracts, compounds eluting at particular retention times were examined for their mass spectra. Compounds 1, 3, 6 and 8 were not resolved. The m/z values obtained from mass spectra of the molecular ions (M^+) and fragment ions of selected compounds are shown in Table 2.

Table 2: m/z values of selected compounds.

	Retention time / Compound		Mass/charge, m/z					Molecular Ion, M^+
			Fragment ions					
1	7.5	unresolved						
2	9.2	Benzoic acid	51	65	77	94	105	122
3	12.2	unresolved						
4	17.0	Myristic acid	60	73	85	129	185	228
5	19.2	Palmitic acid	60	73	85	129	213	256
6	19.5	unresolved						
7	21.0	Linoleic acid	67	81	95	109	123	280
8	21.2	unresolved						
9	24.4	Nordihydrocapsaicin	43	122	137	152	195	293
10	25.4	Capsaicin	43	122	137	152	195	305
11	25.7	Dihydrocapsaicin	43	122	137	152	195	307
12	36.9	Vitamin E	43	57	71	165	205	430

As mentioned before, the pungent capsaicinoids have been considered as major indicators of chilli product quality. Typical mass spectra of dihydrocapsaicin is shown in *Figure 3*. The molecular ions (M^+) of the capsaicinoid compounds were confirmed from their mass spectra. The base peak of each compound was found to be common at m/z = 137. Other fragment ions had m/z = 43, 122, 152 and 195.

Figure 2: The capsaicinoids commonly found in chilies.

A possible empirical formula for fragment ion m/z = 137 from isotopic abundance calculation is $C_8H_9O_2$. An achievable fragment ion is shown below as:-

m/z = 137   m/z = 137

The resonance stabilization of this fragment ion suggested its occurrence as the base peak [5].

Figure 3: Mass spectrum of dihydrocapsaicin.

The isotopic abundance calculation of the fragment ion m/z = 195 suggested an empirical formula of $C_{10}H_{13}O_3N$. A possible fragment ion is shown in the decomposition reaction below [6]:-

m/z = 195

$H_2C\!=\!\!=\!CHR$

Fragment ions with m/z = 153 and 152 were perhaps due to the ion decomposition reaction below:-

Multivariate correlation analysis

From the correlation matrix for GC peaks, peak no. 1 and no. 3 correlate strongly ($r = 0.9861$); followed by inter-correlation between peaks no. 9, nordihydrocapsaicin, no. 10, capsaicin and no. 11, dihydrocapsaicin. Others correlate moderately or weaker. The strong correlation between nordihydrocapsaicin, capsaicin and dihydrocapsaicin is expected because these compounds are the major pungent capsaicinoids in capsicum fruits. In other word, we can easily conclude that capsaicinoids present in chili sauces or natural chili are in a constant ratio. On the other hand, we suspect that the unknown peaks no.1 and no.3 also show similar characteristics as the capsaicinoids, but this needs further investigation.

Cluster analysis

CA is a well known technique of data analysis, commonly applied before other mutivariate procedures owing to its unsupervised character, that reveals the natural clusters existing in a data set on the basis of the information provided for the measured variables. The results obtained for the case at hand, using the Ward's method and Euclidean distance are presented as a dendrogram in Figure 4. At distance 700, 3 clusters that can be identified as 'similar' were found: from the top, the first cluster is composed of general sauces including a sub-cluster of hot sauces. The second cluster is a group made up of sauces containing benzoic acid as preservative. The last cluster is those sauces with the addition of garlic.
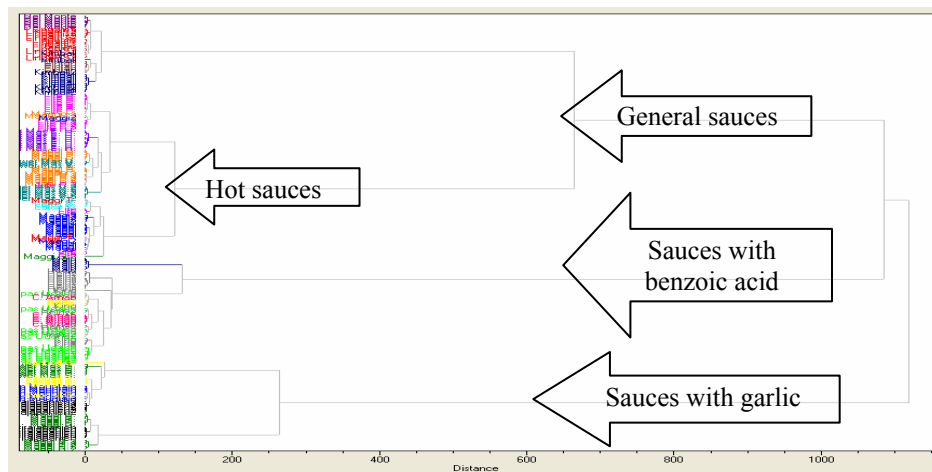
Figure 4: Dendrogram of Cluster analysis.

Principal component analysis

By performing PCA on the dataset, which was initially preprocessed from GC/MS data of the chili sauces extracts, a series of principal components (PCs) could obtained. Each PC is associated with an eigenvalue. PC1 has the largest eigenvalue and carries the largest variance of the original data, and subsequent PCs carry variance in a decreasing order.
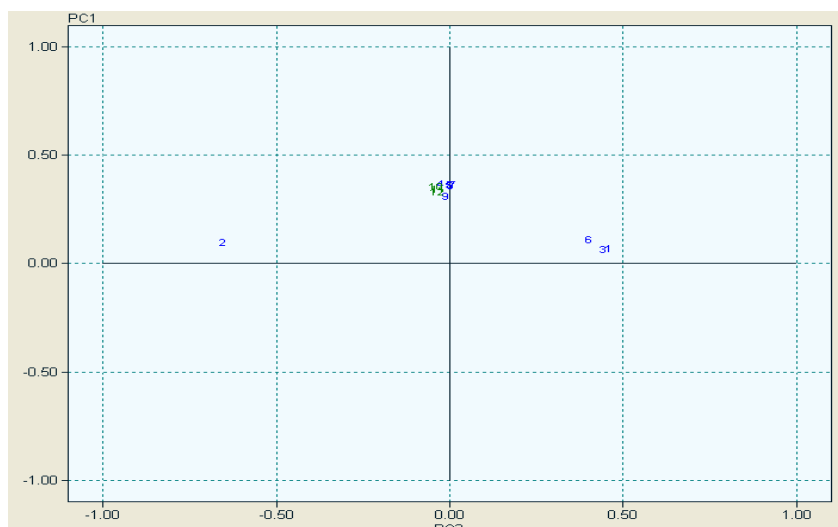
Figure 5: Loading Plot: PC1 vs. PC2.

Loadings graph (Figure 5) is used to determine which variables are important for describing the variation in the original data set, and there are no variables with loading close to ±1, revealing that no PC is closely aligned with any peaks. For PC1, peaks no. 1, 2, 3 and 6 do not contribute much to the variance described by PC1. For PC2, it is the other way round; peaks no. 4, 5, 7, 8, 9, 10, 11 and 12 have near zero loading. In addition, peak no. 2 show high negative loading value, which indicates benzoic acid is a meaningful parameter for PC2.

The final result of PCA, Figure 6, shows a plane spanned by first two PCs, representing 95.87 of the variation in the data. There are crowds of points discriminated by PC2 while PC1 primarily determines the spread of scores. Four major separable classes namely general sauces, hot sauces, sauces with benzoic acid and sauces with garlic can be observed from the plot.
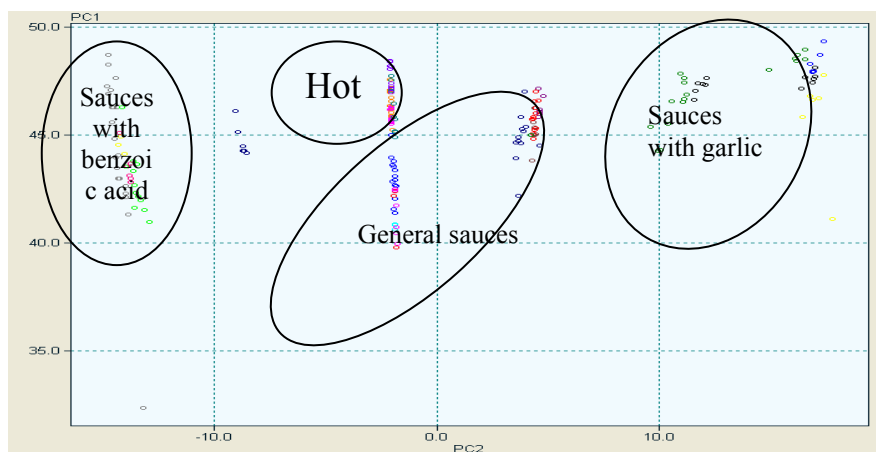
Figure 6: Score Plot of PC1 vs. PC2.

As had been discussed, peaks no. 1, 2, 3 and 6 are the dominant features in PC2. From scores plot, it is demonstrated that those sauces with benzoic acid clusters on the negative area of axis PC2 corresponding to its' negative loading, while those sauces with garlic are on the positive side. These indicates that the unknown peaks no. 1 and 3 should correspond to the garlic content of the sauces.

Conclusion

In this study, the feasibility of using just GC profiles to distiguish between chili sauces variety was investigated with multivariate chemometric methods. CA and PCA methods have demonstrated similar results; that using certain peaks in the GC profiles as multivariate parameters we are able to reveal the natural clusters existing in the chili sauce samples studied.

Acknowledgements

References

1. Grading Manual for Chili Sauce, United State, Department of Agriculture, Agricultural Marketing Service, Food and Vegetable Division, Processed Product Branch, 1954.
2. Beebe, K. R., Pell, R. J. and Seasholtz, M. B. 1998. Chemometrics: A Practical Guide, John Wiley & Sons, Inc., New York.
3. Rachaneewan Karnka, Mongkon Rayanakorn, Surasak Watanesk and Yuthsak Vaneesorn. 2002. Optimization of High Performance Liquid Chromatographic Parameters for Determination of Capsaicinoid Compounds Using the Simplex Method. Analytical Sciences. 18, 661-665.
4. Padin, P. M., Pena, R. M., Garcia, S., Iglesias, R., Barro, S. and Herrero. 2001. Characterization of Galician (N.W. Spain) quality brand potatoes: a comparison study of several pattern recognition technique. Analyst, 126, 97-103.
5. Ahmad Ab. Wahab. 1984. A Combined Gas Chromatography-Mass Spectrometry (GCMS) study on Pungent Principles in Chillies (Capsaicum Species), MARDI Res. Bull. 12,3, 290-297.
6. McLaferty, F.W. 1980. Interpretation of mass spectra. 3rd Ed. Mill Valley, California: University Science Books.

CO₂ / H₂ METHANATION ON NICKEL OXIDE BASED CATALYST DOPED WITH VARIOUS ELEMENTS FOR THE PURIFICATION OF NATURAL GAS

Nor Aziah Buang*, Wan Azelee Wan Abu Bakar, Faridah Mohd Marsin, Mohd Hasmizam Razali

Department of Chemistry, Faculty of Science, Universiti Teknologi Malaysia, 81310, Skudai, Johor.

Abstract

Nickel possess characteristics similar to noble metals, apart from being easily deactivated by carbon deposition and poisoning. In this study, the activity of prepared nickel based catalysts doped with selected elements (Mg, Zr, Mo, Mn, Co, Fe, and Cu) that were presumed to help nickel active sites has been investigated for the CO_2 elimination in the presence of H_2 in the hopes for a methanation reaction. With the addition of lanthanide series as co-dopant in the catalyst, the synthesized catalysts were tested for its catalytic activity and reproducibility by FTIR spectroscopy. It was found that only several elements can boost CO_2 elimination, namely magnesium, cobalt and ferum, with cobalt showing the highest conversion for both ratios, Ni/Co/Pr 60:30:10 and 60:10:30. Furthermore, Ni/Co/Pr with the ratio of 60:30:10 was proven superior as it yielded highest CH_4 in the lowest conversion temperature of approximately 350 °C. Further characterization on Ni/Co/Pr with the ratio of 60:30:10 showed the supremacy towards the conversion of CO_2 to CH_4. Single point BET analysis showed that Ni/Co/Pr did not have any changes in the surface area, as it did not adsorb CO_2. This statement is in agreement with the XRD and EDX results obtained whereby there are no traces of carbon deposition. From TPD results showed CO_2 desorption peaks at low and high temperature indicated intermediate bonding of CO_2 on the surface of the catalyst. This shows the presence of dopant will result in the enhancement of CO_2 elimination to a 100%.

Abstrak

Nikel mempunyai ciri-ciri yang menyamai logam yang mahal (paladium, platinum). Walau bagaimanapun ia mudah terencat dengan kehadiran karbon dan keracunan mangkin. Dalam kajian ini, aktiviti pemangkinan bagi mangkin Ni yang didop dengan bahan pendop terpilih (Mg, Zr, Mo, Mn, Co, Fe, and Cu) untuk meningkatkan keupayaan pemangkinan disamping memberi ketahanan kepada keracunan mangkin dalam proses menukarkan CO_2 kepada gas metana. Dengan penambahan praseodymium daripada kumpulan lantanida, mangkin tersebut telah di uji dari segi keupayaan pemangkinan dan ketahanan menggunakan analisis FTIR. Kajian telah mendapati bahawa hanya beberapa elemen sahaja yang boleh menyingkirkan CO_2, iaitu magnesium, ferum dan cobalt. Cobalt menunjukkan keupayaan pemangkinan yang tinggi dalam kedua-dua nisbah Ni/Co/Pr 60:30:10 dan 60:10:30. Selain itu, Ni/Co/Pr dengan nisbah 60:30:10 merupakan mangkin yang paling efektif untuk menyingkirkan CO_2 disamping menukarkannya kepada CH_4 pada suhu lebih kurang 350ºC. Kajian pencirian mangkiin menunjukkan bahawa Ni/Co/Pr dengan nisbah 60:30:10 lebih berkesan menukarkan CO_2 kepada CH_4. Kajian luas permukaan BET menunjukkan bahawa Ni/Co/Pr tidak menunjukkan sebarang perubahan dalam luas permukaan, bermakna ia tidak menyerap CO_2. Analisis XRD and EDX menunjukkan tiada perubahan struktur dan tiada karbon terbentuk di atas permukaan mangkin. Analisis TPD menunjukkan puncak penyahjerapan CO_2 berada pada kedua-dua suhu yang rendah dan tinggi. Ini menunjukkan terdapat penjerapan CO_2 di atas permukaan mangkin. Ini semua menunjukkan peningkatan kepada keupayaan mangkin untuk menyingkirkan CO_2 100%.

Introduction

The necessity of natural gas purification into high quality products boosted both the applied and academic research activity. In recent years, renewed interest in CO_2 elimination process has arisen. Noble metals such as Rh, Ru and Ir exhibit high stability and less sensitivity in catalytic process [1-2], cost and limited avaibility of these metals discourage their widespread industrial applications. Nickel oxide exhibited high activity and selectivity of methane due to the ability of NiO to undergo reduction process owing to the presence of defect sites of the surface [3]. Despite of the fast catalyst deactivation and carbon deposition, NiO catalyst was still favored for its high thermal stability [4], and its low price [5]. Therefore, it is very important to develop stable and effective nickel oxide catalyst with improved resistance to deactivation caused by coking and poisoning. A study by Valentini *et al.* [6] found that the catalytic properties, metal dispersion and the structural features of

species depend on the method to process these materials and on the support used. The addition of dopant into nickel oxide base catalyst was found to enhance the capability of the catalyst. The usage of catalyst will depend on the dopant used in order to form a durable, sulfur tolerant, high catalytic activity catalysts. The selected dopants studied were magnesium (Mg), zirconium (Zr), molybdenum (Mo), manganese (Mn), ferum (Fe), cobalt (Co), and copper (Cu).

Cobalt was mainly used for Fisher-Troposh Synthesis (FTS) and was chosen due to its reducibility of CO. Jacobs *et al.* [7] found that addition of Ru and Pt exhibited a similar catalytic effect on decreasing both the reduction temperatures of cobalt oxides. The hydrogenation of CO and CO_2 were found to catalyze by the larger cobalt clusters formed by three incipient wetness impregnations [8]. Other research by Guczi *et al.* [9] found that Co–Pd samples are fully reducible and form bimetallic particles which can be reversibly oxidized/ reduced. CO hydrogenation takes place in the range of 200–300°C producing mainly alkenes on pure cobalt catalyst with short chains. Synergism on the addition of small amount of palladium to cobalt is observed and the rate of the CO hydrogenation significantly increases.

In this research, Nickel based catalyst was doped with selected metal elements and praseodymium, to alter the surface and bulk structure of the catalyst so it will become polycrystalline. Different ratios of dopant was introduced into the catalyst matrices and was then used to eliminate CO_2 with the presence of H_2 with the hopes for CO_2 hydrogenation to occur. The reducibility and characteristics of the doped Nickel based catalysts were tested by means of FTIR for catalytic activity of the CO_2 removal and methane production, X-Ray Diffraction for phase or structural changes, Temperature Programmed Desorption(TPD) for the determination of active site, and BET Surface Area of the catalyst.

Experimental

Catalyst preparation
Ni/M*/Pr (M*= Mg, Zr, Mo, Mn, Fe, Co, and Cu) in both higher and lower atomic ratios of selected dopant, 60:30:10 and 60:10:30, were prepared via optimized sol gel method. This method includes the addition of its specific metal salts with its base metal, $Ni(NO_3)_2.6H_2O$, and second dopant, $Pr(NO_3)_3.6H_2O$. it was then aged at 75°C for 48 hours before it was calcined at 400°C for 17 hours.

Catalytic activity measurement
The prepared samples were tested for its activity towards CO_2 removal via methanation reaction. This was done using a flow bed reactor of 10 mm inner diameter under atmospheric pressure. The reaction gas mixture of CO_2 and H_2 was passed continuously through the catalyst which flows through the FTIR whereby the CO_2 peaks elimination and CH_4 formation will be detected and monitored.

Characterization
X-ray Diffraction Analysis : The catalyst samples were characterized by using a Philips D5000 X-Ray Diffractometer (Cu-K$_\alpha$ radiation) with 2θ values ranging from 10-80°,
Single Point BET Surface Area: the surface area of samples before and after exposure to CO_2/H_2 were measured using Micromeritics ASAP, whereby it uses nitrogen as the adsorption gas for the physical characterization of the catalyst.
Temperature Proggrammed Desorption Analysis: the H_2 and CO_2 desorption from the catalyst were taken into account using the Thermofinnigan TPD/R/O 1100.

Results and disscussion

Catalytic activity
For the lower ratio of the selected dopant, Ni/M*/Pr (M =Mg, Zr, Mo, Mn, Co, Fe, and Cu) with the ratio of 60:10:30, from the results it indicated that for the lower addition of various metals as dopants, most of the catalyst exhibit CO_2 elimination properties. The three highest CO_2 elimination catalysts were Ni/Mg/Pr, Ni/Fe/Pr, and Ni/Co/Pr. Starting from 300°C, Ni/Mg/Pr has already eliminated over 80% of the CO_2. The highest CO_2 elimination is at 330°C with 93.26%. For Ni/Fe/Pr and Ni/Co/Pr, the light off temperature (T_{LO}) were both at 250°C, while complete elimination of CO_2 was also both at around 427°C. Ni/Mo/Pr and Ni/Cu/Pr also showed response in the CO_2 elimination whereby at 300°C, the catalyst eliminated 17.69% and 40% respectively. Hence the CO_2 elimination for Ni/Cu/Pr terminated at 430°C with a maximum elimination of 67%,

while after 50% of elimination, the performance of Ni/Mo/Pr declined at 450°C. Ni/Mn/Pr, and Ni/Zr/Pr did not show any significant CO_2 elimination throughout the catalytic measurement.

Figure 1 showed the catalytic activity of Ni/M*/Pr (M =Mg, Zr, Mo, Mn, Co, Fe, and Cu) with catalyst ratio 60:30:10 for CO_2 elimination that were calcined at 400°C for 17 hours and tested under stoichiometric conditions, consisting of CO_2 and H_2, from 300-500°C.

Results indicated that for the higher loading of various metals as dopants, most of the catalysts performances have been suppressed in eliminating CO_2 in the system. Most of the catalyst eliminated less than 20% of CO_2, except for the Ni/Co/Pr catalyst. The later maintained its performance in eliminating CO_2 at T_{LO} of 300°C with 20% elimination, and further elimination at 400°C with highest percentage of 97.42%.
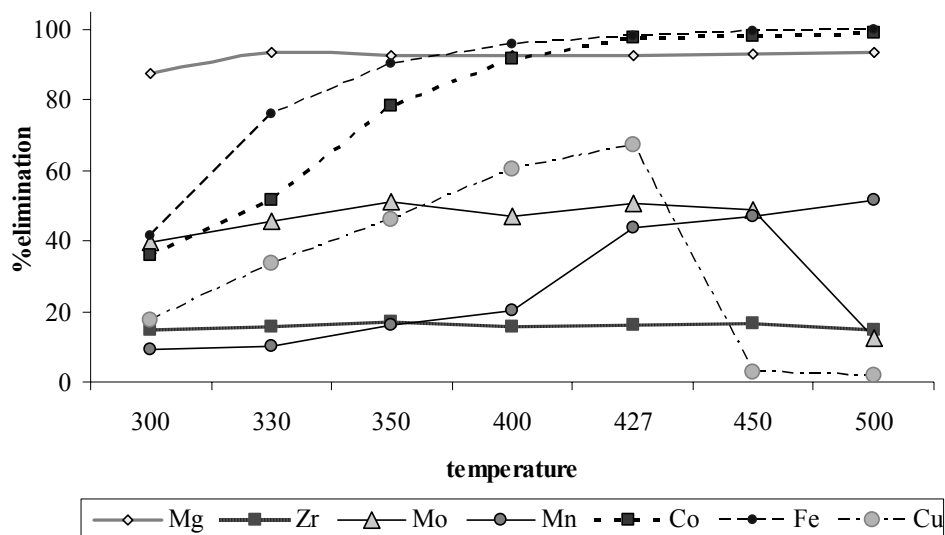
Figure 1: Catalytic activities of Ni/M*/Pr (M =Mg, Zr, Mo, Mn, Co, Fe, and Cu)
ratio 60:10:30 for CO_2 elimination versus temperature
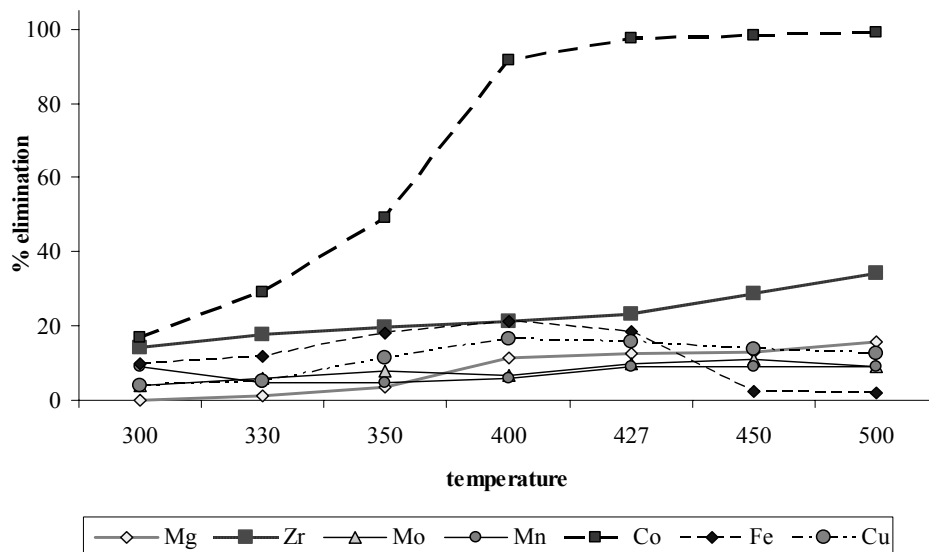
Figure 2: Catalytic activities of Ni/M*/Pr (M =Mg, Zr, Mo, Mn, Co, Fe, Cu, and Zn) ratio 60:30:10
for CO_2 elimination versus temperature
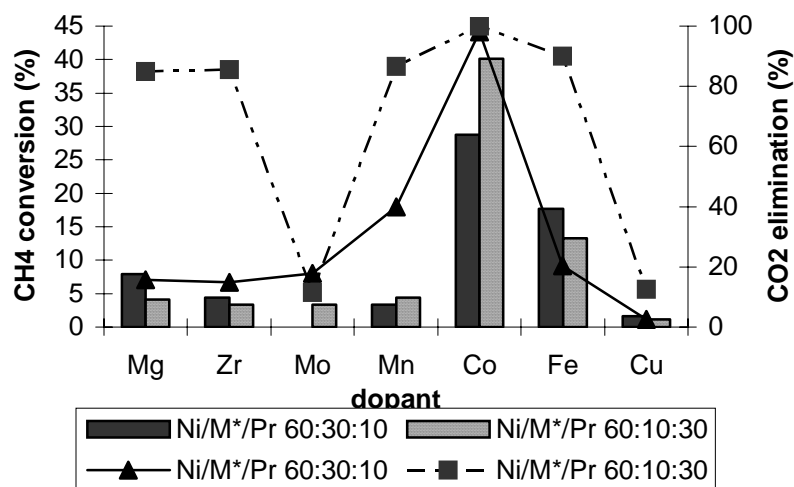
Figure 3: Catalytic activities of Ni/M*/Pr (M =Mg, Zr, Mo, Mn, Co, Fe, Cu, and Zn)
ratio 60:30:10 and 60:10:30 for CO_2 elimination and CH_4 conversion at 400ºC

As we compare the dopants according to ratios shown in Figure 2 and Figure 3, we can see significant difference in each ratio for each dopant. The line chart in Figure 3 showed the CO_2 elimination for the catalyst indicated that the catalyst doped with cobalt for both higher and lower amount of dopant, were superior from the rest. It was observed in the Ni/Co/Pr catalyst, which has special features itself, showed that, it still does the function of eliminating CO_2 and forming CH_4 as the product. Further study on the cobalt doped catalyst shows that the optimum ratio of the dopant added to Ni/Co/Pr are with the ratio of 60:35:5. with only low addition of praseodymium, the catalyst structure was altered to a suitable structure for methanation catalyst.

Characterization
In order to further understand the performance of the catalyst and role of dopant in the enhancement of the catalytic performance material, the best catalyst was characterized by various techniques.

X-Ray Diffraction(XRD)
XRD analysis was carried out on Ni/Co/Pr with the ratio of 60:35:5 prepared by calcination at 400ºC for 17 hours. From Figure 4, it was found out that the catalyst formed a polycrystalline phase, a form of mixture of amorphous and crystalline phases, which indicates a good catalyst. We can clearly see formation of spinel compound of Co_3O_4 on the surface of catalyst. This was preferred because the spinel compound is a combination of two oxidation state that is CoO and Co_2O_3 which served as an active site on the surface. The particle size calculated from Scherrer's equation is 17.65nm. From the XRD analytical data, we presumed that spinel compound that formed in the catalyst plays a major role in enhancing the performance of the catalyst. Meanwhile, the addition of Pr has also played a part in the enhancement of physical properties of the catalyst which probably affected the physical structure by making it more amorphous and also contributes in the CO_2 conversion mechanism to form methane.
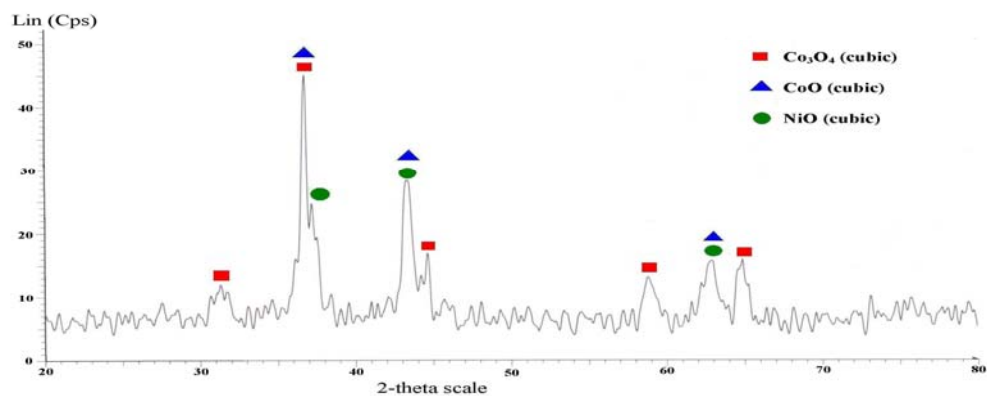
Figure 4: X-Ray Diffraction pattern for Ni/Co/Pr with the ratio of 60:35:5 calcined 400°C for 17 hours

BET surface area

Ni/Co/Pr 60:35:5 catalysts was sent for the surface area analysis. Table 1 showed the comparison between the previous studied catalyst Ni/Pr with the ratio of 60: 40 and Ni/Co/Pr 60: 35: 5. It seems that the surface areas for Ni/Pr 60:40 and Ni/Co/Pr 60:35:5 catalysts have only had a slight difference in the surface area. While Ni/Co is about half of Ni/Co/Pr, which means that, the surface area of the new modified catalyst have similarity of the previous catalyst and we can presume that the catalytic activity should be the same. This also showed that the addition of Pr change the physical properties by increasing the surface area of the catalyst

Table 1: BET surface area of catalysts

Catalyst	BETsurface area (m^2/g)
Ni/Pr [11]	75.58
Ni/Co/Pr	59.86
Ni/Co	38.49

Temperature Programmed Desorption

To determine the sorption profile of CO_2 and H_2 on the surface of catalyst, TPD was used whereby the ability of Ni/Co/Pr with the ratio of 60: 35: 5 to absorb CO_2 and H_2 was studied. The TPD profile of CO_2 by the catalyst is shown in Figure 5. Three desorption peaks at 270°C, 600°C and 750°C can be distinguished. Peak evolve at a lower temperature and two remain peaks are at a higher temperature. This was probably due to the different bonding modes of CO_2 with the active sites, during the adsorption on the surface.
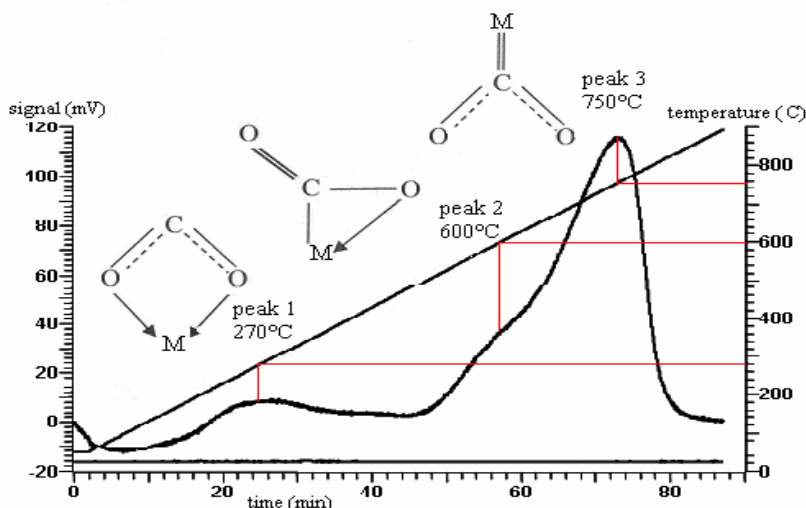
Figure 5: TPD profile of CO_2 for Ni/Co/Pr with the ratio of 60:35:5

A study by Cox [11], mentioned that the coordination of CO_2 onto metal oxide has different energies, which will cause different desorptions profile. The peak at lowest temperature of 270°C is due to desorption of the weakest bonding mode of CO_2 onto the catalyst surface. It was proposed that three bonding modes occurred. The peak area showed the amount of CO_2 sorption of the species. It was clearly seen that the metal carbene (M=CO_2) primarily dominated the bonding mode on the surface of the catalyst. This means that the catalyst that formed strong bonds with CO_2, and needed high temperature to produce more energy for desorption the CO_2. The sorption sites of H_2 on the surface of the catalyst were also being studied. Two significant peaks were detected at 350°C and 780°C. It was probably due to the sorption of hydrogen between the NiO or CoO lattices to form metal hydrates (M-H). Nevertheless, H_2 sorption correlates with the CO_2 sorption at the higher temperature of 780°C. It can be concluded that the chance for formation of methane at lower temperature is less compared to catalyst at higher temperature. But the lower desorption peaks can still be accounted because it still can convert to methane

Conclusion

The catalytic testing of all the catalyst with higher and lower loading of dopants (ratio 60:30:10 and 60:10:30 respectively), the testing showed that addition of specific dopants resulting in a high catalytic activity, and some suppress the catalytic activity of the catalyst. For the ability of the catalyst to eliminate CO_2 as well as to converted to methane simultanously, the Ni/Co/Pr with an optimum ratio of 60:35:5 was identified to be able to do almost 100% of CO_2 elimination.

Characterization of the best performance catalyst was studied in depth. XRD analysis found that the catalyst consists of a cubic NiO, and a spinel compound of Co_3O_4 which consist of mixture of cubic CoO and Co_2O_3. The present of Co_3O_4 was identified to be the major contribution to the catalytic activity enhancement of the Ni/Co/Pr catalyst. The single point BET analysis, obtained for the Ni/Co/Pr (60:35:5) showed high surface area of 59.86m^2/g when compared to the Ni/Co 60:40 (38.50m^2/g). It was predicted that the incorporation of Pr attributed to the surface area and thus making it superior. Commencing the TPD analysis of the catalyst, three major peaks for the sorption of CO_2 and two major peaks for the sorption of H_2 were depicted. As the lower peaks contributed to the elimination of CO_2 at lower temperature (270°C) with the high formation of methane (350°C), the actual desorption of both CO_2 and H_2 occured at higher temperature. This means that the Ni/Co/Pr catalyst full potential towards methanation reaction lies in the temperature ranging from 600-800°C.

From the characterization, we can conclude that the addition of Co as dopant enhanced the catalytic activity of the Ni/Co/Pr catalyst as it contributed to the formation of additional active sites and change the chemical properties of the catalyst. Hence,the incorporation of Pr cause changes in the physical properties of the Ni/Co/Pr catalyst.

References

1. Kudo, K., and Komatsu, K. (1999). Reduction of alkali metal carbonate to methane with water in the presence of Raney alloy. *J. of Molec. Catalysis. A: Chemical.* 145: 159–167
2. Cattenot, M., Geantet, C., Glasson, C., and Breysse, M. (2001). Promoting effect of ruthenium on NiMo/Al$_2$O$_3$ hydrotreating catalysts". *Appl. Catalysi. A: General.* 213: 217–224.
3. Jose, A., R., Jonathan, C., H., Anatoly, I., F., Jae, Y., K. and Manuel, P. (2001). Experimental and Theoretical Studies on the Reaction of H$_2$ with NiO. Role of O Vacancies and Mechanism for Oixde Reduction. *J. Am. Chem.Soc.* 124, 346-354
4. Wang, L., Murata, K., and Inaba, M. (2004). Control of the Product Ratio of CO$_2$/ (CO+CO$_2$) and Inhibition of Catalyst Deactivation for Steam Reforming of Gasoline to Produce Hydrogen. *Appl. Catalysis B: Environmental.* 48: 243-248
5. Hou, Z., Yokota,O., Tanaka, T., and Yashima, T. (2004). Surface Properties of a Coke-free Sn Doped Nickel Catalyst for the CO$_2$ Reforming of Methane. *Appl. Surf. Sci..* 233: 58-68.
6. Valentini, A., Carreno, N.L.V., Probst, L.F.D., Lisboa-Filho, P.N., Schreiner, W.H., Leite, E.R., and Longo, E. (2003). Role of vanadium in Ni:Al$_2$O$_3$ catalysts for carbon dioxide reforming of methane. *Appl. Catalysis A:General* 255: 211-220
7. Jacobs, G., Das, T.K., Zhang, Y., Li, J., Racoillet, G., and Davis, B.H. (2002). Fisher-Troposh synthesis: support, loading, and promoter effects on the reducibility of cobalt catalyst. *Appl. Catalysis A: General* 233: 263-281.
8. Zhang, Y., Jacobs, G., Sparks, D.E., Dry, M.E., and Davis, B.H. (2002). CO and CO2 hydrogenation study on supported cobalt Fisher-Troposh synthesis catalysts. *Catalysis Today* 71: 411-418
9. Guczi, L., Schay, Z., Stefler, G., and Mizukami, F. (1999). Bimetallic catalysis: CO hydrogenation over palladium–cobalt catalysts prepared by sol gel method. *J. of Molec. Catalysis A: Chemical.* 141: 177–185.
10. Mohd Hasmizam, R. (2005). CO$_2$ Methanation on Nickel-Based Catalysts. MSc thesis, UTM.
11. Cox, P., A. (1995). *The Elements on Earth-Inorganic Chemistry in the Environment*. Oxford. Oxford University Press. 147-158.

PENGHASILAN SURFAKTAN TAK BERION BERASASKAN LAURIL ALKOHOL DARIPADA TERBITAN MINYAK KELAPA SAWIT

Norhafipah Mohamad*, Zarina Edris dan Mohd Ambar Yarmo

*Makmal Pemangkinan, Pusat Pengajian Sains Kimia dan Teknologi Makanan, Fakulti Sains dan Teknologi,
43600 Universiti Kebangsaan Malaysia, Bangi, Selangor.*

Kata kunci: Tindak balas pengetoksilan, lauril alkohol teretoksilat, etilena oksida, minyak sawit

Abstrak

Penghasilan surfaktan tidak berion jenis lauril alkohol teretoksilat (LAT) berasaskan produk lauril alkohol daripada minyak kelapa sawit berjaya dilakukan. Sintesis ini melibatkan tindak balas pengetoksilan antara gas etilena oksida (EO) dengan lauril alkohol (C_{12}). Antara parameter yang dikaji dalam kajian ini adalah kesan perbezaan bilangan mol EO, tekanan dan suhu tindak balas. Tindak balas dilakukan menggunakan kalium hidroksida (KOH) sebagai mangkin homogen. Hasil terbentuk dianalisis menggunakan teknik HPLC, FTIR, ujian pembuihan, nilai Keseimbangan Hidrofilik-Lipofilik (HLB) dan Ujian Detergensi (peratus penyingkiran kotoran). Pembentukan molekul LAT dapat ditunjukkan melalui spektroskopi FTIR yang menandakan wujudnya puncak regangan C-O (kumpulan eter) pada jarak gelombang 900 – 1350 cm^{-1}. Manakala pencirian menggunakan teknik HPLC menunjukkan masa penahanan produk ialah 6.201 min untuk LAT-3 EO, 6.261 min untuk LAT-5 EO dan 6.260 min untuk LAT-7 EO. Pencirian surfaktan melalui ujian pembuihan menunjukkan produk LAT yang diperolehi mempunyai kestabilan dan kekuatan buih yang baik. Secara umum hasil menunjukkan produk yang diperolehi berpotensi untuk digunakan sebagai detergen dan kegunaan industri.

Abstract

Non-ionic surfactant type of ethoxylated lauryl alcohol (LAT) based on lauryl alcohol product from palm oil was produced successfully. Ethoxylation reaction was carried out between EO with lauryl alcohol (C_{12}). Different moles ratio of EO, reaction temperature and pressure were among various parameters investigated. The reaction was performed with KOH as a homogenous catalyst. LAT products were analyzed using FTIR, HPLC, foaming test, value of Hydrophilic-Lipophilic Balance (HLB) and detergency. The formation of LAT molecule was indicated by the C-O stretching peak (ether group) at 900 – 1350 cm^{-1} of the FTIR spectrum. Characterization using HPLC showed the retention time of 6.201 minutes for LAT-3 EO, 6.261 minutes for LAT-5 EO and 6.260 minutes for LAT-7 EO. Generally, the ethoxylated product has a good potential to be used as detergent and for industrial application.

Pengenalan

Malaysia merupakan negara pengeluar dan pengeksport terbesar minyak sawit. Sebanyak 90% minyak sawit yang dikeluarkan diguna dalam industri makanan dan industri oleokimia seperti pembuatan kosmetik, detergen dan sebagainya [1]. Disebabkan pasaran turun naik bagi bahan mentah surfaktan yang berasaskan minyak petroleum, maka satu alternatif baru telah diberi perhatian iaitu penggunaan bahan mentah yang berasaskan bahan semulajadi seperti kelapa sawit dan sayur-sayuran sebagai menggantikan penggunaan produk berasaskan petrokimia. Ini berikutan daripada tren dunia tentang penjimatan kos dan juga konsep yang lebih mesra alam.

Surfaktan yang mempunyai 2 bahagian iaitu hidrofilik (suka air) dan hidrofobik (suka minyak).meliputi kimia organik sintetik yang mana ia membantu dalam pembuihan, pemelarutan, pengemulsian, penyerakkan dan pembasuhan. Walaupun demikian, tidak kesemua surfaktan mempunyai ciri-ciri yang sama kerana ia sangat bergantung kepada struktur kimia molekul tersebut [2].

Industri surfaktan kini semakin terus berkembang pesat di mana penggunaan surfaktan dunia terus meningkat kepada 11 juta ton setiap tahun. Di samping itu penggunaan bahan pengemulsi, agen pembasah dan lain-lain lagi telah lama berkembang dalam sektor perindustrian. Surfaktan juga banyak digunakan dalam industri pemprosesan seperti industri makanan, farmaseutikal dan penjagaan diri. Surfaktan bukan sahaja penting sebagai juzuk yang aktif tetapi juga penting sebagai pengemulsi, penstabil dan pelembut fabrik. Rajah 1 menunjukkan kegunaan lemak dan minyak dunia. Pada 1990, pengeluaran surfaktan dunia mencapai sehingga 81 juta ton yang mana 11.4 juta ton menggunakan proses teknikal dan kimia [3].
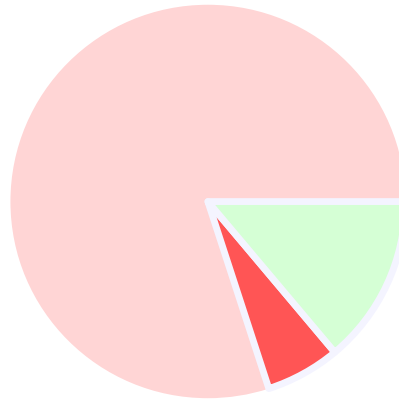
Kegunaan lemak dan minyak dunia

Industri surfaktan telah meningkat pada akhir dekad dan penggunaan bahan mentah semulajadi telah diberi perhatian bagi menggantikan produk yang berasaskan petrokimia seperti penghasilan gula berasaskan surfaktan seperti alkil glukosida [4]. Sebanyak 20 million ton bahan mentah kimia yang dikitar semula telah diguna seluruh dunia setiap tahun seperti karbohidrat 15 % (55 % daripada minyak dan lemak), glukosa, sukrosa dan bahan sorbitol (daripada penghidrogenan glukosa) merupakan sebatian polihidroksi daripada bahan semulajadi. Sebatian-sebatian ini boleh diguna tanpa had, mempunyai ekologi yang bagus, berketulenan tinggi serta kurang toksik. Oleh kerana itu, kajian secara menyeluruh tentang penggunaannya dilakukan [3].

Lemak alkohol teretoksilat merupakan salah satu daripada kelas surfaktan tidak berion yang penting. Tindak balas pengetoksilan lemak alkohol ini dilakukan dengan kehadiran mangkin. Mangkin aluminium alkoksida sulfat telah dikaji tentang keberkesanannya dalam tindak balas pengetoksilan. Hasil yang diperolehi adalah lebih tinggi berbanding mangkin bes. Namun demikian banyak produk sampingan yang terhasil [5]. Sehingga kini, mangkin bes seperti KOH dan NaOH banyak digunakan dalam industri [6].

Kajian tindak balas pengetoksilan telah dilakukan terhadap nonifenol oleh Santecaseria [6]. Kajian ini mengenai kinetik nonilfenol teretoksilat dengan menggunakan mangkin KOH. Selain itu, kajian tindak balas pengetoksilan juga telah dilakukan dengan menggunakan 1-dodekanol dan 4-nonilfenol sebagai reaktan. Kajian dilakukan untuk melihat keberkesanan tindak balas pada pelbagai suhu tindak balas dilakukan [7]. Formula umum bagi poliglikol eter yang terhasil daripada tindak balas pengetoksilan seperti kajian yang telah dilakukan oleh Alfonso *et.al.* pada 2004 [1] adalah seperti berikut:

$$CH_3 (CH_2)_m\text{-}(OCH_2CH_2)_nOH$$
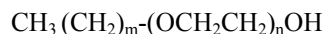
Eksperimen

Penyediaan mangkin
Mangkin KOH dalam bentuk pallet dengan ketulenan 99.9 % daripada Aldrich Chemical digunakan. Sebanyak 1.34 g KOH dilarutkan dalam campuran 0.56 ml air suling dan 0.804 ml metanol daripada Fischer Scientific dengan ketulenan 99.99 %.

Bahan kimia dan reaktor
Kalsium karbonat daripada Fluka sebagai peneutral dalam bentuk serbuk dilarutkan dengan air suling, lauril alkohol berketulenan 99 % daripada Cognis Oleochemical sebagai bahan hidrofobik, gas etilena oksida (EO) daripada Fluka sebagai bahan hidrofilik dengan ketulenan 99% dan cecair nitrogen daripada Taylor Wharton berfungsi sebagai pemerangkap atau pemegun wap metanol.

225

Pelarut dan bahan untuk ujian pencirian surfaktan
Pelarut kalium bromida (KBr) digunakan dalam penyediaan sampel untuk analisis FTIR. Air suling dan metanol berketulenan 99% (Gred HPLC) daripada Fischer Scientific sebagai pelarut untuk HPLC. *Cotton AS9 pigment/oil* digunakan dalam ujian detergensi untuk menentukan peratus penyingkiran kotoran.

Kaedah Tindak balas Pengetoksilan
Reaktor pengetoksilan yang digunakan adalah daripada Vinci Technology dari Perancis. Reaktor ini mempunyai sistem keselamatan yang tinggi bagi mengendalikan gas EO. Secara umumnya reaktor tersebut terdiri daripada tangki EO, sistem vakum, penimbang EO, pam gas EO, reaktor(sistem pengetoksilan), pengawal suhu reaktor, sistem pembuangan gas EO dan sistem kawalan komputer seperti dalam skema reaktor dalam Rajah 2.
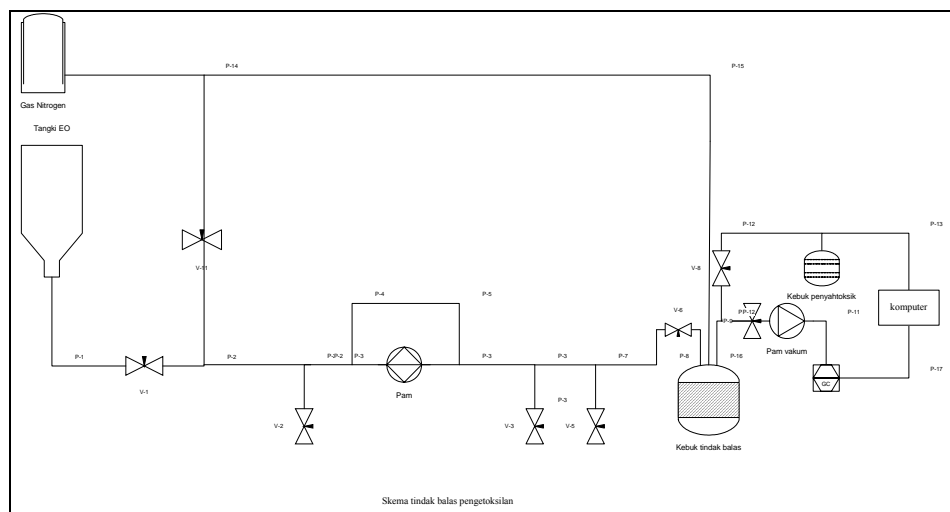
Skema reaktor pengetoksilan.

Reaktor pengetoksilan dilengkapi dengan gas EO sebagai reaktan dan gas nitrogen sebagai gas pembawa. Gas EO akan ditukar kepada bentuk cecair melalui pam EO. Kemudian cecair EO yang terhasil akan disuntik ke dalam reaktor pengetoksilan. Rajah 3 menunjukkan reaktor pengetoksilan yang diguna dalam menghasilkan surfaktan tidak berion.

Kaedah sintesis LAT merupakan satu tindak balas pengetoksilatan iaitu antara molekul etilena oksida (EO) terhadap lauril alkohol. Sebelum itu mangkin bes iaitu 1.34 g KOH dilarutkan dalam campuran 0.56 ml air dan 0.804 ml metanol. Larutan ini dimasukkan ke dalam reaktor dan dipanaskan di bawah vakum pada suhu 90°C selama 1 jam di dalam reaktor pengetoksilan. Selepas 1 jam, larutan ini akan kelihatan seperti gel berwarna putih.

Seterusnya suhu reaktor terlebih dahulu dinaikkan sehingga 100 °C. Setelah itu lauril alkohol dimasukkan ke dalam reaktor dan apabila suhu berada dalam keadaan stabil iaitu pada 70 °C, EO pula disuntik masuk melalui sistem reaktor mengikut bilangan mol yang ditetapkan. Tindak balas pengetoksilan berlaku sejurus EO masuk ke dalam reaktor. Pengacauan terus dilakukan sepanjang proses tindak balas. Selepas tamat tindak balas, suhu reaktor diturunkan dan gas nitrogen dilalukan dalam reaktor bertujuan untuk menyingkirkan lebihan EO yang mungkin tidak bertindak balas.

Rajah reaktor pengetoksilan.

Pencirian

Produk yang diperoleh dianalisis menggunakan teknik FTIR jenis Perkin Elmer Model GX dan HPLC jenis Agilent Technologies Siri 1100 dengan menggunakan pengesan ELSD jenis Altech Model 2000. Pencirian seterusnya dilakukan bagi menentukan tahap pembuihan dan kestabilannya serta peratus penyingkiran kotoran dengan melakukan ujian pembuihan dan ujian detergensi.

Ujian Pembuihan LAT

Ujian LAT dilakukan untuk ujian pembuihan telah dilakukan terhadap surfaktan yang diperolehi iaitu keupayaan pembuihan (foaming power) dan kestabilan pembuihan (foaming stability).

Kaedah yang digunakan ini diperoleh daripada kaedah dalaman AOTD. Kaedah ini menggunakan silinder 500 ml yang diisi dengan larutan surfaktan (0.2 g dalam 200 ml air ternyahion). Larutan dikocak menggunakan rod selama 30 kali pada kadar yang tetap. Apabila buih terbentuk, bacaan diambil bagi mengira kadar keupayaan pembuihan iaitu kemampuan surfaktan menghasilkan buih, berdasarkan persamaan :-

$$\text{Keupayaan pembuihan} = (\text{takat atas}) - \frac{(\text{takat bawah})}{\text{Jumlah ketinggian}}$$

Manakala kestabilan pembuihan pula diukur selepas 5 minit kocakan. Kestabilan pembuihan adalah kemampuan surfaktan mengekalkan tahap pembuihan dalam masa tertentu dan ia diukur berdasarkan persamaan:-

$$\text{Kestabilan pembuihan} = (\text{takat atas}) - \frac{(\text{takat bawah})}{\text{Jumlah ketinggian}}$$

Peratus penyingkiran kotoran
Dalam pencucian, % keupayaan detergen diuji dengan menggunakan spektrofotometer CM36000. Dalam eksperimen ini, detergen diuji ke atas *cotton AS9 pigment/oil*. Surfaktan terhasil dicairkan dengan menggunakna 100 ml air suling dan dicampur dengan 50 ppm air liat (*hard water*) selama 3 minit. Selepas proses pencampuran, *cotton AS9 pigment/oil* dimasukkan ke dalam bekas untuk pencucian selama 10 minit. Akhir sekali, *cotton AS9 pigment/oil* dibilas sebanyak 2 kali dengan 1000 ml dan 500 ml air liat. Peratus penyingkiran kotoran dikira berdasarkan:

$$\% \, \text{Penyingkiran kotoran} = \frac{(AW - BW)}{(BS - BW)} \times 100$$

AW = intensiti kecerahan selepas cucian terhadap *cotton AS9 pigment/oil*
BW = sebelum cucian terhadap *cotton AS9 pigment/oil*
BS = sebelum cucian dalam *standard clothes*

Hasil dan Perbincangan

Proses pengetoksilan
Proses pengetoksilan lauril alkohol berjaya dijalankan pada julat suhu $100 \, ^0C$ - $135 \, ^0C$ dengan masa tindak balas selama 2 jam. Tindak balas yang berlaku adalah seperti berikut:

$$CH_3(CH_2)_{11}\text{-OH} \quad + \quad n(CH_2CH_2O) \rightarrow CH_3(CH_2)_{11}\text{-}(OCH_2CH_2)_nOH$$
(Lauril alkohol)   (EO)   (LAT)
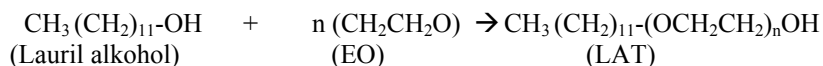
Kenaikan suhu reaktor dapat dilihat secara mendadak semasa EO disuntik ke dalam reaktor iaitu dari $60 \, ^0C$ sehingga $120 \, ^0C$ melebihi suhu yang diset pada monitor. Ini menandakan tindak balas eksotermik telah berlaku pada tindak balas pengetoksilan tersebut. Rajah 4 (i) menunjukkan profil perubahan suhu reaktor semasa tindak balas pengetoksilan berlaku dan rajah 4 (ii) pula menunjukkan graf suhu yang telah diset pada monitor.

Suhu reaktor dikawal sepenuhnya oleh komputer. Pada awalnya suhu dinaikkan sehinnga $90 \, ^0C$ dan pada ketika suhu mencapai $50 \, ^0C$ lauril alkohol dimasukkan ke dalam reaktor (a). reaktor dibiarkan seketika sehingga suhu yang tercatat pada komputer adalah stabil iaitu pada 70^0C dan pada ketika ini, EO disuntik (b). Peningkatan suhu secara mendadak dapat dilihat setelah EO habis disuntik iaitu daripada suhu $60 \, ^0C$ dan meningkat sehingga $120 \, ^0C$. Ini menandakan tindak balas eksotermik berlaku. Ini adalah kerana kereaktifan molekul EO dan aktiviti mangkin yang digunakan.

Pencirian LAT
a) FTIR
Perubahan warna daripada warna jernih lauril alkohol kepada warna kuning keemasan setelah proses pengetoksilan tamat menandakan wujudnya sebatian baru iaitu LAT. Produk yang terhasil dianalisis dengan menggunakan teknik FTIR. Sampel disedia dengan menggunakan teknik lazim. Kumpulan berfungsi yang wujud dalam sebatian yang dikaji dapat diketahui melalui maklumat yang diperolehi daripada spectrum FTIR. Rajah 5 menunjukkan spektrum bagi lauril alkohol dan sebatian-sebatian LAT yang diperolehi.
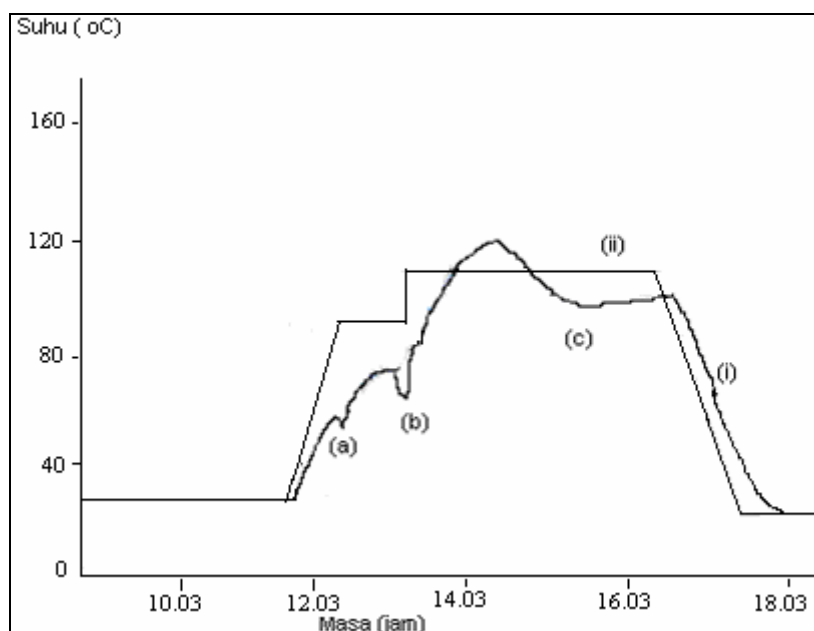
Profil suhu tindak balas pengetoksilan LAT.

(a) = Kemasukkan lauril alkohol.
(b) = EO disuntik.
(c) = Masa tindak balas.
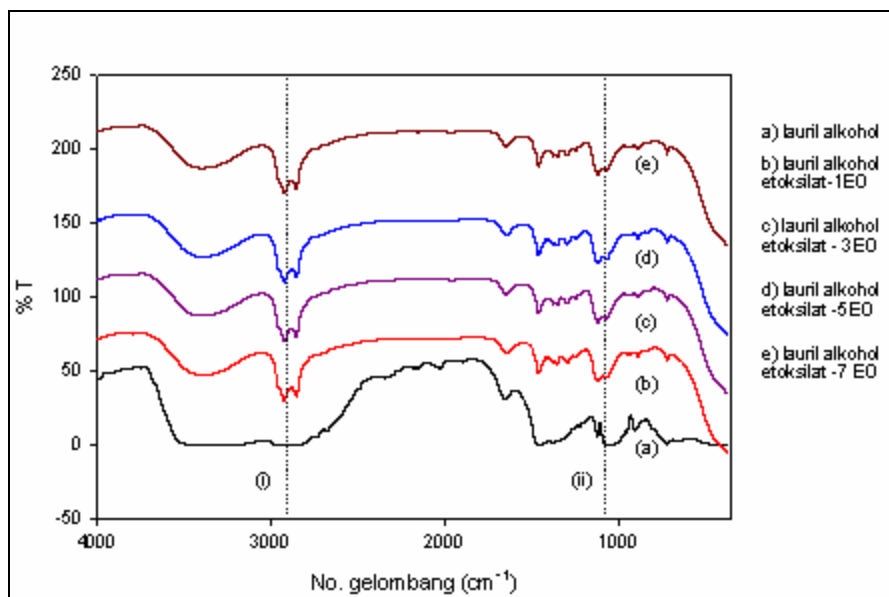
Spektrum FTIR bagi produk LAT dan lauril alkohol.

Spektrum FTIR bagi semua siri LAT dan lauril alkohol yang diperolehi menunjukkan wujudnya puncak ikatan O-H (i) pada jarak gelombang 2500 – 3450 cm^{-1} dan puncak regangan C-O (ii) pada jarak gelombang 900 – 1350 cm^{-1}. Regangan C-O menandakan bahawa hasil yang diperolehi adalah sebatian yang mempunyai kumpulan eter.

b) HPLC

Setelah itu, LAT yang diperolehi dianlisis dengan menggunakan teknik HPLC. Turus jenis Zorbax 300 SB-C18 digunakan bagi mendapatkan spektrum LAT. Pelarut yang digunakan adalah metanol dan air dengan nisbah 90:10. Sampel disuntik pada kadar 2 μl dengan kadar alir bagi teknik ini adalah 1ml/min. Rajah 6 menunjukkan kromatogram HPLC bagi LAT yang diperolehi.

(a)   (b)

(c)   (d)
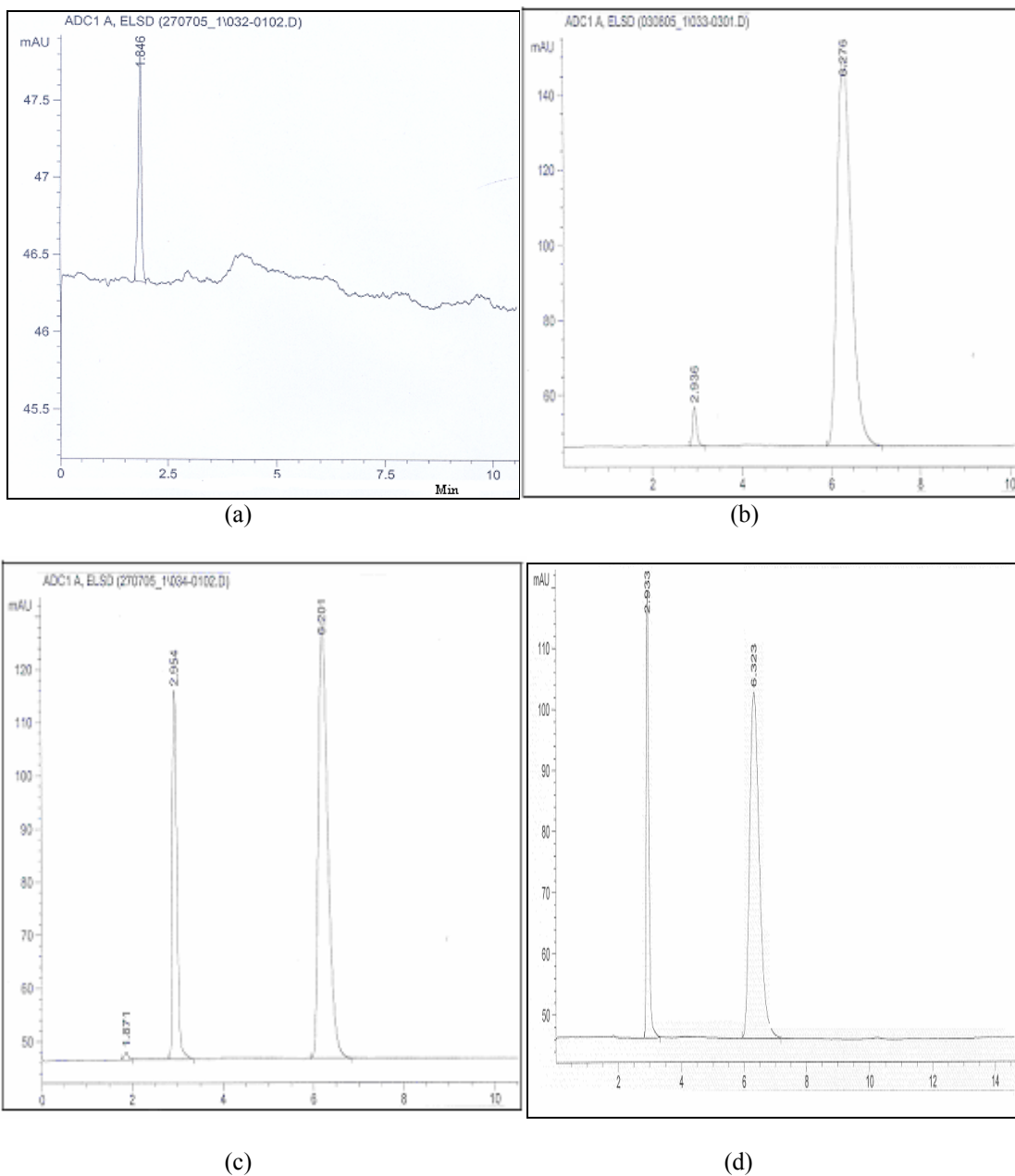
Kromatogram HPLC bagi sebatian lauril alkohol (a), LAT-3EO (b), LAT-5EO (c) dan LAT-7EO (d).

Peratus penukaran produk diperolehi berdasarkan teknik ini. Daripada analisis kromatogram, peratus penukaran produk bagi LAT hampir mencapai 100 % seperti yang tercatat dalam jadual 1 di bawah.

Hasil analisis berdasarkan kromatogram HPLC.			
Produk	Bilangan mol EO	Masa penahanan (min)	Peratus penukaran produk
	0	1.846	0
Lauril alkohol	3	6.201	70.6
teretoksilat (LAT)	5	6.261	97.6
	7	6.260	79.8

c) Ujian Detergensi

Ujian pencucian dilakukan terhadap LAT yang terhasil bagi menentukan peratus penyingkiran kotoran. Dalam proses ini, 3 elemen diambil kira iaitu substrat, jenis kotoran dan larutan pembersih dalam menentukan keberkesanan pencucian. Struktur kimia bagi panjang rantai kumpulan hidrofobik dan hidrofilik menentukan peratus pencucian kotoran. Panjang rantai karbon yang lurus adalah lebih baik daripada rantai karbon bercabang bagi kumpulan hidrofobik dan peningkatan panjang rantai kumpulan ini akan meningkatkan lagi keberkesanan pemindahan kotoran berminyak [8].

Manakala peningkatan kumpulan hidrofilik dalam rantai polioksietilena (POE) menunjukkan penurunan keberkesanan jerapan surfaktan ke atas suatu bahan dan ia berkaitan dengan penurunan dalam detergensi, contohnya dalam ujian detergensi kain kapas pada suhu 30 ^{0}C oleh POE nonilfenol dalam air suling menurun dengan peningkatan kumpulan EO daripada 9 kepada 20 [9]. Rajah 7 menunjukkan peratus penyingkiran kotoran LAT (surfaktan tidak berion) yang diperolehi.
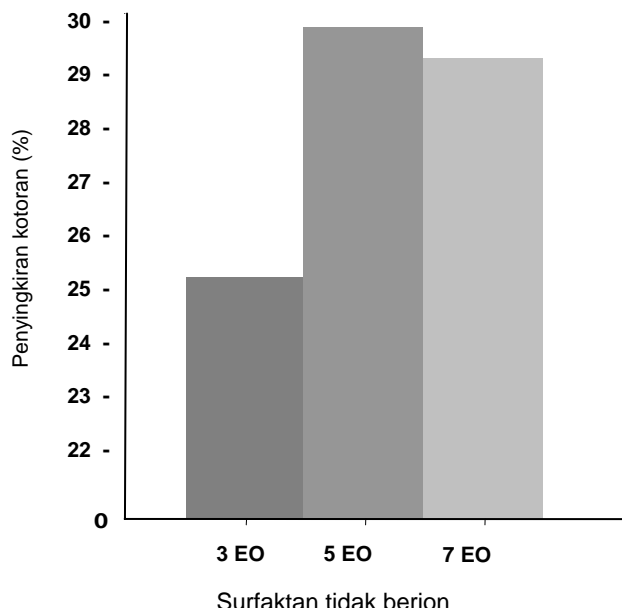
Peratus penyingkiran kotoran bagi surfaktan tidak berion.

Peratus penyingkiran kotoran bagi LAT-5 EO adalah lebih tinggi berbanding LAT-3 EO dan LAT-7 EO. Ini menunjukkan panjang rantai EO iaitu kumpulan hidrofilik mempengaruhi peratus penyingkiran kotoran, iaitu semakin panjang EO maka semakin rendah peratus penyingkiran kotoran. Namun demikian, rantai EO terlalu pendek juga mempengaruhi peratus pencucian. Oleh sebab itu, LAT dengan 5 mol EO adalah amat sesuai digunakan dalam detergen berdasarkan ujian detergensi yang dilakukan.

d) Ujian Pembuihan

Ujian pembuihan bergantung kepada panjang rantai alkil, darjah pengetoksilan dan nisbah surfaktan yang hadir. Peningkatan darjah pengetoksilan akan menghasilkan surfaktan yang lebih larut air [10].

231

Semasa pembuihan, permukaan udara-air terbentuk. Secara amnya ia akan menghasilkan luas permukaan yang tinggi bagi jerapan surfaktan yang tidak lengkap. Luas permukaan akan menurun dengan masa dan ini merupakan peningkatan jerapan surfaktan. Ujian pembuihan menentukan tahap keupayaan buih dan kestabilan buih yang terhasil. Rajah 8 menunjukkan keupayaan dan kestabilan pembuihan bagi LAT yang diperolehi.
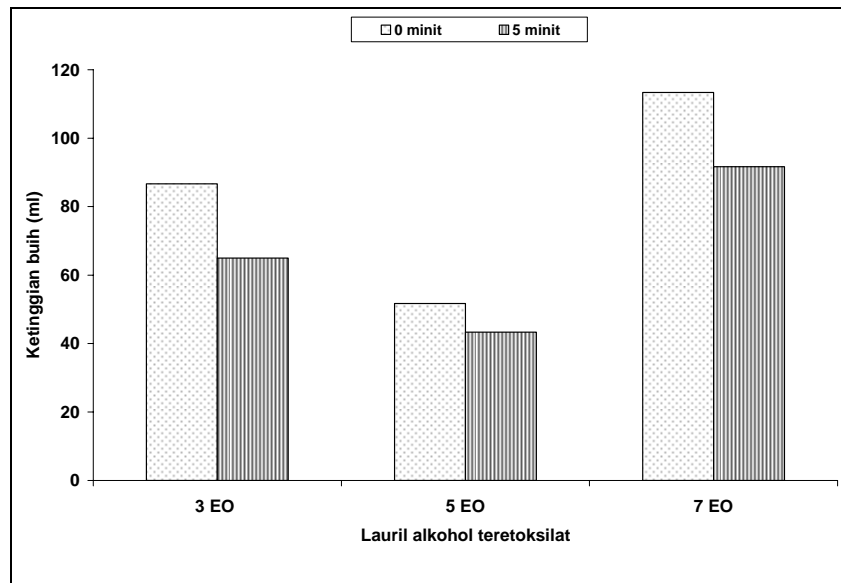
Keupayaan dan kestabilan pembuihan bagi semua siri LAT.

Keupayaan pembuihan LAT-7 EO yang terhasil adalah lebih tinggi berbanding LAT-3 EO dan LAT-5 EO. Namun, LAT-5 EO memberikan kestabilan pembuihan yang lebih baik berbanding LAT-3 EO dan LAT-7 EO. Secara amnya peningkatan bilangan kumpulan EO dalam surfaktan tidak mempengaruhi peningkatan dalam keupayaan pembuihan dan kestabilan pembuihan.

e) Nilai Keseimbangan Hidrofilik-Lipofilik (HLB)
Produk LAT yang diperolehi dihitung nilai HLBnya berdasarkan persamaan (i). Jadual 2 di bawah menunjukkan peratus hasilan lauril alkohol teretoksilat (LAT) yang diperolehi. Berdasarkan jadual 3, nilai HLB bagi produk LAT yang diperolehi menandakan ia mempunyai ciri-ciri sebagai agen pengemulsi yang sesuai digunakan dalam penghasilan detergen.

$$\text{HLB} = \frac{20xMh}{Mh + Ml} \qquad \text{Persamaan (i)}$$

Mh = berat bahagian hidrofilik
Ml = berat bahagian hidrofobik

LAT yang terhasil dengan berat molekul, nilai HLB dan peratus hasilannya.

Produk	Berat molekul	Nilai HLB	% Hasilan
LAT + 3 EO	318	8.30	91.52 %
LAT + 5 EO	406	10.84	88.96 %
LAT + 7 EO	494	12.47	99.63 %

Ciri-ciri surfaktan berdasarkan nilai HLBnya.

Nilai HLB	Ciri-ciri surfaktan / Potensi kegunaan
3 – 6	air dalam pengemulsi minyak
7 – 9	agen pembasah
8 – 15	minyak dalam pengemulsi air
12 – 15	bersifat detergen
15 – 18	bersifat keterlarutan

Kesimpulan

Bahan kimia berasaskan bahan semulajadi daripada minyak sawit digunakan iaitu lauril alkohol. Ini berikutan banyak kelebihan yang boleh diperolehi daripada bahan semulajadi ini. Selain daripada senang diperolehi dan murah, penggunaannya juga akan menghasilkan produk yang tidak toksik dan mudah terbiodegradasi.

Hasil analisis menunjukkan bahawa LAT telah berjaya dihasilkan berdasarkan teknik FTIR dan HPLC. Teknik FTIR menunjukkan wujudnya satu sebatian baru selepas tindak balas pengetoksilan dilakukan terhadap lauril alkohol. Terdapat puncak ikatan O-H pada jarak gelombang $2500 – 3450$ cm^{-1} dan puncak regangan C-O pada jarak gelombang $900 – 1350$ cm^{-1}. Regangan C-O menandakan hasil yang diperolehi adalah sebatian yang mempunyai kumpulan eter. Sebagaimana yang diketahui, melalui tindak balas pengetoksilan lemak alkohol akan menghasilkan sebatian poliglikol eter.

Manakala melalui teknik HPLC menunjukkan peratus penukaran produk yang tinggi iaitu menghampiri 100 % bagi produk-produk LAT ini. Setelah pelbagai pencirian surfaktan dilakukan ke atas semua siri produk LAT, dapat disimpulkan bahawa produk LAT-5 EO adalah lebih sesuai untuk kegunaan industri dan detergen. Ini adalah berdasarkan pada nilai HLBnya iaitu 10.84 dan ujian detergensi yang dilakukan menunjukkan peratus pencucian bagi LAT-5 EO adalah tinggi daripada LAT-3 EO dan LAT-7 EO dan mempunyai keupayaan pembuihan yang rendah berbanding LAT yang lain. Sebagaimana yang diketahui pembuihan yang tinggi tidak menentukan detergen yang baik. LAT-5 EO adalah lebih berpotensi dalam penggunaan detergen berbanding produk LAT yang lain berdasarkan ujian-ujian yang dilakukan ke atasnya.

Penghargaan

Rujukan

1. Alfonso, E. S., Citterio. A., Ramis-Ramos, G., Righetti, P. G. & Sebastiano, R. (2004) "Separation of Fatty Alcohol Polyethoxylates by Capillary Electrophoresis Through Easy Electroosmotic Flow Control with a Queternary Diammonium Salt" *Journal of Chromatography A* 1053. 235-239.
2. Ishikawa, Y., Modler, R. & Mueller, S. (2004) Surfactants.
3. Baumann, H. & Biermann, H. (1992) "Oleochemical Surfactants Today" *The International Journal of Oil Palm Research & Development* 6 (1).
4. Johansson, I. & Svensson, M. (2001) "Surfactants Based on Fatty Acids and Other Natural Hydrophobes" *Current Opinion in Colloid & Interface Science* 6. 178-188.
5. Bruni, S., DiSerio, M., Gobetto, R., Iengo, P. & Santacesaria E. (1996) "Ethoxylation of Fatty Alcohols Promoted by an Aluminium Alkoxide Sulphate Catalyst" *Journal of Molecular Catalysis A: Chemical* 112. 235-251.
6. Massey, N. (2005) "Predicting The Distribution of Ethoxylation Homologues with a Process Simulator" *Chemstation, Inc*. 1-9.
7. DiSerio M., Santacesaria E. & Tesser R. (1995) "Role of Ethylene Oxide Solubility in the Ethoxylation Processes" *Catalysis Today* 24. 23-28.
8. Rosen, M. H. (1978) "Surfactants and Interfacial Phenomena" A. *Wiley Interscience Publication*. 272-291.
9. Schwuger, A. M. (1971) *Journal Am Oil Chemistry Society* 48. 566.
10. Sawicki, G. C. (2005) "Impact of Surfactant Composition and Surfactant Structure on Foam Control Performance. Colloids and Surfaces" *Physicohhem. Eng. Aspects* 263. 226-232.
11. Carter, D. K., Hill, E. A. & Monroe, K. R. (2005) "Surfactant Parameter Effects on Cleaning Efficiency" *Research Triangle Institute*. 405-414.
12. Mccoy, M. (2005) "Soap and Detergents", C & EN Northeast News Bureau.
13. http://media.wiley.com (2005).
14. www.epu.jpm.my (2005).

233

TOXICITY AND ANTITERMITE ACTIVITIES OF THE ESSENTIAL OILS FROM *PIPER SARMENTOSUM*

T. C. Chieng., Z. B. Assim and B. A. Fasihuddin

Faculty of Resource Science and Technology, Universiti Malaysia Sarawak, 94300 Kota Samarahan, Sarawak

Abstract

The leaves of *Piper sarmentosum* were hydrodistilled using the modified Clevenger-type apparatus, and an average yield of essential oil of 1.10% (v/dry weight) was obtained. The leaf oils were analyzed by GC and GC-MS. A total of 31 components were identified. Spathulenol (21.0%), myristicin (18.8%), β-caryophyllene (18.2%) and (*E,E*)-farnesol (10.5%) were the major compounds found in the leaf oil. The leaf oil showed inhibitory activity against the larvae of *Artemia salina* with LC_{50} value of 35.2 µg/mL, and 100% mortality within two days at 1% concentration against the subterranean termite (*Coptotermes* sp.). The crude extract was then subjected to bioassay-guided isolation using silica gel column chromatography, and eluted with hexane containing increasing volumes of ethyl acetate and yielded three pure compounds. Their toxicity and antitermite activities of the three compounds were determined. Compound **2** showed the most potent activity against the larvae of *A. salina* with LC_{50} value of 7.5 µg/mL, while the LC_{50} values for compound **3** and compound **1** were 17.2 µg/mL and 22.5 µg/mL respectively. Compound **3** showed the strongest inhibitory activity against the subterranean termite (*Coptotermes* sp.) with 100% mortality after 3 days at 0.1% concentration followed by compound **2** with the same mortality rate at 0.5% concentration. Compound **1** showed the weakest inhibitory activity with 80% mortality after 3 days at 2% concentration. Based on spectroscopic data and comparison with published information, compound **1** and **2** have been identified as caryophyllene and myristicin respectively. Compound **3** is still being studied in order to elucidate its structure.

Introduction

The genus *Piper* belongs to the family Piperaceae, comprising more than 700 species distributed throughout the tropical and subtropical regions of the world [1]. Most of the species in this genus are aromatic, woody perennial climbers and rarely shrub. The *Piper* species have high commercial, economical and medicinal importance. Many species have been shown to possess antimicrobial, antifungal, antioxidant, insecticidal, allelopathic and antitumour activities [1]. Various compounds, including alkaloids/amides, propenylphenols, lignans, neolignans, terpenes, steroids, kawapyrones, chalcones, flavones and flavanones have been isolated from different *Piper* species. The chemistry of *Piper* species has been reviewed by several researchers [2, 3].

Piper sarmentosum Roxb., locally known as "kaduk", is a creeping herb with erect, slender branchlets about 30 cm tall. It is commonly found in damp open spaces, riverbanks cleared and cultivated lands in Sarawak [4]. The leaves are used in folk medicine as counter-irritants in poultices for headaches and pains in bones. A decoction of the boiled leaves may be utilized to treat coughs, influenza, toothaches and rheumatism. The root is also a remedy for toothache and may be made into a wash for fungoid dermititis on the feet [5]. A bioactive compound, isoasarone has been isolated from the roots of *P. sarmentosum* and showed insecticidal property similar to DDT [6]. Four phenylpropanoids isolated from the benzene-soluble fraction of the methanolic leaf extract showed antimicrobial activity against *Escherichia coli* and *Bacillus subtilis* [7], and the methanol extract of the leaves was found to possess a profound neuromuscular blocking activity in rat nerve-hemidiaphragm preparation [8]. The chloroform extract of the plant showed considerable antimalarial activity against *Plasmodium falciparum* and *Plasmodium berghei* parasites [9], while the water extract of the whole plant had a hypoglycaemic effect in rats [10]. In addition, some amides isolated from the hexane and methanol extracts of fruits exhibited antituberculosis and antiplasmodial activities [11]. A resent study showed that this plant is a good source of natural antioxidants as the methanol extracts were found to possess high antioxidant activity, which may be attributed to the high contents of vitamin E and xanthophylls [12].

This paper reported three compounds isolated by means of bioassay-guided chromatographic separation from the essential oil extracted from the leaves of *P. sarmentosum*. The bioactivity of these compounds against brine shrimp larvae and subterranean termites were also studied.

Experimental

Plant materials
The leave samples of *Piper sarmentosum* was collected around Kuching area. Sample was identified and authenticated by a plant taxonomist. A voucher specimen was deposited at the Herbarium of Universiti Malaysia Sarawak.

Extraction and analysis
The randomly picked leaves were air dried and ground. About 100 g of the ground samples were hydrodistilled using the modified Clevenger-type apparatus for 6 hours, and the oily layers obtained were separated and dried over anhydrous sodium sulphate and stored in vial at $4-5^{\circ}$C. The yield was calculated based on dry weight of the plant material.

The oils were analyzed on a Shimadzu GC-17A chromatograph equipped with a flame ionization detector using fused silica capillary column DB-5 (25 m $\times$ 0.22 mm ID and film thickness 0.25μm). The operation parameters were: N_2 as carrier gas at flow rate of 20 cm^3 min^{-1}, splitless, injector temperature 280°C, and detector temperature 320°C. The column was programmed initially at 50°C for 2 minutes, and ramped to 300°C at a rate of 6.5°C min^{-1} and held for 7 minutes.

The oils were also analyzed using GC-MS (Shimadzu GC-17A) fixed with the same type of capillary column as GC and under ionization energy of 70 eV. The operation parameters were: He as carrier gas at flow rate of 20 cm^3 min^{-1}, splitless, injector temperature 250°C, and detector temperature 280°C. The column was programmed initially at 50°C for 2 minutes, and then ramped to 300°C at a rate of 6.5°C min^{-1} and held for 7 minutes.

The components were identified tentatively by comparing their Kovat's retention indices with literature values and their mass spectral data with those from NIST mass spectral database. The retention indices were calculated for all components using a homologous series of n-alkanes as standards [13]. For mass spectral analysis, the components were identified by matching the MS with those of authentic standards held in the NIST library. Only similarity indices of 85 or higher were taken as proof of identity [14].

Bioassay-guided fractionation
The biological activity of the extract was performed against brine shrimp larvae (*A. salina*) and termites (*Coptotermes* sp.) using the methods described below.

About 2.0 mL of the essential oil was applied to a silica gel column, and eluted with hexane and a gradient mixture of hexane:EtOAc (19:1, 9:1, 4:1, 1:1). A total of 70 fractions (25 mL each) were collected and combined into 6 groups (PS1 to PS6) based on the similarities in TLC profiles. The activity against larvae of *A. salina* was found in fractions PS1, PS4 and PS6. These 3 fractions were then submitted to further fractionation and purification. Fraction PS1 (352 mg) was subjected to CC on silica gel and eluted with gradient mixture of hexane:EtOAc (9:1, 4:1) yielding 30 fractions, which were pooled into 3 groups. Preparative TLC of group 1[hexane:EtOAc (9:1)] yielded 252 mg of compound (**1**). Fraction PS4 (212 mg) was subjected to CC on silica gel and eluted with a mixture of hexane:benzene:chloroform (3:1:2) yielding 15 fractions, which were pooled into 3 groups. Preparative TLC of group 2 [hexane:benzene:chloroform (3:1:2)] yielded 157 mg of compound (**2**). Fraction PS6 (272 mg) was subjected to CC on silica gel and eluted with gradient mixture of hexane:EtOAc (4:1, 1:1) yielding 15 fractions, which were pooled into 3 groups. Preparative TLC of group 2 [hexane:EtOAc (4:1)] yielded 136 mg of compound (**3**). The bioactivities of these three compounds were determined against larvae of *A.salina* and termites (*Coptotermes* sp.)

Toxicity assay
The protocol established by Mclaughlin [15] was adopted for the toxicity assay against the larvae of *A. salina*. The test samples were prepared by dissolving separately 2 mg of each extract in 2 mL of methanol. From these solutions, 500, 50, and 5 μL were transferred to vials. The solvent was removed under vacuum and 5 mL of artificial seawater was added to each vial, resulting in final concentrations of 100, 10 and 1 μg mL^{-1}

respectively. Then 2 mL of these diluted solutions were transferred to 24 well multidish and second instar larvae of *A. salina* (10 per well) were added. After 24 hours contact, the number of dead larvae in each well was counted and the percentage of death was plotted against the concentrations (on a log scale). The LC_{50} values were determined graphically. The LC_{50} is defined as the lethal concentration of the sample at which 50% of the larvae do not show visible mobility. Controls with and without thymol (10 µg mL^{-1}) were run simultaneously. All experiments were run in triplicate.

Antitermite assay

 The modified method established by Sakasegawa *et al* [16] was used for the antitermite assay against a *Coptotermes* sp. collected around Kuching area. The termites were cultured for 2 – 3 days in a plaster container at room temperature. In the bioassay for termiticidal activity, cut filter paper (diameter 35 mm) were placed in each well of a 6-well multidish (3 rows × 2 lines, hole diameter 35 mm). The samples were diluted to 10.0%, 1.0% and 0.1% with methanol. Exactly 80 µL of these diluted samples were pipetted onto the filter paper in each well of one line. Exactly 80 µL of methanol were placed on the filter paper in each well of the other line, which acted as control. The methanol was allowed to evaporate from the filter paper for several hours. 6 termites (5 undifferentiated workers and a soldier) were placed on each well. The absence of soldier causes the initiation of physiological process in which a certain number of workers become soldiers [17]. The multidishes were closed tightly and kept at 25°C in an incubator. The numbers of living termites were counted each day. Each treatment was performed 6 times (3 wells/multidish × 2 times).

Results and Discussion

Hydrodistillation of the air dried leaves of *P. sarmentosum* yielded 1.10% (v/dry weight) of essential oil. There were 31 components (greater than 0.1%) identified in the leaf oil of *P. sarmentosum* (Table 1)*.* Sesquiterpenoids were the main constituents with sesquiterpene hydrocarbons representing 30.3% and oxygenated sesquiterpenes 61.0% of the oil. The major component of the sesquiterpenes hydrocarbons was β-caryophyllene (18.2%) while spathulenol (21.0%), myristicin (18.8%) and (*E,E*)-farnesol (10.5%) were the main oxygenated sesquiterpenes. Monoterpenoids only made up of 5.1% of the oils with α-phellandrene the only monoterpene hydrocarbon present.

This leaf oil showed inhibitory activity against the larvae of *A. salina* with LC_{50} value of 35.2 µg/mL, and 100% mortality within two days at 1% concentration against the subterranean termite (*Coptotermes* sp.). After first fractionation, the fractions obtained were subjected to biological activity. The biological activity against larvae of *A. salina* was found in fractions PS1, PS4 and PS6 with all showing LC_{50} value of less than 30 µg/mL after 24 hours of contact (Table 2). The result showed that the three fractions might contain bioactive components.

Bioassay-guided chromatographic separation of the three active fractions afforded three compounds. All the three compounds were subsequently tested against *A. salina* and subterranean termite (*Coptotermes* sp.). Compound **2** and **3** showed stronger biological activity against the larvae of *A. salina* and termites compared to compound **1**. Compound **2** showed the most potent activity against the larvae of *A. salina* with LC_{50} value of 7.5 µg/mL, while the LC_{50} values for compound **3** and compound **1** were 17.2 µg/mL and 22.5 µg/mL respectively.

Compound **3** possess the strongest inhibitory activity against the subterranean termite with 100% mortality after 3 days at 0.1% concentration (Figure 1) followed by compound **2** with the similar mortality rate at 0.5% concentration (Figure 2). Compound **1** showed the weakest inhibitory activity with 80% mortality after 3 days at 2% concentration (Figure 3). However, detailed structure-activity relationship should be further investigated. Based on spectroscopic data and comparison with published information, compound **1** and **2** has been identified as caryophyllene and myristicin respectively. Compound **3** is still being studied in order to elucidate its structure.

As there is no previous report on the activity of these three volatile oil components on termites, the data obtained will be used for further study to develop environmental friendly termiticital compounds.

The Malaysian Journal of Analytical Sciences Vol. 12 No. 1 (2008)

Table 1: Chemical composition of the essential oils from the leaves of *P. sarmentosum*

Compound	Kovat's Index		% RA
	KI[1]	KI[2]	
α-Phellandrene	1005	1007	0.78
Piperitone	1245	1245	0.67
Cinnamyl alcohol	1314	1312	0.18
Eugenol	1366	1364	1.80
α-Copaene	1377	1377	0.29
Methyl eugenol	1407	1407	1.63
α-Ionone	1422	1422	2.96
γ-Elemene	1426	1425	2.48
β-Caryophyllene	1465	1467	18.19
α-Humulene	1469	1467	0.86
β-Guaiene	1481	1483	0.43
Germacrene D	1488	1487	1.26
Ethyl laurate	1494	1494	1.09
α-Farnesene	1499	1500	0.21
Elemicin	1512	1514	0.88
Bicylogermacrene	1516	1517	0.34
δ-Cadinene	1519	1519	0.72
Cadinadiene	1526	1527	0.96
Myristicin	1533	1532	18.77
γ-Cadinene	1543	1543	2.26
Germacrene B	1562	1562	2.26
Guaiol	1587	1589	0.69
Dehydrocarveol	1591	1593	0.85
Spathulenol	1617	1619	20.98
T-Muurolol	1636	1635	0.21
β-Eudesmol	1648	1648	0.58
β-Bisabolol	1668	1666	0.26
δ-Cadinol	1673	1674	0.29
α-Cadinol	1677	1676	0.70
E,Z-Farnesol	1696	1696	2.19
E,E-Farnesol	1720	1722	10.50

KI[1] = Kovat's retention indices obtained on a DB-5 column using the series of n-alkanes.
KI[2] = Kovat's retention indices from literature. [13]
RA = Relative area (peak area relative to total peak area).

Table 2: LC$_{50}$ values against larvae of *A.salina*.

Fraction	PS1	PS2	PS3	PS4	PS5	PS6
LC$_{50}$ (µg/mL)	29.1	>100	nd*	21.6	82.0	23.5

nd* – not done due to inadequate amount of sample
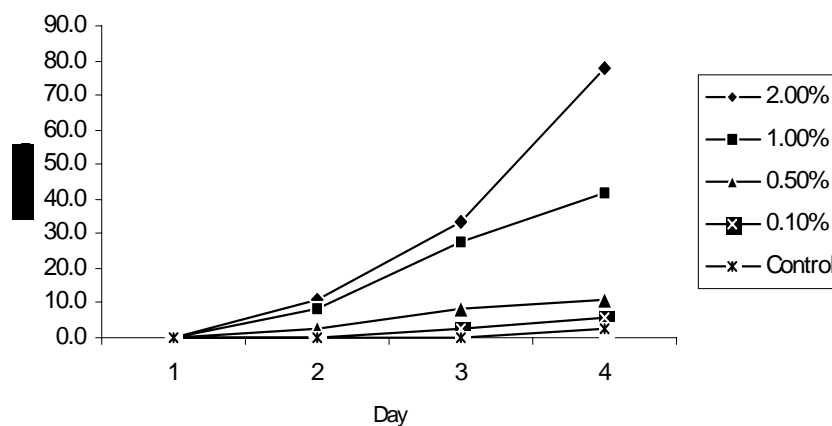
Figure 1: Antitermite activity of Compound (**1**) at different concentrations

237
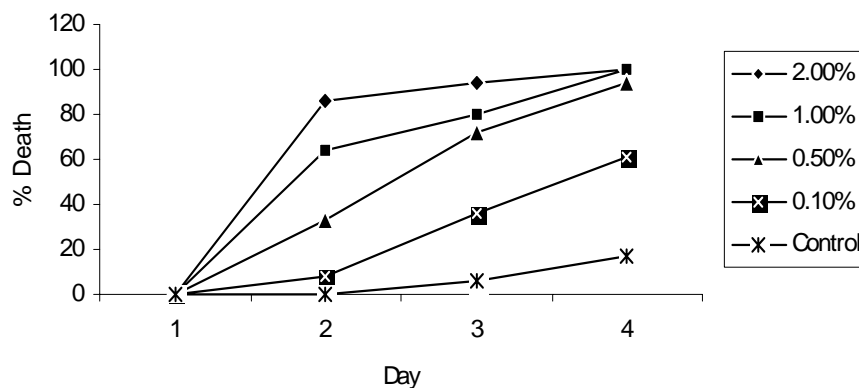
Figure 2: Antitermite activity of Compound (**2**) at different concentrations
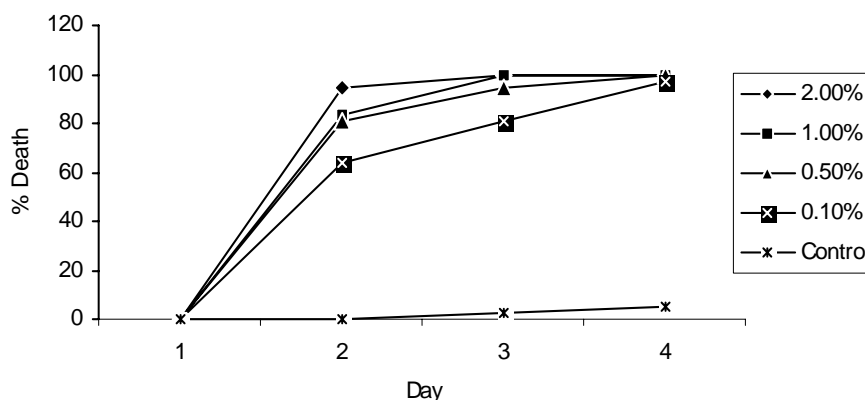
Figure 3: Antitermite activity of Compound (**3**) at different concentrations

Conclusion

The finding of this study showed that essential oil from leaves of *P. samentosum* contains larvicidal and termiticidal components. Further studies are required to increase the lethality of these components due to the synergy achieved by the presence of other minor components of the oil.

Acknowledgement

References

1. Sumathykutty, M.A., Rao, J.M., Padmakumari, K.P., & Narayanan, C.S., 1999. Essential oil constituents of some *Piper* species. Flavour Fragrance. J., **14**, 279 - 282.
2. Sengupta, S., & Ray, A.B., (1987). The chemistry of *Piper* species: a review. *Fitoterapia*, **58**, 147-165
3. Parmer, V.S., Jain, S.C., Bisht, K.S., Jain, R., Taneja, P., Jha, A., Tyagi, O.D., Prasad, A.K., Wengel, J., Olsen, C.E., & Boll, P.M., 1997. Phytochemistry of the Genus *Piper*. *Phytochemistry*, **46 (4),** 597 – 673.
4. Tawan, C.S. & Ipor, I.B., (1993). Some common wild *Piper* of Sarawak. In: Ibrahim, M.Y., Bong, C.E.J. & Ipor, I.B. (Eds). *The Pepper Industry: Problems and Prospect*. Universiti Pertanian Malaysia, Bintulu Campus, 72 – 78.
5. Muhammad, Z. & Mustafa, A.M., (1994). *Traditional Malay Medicinal Plants*. Fajar Bakti, Kuala Lumpur.
6. Satariah, H., Hapipah, M.A., Khalijah, A., Abdul Aziz, K., Habsah, A.K., Kamaliah, M. & Hadi, A.H., (1999). Chemical constituents and insecticidal activity of *Piper sarmentosum*. In: Manaf Ali, A., Khozirah, S & Zuriati, Z. (Eds.), *Phytochemical and Biopharmaceutins from the Malaysian Rain Forest*. FRIM, Kepong, 62-66.
7. Masuda, T., Inamuzi, A., Yamada, Y., Padolina, W.G., Kikuzaki, H. & Nakatani, N., (1991). Antimicrobial phenylpropanoids from *Piper sarmentosum*. *Phytochemistry* **30**, 3227–3228

8. Ridtitid, W., Rattanaprom, W., Thaina, P., Chittrakarn, S., & Sunbhanich, M. (1998). Neuromuscular blocking activity of methanolic extract of *Piper sarmentosum* leaves in the rat phrenic nerve–hemidiaphragm preparation. *J. Ethnopharmacol.*, **61**, 135–142.

9. Najib Nik, A., Rahman, N., Furuta, T., Kojima, S., Takane, K., & Ali Mohd, M., (1999). Antimalarial activity of extracts of Malaysian medicinal plants. *J. Ethnopharmacol*. **64**, 249–254

10. Peungvicha, P., Thirawarapan, S., Temsiririrkkul, R., Watanabe, H., Prasain, J. K., & Kadota, S. (1998). Hypoglycemic effect of the water extract of *Piper sarmentosum* in rats. *J. Ethnopharmacol.*, **60**, 27–32.

11. Rukachaisirikul, T., Siriwattanakit, P., Sukcharoenphol, K., Wongvein, C., Ruttanaweang, P., Wongwattanavuch, P. & Suksamrarn, A. (2004). Chemical constituents and bioactivity of *Piper sarmentosum*. *J. Ethnopharmacol.*, **93**, 173-176.

12. Chanwitheesuk, A., Teerawutgulrag, A. & Rakariyatham, N. (2005). Screening of antioxidant activity and antioxidant compounds of some edible plants of Thailand. *Food Chemistry*, **92**, 491-497.

13. Acree, T. and Arn, H. (2004). http://www.Flavornet.com. [online], retrieved on 7 March, 2005.

14. Adam, R.P., 1995. Identification of Essential Oil Components by Gas Chromatography/Mass Spectrometry. Allured, Carol Stream, IL., USA.

15. McLaughlin, J.L., (1991). Grown gall tumours on potato disc and brine shrimp lethality: two simple bioassay for higher plants screening and fractionation. In: Hostettmann, K. (Ed), *Assays for Bioactivity*, Academic Press, San Diego, 2-32.

16. Sakasegawa, M., Hori, K. & Yatagai, M., (2003). Composition and antitermite activities of essential oils from *Melaleuca* species. *J. Wood Science*, **49**, 181-187.

17. Tellez, M.R., Khan, I.A., Kobaisy, M., Schrader, K.K., Dayan, F.E. and Osbrink, W., (2002). Composition of the essential oil of *Lepidium meyenii* Walp.. *Phytochemistry*, **61**, 149-155.

PERTUKARAN FASA ZEOLIT ASLI KE FASA ZEOLIT SINTETIK YANG DICIRIKAN OLEH XRD BAGI MENGHASILKAN BAHAN PENUKAR ION

Zainab Ramli*, Dewi Jamaliah Kamsiar dan Hasidah Mohd Arsat

Jabatan Kimia, Fakulti Sains,Universiti Teknologi Malaysia,
81310 UTM Skudai, Johor, Malaysia.

Abstrak

Dalam kajian ini, modernit asli diubahsuai kepada zeolit yang rendah nisbah Si/Al untuk mendapatkan sifat penukar ion yang lebih baik. Pengubahsuaian dilakukan secara pemanasan hidroterma pada suhu 100˚C dan pada julat masa 0 hingga 24 jam. Hasil yang diperolehi dicirikan menggunakan kaedah XRD dan spekstroslopi Inframerah. Keputusan pencirian mendapati fasa hablur yang terhasil ialah campuran zeolit X dan P. Zeolit P lebih dominan untuk pemanasan melebihi 6 jam manakala zeolit X yang lebih tulin terbentuk pada pemanasan 6 jam. Keupayaan penukar ion sampel zeolit asli dan sampel pada pemanasan 6 jam dan 24 jam menggunakan ion Ca^{2+} sebagai kation contoh memberikan hasil penukaran ion sampel 24 jam (83.57%) diikuti dengan sampel pada 6 jam (72.50%) dan yang paling rendah zeolit asli (69.45%). Ini menunjukkan sampel yang mengandungi zeolit P mempunyai kapasiti penukar ion Ca^{2+} paling baik iaitu sebanyak 21 mg Ca^{2+}/g zeolit, peningkatan sebanyak 23% berbanding zeolit asli.

Abstract

In this study, natural mordenite was modified to other zeolites phases having low Si/Al in order to increase the cation exchange capacity of the material. Modification was carried out hydrothermally at 100oC in time range between 0 to 24 hours. The samples obtained were characterized by XRD and infrared spectroscopy. Results showed that a mixture of zeolite X and P were formed zeolite X was the dominant zeolite at 6 hrs heating time while zeolite P were dominant after 6 hrs. Ion Exchange capacity of natural mordenite, samples at 6 hr and 24 hrs heating, performed using Ca^{2+} cation gave cation exchange in the decreasing order of 83.57% , 72.50%, 69.45% for sample 24 hrs, 6 hrs and natural mordenite respectively. It indicates that sample having zeolite P phase is the best cation exchange capacity with 21 mg Ca^{2+}/g zeolite with an increased of 23% capacity compared to natural zeolite.

Pengenalan

Zeolit asli jenis mordenit merupakan ahli kumpulan zeolit mineral dengan formula kimianya $(Ca,Na_2,K_2)Al_2Si_{10}O_{24}$ [1] Kegunaan umum mordenit asli adalah dalam rawatan air berammonia dan sebagai baja dimana zeolit berfungsi sebagai penukar ion [2-4]. Mordenit asli jarang digunakan bagi penghasilan zeolit lain tetapi penggunaannya masih boleh dikembangkan. Berasaskan kandungan utama sebatian yang terdapat dalam zeolit asli iaitu silika dan alumina, ia berkemungkinan diubah kepada fasa zeolit lain, dengan mengubah nisbah oksida bahan mula bagi mensintesis zeolit yang dikehandaki. De las Pozas *et al* [5] telah melaporkan pertukaran klinoptilolit asli kepada fasa zeolit Y dan P manakala Shan Wan et al [6] telah berjaya menyediakan MCM-41 mesoporous daripada mordenit bagi tujuan permangkinan. Abu terbang yang juga mengandungi campuran silika dan alumina sebagai bahan utama telah berjaya menghasilkan fasa zeolit P [7-9] telah berjaya menghasilkan berbagai zeolit yang mempunyai kandungan Si/Al yang rendah.

Mordenit asli yang didapatkan daripada lapangan biasanya tidak tulen dan mengandungi oksida logam lain sehingga merendahkan keupayaan penukarionnya. Oleh itu dalam kajian ini mordenit asli akan cuba diubahsuai kepada fasa zeolit lain terutama zeolit yang mempunyai nisbah Si/Al yang lebih rendah seperti zeolit A, X, Y dan P untuk meningkatkan kapasiti penukarionan zeolit asli tersebut.

Eksperimen

Pengubahsuaian zeolit asli secara hidroterma

Dalam sintesis ini komposisi oksida yang digunakan adalah 6 NaO_2 : Al_2O_3 : 8 SiO_2 : 112 H_2O. Mordenit (5.0 g) dan RHA (3.5 g) dimasukkan ke dalam botol teflon. $NaAlO_2$ (1.6 g) dan NaOH (5.4 g) dilarutkan dalam 40 mL air suling dan larutan aluminat ini dimasukkan ke dalam botol teflon yang mengandungi mordenit asli dan RHA tadi.. Campuran diaduk semalaman untuk menghomogenkan dan seterusnya dipanaskan dalam ketuhar pada suhu 96-100 ºC. Pemanasan dilakukan pada julat masa tertentu antara 0-24 jam. Pepejal yang terhasil pada setiap waktu pemanasan dituras dan dicuci dengan air suling sehingga pH air basuhan antara 7 - 10. Hasil sintesis dikeringkan semalaman di dalam ketuhar pada suhu 100°C. Setelah kering hasil sintesis dicirikan dengan menggunakan XRD dan IR untuk mengesahkan jenis fasa zeolit yang terbentuk.

Kapisiti Penukar Ion

Kation Ca^{2+} digunakan sebagai model kation contoh untuk mengkaji kapisiti penukar ion hasil sintesis berbanding mordenit asli. Bagi penyediaan penukargantian ion ini, berat sampel, kepekatan dan isipadu larutan kalsium silikat yang digunakan adalah ditetapkan. Di dalam proses penukarionan ini sebanyak 0.2 g sampel dan 50 mL 100 ppm kalsium silikat digunakan. Analisis kepekatan ion Ca^{2+} dilakukan menggunakan kaedah fotometeri nyala

Keputusan dan Perbincangan

Perubahan Fasa Zeolit Asli

Difraktogram semua sampel selepas sintesis pada masa pamanasan yang berlainan ditunjukkan dalam Rajah 1. Daripada difraktogram jelas menunjukkan terdapat perubahan fasa zeolit asli terhadap masa pemanasan. Sampel yang dipanaskan selama 1 jam menunjukkan kebanyakan puncak bagi fasa mordenit telah berubah kefasa baru. Kehadiran puncak pada sudut rendah 2θ 6.49°, adalah salah satu petunjuk atau ciri bagi pembentukan fasa zeolit X yang menunjukkan pembentukan keliangan besar pada sistem bingkaian fasa hablur baru. Sampel selepas pemanasan 3 jam telah mula bertukar menunjukkan pembentukan fasa zeolit X sebagai fasa utama dengan memberikan 5 puncak pembelauan yang mewakili puncak zeolit X dengan beberapa puncak fasa yang tidak boleh dikenalipasti.

Sampel pada pemanasan selama 6 jam, memberikan pola pembelauan bagi fasa zeolit X yang paling utama. Puncak-puncak pembelauan tersebut adalah pada 2θ 10.07°, 15.50°, 17.57°, 20.17°, 24.40°, 26.74°, 28.61°, 31.14° dan 31.79°. Manakala puncak pembelauan 2θ 12.44° dikenal pasti adalah fasa zeolit P. Difraktogram pemanasan pada 9 jam, beberapa puncak bagi fasa zeolit P mula terbentuk dengan jelas yang masih bercampur dengan fasa zeolit X. Pemerhatian ini mencadangkan fasa zeolit X telah mula berubah bentuk kepada fasa zeolit P yang lebih stabil secara termodinamik. Keputusan ini juga menunjukkan yang fasa zeolit X adalah metastabil yang mengalami penyusunan semula bingkaian melalui pemelarutan semula bingkaian zeolit X dan pembentukan nuklius zeolit P. Puncak pembelauan utama zeolit P ditunjukkan pada 12.50°, 17.74° dan 21.70° dan 28.06. Pertukaran fasa zeolit X berlaku sepenuhnya kepada fasa zeolit P seperti yang ditunjukkan oleh difraktogram bagi sampel pada pemanasan 12 jam. Puncak pembelauan fasa zeolit P adalah 2θ 12.49°, 17.67°, 28.08° dan 33.42° dengan satu puncak yang tidak dapat dikenalpasti terdapat pada 21.66°. Kestabilan zeolit P terhadap masa pemanasan dibuktikan oleh sampel pada pemanasan 24 jam sudut pembelauan 12.49°, 17.64°, 21.65°, 28.06° dan 33.35° bagi zeolit P yang tulen. Rajah 2 memperlihatkan graf ringkasan kepada perubahan fasa zeolit asli terhadap masa yang menunjukkan zeolit X adalah fasa yang lebih dominan pada pemanasan selama 6 jam dan zeolit P pada pemanasan lmelebihi 6 jam

Dalam spektrum inframerah pada Rajah 3 menunjukkan pola regangan yang biasa bagi zeolit modernit, zeolit X (sampel 6 jam) dan zeolit P. Jika diperhatikan dengan lebih teliti, sampel pada masa 6 jam ada menunjukkan sedikit kehadiran zeolit P (ditanda * dalam spektrum). Zeolit asli memberikan tiga getaran utama pada 1011.6 cm^{-1}, 607.5 cm^{-1} dan 437 cm^{-1} yang berkaitan dengan regangan asimetri TO_4, regangan simetri TO_4 dan bengkokan T-O. Sampel hasil sintesis pada 6 jam dan 24 jam menunjukkan regangan asimetri TO_4 telah beranjak ke frekuensi lebih rendah, 1002.0 cm^{-1}. Anjakan ke frekunsi rendah menunjukkan kebanyakan ikatan Si-O-Si dalam sampel zeolit asli telah bertukar membentuk ikatan Si-O-Al [10]. Ini disebabkan sampel ini mempunyai ikatan Al-O yang lebih panjang berbanding ikatan Si-O. Ini membuktikan zeolit yang lebih rendah nisbah Si/Al telah terbentuk. Penyusutan nombor gelombang daripada zeolit X dan seterusnya zeolit P menunjukkan
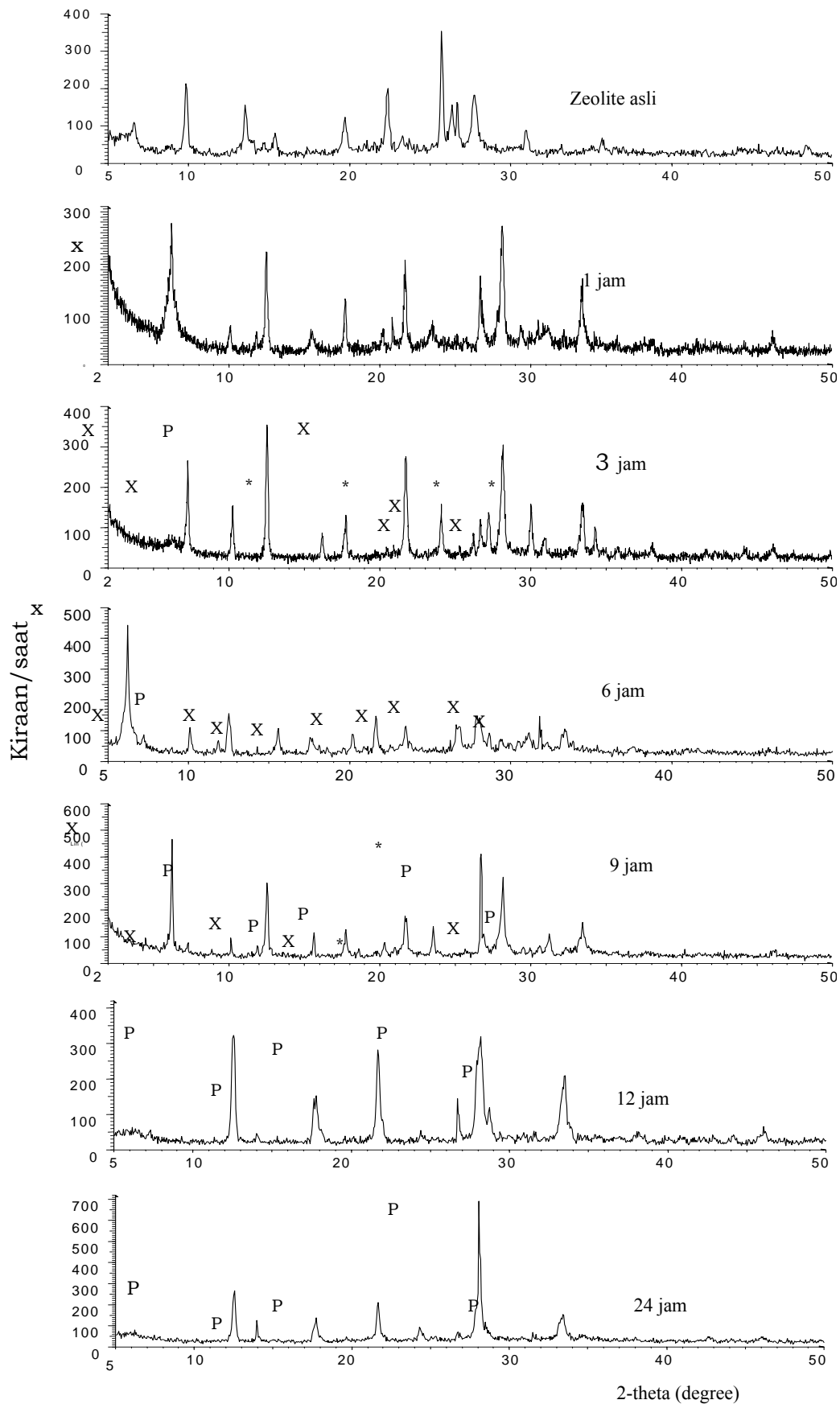
Rajah 1 **:** Difraktogram bagi sample zeolit asli yang disintesis pada masa yang berlainan
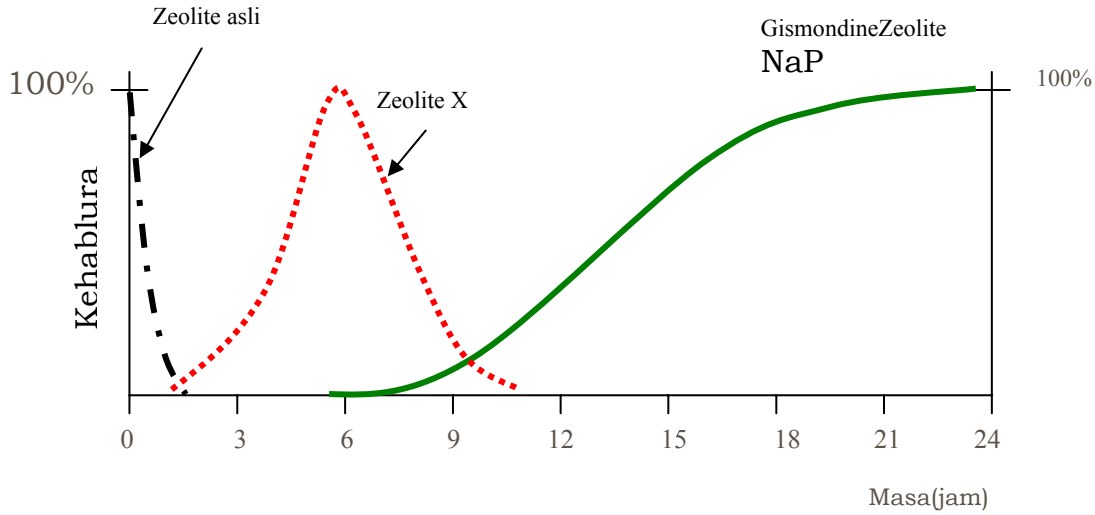
Rajah 2. Ringkasan perubahan fasa zeolit asli terhadap masa pemanasan
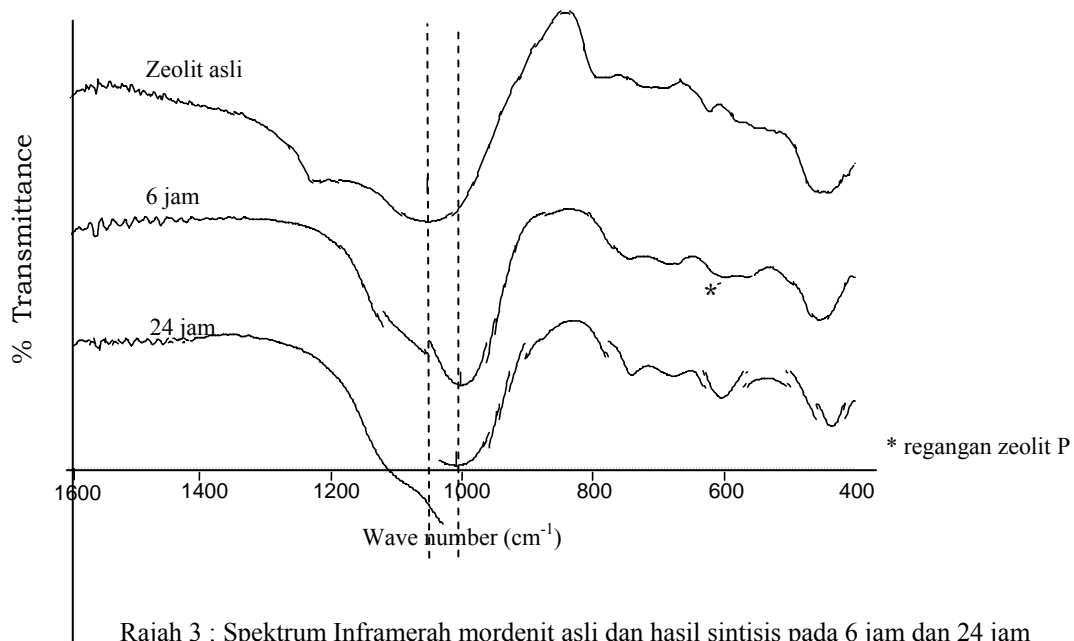
Rajah 3 : Spektrum Inframerah mordenit asli dan hasil sintisis pada 6 jam dan 24 jam

fasa zeolit X adalah dalam keadaan metastabil dalam medium sel beralkali dan mudah bertukar kepada fasa yang lebih stabil iaitu zeolit P.

Keupayaan Penukar Ion

Zeolit asli dan zeolit yang disintesis secara amnya adalah dalam bentuk natrium, Na-zeolit. Proses penukarion yang berlaku adalah ion kation Na^+ dalam zeolit dengan ion yang ingin ditukar ganti. Persamaan penukar ion diberikan oleh persaman dibawah.

$$2 \text{ Na-zeolit (p)} + Ca^{2+}(ak) \longleftrightarrow Ca\text{-zeolit (p)} + 2Na^+(ak)$$
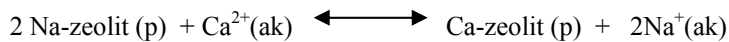
Sampel hasil sintesis pada masa 6 jam (fasa utama zeolit X) dan 24 jam(fasa zeolit P) bersama zeolit asli dilakukan pertukaran ion dengan ion Ca^{2+}. Keupayaan penukar ion setiap sampel ditunjukkan dalam Rajah 4.

243

Secara am proses penukaran ion berlaku dengan pantas dengan semua sampel dapat melakukan penukaran ion sebanyak 50% dalam masa 15 minit. Keputusan menunjukkan yang kapasiti penukar ion adalah berkadar langsung dengan masa. Semua sampel selepas pengubahsuaian memberikan keupayaan penukarion sebanyak > 55% dalam masa 15 minit manakala zeolit asli memberikan 53%. Sampel pada masa 24 jam yang merupakan sampel zeolite P menunjukkan keupayaan penukar ion paling baik dengan peratus penukar ion sebanyak 84 % pada masa pengadukan 60 minit. Seterusnya kapasiti penukar ion bagi setiap sampel adalah zeolit asli, sampel pada masa 6 jam dan sampel pada masa 24 jam ialah 17, 18 dan 21 mg Ca^{2+}/g zeolit. Dalam hal ini peningkatan sebanyak 23 % kapasiti penukar ion zeolit yang disentisis berbanding sampel zeolite asli.
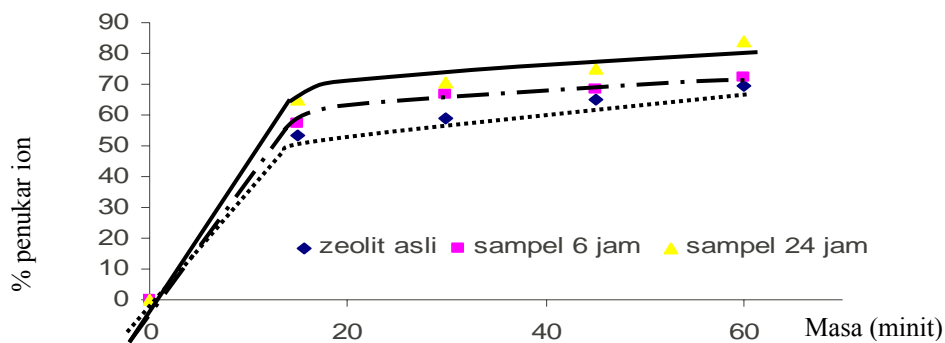
Rajah 4 : Graf kapasiti penukar ion Ca^{2+} bagi sampel zeolit asli, sampel pada 6 jam dan 24 jam

Kesimpulan

Dalam kajian ini, mordenit asli telah berjaya ditukarkan kepada fasa zeolit lain iaitu zeolit X dan zeolit P. Zeolit X adalah merupakan zeolit yang metastabil dan berubah kepada zeolit P yang lebih stabil pada pemanasan yang melebihi 6 jam. Zeolit P didapati merupakan zeolit dominan untuk pemanasan melebihi 6 jam. Keupayaan penukar ion sampel dengan fasa zeolit P menunjukkan sifat penambahan sifat penukar ion dengan peningkatan % penukar ion sebanyak 23% berbanding zeolit mordenit asli.

Rujukan

1. L. B. Sand and F. A. Mumpton (1978), "Natural Zeolites, Occurrence, Properties, Use", Tucson : Pergamon
2   R. Moreno-Tost, J. Santamaría-González, E. Rodríguez-Castellón, A. Jiménez-López, M. A. Autié, E. González, M C. Glacial and C. De las Pozas (2004)Selective catalytic reduction of nitric oxide by ammonia over Cu-exchanged Cuban natural zeolites, *Applied Catalysis B: Environmental* **50**, 279-288.
3. L.R. Weatherley and N.D. Miladinovic (2004) Comparison of the ion exchange uptake of ammonium ion onto New Zealand clinoptilolite and mordenite *Water Research,* **20,** 4305-4312
4. Marlene Seijó Echevarría, Ruben Del Tóro Déniz, Eugenio Martinez Castellanos, Gerard A. Sherbakov, Juan Jose Rodriguez Moya (1997**)** "Uses of natural zeolite in the removal of Pb^{2+} from contaminated water" *Eclética Química*, **22**.
5. Carlos de las Pozas, David Diaz Quintanilla,Joaquin Perez-Pariente, Rolando Roque-Malherbe and M. Magi (1989) Hydrothermal transformation of natural clinoptilolite to zeolites Y and P$_1$: Influence of the Na, K content' *Zeolites*, **9**, 33-39
6   Shan Wang, Tao Dou, Yuping Li, Ying Zhang, Xiaofeng Li and Zichun Yan (2004) **"**Synthesis, characterization, and catalytic properties of stable mesoporous molecular sieve MCM-41 prepared from zeolite mordenite" *J. Solid State Chem*. __177__, 4800-4805.
7. Miki Inada, Yukari Eguchi, Naoya Enomoto and Junichi Hojo, (2005) Synthesis of zeolite from coal fly ashes with different silica–alumina composition *Fuel*, **84**, 299-304.
8. Hidekazu Tanaka, Yasuhiko Sakai and Ryozi Hino (2002) Formation of Na-A and -X zeolites from waste solutions in conversion of coal fly ash to zeolites' *Material Research Bulletin*, **37**, 1873-1884
9. Nor Idah Taib (1999) Sintesis Zeolit Daripada Abu Terbang, Tesis Projek Sarjana Muda. UTM
10 E.M. Flanigen, H. A Szymanski dan H.Khatami(1971), Infrared Structural Studies of Zeolite Framework., *Adv. Chem.Ser.*, 201-229

KAJIAN KRISTALOGRAFI SINAR-X KOMPLEKS [μ-1(2-PIRIDIL-κ*N*)ETANON 4-FENILTIOUREASEMIKARBAZONATO-κ²*N*¹, *S*]BIS[IODOMERKURI(II)] DAN BIS(*N*-4-METOKSIBENZOIL) -*N*'-*O*-TOLILTIOUREA-κ*S*)DIIODOMERKURI(II)

Mohd Sukeri Mohd Yusof[1]* & Bohari M. Yamin[2].

[1]*Jabatan Sains Kimia, Fakulti Sains dan Teknologi Malaysia, Universiti Malaysia Terengganu,t, 21030 K. Terengganu.*
[2]*Pusat Pengajian Sains Kimia dan Teknologi Makanan, Fakulti Sains dan Teknologi, Universiti Kebangsaan Malaysia, 43650 Bangi, Selangor.*

Kata kunci: Merkuri kompleks, tiourea, benzoiltiourea

Abstrak

Kompleks   [μ-1(2-piridil-κ*N*)etanon   4-feniltioureasemikarbazonato-κ²*N*¹,*S*]bis[iodomerkuri(II)],   dan   Bis(*N*-4-metoksibenzoil)-*N*'-*o*-toliltiourea-κ*S*)diiodomerkuri(II), mempunyai formula molekul masing-masing $Hg_2(L)_2I_2$ dan $Hg(L)_2I_2$. Kedua-dua kompleks, mempunyai sistem hablur monoklinik dengan kumpulan ruang masing-masing adalah C2/c, a=18.466(3)Å, b=16.745(2)Å, c=13.9140(19)Å, β=129.174(2)º dan P2₁/c, a=10.848(3)Å, b=24.474(7)Å, c=14.038(4)Å, β=92.206(4)º. Dalam kompleks merkuri-bes Schiff, atom Hg mempunyai geometri segi empat pyramid di mana ligan terikat secara tridentat melalui atom *NNS*. Atom Sulfur kedua-dua ligan membentuk jejambat menghubungkan dua atom Hg menjadikan bentuk keseluruhan molekul seperti kotak. Sebaliknya, dalam kompleks merkuri-tiourea atom merkuri berkoordinat dengan ligan melalui atom S kumpulan tion secara monodentat dan bersifat dimerik, menjadikan geometri Hg tetrahedron terherot.

Abstract

Both   [μ-1(2-pyridyl-κ*N*)ethanone   4-phenylthioureasemicarbazonato-κ²*N*¹,*S*]bis[iodomercury(II)],   and   Bis(*N*-4-methoxybenzoyl)-*N*'-*o*-tolylthiourea-κ*S*)diiodomercury(II), complexes have the molecular formula of $Hg_2(L)_2I_2$ and $Hg(L)_2I_2$ where L is the ligand, respectively. They also crystallized in   monoclinic system, but having space group is C2/c, a=18.466(3)Å, b=16.745(2)Å, c=13.9140(19)Å, β=129.174(2)º and P2₁/c, a=10.848(3)Å, b=24.474(7)Å, c=14.038(4)Å, β=92.206(4)º, respectively. In the first complex, the Schiff base ligands are coordinated to the mercury atom via their (*NNS*) donor atoms in a tridentate manner. The sulfur atoms act as a bridge connecting the Hg atoms, forming a rectangular base that almost perpendicular to the ligand planes, resulting in an open box-like structure. The geometry of the mercury atom is close to a square pyramid. However, the mercury atom in the mercury-thiourea complex is coordinated to the ligands via the thiono sulfur atoms in a monodentate manner and form a distorted tetrahedral geometry.

Pengenalan

Masalah pencemaran oleh logam berat terutama dalam sistem akueus seperti air buangan yang disalurkan ke sungai masih merupakan ancaman hingga ke hari ini. Kilang-kilang yang bertanggung jawab sudah pasti sepatutnya menerima baik sebarang kaedah atau teknik yang boleh memisahkan logam berat dan toksik di loji masing-masing daripada menyalurkan ke dalam sungai. Untuk itu penyelidikan mencari bahan dan teknik yang murah, mudah dan cekap untuk memisahkan logam-logam toksik terus berkembang. Satu daripada kaedah pemisahan logam tersebut adalah melalui pengkompleksan dan seterusnya terpisah daripada larutan. Kajian awal kami mendapati terbitan tiourea mampu membentuk kompleks dengan beberapa logam kini mendapat tumpuan. Baru-baru ini benzoiltiourea yang diubahsuai di atas silica mesoporos MCM-48 didapati menjerap raksa daripada larutan akueus [1]. *N*-benzoiltiourea yang diubahsuai bersama polimer PAMAM dapat memisah secara terpilih dan mengumpul semula ion logam berat daripada buangan akueus [2]. Beberapa sebatian terbitan tiourea telah menunjukkan kemampuan yang tinggi untuk membentuk kompleks dengan logam berat terutamanya raksa dan kadmium [3]. Kajian struktur tentang kompleks merkuri-tiourea telah banyak dilaporkan, tetapi kebanyakannya adalah kompleks merkuri-siklotiourea seperti $Hg(C_8H_{16}N_4S_2)Cl_2$, $Hg(C_8H_{16}N_4S_2)Br_2$, $Hg(C_8H_{16}N_4S_2)I_2$, $Hg(C_8H_{16}N_4S_2)(SCN)_2$ dan $Hg(C_8H_{16}N_4S_2)(CN)_2$ [4]. Hanya terdapat beberapa laporan tentang kompleks merkuri-tiourea (gelang terbuka) seperti Bis(o-klorofenilbenzoiltiourea-κ*S*)-diiodomerkuri(II) [5] dan bis{μ-kloro-kloro[(*N*-dietilaminotiokarbonil)benzimido-*O*-metil   ester-*S*]merkuri(II)   [6].   Kertas   ini membincangkan struktur kompleks merkuri-bes Schiff dan merkuri-tiourea.

Eksperimen

Tindak balas pengkompleksan dilakukan dengan merefluks ligan *N*-fenil-2-(1-piridin-2-iletil)hidrazinakarbotioamida dan *N'*-4-metoksibenzoil)-*N'*-*o*-toliltiourea masing-masing dengan merkuri iodida (HgI$_2$) dalam pelarut etanol selama 3 jam. Hasil refluks dituras dan dibiarkan menyejat pada suhu bilik dan menghasilkan hablur yang kekuningan. Hablur yang diperoleh dianalisis untuk menentukan struktur hablur dengan menggunakan alat pembelauan sinar-X hablur tunggal.

Keputusan dan Perbincangan

Kompleks Bis[μ-1(2-piridil-κ*N*)etanone 4-feniltioureasemikarbazonato-κ$^2N^1$,*S*]bis[iodomerkuri(II)], Hg$_2$(C$_{14}$H$_{13}$N$_4$S)$_2$I$_2$], (I) dan Bis(*N*-4-metoksibenzoil)-*N'*-*o*-tolyltiourea-κ*S*)diiodomerkuri(II), Hg[C$_{16}$H$_{16}$N$_2$O$_2$S]$_2$I$_2$, (II), masing-masing mempunyai sistem hablur monoklinik dengan kumpulan ruang C2/c, sel unit a=18.466(3)Å, b=16.745(2)Å, c=13.9140(19)Å dan β=129.174(2)º dan P21/c, a=10.848(3)Å, b=24.474(7)Å, c=14.038(4)Å dan β=92.206(4)º. Data hablur dan parameter penghalusan kedua-dua kompleks ditunjukkan dalam Jadual 1.

Jadual 1: Data hablur dan penghalusan data hablur kompleks (I) dan (II)

Perkara	Kompleks I	Kompleks II
Formula empirik	Hg$_2$(C$_{14}$H$_{13}$N$_4$S)$_2$I$_2$	Hg[C$_{16}$H$_{16}$N$_2$O$_2$S]$_2$I$_2$
Berat molekul	1193.67	1055.13
Sistem hablur, kumpulan ruang	Monoklinik, C2/c	Monoklinik, P21/c
Dimensi sel unit	a = 18.466(3)Å	a=10.848(3)Å, b=24.474(7)Å,
	b = 16.745(2)Å	c=14.038(4)Å
	c = 13.9140(19)Å	β=92.206(4)º
	β = 129.174(2)º	
Isipadu	3335.3(8) Å^3	3724.2(18)
Z, ketumpatan	4, 2.377 Mg/m^3	4, 1.882 Mg/m^3
Saiz hablur	0.38 x 0.18 x 0.13 mm	0.47 x 0.39 x 0.07 mm
Kawasan theta untuk pungutan data	1.8 hingga 27.6º	1.66 hingga 27.50
Set data	-24<=h<=24, -21<=k<=21, -18<=l<=18	-14<=h<=14, -31<=k<=21, -18<=l<=18
Pungutan pantulan/ unik	3875 / 3277 [R(int) = 0.033]	40517/8483[R(int) = 0.053]
Kesempurnaan kpd. theta=27.6/27.5 º	99.5%	99.1%
Pembetulan serapan	Multi-scan	Multi-scan
Mak. dan min. transmisi	0.9288 dan 0.8624	0.6811 dan 0.1667
Kaedah pemprosesan	Kuasa dua terkecil matriks-lengkap	Kuasa dua terkecil matriks-lengkap
Data / kekangan / parameter	3175 / 0 / 193	8483/0/406
Nilai ketepatan struktur (GooF)	1.081	1.084
Indeks akhir R [I>2sigma(I)]	R1 = 0.0423, wR2 = 0.1124	R1 = 0.0413, wR2 = 0.0911
Indeks R (semua data)	R1 = 0.0506, wR2 = 0.1189	R1 = 0.0560, wR2 = 0.0975
Perbezaan puncak dan lubang	0.219 dan -0.237 e. Å^{-3}	1.343 dan -0.842 e. Å^{-3}

Bagi kompleks (I), ligan *N*-fenil-2-(1-piridin-2-iletil)hidrazinakarbotioamida merupakan ligan tridentat iaitu berkoordinat dengan atom Hg1 melalui atom N3, N4 dan S1^i (Rajah 1). Ini adalah satu contoh logam merkuri berkoordinat lebih daripada 2 yang jarang berlaku. Molekul kompleks adalah dimerik dengan dua atom Hg dihubungkan dengan dua ikatan jejambat daripada dua atom S dan molekul berbentuk seperti kotak yang terbuka. Panjang ikatan Hg-S [2.6840(16)Å] dalam kompleks I adalah pendek sedikit berbanding dalam kompleks bis(*o*-klorofenilbenzoiltiourea-κ*S*)-diiodomerkuri(II) [7]. Panjang Ikatan C7-S1, 1.768(4) Å adalah lebih panjang dibandingkan dengan kompleks bis(*o*-klorofenilbenzoiltiourea-κ*S*)-diiodomerkuri(II) [1.690(6) Å]. Panjang ikatan dan sudut yang lain adalah dalam jarak yang normal [8,9] dan juga bersamaan dengan kompleks bes-Schiff yang lain seperti [Mn(C$_{14}$H$_{13}$N$_4$S$_2$)$_2$]. Sudut dihedral bagi kedua-dua ligan ialah 9.07(11)º.
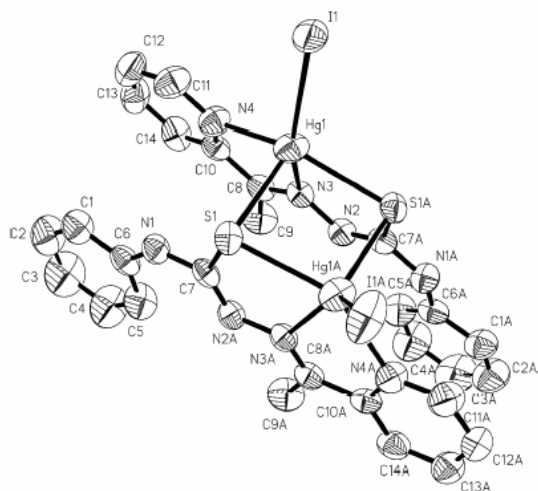
Rajah 1: Gambarajah ORTEP molekul kompleks (I) pada kebarangkalian
30% tanpa atom H untuk gambaran lebih jelas.

Geometri bagi kedua-dua atom Hg adalah antara trigonal bipiramid dan piramid planar tetapi mendekati kepada piramid planar. Atom N3, N4, S1^i dan I1 adalah sesatah dengan pesongan maksimum sebanyak 1.491(1) Å. Sudut pusat atom Hg adalah antara 67.63(12) dan 107.74(2)º.

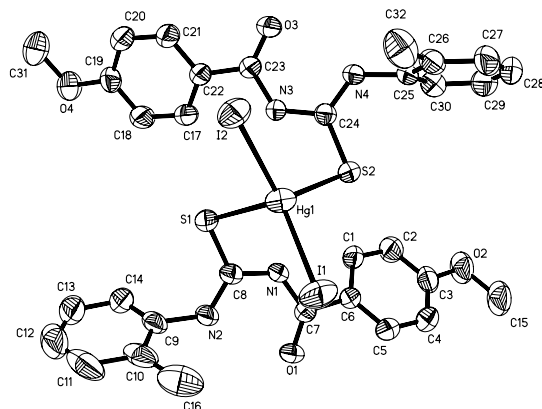Jadual 2: Panjang ikatan dan sudut ikatan dalam kompleks (I)

Ikatan	Panjang Ikatan, Å	Ikatan	Sudut Ikatan, º
Hg1-N4	2.387(4)	N4-Hg1-N3	67.63(2)
Hg1-N3	2.398(3)	N4-Hg1-S1^i	140.71(9)
Hg1-S1^i	2.6173(11)	N3-Hg1-S1^i	73.32(9)
Hg1-S1	2.6490(12)	N4-Hg1-S1	95.73(9)
Hg1-I1	2.6635(4)	N3-Hg1-S1	97.71(8)
N2-C7^i	1.290(5)	S1^i-Hg1-S1	93.48(3)

Molekul kompleks distabilkan oleh ikatan hidrogen inter-molekul, N1-H1A···I1^{ii}, [simetri kod; (ii) 3/2-x,1/2-y,1-z] membentuk rantaian *zig-zag* yang selari pada paksi-*a* (Rajah 2).
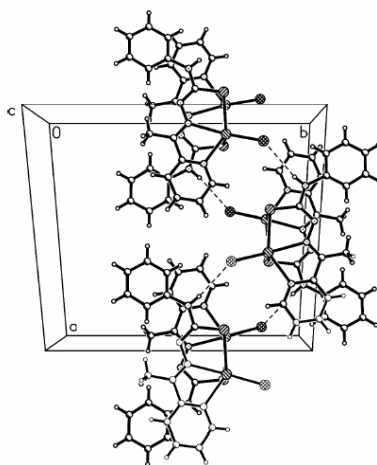
Rajah 2: Gambarajah padatan molekul dalam sistem hablur, dilihat ke dalam paksi *c*.
Garisan putus-putus menunjukkan ikatan hydrogen inter-molekul N-H···I.

Kompleks (II) adalah dimerik (Rajah 3) dengan dua molekul ligan berkoordinat dengan atom pusat, Hg1 melalui atom sulfur, S. Atom pusat Hg1 mempunyai geometri tetrahedral terherot dengan sudut antara 96.18(4)º dan 133.75(2)º. Panjang ikatan dan sudut ikatan adalah normal [8,9] dan berpadanan dengan kompleks bis(*o*-klorofenilbenzoiltiourea-κ*S*)-diiodomerkuri(II) (Jadual 4).


Rajah 3: Gambarajah ORTEP molekul kompleks dengan kebarangkalian 50%
tanpa atom H untuk gambaran lebih jelas.

Jadual 3: Panjang ikatan dan sudut ikatan dalam kompleks

Ikatan	Panjang Ikatan, Å	Ikatan	Sudut Ikatan, º
Hg1-I1	2.6558(6)	I1-Hg1-I2	133.75(2)
Hg1-I2	2.6700(6)	I1-Hg1-S2	104.47(3)
Hg1-S1	2.6762(13)	I2-Hg1-S2	110.47(3)
Hg1-S2	2.7192(14)	I1-Hg1-S1	108.21(3)
S1-C8	1.698(5)	I2-Hg1-S1	97.31(3)
S2-C24	1.709(4)	S2-Hg1-S1	96.18(4)

Panjang ikatan Hg1-I1 dan Hg1-I2 [2.6558(6)Å dan 2.6700(6)Å], didapati lebih pendek jika dibandingkan dalam kompleks $Hg(C_8H_{16}N_4S_2)I_2$ [2.7123(5)Å] [4] tetapi bersesuaian dengan panjang ikatan seperti dalam kompleks bis(*o*-klorofenilbenzoiltiourea-κ*S*)-diidomerkuri(II) [2.6582(6)Å] [5]. Ikatan Hg1-S1 [2.7192(14)Å adalah lebih panjang berbanding dalam kompleks bis(*o*-klorofenilbenzoiltiourea-κ*S*)-diidomerkuri(II) [2.6840(16)Å].
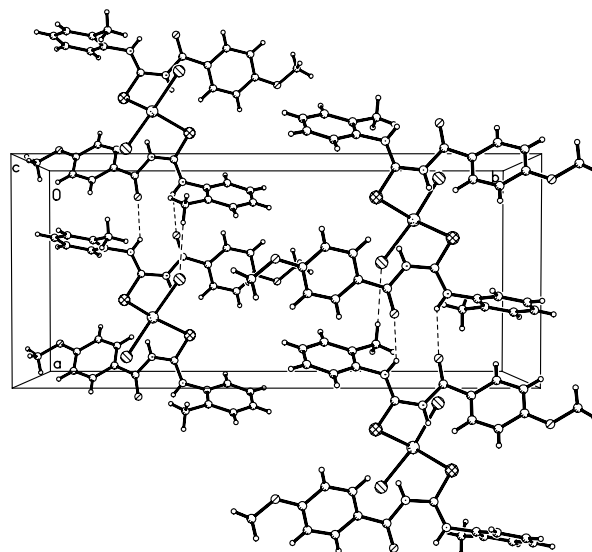
Rajah 4: Gambarajah padatan molekul kompleks yang dilihat pada permukaan *ab*. Garisan putus-putus menunjukkan ikatan hidrogen inter-molekul N-H···O dan C-H···I.

Terdapat enam ikatan hydrogen intra-molekul, N-H···S, N-H···O dan C-H···N [Jadual 3] yang memberikan 4 gelang pseudo-enam ahli (Rajah 3). Dalam sistem hablur, molekul terikat melalui ikatan hidrogen inter-molekul N-H···O dan C-H···I (Jadual 4) membentuk dimer yang dilihat melalui permukaan *ab* (Rajah 4).

Jadual 4: Senarai ikatan hidrogen intra- dan intermolekul dalam kompleks (Å,°).

D-H···A	*D*-H	H···A	D···A	*D*-H···A
N1-H1A···S2	0.86	2.76	3.5135	147
N2-H2A···O1	0.86	1.98	2.6558	134
N3-H3A···S1	0.86	2.76	3.5762	159
N4-H4A···O3	0.86	1.98	2.6419	133
C16-H16A···N2	0.96	2.38	2.8546	110
C32-H32A···N4	0.96	2.38	2.8660	111
N2-H2A···O3^i	0.86	2.36	3.0661	139
N4-H4A···O1^{ii}	0.86	2.32	3.0124	137
C16-H16B···I2^i	0.96	2.97	3.9245	173

Simetri kod; (i) 1+x,y,z; (ii) -1+x,y,z

Rujukan
1. Olkhovyk, O., Antochshuk, V., & Jaroniec, M. 2004. Benzoylthiourea-modified MCM-48 mesoporous silica for mercury(II) adsorption from aqueous solutions. *Colloids and Surfaces A: Physicochemical and Engineering Aspect.* **Vol. 236**, 1-3:69-72.
2. Rether, A. & Schuster, M. 2003. Selective separation and recovery of heavy metal ions using water-soluble *N*-benzoylthiourea modified PAMAM polymers. *Reactive and Functional Polymers, Vol. 57, 1:13-21.*
3. Yusof, M. S. M. & Yamin, B. M. 2004. *N*-Benzoyl-*N'*-(2-chlorophenyl)thiourea. *Acta Cryst.* **E60**: 1403-1404.
4. Popovic, Z., Pavlovic, G., Matkovic, D., Soldin, Z., Rajic, M., Vikic, D., & Kovacek, D. 2000. Mercury(II) complexes of heterocyclic thiones.: Part 1. Preparation of 1:2 complexes of mercury(II) halides and pseudohalides with 3,4,5,6-tetrahydropyrimidine-2-thione. X-ray, thermal analysis and NMR studies. *Inorganica Chimica Acta,* **Vol. 306: Issue 2**:142-152.

5.   Yusof, M. S. M., Yamin, B. M. & Kassim, M. B. 2004. Bis(*o*-chlorophenylbenzoyl thiourea-*S*)diiodomercury(II). *Acta Cryst.* **E60:** m98-m99.
6.   Leßmann, F., Beyer, L., & Sieler, J. 2000. Synthesis and X-ray structure of the first chloro-bridged thiourea mercury(II) complex [$C_6H_5C(OCH_3)NC(S)N(C_2H_5)_2HgCl_2$]$_2$. *Inorganic Chemistry Communications.* **Vol 3: Issue 2**:62-64.
7.   Yusof, M. S. M., Yamin, B. M. & Shamsuddin M. 2003. *N*-(*N*-Benzoylhydrazino carbothioyl)benzamide. *Acta Cryst.* **E59**: o810-o811.
8.   Allen, F.H., Kennard, O., Watson, D.G., Orpen, A.G. & Taylor, R. 1987. J. *Chem. Soc. Perkin Trans.* **2**:S1-19.
9.   Orpen, A.G., Brammer, L., Allen, F.H., Kennard, O., Watson, D.G., & Taylor, R. 1989. J. *Chem. Soc. Dalton Trans.* S1-83.

SYNTHESIS AND FLUORESCENCE CHARACTERISTIC OF 2-SUBSTITUTED AND 6-SUBSTITUTED PURINES

Zanariah Abdullah, *Maizatul Akmam A. Bakar, Ernie Iryana Awang Din, Nadiah Rifhan Abd. Rani, Noordini Mohd Salleh, Goh Poh Leong, Liow Pei Ling and Zaharah Aiyub

*Chemical Synthesis Group, Department of Chemistry, Faculty of Science,
University of Malaya, 50603, Kuala Lumpur
email: zana@um.edu.my*

Abstract

2-Fluoropurine was prepared from 2–aminopurine through a diazotization reaction, followed by treatment with fluoroboric acid. 2-Aminopurine was obtained from a series of reactions, using 5-nitrouracil as the starting material. 2-Piperidino and 2-anilinopurines were obtained by treating 2-fluoropurine with piperidine and aniline respectively. 6-Piperidino and 6-anilinopurines were obtained by treating 6-chloropurine with piperidine and aniline. Fluorescence studies was carried out in various solvents and maximum fluorescence was observed in 75% ethanol. 2-Aminopurine showed the highest fluorescence intensity, followed by 2-anilino and 2-piperidinopurines. 6-Substituted purines showed stronger fluorescence intensities compared to 2-substituted purines.

Abstrak

2-Fluoropurina disediakan daripada 2-aminopurina melalui tindak balas pendiazoan diikuti dengan pengolahan dengan asid fluoroborik. 2-Aminopurina diperolehi melalui beberapa peringkat tindak balas bermula dengan 5-nitrourasil. 2-Piperino dan 2-anilinopurina diperolehi apabila 2-fluoropurina ditindak balas dengan piperidina dan anilina. 6-Anilino dan 6-piperidinopurina pula diperolehi apabila 6-kloropurina ditindak balaskan dengan piperidina dan anilina. Kajian pendarfluor dilakukan menggunakan berbagai pelarut dan kadar pendarfluor maksimum diperolehi dalam 75% etanol. 2-Aminopurina menunjukkan kadar pendafluor yang tinggi diikuti dengan 2-anilino dan 2-piperidino purina. Purina tertukar ganti di kedudukan 6 menunjukkan kadar pendafluor yang lebih tinggi berbanding dengan purina tertukar ganti di kedudukan ke 2 yang setara.

Introduction

The purine system is one of the most important systems present in living systems. The purine system or rings can be found in many natural products, including nucleotides, co-enzymes and several compounds which are valuable for treatment of cancer. Even though many of its rings can be found in the natural occurring products, the parent compound itself cannot be found in nature.

The first pure purine, uric acid, was obtained by the isolation from kidneystones in 1776 [1] but its structure was confirmed one hundred year later by Medicus [2]. But the chemistry of purines flourished from 1906 onwards [3-5] until today.

The purine ring can be synthesized using two main synthetic route, either using pyrimidine or imidazole as the precursor. The most extensively used method is the Traube Sythesis which involved the use of diaminopyrimidines, whereby the diaminopyrimidines are condensed with a simple compound to supply a one-carbon fragment to bridge the two pyrimidine amino nitrogen atoms to form a five-membered ring. In this work, the Traube method was used in the synthesis of 2-fluoropurine.

The fluorescence characteristic of purines or other heterocycles are not extensively studied, eventhough a wide variety of heterocyclic compounds are known to be fluorescent [6]. Fluorescence studies of these compounds are made more difficult because their fluorescence characteristics are often dependent on the solvents used. The aim of this work is to study the fluorescence charateristic of selected alkylaminopurines and the effect of solvent on

the fluorescence characteristic. In this paper, only the characteristic of 2- and 6- anilino, 2- and 6-piperidino purines will be discussed.

Experimental

Synthesis of 2-fluoropurine
2,4-Dichloro-5-nitropyrimidine [7]
5-Nitrouracil (26 g), phosphoryl chloride (130 ml), and dimethylaniline (32 ml) were heated with occasional shaking until the reaction commerced. When this has subsided, the mixture was refluxed for 1.5 hours, cooled and phosphoryl chloride was evaporated off. The residue was poured onto crushed ice with vigorous stirring, and extracted with ether (500 ml). The ether extracts were washed with water and dried over anhydrous sodium sulphate. Removal of ether and vacuum distillation gave pure product.
89%, IR (cm^{-1}):1670, 1620, 1350, 785; ^{1}H NMR (CDCl$_3$) δ:9.26, s, 1H, (H$_6$).

2, 4-Diamino-5-nitropyrimidine [8]
2, 4-Dichloro-5-nitropyrimidine (10.3 g) and phenol were heated under reflux while a stream of ammonia was passed into the mixture for four hours. The phenol was distilled off and the residual suspension was cooled and filtered. The crystals of 2, 4-diamino-5-nitropyrimidine were washed with water, followed by ethanol and dried.
90%, IR (cm^{-1}): 3345, 1675, 1630, 1350; ^{1}H NMR (CDCl$_3$) δ: 9.15, s, 1H, (H$_6$), 7.20, b, 2H (NH$_2$ of C$_4$), 6.50, b, 2H (NH$_2$ on C$_2$).

2, 4, 5-Triaminopyrimidine [8]
Finely powdered 2, 4-diamino-5-nitropyrimidine (8.9 g) was heated to 80 ^{o}C with water (15 ml) and mechanically stirred. Sodium dithionite (3.75 g) was added during 3 - 4 minutes. The resulting solution was stirred until 60 ^{o}C, followed by addition of powdered anhydrous sodium carbonate (5.5 g). The thick suspension was taken to dryness in an open basin on water bath. The solid was machine ground and extracted for 20 minutes with stirred boiling alcohol (22 ml) which was filtered while hot. The filtrate was taken to dryness and the product was re-extracted with ethanol (7.5 ml) to remove sodium carbonate. Evaporation of filtrate gave the pure product.
71%; IR (cm^{-1}): 3363, 1670, 1625; ^{1}H NMR (DMSO-d6) δ: 7.25 s, 1H (H$_6$), 6.00, b, 4H (NH$_2$ of C$_2$ and C$_4$), 5.10, b, 2H (NH$_2$ of C$_5$).

2-Aminopurine [9]
2, 4, 5-Triaminopyrimidine (0.3 g), formyl morpholine (1.2 ml) and formic acid (0.6 ml) was heated under refluxed for one hour in nitrogen atmosphere. Acetone (2 ml) was added to precipitate 2-aminopurine which was dissolved in boiling water (3 ml). The solution was passed through a wide filter, cooled to 50 ^{o}C and diluted with 3N nitric acid and refrigerated. The nitrate was filtered off. The solution was then suspended in boiling water and brought to pH 6.8 with sodium citrate and 6N sodium hydroxide solution. The solution was boiled with charcoal, giving buff-coloured crystals of 2-aminopurines. Crystallisation with boiling water gave colourless crystals.
40%, IR (cm^{-1}): 3245, 1670, 1620; ^{1}H NMR (D$_2$O) δ: 8.70, s, 1H (H$_6$), 8.00 s, 1H (H$_8$) 6.25, b, 2H (NH$_2$), 6.50, b, 1H (NH).

2-Fluoropurine (improved method) [10, 11]
An aqueous solution of sodium nitrite (800 mg in 4 ml of water) was added with stirring to a solution of 2-aminopurine (200 mg) in 48% fluoroboric acid (22 ml) at the rate of 0.1 ml per minute at -11 ^{o}C. After the addition was completed, the mixture was stirred for one hour between - 10 to 0 ^{o}C. The mixture was then neutralized with 50% sodium hydroxide solution. The neutral slurry was evaporated to dryness. The crude purine was isolated by extraction of dry residue with ether in a soxhlet extractor. Evaporation of ether gave crude product, which was recrystallised from water.
35%, IR (cm^{-1}): 3325, 1673, 1623, 1132; ^{1}H NMR (DMSO-d6) δ:8.70 s, 1H, (H$_6$), 8.00 s, 1H (H$_8$), 6.50, b, 1H (NH).

2-Piperidinopurine
Piperidine (20 mg) in ethanol (4 ml) was added to a solution of 2-fluoropurine (40 mg) in ethanol (7 ml) and the mixture was refluxed for 1 hour at 100 ^{o}C. The mixture was cooled and ethanol was evaporated off. The slurry was extracted twice with ether. The ethereal layer was washed with water and dried over anhydrous sodium sulphate. Evaporation of ether gave crude product, which was recrystallised from petroleum ether.

50%, decomposed above 215, IR (cm^{-1}): 3115, 1673, 1620; ^{1}H NMR δ: 8.70, s, 1H (H$_6$), 8.00, s, 1H (H$_1$), 3.35, m, 4H (H$_{2'}$, H$_{6'}$), 1.68, m, 6H (H$_{3'}$, H$_{4'}$, H$_{5'}$); M^{+}: 203.1163.

2-Anilinopurine

2-Fluoropurine (80 mg) was added to aniline (3 ml) and warmed at 60 ^{o}C for four hours. The mixture was cooled and refrigerated overnight. 2-Anilinopurine was crystallized out of the reaction mixture. The crystal was filtered, washed with ice-cold water and dried. Pure product was obtained after recrystallisation from dichloromethane. 73.5%, decomposed above 200°, IR (cm^{-1}): 3330, 1670, 1630; ^{1}H NMR (DMSO-d6) δ: 8.65, s, 1H (H$_6$), 8.00, s, 1H (H$_8$), 7.20, m, 3H (H$_{3'}$, H$_{4'}$, H$_{5'}$), 6.90, d, 2H (H$_{2'}$ and H$_{6'}$), 5.40, d, 2H, (N-H); M^{+}:211.0858.

6-Piperidinopurine

Piperidine (0.5 ml) in ethanol (3 ml) was added to 6-chloropurine (0.232 g) [11-12] and the mixture was refluxed for 2 hours. The mixture was cooled and ethanol was evaporated off. The slurry was extracted twice with ether; the ethereal layer was washed with water and dried over anhydrous sodium sulphate. Evaporation of ether gave grey product, which was recystallised from petroleum ether. 30%, decomposed above 270, IR (cm^{-1}): 3115, 1673, 1620; ^{1}H NMR (DMSO-d6) δ: 8.23, s, 1H (H$_2$), 8.15, s, 1H (H$_8$), 2.62, m, 4H (H$_{2'}$, H$_{6'}$), 1.66, m, 6H (H$_{3'}$, H$_{4'}$, H$_{5'}$); M^{+}: 203.1163.

6-Anilinopurine

2-Chloropurine (0.161 g) was added to aniline (0.3 ml) in ethanol (3 ml) and refluxed for 3 hours. The mixture was cooled and the solvent was evaporated. The slurry was extracted with ether, washed with water and dried over anhydrous sodium sulphate. Evaporation of ether gave light brown solid. 50.3%, decomposed above 280°, IR (cm^{-1}): 3330, 1670, 1630; ^{1}H NMR (DMSO-d6) δ: 9.81, s, 2H (N-H), 8.43, s, 1H (H$_2$), 8.34, s, 1H (H$_8$), 8.01, d, 2H (H$_{2'}$ and H$_{6'}$), 7.38, t, 2H (H$_{3'}$, H$_{5'}$), 7.08, t, 1H (H$_{4'}$); M^{+}: 211.0858.

Spectroscopic Analysis

All solvents were redistilled before use. Melting points were determined with Electrothermal Melting Point Appararus and were not corrected. Infrared spectra were recorded using Perkin Elmer 298 Infrared Spectrometer and FTIR Perkin Elmer 1600 Series. ^{1}H NMR spectra were recorded on Bruker WP-80 and Bruker AM 250.

Fluorescence Studies

2- and 6-Substitued purines at the same concentration were prepared in various solvents. Quinine sulphate with the same concentration as the compounds under studied were also prepared and used as the standard. The fluorescence intensity of quinine sulphate was taken to be 1.00. The fluorescence measurement was carried out using Hitachi Fluorescence Spectrometer Model F-2000.

Results and Discussion

The synthetic route of 2-fluoropurine is as shown in Scheme 1 below:-

Scheme 1
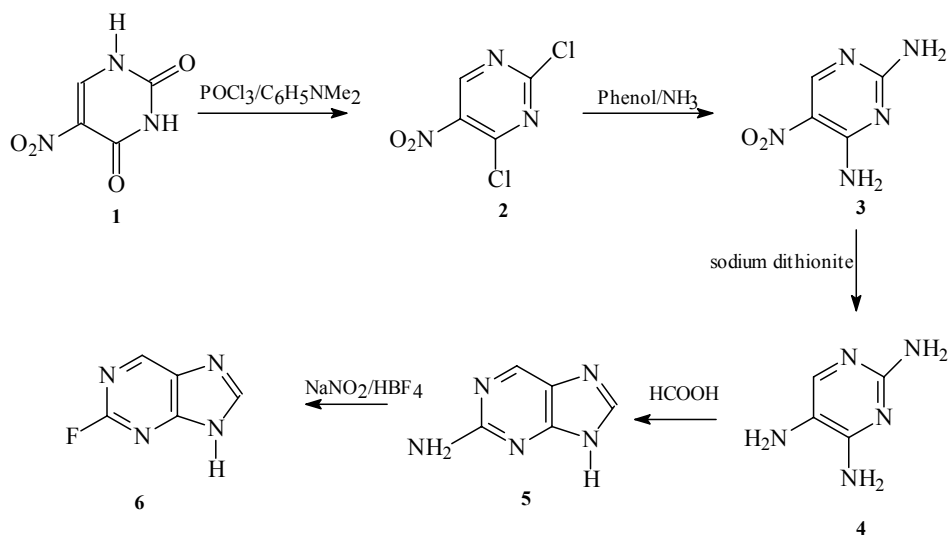
The preparation of 2-fluoropurine was carried out according to the Brown method [4], using 5-nitrouracil (1) as the starting material. Purine ring was obtained through cyclisation reaction of 2, 4, 5-triaminopyrimidine (4) with formic acid to give 2-aminopurine (5). Compound 5 undergoes diazotization reaction, followed by treatment with HBF_4 to give 2-fluoropurine (6). Low percentage yield was obtained in the synthesis of 6-chloropurine. Due to low percentage yield obtained, 6-chloropurine used in this work was obtained commercially.

Treatment of 2-fluoropurine and 6-chloropurine with aniline and piperidine are as shown in Schemes 2 and 3.
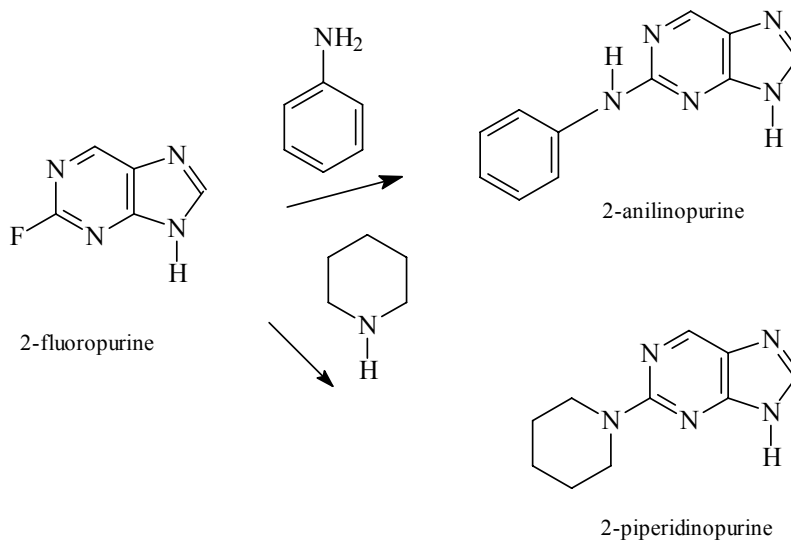
Scheme 2
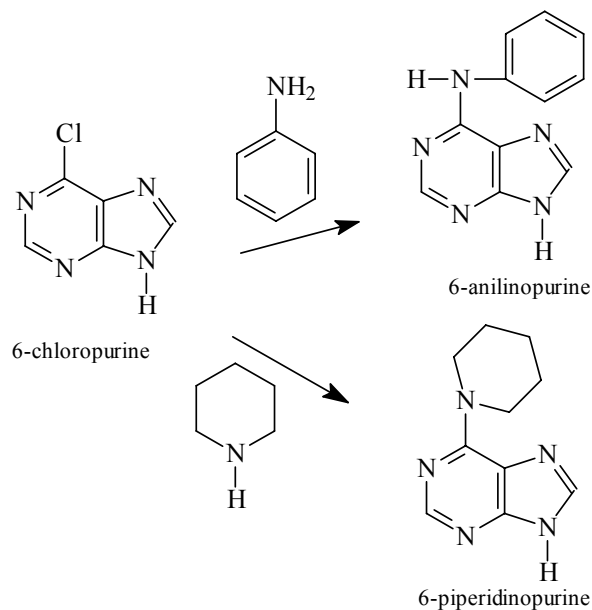
Scheme 3

The structures of 2- and 6- substituted purines were confirmed by ^{1}H NMR and mass spectra as given in the experimental section.

The fluorescence studies of 2- and 6-substituted purines were carried out in 75% ethanol. Quinine sulphate at the same concentration as the compounds studied was used as the standard and its fluorescence intensity was taken to be 1.00. The fluorescence band of 2- and 6-substituted purines were given in Table 1.

Table 1: Fluorescence peaks of 2- and 6- substituted purines in 75% ethanol

Purine	Solvent	Excitation wavelength/nm	Fluoresence wavelength/nm	Rel. Fluorescence intensity
2-fluoro	75% EtOH	350	430	0.640
2-amino	75% EtOH	340	380	0.964
2-anilino	75% EtOH	340	473	0.371
2-piperidino	75% EtOH	340	390	0.307
6-chloro	75% EtOH	330	420	0.650
6-anilino	75% EtOH	340	480	0.452
6-piperidino	75% EtOH	340	395	0.351

It can be seen from the table that, the fluorescence intensity of 6-substituted purines is stronger than 2-substituted derivatives. This is probably due to at the 6- position, the substituent is not sandwich between the two nitrogen atoms as in the 2nd position. As the result, the electrons can move freely from the substituent to the rest of the ring.

Anilinopurines showed stronger fluorescence intensities and fluoresced at a higher wavelength compared to the piperidinopurines. The fluorescence peak observed at a higher wave length is believed to be due to the increase in the degree of conjugation in the anilinopurines compared to piperidinopurines. The same phenomena was observed with pyrimidine derivatives studied earlier [13]. Lower fluorescence intensity was recorded with piperidinopurines in 75% ethanol. This is probably due to the piperidino ring flipping from one conformation to another, resulted in the loss of energy in the transition state. As the result, low fluorescence was observed.
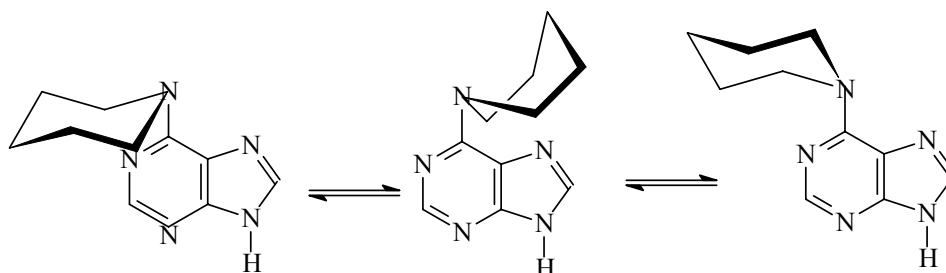
Flipping of piperidino ring

2- and 6-Piperidino purines were less rigid compared to 2- and 6- anilino purines. Some energy may also loss in the transition state, which also resulted in low fluorescence intensity observed.

2-Aminopurines showed the highest fluorescence intensity amongst all the derivatives of purines studied. This is probably due to the electron donating nature of the amino group which enhances the mobility of electron in the system. The free mobility of the electron enhances the   to   transitions, which resulted in high fluorescence intensity.

Conclusion

All the 2- and 6-substituted purines studied are fluorescent compounds. 2-Aminopurine is the most fluorescent and the fluorescence intensity depending on the type of the substituents. Substituent with high degree of conjugation, as in the case of anilinopurine showed higher fluorescence intensity and fluoresced at a higher wavelength. The purine system with unconjugated substituent (in the case of piperidinopurines) fluoresced at a lower wavelength. Further work on the purine system and other heterocyclic systems are still under going before any concrete conclusion can be made on solvent-structure-fluorescence and substituent-fluorescence relationship.

Acknowledgement

References

1. Scheel K. W., Opuscula, (1776), **2**, 73.
2. Medius, V. L. (1875), Annalen, **175**, 230.
3. Baxter, R. A. and Spring F. S., (1944), Nature, **154**, 462.
4. Brown D. J. and Waring P., (1974), J. Chem. Soc. Perkins Trans. II, 204.
5. Tong Y. C., (1975), J. Heterocyclic Chem., 451.
6. Abdullah Z., PhD. Thesis, (1989), Queen Mary & Westfield College, Uni. of London.
7. Whittaker N., (1951), J. Chem Soc., 1565.
8. Brown D. J., Albert, A. and Cheeseman G. (1951), J. Chem Soc., 474.
9. Albert A. and Brown D. J., (1954), J. Chem Soc., 2060.
10. Montgomery J. A. and Hewson J., (1960), J. Amer. Chem. Soc., **82**, 463.
11. Abdullah, Z. and A. Bakar M. A. (2005), sent to Jour. of Organic Chem.
12. Robins R.K., Dille K.J., Willits L.H. and Christensen K., (1975), J.Amer. Chem. Soc., 388.
13. Abdullah, Z., Mohd Tahir N., Abas M. R., Low B. K. and Aiyub Z. (2004), Molecules, 9, 520-26.

ARIMA AND INTEGRATED ARFIMA MODELS FOR FORECASTING AIR POLLUTION INDEX IN SHAH ALAM, SELANGOR

Lim Ying Siew, Lim Ying Chin and Pauline Mah Jin Wee

International Education Centre (INTEC), Universiti Teknologi MARA Section 17 Campus,
40200 Shah Alam, Selangor.

Abstract

Air pollution is one of the major issues that has been affecting human health, agricultural crops, forest species and ecosystems. Since 1980, Malaysia has had a series of haze episodes and the worst ever was reported in 1997. As a result, the government has established the Malaysia Air Quality Guidelines, the Air Pollution Index (API) and Haze Action Plan, to improve the air quality. The API was introduced as an index system for classifying and reporting the ambient air quality in Malaysia. The API for a given period is calculated based on the sub-index value (sub-API) for all the five air pollutants, namely sulphur dioxide (SO_2), nitrogen dioxide (NO_2), ozone (O_3), carbon monoxide (CO) and particulate matter below 10 micron size (PM_{10}). The forecast of air pollution can be used for air pollution assessment and management. It can serve as information and warning to the public in cases of high air pollution levels and for policy management of many different chemical compounds. Hence, the objective of this project is to fit and illustrate the use of time series models in forecasting the API in Shah Alam, Selangor. The data used in this study consists of 70 monthly observations of API (from March 1998 to December 2003) published in the Annual Reports of the Department of Environment, Selangor. The time series models that were being considered were the Integrated Autoregressive Moving Average (ARIMA) and the Integrated Long Memory Model (ARFIMA) models. The lowest MAE, RMSE and MAPE values were used as the model selection criteria. Between these two models considered, the integrated ARFIMA model appears to be the better model as it has the lowest MAPE value. However, the actual value of May 2003 falls outside the 95% forecast interval, probably due to emissions from mobile sources (i.e., motor vehicles), industrial emissions, burning of solid wastes and forest fires.

Introduction

Air pollution is one of the major issues that has been affecting human health, agricultural crops, forest species and ecosystems. Air quality monitoring is part of the initial strategy in the pollution prevention program in Malaysia. Since 1980, six major haze episodes were officially reported in Malaysia that is in April 1983, August 1990, June 1991, October 1991, August to October 1994 and July to October 1997. The 1997 haze episode was the worst ever experience in the country [3]. As a result, the government has established the Malaysian Air Quality Guidelines, the Air Pollution Index (API) and the Haze Action Plan in an attempt to improve the air quality.

There are possible health effects of exposure to air pollution. Recent studies have examined possible health effects of the 1997 forest fires. For example, respiratory disease outpatient who visited the Kuala Lumpur General Hospital increased from 250 to 800 per day and the data assembled indicated an increase in cases of asthma, acute respiratory infection, and conjunctivitis [1]. A study conducted by Nasir *et al*. [8] suggested that in the 1997 haze episode the total health effects were estimated to include 285,227 asthma attacks, 118,804 cases of bronchitis in children, 3889 cases of chronic bronchitis in adults, 2003 respiratory hospital admission, 26,864 emergency room visits and 5,000,760 restricted activity days. In addition, among the five pollutants, ozone was demonstrated to cause stress to the skin. It possesses a strong oxidizing potential and is therefore very reactive to the affected part [7]. Blockage of sunlight may also promote the spread of harmful bacteria and viruses that would otherwise be killed by ultraviolet B. Components of smoke haze, including polycyclic aromatic hydrocarbons known as carcinogens are also potentially dangerous and their effects may not be apparent for

years. The consequences may be more severe to children, for whom the particulates inhaled are high relative to their body size [4].

Since 1996, the National Environmental Research Institute [9], Denmark, has developed a comprehensive and unique integrated air pollution forecasting model system, called the THOR system. The system has been used to forecast the air pollution from accidental releases such as power plants, industrial sites and natural or human made fires. Dominici *et al.* [6] studied on the improved semi-parametric time series models of air pollution and mortality.

Clearly then from the above discussions, the modelling and ability to forecast API in Malaysia can be useful to many organisations like Environmental Agencies, Medical Research Institutes, Hospitals, etc. and the public at large. Therefore, the objective of this research is to model the API time series data in Shah Alam, Selangor so that such a model may be able to provide somewhat an estimate of the future API values.

Methodology

The Data Set

The Air Pollution Index (API) was introduced as an index system for classifying and reporting the ambient air quality in Malaysia. The API for a given period is calculated based on the sub-index value (sub-API) for all the five air pollutants, namely sulphur dioxide (SO_2), nitrogen dioxide (NO_2), ozone (O_3), carbon monoxide (CO) and particulate matter below 10 micron size (PM_{10}) which are included in the Malaysia API system. The API reference value has been based on the Malaysia Ambient Air Quality Guidelines (MAQG) of 1989 as shown in Table1 [2].

Table 1: API and Health Effect

API readings	Alert level	Health Effect Descriptor
0-50	No alert	Good
51-100	No alert	Moderate
101-150	Early alert	Unhealthy
151-200	Early alert	Unhealthy
210-300	On alert	Very unhealthy
301-500	Warming	Hazardous
>500	Emergency	Hazardous

Alam Sekitar Malaysia Berhad (ASMA) is a company that monitors the ground level ambient air continuously 24 hours a day. ASMA is responsible to install, operate, and maintain a network of 50 continuous air quality monitoring stations throughout Malaysia for the Department of Environment, DOE [7].
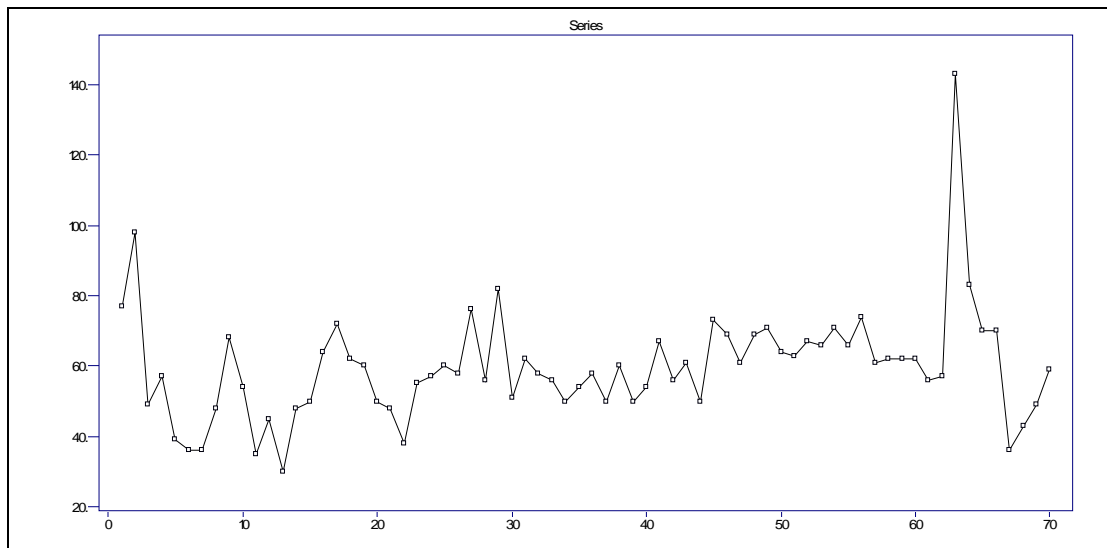

Figure 1: The time series plot of the monthly API data observed at the Shah Alam
monitoring station from March 1998 to December 2003

258

The data used in this study consists of 70 monthly observations of API (from March 1998 to December 2003) published in the Annual Reports of the Department of Environment, Selangor [10]. The time series plot of API is shown in Figure 1.

Time Series Modelling Procedure
For the purpose of time series modelling in this study, the first 58 observations (March 1998 to December 2002) were used to fit the ARIMA and integrated ARFIMA models while the subsequent 12 observations (from January 2003 to December 2003) were kept for the post sample forecast accuracy check.

A brief description of the time series models and definitions used in this study are as follows. A stationary ARMA (p, q) model is defined as a sequence of random variables $\{X_t\}$, given by

$$X_t - \phi_1 X_{t-1} - \cdots - \phi_p X_{t-p} = Z_t + \theta_1 Z_{t-1} + \cdots + \theta_q Z_{t-q}$$

where $\{Z_t\}$ is a sequence of uncorrelated random variables with zero mean and constant variance, denoted as $\{Z_t\} \sim WN(0, \sigma^2)$, [5].

A process $\{X_t\}$ is called an ARIMA (p, d, q) process [5] if d is a nonnegative integer such that $(1-B)^d X_t$ is a causal ARMA (p, q) process. The ARIMA (p, d, q) processes satisfies the difference equation of the form

$$\phi^*(B) \equiv X_t \phi(B)(1-B)^d X_t = \theta(B)Z_t, \ \{Z_t\} \sim WN(0, \sigma^2),$$

where $\phi(z)$ and $\theta(z)$ are polynomials of degrees p and q respectively, and $\phi(z) \neq 0$ for $|z| \leq 1$. The $\phi^*(z)$ has a zero of order d at $z = 1$. The process $\{X_t\}$ is stationary if and only if $d = 0$, in which case it reduces to an ARMA (p, q) process.

A long memory process [5] or a fractionally integrated ARMA, ARFIMA (p, d, q) processes with $0 < |d| < 0.5$ is a stationary process with much more slowly decreasing autocorrelation function $\rho(k)$ at lag k as $k \to \infty$ which satisfies the property of $\rho(k) \sim Ck^{2d-1}$. The ARFIMA processes satisfy the difference equation of

$$(1-B)^d \phi(B)X_t = \theta(B)Z_t, \text{ where } \{Z_t\} \sim WN(0, \sigma^2),$$
$$\phi(z) = 1 - \phi_1 z - \ldots - \phi_p z^p \text{ satisfying } \phi(z) \neq 0 \text{ and}$$
$$\theta(z) = 1 + \theta_1 z + \ldots + \theta_q z^q, \text{ satisfying } \theta(z) \neq 0$$

for all z such that $|z| \leq 1$, and B is the backward shift operator. The operator $(1-B)^d$ is defined by the binomial expansion of

$$(1-B)^d = \sum_{j=0}^{\infty} \pi_j B^j \text{ with } n_0 = 1 \text{ and } \pi_j = \prod_{0 < k \leq j} \frac{k-1-d}{k} \text{ for } j = 0, 1, 2, \ldots.$$

For the purpose of this study, we let $\{Y_t\}$ be the time series that represents the API and $\{y_t\}$ be the observed time series. Since there is a gradual decrease in level of $\{y_t\}$, we differenced the series at lag 1 to obtain a new series that is more or less constant in its level and this we denote it by $\{X_t\}$. To this $\{X_t\}$, we fitted an ARMA (p, q) process. The entire process of model fitting was done using the computer software "ITSM 2000, version 7.0", [5].

The criteria chosen to measure the accuracy of the forecast in this study are the mean absolute error (MAE), the root mean squared error (RMSE) and the mean absolute percentage error (MAPE) are given below.

$$\text{MAE} = \frac{\sum_{i=1}^{n} |x_i - \hat{x}_i|}{n}, \qquad \text{RMSE} = \sqrt{\frac{\sum_{i=1}^{n} (x_i - \hat{x}_i)^2}{n}}, \qquad \text{MAPE} = \frac{\sum_{i=1}^{n} \left| \dfrac{x_i - \hat{x}_i}{x_i} \right|}{n} \times 100\%$$

where x_i and $\hat{x}_i$ are the actual observed values and the predicted values respectively while n is the number of predicted values.

Results

In this section, we present the results of the study.

Let $\{ Y_t \}$ be the API and $X_t = \nabla Y_t$ where $\{ X_t \}$ is an ARMA (p, q) process. The best model fitted based on the AICC criterion that is given as follows:

$$X_t = 1.047 X_{t-1} - 0.6656 X_{t-2} - 0.1976 X_{t-3} + Z_t - 1.771 Z_{t-1} + 1.772 Z_{t-2} - 0.7764 Z_{t-3}$$

where $\{ Z_t \} \sim WN(0, 0.027020)$.

The monthly forecast results of the API values using the ARIMA (3, 1, 3) model for the year 2003 are shown in Table 2.

Table 2: Forecasts of the API values from January 2003 to December 2003
using the ARIMA (3, 1, 3) model

Month	Actual	Forecast	95% Confidence Interval
January	62	61.23	(44.36, 84.50)
February	62	63.20	(45.25, 88.27)
March	56	65.61	(44.43, 96.88)
April	57	66.76	(43.81, 101.73)
May	143	65.70	(42.73, 101.04)
June	83	63.20	(41.08, 97.22)
July	70	60.93	(39.60, 93.73)
August	70	60.18	(39.03, 92.79)
September	36	61.15	(39.08, 95.68)
October	43	62.96	(39.12, 95.68)
November	49	64.17	(38.88, 105.92)
December	59	63.81	(38.23, 106.52)

In Figure 2, the graph of the predicted values given by the ARIMA (3, 1, 3) model and the actual values of the API, together with their 95% forecast intervals are shown. We note that the actual API values fall within the 95% confidence interval.
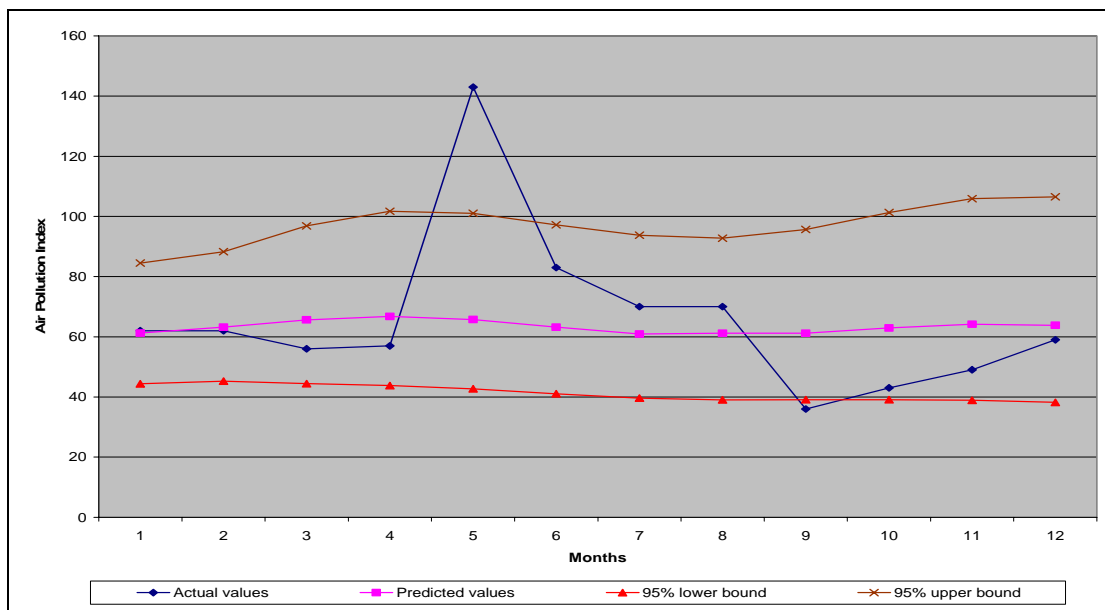
Figure 2: Graph of the API values with 12 predicted values of the ARIMA (3, 1, 3) model and the actual values
from January 2003 to December 2003

For ARFIMA modelling, again, we let $\{Y_t\}$ be the API and $X_t = \nabla Y_t$ where $\{X_t\}$ is now an ARFIMA (p, d, q) process given by,

$$(1-B)^{-0.5} X_t = Z_t - 0.001520 Z_{t-1} + 0.3578 Z_{t-2},$$

where $\{Z_t\} \sim WN(0,0.036980)$.

The monthly forecast results of the API values using the integrated ARFIMA (0, −0.5, 2) model for the year 2003 are shown in Table 3.

Table 3: Forecasts of the API values from January 2003 to December 2003
using the integrated ARFIMA (0, −0.5, 2) model

Month	Actual	Forecast	95% Confidence Interval
January	62	59.18	(33.60, 85.98)
February	62	58.56	(30.31, 87.25)
March	56	58.53	(25.18, 92.55)
April	57	58.13	(22.56, 94.44)
May	143	57.70	(20.60, 95.52)
June	83	57.26	(19.00, 96.22)
July	70	56.84	(17.63, 96.71)
August	70	56.44	(16.41, 97.05)
September	36	56.05	(15.31, 97.29)
October	43	55.68	(14.31, 97.46)
November	49	55.32	(13.38, 97.58)
December	59	54.97	(12.51, 97.65)

Figure 3 shows the predicted values given by the integrated ARFIMA (0, −0.5, 2) model and the actual values of the API, together with their 95% forecast intervals. The actual API values all fall within the 95% forecast intervals.
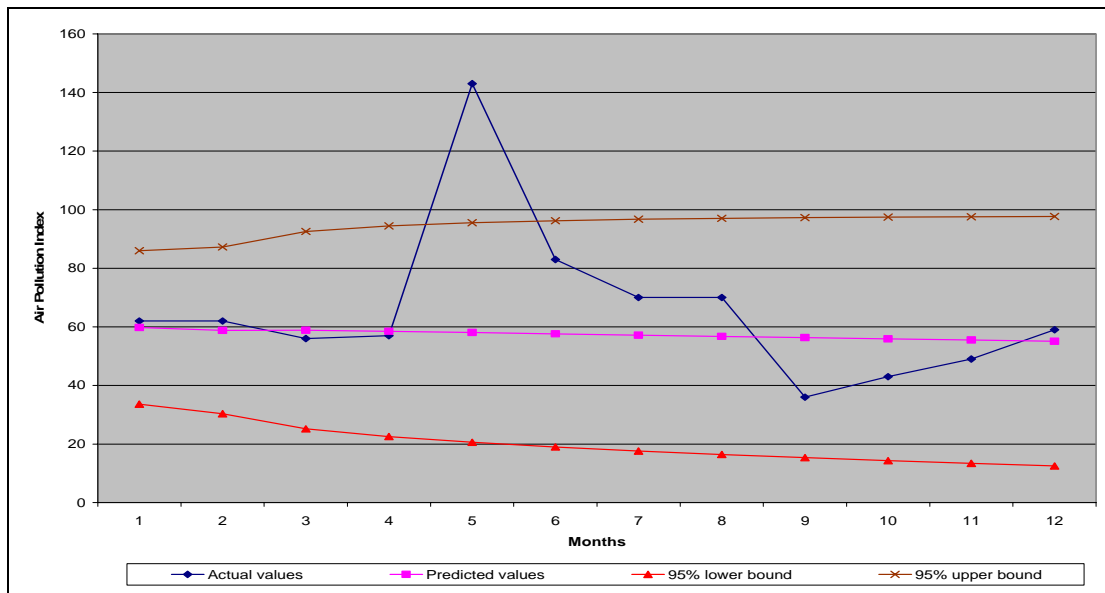
Figure 3: Graph of the API values with 12 predicted values of the integrated
ARFIMA (0, −0.5, 2) model and the actual values from January 2003 to December 2003

In Table 4, the MAE, MAPE and RMSE values of the ARMA (3, 1, 3) and the integrated ARFIMA (0, −0.5, 2) models are shown.

Table 4: The MAE, MAPE and RMSE values of the ARMA (3, 1, 3) and the integrated
ARFIMA (0, −0.5, 2) models

Model	MAE	RMSE	MAPE
ARIMA (3, 1, 3)	16.786	25.821	24.70%
ARFIMA (0, −0.5, 2)	15.896	27.299	20.86%

The MAE and MAPE values of the integrated ARFIMA (0, −0.5, 2) model are smaller when compared to those of the ARIMA (3, 1, 3) model. The RMSE value for ARIMA (3, 1, 3) is found to be smaller than the ARFIMA (0, −0.5, 2) model. The actual API value for May 2003 falls outside the 95% forecast intervals when forecasting using both the ARIMA (3, 1, 3) and ARFIMA (0, −0.5, 2) model. The ARIMA (3, 1, 3) model seem to be unable to forecast well as the actual API value for September 2003 is also found to be below the 95% lower bound of the forecast interval.

Conclusion

Based on this data set, the integrated ARFIMA model appears to have a slightly better forecasting performance compared to that of the ARIMA although both models are unable to forecast all values within the 95% forecast interval.

The actual API value of May 2003 which falls outside the 95% upper bound of the forecast interval may be due to the emissions from mobile sources like motor vehicles, industrial emissions, burning of solid wastes and forest fires. As such, factors which could affect the API should be taken into consideration in modelling of API for a better forecast ability as the modelling processes in this project were done based on the data of API only.

References

1. Awang M. B., Jaafar A. B., Abdullah A. M., Ismail M.B., Hassan M.N., Abdullah R., Johan S. and Noor H. (2000), Air Quality In Malaysia: Impacts, Management Issues And Future Challenges, *Respirology*, Vol. 5, pp 183-196.
2. Afroz R., Hassan M.N. and Ibrahim N.A. (2003), Review Of Air Pollution And Health Impacts In Malaysia, Environmental Research, Volume 92, Issue 2, pp 71-77.

3. Nasir M.H., Choo W.Y., Rafia A., Theng L.C., Noor M. M. H (2000), Estimation Of Health Damage Cost For 1997-Haze Episode In Malaysia Using the Ostro model, *Proceeding Malaysian Science And Technology Congress*, Confederation Of Scientific And Technological Association In Malaysia,COSTAM, Kuala Lumpur, in Press.
4. Faridah Mohamad (2002), Impacts Of Exposure To Ambient PM_{10} On Hospital Outpatient Visits For Haze-Related Diseases And School Children Lung Function, *Masters Thesis*. Universiti Putra Malaysia, Malaysia.
5. Beardsley R., Bromberg P.A., Costa D.A., Devlin R., Dockery D. W., Frampton M. W., Lambert W., Samet J. M., Speizer F. E., Utell M.(1997), Smoke Alarm: Haze From Fires Might Promote Bacterial Growth. *Science America*, pp 24-25.
6. National Environment Research Institute, NERI (2003), THOR. http://www.dmu.dk/1_viden/2_miljoe-tilstand/3_luft/4_spredningsmodeller/5_thor/default_en.asp. Accessed on 27 April 2004.
7. Dominici, F., McDermott, A., Hastie, T. J.(2004), Improved Semi-Parametric Time Series Models Of Air Pollution And Mortality. http://www-stat.stanford.edu/~hastie/Papers/dominiciR2.pdf. Accessed on 27 April 2004.
8. Awang M.B., Hassan M.N., Noor Alshurdin M.S., Abdullah A.M. (1997), Air pollution in Malaysia, in *IMR Quaterly Bulletin*, No. 43, pp 26-42.
9. *Annual Report* (1998-2003), Department of Environment, Selangor.
10. Brockwell, P.J. and Davis, R.A. (2002), *Introduction To Time Series And Forecasting*, 2nd Edition, Springer-Verlag, New York.

COMPARISON OF VARIOUS SOURCES OF HIGH SURFACE AREA CARBON PREPARED BY DIFFERENT TYPES OF ACTIVATION

Abdul Rahim Yacob, Zaiton Abdul Majid, Ratna Sari Dewi Dasril and Vicinisvarri a/p Inderan

Department of Chemistry, Faculty of Science, Universiti Teknologi Malaysia, 81310 UTM Skudai, Johor, Malaysia.

Abstract

Activated carbon has been known as an excellent adsorbent and is widely used due to its large adsorption capacity. Activation condition and types of activation influence the surface area and porosity of the activated carbon produced. In this study, palm kernel shells and commercially activated carbon were used. To convert palm kernel shells into coal, two methods were employed, namely chemical activation and physical activation. For chemical activation, two activating agents, zinc chloride and potassium carbonate, were used. The activated carbons were analyzed using Fourier Transform Infrared (FTIR) spectroscopy, single point BET and free emission scanning electron microscopy (FESEM). The commercial activated carbon was also characterized. FTIR results indicate that all the palm kernel shells were successfully converted to carbon. Single point BET surface area of all the carbons prepared were obtained. From FESEM micrograph, the chemically activated palm kernel shells shows well highly defined cavities and pores. This study also shows that palm kernel shells can be used to be a better source of high surface area carbon.

Karbon teraktif dikenali sebagai bahan penjerap yang baik dan digunakan secara meluas kerana kapasiti penjerapannya yang tinggi. Kaedah dan jenis pengaktifan yang digunakan mempengaruhi luas permukaan dan sifat keliangan karbon teraktif yang dihasilkan. Dalam kajian ini, tempurung kelapa sawit dan karbon teraktif komersial digunakan. Bagi menukarkan tempurung kelapa sawit kepada arang, dua kaedah digunakan iaitu, pengaktifan secara kimia dan fizikal. Bagi pengaktifan secara kmia, dua jenis agen pengaktifan digunakan, zink klorida dan kalium karbonat. Karbon yang telah diaktifkan seterusnya dianalisis menggunakan spektroskopi Inframerah Transformasi Fourier (FTIR), penjerapan titik tunggal BET dan mikroskopi imbasan electron pancaran bebas (FESEM). Karbon teraktif komersial juga turut dianalisis. Keputusan FTIR menunjukkan bahawa kesemua tempurung kelapa sawit berjaya ditukarkan kepada karbon. Luas permukaan penjerapan titik tunggal BET bagi kesemua sampel telah diperolehi. Daripada mikrograf FESEM, tempurung kelapa sawit yang diaktifkan secara kimia menunjukkan liang dan rongga yang jelas. Kajian ini juga menunjukkan bahawa tempurung kelapa sawit boleh menjadi sumber karbon berluas permukaan tinggi yang lebih baik.

Introduction

Activated carbons are disordered, microporous forms of carbon, with very high porosity and surface area. They can be prepared from a large number of raw materials, especially agro-industrial by-products such as olive stones [1], coconut shells [2], walnut shells [3] and macadamia nutshells [4]. These by-products are often considered as wastes and have caused significant disposal problems in some countries. Their utilization in the activated carbon industries is a feasible solution to this environmental issue.

In Malaysia, palm kernel shell is one of the main agriculture wastes from the palm oil industries. It is estimated that for every one million tonnes of palm oil produced, 0.8 million tonnes of palm shells is created [5]. Based on a total oil production of 7.4 million tonnes in 1993, the amount of palm shell generated in that year alone was about 6 million tonnes. Palm kernel shell is proposed to be used as a prospective starting material for activated carbon because of its relatively high fixed carbon content (about 18 %w/w), low ash content (less than 0.1 % w/w) and the presence of inherent porous structures [6].

Activated carbon is widely used for a number of applications, such as separation of gases, recovery of solvent, removal of organic pollutants from drinking water and as a catalyst support, among many other operations. It is most widely used because of its large adsorption capacity and low cost. Activated carbons are important adsorbents in various industrial sectors such as the food, pharmaceutical and chemical industries [7]. For an

example, Ghana imports large quantities of activated carbon annually especially for gold mining industries to recover gold from cyanide solution using the carbon-in-pulp or carbon-in-leach processes [8]. Furthermore, as environmental pollution is increasingly becoming a serious problem, the demand for activated carbon is growing.

The process for manufacturing activated carbons involves two steps; the carbonization of raw carbonaceous materials and the activation of the carbonized product. Two methods are used to prepare activated carbons, namely physical activation and chemical activation. In the physical activation, the raw material is carbonized and consequently the prepared char is reacted with steam or CO_2. In chemical activation, the raw material is mixed with an activation reagent and the mixture is heated in an inert atmosphere.

The carbonization leaves an imprint effect on the final product [5]. The purpose of carbonization process is to enrich the carbon content and to create an initial porosity in the char. The activation process further develops the porosity and creates some ordering of the structure to generate a highly porous solid as the final product.

In this study, three types of activated carbon were prepared using palm kernel shell as the starting materials. Both chemical and physical activation were employed. For chemical activation, two activating agents were used; zinc chloride ($ZnCl_2$) and potassium carbonate (K_2CO_3). As a comparison, commercial activated carbon was used. $ZnCl_2$ was chosen because it is the most widely used chemical in the production of activated carbons. On the other hand, K_2CO_3 was used because it is non deleterious such as KOH or NaOH since it is also used as food additive [9]. As for physical activation, direct heating under vacuum atmosphere was carried out where the carbonization and activation steps proceed simultaneously.

EXPERIMENTAL

Reagents
Commercial activated carbon (99.9%) with molecular weight of 12.01 $gmol^{-1}$ was purchased from Scharlau Chemise S.A. Zinc chloride ($ZnCl_2$) and sodium carbonate (Na_2CO_3) from Goodrich Chemical Enterprise were used along with concentrated hydrochloric acid (HCl), 37% w/w purchased from J.T. Baker. Potassium carbonate (K_2CO_3) was obtained from Fluka Chemie AG. The palm kernel shell was obtained from Kulai palm oil mill.

Chemical Activation
100 g of $ZnCl_2$ was added to 100 g of palm kernel shell in a beaker of 1 L. $ZnCl_2$ acts as the chemical activating agent. 100 mL of concentrated HCl (37% w/w) and 10 mL deionized water were added to the beaker. The mixture was stirred and heated at 100 - 110°C until it was fully dried. The treated char was kept in oven overnight for dehydration purpose. About 0.5 g of the dehydrated char was placed in a quartz tube and then connected to a vacuum line system. The sample was then heated at 800°C for two and four hours respectively under 1×10^{-3} mbar pressure. The activated samples were neutralized with diluted Na_2CO_3 solution and deionized water. The washing process was repeated until the pH is approximately 7. Sample was then dehydrated in oven at 100°C. The sample obtained was labeled as CZ-AC 2h and CZ-AC 4h.

As for the second activating agent, 100 g of K_2CO_3 was added to 100 g of palm kernel shell in 1 L beaker. 100 mL of distilled water was added to the beaker. The mixture was then treated with the same heating and activation processes as above. The activated samples were then neutralized using hot distilled water. The washing process was also repeated until the pH is approximately 7. The sample was then dehydrated in oven at 100°C. The sample obtained was labeled as CK-AC 2h and CK-AC 4h.

Physical Activation
About 0.5 g of crushed palm kernel shells was placed in a quartz tube. The sample was subjected to the same activation under vacuum atmosphere for two and four hours as described above. The samples were heated at 800°C. The samples obtained were labeled as P-AC 2h and P-AC 4h.

Characterization of Samples
Fourier Transform Infrared (FTIR) analysis was carried out using Shimadzu 8300 spectrometer with wave number ranging from 400 to 4000 cm^{-1}. Single point BET surface area was measured at temperature of   77 K

using Micromeritics Pulse Chemisorb 2705. Free emission scanning electron microscopy (FESEM) and energy disperse analysis through X-ray (EDAX) were performed using SUPRA 35VP.

Results and Discussion

Fourier Transform Infrared Spectroscopy

Figure 1 shows the FTIR spectra of raw palm kernel shell (PKS), commercial activated carbon, X-AC and samples activated for two hours, CZ-AC 2h, CK-AC 2h, and P-AC 2h. The X-AC FTIR spectrum was used as a reference for comparison with other synthesized activated carbon. Figure 2 also shows the raw PKS and X-AC spectra along with samples activates for four hours, CZ-AC 4h, CK-AC-4h and P-AC 4h. By interpreting the infrared transmittance spectrums, the functional group in the sample can be determined.
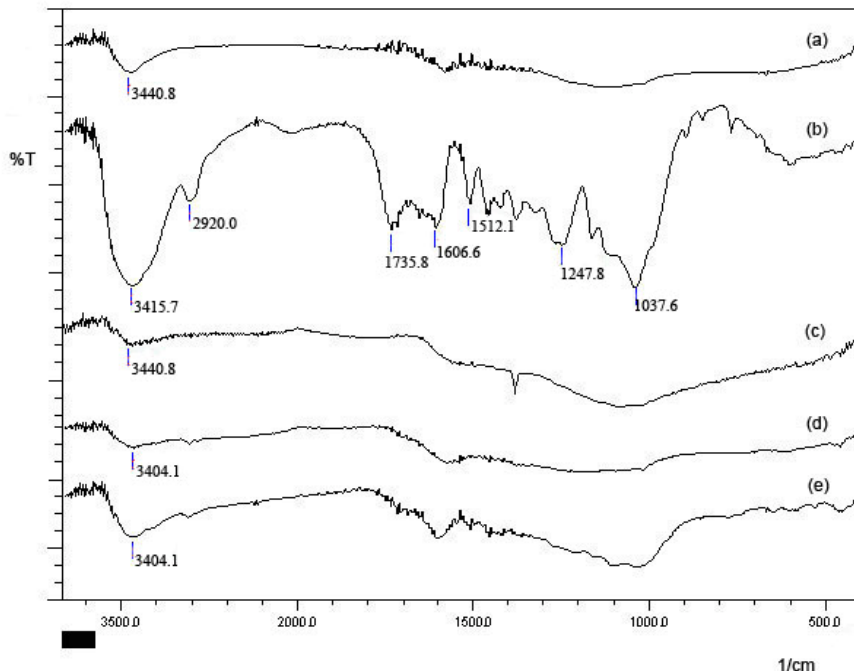

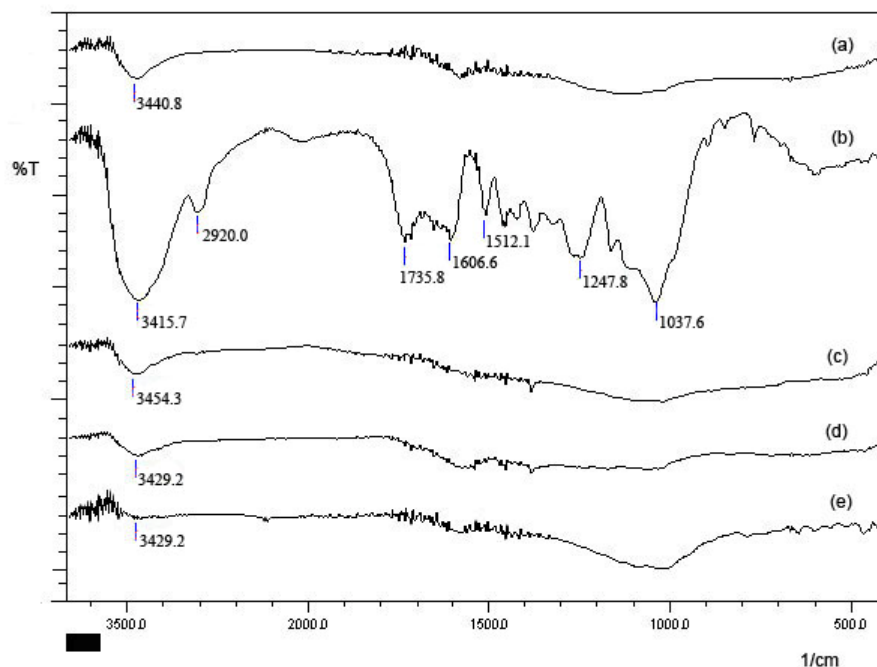Figure 1. FTIR spectra for (a) X-AC, (b) raw PKS, (c) CZ-AC 2h, (d) CK-AC 2h and (e) P-AC 2h

266

Figure 2. FTIR spectra for (a) X-AC, (b) raw PKS, (c) CZ-AC 4h, (d) CK-AC-4h and (e) P-AC 4h

Based on both Figure 1 and Figure 2, only raw PKS shows the most complicated and apparent spectrum. A strong and broad adsorption peak appeared at 3415.7 cm^{-1}, corresponding to the stretching of O–H functional group and this indicates the presence of bonded hydroxide in the raw sample. There was another peak observed at 2920.0 cm^{-1} corresponding to the C–H sp^3 stretching. A strong C=O peak could be observed at 1735 cm^{-1}. This sample also shows two important absorption peaks at 1247.8 and 1037.6 cm^{-1} which represents the stretching of C–O functional group.

Unlike the FTIR spectrum showed by raw PKS, spectra of CZ-AC 2h, CZ-AC 4h, CK-AC 2h, C-AC 4h, P-AC 2h and P-AC 4h illustrate less absorption peaks. Although the samples were prepared via various activation method, there was a similarity in the adsorption patterns. Basically all the samples showed a weak broad peak around 3350 – 3450 cm^{-1} which indicates the presence of hydroxide in the samples. It is suggested that the samples traps moisture on its surface during sample handling due to their adsorptive nature.

From the samples spectra obtained, clearly, most of the absorption peaks of functional groups were diminished. During the carbonization and activation processes, the functional groups as observed from the raw PKS spectrum were evaporated as volatile materials when heat was applied to the samples. This proved that the activation process have taken place successfully.

The trends of all the samples spectra were almost similar with the commercial activated carbon spectrum which was used as the reference sample. Consequently, this indicates that all the prepared samples were successfully converted into carbon. Table 1 summarized the FTIR absorption data incorporating functional groups from the FTIR spectra shown in both Figure 1 and Figure 2.

Furthermore, both figures shows apparent decrease in the broad C–O peak around 1250 – 1000 cm^{-1} and C=C absorption band around 1650 – 1500 cm^{-1} for the prepared samples spectra towards the raw PKS spectrum. Samples activated for four hours showed clearer peaks reduction than the two hours activation. This is best explained particularly by the P-AC 2h and P-AC 4h spectrums. The decreasing bands suggest that activation time influenced the prepared samples. This indicates that four hours activation time is favorable than two hours activation time.

Table 1. Absorption frequencies and functional groups of the samples

Sample	Absorption frequencies (cm^{-1})	Functional Group
raw PKS	3415.7	O – H stretching
	2920.0	C – H (sp^3) stretching
	1735.8	C = O stretching
	1606.6 , 1512.1	C = C (aromatic) stretching
	1247.8 , 1037.6	C – O stretching
X-AC	3440.8	O – H stretching
CZ-AC 2h	3440.8	O – H stretching
CZ-AC 4h	3454.3	O – H stretching
CK-AC 2h	3404.1	O – H stretching
CK-AC 4h	3429.2	O – H stretching
P-AC 2h	3404.1	O – H stretching
P-AC 4h	3429.2	O – H stretching

Single Point BET Surface Area

The single point BET surface area analysis at temperature of 77 K was performed to determine the surface area obtained for the activated carbon prepared by different activation method. All the data collected, including the raw PKS and commercial activated carbon were presented in the form of a bar chart in Figure 3.
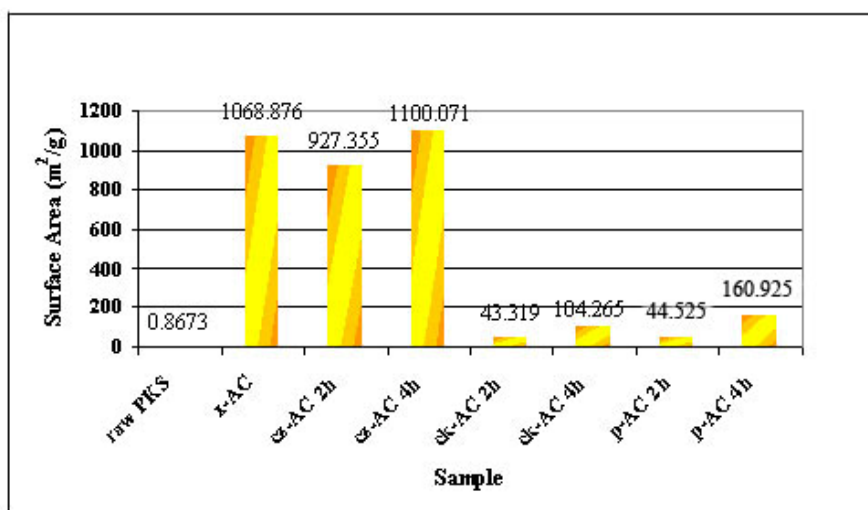

Figure 3. Single Point BET surface area of raw PKS, X-AC and synthesized carbons

Raw PKS gives only 0.8673 m^{2}g^{-1} of BET surface area. From the graph, all the synthesized carbon gave extensively higher BET surface area which drastically increased after the activation process. Based on the results obtained, CZ-AC 4h showed the highest BET surface area among the prepared carbons with 1100.071 m^{2}g^{-1}. Moreover, CZ-AC 4h also exhibits slightly higher surface area compared to the commercial activated carbon with only 1068.876 m^2 g^{-1}.

It is also found that CK-AC 2h, CK-AC 4h, P-AC 2h and P-AC 4h gave relatively low BET surface area. When it was compared to CZ-AC 4h and CZ-AC 2h obviously there was a pronounced decrease in the BET surface area. This result suggests that the chemical activating agent used, ZnCl$_2$, has contributed to the higher surface area. The used of ZnCl$_2$ as the activating agent resulted in more new pores being created and the existing pores widened to give activated carbon with higher BET surface area [10].

From the results obtained, samples activates for four hours shows relatively higher BET surface area than

samples activates for only two hours. This findings support the previous results obtain from FTIR that suggested that the activation duration affects the final product in preparing high surface area activated carbon. However, the surface areas for CK-AC 2h, CK-AC 4h, P-AC 2h and P-AC 4h which are, 43.319, 104.265, 44.525 and 160.925 m^2g^{-1} respectively didn't achieve the range of activated carbon surface area. Typically, the surface area of activated carbon ranges from 500 to 1400 m^2g^{-1} [8].

Free Emission Scanning Electron Microscopy
The surface morphology of the samples was studied using FESEM. Figure 4 shows the micrograph of X-AC. The commercial activated carbon was in highly amorphous form. From the micrograph, no pores could be detected even though it has a high BET surface area results. It is suggested that the pores were diminished during the product manufacturing in order to get a powder form. Nevertheless, the micrograph also illustrate that the X-AC have fine particle size.
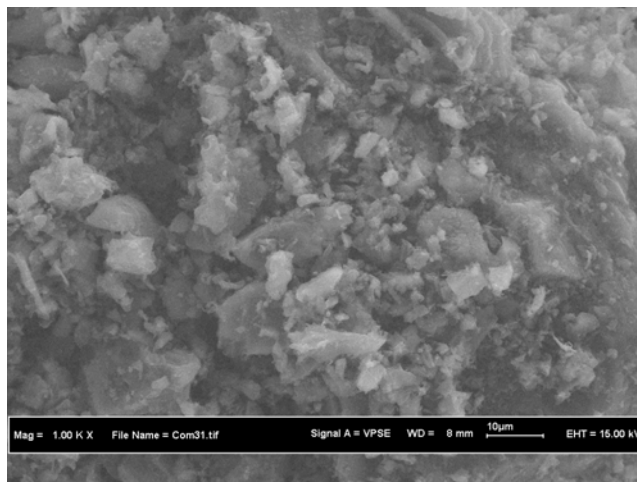

Figure 4**.** Micrograph for X-AC with magnification of 1000×

Figure 5(a) shows the micrograph for raw PKS. The surface was rough and dented. Small pores are also evident on the surface. Figure 5 (b) shows the P-AC 4h micrograph. Generally, the morphology is similar with the raw PKS except, larger pores are observed, resulted in the formation of larger pores from activation. Figures 5(c) and (d) show the micrograph of CZ-AC 4h and CK-AC 4h respectively. The CZ-AC 4h micrograph shows highly defined pores and cavities. The surface differs from the raw PKS surface in that it is cleaner and smooth. However, small particles are randomly scattered among the pores.

As for the CK-AC 4h micrograph, major development of pores could be seen. However, the pores size distributions are non-uniform. Similar to CZ-AC 4h, the surface is clean and smooth. The pore development was so rapid, resulting in too much cavity and lead to cracks formation. The pores are large and are external pores. This explains why the BET surface area value for CK-AC 4h was lower than CZ-AC 4h.

It is also identified that the pores and cavities for CZ-AC 4h were internal pores because the pores could only be seen under the FESEM after being crushed into smaller fraction, though this damages some of the pores formed. This finding corroborates the BET surface area results gathered earlier.
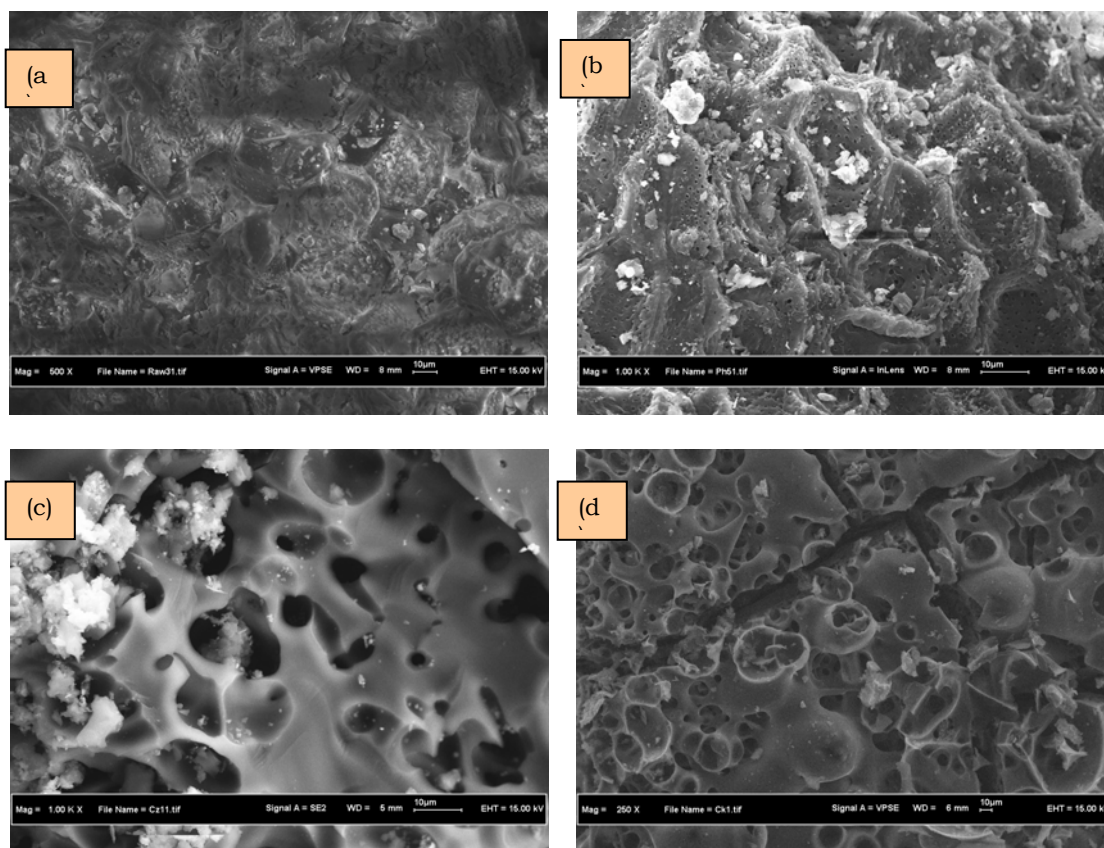
Figure 5. Micrograph for (a) raw PKS with magnification of 500×, (b) P-AC 4h with magnification of 1000×, (c) CZ-AC 4h with magnification of 1000× and (d) CK-AC 4h with magnification of 250×

Energy Disperse Analysis through X-ray Spectroscopy

Table 2 shows the element weight percent (wt %) obtained from EDAX analysis. The raw PKS showed the presence of carbon, oxygen, aluminum and silicon with 46.18, 45.08, 3.47 and 5.27 wt % respectively. While X-AC showed only two elements that are carbon and oxygen with 91.28 and 8.72 wt % respectively. The raw PKS exhibits lower carbon content and higher oxygen content compared to the X-AC. P-AC samples also have the same elements as the raw PKS. However, after the activation process, the carbon content was enriched to 75.77 wt % and the percentage of oxygen, aluminum and silicon are reduced. From the table, CZ-AC 4h showed the highest carbon content among the three prepared samples with 79.47 wt % and the lowest oxygen content, 13.67 wt %. However, CZ-AC 4h exhibits the highest aluminum content. No silicon was observed in this sample. Additional element, zinc, could be detected in this sample with 5.68 wt % suggesting that the chemical impregnation of $ZnCl_2$ took place during the sample preparation.

As for CK-AC 4h sample, it exhibits the lowest carbon content with 69.95 wt % and 19.22 wt % of oxygen. In contrary to CZ-AC 4h, CK-AC 4h shows the lowest aluminum content. No silicon was observed as in CZ-AC 4h. This suggests that the chemical activation removes silicon from the raw PKS. Potassium could be seen as expected for chemical impregnation with 10.22 wt %.

Table 2. Elemental analysis carried out by EDAX Spectroscopy

Sample	Element (wt %)						Total
	C	O	Al	Si	Zn	K	(wt %)
raw PKS	46.18	45.08	3.47	5.27	-	-	100
X-AC	91.28	8.72	-	-	-	-	100
CZ-AC 4h	79.47	13.67	1.18	-	5.68	-	100
CK-AC 4h	69.94	19.22	0.62	-	-	10.22	100
P-AC 4h	75.77	21.2	1.12	1.91	-	-	100

EDAX analysis strengthens the fact that CZ-AC 4h is the best activated carbon prepared with the highest carbon content and the lowest oxygen content. Still, the X-AC showed higher and finer form of activated carbon.

Conclusions

In this study, three different types of carbons were successfully prepared. The study showed that the type, condition and time of the activation process influenced the physical properties of an activated carbon. FTIR results indicate that all the palm kernel shell was successfully converted into carbon. Single point BET surface area of all the carbons prepared were obtained and CZ-AC 4h showed the highest surface area with 1100.071 m^2 g^{-1}, even higher surface area than the commercially activated carbon. From FESEM micrograph, the chemically activated palm kernel shells showed well developed pores and clean surface compared to the raw PKS. CZ-AC 4h exhibits internal and highly defined cavities and pores. EDAX analysis strengthens the fact that CZ-AC 4h is the best activated carbon prepared. This study also shows that palm kernel shells can be used to be a better source of high surface area carbon.

Acknowledgement

References

1. Rodriguez-Reinoso, F., Molina-Sabio M. and Gonzalez M.T. (1995) "The Use of Steam and CO_2 as Activating Agents in the Preparation of Activated Carbons" *Carbon*. 33. 15-23.
2. Zhonghua Hu and Srinivasan M. P. (1999) "Preparation of High Surface Area Activated Carbons from Coconut Shell" *Microporous and Mesoporous Mat.*. 27. 11-18.
3. Zhonghua Hu and Vansant E. F. (1995) "Carbon Molecular Sieves Produced from Walnut Shell" *Carbon*. 33. 561-567.
4. Ahmadpour A. and Do D. D. (1997) "The Preparation of Activated Carbon from Macadamia Nutshell by Chemical Activation" *Carbon*. 35. 1723-1732.
5. Wan Mohd Ashri Wan Daud, Wan Shahbudin Wan Ali and Mohd Zaki Sulaiman. (2000) "The Effects of Carbonization Temperature on Pore Development in Palm-Shell-Based Activated Carbon" *Carbon*. 38. 1925-1932.
6. Aik C. L. and Jia G. (1998) "Preparation and Characterization of Chars from Oil Palm Waste" *Carbon*. 36. 1663-1670.
7. Hayashi J., Uchibayashi M., Horikawa T., Muroyama K. and Gomes V. G. (2002) "Synthesizing Activated Carbons from Resins by Chemical Activation with K_2CO_3" *Carbon*. 40. 2747-2752.
8. Lartey R. B., Acquah F. and Nketia K. S. (1999) "Developing National Capability for Manufacture of Activated Carbon from Agricultural Wastes" The Ghana Engineer.
9. Hayashi J., Horikawa T., Takeda I., Muroyama K. and Farid Nasir Ani. (2002) *Carbon*. 40. 2381-2386.
10. Zhonghua Hu, Srinivasan M. P. and Yaming Ni. (2001) "Novel Activation Process for Preparing Higly Microporous and Mesoporous Activated Carbons" *Carbon*. 39. 877-886.

271

KETOHYDRAZONE COMPLEXES AS POTENTIAL EMITTING MATERIAL IN OLED

Haznita Rose Bahari[1], Mohd Nordin Garif[1] and Mustaffa Shamsuddin[1]

[1]Department of Chemistry,
Faculty of Science,
Universiti Teknologi Malaysia,
81310 UTM Skudai, Johor Bahru, Malaysia.
Email: nordin@kimia.fs.utm.my

Abstract

Ketohydrazone is a molecule that is able to act as a bidentate ligand through the O of C=O and N of N=C in the molecule. Three ketohydrazone ligands had been fully synthesized through the condensation reaction between 2-hydroxynaphthaldehydes with various hydrazides: salisylic hydrazide, benzyhydrazide and 2-furoic acid hydrazide in a 1:1 stoichiometry. The ligands had been characterized using infrared, ^{1}HNMR and ultraviolet-visible spectrometer. Complexation reaction between all ligands and metals, with a stoichiometry of 1:2 for Zn (II) : ligand and 1:3 for Al(III) : ligand were carried out. All six complexes obtained were characterized using FTIR and UV-Vis spectrometer. The fluorescence properties of each ligands and complexes were investigated using luminescence spectrofluorometer excited at 406 nm. It was found that the compounds emitted blue light at λ_{max} = 470 nm. Results showed that all the ligands and molecules synthesized have the fluorescence properties and complexation with metal enhanced the intensity of the fluorescence. It was observed that complex of Al(NDB)$_3$ showed the best potential as an emitting material for OLED as it has the highest fluorescence intensity compared to others.

Abstrak

Ketohidrazon merupakan sebatian molekul yang berupaya berfungsi sebagai ligan bidentat melalui O daripada C=O dan N daripada N=C di dalam molekulnya. Tiga ligan ketohidrazon telah berjaya disintesis melalui proses kondensasi antara 2-hidroksinaftaldehida dan beberapa kumpulan hidrazida, salisilik hidrazida,, 2-furoik hidrazida, dan benzihidrazida.mengikut nisbah stoikiometri 1 : 1. Semua ligan yang telah disintesis dicirikan melalui spektroskopi IR, UV-Vis dan ^{1}H-RMN. Tindak balas pengkompleksan antara ligan yang telah disintesis dengan dua logam yang berasingan, iaitu aluminium dan zink telah dijalankan dengan nisbah ion ligam : ligan 1 : 3 bagi pengkompleksan dengan aluminium dan 1 : 2 bagi pengkompleksan dengan zink. Enam kompleks yang terhasil dicirikan melalui spektroskopi IR dan UV-Vis. Ciri-ciri pendarfluor bagi tindak balas pengkompleksan dan ligan yang terhasil telah dikaji menggunakan spektrometer pendarfluor pada panjang gelombang pemancaran 405nm. Didapati sebatian-sebatian tersebut memancarkan cahaya biru pada λ_{max} = 470 nm. Hasil yang diperolehi menunjukkan bahawa semua ligan dan kompleks yang disintesis menunjukkan sifat pendarfluor dan pengkompleksan dengan logam dapat meningkatkan keamatan pendarfluornya.. Kompleks Al(NDB)$_3$ menunjukkan potensi yang terbaik sebagai bahan pemancar dalam diod pemancar cahaya organik (OLED) memandangkan kompleks ini menunjukkan keamatan pendarfluor yang tertinggi.

Introduction

Since organic light-emitting diodes (LEDs) using 8-hydroxyquinoline aluminum as the emitting layer was reported to emit green light in 1987 [1], organic LEDs have received considerable attention due to their potential application in various displays. Emitting material for organic LEDs can be classified into three types according to their molecular structure: organic dyes, chelate metal complexes and polymers. Complexes of chelating ligands are in general more stable thermodynamically than those with an equivalent number of monodentate ligands. These organic molecules were useful due to their solubility. They could be applied to a surface as a film via evaporation of their solvent.

Ketohydrazone, a chelating ligand with both oxygen and nitrogen donors coordinated to metal ion formed a stable complex. From earlier studies, the metal–chelate complex is believed to be a promising emitting material. Oxadiazole compounds are also known to have excellent electron transport ability and efficient fluorescence

properties. Several research groups reported efficient bluish-green emission in the devices using the oxadiazole compounds [2]. From Suning Wang study, he reported fluorescence properties for two derivatives of 7-azaindole complexes with aluminium. Although the compounds has a blue emission band at ca. 450 nm, it is very weak and the steric factors may be responsible for the problem[3].

There is a big challenge in developing emitting materials which can exhibit highly efficient blue-light emission. Thus, the research was focused on synthesizing the new complexes as blue light emitting material and their potential as the emitting material in OLED.

Experimental

Synthesis of Ligands

2-Hydroxynaphthaldehyde was dissolved in absolute methanol in a 3-necked round bottomed flask. Solution of 4-Hydroxybenzhydrazide in absolute methanol was added into the flask. The reaction mixture was then heated with stirring under nitrogen at 80^0C, for 2.5 hours. The light yellow precipitate formed was filtered by suction and dried in a vacummed dessicator. The product, 2-hydroxynaphthaldehyde benzoilhydrazide was then recrystallized using methanol. The same procedure was repeated for preparation of other ligands by replacing benzhydrazide with salicylichydrazide for 2-Hydroxynaphthaldehyde salicyloilhydrazide (NDS) ligand and 2-furoic acid hydrazide for 2-Hydroxynaphthaldehyde furoilhydrazide (NDF) ligand. All the ligands obtained were characterized using NMR, UV-Vis and IR spectroscopy.

Determination of Ligand-Metal Stoichiometry

By using Job method [4], absorption of different mole fraction of ligand and metal was plotted. Metal solution and ligand solution with different mole fraction were mixed together followed by addition of buffer solution at pH 5.1, which was made up from sodium acetate trihydrate and glacial acetic acid followed by addition of deionized water. After 5 minutes, UV-Vis spectrum was recorded. By using the following formula;

$$n \quad = \quad X_{max} / (1-X_{max})$$

$$n \quad = \quad \text{no. of mole ligand bonded with metal}$$
$$X_{max} = \text{mole of ligand at maximum absorption}$$

the value of n was calculated.

It was found that the metal : ligand stoichiometry are 1:2 for zinc complexes and 1:3 for aluminium complexes.

Synthesis of Complexes

tris(2-hydroxynaphthaldehyde 4-hydroxybenzhydrazide Aluminium(III) (Al(NDB)₃) Complex.

A quantity of NDB ligand (0.0918 g, 3 mmol), was weighed and dissolved in absolute ethanol in a 3-necked round-buttomed flask. The solution was stirred under nitrogen at room temperature. Aluminium nitrate nonahydrate (0.0375 g, 1 mmol) was added to the solution. The mixture was stirred under nitrogen until a yellow precipitate was formed. The solid was collected by suction filtration and dried in vacuum dessicator. By taking note that aluminium : ligand stoichiometry is 1:3, the same procedure were repeated for synthesis of tris(2-hydroxynaphthaldehyde salicyloihydrazide Aluminium(III) (Al(NDS)₃) and tris(2-hydroxynaphthaldehyde furoilhydrazide Aluminium(III) (Al(NDF)₃).

Tris(2-hydroxynaphthaldehyde benzoilhydrazide Aluminium(III) (Al(NDB)₃) Complex.

 A quantity of NDB ligand (0.0612 g, 2 mmol), was weighed and dissolved in absolute methanol in a 3-necked round-buttomed flask. The solution was stirred under nitrogen at room temperature. Zinc acetate dihydrate (0.0220 g, 1 mmol) was added to the solution. The mixture was stirred under nitrogen until a yellow precipitate was formed. The solid was collected by suction filtration and dried in vacuumed dessicator. By taking note that zinc : ligand stoichiometry is 1:2, the same procedure were repeated for synthesis of di(2-hydroxynaphthaldehyde salicyloihydrazide Zinc(II) (Zn(NDS)₂) and di(2-hydroxynaphthaldehyde furoilhydrazide Zinc(II) (Zn(NDF)₂).

All the complexes obtained were characterized using UV-Vis and IR spectrometer.

Determination of Fluorescence Intensity of Ligands

Ligand solution (1 mL, 1×10^{-4} M) was pipeted into a 10 mL Erlenmeyer flask. Buffer solution (3 mL, pH 5.1), which was made up from sodium acetate trihydrate and glacial acetic acid in distilled water, was added to the solution. Deionized water was added until the mark. The flask was swirled to give a homogeneous solution.

After 5 minutes, fluorescence spectrum was recorded using Perkin Elmer Luminescence Spectrometer model LS55. The ligands were excited at 406 nm.

Determination of Fluorescence Intensity of Complexes
Ligand solution (3 mL, $1x10^{-4}$ M) was pipeted into 10 mL volumetric flask. Metal solution (1 mL, $1x10^{-4}$M) was added to the solution followed by buffer solution with pH 5.1 (2 mL). The mixture was then added with deionized water until the mark. The complexes were ecited at 406 nm.

Results and Discussion

The percentage yield for NDB ligand is 64%, NDF ligand is 69% and NDS ligand is 74%. Each of the ligands is yellow in colour and has melting points higher than 200^0C. Figure 1 shows the structure for ligands. Based on the IR, UV-Vis and ^{1}H-NMR data obtained, as discussed below we expected that all ligands were successfully synthesized.
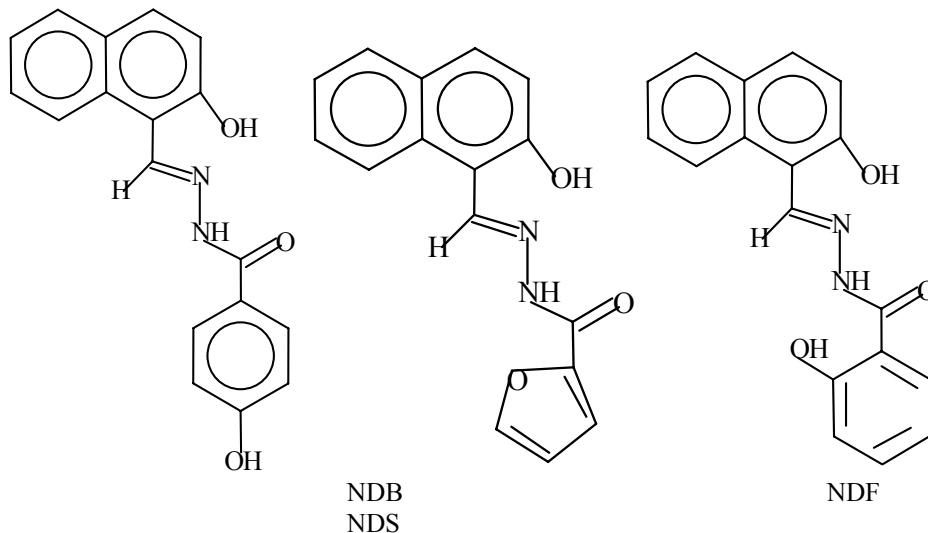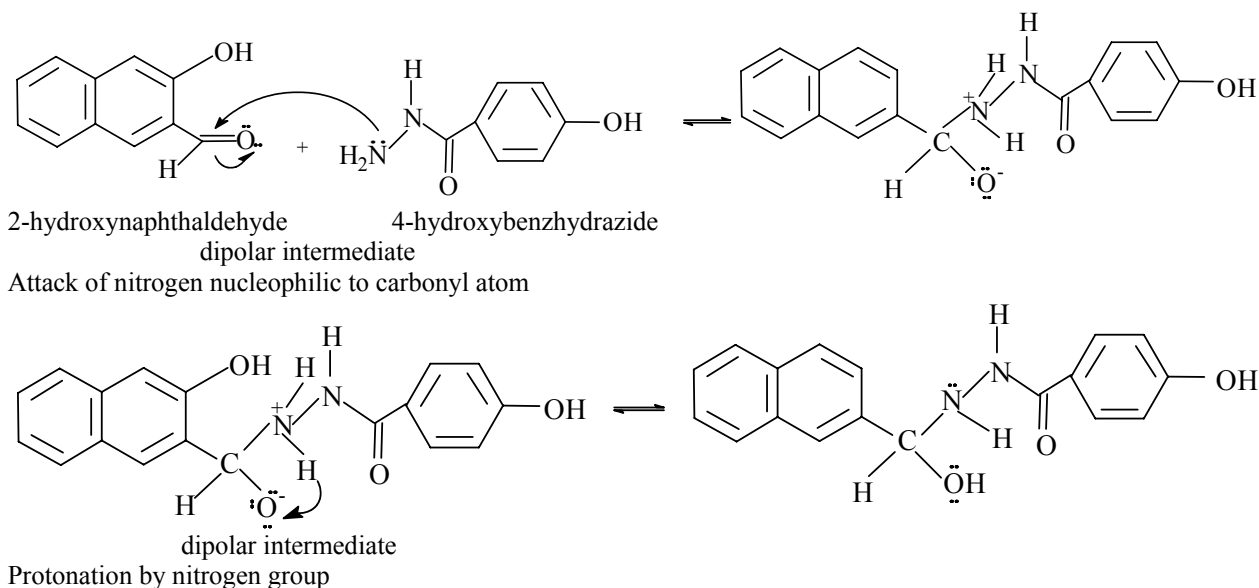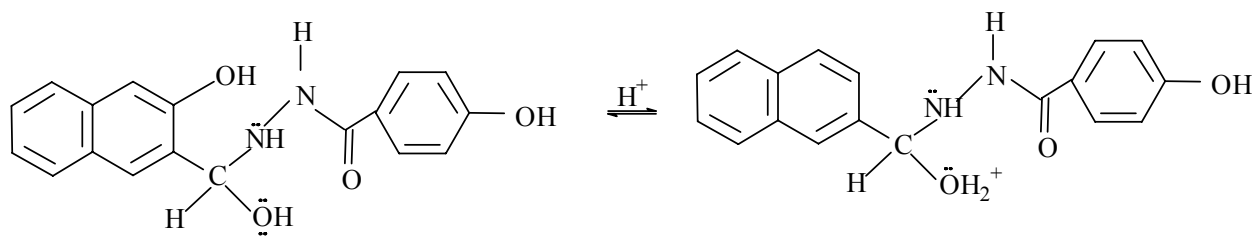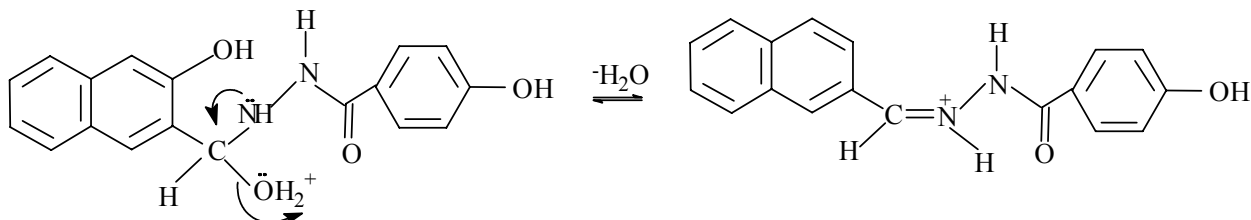

NDB

NDS

NDF

Figure 1 : Molecular structures of ligands.

2-hydroxynaphthaldehyde   4-hydroxybenzhydrazide
                    dipolar intermediate
Attack of nitrogen nucleophilic to carbonyl atom
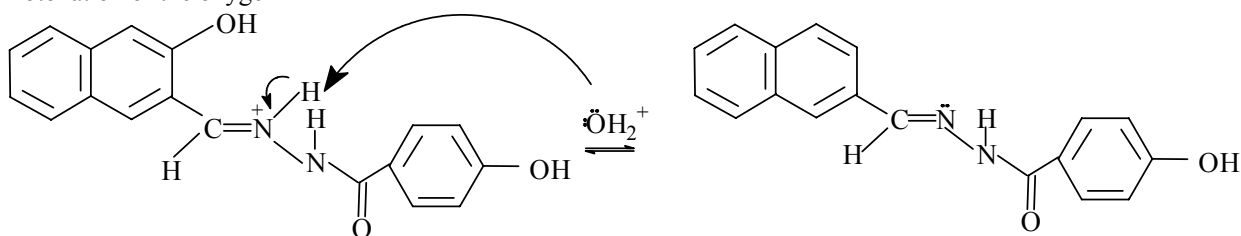

dipolar intermediate
Protonation by nitrogen group

protonated amino

alcohol
Protonation of hydroxyl group

iminium ion

Protonation of the oxygen

2-hydroxynaphthaldehyde4-hydroxybenzhydrazide

Table 1 : Main absorption bands according to types of electronic transition in UV-Vis spectra of ligands.

Ligands	Electronic Transition (nm)				
	$\pi \rightarrow \pi^*$			$n \rightarrow \pi^*$	
	C=O	C=N	Aromatic ring	C=O	C=N
NDB	311	325	361 and 375	425	425
NDS	314	327	363 and 385	426	426
NDF	313	326	364 and 377	433	433

Table 1 shows the UV-Vis data for ligands. Substitution on the carbonyl group by an auxochrome with lone pair of electrons, -NHR, gave a pronounced hypsochromic effect on the $n \rightarrow \pi^*$ transition. The auxochrome attached to the carbonyl group on ligands caused a bathochromic shift on the $\pi \rightarrow \pi^*$ transition [5]. Overall, absorption caused by transition of $n \rightarrow \pi^*$ for C=O and C=N occurred at lower energy level compared to the transition of $\pi \rightarrow \pi^*$. It is due to the energy barrier between molecule π and π^* is larger than between n and π^*. Thus, higher energy is needed for the transition from orbital π to π^*.

Table 2 : IR data for ligands

Ligands	Frequency(cm^{-1})					
	OH	**NH**	**C=O**	**C=N**	**C-O**	**C=C Aromatic**
NDS	3500-3200	3059.9	1644.2	1603.7	-	1457.1 and 1388.7
NDB	3210	3167.9	1635.5	1590.2	-	1538.1 and 1497.1
NDF	3437.9	3138.9	1642.3	1602.7	1196.7	1465.8 and 1392.5

Table 2 shows the data for IR spectra of ligands. From IR data , the observed band at 3500-3200 cm^{-1} are assigned as the bonded O-H. The sharp and intense band at 3167.9 cm^{-1} for NDB ligand, 3059.9 cm^{-1} for NDS ligand and 3138.9 cm^{-1} for NDF ligand is consistent with the presence of a N-H group while the band of medium intensity 1605 – 1590 cm^{-1} is characteristic of the amine C=N, formed through the condensation between aldehyde and hydrazide. The absorption band for N-H had shifted to a lower frequency that maybe due to the formation of the enol form of the ligands. The strong band at 1642.3 cm^{-1} for NDF ligand, 1635.5 cm^{-1} for NDB and 1644.2 cm^{-1} for NDS are assigned to the C=O group of the hydrazide. The presence of the C=N and C=O absorption bands in the spectrum confirmed the completeness of the condensation reaction.

Table 3 : NMR data for ligands

Ligand	Chemical Shift				
	OH	**NH**	**N=CH**	**Aromatic**	**C=CH**
NDB	12.90 s, 12.00 s	10.25 s	9.49 s	6.9-8.2 m	-
NDF	12.63 s	12.25 s	9.50 s	7.3-8.2 m	7.2 d
NDS	12.72 s, 11.99 s	11.69 s	9.51 s	6.9 m-8.3 m	-

Table 3 shows the NMR data for ligands dissolved in d_6-DMSO. The presence of amide O=C-NH proton resonance in the ^{1}H NMR spectrum indicated that the ligand exists as the keto form .

Figure 2 shows the molecular structure of Al(NDB)$_3$ and Zn(NDF)$_2$. the characterization of complexes were discussed below.
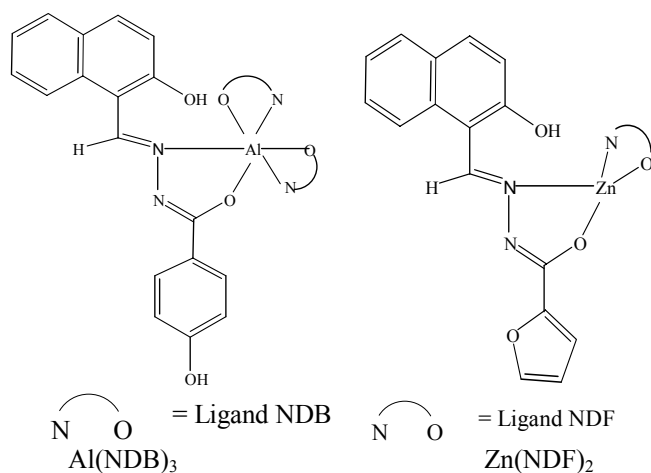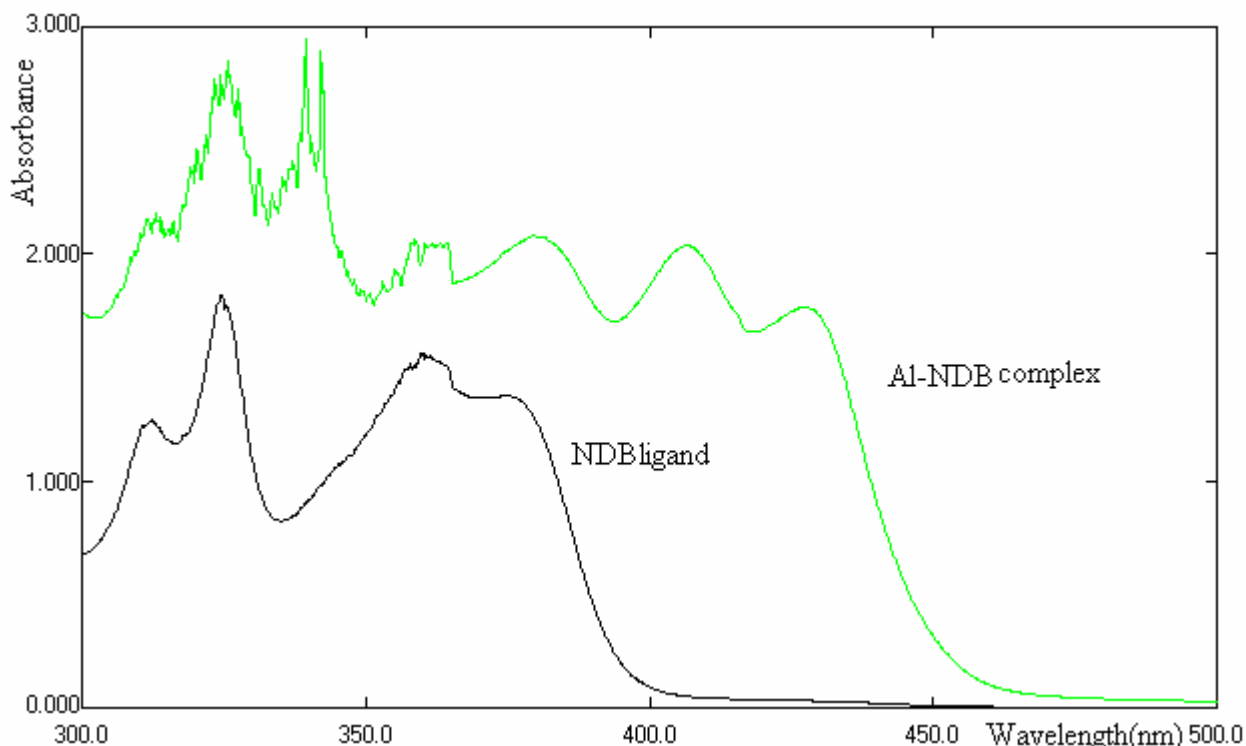
Figure 2 : Structure for complexes

Figure 3 : UV-Vis spectra for NDB ligand and Al(NDB)₃ complex

Figure 3 shows the UV-Vis spectrum for NDB ligand and Al(NDB)$_3$ complex as representative spectrum for the complexes. UV-Vis spectrum for complex shows that absorption due to electronic transition in C=O and C=N had shifted to longer wavelength. Batochromic shift for aromatic complex occurred at 410 nm and new absorption band formed at 435 nm that could be assigned as the charge transfer transition between metal and ligand [6].

Table 4 shows IR data for complexes. By comparing the FTIR spectrum between ligands and complexes, we can observed the presence of OH group bonded to the aromatic ring, in the region of 3300-3450 cm^{-1}. This indicates that this group did not involved in the coordination with metal. However, the stretching frequency of C=N had shifted to a higher frequency due to the bonding of N atom to the metal.

Table 4: IR data for complexes

Complex	Frequency(cm^{-1})			
	OH	C=O	C=N	NO_3^-
NDB Complex	3394 (3200-3500)	Not observed	1605.6 (1604.7)	1384.8 1390.6
NDF Complex	3436.9 (3425.3)	Not observed	1619.1 (1617.2)	1385.8 1382.9
NDS Complex	3450.4 (3200-3500)	Not observed	1604.7 (1604.7)	1386.7 (1388.5)

*Bracket indicates value for zinc complexes

It was also observed that the absorption of NH in amide group had disappeared, suggesting the fornnation of enol group and the formation of C=N-O⁻ before the bonding of oxygen atom with the metal occurred. This also explain why the C=O band is not observed.

Figure 4 shows the spectra of ligand and complex being excited at the same wavelength. Similar spectrum also observed for other complexes.
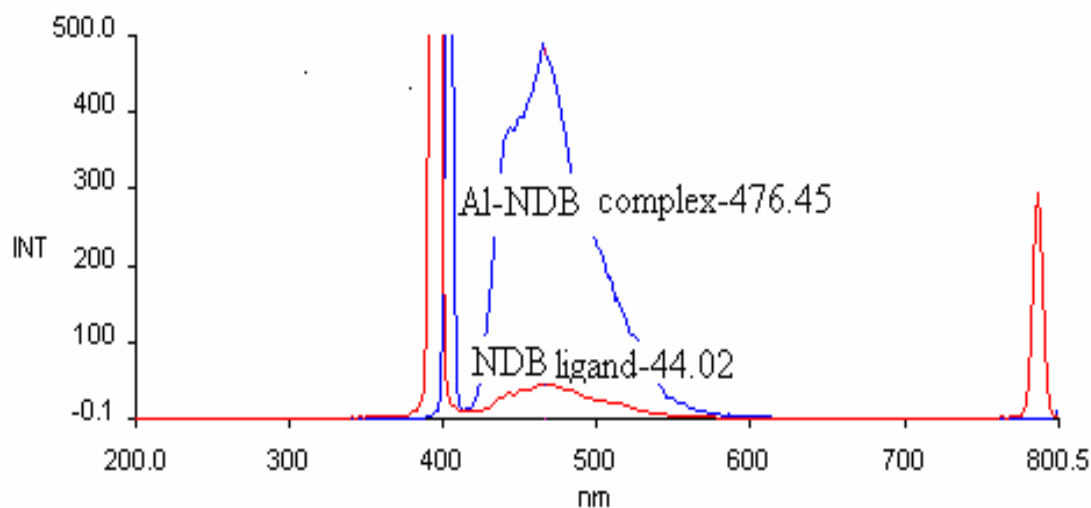

Figure 4 ;   Fluorescence spectra of NDB ligand and Al(NDB)₃ complex

Table 5 shows the intensity of fluorescence excited at λ_{max} 406nm and emit blue light at λ_{max} 470 nm. It shows that Al(NDB)₃ complex has the highest intensity compared to the others and all the aluminium complexes shows higher fluorescence intensity compared to zinc complexes which maybe attributed by more number of ligands bonded to aluminium.

Normally, a rigid molecule has the ability to emit high fluorescence radiation. It is because rigidity of molecules able to decrease the rate of collisional quenching, thus give more time to form emission. For chelate ligand, the intensity of fluorescence increases when it forms complex. Ketohydrazone, under the influence of metal, forms a rigid chelate ring. The central metal ion does not exhibit flourescent characteristic [8].

Table 5 : Fluorescence intensity of ligands and complexes

Compound	Fluorescence intensity (a.u)
NDF	37.99
NDS	56.22
NDB	44.02
Al(NDF)$_3$	194.56
Al(NDB)$_3$	476.45
Al(NDS)$_3$	249.00
Zn(NDF)$_2$	94.04
Zn(NDS)$_2$	102.10
Zn(NDB)$_2$	196.20

Conclusions

Three ketohydrazone ligands had been successfully synthesized and characterized. Complexation with metal increased the fluorescence intensity of the compounds as it causes the increase in rigidity of molecule especially with chelating ligand. Al(III) complexes shows better fluorescence intensity than Zn(II) complexes as it has a higher coordination number and thus increases the rigidity of molecules. All compounds emitted light in blue region.

As a conclusion, Al(III) complexes show a better potential to be the emitting material for OLED devices as it shows a better fluorescence properties compared to Zn(II) complexes. However, among all the complexes, Al(NDB)$_3$ had the best potential for this purpose as it shows the highest intensity of fluorescence.

Acknowledgement

References

1. Gui Y., Yang S. (2001). A New Blue Light-Emitting Material. *Synthetic Metals*. **117**. 211-214
2. Shizuo T., Noda K., Hiromitsu T. (2000) "Organic Light-Emitting Diodes using Novel Metal–Chelate Complexes". *Synthetic Metals*. **111.** 393–396.
3. Suning W. (.2001) "Luminescence and Electroluminescence of Al(III), B(III), Be(II) and Zn(II) Complexes with Nitrogen Donors". *Coordination Chemistry Reviews*. **215**. 79–98.
4. Constable, E.C. (1996). *Metals and Ligand Reactivity: An Introduction to the Organic Chemistry of Metal Complexes*. New York: VCH Publishers. 22-44.
5. Donald, L.P, Gary, M.L, and George, S.K. (1996). "Introduction to Spectroscopy". 2nd Edition. Saunders College. USA. **53**. 162-164.
6. UV Spectrometry Group (1993). *UV Spectroscopy Techniques : Instrumentation, data handling*. London : Chapman & Hall. 26-30
7. Tao Y. T. (2001). "Organic Light-Emitting Diodes Based on Variously Substituted Pyrazoloquinolines as Emitting Material". *Chem. Mater.* **13**, 1207-1212.
8. Chen B. J. and Sun X. W (2003). "Influences of Central Metal Ions on the Electroluminescence and Transport Properties of tris –(8-hydroxyquinolinoline) Metal Chelates". *Applied Physics Letter*. **82**. 3017-

The Malaysian Journal of Analytical Sciences
ISSN 1394—2506

Instructions for Authors

Authors are encouraged to submit high quality, original work that has not appeared in nor is under consideration by, other journals. Papers that have appeared in conference proceedings may also be considered, but this should be so indicated at the time of submission. Papers may be written in Malay or English.

The Malaysian Journal of Analytical Sciences requires that manuscripts be camera ready and of a specified page size, format, font, and point size. The Editor will not be responsible for any retyping, pasting in figures, tables etc. The only information that will be added by the Editor will be the journal title, page numbers and dates the paper was received and accepted.

Please read these instructions very carefully and refer to articles published in past issues for guidance on how the manuscript must be prepared. Please note that the measurements for indentations etc. may vary slightly depending on the spacing used in the word processing program.

1. The maximum paper length is 15 pages for the complete, camera-ready manuscript.

2. The text on first page should occupy a box 16.0 cm width and 22. 0 cm length. Begin Title at least 3.5 cm from top of page.

3. The text on other pages should be 16.0 cm x 23.5 cm. Begin text at least 2.0 cm from the top of page. The preferred typeface is Times New Roman.

Some Specific Points

1. Title of Paper
All upper case, 14 point text 16.0 cm in width, centered on page. Leave one space between title and authors.

2. Authors
Use 10 point font. Use initials followed by family name, otherwise use full name. Use comma between authors and use superscript 1, 2, 3 etc. to indicate affiliation. Center author names. Leave one space between authors and addresses.

3. Addresses
Use 9 point font italic, full page width, centered. Indicate authors' affiliation with superscript 1, 2, 3 etc. and start each address on new line. Leave 3 spaces between addresses and key words.

4. Key words
Use English key words maximum 6. Use 9 point font and centered. Leave one space before abstract.

5. Abstract
Maximum 200 words in English and Malay. Use 9 point font with text left and right justified. Leave two spaces before text of paper.

6. Headings
Organise paper into Introduction, Experimental, Results and Discussion, and References. All first order headings use 10 point font, bold and centered. Second order headings should be italics, 10 point font and unindented.

7. Text of Paper
Should be in 10 point font size. Unindented. The text should be left and right justified. Metric units should be used in their accepted abbreviated form. Chemical symbols should be specified and spelled out for the first time, thereafter the symbol used.

8. References Cited
Used sequential numerals in square brackets [2] for indicating references. References should be listed in numerical order in the References section and should be in 9 point font text with the format, authors, years, title of paper, abbreviated journal tide, volume, issue number, and pages.

9. Tables
Must be included in body of the text. Table text and caption should be in 9 point font centered over full page width. Table number and heading should be centered above the table.

10. Illustrations
Figures must be located in the body text and centered. The figure number and caption in 9 point font should be centered below the figure using the full page width. Only good contrast, original line drawings are accepted. Poor quality illustrations will be returned.

11. Acknowledgement
This should be included whenever appropriate as a separate section before Reference section. Use 10 point text.